Methods of Evaluating Slate and their Application to the Scottish Slate Quarries

This Thesis is submitted for the Degree of

Doctor of Philosophy

Division of Earth Sciences

Department of Geography and Topographic Science

University of Glasgow

Glasgow, Scotland

Summer 1999

Declaration

The material presented in this Thesis is the product of independent research undertaken by the undersigned within the Department of Geography and Topographic Science. Any published or unpublished work by other authors has been given full acknowledgement in the text.

Joan A Walsh

Summary

This research Project was initiated by Historic Scotland, with the objective *of selecting appropriate Scottish quarries for further investigation with a view to reopening. It is hoped thereby to ensure the continued availability of this traditional roofing material of proven quality and durability and thus to maintain and restore the indigenous character of Scottish architecture.*

Methodology The basis of the research was to identify those physical, chemical and geological attributes of slate which make it a good roofing material. These were then related to specific Scottish quarries in order to select those which showed the best potential for resumed production. However, as no fresh samples of Scottish slate were available, the work was based initially on slate of known and reliable quality from producing quarries elsewhere. The parameters examined were mineral composition, metamorphic grade, fabric and weathering properties. When the parameters most closely related to the quality of finished slates were established then the Scottish slate was examined for these same parameters.

- ***Mineral Composition*** Recent progress in the determination of the chemical formulae of the phyllosilicates of fine-grained material has enabled the mineral composition of slate to be calculated from its total oxide composition. Calculations based on representative samples from each group of quarries gave good results when taken from sites in close proximity, but application to samples from more remote sites gave a weaker correlation.

- ***Metamorphic Grade*** Metamorphic grade affects the crystallinity and the grain size of a material. Traditionally for sedimentary rocks both properties were evaluated by the sharpness of peaks in XRD analysis, using Full Width at Half Magnitude (FWHM) as the criterion. However, this method is not effective when applied to slate, and an alternative method of determining its crystallinity was developed, based on the intensities of peaks of the main minerals.

- ***Fabric of Slate*** A relationship was developed between the characteristics of slaty cleavage and the potential minimum thickness of the finished roofing slate. A Fabric Points Scheme (FPS) was devised and used initially to relate the fabric of slates from producing quarries with the actual thickness of the finished slates. This relationship was then used to predict the potential minimum thickness of Scottish slate and verified where possible by comparing the actual thicknesses of used Scottish slates.

- ***Weathering Properties*** Estimates of the durability of slate were made by experimentally weathering new slates using a wetting and drying test, and measuring the increase in ability of the slate to absorb water. It was found that 5 to 12 wetting and drying cycles were equivalent to one year of natural weathering. It was then possible to estimate the life of a slate to the point at which water absorption reached a value of 0.3% which is the limit specified by the British Standard for slate, BS 680.

Resources of Scottish slate There was a satisfactory degree of agreement between the quality of the various slates as established using the above parameters and their performance or to their reputation. Based on the data thus obtained, an assessment was made of the potential of each of the known Scottish slate quarries.

- The best Scottish slate is found at ***Ballachulish***, and there are sufficient resources to merit further investigation.
- There are large resources of very durable ***Macduff*** slate on the north slopes of the Slate Hills Aberdeenshire.
- The mineralogy of ***Highland Border*** slate suggests that it would have good potential as a roofing material. Other properties however vary considerably from quarry to quarry and for producing units within a quarry.
- No quarry in the ***Easdale*** area was particularly suitable for further investigation, but one suggestion has been made.

The following quarries are recommended for further investigation:

1.	Ballachulish	Khartoum
2.	Macduff	Kirkney
3.	Highland Border	Craiglea
4.	" "	Aberfoyle
5.	Easdale	Breine Phort

Table of Contents

List of Figures

List of Tables

Abbreviations

BGS	British Geological Survey
BRE	Building Research Establishment
BSE	Back scatter electron
BSI	British Standards Institution
C of V	Coefficient of Variation
CD	Cleavage domains
FPS	Fabric Points Scheme
FWHM	Full Width at Half Magnitude
H	Thin section parallel to cleavage surface
HS	Historic Scotland
IC	Illite crystallinity
L	Thin section perpendicular to cleavage surface
LOI	Loss on Ignition
ML	Microlithon
PPL	Plane Polarised Light
SEM	Scanning Electron Microscope
St Dev	Standard deviation
W/D	Wetting and drying
XP	Cross polars
XRD	X-ray Diffraction
XRF	X-ray Fluorescence
Z	Atomic number
μ	Attenuation coefficient

Acknowledgements

Firstly I would like to thank Ingval Maxwell of Historic Scotland, whose vision of reviving the Scottish slate industry first led to this Project. Together with him, my Project Managers Robin Kent and subsequently Audrey Dakin gave me their support throughout its execution.

I would then like to thank Brian Bluck for choosing me to carry out the Project and for his supervision throughout its duration, not least for his giving me the freedom to develop it as I saw fit.

I would like to thank all the staff of the Department of Earth Sciences who, during a difficult period of reorganisation, never failed to give of their time to discuss aspects of the work. No member of staff entirely escaped my questions but I would like to mention in particular Alan Hall for his advice on XRD work and Tim Dempster for advice on microprobe work

On a sad note I would like to remember Roddy Morrison, who died so soon after retiring, for his moral support during my time in the Department. He is sadly missed.

I received considerable help with the practical aspects of this research from Murdo Macleod (now retired) and Bill Hickson. I would also like to express my gratitude to Douglas Maclean for the care he gave to the development of the photographs, even to the extent of coming out of retirement to redo those chosen to be included in this Thesis. Kenny Roberts is thanked for his help with computers, John Gilleece for the preparation of polished sections and Robert McDonald for assistance with the microprobe.

I would like to thank A Williams, Elfed Williams and David Bailey of the Cwt y Bugail Slate Co. for all the help and invaluable information they gave me in the early stages of this research, providing the basis for much of the subsequent work

I would also like to express my gratitude to Donald Ramsay, formerly of this Department, and Graham Smith at BGS for reading the Quarry Reports and for their very useful comments and suggestions.

I would like to thank the staff at BRE for giving me access to old records in their archives. In particular I would like to thank John Huston for all his help during the time I spent at the BRE offices in Watford.

My thanks too, to Jeff Harris for arranging to carry out XRF work at Edinburgh University and to Godfrey Fitton and Dodie James for their help during my few weeks there.

I thank my son Ronan for a long discussion on Scottish Industrial History and my son Kieran for advice on statistics and much more. I am also very grateful to my father John Walsh who in his ninth decade was delighted to join me when visiting quarries and in particular arranged my visits to the various Irish slate quarries.

It is not possible to mention by name all the people who freely gave of their time, generously gave me information on slate quarries and allowed me to visit quarries on their land. To all, I am extremely grateful for their help.

And finally I would like to express my deepest gratitude to David for his never ending support both moral and practical, not least in the tedious task of editing and re-editing this Thesis.

This project was funded by Historic Scotland.

Chapter 1 Introduction

Slate is a rock derived from fine-grained mudstones or siltstones, or in some cases volcanic tuffs, which have undergone low-grade metamorphism and deformation due to tectonic compression. It is made up of a high proportion of platy minerals i.e. phyllosillicates. These phyllosilicates align during deformation, imparting a schistosity or cleavage to the rock along which it can be split into thin sheets. It is the ability to be split along planes of cleavage that make slate suitable for use as a building material, in particular a roofing material

1.1 Aim

Much of the urban landscape of Scotland consists of slate roofs, and slate is the roofing material for many historic buildings. However, there are no longer any slate quarries in production in Scotland and any repairs or renovations to such buildings must rely on second hand slates or on supplies from outside Scotland. It was with this in mind that this research Project was initiated by Historic Scotland, with the objective ***of selecting appropriate Scottish quarries for further investigation with a view to reopening. It is hoped thereby to ensure the continued availability of this traditional roofing material of proven quality and durability and thus to maintain and restore the indigenous character of Scottish architecture.*** This Thesis is concerned with the development of methods suitable for the analysis of slates in terms of their mineralogy, crystallinity, fabric and weathering properties. Individual quarries are described in Appendix A The Scottish Slate Quarries. Because this is to be published as a separate document in the form of a Technical Advice Note (TAN) by Historic Scotland some parts of the Thesis have been duplicated in the Appendix so that it can stand alone.

1.2 Methodology

The emphasis of the original Historic Scotland contract was on Scottish slate, with particular importance placed on updating the last article written on Scottish quarries

by Richey and Anderson in 1944. Therefore to comply with the contract necessitated looking at over 100 individual quarries spread over a large area. As a result it was not possible to map any quarry in great detail, and only a few representative samples were analysed from each quarry. In addition some laboratory test methods had to be rejected as too time consuming, because of the need to include such a large data set. However, to assess the quality of Scottish slate it is necessary firstly to determine those properties of slate in general which make it a good roofing material. The lack of any working quarries in Scotland meant that no recently finished samples of Scottish slate were available. Initially therefore, slate samples were collected from producing quarries in North Wales and Cumbria, where the product is of known and reliable quality. The slates from these areas are very different and provide a reasonably broad spectrum with which to compare Scottish slate. In a further stage of the research it is proposed to look at Scottish slate in relation to that produced world-wide and hence broaden the data base used in all aspects of this work. The samples from these producing quarries which were used in this Project are listed in Appendix 1.1. The samples were analysed in terms of their mineral composition, metamorphic grade, fabric and weathering properties and compared with the graded quality of the finished slate. When the parameters most closely related to the quality of finished slate were established, then the Scottish slates were examined for these same parameters.

The quarries chosen for further study were selected on the basis of their mineralogy, fabric and weathering properties and localities. The next stage of research will be to carry out a site investigation of each chosen quarry. This will look at the rock *in situ* to determine the resources, the proportion of usable slate, and parameters such as the density and orientation of discontinuities, joint patterns, veins etc. which control the size of slate. A larger sample set for an individual quarry will be tested according to the procedures laid out in this Report to identify those seams which have the best fabric and mineral composition.

1.3 Previous Work

While many aspects of slate as a rock have been covered in the literature, there has been very little work done on relating the geological properties of slate to its use as a roofing material. The last definitive article on the Scottish slate industry and Scottish slate quarries was the Wartime Pamphlet No 40 (Richey and Anderson, 1944). As the industry closed in the 1960s, more recent work only makes passing references to Scottish slate (Crockett 1975, Harries-Rees 1991 and Wagner *et al.* 1994 and 1995). An important aspect of the present Study is to update the Wartime Pamphlet in the light of recent developments in our understanding of the geology of the various slate areas and the changes that have taken place within the quarries.

More recent references to working quarries have concentrated on the economics of quarry operations. For example, Tacoume *et al.* (1997) and Le Corre (1970) discuss the effect of the spacing of discontinuities within a quarry, such as joints, on the rate of recovery of slate. But without access to unweathered faces in Scottish quarries, this is only of limited relevance to this Study. Tacoume's *et al.* (1998) work will be useful once a quarry has been chosen for further study with a view to reopening.

Mineralogy: Very little work has been done on quantifying the mineral composition of slate. Analyses of fine grained material have mainly been confined to shales e.g. Schultz (1964) evaluated the composition of Pierre Shale, and Avery and Bullock (1977) classified soils by X-ray techniques. Le Corre (1970) and Marty (1980) discussed slate in terms of its mineralogy, fabric and impurities in fairly general terms. Because of recent developments in the microprobe analysis of fine grained material (Dempster and Tanner 1998), it has been possible to refine the determination of mineral composition with a view to relating it to the properties of the slate.

The metamorphic grade: Considerable research has been devoted to the measuring of metamorphic grade in terms of its illite crystallinity (IC) i.e. the sharpness of the illite X-ray diffraction (XRD) peak. A more general term, Full Width at Half

Magnitude (FWHM), is used in this Report instead of IC. Because the metamorphic grade of slate is at the upper limit of the effectiveness of this FWHM technique there is a loss of sensitivity. It was therefore necessary to develop alternative methods of assessing the metamorphic grade.

Fabric: Apart from some reference to the effect of mineral composition on the ability to split a slate by Le Corre (1970) and Wagner *et al.* (1994), little research has been carried out on the splitting properties of slate. Building on the descriptive method of assessing fabric developed by Powell (1979), a more quantitative approach is developed in this Study to relate fabric to the minimum potential thickness of the finished slate (Chapter 4).

Weathering properties are generally covered by the various national standards for slate and the specifications in trade literature, but only in the case of the American and British standards was the research behind the various standards available.

A comprehensive study of the durability of American slate was carried out by Kessler and Sligh (1932) in preparation for the American standard for slate. In this study, the effects of age on the properties of slate on roofs were compared with similar effects achieved by laboratory tests. Watkins carried out research in 1934 in preparation for the publication of the British Standard for slate, BS 680. This research tried to relate the reputation of slates with properties determined objectively in the laboratory. Various studies into the weathering reactions which take place in slate have been carried out e.g. Roekens *et al.* (1991) and Shayan and Lancuck (1987).

The various national standards for slate address the problem of how best to determine the durability of a slate. A précis of those national standards referred to in this Report is given in Appendix B.

1.4 Scottish Slate Industry

Slate quarrying was one of Scotland's most significant building material industries throughout the 18th, 19th and early 20th centuries. It was concentrated at four geological areas (Fig.1.1) namely:

1. Ballachulish near the Great Glen fault.
2. The Slate Islands near Oban, of which Easdale is the best known.
3. A series of quarries just north of the Highland Boundary Fault stretching from Arran in the west to Dunkeld in the east.
4. A group of quarries near Huntly in Aberdeenshire located in high ground called the Slate Hills.

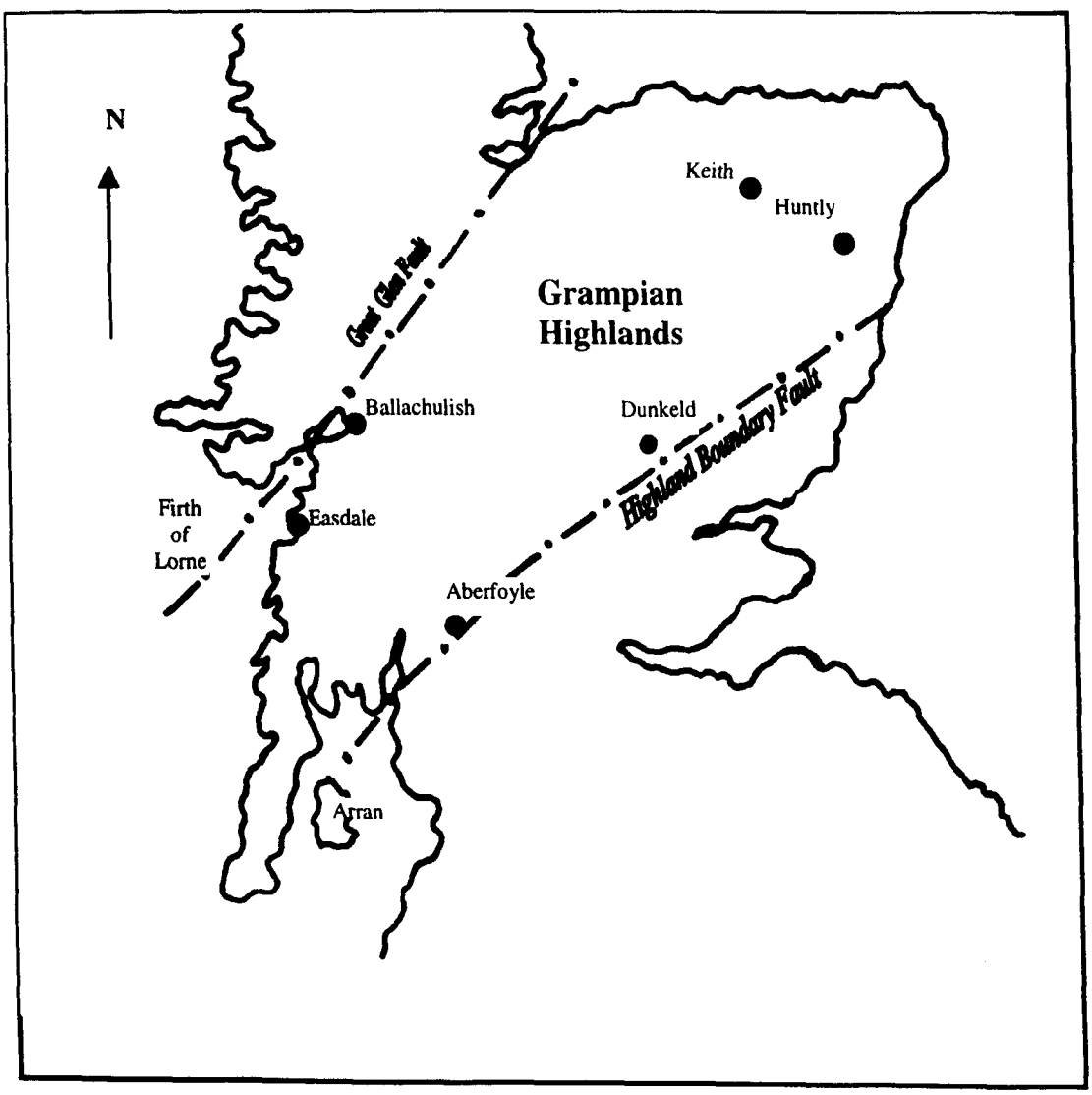

Fig. 1.1 Location of the principal centres of slate production in Scotland.

Slate has made a significant contribution to Scottish architecture in the past. *"Slates are very versatile as a roofing material, permitting carpenters to adopt various shapes of roofs and complicated intersections. The slates could be dressed to form mitres in hips and valleys, to be fixed round curves in turrets and the rounded cheeks of dormers"* (Naismuth 1985). This versatility allowed builders to incorporate intricacies in their designs that were impossible to achieve in other materials and contributed significantly to Scottish architectural tradition.

1.4.1 Brief History of the Scottish Slate Industry

The origins of the Scottish slate industry are unknown. However, re-used slates believed to come from the Easdale slate belt were identified in a wall *"tentatively ascribed as 14th century"* in the Finlaggan Project on Islay in the Inner Hebrides (Per. com. Ruckley 1997). The industry was already established in the 15th century although our knowledge is episodic, for instance in 1445 the Royal Chamberlain paid 11/10d for 130,000 slates quarried on Bute to repair the Kings Castle in Dumbarton (Hewison 1845).

Records improved in the 18th century when the Scottish slate industry was centred on Easdale and the surrounding Slate Islands, part of the Earl of Breadalbane's estate (Tucker 1977). Thanks to the good accounts maintained by the Marble and Slate Company of Netherlorn which the Earl set up in 1745, the expansion of the industry can be followed. At the time of the establishment of this company, seven crews each of 4 or 5 men were employed producing over a million slates annually. These were supplied throughout Scotland but mainly to the east coast. Transport was by sea in ships capable of carrying cargoes of 20,000 to 30,000 slates. As these ships were loaded from small boats off the rocky coastline of Argyll, it is not surprising that many cargoes were lost. In 1751 new quarries were opened at Ellenabeich and Luing and in 1766 further quarries at Luing, Belnahua and Kilchattan with annual production increasing to 4-5 million slates at the end of the century[1].

[1] Journals of the Company at Scottish Record Office GD112/18 54

In 1799 a tax was introduced on all slates carried by sea. The cost of transport was a major part of the cost of the slate and this tax was levied at 20% on the price at the point of delivery (Tucker 1977). It had a detrimental affect on the industry not only in Scotland but throughout Britain as a whole. In spite of opposition from slate proprietors, the tax was not removed until 1831.

During the 19th century, the records kept by the Marble and Slate Company of Netherlorn were not as good, probably indicating that the business was in difficulty. The price of slates dropped from £1 per 1000 in the boom of the 1750s to 17/- per 1000 in 1825 and 15/- per 1000 in 1827 (Tucker 1977). It was reported at this time that Ballachulish was prepared to accept 12/6 per 1000 from a Glasgow dealer. By 1838 the manager James Robertson was being told not to spend money on new leases and removal of tips. When the fifth Earl of Breadalbane died in 1862 the company was broken up into several smaller enterprises. A dramatic end to quarrying at Ellenabeich occurred on 22nd of November 1881 during a great gale when a tidal wave broke the retaining wall and flooded the quarry, preventing it from ever again being worked. The initial monopoly enjoyed by the Easdale slate quarries in the 18th century was over, but the Slate Islands continued to be a major contributor to the overall Scottish production during the 19th and 20th centuries until the final demise of the industry in the 1960s.

One factor in the decline of the fortunes of the Easdale quarries was the rise in the level of production in other areas. In the early 19th century production of slate in Banffshire and Aberdeenshire was increasing, e.g. the Foudland Quarry maintained an annual production of 800,000 for 30 years rising to a peak of 1,000,000 in 1826/27 selling at 10/- per 1000. *"The quantity of slates made in the Foudland, Tillymorgan and Gartly quarries has occasioned a great diminution in the consumption of the Easdale and Ballachulish slate in Aberdeenshire, only two cargoes of the former and one of the latter having been imported at Aberdeen in 1810"* (Blaikie 1834).

Easdale would also have been affected by the opening of the Ballachulish West Quarry in 1693 and the larger East Quarry in 1694 (Fairweather 1994)[2]. Ballachulish

[2] According to Bremmer (1869) this quarry was not opened until 1780!

expanded rapidly during the 19th century. According to Smith's account (1825), production at that time was half the level of that from Easdale. This rose to double that from Easdale by the 1860s onwards. Employment grew from 300 men in 1845 to 587 men in 1875. From 1882 to 1888 Ballachulish was producing 15 million slates annually (Tucker 1977).

The Welsh slate industry was also expanding rapidly, from 20 million slates in 1786 to over 100 million in 1831 (Tucker 1977). The expansion of the railway system in the second half of the 19th century facilitated the transport of cheaper Welsh slates and heralded the decline of the Scottish slate industry as a whole.

The inroads made by the Welsh industry were not felt immediately as production in Scotland continued to increase, reaching its peak at the end of the 19th century. This was a time of rapid growth in urban population with concomitant demand for new housing and hence slates, e.g. in 1896 45,000[3] tonnes (approximately 45 million slates) were produced. Production started to decline soon after 1900 and had already dropped to half its maximum level by 1910. Production ceased completely during World War I due to lack of manpower. The industry partly recovered in the 1920s and 1930s to between 15,000 and 20,000[4] tonnes per annum (15 - 20 million slates), but by then manufactured tiles had become a major competitor taking an increasing proportion of the roofing market. No separate figures for slate production were reported for Scotland between 1945 and 1964 but the last return in the statistical accounts recorded 5 tonnes in 1966.[5]

Although resources are still abundant, the one time buoyant industry is now defunct. A more detailed account of the history of Scottish quarries is given in the appraisals of individual quarries (Appendix A). Descriptions of the quarries of Wales, Cumbria, Devon and Cornwall are given in Hart's account (1991).

---

[3] 1895-1896 Mineral Statistics; Home Office

[4] 1921-1938 Annual Report of the Secretary of Mines; Mines Department, Board of Trade

[5] 1950-1973 U.K. Mineral Statistics; Institute of Geological Sciences

1.4.2 Methods of Working

Until the late 17th century the production of slates was from faces exposed above the shore. On Easdale the tide was utilised to loosen blocks between high and low water by means of wooden wedges which expanded when wet. It was not possible to use the tide at Ballachulish as the quarries were at a higher level, but instead water was poured over the wood.

Removal of surface water was always a problem especially in quarries close to the shore. At Easdale sluices allowed for the disposal of water at low tide. In the early 19th century improved drainage devices, including a steam pump and a windmill, were introduced with varying success, to allow quarrying below sea level. Ellanabeich was 60m (200ft) deep at the time it was flooded.

In the early days slate blocks were transported in creels to the slate cutting banks. Later, tramways were introduced and the blocks transported in wagons drawn by horses. On Easdale the problem was to lift the slate up to ground level from approximately 45m (150ft) below. For this cranes and inclined planes were used. Both Ballachulish and Easdale had extensive tramway networks in place at the end of the 19th century. Stationary engines were used on inclined planes from the quarry faces to the dressing sheds, and locomotives between the quarries and quays (Tucker 1977).

Holes were drilled by hand and filled with black powder, which dislodged the slate blocks on being exploded. Not until 1926 was the time consuming procedure of drilling manually mechanised by using compressed air. The size of blocks was limited by the spacing of discontinuities such as joints. Blocks were split along cleavage into slabs about 25mm (1 inch) thick. These were then conveyed to the dressing sheds by the trammers. The dressers split the slabs into slates using a ***gilb*** (thin chisel) driven by blows from a ***fairchean*** (mallet). Placing the slate on a ***clach eimile*** (iron plate) the dresser finished the slate into a rectangular shape using his ***corc sgleit*** (long heavy knife) (Peach *et al.* 1909). The slates were then ready for transport to their markets.

Before a possible revival of the Scottish slate industry it is necessary to look at modern slate production. Crockett reviewed the British industry in 1975, Harries-Rees and Wagner *et al.* the European market in 1991 and 1995 respectively. A review of modern working practices is outside the scope of this work.

1.5 Slate Industry Today

At present there is a ready supply of second-hand Scottish slates, reflected in their relatively low cost. However, demolition and redressing losses are leading to diminishing stocks. Theft of slate from restorable buildings, even occupied buildings, is increasing as demand outstrips supply. Although the second-hand Scottish slate is mainly used in historic building repair and restoration, there has also been a return to the use of natural slate on new roofs. While concrete tiles still dominate, over 20% of new roofs are currently covered in natural slate. In 1990, 42,000 tons of British slate were produced at £1000/ton and 43,000 tons were imported, mainly from Spain, at a price approximately 25% less than that of the indigenous supply. More recently, even cheaper slates are being imported from Brazil and China. (Richards 1995).

Historic Scotland is aware that the use of non-indigenous roof covering has led to the streetscapes of many Scottish cities, towns and villages losing much of their original character. Rural buildings too have been greatly changed in appearance. To quantify this loss, they commissioned a second research project to run in parallel with this Project at the Department of Town and Regional Planning, Dundee University. The aim of the Dundee project is to assess the historical and aesthetic importance of Scottish slate and the technical, financial and aesthetic issues involved in using traditional Scottish slate. It also includes a survey of sources and levels of demand as well as the attitudes of architects, conservation bodies, local authorities and developers to the use of slate.

This Report concentrates on the inherent properties of slate which relate to its performance as a roofing material, methods of measuring these and draws conclusions on the potential for reopening one or more Scottish quarries.

Chapter 2 Mineralogy

2.1 Introduction

Slate is a rock derived from argillaceous sediments or fine-grained volcanic ashes. It is produced by metamorphism and deformation and characterised by cleavage along planes which are independent of the original bedding. This Study shows that many of the properties of slate are largely dependent on its mineral composition: the proportion of platy minerals controls its splitting, quartz controls its hardness and durability, while the presence of some minor minerals adversely affects its durability. Therefore the relative proportions of the major minerals present is an important criterion in determining the properties of a slate. However, due to the fine-grained nature of the material, determination of its mineral composition is not straightforward, ***and the aim of this Chapter is to evaluate the accuracy of different analytical methods for determining the mineral composition of slate and to present the results of these analyses.***

2.2 Background

The essential minerals of slate are quartz and the phyllosilicates (white micas and chlorite) and various accessory minerals. The determination of the relative abundance of constituent minerals in fine grained rocks has been the subject of a number of publications (Schultz 1964, Carroll 1970, Brindley 1961, Avery and Bullock 1977) but these have concentrated on the proportions in clays and their techniques are not directly applicable to slate. At the level of metamorphism observed in Scottish slate, most of the clay minerals have been converted to white mica and chlorite. Schultz (1964) did determine a proportionality constant between the areas of quartz and carbonate XRD peaks and their concentration. His work was done using copper radiation while cobalt radiation was used in this Study, so no direct comparison was possible. As this chapter evaluates the methods of mineral identification, some of the characteristics of the minerals involved are first briefly reviewed.

2.2.1 Quartz

Formula SiO_2 Hardness 7

Quartz, the most common of minerals, is present in nearly all types of rock and is always present in slate. Structurally, it is made up of silicon tetrahedra (Fig. 2.1) in which all the oxygens are shared with neighbouring tetrahedra forming a three dimensional framework without cleavage. It is the most persistent of the common minerals and survives transportation, weathering prior to sedimentation and the increased temperature and pressure of low-grade metamorphism. Although less abundant in the finer grained mudstones that are the precursors of slate, its presence is nevertheless significant. Detrital grains of primary quartz become more elongated during the development of the slaty cleavage and are orientated with their long axis parallel to the cleavage. Secondary quartz grows during metamorphism in a number of ways. It may grow around pre-existing quartz grains, as clusters of new grains in the pressure shadows of the larger grains of any mineral, or independently in veins filling fissures caused by joints and faults. These veins can range in size from those visible to the naked eye, distorting cleavage on a large scale, to minor clusters, only detected at microscopic level, which destroy the homogeneity necessary to produce a regular slate surface.

Although some quartz is necessary to strengthen a slate, too much quartz, especially if too coarse-grained, impairs the ability of slate to be split into thin sheets, and is therefore detrimental to the production of higher-grade thin slates. The amount of quartz found in Scottish slate is 15%-35%.

2.2.2 Phyllosilicates

Formula variable (see below) Hardness 2-3

Phyllosilicates is a group of minerals which derive their name from the Greek word *phyllon* for leaf which reflects their platy habit. They belong to a group of silicate minerals characterised by their perfect cleavage and elasticity, reflecting their layered atomic structure. Next to quartz, phyllosilicates are the most common sedimentary and low-grade metamorphic minerals, and include clays, illites, and micas such as white micas, chlorite

and biotite. The bulk of slate is made up of white micas and chlorite. The structure and formulae of phyllosilicates are discussed in some detail as these control the physical and chemical properties of slate (Bailey 1984).

2.2.2.1 Layered Structure of Phyllosilicates

The atomic structure of phyllosilicates is comprised of tetrahedral and octahedral layers

i **Tetrahedral layers** consist of silicate tetrahedra SiO_4^{4-} bound together so that three of the four oxygens are shared by neighbouring silica giving a hexagonal grid. The remaining oxygen at the apex of each tetrahedron is normal to the sheet and is co-ordinated to the cation forming the octahedral layers. The overall formula of the tetrahedral sheet is $Si_2O_5^{2-}$ (Fig. 2.1).

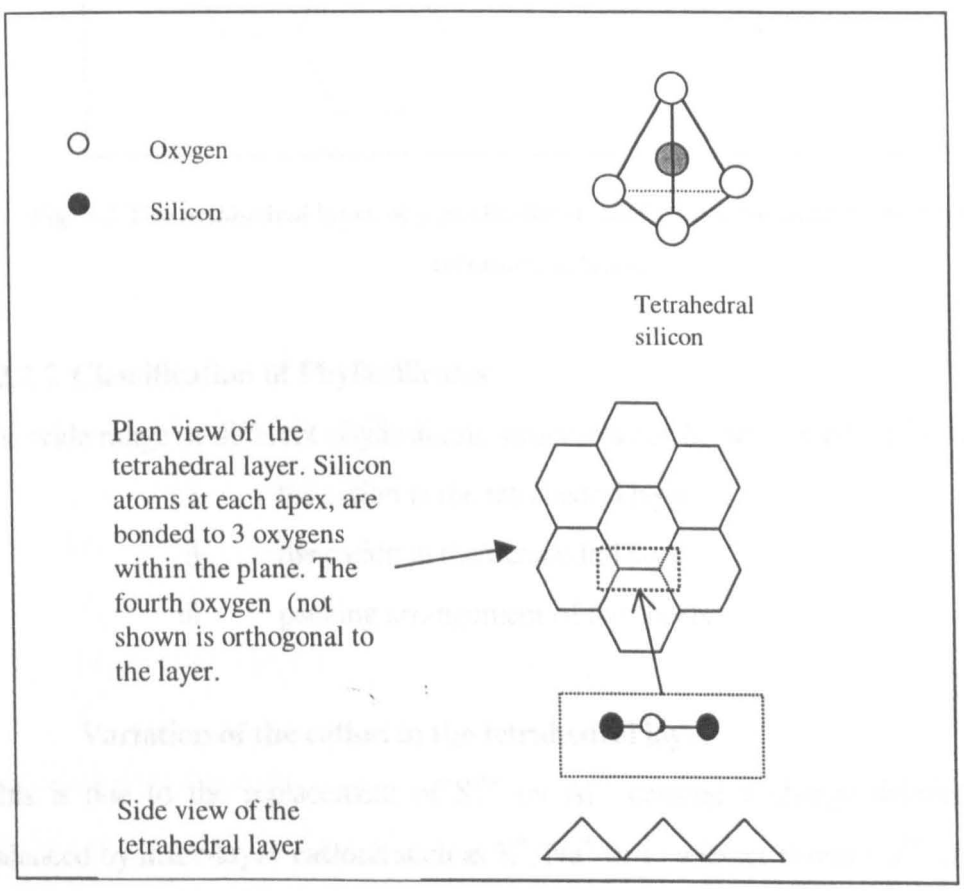

Fig. 2.1 Tetrahedral layer of a phyllosilicate

ii **Octahedral layers** consist of octahedrally bound cations typically magnesium Mg^{2+} or aluminium Al^{3+} forming a brucite or gibbsite layer respectively The cations are bonded to the oxygens at the apex of the tetrahedra as described above, as well as to

hydroxyl ions OH^- found at the centre of each hexagon (Fig.2.2).

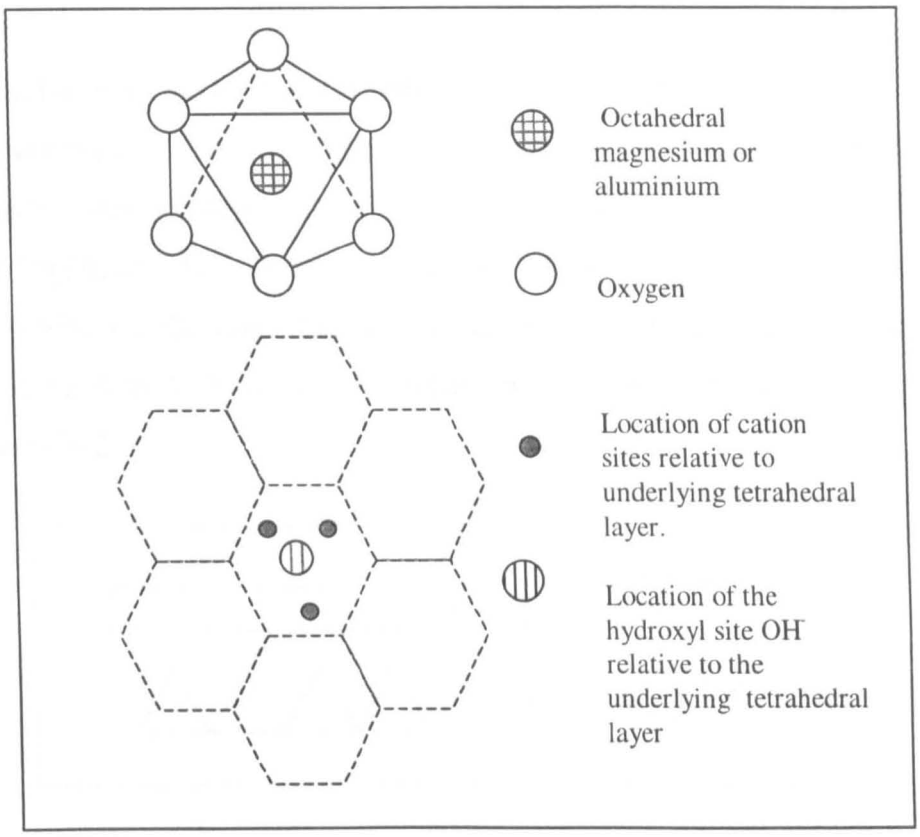

Fig. 2.2 The octahedral layer of a phyllosilicate and its relationship to the underlying tetrahedral layer.

2.2.2.2 Classification of Phyllosilicates

The wide range of different phyllosilicate structures can be accounted for by variation of:

i the cation in the tetrahedral layer

ii the cation in the octahedral layer

iii packing arrangement of the sheets

i. Variation of the cation in the tetrahedral layer

This is due to the replacement of Si^{4+} by Al^{3+} causing a charge deficiency which is balanced by **inter-layer cations** such as K^+, Na^+ or to a lesser extent Ca^{2+} or Mg^{2+}.

ii. Variation of the cations in the octahedral layer.

Three cation sites are generated by each hexagon in the tetrahedral layer. If all three are occupied by a divalent cation such as Mg^{2+} the structure is termed a **trioctahedral layer.** If on the other hand two of the sites are occupied by a trivalent cation such as Al^{3+} the structure is called a **dioctrahedral layer**. The mineral formed is controlled by the

primary composition of the protolith.

iii. Variation in packing arrangement

a) **1:1 Layer type** This is simplest arrangement consisting of alternating layers of tetrahedral and octahedral sheets, often abbreviated to a **t-o** layer. Serpentine minerals $Mg_3Si_2O_5(OH)_4$ are the trioctahedral version while kaolin (clay) minerals $Al_2Si_2O_5(OH)_4$ are the dioctahedral equivalent. This type of phyllosilicate has a spacing of 7.2 Å to 7.3Å and gives a prominent peak in X-ray diffraction patterns at this value (Fig.2.3).

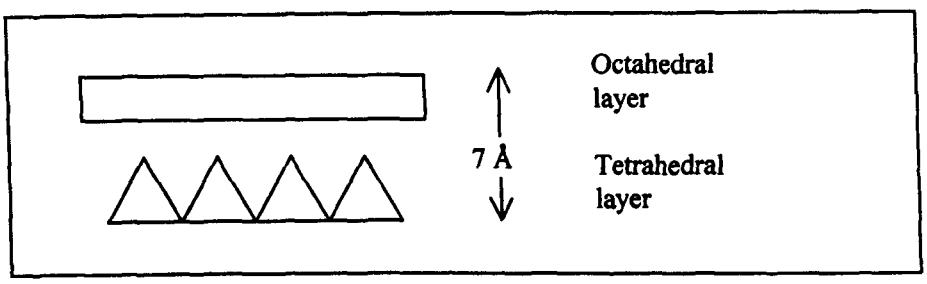

Fig. 2.3 Layered structure of a clay mineral

b) **2:1 Layer type** The next simplest stacking is seen in micas such as muscovite and white mica. Here two tetrahedral layers both point towards the octahedral layer in a **t-o-t** structure. The characteristic spacing of this structure is approximately 10 Å as seen in X-ray diffraction patterns. Examples of minerals with this type of structure are talc, muscovite and paragonite (Fig. 2.4).

Talc	trioctahedral	$Mg_3Si_4O_{10}(OH)_2$
Muscovite/Paragonite	dioctahedral	$(K, Na)Al_2(AlSi_3O_{10})(OH)_2$

In white micas the extra negative charge caused by the replacement of 1 out of 4 Si^{4+} by Al^{3+} is balanced by inter-layer alkali metals such as K^+ giving muscovite or Na^+ giving paragonite. The *illite group* of white micas differs from muscovite in having a higher Si^{4+}:Al^{3+} ratio in the tetrahedral sheet and hence fewer inter-layer cations holding the structure together i.e. illites are white micas which are deficient in K^+. The sodium equivalent is *brammallite,* but this term is only rarely used.

Phengite is a member of the illite group in which excess silica in the tetrahedral sheet

is compensated by replacement of trivalent Al by bivalent Mg and Fe in the octahedral site, and the sum of the interlayer cations is approximately equal to that of muscovite. The naming of white micas in the literature is not consistent and the terminology used by Deer *et al.* (1992) is shown in Table 2.1. The general term white mica has been used in this Report.

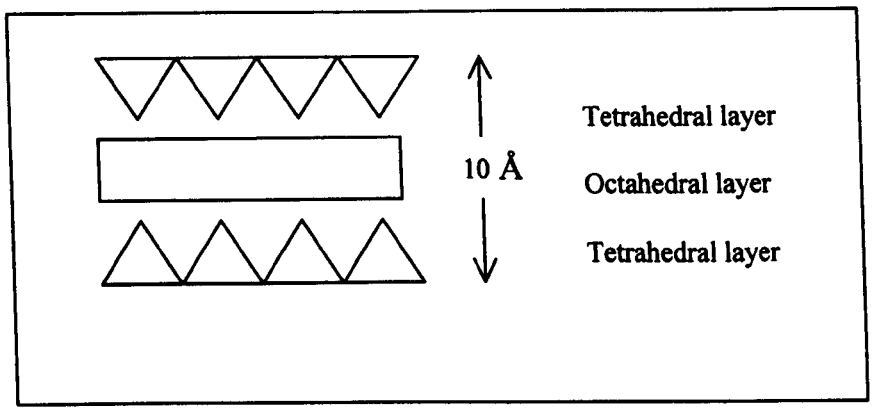

Fig. 2.4 Layered structure of white micas including muscovite.

	Mineral	Inter-layer cations	Octahedral cations	Tetrahedral cations
White micas	Muscovite	K_1	Al_2	Si_3Al
	Illite	K_{1-x}	Al_2	$Si_{3+x}Al_{1-x}$
	Phengite	K_1	$Al_{2-x}(MgFe)_x$	$Si_{3+x}Al_{1-x}$

Table 2.1 Classification of white micas according to the chemical composition after Deer *et al* (1992).

c) **2:1:1 Layer type** This layer structure consists of a t-o-t layer and an extra octahedral layer, giving it a basal spacing of 14.2 Å which is used to identify chlorites in XRD analysis (Fig. 2.5). Chlorite is a primary mineral found in low-grade metamorphic rocks growing at the expense of clay in argillaceous rocks. The colour of chlorite gives greenschists their name.

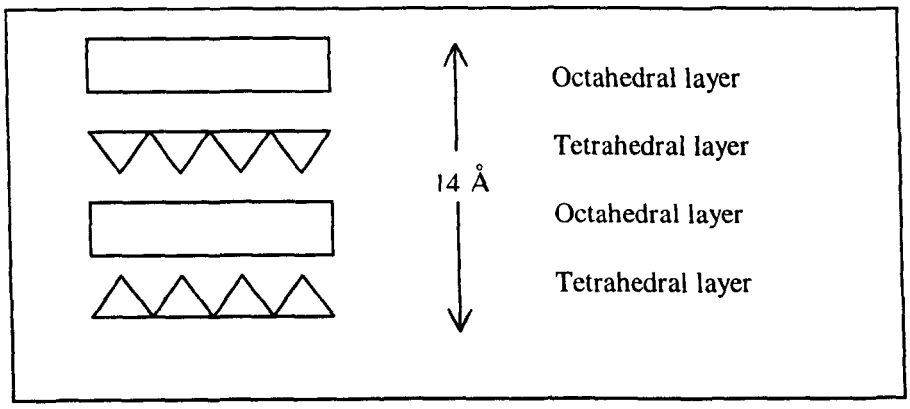

Fig. 2.5 Layered structure of a chlorite

The general formula of chlorite is $(Mg, Fe, Al)_6(Al, Si)_4O_{10}(OH)_8$, with considerable chemical variation due to isomorphous substitution. These isomorphous replacements have been used to classify chlorites by Foster (1962), but the system is arbitrary and carries no generic significance (Casthelineau & Nieva, 1985). It is however the classification most often used in the literature and is included here for completeness (Fig. 2.6). The actual composition of the chlorite reflects the original composition of the rock and does not change in a systematic way with increasing temperature and pressure (Casthelineau & Nieva, 1985).

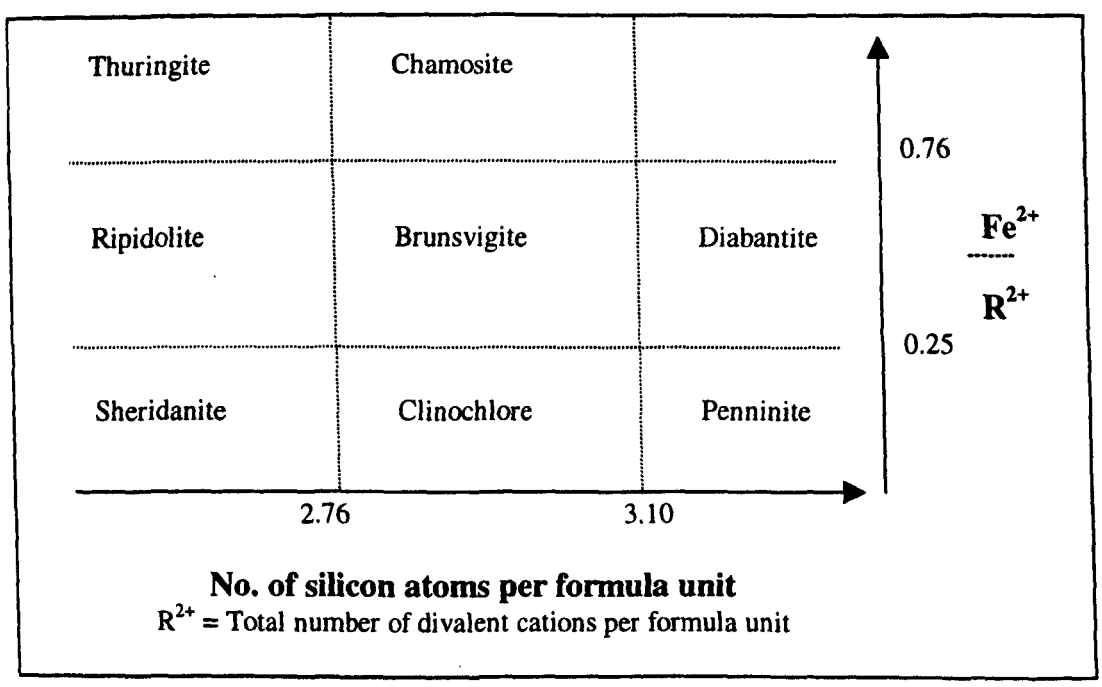

Fig. 2.6 Classification of chlorite based on the two principal types of ionic replacement after Foster (1962).

Swelling chlorites:

Stephen and MacEwan (1950,1951) identified a type of chlorite whose basal spacing expanded from 14Å to 17Å when glycolated. There is some controversy about the nature of this special group of chlorites and some authors have regarded them as a variant of mixed layered minerals (Carroll 1956). Because any swelling phyllosilicates, whatever their classification, would have a detrimental effect on the durability of a slate, their presence was tested by glycolation as discussed in Section 5.6.1.

2.2.2.3 Polytypes

As well as variation in the chemical composition of the different layers of a phyllosilicate, there is also variation in the way they are stacked. The unbound oxygen of the tetrahedral layer is used to bond with the cation of the octahedral layer. The geometry of this arrangement requires that each hexagon of the tetrahedral layer is staggered by a/3 relative to the hexagon on the adjacent layer. There are six possibilities for the direction of each shift (Fig. 2.7). If the direction of stagger differs from layer to layer in some regular fashion the mineral is said to exhibit polytypism (Bailey 1984). While in theory numerous polytypes are possible, only a few are found to occur naturally. They are named systematically as follows:

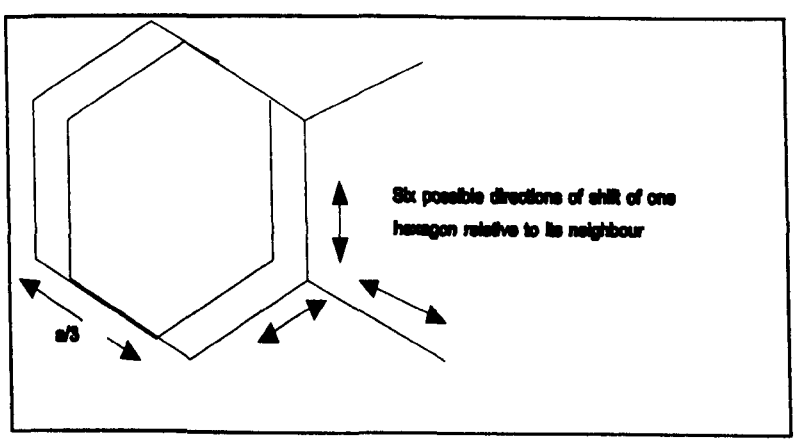

Fig. 2.7 Staggered stacking of the tetrahedral layers.

Naming of white mica polytypes

Different polytypes are denoted by $\mathbf{nX_i}$

n is an integer denoting the number of layers in the repeat unit.

X is a letter representing the symmetry such as M for monoclinic or T for triclinic

i is an integer differentiating between polytypes with similar periodicity and symmetry

Naturally occurring polytypes found in white micas

Composition seems to dictate the layer sequence found naturally e.g. the $2M_1$ is the predominant one for dioctahedral muscovite with $1M_1$, 3T & $2M_1$ less abundant (Srodon *et al.* 1984)

White micas exists as three common polymorphic variations $1M_d$, 1M & 2M

$1M_d$ a disordered form that develops during weathering

1M regressive diagenesis

2M most stable form in micas or detrital illites from source areas where a cold and dry climate did not favour hydrolysis. ***This is the polytype of white micas usually found in slate*** and its significance is discussed further in Section 3.2.3.2.

Chlorite micas also exhibit polymorphism.

Because of the extra layer in the chlorite structure there is a large number of theoretical polytypes (Brown and Bailey, 1962). However, 80% of naturally occurring chlorites are the polytype $2II_b$ in which the structure is a monoclinic cell. This is the stable structure found in low grade metamorphic rocks such as slate.

Significance of the crystalline structure of the phyllosilicates

The platy structure of the phyllosilicates gives slate its splitting property. Slate with insufficient ordering of the phyllosilicates' basal planes would be difficult to cleave. Excessive ordering, on the other hand, as seen in a pure muscovite with a flaky texture, would lack cohesive strength. The optimum degree of regularity of crystalline structure for a good slate is not known, but it can be assumed to lie between these two extremes.

2.2.3 Other Minerals

Other minerals present are feldspar, the ore minerals, carbonates and graphite. Although often present in only small amounts some of these minerals are easily weathered and their presence may have a disproportionate effect on the durability of a slate.

2.2.3.1 Feldspars

Formulae		
Plagioclase	$NaAlSi_3O_8$- $CaAl_2Si_2O_8$	Albite to Anorthite
Alkali Feldspars	$KAlSi_3O_8$ - $NaAlSi_3O_8$	Orthoclase to Albite

Hardness ≈ 6

Feldspars are common minerals found in all type of rocks, and are usually present as albite in the greenschist facies of slate. They have an atomic structure similar to quartz in that all four oxygens of the silicate tetrahedron are shared with neighbouring tetrahedra. (Section 2.2.1). In feldspars, some silicon atoms are replaced by aluminium and concomitant cation in order to maintain balanced charge. In the case of the alkali feldspars, this coupled substitution can be represented as follows:

$$Si^{4+} \rightarrow Al^{3+} + M^{+} \text{ where } M^{+} = Na^{+} \text{ or } K^{+}$$

Similarly in the case of the plagioclases, this coupled substitution can be represented as follows:

$$2Si^{4+} \rightarrow 2Al^{3+} + M^{2+} \text{ where } M^{2+} = Ca^{2+}$$

In chemical reactions feldspars are weathered to clay.

$$2NaAlSi_3O_8 + 2H^{+} + H_2O \rightarrow Al_2Si_2O_5(OH)_4 + 4\,SiO_2 + 2Na^{+}$$

The relative durability of the different feldspars is discussed further in Section 5.2.2.

2.2.3.2 Carbonates

This mineral is made up of anions of CO_3^{2-} which are electrically balanced by a range of positively charged cations such as Ca, Mg and Fe, the most common of these being calcium carbonate, calcite (Table 2.2). All carbonates are susceptible to attack by acid, giving off carbon dioxide and water, e.g.

$$Ca\,CO_3 + 2HCl \text{ ---------> } CaCl_2 + CO_2 + H_2O$$

making slates with carbonates present especially vulnerable to weathering in an urban environment with an acidic atmosphere. Their relative stability is covered in greater detail in Section 5.2.2.

Mineral	Formulae
Magnesite	$MgCO_3.3H_2O$
Calcite/Aragonite	$Ca\,CO_3$
Siderite	$Fe\,CO_3$
Dolomite	$CaMg(CO_3)_2$

Table 2.2 Common carbonates found in slate.

All the carbonates show some chemical variation due to solid solution. Because of the important role carbonates play in chemical-weathering reactions they are discussed at greater length in Section 5.2.2.

The variation in carbonate content from 100% in a pure limestone to 0% in a pure clay has been used as the basis of classification of sedimentary rocks as specified in the European standard for building stone prEN 12407: 1996. Wagner *et al.* (1994) extrapolated this when they based their classification of slate on the carbonate content of its sedimentary precursor, e.g. argillaceous sediment is composed of >97.5% clay which is metamorphosed into an argillaceous slate (Table 2.3).

Pure clay	0-2.5% Carbonate	Argillaceous slate
Marly clay	2.5- 10%	Marly argillaceous slate
Clayey marl	10%-25%	Argillaceous marly slate
Marl	25-65%	Marly slate

Table 2.3 Classification of slate based on the protolith after Wagner *et al.* 1994.

2.2.3.3 Iron Ore Minerals

The most common ore minerals found in slate are the oxides and sulphides of iron. The stability of these minerals is crucial in determining the durability of a slate. Iron is found as the Fe^{2+} ferrous ion and the Fe^{3+} ferric ion. Weathering usually involves oxidising the more reduced ferrous ion to the oxidised ferric ion such as in limonite $FeO.OH.nH_2O$ (see Section 5.2.3.5 for more details).

i ***The oxides of iron***

Haematite Fe_2O_3

Magnetite Fe_3O_4

These are both relatively oxidised forms of iron and as such their presence in slate is harmless.

Limonite $FeO.OH.nH_2O$

This is a field term to describe hydrated oxides of iron with poor crystalline structure. It is yellow to brown in colour and readily dissolved in HCl (see Section 5.2.3.5 for more details).

ii ***The sulphides of iron***

Pyrite FeS_2

This is the most common form of iron sulphide found in sedimentary rocks. It is often formed as a result of bacterial reduction of aqueous sulphate to sulphide, which then reacts with ferrous iron to form pyrite. ***Marcasite*** is a polymorph of pyrite found in acidic aqueous environments.

Pyrite occurs as large euhedral crystals, or disseminated throughout the rock. The large cubic crystals are usually resistant to weathering. When it does break down, it weathers to limonite.

Marcasite is usually associated with pyrite and weathers more easily than pyrite to limonite

Pyrrhotite ~FeS_{1+x} non stoichiometric

This is a less stable iron sulphide than pyrite and is easily decomposed by HCl while

pyrite is not. In weathering reactions it is oxidised to sulphates, carbonates and oxides. In slate deposits pyrrhotite is found in contact metamorphic deposits as pseudomorphs of pyrite.

The iron mineral present in slate is a function of the pH and the Eh of the environment and the activity of the various ions during formation. Therefore haematite is found in moderate to high oxidising conditions while pyrite, siderite and magnetite form in reducing conditions. The formation of pyrite or siderite depends on the concentration of sulphur and carbonate in the pore fluids.

iii Other ore minerals

Rutile and Anatase TiO_2

Rutile is the most common form of TiO_2, being the high temperature polymorph. Anatase is the low temperature polymorph and is found as an alteration product of Ti-bearing minerals such as ilmenite. It is a common detrital mineral in sediments where it is often of authigenic origin (Deer *et al.* 1993).

Ilmenite $FeTiO_3$

There is extensive solid solution between the end members of (Fe, Mg, Mn)TiO_3 i.e. the iron end member is ilmenite $FeTiO_3$. This mineral lacks cleavage, which enables it to survive sedimentation processes thus making it a common detrital mineral.

2.2.3.4 Miscellaneous Minerals

Other accessory minerals are often found in slate such as graphite, apatite, chloritoid, tourmaline and zircon. Of these, graphite is the one with the greatest effect on the properties of slate.

Graphite is derived from organic matter which has been preserved in reducing conditions. This organic matter is later metamorphosed to graphite, a dimorphous form of carbon, and is found disseminated throughout the rock or in local concentrations. Its presence during metamorphism inhibits the growth of minerals and as a result it is associated with less crystalline material. It acts as a catalyst in chemical reactions and

plays a significant role in the weathering of slate (Kessler & Sligh 1932).

2.2.4 Conclusion

The principal minerals of slate are quartz, white micas and chlorite, which in the case of true argillaceous slate make up over 95% of the total. The relative amounts can vary considerably as can individual workers' interpretation of what makes a good slate (Table 2.4).

Source	% Phyllosilicates		%Quartz
	%Illite	%Chlorite	
Le Corre (1970).	70-87* No differentiation		13-30*
Crockett (1975)	38-40	6-18	31-45
Wagner *et al*(1994)	40	20	30

Table 2.4 Composition of slate according to different authors.

* Depending on the grain size of the quartz.

Slate properties are controlled by the proportions of quartz, phyllosilicates and, when present in sufficient concentrations, feldspars. Because of its three-dimensional tetrahedral structure, quartz is a hard mineral (Mohs hardness = 7) without cleavage making it very durable and giving cohesion to the slate. The feldspars too have a three-dimensional tetrahedral framework giving them a hardness of 6 in the Mohs scale. However the coupled substitution for some of the silicon atoms by aluminium and either alkali cations such as K+ and Na+ or alkali earth cations such as Ca^{2+} (Section 2.2.3.1) makes them more vulnerable to weathering than quartz. The layered structure of the phyllosilicates gives the splitting ability to slate. However these multi-layered structures are only held together by weakly bonded alkali cation layers or weak Van der Waal's bonding. The multi layered structure is the conduit for water, which is the principal agent in all weathering reactions, to penetrate the slate.

More research is needed to correlate the mineralogy of rocks in general with their mechanical properties. However, it can be assumed that there is an optimum range of quartz content sufficient to impart enough hardness to the slate yet not so much as to

destroy the splitting property of the phyllosilicate. The amount and type of deleterious minerals present affect the vulnerability of a slate to chemical weathering.

2.3 Samples

Unweathered and weathered samples were collected from producing quarries in North Wales and Cumbria. They were taken from different producing units (*veins*[1]) within a quarry and in the case of Ffestiniog they were also collected from areas between producing units or veins, i.e. areas deemed unsatisfactory for slate at this particular quarry.

As there are no working quarries in Scotland, Scottish samples were collected from many different sources, ranging from slate tips and outcrops in the quarries to second-hand slate merchants. It was generally found that bands of rock left *in situ* in a quarry were coarser grained than those found in the intervening waste tips. Hence samples from the tips located near the producing seams were considered to be more representative of the slate produced. The collection included some samples from all the quarries mentioned in the quarry reports (Appendix A). One or more samples were selected as representative of each group of Scottish quarries, as well as one Welsh slate from the Oakley Quarry in Ffestiniog, and used as standards for the area (Table 2.5).

Over a hundred grams of powder was prepared from each sample for use in all the analyses except in the case of standard samples where 200 grams was prepared. The same sample was used in all tests, except for the experimental weathering of slates where test pieces 5cm x 5cm were needed. These were cut from finished roofing slates.

[1] The part of the formation used in the production of roofing slates are called veins in the Welsh slate industry. The equivalent term used in the Scottish slate industry was *seam*

Quarry Group	Location	Quarry	Sample No	Quarry Report Reference
Wales	Ffestiniog	Oakley	W/F1	
Ballachulish		East Laroch	El-10	2.5.1
Easdale	Seil Island	Breine Phort	SB-6	3.5.3
	Luing Island	Port Mary	LP-5	3.5.7
Highland Border	Bute Island	Hilton Quarry	B2	4.5.2
	Aberfoyle	Aberfoyle	Ab-5	4.5.4
	Dunkeld	Newtyle North	DN-4	4.5.7
Macduff	Kirkney Hill	Kirkney	MK-4	5.5.1

Table 2.5 Samples selected as representative of each Scottish group of quarries and one Welsh slate.

W/F-1 This is a dark grey very fine-grained slate; cleavage surface is flat and smooth, no bedding features are visible. There is slight brown staining after storage.

El-10 This is a dark grey fine-grained slate; cleavage surface is fairly smooth with a slight sheen and faintly crenulated in places. Lineation is subparallel to the pillaring line; no bedding features are visible. Pyrites are less than 1mm in size and brown in colour but there is no leaching. There is slight superficial staining on the weathered surfaces.

SB-6 This is a dark grey, fine to medium-grained slate. The cleavage surface is flat but crenulated. Pyrites are 1-2mm in size; those on the surface are weathered and have leached. Surfaces are superficially weathered.

LP-5 This is a dark blue-grey, fine to medium-grained slate; the cleavage surface is fairly flat but crenulated, with a slight sheen. Pyrites are bimodal; the smaller ones are less than 1mm in size and superficially rusty, the larger ones are 4mm square and have a fresh metallic appearance. There is faint colour banding due to bedding which is at a high angle to cleavage.

B2 This is a dark blue-grey, fine to medium-grained slate. The cleavage surface is

flat and smooth with a slight sheen. No bedding features are visible apart from a slight darkening of the surface. There is no superficial weathering.

Ab-5 This is a dark blue-grey, fine to medium-grained slate with individual white mica grains visible on the cleavage surface, which is flat and smooth. No bedding features are visible apart from a slight darkening of the surface. There is no superficial weathering.

DN-4 This is a dark blue-grey fine to medium-grained slate; the cleavage surface is flat and smooth. No bedding features are visible apart from a slight darkening of the surface. There is no superficial weathering.

MK-4 This is a blue-grey, medium-grained slate with individual white mica grains visible on the cleavage/bedding surface. The cleavage surface is flat but slightly rough in texture. Bedding is sub-parallel to the cleavage surface. Apart from slight pale brown staining on the surface, there is no superficial weathering. Unlike many slates in the Macduff area, this sample is not a hornfels.

2.4 Qualitative Analysis

Identification of minerals

The minerals present in the slate were identified in thin sections as quartz, white mica, chlorite and opaque ore minerals, with accessory feldspar and carbonates. However the fine-grained nature of slate and the intergrowth of minerals makes distinguishing between minerals with similar optical properties very difficult. For example, quartz and feldspar have similar birefringence colours and relief and in fresh samples the feldspar are relatively unaltered giving then a similar appearance to quartz in plain polarised light. Therefore in the absence of twinning in the feldspars, quartz and feldspars can only be distinguished by their interference figures, which is not possible given the small grain size of the samples. It was necessary to use XRD analyses to distinguish between white mica and paragonite, and to identify the different carbonates, iron ore minerals and accessory minerals.

The formulae of the phyllosilicates

The formulae of the phyllosilicates were determined by electron microprobe analyses.

2.4.1 Determination of Minerals present in Slate using XRD Analysis

When crystalline material is bombarded with X-rays, constructive interference occurs in the diffracted beam. This forms a peak when the angles of incidence and the inter-layer spacing of the crystalline lattice satisfy the Bragg (1912) relationship.

$$n\lambda = 2d\sin\theta$$

The inter-atomic spacing **d** controls the position of peaks, measured in terms of the angle θ, which is used as a means of identifying the minerals present in slate.

2.4.1.1 Equipment

The following equipment was used throughout this work:

Diffractometer

Philips PW 1050/35 X-ray diffractometer with vertical goniometer run at 36kV and 20mA

Source of radiation was Co filtered by Fe.

Detector: HV= 535 Window = 300 Lower level = 360 Response sec = 3

Slits: divergence 1°; receiver 0.1°; anti-scatter 1°

Scanning speed variable measured in °2θ/min

Rate 300 counts/sec

Radius of goniometer 173mm

Computer

Sie Ray 122 XRD Automation system

Sie Ray 122D Automation interface

PC using Sie 122D software

'Traces' program run under Microsoft Windows.

(Traces is a Diffraction Technology Ltd. Software package)

For identification of minerals the XRD scans were run from 4° to 64° 2θ at 2 2θ/min; step = 0.2

2.4.1.2 Principles of XRD Analysis

X-rays are part of the electromagnetic spectrum with wavelengths between 0.1 and 45Å (Krauskopf 1953). This range of wavelengths is the same order of magnitude as the inter-atomic spacing between the planes of atoms that make up the regular structure of a crystalline lattice (Section 2.2.2). When a crystalline substance is bombarded by monochromatic X-rays the beam is diffracted, producing a pattern unique to each mineral. This characteristic is used in X-ray Diffraction (XRD) analysis.

Most rocks, including slate, are made up of a variety of minerals each characterised by its own diffraction pattern or trace. The best X-ray traces are produced by homogeneous materials with a small grain size, so that a representative sample of minerals is bombarded in each scan. This makes X-ray diffraction one of the best analytical methods for the study of slate, which satisfies both requirements of homogeneity and grain size.

2.4.1.2.1 Atomic Structure

X-rays are the energy released when electrons surrounding the nucleus of an atom jump from a higher to a lower energy level. Electrons in the atom occupy discrete shells to which Bohr gave the numbers 1,2,3... etc. (The older notation of K, L, M etc has been retained in the XRD nomenclature). Within each shell are subshells called s, p and d which define the shapes of the orbit (These letters come from an early attempt in the 19th century to qualify the spectra of an atom into sharp, principal and diffuse lines). Each orbit has a characteristic energy associated with it, the lowest energy level being 1s, followed by the 2s and the 2p. The energy of the X-ray emitted depends on the transition made by the electron. These transitions are not random but governed by rules which are within the realms of Quantum Mechanics and outside the scope of this Report.

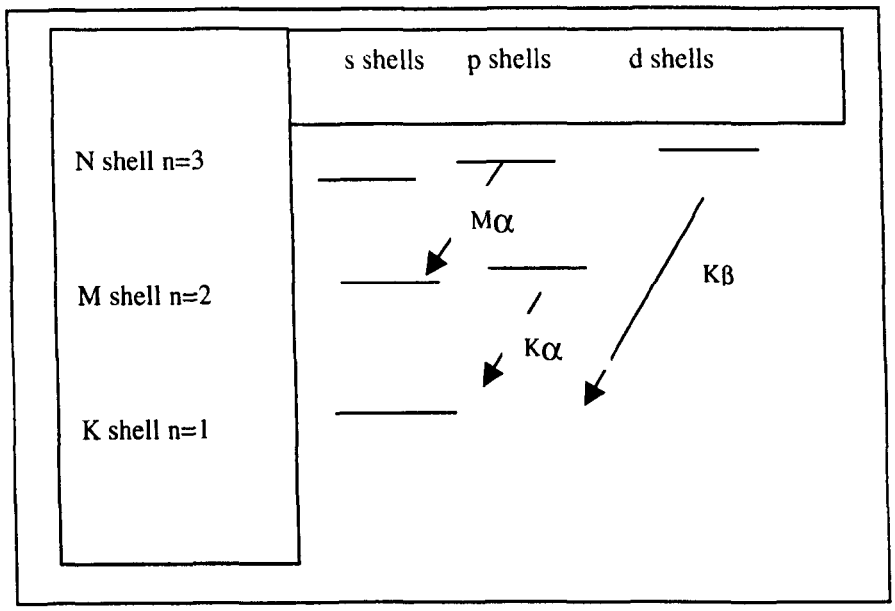

Fig. 2.8 Diagrammatic representation of the lower energy levels of electrons in an atom.
Possible transitions which accompany emission of X-rays
K series filling of vacancy in the K (n=1) shell
M series filling of vacancy in the M (n=2) shell
α when Δ n =1 β when Δn = 2

2.4.1.2.2 X-ray Generation

When a beam of electrons accelerated through 30kV strikes a metal target such as copper or cobalt the metal is ionised, i.e. loses electrons. When electrons from the lowest energy levels, i.e. the innermost 1s shell, escape, electrons from higher energy levels such as the 2p or 3s drop down to fill the vacant 1s. Photons of energy are then released giving rise to the spectrum characteristic of the metal (Fig. 2.8). The lowest energy transition is isolated by filtering out all but the Kα X-rays and so producing a monochromatic beam (More precisely a doublet is produced due to a minute difference in energy levels between different 2p sub-orbits).

Copper 2p ----> 1s Kα $\lambda = 1.5418$Å

This monochromatic peak is superimposed on white radiation due to the general interaction of high velocity electrons with matter.

Copper radiation filtered by nickel is the source generally quoted in the literature. However fluorescence by iron in the sample makes it less suited for many minerals. Fluorescence occurs when the primary beam ejects electrons of low energy from atoms

in the sample. Again electrons from higher energy levels drop down to fill the gaps emitting X-rays as they do so. In effect the sample acts as a secondary source of electrons. The problem of fluorescence is greatest when the incident radiation has a wavelength only slightly shorter than the ionisation potential of the metal, which is the case for copper radiation on iron bearing minerals. To minimise iron fluorescence there is now a trend to using cobalt radiation filtered by iron.

Cobalt 2p ----> 1s Kα λ wavelength = 1.79021 Å

2.4.1.2.3 Diffraction

Diffraction from a 1 dimensional crystal is equivalent to that of light by an optical grating. When the X-rays from successive layers of the crystal are in phase, constructive interference occurs and the diffracted beam is detected as a peak. This is a function of the angle of the incident beam, the wavelength of the X-ray and is given by the Laue equation (Nuffield 1966).

$$a\sin\theta = n\lambda$$

For a three dimensional crystal, three simultaneous equations need to be solved, one for each Cartesian co-ordinate. Fortunately a simpler empirical method can be used. This treats diffraction of X-rays as if individual layers of the crystal were acting as semi transparent mirrors. Constructive interference occurs when the Bragg (1912) equation is satisfied (Fig. 2.9):

$$n\lambda = 2d\sin\theta$$

n is an integer

θ is the angle of diffraction

λ is the wavelength in Å

d is the inter-atomic spacing in Å

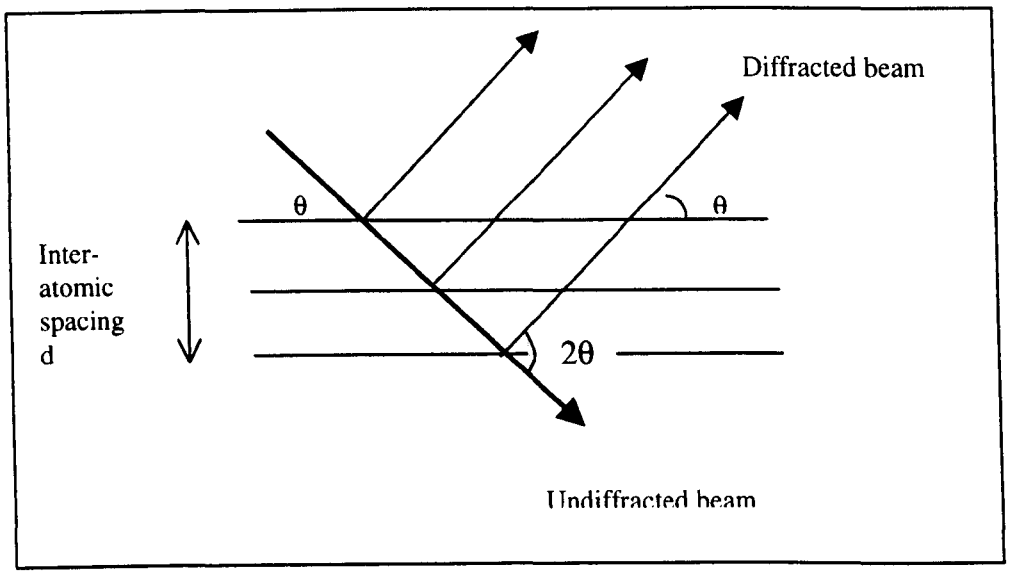

Fig. 2.9 Condition for reflection according to Bragg's Law after Nuffield 1966

While X-rays are not reflected by atoms, only diffracted, the results of this approach agree with observations.

2.4.1.3 Interpretation of XRD Profiles

In modern X-ray powder techniques the sample is scanned by increasing the angle between the diffracted and the undiffracted beams (2θ), (Fig. 2.9) at a constant rate of 2θ/min. Three aspects of the XRD profile produced give information about the atomic structure of the lattice.

- Position of the peaks
- Intensity of the peaks
- Shape of the peaks

2.4.1.3.1 Position of Peaks

The position of peaks is a measure of the distance between planes within the crystal, the **d-spacings,** and is used to identify the minerals present. Small shifts in these peaks give information about the chemical content. X-ray diffraction is particularly suitable for this type of qualitative analysis. Because the position of peaks varies slightly with operating conditions it is necessary to calibrate with respect to quartz when a high degree of precision is required (Section 2.4.1.6).

2.4.1.3.2 Intensities and Areas of Peaks

The intensity and area of a peak of a particular mineral is proportional to the total amount of that mineral present. Unfortunately it is not a direct relationship, as the intensity is affected by numerous factors of which two are relevant to the analysis of slate. Both the orientation of crystals and their size affect the area and intensity of peaks. By grinding the sample to 1-10μ both of these problems can be minimised. The intensities of XRD peaks were used as a measure of crystallinity (Section 3.4) while the areas of XRD peaks were used to estimate the mineral composition of slates (Section 2.5.5).

2.4.1.3.3 Peak Shape

The shape of the peak is used to measure the increase in crystallinity of a slate and is discussed in detail in Section 3.4.

2.4.1.4 Computer Software

Traces' is a computer software package, which is used to process the X-ray profile and which attempts to quantify the three aspects of the scan discussed above. Minerals are identified by comparison with standards. Relative intensities of peaks are determined and concentrations are estimated based on a similar rock with known composition.
The program is invaluable in handling the data, especially in determining peak heights, areas under curves, full width at half magnitudes FWHM (Section 3.4) as well as storing and retrieving XRD profiles. However, the algorithm used in some of the quantification procedures was not found satisfactory and these were done manually.

2.4.1.5 Method

Sample Preparation

Slurry was prepared from each sample by mixing the powdered slate with acetone, pouring on to a glass slide and allowing to dry. The size of the sample was 25mm x

25mm. To minimise the alignment of the platy minerals parallel to the slide, the sample was continually stirred as it was being poured onto the slide. In addition, a rapidly-drying solvent i.e. acetone was used to minimise the settling time. The areas and intensities of the white mica and chlorite peaks were compared with the average values obtained for two rock samples, one taken parallel to cleavage and the other perpendicular to cleavage (Table 4.1). Areas of the white mica peaks and the chlorite peaks were +40% and –7% relative to the average values respectively. Similarly, the respective intensities were +4% and –22% relative to the average values. Both the area and intensity of the quartz peak were +28% relative to the average for the two rock samples. Hence the degree of alignment is white mica > quartz > chlorite.

2.4.1.6 Results

As most samples contain quartz, the position of the quartz [100] peak was used as an internal standard at 24.26°. This was particularly important in the identification of the iron ore minerals, as the main peaks of both pyrite and haematite are very close.

Results are given in Appendix 2.1. The major minerals, quartz, white mica and chlorite are present in all slate, however it is possible to make some general comments on of the mineralogy of a slate producing area, in terms of the type of carbonate and iron ore present. These generalisations are summarised in Table 2.6.

Area	Ballachulish	Easdale	Highland Border	Macduff
Carbonate	Dolomite	Dolomite/ Magnesite	Calcite	None
Iron Ore	Pyrite/Pyrrhotite	Pyrite/Pyrrhotite	Haematite	Haematite
Distinctive Mineral	Amphibole	-	Bute slate has a separate paragonite phase	

Table 2.6 Summary of the accessory minerals found in Scottish slate. For a more detailed review see Quarry Reports Appendix A

The intensities of the major minerals were determined and used for crystallinity

measurements (Section 3.4.2).

2.4.2 Determination of the Chemical Composition of the Phyllosilicates

Chemical composition of the phyllosilicates was determined by electron microprobe analysis. In this techniques a high energy beam of electrons is finely focussed onto the polished carbon coated surface of the sample.

The source of electrons, called an "electron gun", is a tungsten filament which emits a cloud of electrons when heated. This cloud of electrons is converted into a beam by passing through a cylindrical metal cup and accelerated towards an anode with a positive potential difference of approximately 10kV. Having passed through an aperture in the anode, the beam is focused by passing through cylindrical electromagnets so that it attains its smallest diameter at the specimen. When bombarded with electrons the specimen gives off X-rays which are characteristic of the elements within. These X-rays are analysed by X-ray dispersive spectrometers, whereby the beam is separated into peaks by diffraction by a crystal lattice according to Bragg's law as described (Section 2.4.1.2.3). However in the case of electron microprobe procedure, several crystals of different inter-atomic spacing are needed to cover the whole range of wavelengths which need to be analysed. This generates an X-ray spectrum characteristic of each element present, the intensity of which is proportional to the concentration of that element. This concentration is measured by comparing the intensity of the peak corresponding to a particular element to that observed in a standard. In addition, it is necessary to correct for differences between the composition of the specimen and that of the standard. This is caused by the interaction of the X-rays with all the major minerals present in the specimen due to back-scattering (Z), absorption (A) and fluorescence (F). The correction procedure, called ZAF, is done on-line to enable each analysis to be checked before the next analysis (Reed 1996). The chemical compositions of the white micas and chlorites present in the slate standards (Table 2.5) were determined by this technique.

2.4.2.1 Method

Machine Conditions:

The electron microprobe used was the Camebax SX-50 with four spectrometers operated at 10kV accelerating voltage with a 6nA beam current and a finely focused beam.

Spect1, TAP { Na (5s), Al(5s) }; Spect2 LIF {Fe(20s), Mn(10s)}; Spect3 TAP {Si(5s),Mg(10s)}; Spect4 PET {K(5s), Ca (10s), Ti(10s) }

The problem of spot analyses of white micas is loss of the relatively volatile alkalis during analysis. Some workers avoid this by defocusing the electron beam but this results in a larger area being targeted and in fine-grained materials the resultant analysis is of a mixture of minerals. Apart from current, the conditions used in this Study were those developed by Dempster and Tanner (1997) whereby a finely focused beam is used to analyse fine grained micas. This has been further modified to minimise the loss of alkalis in white micas by reducing the beam current from 20nA to 6nA (Per. com. Dempster). The effectiveness of this was tested by analysing the same location twice and it was found that the loss of K and Na was less than 15% in the second analysis. All operating conditions were checked by the analysis of in-house standards of known composition and compared with results obtained at other laboratories. Because of these low beam currents and the fine grain size, it was not possible to identify individual minerals visually and many analyses showed a mixture of both chlorite and white mica and hence were discarded. Satisfactory analyses were identified as follows:

- for white micas by selecting analyses with total oxides of approximately 95%, total alkali cations of approximately 1 per formula unit and low Fe+Mg values.
- for chlorite by selecting analyses with total oxides of approximately 90% and low total alkali cations. There was obviously no problem with loss of alkalis.

2.4.2.2 Results

The chemical compositions of the white micas and chlorites were calculated based on total cation charges of +22 and +28 respectively. Over 10 satisfactory analyses were

obtained for both the chlorite and white micas in each standard sample. The precision of the results was measured by the coefficient of variation[2] (C of V) e.g. for Ballachulish slate (standard EL-10) the C of V was 0.03-0.04 for the main elements in[2] chlorite and slightly less for those in the white micas (Appendix 2.2.) In the case of alkalis in the white mica the C of V was determined for the total alkalis present (Na + K), as individually there was considerably greater variation. Average results are given in Table 2.7.

Ballachulish Slate		
EL-10	White Mica	$Na_{0.13}K_{0.81}Al_{1.81}Mg_{0.15}Fe_{0.08}(Al_{0.87}Si_{3.13}O_{10})(OH)_2$
	Chlorite	$Al_{1.47}Fe_{1.85}Mg_{2.58}Mn_{0.01}(Al_{1.34}Si_{2.66}O_{10})\ (OH)_8$
Easdale Slate		
SB-6	White Mica	$Na_{0.13}K_{0.63}Al_{1.80}Mg_{0.17}Fe_{0.12}(Al_{0.80}Si_{3.20}O_{10})(OH)_2$
	Chlorite	$Al_{1.62}Fe_{1.97}Mn_{0.01}Mg_{2.18}(Al_{1.22}Si_{2.78}O_{10})\ (OH)_8$
LP-5	White Mica	$Na_{0.13}K_{0.68}Al_{1.84}Mg_{0.14}Fe_{0.08}(Al_{0.80}Si_{3.20}O_{10})(OH)_2$
	Chlorite	$Al_{1.39}Fe_{1.91}Mn_{0.03}Mg_{2.66}(Al_{1.37}Si_{2.63}O_{10})\ (OH)_8$
Highland Border Slate		
B2	White Mica	$Na_{0.21}K_{0.74}Al_{1.61}Mg_{0.27}Fe_{0.26}(Al_{0.84}Si_{3.16}O_{10})(OH)_2$
	Chlorite	$Al_{1.35}Fe_{1.56}Mg_{3.00}(Al_{1.32}Si_{2.68}O_{10})\ (OH)_8$
Ab-5	White Mica	$Na_{0.23}K_{0.68}Al_{1.75}Mg_{0.12}Fe_{0.22}(Al_{0.88}Si_{3.12}O_{10})(OH)_2$
	Chlorite	$Al_{1.46}Fe_{2.23}Mg_{2.13}(Al_{1.36}Si_{2.64}O_{10})\ (OH)_8$
DN-4	White Mica	$Na_{0.20}K_{0.73}Al_{1.76}Mg_{0.12}Fe_{0.19}(Al_{0.85}Si_{3.15}O_{10})(OH)_2$
	Chlorite	$Al_{1.53}Fe_{2.10}Mg_{2.19}(Al_{1.32}Si_{2.68}O_{10})\ (OH)_8$
Macduff Slate		
MK-4	White Mica	$Na_{0.32}K_{0.63}Al_{1.88}Mg_{0.04}Fe_{0.15}(Al_{0.99}Si_{3.01}O_{10})(OH)_2$
	Chlorite	$Al_{1.64}Fe_{2.47}Mg_{1.6}(Al_{1.37}Si_{2.63}O_{10})\ (OH)_8$
Welsh Slate		
W/F-1	White Mica	$Na_{0.11}K_{0.78}Al_{1.86}Mg_{0.04}Fe_{0.07}(Al_{0.85}Si_{3.15}O_{10})(OH)_2$
	Chlorite	$Al_{1.77}Fe_{2.75}Mg_{1.02}(Al_{1.35}Si_{2.65}O_{10})\ (OH)_8$

Table 2.7 Formulae of white micas and chlorites as determined by microprobe analyses. Iron assumed to be present as Fe^{2+}.

[2] Coefficient of variation = s/ x sample deviation /mean

2.5 Quantitative Analysis

Because of the fine grain size and the inter-growth of minerals in slate, their relative amounts are difficult to evaluate by conventional methods such as point count analysis. Some workers simply denote the minerals as major and minor. Although XRD is the best method to determine what minerals are present, it is only semi-quantitative when used to determine the proportions of the different minerals. For this a combination of different methods was necessary.

The following methods have been investigated:

1 Spiking with known amounts of quartz
2 XRF analysis
3 SEM back scatter analysis
4 Traditional chemical analysis
5 XRD semi-quantitative analysis

A comparative assessment of the different methods is given in Section 2.6.

2.5.1 Determination of the amount of Quartz: Spiking

To determine the amount of quartz present in a slate sample, known amounts of quartz were added and the increases in area and intensity of the quartz peak in an XRD scan were measured. The sample chosen was the Macduff standard MK-4, to which were added known amounts of Loch Aline sand, a source of quartz known for its purity. To ensure adequate mixing, samples were ground together for 5 minutes, mixed manually for 15 minutes, and this was then followed by mechanical mixing for a further 15 minutes. Samples were scanned by X-ray using three cavity mounts so that the same sample could be remixed and reused. Each was scanned five times from 4° to 30° 2θ at 1° 2θ/min. The scan of a sample analysed in a cavity mount was compared with one prepared by the slurry method and no appreciable difference was found.

Both the intensities and the areas of the [100] quartz peaks at 24.26° 2θ were determined and average values were plotted against the percentage of quartz added. In both cases the best-fit lines were linear and gave a correlation value of R^2 >0.96 (Fig.

2.10). The amount of quartz present in the original sample was calculated using the regressional lines determined in Fig. 2.10 which in the case of area of peaks was as follows:

$$\mathbf{y = 4591.4x + 2321.7}$$

x = total amount of quartz present in the spiked sample

y = area of peak in counts

Assume that the area of a peak is proportional to the amount of quartz present

Let q = amount of quartz present in the slate sample

Let k = proportionality constant

Area of peak $y = kx$

At 0% quartz added $y = kq = 2321.7$

$$k = \frac{2321.7}{q}$$

At 50% quartz added $y = k(0.5q + 0.5) = 4617.4$

$$k = \frac{9234.8}{q+1}$$

$$\frac{2321.7}{q} = \frac{9234.8}{q+1}$$

$$\mathbf{q = 0.335} \qquad \mathbf{(33.5\%)}$$

Similarily, by using the increase in intensity of the quartz peak, the quartz present in the original slate sample was calculated as 27%.

There was poor agreement between the two methods i.e. the area-of-peaks method gave a value of 33.5% and the intensity-of-peaks gave a value of 27%.

As the percentage weight of quartz increased there was a corresponding reduction in the percentage weight of white mica and chlorite. This data set was used for evaluating the precision of XRD semi-quantitative analyses (Section 2.5.5.2).

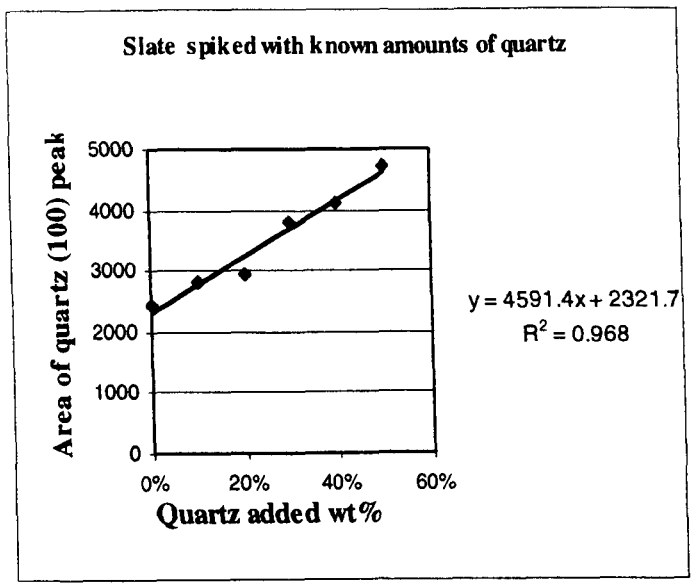

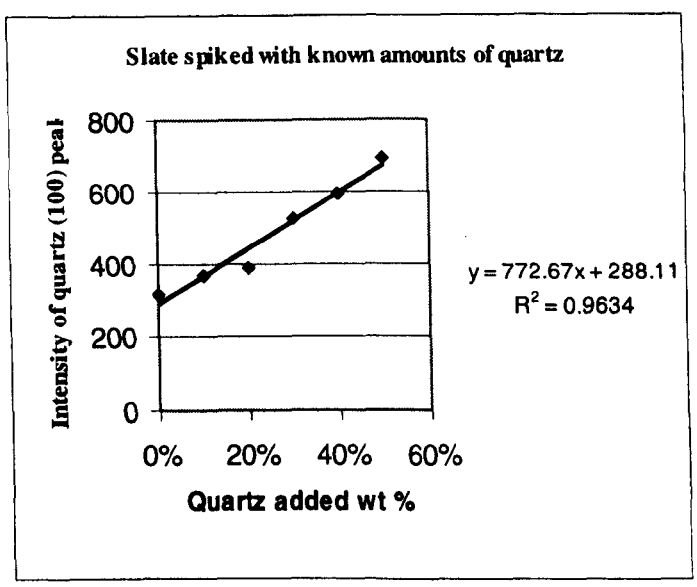

Fig. 2.10 Determination of quartz content of a sample of Macduff slate (MK-4) by spiking with known amounts of quartz. a) The increase in the area of the quartz (100) peak with the amount of quartz added. b) The increase in the intensity of the quartz (100) peak with the amount of quartz added.

2.5.2 X-Ray Fluorescence Spectroscopy: XRF Analysis

XRF analysis is a standard technique for determining the bulk chemical composition of rocks. Powdered samples which have been fused into discs are bombarded with X-rays and emit secondary radiation which is characteristic of the elements present.

In this procedure, a metal anode is bombarded by a beam of electrons emanating from

a heated tungsten filament. The anode gives off a continuous spectrum of X-rays superimposed on which are the characteristic peaks of the metal of the anode. When the sample is bombarded with these X-rays, it gives off secondary radiation due to the filling of inner shells as described in Section 2.4.1.2.2. The choice of anode affects the intensity of the radiation, e.g. a metal with higher Z produces the more intense continuous radiation. However, the intensity of the secondary radiation produced by the sample is greater when the energy of the primary radiation is only slightly greater than the K peak of the elements present (Section 2.4.1.2.3). Some laboratories use tungsten (W, Z = 74) for heavy element analyses and chromium (Cr, Z = 24) for light. However, in this work the metal rhodium (Rh), which has an intermediate value for Z of 45, is used in all elemental analyses. The radiation entering the spectrometer consists of the secondary radiation produced by the sample which is superimposed on the primary radiation of the anode. The radiation is dispersed by several analysing crystals and analysed by wave length dispersive spectrometers (Section 2.4.2).

In quantitative analyses, the intensity of the radiation from each element present in the sample is compared with that from standards of known composition. Systematic errors, such as dead time, line overlap, X-ray absorption and enhancement, can occur due to interaction of the X-ray beam with the sample. Corrections are done iteratively by the instrument, based on the assumption that the sample is homogeneous. In the case of major elemental analyses which have long wavelengths that only penetrate to a shallow depth, the sample appears heterogeneous however small the grain size. The sample is therefore homogenised by fusing it into a glass with a flux such as lithium borate. The presence of the flux dilutes the sample however, so that this procedure is used only for elements present at high concentrations i.e. the major elements. Results are given as the percentage weights of oxides of the major elements (Fitton 1997).

2.5.2.1 Method

A sample of approximately 1gm was weighed precisely with 5 times the amount of flux (Spectroflux 105), ignited in a furnace at 1100°C, and then quenched into glass beads. Samples were analysed using a Philips PW1480 λ dispersive sequential X-ray spectrometer. One problem arose from the presence of small amounts of graphite in

many slates which was not completely oxidised during ignition. Trace amounts of scum were left, from which cracks in the glass beads would have propagated. To prevent this happening, a small amount (0.25gm-0.3gm) of the oxidising agent ammonium nitrate (NH_4NO_3) was added to each sample, thus ensuring complete conversion of the graphite to CO_2 and its loss with the rest of the volatiles.

Over 100 samples were analysed using the XRF technique and the major elements are shown in Appendix 2.3 expressed as percentage weights of oxides, all iron being assumed to be present as Fe_2O_3.

To determine the precision of the analyses, one sample was processed 5 times and one glass bead analysed five times. The results are given in Appendix 2.4 and a summary in Section 2.5.2.2.

2.5.2.2 Results

The minerals present in each sample are known from the XRD whole rock analyses. XRF analysis determines the percentage weight of each oxide (iron was assumed to be present as Fe_2O_3). Allocating the individual oxides to different minerals is complicated by the fact that nearly every element is found in more than one mineral e.g. silicon is present in every mineral apart from the iron ore minerals and carbonates. Therefore any algorithm used to determine the relative amounts of each mineral involved approximations.

2.5.2.2.1 Algorithm used in the determination of the percentage weight of each mineral

1. The Loss on Ignition (LOI) was taken as the difference between 100% and the total percentage of all the oxides.

2. The weight of iron was recalculated to account for the presence of ferrous iron, using the ratio of reduced to total iron. This ratio was determined independently by wet chemical analysis (Section 2.5.4.3). The percentage volatiles were adjusted by adding the increase in weight due to oxidation of the

reduced iron. The XRF results were then normalised to account for this adjustment.

% volatiles = % LOI + 0.112 x % wt FeO

3. The percentage by weight of each oxide was converted to the number of moles of each cation.

4. The amount of apatite present was calculated based on the moles of phosphorus and the amount of calcium, then determined stoichiometrically and subtracted from the total.

5. Excess calcium if present was attributed to carbonate, calcite or dolomite depending on which mineral was detected by XRD analysis. The related amounts of volatiles were adjusted according to the chemical formula.

6. The moles of white mica were based on the amount of potassium (**K**) present, using the formulae determined by the probe as described above. The amounts of sodium (**Na**) and other elements in the phengite were calculated using the formula and then the residue of each determined.

7. Excess **Na** was attributed to albite, the associated silica and aluminium calculated and the residue found as before.

8. The moles of chlorite present were determined as a function of the amount of excess **Mg** present. The associated elements were calculated according to the formula determined by microprobe analysis and subtracted from the residues.

9. Excess aluminium (**Al**) was allocated to clay, and the associated silicon and water was calculated using the formula for halloysite $SiAl_2O_5.2H_2O$ and subtracted from the residues.

10. Excess silicon (**Si**) was attributed to quartz.

11. Excess iron (**Fe**) was attributed to the mineral detected by XRD analysis i.e. haematite or pyrite. In the case of pyrite the associated sulphur was deducted from the remaining volatiles.

12. The percentage weight of each mineral was calculated from the number of moles times the molecular weight. The unallocated residue of each cation was then calculated as the weight of the oxide.

When there was a high amount of potassium, steps 6 and 7 were adjusted by basing the moles of white mica on the sodium present and attributing the excess potassium to the feldspar orthoclase. An example of the above calculation is given in Appendix 2.2.

The actual clay present was not determined, halloysite with two molecules of water was chosen as it gave the best fit for excess Al_2O_3 and H_2O. The presence of this form of clay was detected in the XRD analyses of some Ballachulish slate.

2.5.2.3 Evaluation of Results

Assumptions:

The white mica and chlorite formulae, as determined for a standard for each area, were assumed to be representative for all the samples in the area. Similarly the percentage of reduced iron was determined for one or two samples per area and taken as representative of the whole.

The precision of XRF analysis was determined as follows:

1 ***Random machine errors:*** one sample was analysed five times, sample deviations s for individual oxides were found to be <=0.06 and the coefficient of variation 0.005 (Appendix 2.4).

2 ***Sample preparation errors:*** five beads were prepared for analysis from one sample. The sample standard deviation s was 0.14 for SiO_2 and for LOI while for all other cations it was <=0.06. The coefficient of variation was 0.007 (Appendix 2.4).

The precision of the XRF analyses was high so that the results were suitable for calculating the modal analysis. One problem, difficult to assess, is the interdependency of results e.g. albite and white mica are interdependent and underestimating the white mica increases the apparent albite content. There is similar interdependence between chlorite and haematite, which is particularly sensitive due to the large formula weight of chlorite. Haematite and quartz are calculated as "left-overs" after iron and silicon have been allocated to all the other minerals and are therefore subject to cumulative errors. The corollary of this is that if the amount of quartz found by this residual silicon method correlates with the amount of quartz determined by some other analytical method, this suggests that all the results for minerals containing silicon are satisfactory.

The accuracy of the XRF method can be assessed in two ways, by examination of residue both quantitatively and qualitatively and by correlation with independent methods.

The Residue:

Generally the residue was attributable to the trace mineral ilmenite (TiO_2) and to excess volatiles. The fit was good for the standard samples themselves and within the immediate confines of the quarry of origin. In most cases it was also possible to get satisfactory results for samples from surrounding quarries, but with one notable exception. The mineral composition of the Balvicar samples were calculated based on both the Breine Phort, Seil standard and the Port Mary, Luing standard but no satisfactory results were obtained. This was due to the high level of magnesium and the presence of magnesite for which no allowance was made in the algorithm.

Results

The results are given in Appendix 2.5. A triangular plot of the three major minerals, (quartz, white mica and chlorite) is given in Fig. 2.11a. Because in a triangular plot the total of the three minerals is normalised to 100%, this had the effect of making samples with a high proportion of other minerals such as feldspar and clays have an apparently high value of quartz. It was therefore decided that an XY scatter plot, where the

absolute values of quartz as calculated by XRF analyses were plotted, was a better representation of the mineralogy. The axes chosen were quartz and white mica as these are the two most durable minerals in slate and hence give the best representation of the original mineral composition (Fig. 2.11).

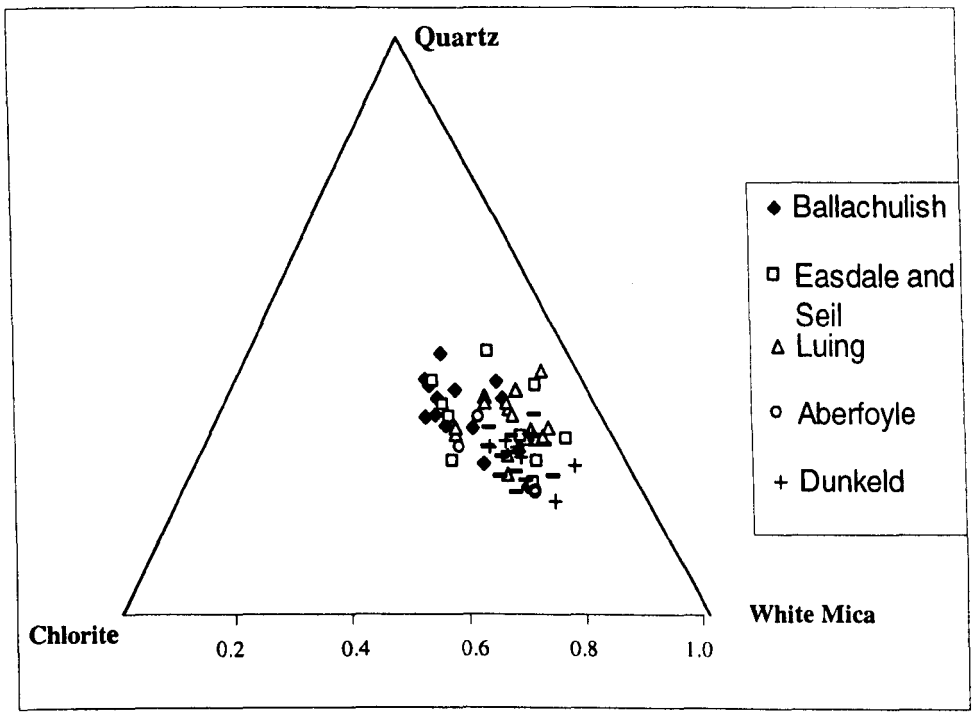

Fig.2.11 Mineral composition of Scottish slate calculated from XRF data. a) A triangular plot showing the relative proportions of the three major minerals.

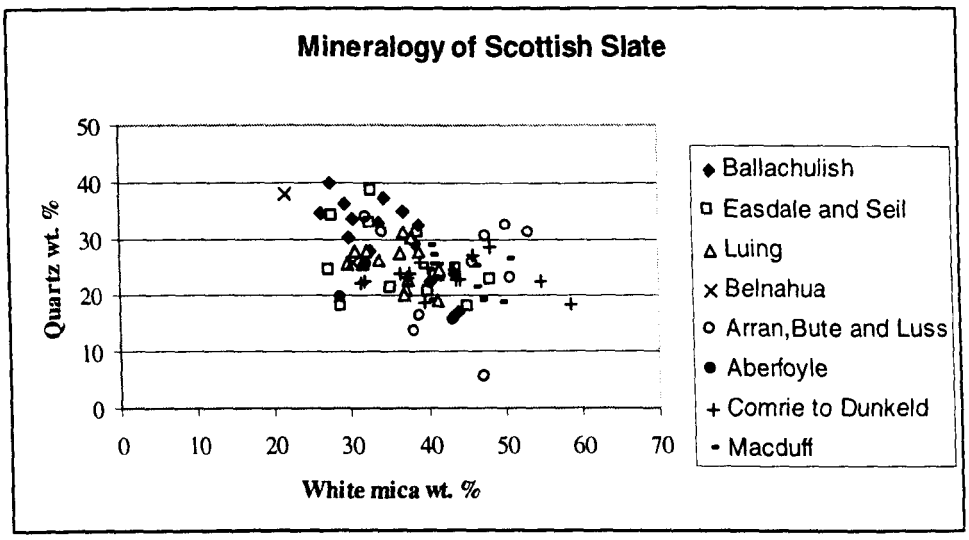

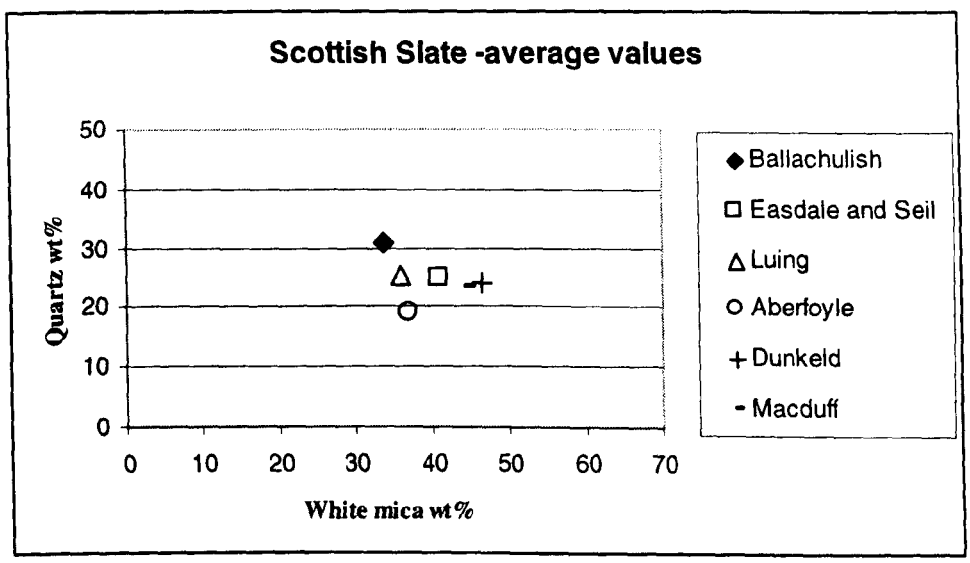

Fig.2.11 (continued) Mineral composition of Scottish slate calculated from XRF data. b) Absolute values of quartz and white micas. c) Average values grouped according to location.

2.5.3 SEM Back Scatter Imaging

A scanning electron microscope (SEM) uses a finely focused high-energy electron beam similar to that used in an electron microprobe (Section 2.4.2) but designed for imaging. In a SEM, the electron beam is scanned across the surface of a specimen in a television-like raster and the signal from an electron detector is displayed on the screen (Reed 1996). Two types of image are produced, one from the secondary electron beam and one from back-scattered electrons. The secondary electrons give an image of topographical features which is used in assessing the slaty cleavage of slates (Chapter 4). In this section the **B**ack-**S**cattered **I**mages (BSI) are used to give information on the compositional variation in a sample.

A Back-Scattered Image is produced by the elastic collisions of the X-rays with the atoms on the surface of the sample. The intensity of BSE (**B**ack **S**catter **E**lectrons) is dependent on **z** the atomic number of the element. This property was used to distinguish between minerals of different mean atomic number i.e. minerals with high average atomic number appeared bright and those with low **z** appeared dark. Approximate modal composition may be determined using the images of mean atomic number.

2.5.3.1 Method

Work was carried out on a Cambridge Instruments Stereoscan 360, using a four Quadrant Back Scatter Detector

Machine conditions

Filament current	I ≈ 2.60A
Probe current	I = 1.5-2.5 nA
Extra high tension	EHT = 20 KV
Working distance	WD ≈ 20mm

The BSI is affected by the surface topography, so polished sections were used. Polished samples were cut parallel and perpendicular to cleavage and carbon coated to

reduce charging.

2.5.3.2 Results

Knowing the minerals present in slate from the preliminary XRD work it was possible to attribute the different tones to the amount of each mineral present. In slate, metal oxides such as haematite appeared very bright, chlorite appeared bright, white mica appeared as mid-grey areas, while quartz and feldspar were a darker grey. It was not possible to distinguish other minerals e.g. dolomite has approximately the same density as white mica and hence was indistinguishable by this method. It was possible to integrate the relative areas of the different minerals using a digipad image analysis program.

It was assumed that the area occupied by the different shades of minerals is directly proportional to the relative *volume* of the different minerals. Given that over 50% of a slate sample is made up of platy minerals and that these mineral show complete orientation as seen from stereo XRD profiles, it was necessary to check this assumption. This was done by comparing the relative areas for two sections, one taken parallel to cleavage and the other at 90° to cleavage. No significant difference was found in the relative area of each mineral for the two orientations in the samples tested (Table 2.8).

MK-4	Very bright %	Bright %	Mid grey %	Dark grey %
Parallel to cleavage	11	8	41	41
Perpendicular to cleavage	7	6	44	44

Table 2.8 Percentage areas of different minerals for two aspects of a slate one parallel to cleavage and one perpendicular.

A much greater problem was caused by the inter-growth of the minerals, which, instead of dividing the area into distinct zones of different tones corresponding to the different minerals, gave an ill-defined graduation from one shade of grey to another. This gave a trace with a high noise to peak ratio (Fig. 2.12). In order to maximise

resolution, adjustments were made to the probe current to increase the contrast, with a corresponding adjustment to the brightness, until the darker minerals were just detectable. However it was impossible to get consistent results for the Aberfoyle and Dunkeld standard samples. Results are given in Table 2.10.

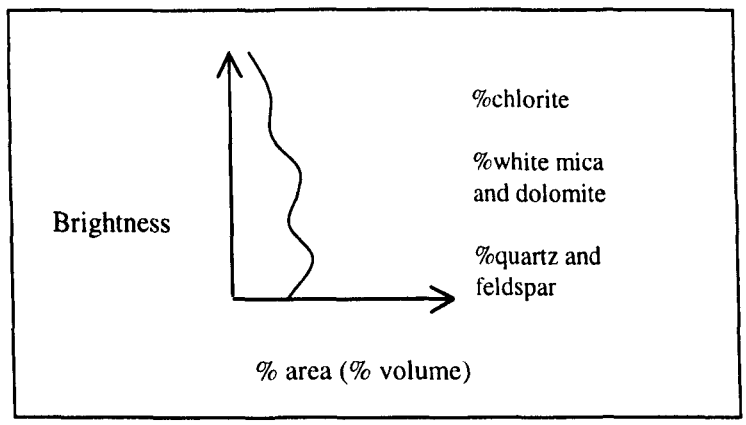

Fig. 2.12 High noise to peak ratio makes interpretation of SEM back scattered images imprecise.

Interpretation of results:

The percentage volume was converted to percentage weight as follows:

% weight = % volume x specific gravity (S.G.)

The densities of quartz and the iron ore minerals were obtained from the literature and a range of values for muscovite and chlorite (Deer *et al.* 1992). Due to the variable chemical composition of chlorite and white mica the apparent specific gravities of these minerals were calculated using the chemical formulae determined by electron microprobe analyses. This was done by taking the molecular weight of the mineral and dividing by the number of oxygens in the formula and standardising with respect to quartz. The percentage volume figures were converted to percentage weights by multiplying by apparent specific gravity and normalising (Table 2.9).

	S.G. gm/cm^3	*Apparent S.G.* gm/cm^3			
Sample Nos		W/F-1	EL-10	MK-4	
Quartz	2.65				
Haematite	5.25				
Pyrite	5.0				
Calcite	2.7				
Dolomite	2.8-2.9				
Feldspar	2.55-2.63				
Chlorite	2.3-3.3	3.15	3.01	3.10	Ripidolite
Muscovite	2.77-2.88	2.92	2.92	2.92	White mica

Table 2.9 Specific gravity of the various minerals found in slate (Deer *et al.* 1992).

The specific gravity for chlorite fell within the range of values recorded by Deer *et al.* (1992), the values varying slightly from one area to the next depending on the proportion of iron present. W/F-1 gave the highest at 3.15. The values for the white micas were slightly higher than those reported for muscovite, due to the presence of small amounts of iron in the former.

	Very bright	Bright	Mid grey	Dark grey	
W/F-1	1	17	46	33	% Volume
	2	19	50	29	% Weight
EL-10	1	7	42	50	% Volume
	2	8	44	47	% Weight
MK-4	7	12	50	31	% Volume
	12	12	49	27	% Weight

Table 2.10 Relative amounts of major minerals by percentage volume and percentage weight

2.5.4 Chemical Analyses

A selection of slate samples were analysed by the following traditional wet chemistry techniques:

1 Loss on Ignition

2. Carbonate Analysis

3 Reduced Iron Analysis

4 Graphite Analysis

2.5.4.1 Loss on Ignition (LOI)

A dried sample was ignited in a furnace at 1100°C for thirty minutes, allowed to cool and weighed. The process was repeated until a constant weight was achieved.

$$\% \text{ volatiles} = \text{LOI} + \% \text{ FeO} \times 0.112$$

2.5.4.2 Percentage Weight of Carbonate

The presence of carbonate was tested by adding a few drops of 10% HCl to the powdered sample and observing effervescence. The smell of sulphurous acid indicated the presence of sulphur in some samples.

Carbon dioxide was determined quantitatively by igniting the sample at 1100°C to 1200°C and removing the volatiles in a stream of nitrogen. Carbon dioxide was absorbed in soda asbestos and determined gravimetrically. Similarly, water was determined by absorption in a tube containing anhydrous magnesium perchlorate and determined gravimetrically. This is the classic method devised by Riley (1958).

The amount of carbonate present was determined in duplicate for a selected number of samples (Table 2.11).

Sample	H_2O % weight		CO_2 % weight	
EL-10	4.36	4.44	4.92	5.02
LS-2	3.36	3.50	0.30	0.24
SB-2	4.78	4.90	2.76	2.82
SB-3	2.90	2.98	13.90	13.98
LP-6	4.04	4.12	1.32	1.30
LT-3	4.04	4.16	10.70	10.94
LT-5	4.32	4.26	5.00	5.06
MK-2	3.61	3.92	0.16	0.16
MH-2	3.56	3.67	0.16	0.17
E/K-1	2.92	3.04	4.66	4.66
E/K-2	2.96	3.10	3.16	3.36
E/EW-1	4.36	4.44	4.92	5.02
E/EW-2	4.64	4.52	5.00	5.04

Table 2.11 Carbonate and water determined gravimetrically for a selection of slate samples.

Pyrite FeS_2

The amount of pyrite present was determined from the amount of sulphur detected in XRF trace analysis (Appendix 2.6).

2.5.4.3 Percentage Weight of Ferrous Oxide

Ferrous oxide was determined by titration with standard potassium dichromate solution after the rock had been dissolved by hydrofluoric acid, sulphuric acid and phosphoric acid (Riley 1958).

The dichromate ion $Cr_2O_7^{2-}$ is an oxidising agent in an acid solution and hence oxidises Fe^{2+} to Fe^{3+} as follows:

$$Cr_2O_7^{2-} + 6\,Fe^{2+} + 14H^+ \rightarrow 2Cr^{3+} + 7H_2O + 6\,Fe^{3+}$$

Using K^+ and SO_4^{2-} as spectator ions, this gives a balanced equation as follows:

$$K_2\,Cr_2O_7 + 7H_2SO_4 + 6FeSO_4 \rightarrow Cr_2(SO_4)_3 + 3Fe_2\,(SO_4)_3 + K_2(SO_4) + 7H_2O$$

Diphenyl amine is used as an indicator, changing from colourless to blue at the end point.

The ratio of reduced to total iron may be typical of the environment of deposition of the original protolith. High values of approximately 90% were found in both the dark grey slates i.e. the Welsh and the Ballachulish samples, which suggests reducing conditions at the time of sedimentation of the original deposits. The presence of both graphite and pyrite is also associated with a reducing environment during deposition. In contrast to the Ballachulish and the Welsh slate, the Macduff slate has a low ferrous content and the iron ore mineral found in such slate is haematite.

	FeO % weight	*$Fe^{2+}/(Fe^{2+}+Fe^{3+})x\ 100$*	*Graphite detected*
EL-10	5.16	89%	yes
SB-6	2.90	66%	yes
SB-7	2.47	52%	yes
LP-5	4.30	66%	yes
B2	1.90	42%	no
AB-5	2.80	33%	no
DN-1	5.66	78%	no
DN-4	2.90	39%	no
MK-4	2.97	28%	no
MF-11	2.58	29%	no
W/F-1	6.92	88%	yes

Table 2.12 Amount of reduced iron and the ratio of reduced to total iron.

The situation is more variable in the Highland Border slate. Two samples from the Newtyle quarries at Dunkeld (Appendix A 4.4.3) showed very different values; the first sample DN-1 has a high ferrous content while the second DN-4 has a low ferrous content. This difference is seen in the colour of the slate whereby the low ferrous content is due to the presence of ferric haematite which imparts a purple colour to the slate. The first sample is green, indicating absence of haematite and not only a high chlorite content. The colour of slate in the quarries follows the bedding direction and hence changes of colour reflect primary differences in oxidation potential (Eh volts).

2.5.4.4 Graphite

The presence of graphite was detected in XRF analysis as discussed (Section 2.5.2.1).

It was also detected during reduced-iron determinations where on dissolving the sample in hydrofluoric acid, the insoluble graphite floated to the surface (Section 2.5.4.3). Results are reported in Table 2.12.

2.5.5 XRD Semi-Quantitative Analysis

The possibility of determining the mineralogy of slate using XRD analysis without reference to a standard was examined.

The area and intensity of the peaks is related to the amount of the mineral present, but the chemical composition of the mineral and preferential orientation also affect the results. In addition problems occur when the sample is small in relation to the incident beam. The intensity of the diffracted X-Ray is proportional to the volume of the sample irradiated; hence there is loss of intensity when the sample size is less than the spread of the incident beam or thinner than that penetrated by the beam. The length of the sample is particularly important at low 2θ angles used in the analysis of phyllosilicates. The 7° 2θ XRD peak, which is unique to chlorite, is particularly affected by this problem. A better peak would be the [002] at 14° 2θ but this is also the location of the [001] peak of several clays. The [001] white mica peak at 10° 2θ is also affected by this problem but to a lesser extent.

The length **L** of a sample is by the geometry of the X ray Diffractor as follows

$$\mathbf{L = R_o\ Tan\ \alpha\ /Sin\theta}$$

α = incident beam slit

R_o = goniometer radius = 17.3cm

θ = angle of the incident beam

(Moore & Reynolds 1997)

°2θ	L cm	intensity/maximum intensity
7	4.9	50%
10	3.5	71%
14	2.5	100%

Table 2.13 Loss of intensity at low 2θ angles for a sample 2.5cm long

At high angles of 2θ, there is an equivalent loss of intensity due to the samples being insufficiently thick. However, simply increasing the thickness affects the position of peaks and defocuses the beam.

Thus there are many problems in determining the mineral composition of a slate by XRD, and quantitative analysis alone is not recommended unless there is no alternative. Instead, the best method is to determine the mineral composition relative to a slate from the same area whose composition is known from XRF and electron microprobe data as already discussed. Then equivalent peaks are compared and the chemical composition calculated on a *pro rata* basis. In this way problems of loss of intensity due to the geometry of the XRD equipment are minimised as well as variation due to differences in chemical composition etc.

Section 2.3 describes how a standard was defined for some quarries by the method of determining the chemical composition of the phyllosilicates (Section 2.4.2). Time constraints made it impossible to determine such a standard for all of the quarries covered in this Report. Therefore the possibility was investigated of determining a rough estimate of the mineral composition based on XRD analyses alone without reference to a standard.

The bulk of slate is made up of the platy minerals, (white mica and chlorite), which have similar grain size and orientation, differences in the intensities of their representative peaks are due to (i) chemical composition (ii)loss of intensity due to the sample length being too small and (iii) abundance. It is possible to correct for the effect of chemical composition by calculating the ***attenuation coefficient*** μ (see below) and applying a correction factor to the peak intensities. It was also possible, using the values shown in (Table 2.13), to correct the intensity of the peaks for loss due to the sample being too short. It then becomes reasonable to attribute the relative intensities and areas of mineral peaks to their relative concentrations. It is not however possible to extend the process to estimate the amount of quartz, due to differences in the crystal structure and degree of orientation. However there is no variation in the intensity of the quartz peaks due to different chemical composition. Following the

standard sample preparation procedure (Section 2.4.1.5) to minimise any variation due sample preparation, it was found that the ratio of the quartz [100] peak to the amount of quartz present (as determined by XRF) was relatively consistent as compared with that found for the white mica (Fig. 2.13). The best-fit line was found using a linear regression analysis and the proportionality constant determined. Using this constant, it is therefore possible to get an approximate quartz content for slates from areas where no more accurate information is available.

2.5.5.1 Determination of attenuation coefficient μ

According to Klug & Alexander 1974 the intensity **I** of an X-ray is related to the weight **w** and attenuation coefficient μ

$$I_I = \frac{w_i}{\mu_i}$$

The attenuation coefficient of a mineral of known composition can be determined using the weighted average of each element present (Table 2.14 & 2.15). Values for white micas and chlorite are given in Table 2.16.

$$\mu = \Sigma w_i \mu_I$$

Z	Element	μ (Co K_α)
8	O	17.4
11	Na	47.1
12	Mg	63.5
13	Al	77.5
14	Si	100.4
19	K	222.0
20	Ca	257.0
22	Ti	300.0
25	Mn	405.0
26	Fe	56.2

Table 2.14 Elemental mass attenuation coefficients extracted from the International Tables for X-ray Crystallography Vol. 4 1974 for Co $K\alpha$ radiation.

Mineral	Formula	μ
Quartz	SiO_2	56.2
Albite	$NaAlSi_3O_8$	52.9
Haematite	Fe_2O_3	44.5
Pyrite	FeS_2	101.5
Calcite	$CaCO_3$	112
Magnesite	$MgCO_3$	29
Siderite	$FeCO_3$	35
Dolomite	$MgCa(CO_3)_2$	74

Table 2.15 Attenuation coefficients for a selection of minerals

Sample	μ chlorite	μ white mica
El-10	46.32	64.60
SB-6	46.23	61.79
LP-5	45.92	62.45
B2	45.70	62.73
AB-5	45.83	61.93
DN-4	46.32	62.71
MK-4	46.39	61.61
Mean	**46.1**	**62.5**
S Dev	**0.28**	**1.0**
C of V	**0.0006**	**0.016**

Table 2.16 Attenuation coefficients for chlorite and white micas in the standard slate samples.

The effect of chemical composition on the chlorite attenuation coefficient is insignificant (s = 0.28) and an average figure of 46.1 was used. Similarly, the average figure for white mica of 62.5 was used (s = 1.0), (Table 2.16).

2.5.5.2 Method

Powdered samples were scanned by XRD from 4 – 30° at 1° 2θ per minute. The areas of the [100] quartz peak at 24.26° 2θ, the [001] white mica peak at 10° 2θ and the [001] chlorite peak at 7° 2θ were determined using the Traces software package.

Precision of XRD results

The following statistical evaluation was carried out:

1 The precision of the software program was assessed by determining the areas of each of the three main peaks over 20 times.

2. Three XRD samples were prepared from the same slate and analysed over an interval of two years.

3. The effect of reducing the concentration was assessed by mixing the slate with quartz (data from spiking experiment, Section 2.5.1)

	Coefficient of variation	Quartz	White Mica	Chlorite
1	Determination of area – Traces software	0.014	0.017	0.027
2	Sample preparation	0.04	0.05	0.05
3	Variation due to concentration		0.16	0.17

Table 2.17 XRD precision measurements.

The results are summarised in Table 2.17, where it can be seen that variation in concentration has the most significant effect on the precision of results. This shows that variation in the results due to sample preparation or interpretation is insignificant compared with imprecision due to differences in the sample itself.

Reliability of XRD results

There is no correlation between the amount of the phyllosilicates of the different standards as determined by XRF analyses and the area of the XRD peaks. (Fig. 2.13). However the quartz content as determined by XRD does show some correlation with the XRF results. This shows that quartz peaks are less affected by preferential orientation than are white micas. In this section this relationship is used to determine the approximate amount of quartz in a slate.

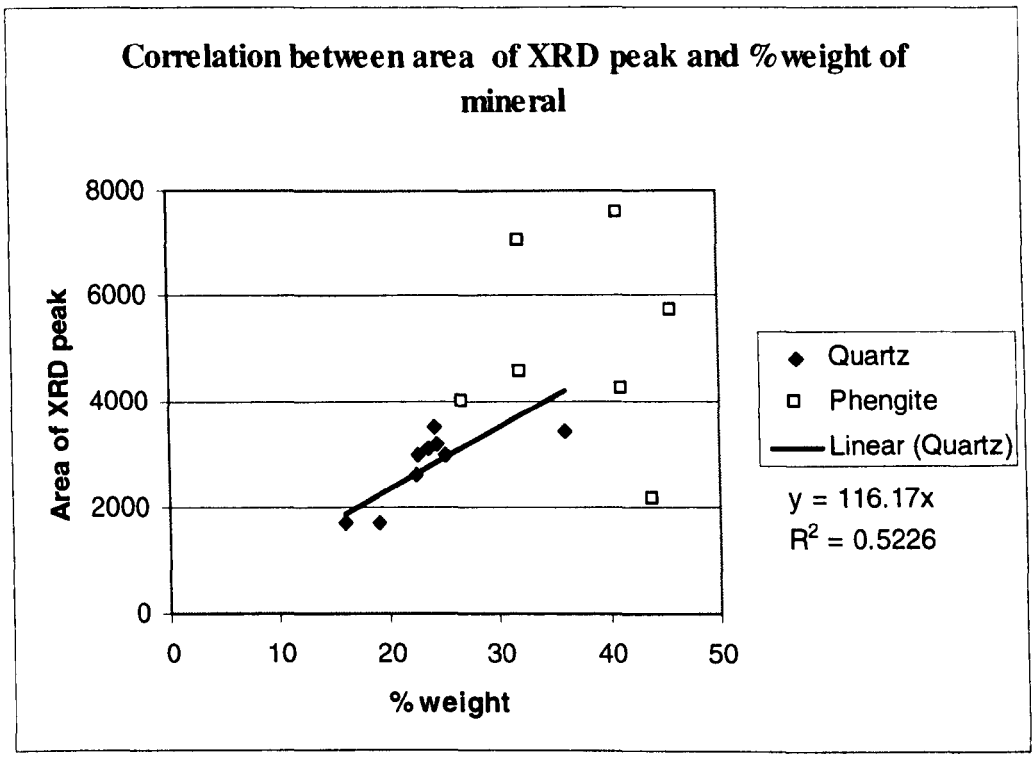

Fig. 2.13 Area of XRD peak relative to the XRF results for different standard samples.

Sample	Counts	% weight
MK-4	2592	22.5
LP-5	1708	19.1
EL-10	3394	36.0
W/F-1	3104	23.6
SB-6	3491	24.3
AB-5	1710	16.0
AB-6	2971	25.2
W/F-9	3177	24.4
DN-4	2948	22.8

Table 2.18 Area of XRD peaks and the quartz content as determined by XRF analysis.

2.5.5.3 Results

XRD is a very simple and convenient procedure and when necessary can be used to give a rough estimate of the mineral composition of a slate as follows:

1. Determination of the percentage weight of quartz at 116 counts per 1% weight (Fig. 2.13).
2. The remainder of the composition is assigned to phyllosilicates in the ratio of their [001] peaks corrected for their attenuation coefficient (Table 2.16) and loss of intensity due to the size of sample being smaller than the spread of the incident X-ray beam (Table 2.13)
3. Some refinement of the above may be necessary in the case of slates with large amounts of feldspar and carbonates.

2.6 Comparison of Results

2.6.1 Evaluation of the Spiking Technique

The values obtained for quartz by this method are substantially different from those obtained in both the SEM and XRF methods i.e. the sample of MK-4 has 22% quartz using XRF method but 33% using the spiking method as determined by the area of the quartz peak. One explanation is that this is due to the difference in grain size and/or crystallinity between the added quartz, and that present in the slate. These values of quartz content were not used in this Report.

2.6.2 Comparison of XRF and SEM Analyses

SEM results (Table 2.10) are compared with those calculated from XRF data (Appendix 2.5) in Table 2.19. When XRF results are grouped according to mineral density e.g. quartz plus feldspar is compared with the dark zone of a SEM back scatter image, there is reasonable agreement between the results (Table 2.18 & Fig. 2.14). However the SEM method is limited in its usefulness. Apart from the difficulties in analysis, it is also unable to distinguish between minerals of similar densities. However it has been useful in giving an independent assessment of the accuracy of the XRF results.

Sample		Quartz	Feldspar	Chlorite	White Mica	Dolomite/ Calcite	Haematite/ Pyrite
	SEM	Dark area		Light grey	Medium grey		Very bright
MK-4	XRF	22.5	5.4	14.6	41.5		7.6
	SEM	27		12	49		12
W/F-1	XRF	23.6	2.6	27.6	45.7		0
	SEM	29		19	50		2
EL-10	XRF	34.6	4.5	21.1	26.3	6.5	2.7
	SEM	30		8	43.5		2

Table 2.19 XRF data grouped according to density of individual minerals for comparison with SEM results.

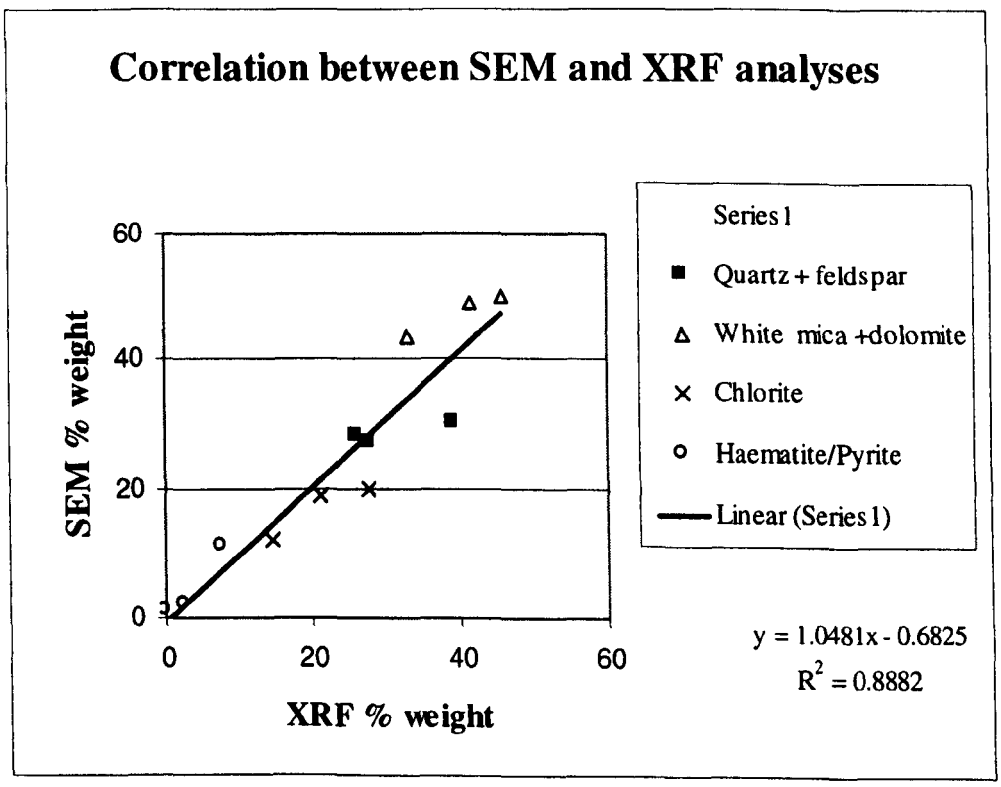

Fig. 2.14 Correlation of XRF/SEM results for minerals of comparable densities e.g. medium density minerals (SEM) relative to white mica + dolomite (XRF).

2.6.3 Comparison of XRF and Traditional Chemical Analyses

The carbonate values determined by XRF (Appendix 2.5) were compared with those produced by wet chemistry. Although the correlation between the percentage CO_2 values determined by the two methods gives $R^2 = 0.9$, there is a systematic difference

whereby the values determined by wet chemistry are consistently higher than those determined from XRF calculations. This could be due to the presence of other carbonates such as siderite, but it is more likely to be due to the oxidation of trace amounts of graphite in the wet chemistry technique. Oxidation of one gram of graphite yields 3.7gm of CO_2. Substantial amounts of magnesite are present in the Balvicar (Appendix A 3.5.4) and the Toberonochy (Appendix A 3.5.5) samples which are not accommodated by the XRF algorithm and hence not used in the correlation.

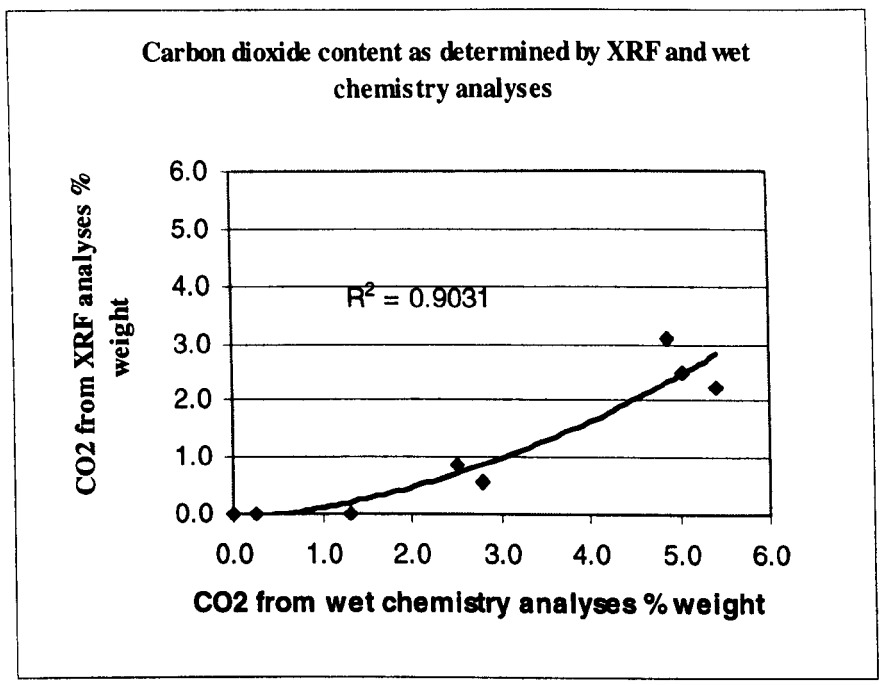

Fig. 2.15 Correlation between CO_2 calculated from XRF analyses and that determined by wet chemistry analyses.

Sample	CO_2 Run 1	Run2	% CO_2 by wt	Difference	CO_2 calculated from XRF	XRF % wt dolomite
EL-10	4.84	4.92	4.88	1.99	3.11	6.5
LS-2	0.30	0.24	0.27	0.27	0.00	0
SB-2	2.76	2.82	2.79	1.42	0.57	1.2
SB-5	2.52	2.52	2.52	1.66	0.86	1.8
BB-2	5.40	5.44	5.42	3.17	2.25	4.7
LP-6	1.32	1.30	1.31	1.31	0.00	0
LT-5	5.00	5.06	5.03	2.54	2.49	5.2
MK-2	0.00	0.00	0.00	0	0.00	0
LT-3	10.7	10.94	10.82		0.81	1.7
SB-3	13.9	13.98	13.94		6.36	13.3

Table 2.20 Comparison of carbon dioxide results obtained by XRF and wet chemistry.

2.6.4 Comparison of XRF and XRD Results.

The mineralogy of slate was calculated from XRD data relative to the relevant standard on a *pro rata* basis by comparing the areas of the different peaks with the equivalent values in the standard. This method should eliminate many of the problems inherent in XRD quantification analyses. There is poor correlation between the XRF and the XRD quantitative analyses when applied to individual minerals, but when the figures for the three major minerals (quartz, white mica and chlorite) are grouped together the weighting of the occasional rogue XRD result is reduced and the correlation is moderately good. For example for Ballachulish slate $R^2 = 0.69$ (Fig. 2.16) although the best-fit line does not have a slope of one, nor an intercept of zero. As XRD results measure crystalline material, while XRF determines the total amount of mineral based on its chemical composition, it was hoped that the ratio of XRD to XRF results would give a measure of the crystalline/amorphous ratio, but this was not possible due to there being too many variables.

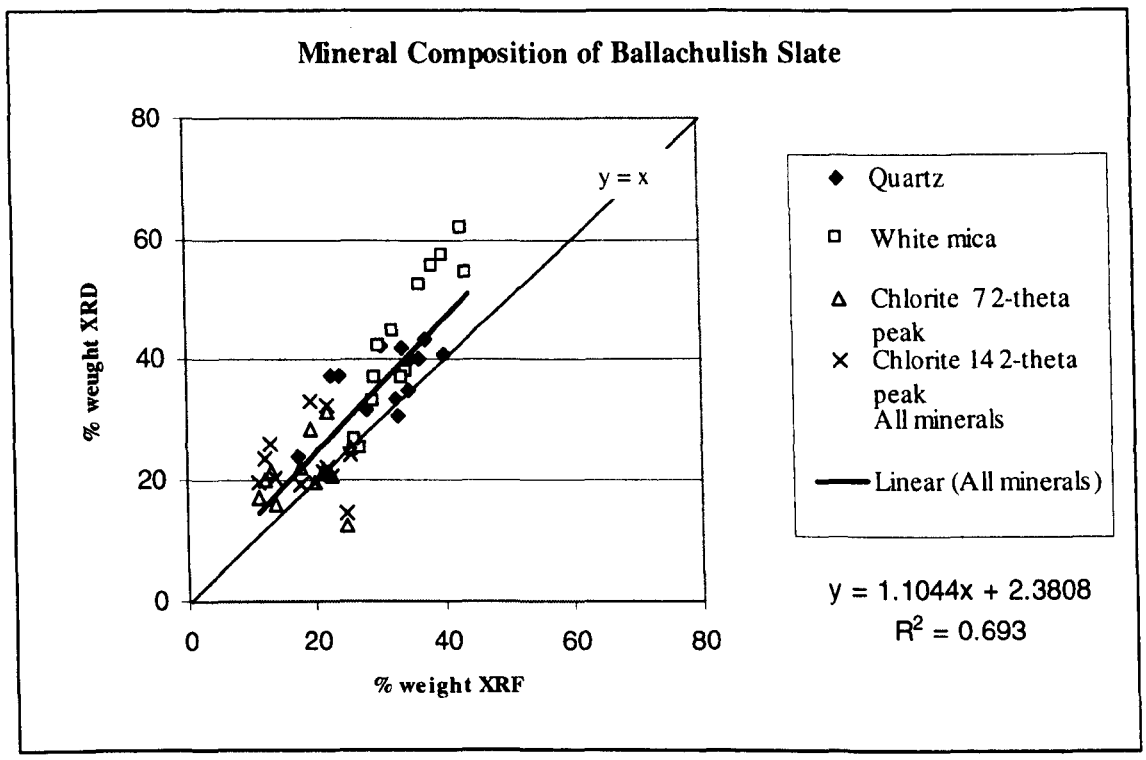

Fig. 2.16 Comparison of the mineral composition of Ballachulish slate as determined by XRD and XRF analyses. The XRD results are calculated on a *pro rata* basis relative to the standard EL-10

The composition of Ballachulish samples was also determined without reference to the standard EL-10 as described in Section 2.5.5.3. In this method the sum of the concentrations of the three major minerals is normalised to 100% i.e. recalculated *pro rata* so that the total equals 100%. Therefore to enable comparison with the XRF results, the sum of the concentrations of the three major minerals as determined by XRF analyses was also normalised to 100%. The correlation figure between XRF and XRD results was $R^2 = 0.64$, with the slope of the graph equal to one and the intercept equal to zero. This shows that it is possible to get a rough estimate of the proportions of the major minerals in slate without supporting electron microprobe and XRF analyses (Fig. 2.17). It is however impractical to extend this method to other minerals present in slate.

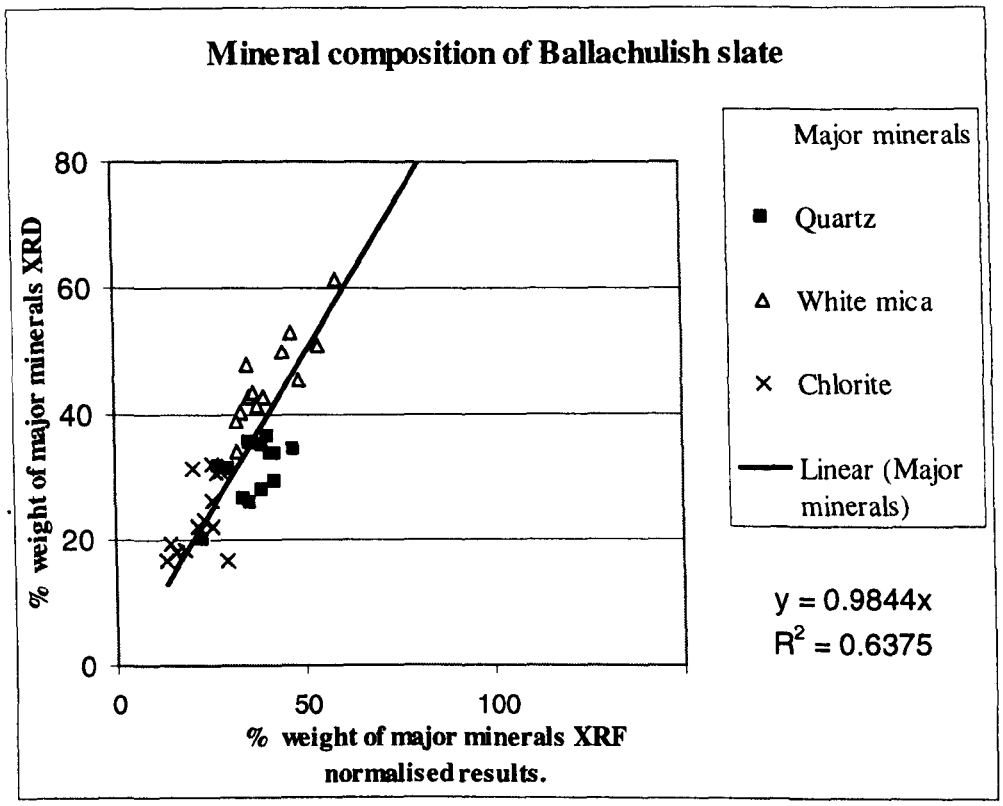

Fig. 2.17 Comparison of the three major mineral composition of Ballachulish slate as determined by XRD (without reference to the standard EL-10) and XRF results have been normalised to 100% i.e. recalculated so that the totals equal 100%

2.7 Conclusions

- To determine the mineralogy of slate is not a straightforward process and a combination of methods is necessary.

- The above work was based on all the slate quarries visited in Scotland, which stretch over a wide area. It is therefore not surprising that using chemical composition of the phyllosilicates from one quarry to determine the mineral composition of slates in another quarry was not always successful.

- The methodology described above would be better suited to determining the mineralogy of the different zones of a quarry chosen for a more detailed study.

1 Determination of the formulae of the phyllosilicates by microprobe analysis for one or more standard samples.
2 Interpretation of bulk chemistry from XRF results to give the composition of the slate in terms of the major minerals present, checking results with SEM quantification where possible.
3 XRD analyses, although less precise, are useful in a fairly homogeneous area and would support the XRF analyses. Where XRF and electron microprobe results are not available the XRD can be used for less precise results.
4 Determination of carbonate and reduced iron for a few samples.

Ideally the mineralogy should be done on un-weathered samples from boreholes. Comparison with the weathered surface would give important information on how the slate of a particular quarry is weathered. Such work is outside the scope of this research.

Chapter 3 The Metamorphic Grade of Slate

3.1 Introduction

The metamorphic grade was investigated as a possible control on the quality of a slate as a roofing material. ***The aim of this chapter is to assess different ways of evaluating the metamorphic grade in slates where temperature and pressure are low, and to relate the grade to the quality of the slate.***

The changes that occur during diagenetic and metamorphic processes are

- growth of new minerals and loss of clay minerals
- change in the chemical composition of phyllosilicates
- increasing crystallinity due to increasing regularity of the atomic structure of individual minerals.
- increase in grain size

The mineral composition of slate and the chemical composition of individual minerals have been discussed in Chapter 2. This section is concerned with the route taken in converting the protoliths of slate, fine-grained clays and silts, into the final product. X-ray diffraction can be used to detect the petrological changes which have taken place in developing a slate, but is particularly useful in assessing the increase in ***crystallinity*** due to increasing regularity of the crystalline structure and grain size.

3.2 Background -Metamorphism

Most slates are derived from clays and silts, which are fine-grained sediments deposited under water. Clay minerals have a grain size of < 0.0039mm (1/256") on the Udden-Wentworth scale while silt has a grain size of 0.0039 - 0.0625mm. (1/256" - 1/16"). When these deposits are subjected to increasing temperature and pressure during burial, they become compacted and minerals recrystallise to form a rock.

Diagenesis is the term used to describe the changes that take place as sediments are converted to a sedimentary rock, i.e. the clays and silts become a mudstone. As the conditions become further and further removed from those at the surface, minerals that were stable in a sedimentary environment begin to dissolve and new minerals begin to grow, i.e. the rock undergoes ***metamorphism.*** There is no agreed divide between diagenetic processes and metamorphic processes. The term ***anchimetamorphism*** was introduced by Kubler (1967) and followed by Dunoyer de Segonzac (1969) and Frey (1970) to cover all those processes which occur between late diagenesis and epigenesis, the earliest stage of metamorphism.

With increasing temperature and pressure the mudstone becomes a ***shale.*** Increasing alignment of the minerals and the shale becomes a ***slate*** and at slightly higher metamorphic grade a ***phyllite.*** If temperature and pressure increase even further, grain size becomes larger, slaty cleavage is lost and the rock becomes a ***schist.***

3.2.1 Types of Metamorphism

There are many processes involved in metamorphism but only those relevant to the genesis of slate are described.

3.2.1.1 Burial Metamorphism

Sediments experience greater temperature and pressure with depth of burial. Whilst the geothermal and geobarometric gradients may vary considerably, average values are taken as 25°C/km and 0.3kbar/km respectively. Under a thick pile of sediments accumulating in a basin therefore, the conditions can be sufficiently extreme for metamorphic processes to take place. This is called burial metamorphism.

3.2.1.2 Regional Metamorphism

It has long been recognised that regional metamorphic rocks occur in belts up to thousands of kilometres long, but only tens of kilometres wide. This type of

metamorphism is related to large scale compression which occurs at lithospheric plate boundaries or points of inter continental compression. In these conditions, rocks are subjected to directed stress, fold, deform and develop cleavage and schistosity. Slate is found in these belts where sediments, sufficiently fine grained, have experienced just the right temperature for characteristic slate minerals to grow and sufficient directed pressure for cleavage to develop.

3.2.1.3 Contact Metamorphism

When an igneous body is intruded into the upper crust, the surrounding country rock is baked, producing a ***hornfels.*** When the country rock is slate, this has the effect of destroying the cleavage in the aureole surrounding the intrusion, except in the outer fringes where the slate is hardened sufficiently to produce a good roofing material. Macduff roofing slates were produced from one such aureole. However, the same process which produced good quality slate also limited its extent (Appendix A 5.2.3).

3.2.2 Metamorphic Zones of the Scottish Highlands

The slate belts of Scotland occur in a classic area of metamorphic geology. They are the product of regional metamorphism and were formed during the Caledonian tectonic events. Barrow (1893,1912) made the first systematic studies of the variation in degree of metamorphism across the Scottish Highlands, setting up a zonal scheme which has been used world wide. Different minerals, e.g. chlorite, biotite, grew at different grades of metamorphism and were used to identify metamorphic zones. He recognised that slates were the least changed from the original sediments and called the area with slaty cleavage the "*zone of undigested clastic micas*". This zone was later renamed the ***chlorite zone*** by Tilley (1925) after the mineral that typifies this level of metamorphism. Slates are generally found in this chlorite zone (also referred to as the greenschist metamorphic zone due to the colour imparted to the rocks by the presence of green minerals such as chlorite).

Barrow's (1893,1912) work formed the foundation for subsequent studies of high grade metamorphism, wherein equilibrium constants of many different metamorphic

reactions are used to determine the geothermal and geobarometric conditions. However, slate is found at a grade where original minerals have not attained equilibrium conditions, so that other methods had to be devised to investigate regional metamorphism at these very low grades.

3.2.3 Diagenetic and Metamorphic Zones

Due to the small grain size of low grade metamorphic rocks and the non-equilibrium conditions, it is not possible to use isograds in the conventional manner. Measurement of metamorphic grade therefore exploits the increasing grain size and increasing crystallinity of individual minerals. A technique frequently used is ***illite crystallinity*** **(IC),** wherein the sharpness of X-ray diffraction peaks (expressed as an angle 2θ) is used to measure both of these properties (Illite crystallinity is discussed at greater length in Section 3.3). Kubler (1967) defined the boundaries of the anchimetamorphic zone ***(anchizone)*** in terms of the observed illite crystallinity and assigned a value of 0.43°2θ to the lower boundary and of 0.21°2θ to the upper boundary (Table 3.1).

Zone	Illite crystallinity (°2θ).
diagenetic zone	> 0.43
anchizone	0.43 - 0.21
epizone	< 0.21

Table 3.1 Limits of diagenetic and metamorphic zones defined by illite crystallinity

The metamorphic grade of Scottish slate spans the boundary between the anchizone and the epizone but most is found in the epizone (See Fig. 3.6).

3.2.3.1 Diagenetic Zone

During diagenesis, water is driven out of the sediments and clay minerals such as kaolin (Section 2.3.2) become unstable and are converted to chlorite and illite. These

changes are not isochemical, as extensive exchange of ions between the sediments and the pore fluids takes place.

With increasing depth of burial, clay minerals with irregular mixed layers give way to a mineral having regular layers called ***allevardite***. At greater depth this in turn is replaced by the simple ordered mineral ***illite***. Chlorite is also formed from irregular clay minerals by the adsorption of Mg^{2+} cations to produce a mineral with mixed layers of chlorite and smectite i.e. ***corrensite***, which on increasing depth of burial gives way to a mineral having regular layers i.e. ***chlorite*** (Dunoyer de Segonzac 1970), (Fig. 3.1). The mineral formed is controlled by the cation in the pore fluids e.g. if K^+ is adsorbed illite is formed and if Mg^{2+} then chlorite is formed.

Roberts and Merriman's (1985) observations, in their regional study of the slate of the Welsh basin, agree with the above conclusion. In what they called "Stage I" the < 2μ fraction has an illite crystallinity of >0.43 °2θ and the polytype is 1Md (Section 2.2.2.3) No cleavage fabric had developed at this stage.

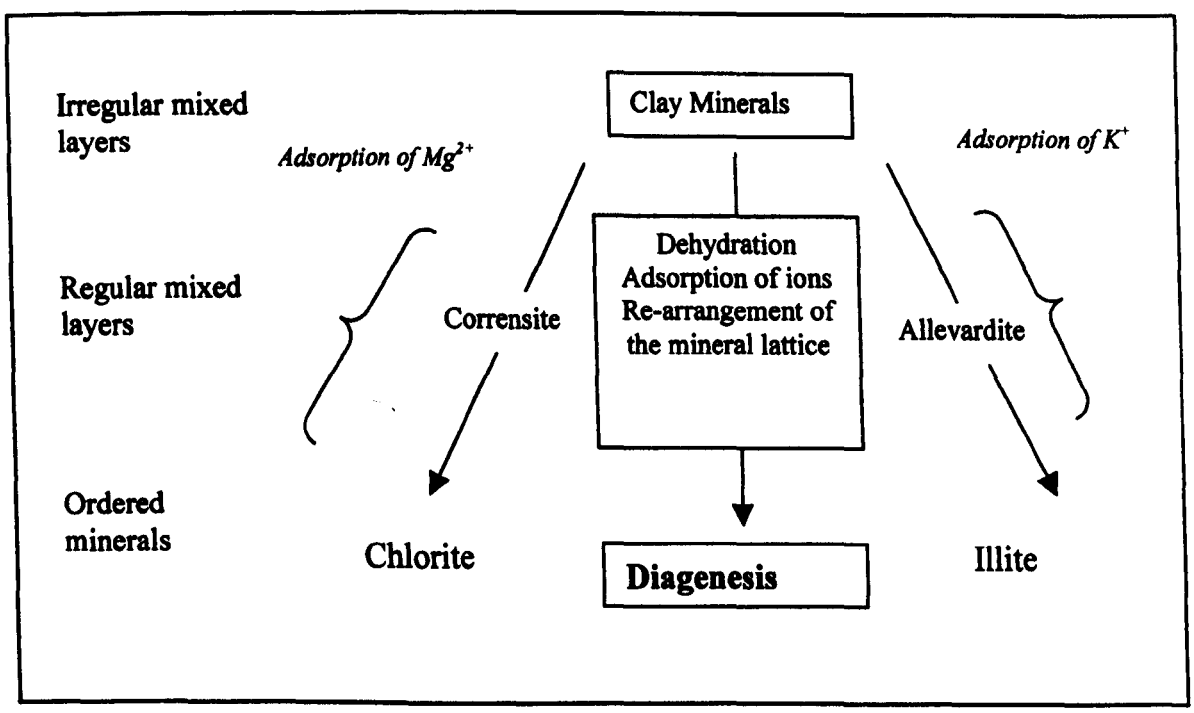

Fig. 3.1 The transformation of clay minerals during diagenesis after Dunoyer de Segonzac (1970)

3.2.3.2 Anchizone

As well as an improvement in illite crystallinity, several other changes have been reported in the anchizone.

a) **Change of illite polytype**

Frey (1970), in his regional study of the Alpine border region in Switzerland, listed a change in polytype as one of several events that take place in the anchizone. The normal trend in the polymorphic variation of illite is $1M_d$ ----> 1M ----> $2M_1$ with increasing temperature (Section 2.2.2.3).

- **The $1M_d$ polytype** This consists of disordered layers, formed as a result of weathering, and is typical of sedimentary clays.
- **The 1M polytype** This polytype is fairly rare although illites rich in Fe and Mg recrystallise preferentially as 1M.
- **The $2M_1$ polytype** This is the most stable form found in micas from metamorphic zones and detrital illites where erosion was sufficiently rapid to prevent weathering. The presence of this polytype was observed in Upper Ordovician periglacial sediment where the detrital illite had hardly weathered (Dunoyer de Segonzac, 1969).

Particle size and chemical composition can affect illite polytype. Small particles are more disordered during sedimentation and more sensitive to weathering. According to Kubler (1964), the crystallinity of illite is a valid marker for metamorphic grade only when crystallinity has become independent of lithology, and its concomitant inherited crystallinity. However from the point of view of the quality of slate the degree of crystallinity is important whatever its origin.

b) **Change in illite composition** The chemical composition of illite approaches phengite with increasing grade (Fig. 3.2) as well as with an increase in the Mg/Fe ratio.

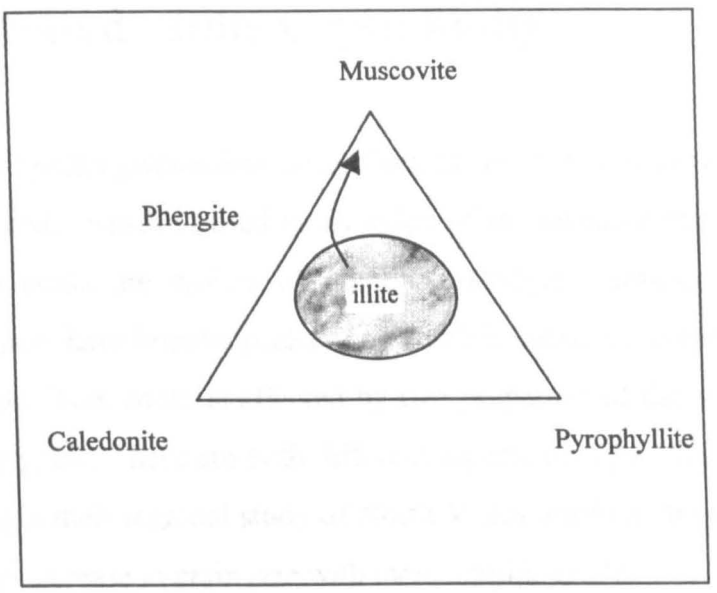

Fig. 3.2 Chemical changes in white mica composition during metamorphism.

c) **Growth of new minerals**

Kisch (1990) in his integrated picture of the changes that occur from diagenesis to what he calls incipient metamorphism i.e. anchimetamorphism also mentions the appearance of paragonite, a sodium muscovite and pyrophyllite as typical of the anchizone. Roberts and Merriman (1985) describe a regular intrastratified sodium and potassium mica in their Stage II and report the appearance of discrete paragonite and K mica in the next zone.

3.2.3.3 Epizone

This is the lowest level of traditional metamorphism, also called the greenschist facies or chlorite zone in the Barrovian scheme. The mineral assemblage typical of this zone is chlorite and phengitic muscovite with variable amounts of quartz, albite, and accessory pyrite. The white mica is characterised by a $2M_1$ polytype with discrete paragonite, not a mixed-layer paragonite/muscovite. TiO_2 is reported as anatase and rutile (Section 2.2.3.3) in the Cambrian and Ordovician slate by Merriman and Roberts (1985) in their excellent description of the slate formations of Wales.

3.3 Background - Illite Crystallinity

The shape of XRD peaks gives information about the regularity of the atomic structure of individual minerals, which is used as an index of the metamorphic grade (Section 2.4.1.3.2). Sharp peaks are typical of highly crystalline substances while poorly crystalline substances have broader peaks. The width is measured at half the maximum height of the peak. This width is affected by two properties of the slate, crystal size and metamorphic grade. These are both different aspects of crystallinity. Roberts and Merriman (1985) in their regional study of North Wales attribute the decrease in illite crystallinity to the increase in grain size with metamorphic grade.

3.3.1 Crystal Size

In large crystals there is efficient destructive interference for all values of 2θ intermediate between the angles producing the peaks. In smaller crystals not every beam diffracted from every incremental plane of atoms has a corresponding beam with equal but opposite phase to cancel it. This incomplete destructive interference has the effect of broadening the peak. The extra peak width above that dictated by the limitations of the X-ray equipment is used in the Scherrer equation to estimate the crystal size t (Moore & Reynolds 1989) as follows:

The Scherrer equation

$$t = 0.9\lambda / B\cos\theta$$ where

λ = wavelength

θ = Bragg angle

$B = B_m^2 - B_s^2$

B_m = measured width

B_s = width of the unbroadened peak, characteristic of the operating conditions.

Before being able to measure grain size it is necessary to determine the width of the unbroadened peak B_s

3.3.2 Illite Crystallinity (IC)

X-ray analysis has long been used to measure systematic trends of increasing grade of metamorphism. Numerous studies have shown that the shape and width of the. mica/illite basal peak at 10 Å changes with depth of burial and grade of metamorphism. Because results are dependent on operating conditions it is difficult to correlate between different workers. Several attempts have been made to devise methods which are independent of operating conditions.

Weaver (1960), in his study of the relative degree of diagenesis and metamorphism of shales and slates from the Ouachita Mountains, defined the Weaver Index as the ratio of the intensity of the peak at 10.5 Å to the intensity at 10 Å, but small differences in the position of the peak affect the result. This was superseded by Kubler (1964), who used the peak width in millimetres at half height as a measure of the degree of crystallinity. Although quick and easy to measure, this method is dependent on operating conditions such as scan rate, chart speed etc. To overcome this problem measurements are now in °2θ which should be more independent of operating conditions. This is called the Kubler Index K.I. or the Full Width at Half Magnitude **FWHM.** Weber (1972) suggested using quartz as an internal standard and defined the relative half height Hh_{rel} as:

$$Hh_{rel} = Hh_{illite}(mm)/Hh_{quartz}(mm) \times 100$$

This he felt would allow comparison of reflection measurements from different X-ray equipment. Kisch (1990) in his critical comparison of illite crystallinity does not adopt the quartz standard as it varies unsystematically with scanning rates and the same sample can have different Hh_{rel} at different instrument settings.

Variation in Illite Crystallinity Values

In the literature, the effects of different operating conditions are evaluated in terms of defining the limits of the anchizone (anchimetamorphic zone of Kubler 1964). Weaver (1960), in his study "Shale-Slate Metamorphism in the Southern Appalachians", found that the rate of change of IC increases significantly at the diagenesis/anchizone and the anchizone/epizone boundaries. This he interpreted as an increase in the rate of crystallisation.

Kubler (1967), taking a statistical approach to IC i.e. 5 samples/outcrop, defined the limits of the anchimetamorphic zone as 0.42 and 0.25 °2θ. Robinson, Warr and Bevins (1990) addressed the problem of inter laboratory comparisons of IC values and attempted to define common limits of the anchizone in terms of IC. They are critical of the "isocryst" approach of Roberts and Merriman (1985), who contoured the North Wales region from 0.17 to 0.70 °2θ using steps of 0.03. However they agree with the major sub divisions of the anchizone into lower and upper divisions.

XRD Operating Conditions

Kisch (1990) looked at the effect of different operating conditions:

1. While the **goniometer scanning** and the **chart speed** can be standardised by evaluating the IC in °2θ the **scanning rate** does affect the peak width. Kisch (1990) found that a fast scanning rate of 2 °2θ/min broadens the peaks by 0.04 - 0.05 °2θ as compared to a slow rate of 0.5 °2θ/min.
2. Kisch also found that an increase in the time constant affected the IC value e.g. by increasing the time constant from 2 to 4 seconds the IC value is reduced by 0.05 °2θ
3. According to Kisch (1990), the effect of a wider **divergence** and **scatter slit** is negligible.
4. The effect of type of radiation was not studied by Kisch (1990). In the literature, most work discussed has been carried out using copper radiation. The effect of the swing to cobalt as a source of X-rays has not been looked at. Comparison of XRD profiles involves conversion of copper peaks to cobalt or *vice versa.*

Sample Preparation

Weber (1972) studied the effects of different sample preparation techniques. Using as a reference value polished rock slabs orientated parallel to cleavage he found the following:

a Thickness of film

Samples were reduced to 1mm and then treated with H_2O_2 for several hours during which time the organic matter was oxidised and the rock disintegrated. A thin film compared well up to $130Hh_{rel}$ or 4.2 Hh, while a thick film had higher IC values but more scatter in the results.

b Grain Size

Sample was separated into fractions with a grain size of (i) <2 μ, (ii) 2-6 μ and (iii) 6-20 μ. using a sedimentation method similar to that described in Section 3.4.1.1. The smaller grain size has a higher IC and is assumed to have a higher ratio of illite to smectite. During rock disintegration a grain size fractionation occurred. However the crystallinity of the various illite fractions becomes equal when $Hh_{rel} \sim 130$.

Chemical Composition

In a sodium-rich samples, Kisch (1990) reports apparent broadening of the 10Å peak due to the coexistence of brammallite and illite (Section 2.3.2) because of superposition of adjacent basal reflections. Other chemical variations may well cause similar problems.

3.3.3 Conclusion

Measurement of Illite Crystallinity in terms of FWHM in units of $^{o}2\theta$ rather than in millimetres eliminates the effect of different plotting technique. Measurements were made using the "Traces" software package (Section 2.4.1.4). The accuracy of these measurements was checked manually and they were found to be accurate.

Operating conditions can affect the results, but for a comparative evaluation of the crystallinity grades of different slates, standardisation of operating techniques eliminates these effects. Similarly a standard routine for preparing samples reduces the effect of different sample thicknesses etc. The effectiveness of this can be assessed by determining the repeatability of results (Table 3.3).

Grain size affects the IC values. In order to determine the metamorphic grade it is necessary to reduce this effect by comparing equivalent grain-size fractions. However, it is the average crystallinity that determines the properties of a slate and grain size is an important element of this crystallinity. Hence for the purposes of this Report it is the average crystallinity value for all grain size fractions which is more appropriate and not the crystallinity of a particular fraction.

The most significant limitation of the IC method of determining crystallinity is the loss of sensitivity within the epizone i.e. when IC is less than 0.21 $^{o}2\theta$. Most commercial roofing slate lies within the epizone. Roberts and Merriman (1985), when mapping North Wales in terms of the metamorphic grade (Section 3.3.2), ascribe the loss in the metamorphic gradient in the epizone to the insensitivity of the IC method and state that an increase in crystal size below IC = 0.16 $^{o}2\theta$ is not accompanied by a reduction in the width of the white mica peak at this grade. This important limitation of the IC method is discussed further in Section 3.4.

3.4 Slate Crystallinity

The crystallinity of a slate is defined as the degree to which individual minerals have developed a regular crystalline structure.

Crystallinity is derived from:

1 The original deposits, which may have retained considerable crystallinity, especially if the original detrital material was relatively unweathered.

2 The increase in crystallinity during subsequent diagenetic and metamorphic processes as minerals became more regular in their crystal structure and any amorphous material is incorporated into new minerals.

3 The increase in grain size associated with these diagenetic and metamorphic changes also contributes to the overall crystallinity.

However, as far as the properties of slate are concerned, it is the actual value of crystallinity that is significant and whether this is inherited from the detrital source or acquired during subsequent metamorphism is not important.

Because XRD detects only the presence of crystalline material it is ideally suited for comparing the relative crystallinity of different slates. Individual XRD peaks become sharper and stronger as the crystal structure of individual minerals approaches the ideal described in Section 2.2. The usual method for determining the sharpness of peaks is IC. In this Report the more general term FWHM (Full Width at Half Magnitude) is preferred (Section 3.3). However, this technique was found to be insensitive at the metamorphic grade observed in slate with 90% of the values clustered between 0.1° and 0.2° 2θ (Fig. 3.4, Section 3.4.1). Other methods investigated, such as the ratio of the trace height to the area, were found to be equally insensitive. Yet it was apparent from the overall shape of the XRD traces (Fig. 3.3) that there was considerable variation in the degree of crystallinity in slate from one area to another, so that it was necessary to devise some method to compare these differences in a quantitative way.

3.4.1 Crystallinity and FWHM

Because of the effect of grain size on the FWHM values, measurements are usually carried out on the $< 2\mu$ or $< 6\mu$ fractions. In order to compare results with those reported in the literature, it was decided to check the effect grain size has on the observed crystallinity.

3.4.1.1 Methodology

Samples were separated into fractions of different grain size by sedimentation. The settling time was assumed to follow Stokes Law for spherical particles where $v \propto r^2$

$$\textbf{Stokes Law} \quad v = \frac{2r^2 g \Delta\rho}{9\eta}$$

v =	velocity
r =	diameter of particle
g =	gravity
$\Delta\rho$ =	density difference
η =	dynamic viscosity

Samples tested: W/F-1, W/F-16, EL-4 and LC-2

Method:

- Samples were ground manually using a pestle and mortar and passed through a 140μ sieve, sieving frequently to prevent over grinding.
- The powder was then disaggregated in an ultrasonic bath for 15 minutes before transferring to measuring cylinders.
- The measuring cylinders were filled with water and the slurries shaken before being allowed to settle for the appropriate length of time (Table 3.2).
- After sedimentation had taken place, the top 10 cms of each liquid was siphoned off and centrifuged at 4500rpm for 30 minutes.
- The supernatant liquids were then decanted and the residues transferred onto ceramic slides and allowed to dry overnight.
- The slides were stored in a desiccator until analysed by XRD.

For the larger grain sizes the remaining liquids in the measuring cylinders were filled to the top and shaken and the rest of the procedure was followed after allowing sedimentation for the appropriate length of settling time for each fraction as per table.

Grain size	<2μ	<6μ	<10μ
Settling time	7hrs 38min	51 minutes	18.3minutes

Table 3.2 Settling times for different grain-size fractions.

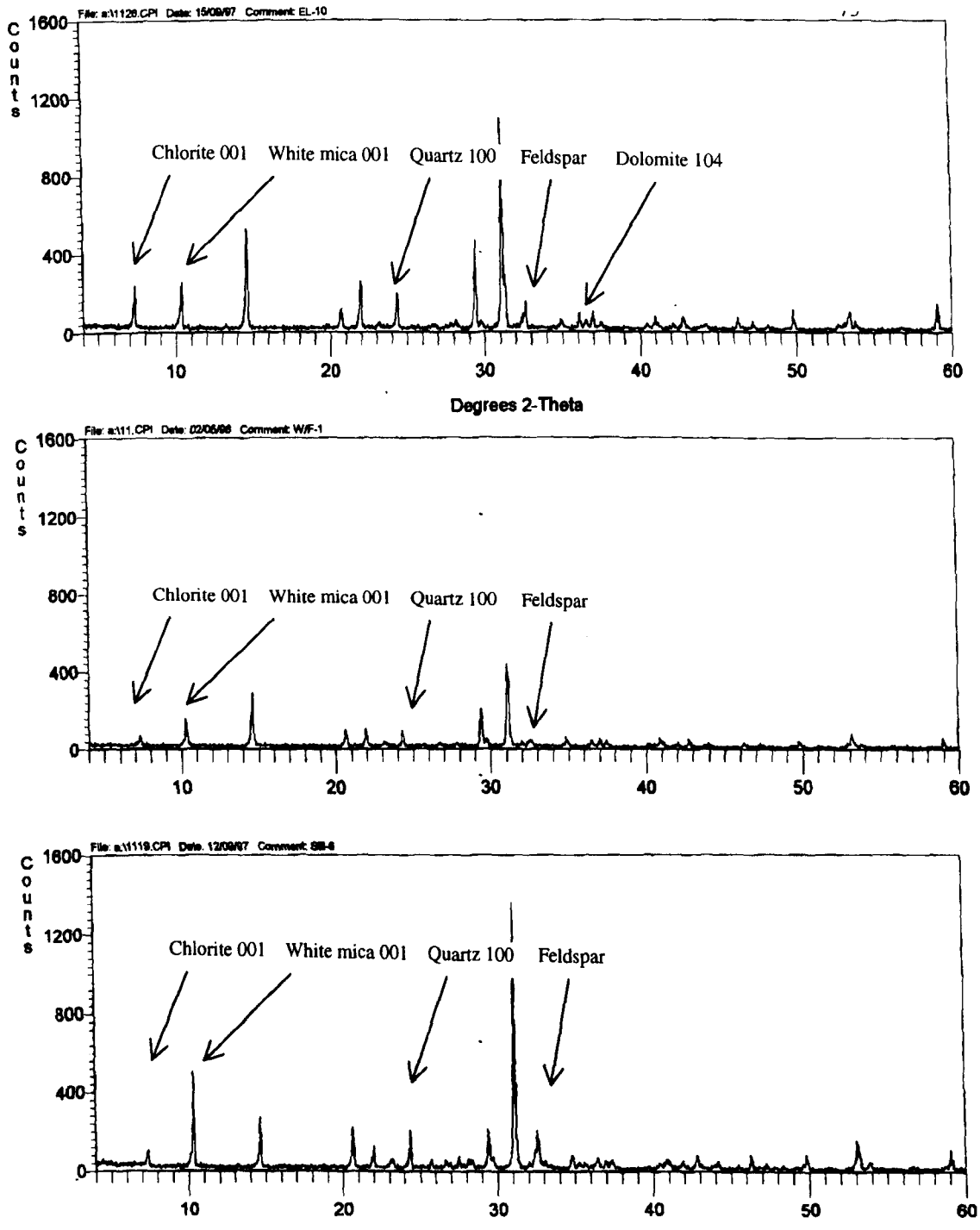

Fig. 3.3 XRD scans for a sample of a) Ballachulish slate EL-10 b) Ffestiniog W/F-1 and c) Seil slate SB-6.

3.4.1.2 Evaluation of Results

The precision of FWHM results was assessed as follows:
The crystallinity of the white mica of samples of Ffestiniog and Cwt y Bugail slate was determined several times at two different scanning rates. The means and variation were calculated and used to determine the precision of FWHM measurements at different scan rates (Table 3.3). The mean values show a slight decrease in FWHM at the higher scan rates, which disagrees with the trend reported by Kisch (1991) (See also Section 3.3.2). This probably reflects the inherent imprecision of the technique. It does show that there is no significant loss of precision at higher scan rates and all subsequent quantitative work was carried out at 1° 2θ/min. The effect of varying the time constant was not assessed.

Sample	<2μ		<6μ		<10μ	
W/F-1	0.314	0.294	0.244	0.238	0.158	0.160
W/F-16	0.228	0.218	0.160	0.172	0.204	0.188
EL-4	0.176	0.174	0.152	0.182	0.218	0.212
LC-2	0.238	0.228	0.162	0.160	0.146	0.154

Quarry	Number of samples	Scan rate 2θ/min	Mean	Standard Deviation	Coefficient of variation
Ffestiniog	10	2	0.149	0.014	0.100
		0.5	0.155	0.023	0.148
Cwt y Bugail	5	2	0.157	0.019	0.122
		0.5	0.164	0.023	0.140

Table 3.3 a) Effect of grain size on FWHM measurements at 0.5° 2θ/min.b) Effect of scan rates on FWHM results and their precision.

The FWHMs were determined for Scottish samples at 1° 2θ/min from 4° to 30°. The procedure was extrapolated to incorporate the principal peaks of the major minerals

and results are given in Appendix 3.2 and summarised in Fig. 3.4 and Table 3.4. The Ballachulish and Easdale samples have lower values than the Highland Border and Macduff slates.

FWHM white micas	Mean	Standard deviation	Coefficient of variation
Ballachulish	0.137	0.022	0.16
Luing	0.143	0.027	0.19
Seil & Belnahua	0.117	0.013	0.11
Bute	0.182	0.068	0.38
Aberfoyle	0.164	0.015	0.09
Dunkeld	0.162	0.014	0.09
Macduff	0.191	0.028	0.14

Table 3.4 Average FWHM values of Scottish slate

3.4.1.3 Discussion

The are several reasons why the FWHM method of measuring metamorphic grade and grain size was considered unsatisfactory:

1. The average FWHM (Table 3.4) values for the various Scottish quarries (apart from a few weathered samples with predictably high values) were clustered between 0.25 and 0.10. However, this range of values is no greater than those for Bute slates considered in isolation i.e. 0.182± 0.07 at 95% confidence. Bute samples do have a significantly greater variation than those from other areas but nevertheless this clustering does limit the usefulness of the FWHM method as discussed in Section 3.3.3.
2. The presence of paragonite in many Scottish slates has the effect of broadening the white mica peaks and hence give an erroneously high FWHM and concomitant low crystallinity.
3. Attempts to use FWHM to determine the grain size using the Scherrer equation as described in Section 3.3.1 were unsuccessful due to the width of the peak approaching the limitation of the X-ray equipment.
4. The procedure is very time consuming and would have been difficult to apply to a large data set.

Although the FWHM values of Ffestiniog and Ballachulish slate are approximately the same, it was noted that there is a large difference in the intensities of the individual XRD peaks (Fig. 3.3) i.e. the intensities of the former are approximately half those of the latter. For a given area, the intensity of a peak correlates inversely with the FWHM. Given the restraints imposed by No 4 above, it was decided to use the intensity of peaks instead of FWHM as a rough method of highlighting differences in the crystallinity of slates.

3.4.2 Crystallinity based on Intensities of XRD Peaks

As already discussed, the FWHM method is too insensitive to measure the crystallinity of slate. For example, Ffestiniog slates have a mean FWHM value of 0.15 $2\theta \pm 0.03$ which approximates to that of Ballachulish slates (0.14 $2\theta \pm 0.04$), yet when their respective XRD profiles are compared, the former have peak heights of < 450 counts while the latter reach a height of >1100 counts (Fig. 3.3). This again indicates that the classical method of determining crystallinity was not suitable in discriminating between different quality slates. Therefore it was necessary to identify the key differences in the XRD scans and devise some method to quantify these observations. Variation in intensities of peaks was seen as the most significant factor and the following discussion describes the approach taken in quantifying these differences to reflect the overall crystallinity of a slate.

3.4.2.1 Methodology

To assess the crystallinity of a slate in terms of the intensity of XRD peaks, it is essential to determine those factors other than the crystallinity, which also contribute to that intensity.

The intensity of XRD peaks is dependent on the following:

- The amount of the mineral present
- Orientation of minerals
- Attenuation coefficient of the mineral
- Machine conditions

The ideal method should be as independent of the apparatus used, and the mineral composition of the slate, as possible.

Mineral Composition: As well as being a measure of the crystallinity, the intensity of a peak is also influenced by the amount of the mineral present. Therefore to make the crystallinity measurement independent of the proportions of individual minerals, it is necessary to determine the total contribution made by all the crystalline minerals. Peak intensity measurements were accordingly taken for all the crystalline minerals present, i.e the three major minerals chlorite, white mica and quartz, and the minor minerals feldspar, carbonate minerals and iron ore minerals, and the results summed.

Orientation of minerals: Only those minerals aligned to satisfy the Bragg angle (Section 2.4.1.2) contribute to the diffracted X-ray peak, therefore the degree of alignment of the different minerals in a sample would impact on the crystallinity value. The slurry method of sample preparation for XRD scans gives a random orientation of minerals (Section 2.4.1) which reduces the effect of varying degrees of orientation. This can be seen in Table 4.1 where the sum of the intensities of the three peaks in the randomly orientated sample approximately equals that of the two orientated samples. (To minimise the imprecision of XRD results the total of the three peaks was used for comparison, rather than a direct comparison between individual peaks).

Chemical Composition: To minimise the effect of chemical composition, the intensity of each peak was adjusted by a correction factor based on the attenuation coefficient of each mineral as described in Section 2.5.5.

Machine Conditions

A correction was also made to intensity values of peaks at low angles of diffraction, to allow for the spread of the X-ray beam in relation to the dimensions of the sample. This is described more fully in Section 2.5.5.

Other variations were minimised by using the same machine settings throughout and by standardising sample preparation.

Samples: Unweathered and weathered samples were collected from producing quarries in North Wales and Cumbria. Samples were taken from different *veins* within a quarry and in the case of Ffestiniog they were also collected from areas of between *veins*. As there are no working quarries, Scottish samples were collected from many different sources such as tips and outcrops in the quarries and second-hand slate merchants as specified in Appendix 1.1.

Using the same XRD scans as described in Section 2.4.1, the data set was processed as follows:

In order to minimize the effect of the chemical composition on the intensity of different peaks, the attenuation factor of each mineral were determined and the intensity was corrected to equal that of quartz. (This was an arbitary decision to keep the range of crystallinity values to less than 2000)

Intensity $_{(mineral)}$ =	Intensity of mineral in total counts
$\mu_{mineral}$	Attenuation factor of mineral
k	Size correction

$$\textbf{Corrected intensity} = \frac{I_{mineral} \times \mu_{mineral} \times k}{\mu_{quartz}}$$

Crystallinity equals the sum of the corrected intensities of the main peaks shown in Table 3.5.

$$\textbf{Crystallinity} = \Sigma I_{Mineral}$$

Mineral		Angle 2θ	D-spacingÅ	[hkl]	μ
Quartz		24.26	4.26	100	56.2
White mica		10	9.8	001	64.8
Chlorite		7.2-7.3	14.2	001	45.1
Feldspar	Plag	32.70-32.50	3.18-3.20	.	52.9
	K Feldspar	31.38	3.31		
Haematite		38.88	2.69	104	44.5
Carbonate	Calcite	34.31	3.04	104	112
	Dolomite	36.1	2.89	104	74
	Magnesite	38.1	2.74	104	29
	Siderite	37.35	2.80	104	35

Table 3.5. Details of the XRD peaks used in determining the crystallinity of slate; Attenuation coefficients μ of the different minerals.

Note. The identification of siderite is difficult due to low peak intensities and, although shown in Table 3.5, identification was sometimes equivocal. In such cases the peak heights for siderite were not included in the value of the total crystallinity.

Results of the crystallinity are given in Appendix 3.1 and plotted against FWHM in Fig. 3.4.

3.4.2.2 Evaluation of Results

The crystallinity values of the different slates is given in Appendix 3.1 and summarised in Fig. 3.5. The crystallinity values calculated are on an empirical scale ranging from 200 to 1800. However it should be emphasised that even the lowest values have a well developed crystalline structure as compared with sedimentary mudstones and shales.

To check the validity of the technique it is important to see that the values obtained by this method are indeed typical of an area. With this in mind several fresh samples, collected from a single quarry, were scanned and found to give approximately the same value indicating that crystallinity is indeed characteristic of

an area. For example, five Cwt y Bugail (Appendix 1.1) samples are in the range of 392 ± 92 (95% confidence level).

Results were then compared with other non-slates such as a Caithness flagstone, a schist and a hornfels (Fig.3.5). The Caithness flags were found to have a ***low*** crystallinity while the schist and hornfels samples were found to have a ***medium*** degree of crystallinity. Although Caithness flags were found to have ***low*** value, this was relative to slates and they were actually very crystalline for a sedimentary rock, due to their detrital source rich in quartz. The fact that the schist and hornfels do not have values higher than the most crystalline slates shows that the technique is not independent of petrology and orientation. But the technique is only intended for use to compare within one rock type, slate, which has considerable similarity in both these properties whatever the source.

When the relationship between FWHM and crystallinity was assessed (Fig. 3.4) a loose correlation was found between the FWHM values of the white micas and overall crystallinity ($R^2 = 0.37$). However little or no relationship was found between the FWHM values of the chlorite and quartz. This suggests that the extrapolation of the FWHM technique to include other minerals was of no value.

Although results show a lot of scatter, there is some correlation between FWHM and crystallinity (Fig. 3.4). The Ballachulish and Easdale slates have the highest crystallinity as measured by both techniques, while the Macduff and some of the Highland Border slates have the lowest.

Other slates vary as follows (Fig. 3.5):

- The Welsh slate has ***low*** crystallinity.
- Due to the high contribution from its calcite content (Appendix 3.1), the crystallinity of Cumbrian slate is ***medium*** to ***high***
- Ballachulish and Easdale slates have ***high*** to ***very high*** crystallinity, in spite of the fact that all Scottish samples have experienced over 60 years of weathering and often substantially more.

- As is to be expected from such a diverse area, the Highland Border slate has a wide range of values.
- Macduff slates are fairly homogeneous reflecting its mineralogy and have crystallinity ***medium***.grade

- The French samples show a correlation between crystallinity and the grade of slate as judged by the quality control in the quarries (Appendix 1.1). The Grade B slates are deemed inferior due to the presence of amorphous pyrite visible to the unaided eye. All three quarries have ***medium*** crystallinity at 600 - 700 for Grade A and a value approximately 200 less for their Grade B counterparts e.g. Noyant Grade A has a crystallinity value of 593 and Grade B a value of 353 (Appendix 3.1)

The effect of weathering on the crystallinity of slate is investigated further in Chapter 5. From anecdotal evidence it appears that weathered slates have values lower than that for the source area e.g. the lowest value in the Ballachulish group is for a slate over 100 years old as estimated by Mr. Cummings, second-hand slate dealer (per. com.). Because the rate of weathering is variable depending on the history of the slate there is an increase in the standard deviation for Scottish slate. This suggests that instead of average values being used for comparing the crystallinity of Scottish slate with current producing areas, some positive adjustment should be made to the results. One simple technique would be to use the maximum value as typical of the original material.

Highland Border slate shows considerable variation. The ***low*** crystallinity value for several of the Aberfoyle slate correlates with its reputation of softening within 20-50 years. However, Luss slate has a similar reputation yet the two samples collected have high crystallinity value. Craiglea also has a good reputation and it too has a ***high*** crystallinity value.

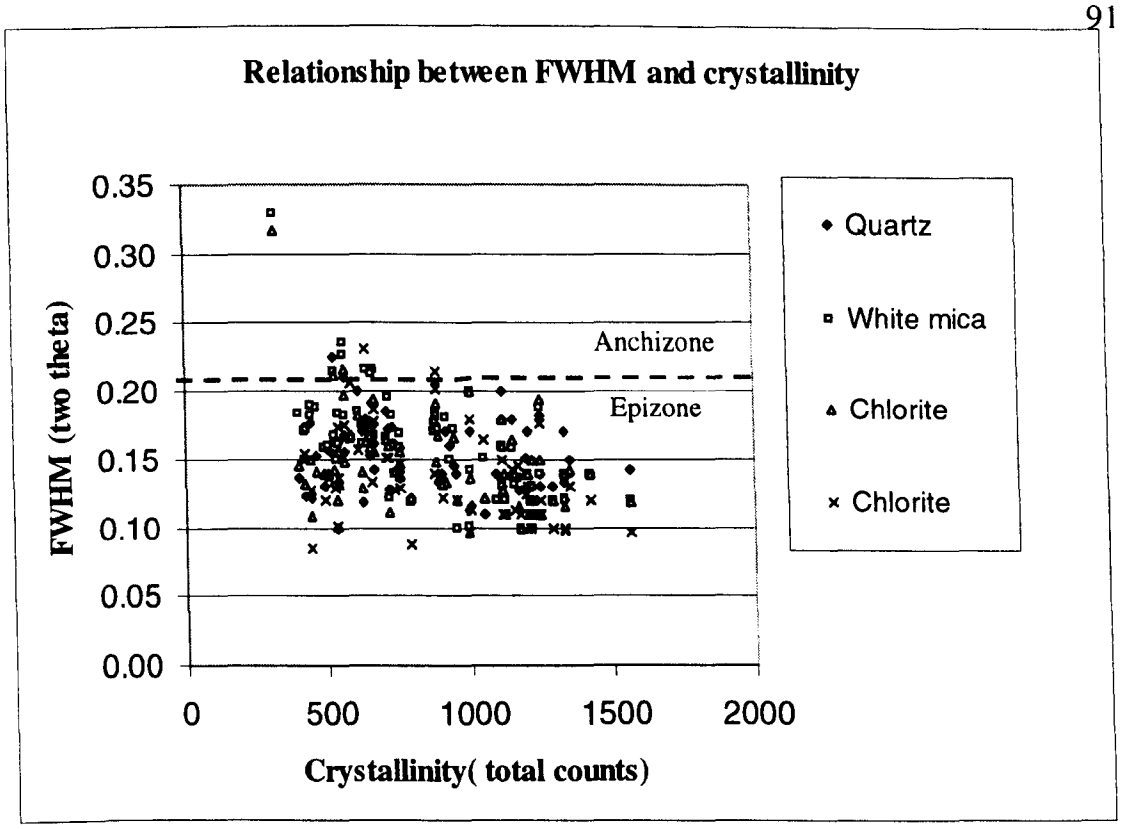

Fig. 3.4 Relationship between FWHM and crystallinity based on intensities of XRD peaks

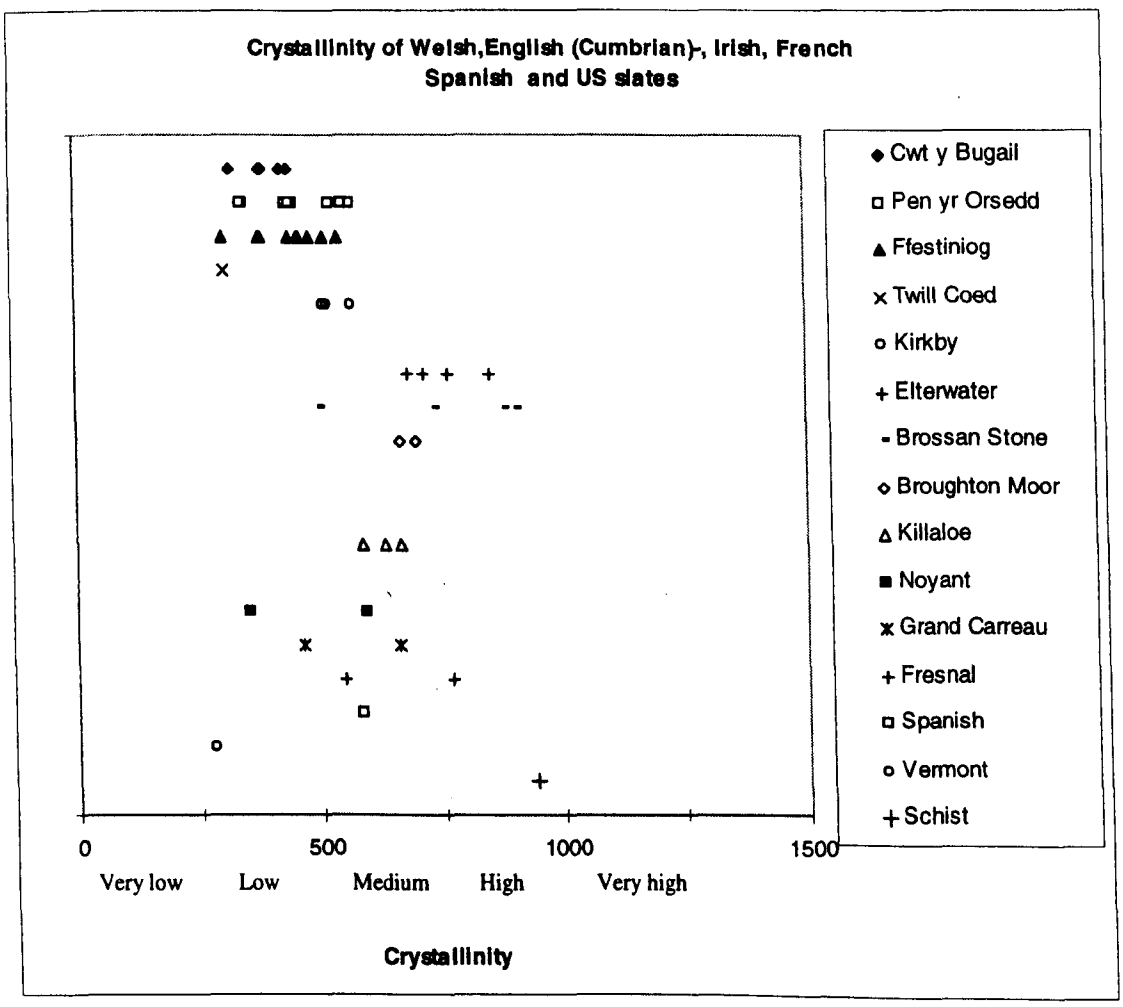

Fig. 3.5 Crystallinity of a selection of non-Scottish slates

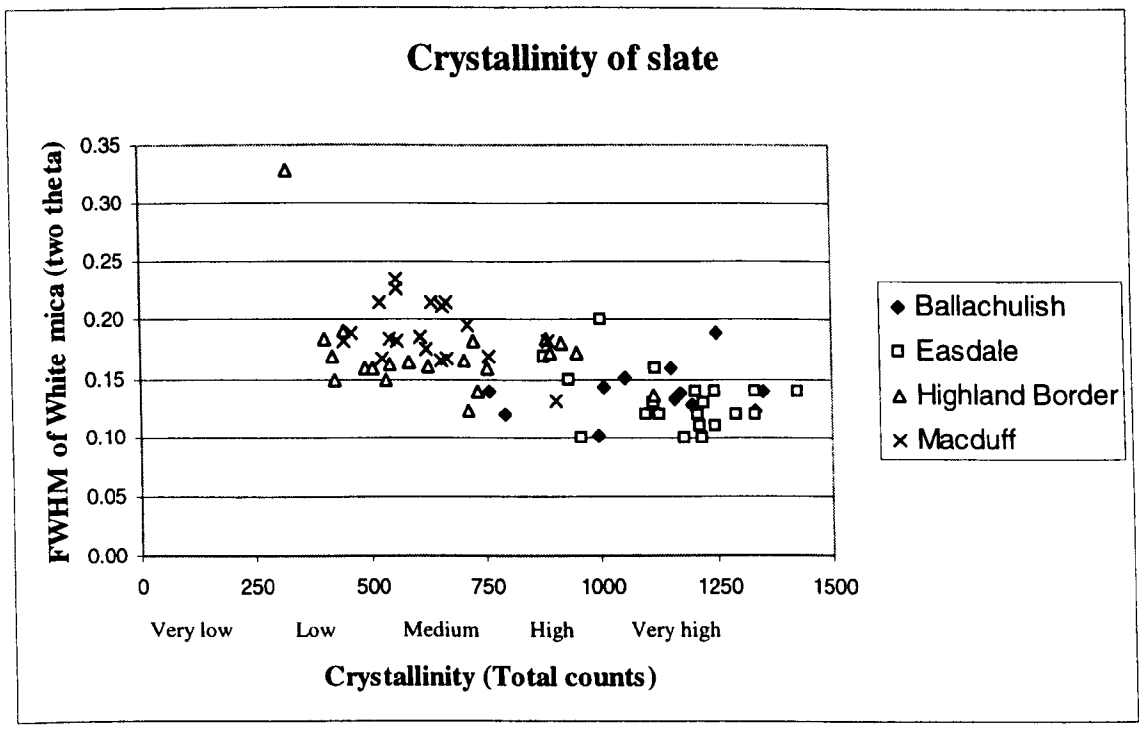

Fig. 3.6 Crystallinity of Scottish slates.

3.4.3 Conclusion

Because of the large number of quarries which needed to be included in this Report, the data sets for some quarries are smaller than desirable. Thus, given the spread of values due to variable weathering the average crystallinity values shown for some quarries may not reflect the true average. Yet with that proviso the following conclusions can be made:

- Crystallinity of slate as measured by FWHM and intensities of peaks is related but the range of values observed in the latter is greater and enables different slates to be more easily graded.

- A crystallinity value is characteristic of an area.

- Crystallinity of a slate does not always correlate with their reputations. For example Pen yr Orsedd slates have similar crystallinity values to that of the

Spanish slate, yet the former have a much greater life expectancy than the later. The longevity of the Pen yr Orsedd slates is due to their high quartz but this is not reflected in the quartz contribution to the overall crystallinity of the slate. However slates containing substantial amounts of calcite such as Cumbrian and Killaloe have medium crystallinity values due to the contribution made by this crystalline mineral which does agree with their reputations. In order to relate crystallinity to longevity of a slate it is necessary to examine the contribution made by the different minerals. This will be discussed further in Chapter 5.

- Determination of the crystallinity as a function of the intensities of the XRD peaks has value in determining the durability of slate. Ballachulish and Easdale slates have high to very high crystallinity in keeping with their reputation for longevity. Highland Border slate is variable, but one example, Aberfoyle, has low crystallinity and a reputation of softening after 20 to 30 years. Macduff slates have low crystallinity values but are very durable, showing that other factors are involved besides the crystallinity. This will be discussed further in Chapter 6.

Chapter 4 The Fabric of Slate

4.1 Introduction

Slate belts are found in mountainous areas where tectonic forces have deformed and shortened the earth's crust. Rocks respond to these compressive forces by folding. At the same time minerals grow normal to the maximum stress and in so doing the rocks develop a cleavage. At a microscopic level, it can be seen that cleavage is due to closely spaced sub-parallel dark seams of phyllosilicates, carbonaceous material and insoluble residues along which the rock can be split (Fig. 4.1). This is the property of a fine-grained rock that allows it to be split into thin sheets suitable as a roofing material.

Evaluating the fabric of a slate in terms of its cleavage properties is an important aspect in determining its suitability for exploitation as a roofing material. The aim of this part of the research is to devise a technique to carry out this evaluation.

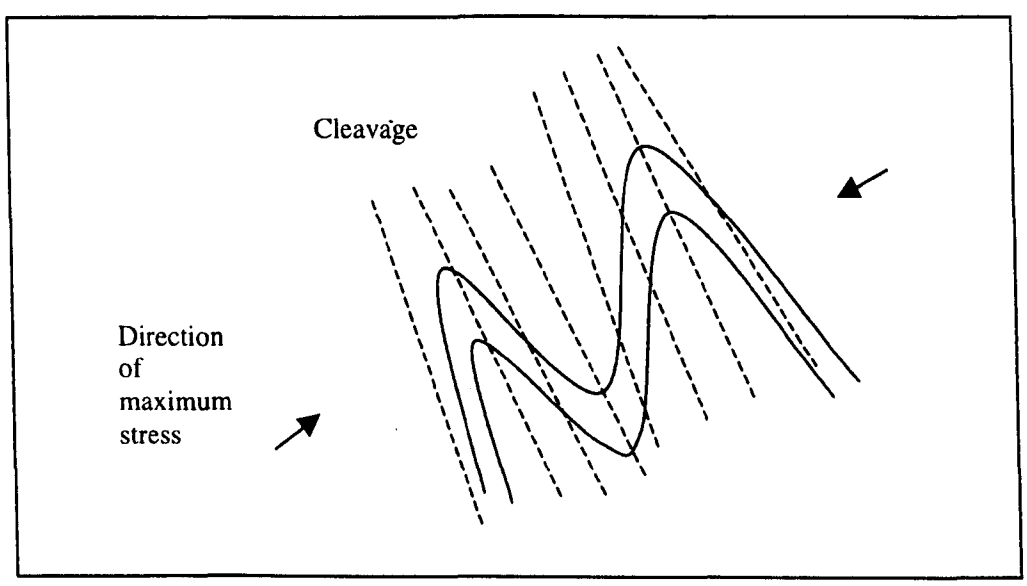

Fig. 4.1 Cleavage develops parallel to the axial plane of the fold and normal to the direction of maximum stress.

4.2 Background

As there is still controversy about the way cleavage develops, a generic categorisation is not possible. In his definitive classification Powell (1979) used a descriptive method based on the morphology and this approach has been used throughout this report.

4.2.1 Classification

A cleaved rock is divided into two domains; cleavage domains consisting of strongly aligned minerals (Fig. 4.2) which are separated by microlithons where the minerals may or may not be aligned. Most rocks exhibit this domainal property of cleavage; even the type called continuous cleavage is so called only because the spacing between the cleavage domains is so small that it is not resolvable by the optical microscope.

Factors used in classification (after Powell 1979)

- Shape of cleavage domains:
- Spacing between cleavage domains
- Proportion of rock occupied by cleavage domain.
- Fabric of the microlithon

Fig. 4.2. Photomicrograph of microfabric in slaty cleavage in an Aberfoyle slate. Mica rich cleavage domains anastomose around large quartz and chlorite grains in the microlithons.

1. ***Shapes*** of cleavage domains (CDs) are divided into four groups; stylolitic, anastomosing, rough and smooth depending on their smoothness and regularity (Fig.4.3). The most irregular shape is *stylolitic* where the CDs are long and continuous but very jagged. In *anastomosing* fabric the CDs are long, continuous and undulating, forming a network of irregular lenticular microlithons. *Rough* cleavage is found in rocks containing abundant sand-size mineral grains; here the CDs are short and discontinuous. *Smooth* cleavage fabric is at the most planar end of the spectrum and consists of smooth and continuous cleavage domains.

Shape and spacing of cleavage domains	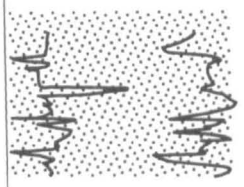	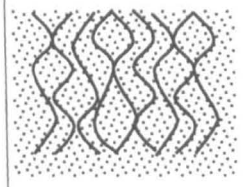	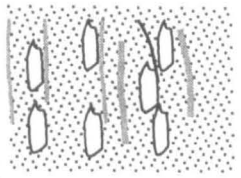	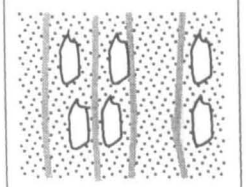
Cleavage domain ———			Microlithon 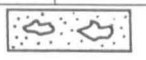	
Spacing	1-5cm	0.5 – 1 cm	< mm	10-100μm
Style	Styolitic	Anastomosing	Rough	Smooth

Fig. 4.3 Different shapes of cleavage domains

2. ***Spacing*** is a measure of the distance between cleavage planes. This is easy to determine when the planes are planar and parallel but in anastomosing cleavage where the enclosed microlithons are discoid or trapezoidal, a judgement must be made whether to take a maximum, minimum or an average value. In spite of this problem spacing is a useful parameter. The spacing of the slaty cleavage found in roofing slate in this Study is generally 10 to 50μm. Although the spacing decreases with increasing metamorphism it is also dependent on the grain size of the protolith and hence cannot be used unconditionally as a measure of the metamorphic grade.

3. ***Proportion*** The proportion of the rock occupied by a cleavage domain generally increases with increasing metamorphism as more of the minerals in the microlithons dissolve and re-precipitate as aligned minerals and become part of the cleavage domains.

4. ***Fabric*** Greater alignment of the minerals in the microlithon develops with increasing metamorphic grade

These four parameters control the thickness and texture of the slate.

4.2.2 Formation of Cleavage

Weber (1981), in his study of slates in the Rheinisches Schiefergebirge and other

areas, has shown that cleavage develops by more than one process:

1. Cleavage without syntectonic phyllosilicate recrystallisation i.e. pressure solution cleavage.
2. Cleavage with syntectonic phyllosilicate recrystallisation increasing with increasing metamorphic grade.

Phyllosilicates are easily sheared because of their layered structure. At the lowest metamorphic grade, cleavage develops mechanically with flexure-like deformation as the platy minerals are drawn into the cleavage domains. If a primary fabric exists e.g. due to settling of micas on a bedding plane, this deformation will give a crenulation cleavage with orthorhombic symmetry in the hinges and monoclinic in the fold limbs. The transition from cleavage domain to microlithon is continuous. Width of the microlithons depends on grain size but generally is in the 10-20 microns range.

At higher metamorphic grades, the deformation mechanisms during prograde strain are no longer purely mechanical but are also chemical, wherein material is transferred from the cleavage lithons to the microlithons by dissolution and recrystallisation. Due to the heterogeneous nature of rocks, stress is partitioned into areas of progressive shearing and progressive shortening (Bell *et al.* 1986). Minerals dissolve in the cleavage domains causing the rocks to shorten normal to cleavage. At the same time in the areas between the cleavage domains, i.e. the microlithons, extension is taking place at right angles to shortening. Micro-fracturing occurs in the direction of extension allowing fluids derived from the cleavage domains to enter the minute cracks and provide the raw material for porphyroblasts of minerals, such as chlorite or white mica, to grow. Basal planes [001] of these porphyroblasts are at a high angle to cleavage indicating growth in the direction of stretching (Ramsay 1976). As cleavage continues to develop, the contact between microlithon and cleavage becomes sharper due to extensive pressure solution.

On the other hand there is another school of thought, believing that cleavage begins to develop at the earlier stage of diagenesis (Maxwell 1962). Roy (1978) attributes the presence of silty dykes parallel to the cleavage lithons to the onset of cleavage development before complete lithification of the sediments.

Crenulation cleavage is also found in slates. This consists of harmonic wrinkles found on the cleavage surface, due to the development of cleavage in a rock with a pre-existing fabric. This type of cleavage is commonly found in Easdale slate and is described in the various quarry reports (Appendix A Section 3.6; an example is shown in Appendix A Fig. 15).

4.2.3 Correlation between Cleavage and Strain

Although there is a relationship between development of cleavage and strain, evaluating the amount of strain necessary to produce cleavage is not direct. Estimates of strain have been deduced from measurements of features in a rock thought to have been originally spherical, such as concretions, and lapilli in tuffs, and especially reduction spots which appear as ellipsoids in slate. These reduction spots formed around a particle of organic matter, which acted as a reducing agent and converted purple ferric oxide to green/yellow ferrous oxide (Fig. 4.4). Such bleached spots are initially spherical and are subsequently deformed into ovoids as the cleavage develops. The relative lengths of the three mutually perpendicular axes of these ellipsoids give an indication of the degree of deformation and hence an estimation of the percentage shortening of the rock perpendicular to cleavage. In a comparative study of the slates of the Caledonides, Wood (1971) found that the ellipsoids of North Wales, an area of open and upright folds, have a mean ratio of 1.6:1:0.27, while in the Taconic slate belt of North America, where the accompanying folds are tight and overturned, the values are 1.7:1:0.17.

However the accuracy of estimates of the amount of deformation undergone by reduction spots is limited by lack of reliable data on loss of volume during the development of cleavage. Cloos (1947), an advocate of pre-lithification cleavage development, assumed that the intermediate axis remained constant which implies a 60% reduction in volume. In contrast Wood (1974) assumed constant volume in his work and hence calculated that the onset of slaty cleavage is found with 30% shortening and 35% extension and that best commercial slates have shortening of 70% and extension of 150%. Other estimations of volume loss have been based on

petrographic and geochemical studies, using as an indication of substantial volume loss the fact that in soluble minerals, cleavage domains are depleted relative to those in insoluble. Yet another approach, based on comparing the density of a typical argillaceous slate (2.8 gm/cc) with that of shale at a depth of 1500m (2.66gm/cc), suggests little non-volatile loss. Using this last method Sorby (1908) estimated the volume loss to be 10%. Ramsay and Wood (1973) examined the shape changes due to both compaction and volume loss during tectonic deformation and found that all slates fall within the field of apparent flattening and the majority lie within the true flattening (Fig. 4.5).

In this Report, the three orthogonal axes are called X, Y and Z where X>Y>Z.
The cleavage plane generally lies in the X-Y plane.
The pillaring line is parallel to the X direction i.e. the stretching direction.
The pillaring surface is generally in the X-Z plane (Fig. 4.10).

Fig. 4.4 Reduction spots in slate: a) Arran slate (NR963504), b) Cumbrian slate (SD250837).

4.2.3.1 Measurement of Strain

Whatever the genesis of these ellipsoidal reduction spots, their degree of flattening is a measure of the submicroscopic fabric of a slate. Using the three orthogonal axes X, Y, Z of the ellipsoid (where X>Y>Z), Flinn (1962) represented the strain by plotting the ratio X/Y versus Y/Z. This was later modified by Ramsay (1976) so that the natural logarithm **ln** of the ratios is plotted as shown in Fig. 4.5. Ellipsoids found in slate always plot in the oblate or flattening area of the graph.

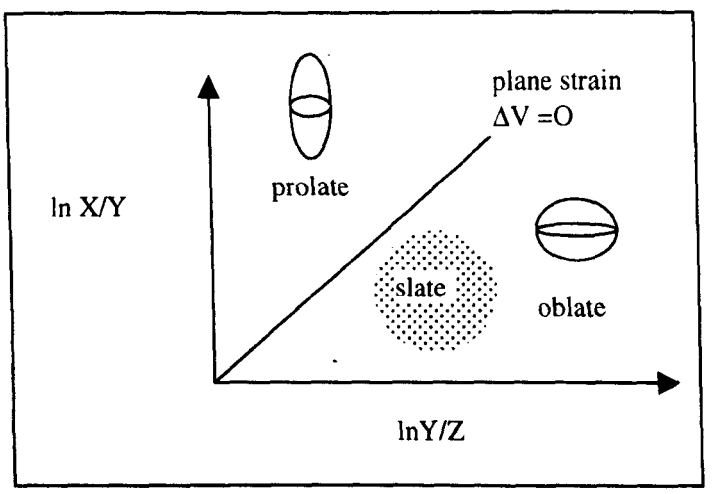

Fig. 4.5 Logarithmic Flinn diagram showing the plane strain boundary between the fields of flattening and constrictional strain at constant volume after Ramsay (1976).

Wood (1974) found that strain changed with variation in the location in geological structures. In folds with variable plunge, strain values correlate well with culminations and depressions so that maximum principal extensions are found in culminations and the greatest flattening producing the most oblate ellipsoids is found in plunge depressions.

Using an X-ray goniometer, Oertel (1970) was able to correlate the degree of ordering of basal planes of chlorite and muscovite with the degree of shortening. The degree of deformation of quartz grains was also used by Wood (1974). In this method, the ratio of the long axis to the short axis of quartz grains gives a qualitative indication of strain. Wood gives the following values of a few slate-producing regions:

long axis: short axis

Welsh and North American slate belt	3: 1
Valdres, Norway	4: 1
Ballachulish, Scotland	6: 1

4.2.4 Correlation between Cleavage Intensity and Metamorphism

Kisch (1991), in his comprehensive review of work done world-wide on cleavage, endeavoured to correlate slaty cleavage and the degree of metamorphism. Metamorphic grade was measured in illite crystallinity which, when converted to 2θ, can be used for comparing data from different sources (Section 3.3.2.3.b), although instrument conditions still affect the values.

Using the literature as a database, Kisch found that comparison of the intensity of slaty cleavage is hampered by insufficient detail of micro fabrics and a lack of uniformity in descriptive methods. Nevertheless his tables of comparison of strain, fabric and metamorphic grade for different tectonic units is a valuable synopsis of work done world-wide. The only reference to Scotland in Kisch's review is to work the of Kemp *et al.* (1985) on the Southern Uplands. Several detailed studies have been carried out in the Welsh slate belts e.g. Merriman & Robert's (1985) work in Snowdonia and Llyn, North Wales.

Lithological controls

Whereas there is a strong link between the onset of slaty cleavage and the degree of metamorphism, lithological effects are also important. Norris and Rupke (1986) found that finer-grained metapelite develops cleavage at a lower grade of metamorphism than coarser-grained rocks such as greywackes The morphology of the cleavage domains is also affected by grain size i.e. the spacing is wider and the shape is rougher in coarser grained protoliths (Kisch 1991).

4.2.5 Discussion

While there is a direct relationship between strain and the first appearance of distinct types of cleavage, there is only a loose relationship between strain and improvement in illite crystallinity IC (Kisch 1991). In pelites, cleavage begins to develop in the diagenetic zone at 0.6-0.42 IC, and smooth cleavage domains and microlithons with fabric are associated with the IC values typical of the anchizone. Equivalent stages of cleavage development appear at slightly higher grades in metagreywackes. Where IC is significantly lower (i.e. more crystalline) than normal, this is due to many factors such as post-kinematic annealing following later intrusion of an igneous body in the region (Kisch 1991).

4.3 The Influence of Cleavage on the Production Roofing Slate

From the industry's point of view, the most important aspect of the slate deposit is the type and intensity of its cleavage. This controls every aspect of production, from ease of extraction to the characteristics of the finished product. ***How cleavage affects the characteristics of slate such as thickness and the texture of its cleaved surface is the subject of this section.***

Consideration of the many criteria governing the selection of the best slate for the job is outside the scope of this work and this discussion is limited to those submicroscopic aspects of cleavage which affect the ability of the rock to be split into thin slabs. The ability to cleave a rock is also affected by geological features such as folding, igneous intrusions, jointing, veins of quartz etc. These macroscopic characteristics are discussed in the various quarry reports (Appendix A).

The ideal slate deposit, from the point of view of its cleavage, is a fine-grained homogeneous material which has been metamorphosed to develop the optimum slaty cleavage.

The optimum cleavage fabric has:

1. Closely spaced, straight cleavage domains (CDs).
2. CDs straight and continuous.
3. CDs regularly spaced.
4. Microlithons (MLs) also having an aligned fabric.

But slate is a natural material and these criteria are rarely achieved. Fabric can range from that observed in slate extracted from the *old vein* at Oakley Quarry, Blaenau Ffestiniog, North Wales to a Westmorland slate from Broughton Moor Quarry, Cumbria. The fabric in the former is fine-grained material with a regular pervasive cleavage (Fig. 4.6) enabling the rock to be split to 3mm thickness without tapering, while the fabric in the latter is coarse-grained producing a thicker slate (Fig. 4.7). Between these two extremes lies an example of Scottish slate from Ballachulish (Fig. 4.8). Here the distinction between the MLs and the CDs can be clearly seen as the continuous CDs are anastomosing around the large microlithons. As the fabric was being strained in the direction of stretching, tensional cracks developed in the MLs allowing fluids to penetrate and other minerals to grow (Bell *et al.* 1986).

Slates were produced from all of these sources in spite of their very different fabrics. The aim of this discussion is to evaluate the fabric of slate from working quarries in such a way that it can be correlated with the thickness of the slates produced, and hence set up a system with which to assess the splitting potential of Scottish slate.

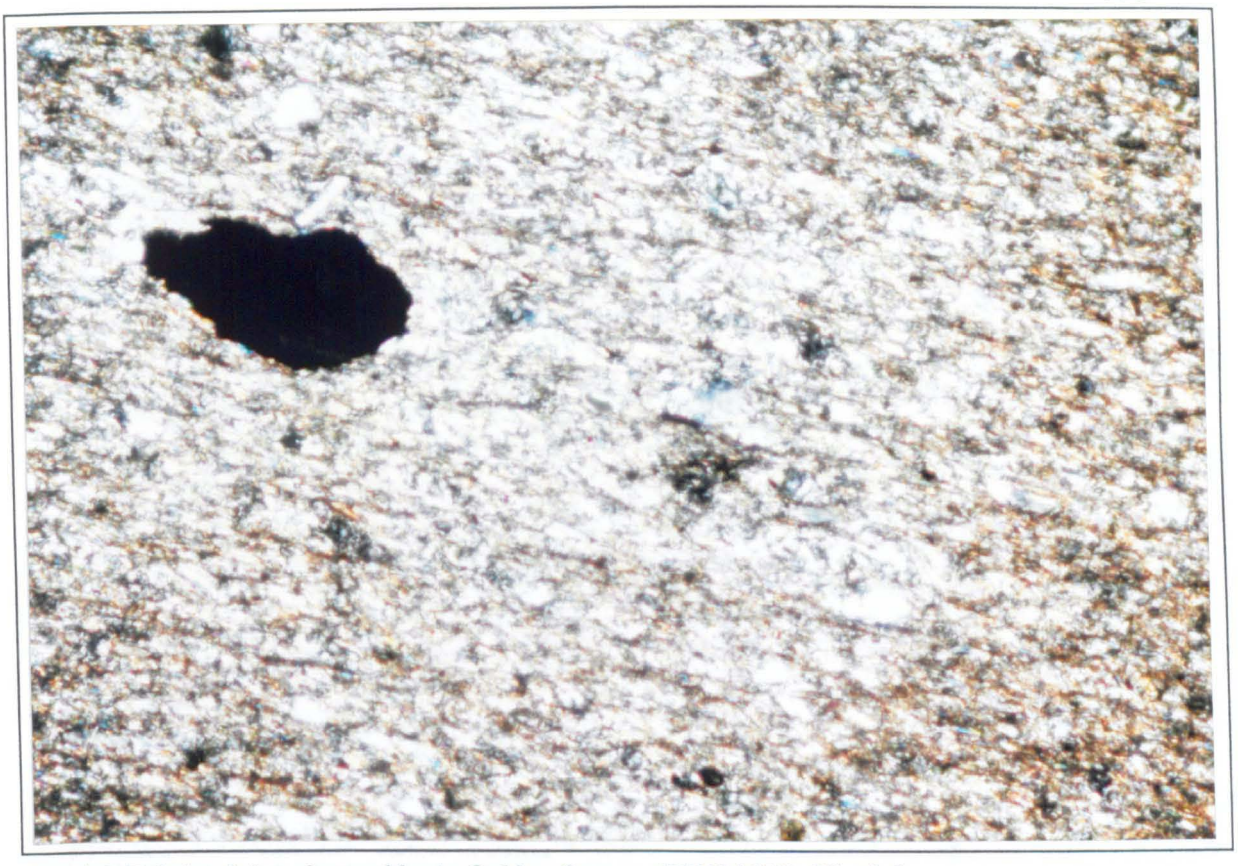

Fig. 4.6 Fabric of slate from *old vein* Oakley Quarry (SH694473), Ffestiniog. ← 0.2mm → Photomicrograph (XP) of the microfabric shows closely spaced and straight cleavage domains in this fine-grained slate. The very dark area is a cluster of pyrite grains.

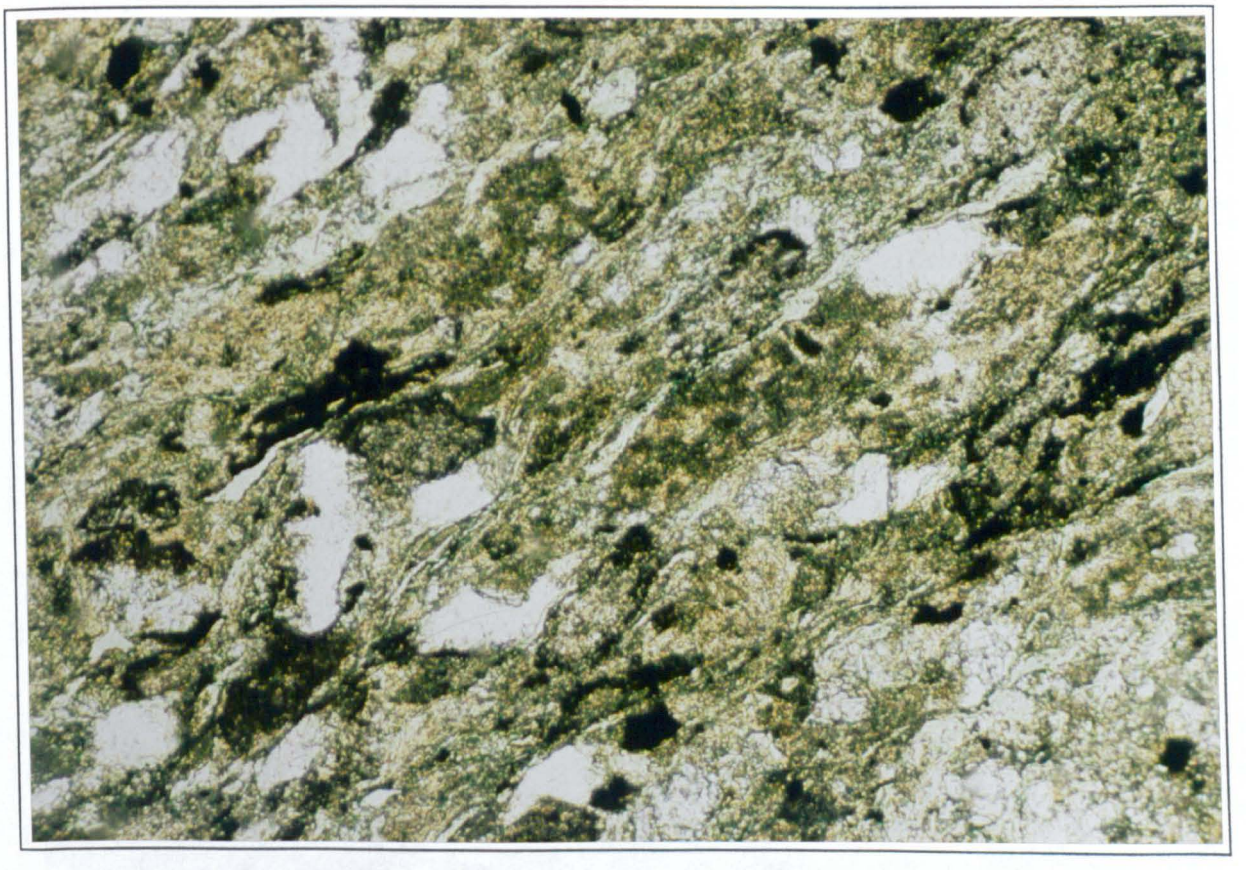

← 0.2mm →

Fig. 4.7 Photomicrograph (PPL) of the fabric of slate from Broughton Moor Quarry (SD254646), Cumbria. The cleavage in this slate is made up of widely spaced anastomosing cleavage domains and microlithons without parallel fabric.

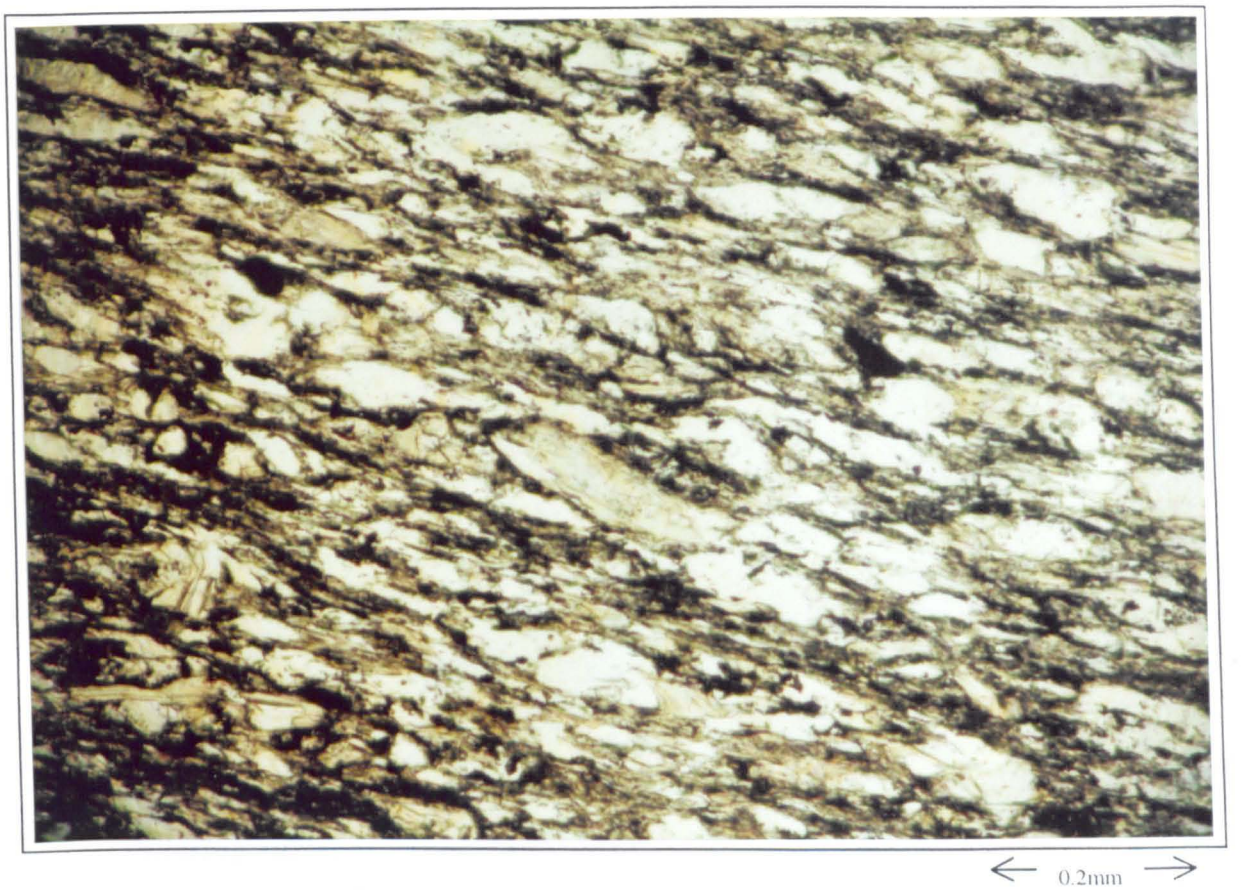

Fig. 4.8 Photomicrograph (PPL) of the fabric of a Ballachulish slate (NN08558). The cleavage in this slate is made up of closely spaced cleavage domains which anastomose gently around the microlithons. Microlithons are quartz-rich and show little parallel fabric.

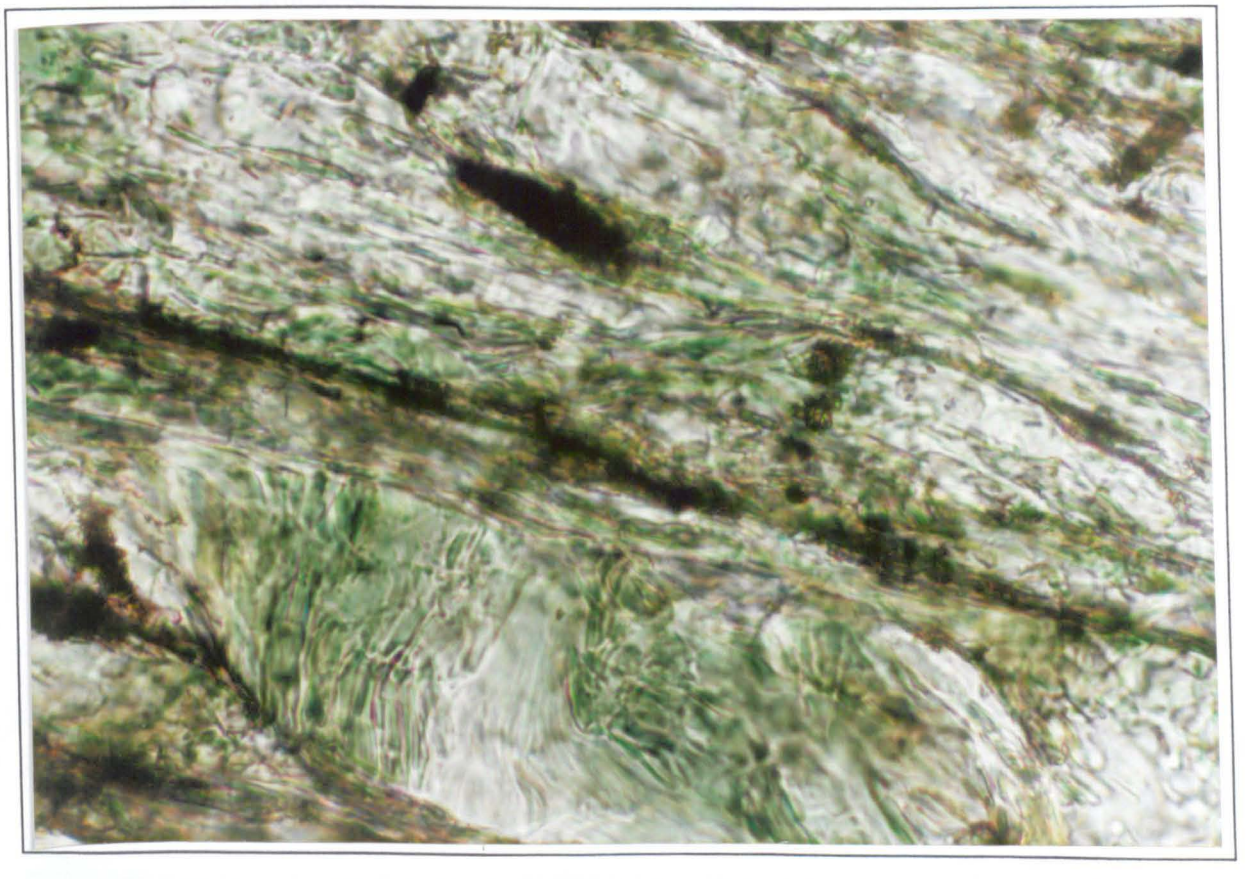

Fig. 4.9 Photomicrograph (PPL) of the relationship between detrital mica grains and chlorite overgrowths in an Aberfoyle slate (NN505030).

4.3.1 Anisotropy of Slate

As slate is an anisotropic material it has different properties depending on direction. One of these properties, and that most relevant to producing roofing slate, is variation of fabric with orientation and the resultant effect on the splitting ability of the slate.

Three orthogonal sections were prepared as follows:

1. ***Cleavage surface***. This is the face parallel to the cleavage face and is perpendicular to the direction of maximum shortening. This is the XY plane and perpendicular to Z. The *grain* of a slate is parallel to the longest axis of the certain minerals due to their elongation during deformation (Fig. 4.10).
2. ***Pillaring surface*** This is the plane perpendicular to the cleavage surface and parallel to the grain of the slate. The intersection of this surface with the cleavage surface is the pillaring line. In most cases this imparts a secondary line of weakness along which the slate can be broken, a property which is always recognised by the quarrymen and exploited in the winning of slate (Fig.4.10).
3. ***Third surface.*** This face is perpendicular to the previous two sections. Due to the tendency of the slate to break preferentially along the other two planes it is not easy to get a natural break in this direction.

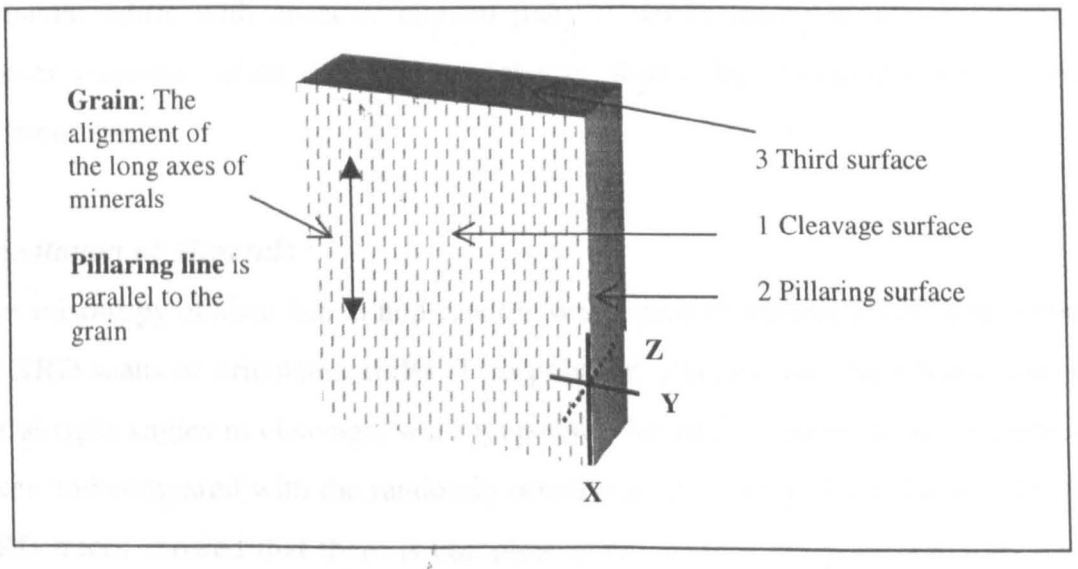

Fig. 4.10 Terms given to the different features of a slate.

This internal fabric of a slate is visually demonstrated by reduction spots as discussed in Section 4.2.3, the ratio of the axes of these oblates giving a measure of the degree of deformation. Several examples of such reduction spots (Fig. 4.4a) were found in Arran Slate Quarry (Appendix A 4.5.1) and the following measurements made:

Average axes X:Y:Z = 1.6:1:0.06

While the X:Y ratio agrees with that found by Wood (Section 4.2.3), Z is exceptionally low. This was due to the reduction spots being found on the cleavage surface and hence the measured Z not being the true value but a minimum due to flaking of the surface. However the slate broke preferentially parallel to the longest axis of the reduction spot, i.e. the pillaring line. Not all slate has a pillaring line e.g. the slate in the Kirkby Quarry in Cumbria. Here the degree of strain in the X and Y axes is the same, hence the lack of a linear fabric and no pillaring line. This is demonstrated by a concretion (Fig. 4.4b), originally spherical, which has been strained into a very oblate shape and appears as circular on the cleavage surface. These two examples are only useful in explaining the fabric and in particular the pillaring line.

The anisotropy of the fabric is demonstrated in a slate from Luing (LC-1), (Fig. 4.11), which shows three orthogonal aspects of the cleavage. The plane of cleavage is a flat flaky texture with no apparent alignment; the pillaring surface shows the domainal fabric with areas of aligned platy minerals interspersed with layers of coarser minerals, while the third aspect also shows the domainal texture from a different angle.

Orientation of Minerals

The anisotropy of slate due to non-random orientation of minerals was demonstrated by XRD scans of orientated slides. Two polished sections, one cut parallel and one cut at right angles to cleavage, were prepared. An XRD scan of these sections was taken and compared with the randomly orientated smear (Fig. 4.12, Table 4.1). The XRD traces showed that there is complete orientation of the platy minerals i.e. no basal peaks were detected on the scan of the perpendicular section and enhanced peaks of greater intensity were detected on the section parallel to cleavage.

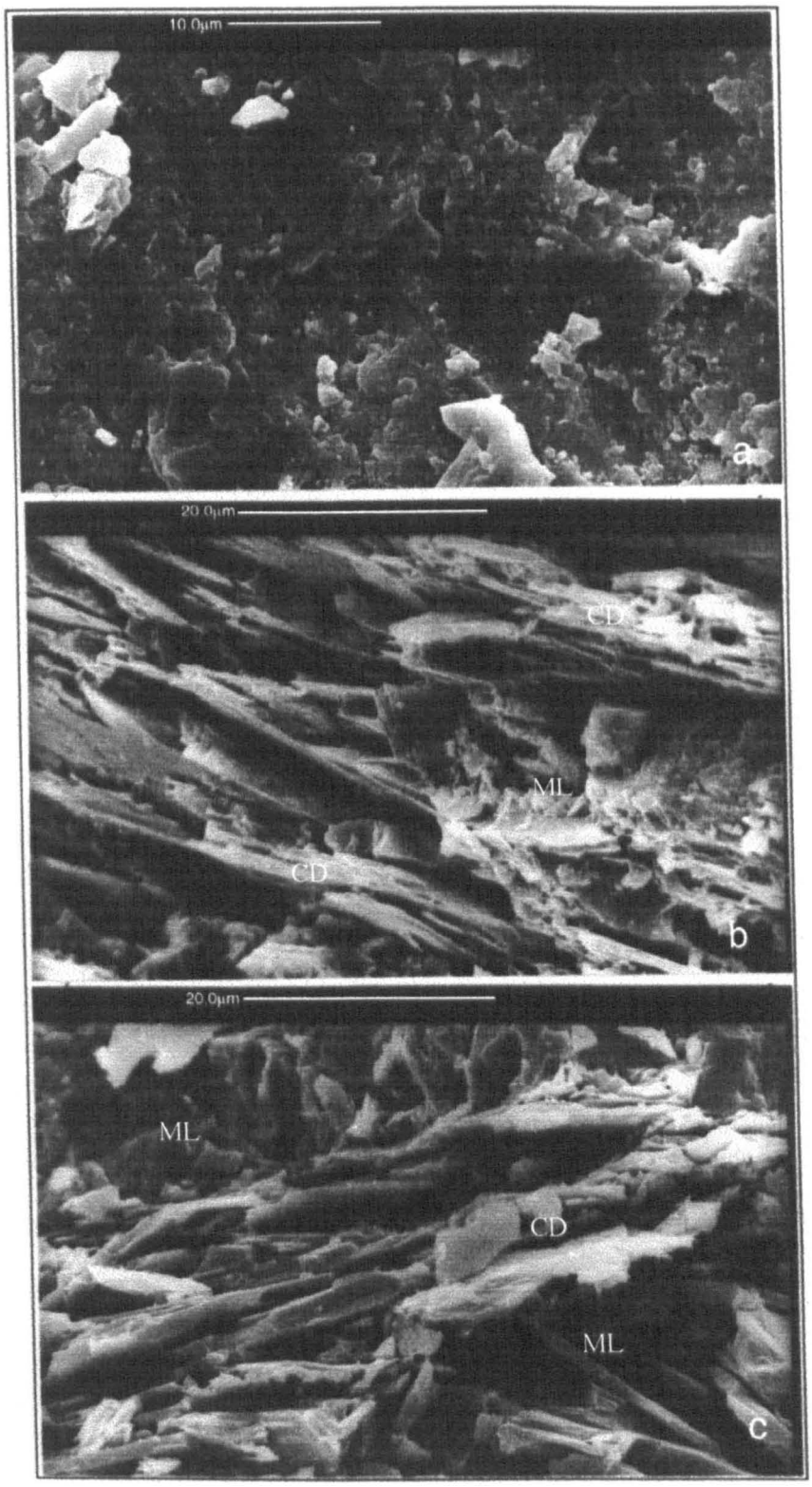

Fig. 4.11 Anisostropy of slate. Three orthogonal aspects of the fabric of an Easdale slate LC-1 a) View of the surface showing a platy fabric with a flaky texture. b) View of the pillaring surface showing the domainal nature of the slaty cleavage c) View of the third surface showing an end-on view of the cleavage.

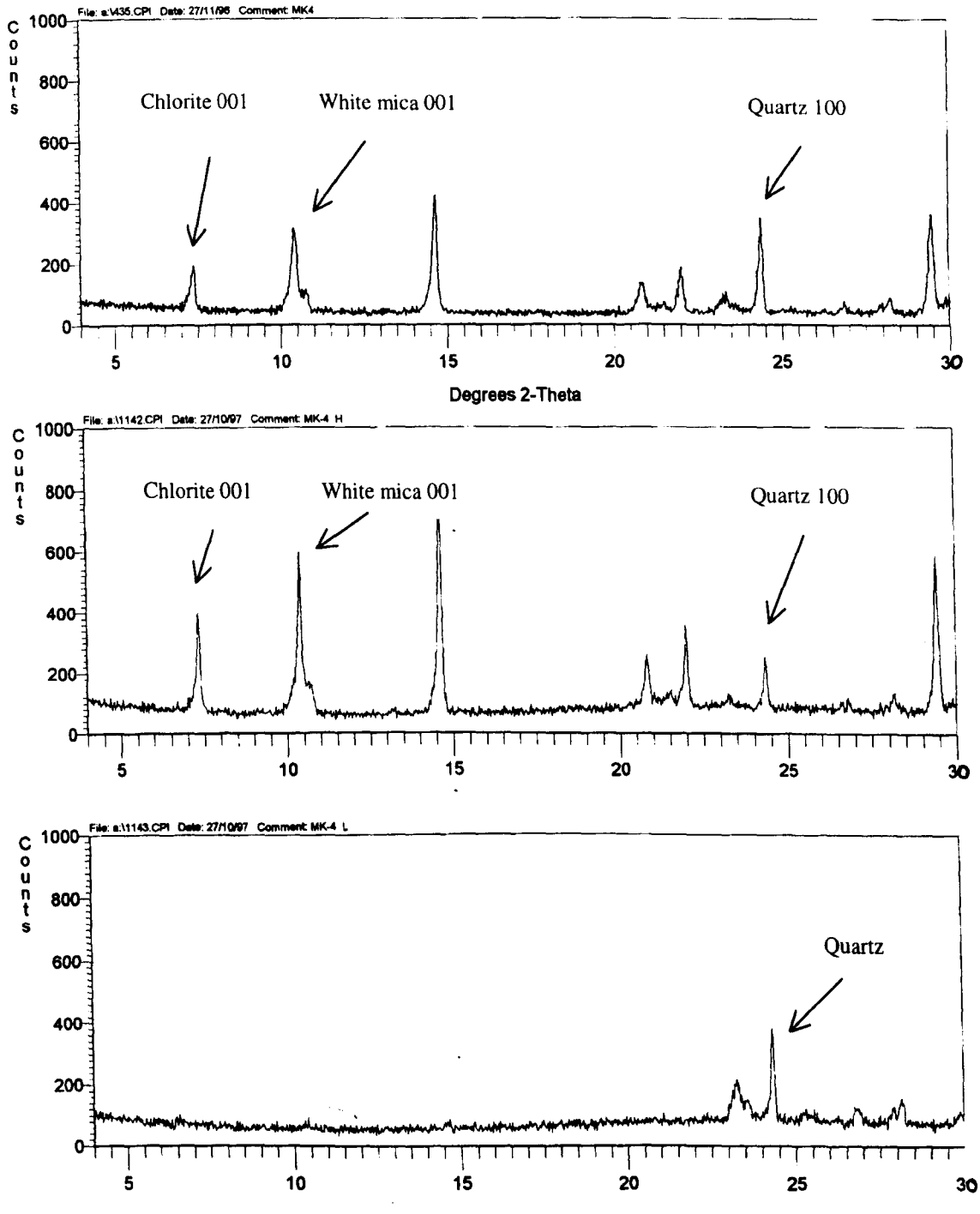

Fig. 4.12 Effect of orientation on XRD scans of a Macduff slate MK-4, a) a powdered sample randomly orientated, b) parallel to the cleavage surface, c) perpendicular to the cleavage surface.

MK-4	Chlorite [001]		White mica [001]		Quartz [100]	
Orientation relative to cleavage	Area	Intensity	Area	Intensity	Area	Intensity
Random	1412	145	3981	271	2277	309
Parallel	3025	370	5695	520	1327	170
Perpendicular	0	0	0	0	2193	313
Mean of parallel and perpendicular values	1513	185	2848	260	1759	242

Table 4.1 Effect of orientation on XRD scans of a Macduff slate. Sample MK-4, a) a powdered sample, randomly orientated, b) parallel to the cleavage surface, c) perpendicular to the cleavage surface.

4.3.2 Measurements of Fabric

To evaluate the fabric of slate, the orientation of phyllosilicates were studied by XRD analyses of rock slabs cut in different orientations relative to the attitude of their bedding and cleavage (Oertel 1970, Sutton 1989). Weber (1981) also used the degree of orientation of the phyllosilicates using X-ray goniometry but this technique was not available in-house. The degree of shortening in best commercial Welsh slates was measured using reduction spots and found to be 70% (Wood 1974). However none of these methods discriminate between different fabrics in terms of their ability to be split into roofing slates of varying thicknesses.

In this Report, several methods of evaluating the anisotropy of a slate were investigated, such as the oblateness of reduction spots, however it was found that reduction spots are too infrequent to be used as a general means of evaluation. Measurement of the degree of orientation of platy minerals using X-ray analyses of rock slabs cut in different orientation relative to cleavage was investigated in Section 4.3.1. However the degree of the orientation was too uniform to be used as a method of discriminating between different types of fabrics. Roofing slate is produced from rocks with a wide range of different fabrics as seen in Figs. 4.6 - 4.9 and it was necessary to develop a general method of assessing and comparing fabrics which is independent of mineralogical differences and therefore applicable to

a wide range of different slates. Individual samples were examined using the scanning electron microscope (SEM) and the splitting potential of the fabric evaluated in a semi-quantitative way. To test the validity of this method a selection of slates from producing quarries was evaluated and compared with their known splitting properties as evaluated by the quality control at the quarry.

4.3.2.1 Methodology

The topography of the pillaring surface was examined using SEM imaging and photography. As sawing the sample destroyed this surface topography, it was necessary to break the sample along natural lines of weakness such as the pillaring line. This was easily done in a slate with a strong pillaring fabric, such as the Welsh slate W/F-1, but slates with little linear fabric have a poorly developed pillaring line, making it difficult to get a natural break along the pillaring surface. However, such slates with a less developed grain are less anisotropic in the planes perpendicular to cleavage. For example, in the Cumbrian slate (Fig. 4.4b) there is no pillaring line and the precise orientation of the section cut perpendicular to the cleavage is not critical.

The method used to prepare the slate was as follows:

- The slate sample was broken using a hammer and chisel and a flat surface with the pillaring surface visible was selected using a hand lens (Fig. 4.10).
- Surface particles were removed by placing in a beaker of water in a sonic water bath for 10 minutes.
- The sample was dried in a oven at 105°C for 30 minutes.
- The sample was placed on a SEM stub, earthed with silver paint and a gold coating.
- The samples were then examined under the SEM. Where possible, the procedures discussed below were carried out at specific magnifications of x 500, 750, 1K and 1.5K to facilitate comparison between different samples.

The following observations and measurements were made:

- ***Spacing: the distance between cleavage domains***

An average value of the spacing between cleavage domains was determined across the field of view. These measurements were made directly on the SEM, which has the facility to measure distances accurately. Whenever possible the distance was measured over several cleavage domains in order to obtain an average value. This was especially important in the case of anastomosing cleavage domains. Spacing was determined at several magnifications but machine conditions were not found to affect the results.

Problems arose when the degree of alignment of minerals was so great that individual CDs were indistinguishable. This arose in slates with good fabrics and any lack of precision was offset by a high alignment value. Problems also arose when the slate was very heterogeneous and the area measured was not typical of the whole slate. An extreme case of this was found in the Cnocfergan *slate*, which is really a flagstone. Here splitting can take place because micaceous minerals form layers between the quartz rich areas of equant minerals. This *slate* was excluded from the analysis.

- ***% Alignment: The proportion of the total surface area occupied by minerals orientated in the direction of cleavage.***

In general, the minerals of a slate are aligned in the cleavage domains and non-aligned in the microlithons. The ratio of the thickness of cleavage domains to that of the microlithons is a measure of the degree of development of the slaty cleavage. However as the degree of alignment within the microlithons increased, it was not always possible to distinguish between the two type of domains. From the point of view of splitting a slate, the proportion of suitably aligned platy minerals i.e. parallel to the cleavage surface, whether in the cleavage domains or microlithons was deemed significant. It was therefore decided to measure the proportion of slate consisting of aligned minerals. Estimates of the percentage alignment were made on screen but better precision was obtained from photographs of SEM images taken at 4-5 locations on each sample. Each photograph was analysed by taking two to three cross sections at right angles to cleavage, and measuring the cumulative length of *zones of alignment* and then calculating the % value relative to the total length of the cross section.

- ***Shape of cleavage domains as described in Section 4.2.1 (Fig.4.2)***

The shapes of the cleavage domains and their degree of continuity were noted.

- ***Microlithon fabric: the degree of alignment of minerals in the zones between the cleavage domains.***

The fabrics of the ML varied from those with complete alignment of elongated minerals to those where the minerals were equant. In cases where the alignment was considerable it was incorporated into the degree of alignment previously described. In some cases it was possible to quantify the degree of alignment in the microlithon fabric by measuring the long and short axes of the minerals and determining the ratio. Other samples could only be evaluated in a semi-quantitative way.

- ***Homogeneity: A measure of the variance in all the properties in the fabric.***

The ideal slate is a uniform material and all imperfections and irregularities affect the splitting value of the slate. The presence of large detrital grains, e.g. of quartz, in an otherwise fine-grained rock would increase the minimum commercial thickness of the roofing slate produced. To assess the heterogeneity of the slate, the degree of variation of the spacing and percentage alignment properties and the overall appearance from one location to the next were used as criteria in evaluating this property but no attempt was made to quantify it numerically.

4.3.2.2 Evaluation of Results

Values of the different measurements are given in Appendices 4.1 and 4.2.

Precision:

Repeated checks of the photographs of the same samples were made and the measurements of properties such as the percentage alignment never differed by more than one point in the Fabric Points Scheme. Operator bias was not a major factor in the process of evaluating the slate.

Sample Precision

Two SEM stubs were prepared from a single sample (W/F-5) from the *old vein* in the Oakley Quarry to assess sample precision and gave similar results (Appendix 4.1). Two samples from the same vein also gave consistent results, based on the initial weightings as discussed in Section 4.3.2.3.

Variation within a vein is attributed to variation in the material itself. For example, a sample taken from the quarry face *old vein* Cwt y Bugail and a finished slate produced earlier from that vein gave values of 18 FP (minimum commercial thickness of 4.2mm) and 15 FP (minimum commercial thickness of 5.6mm) (Appendix 4.1) respectively. Since this work was carried out, roofing slates 4mm thick are being produced from the seam in this quarry with the better slaty fabric.

Using the data for the Welsh and Cumbrian slates, the interdependence of parameters was noted in that there is a strong reciprocal relationship ($R^2 = 0.7479$) between spacing **y** and the degree of alignment **x** (Fig. 4.13). The relationship is as follows:

$$y = k\,x^{-1.05} \qquad k = \text{constant}$$

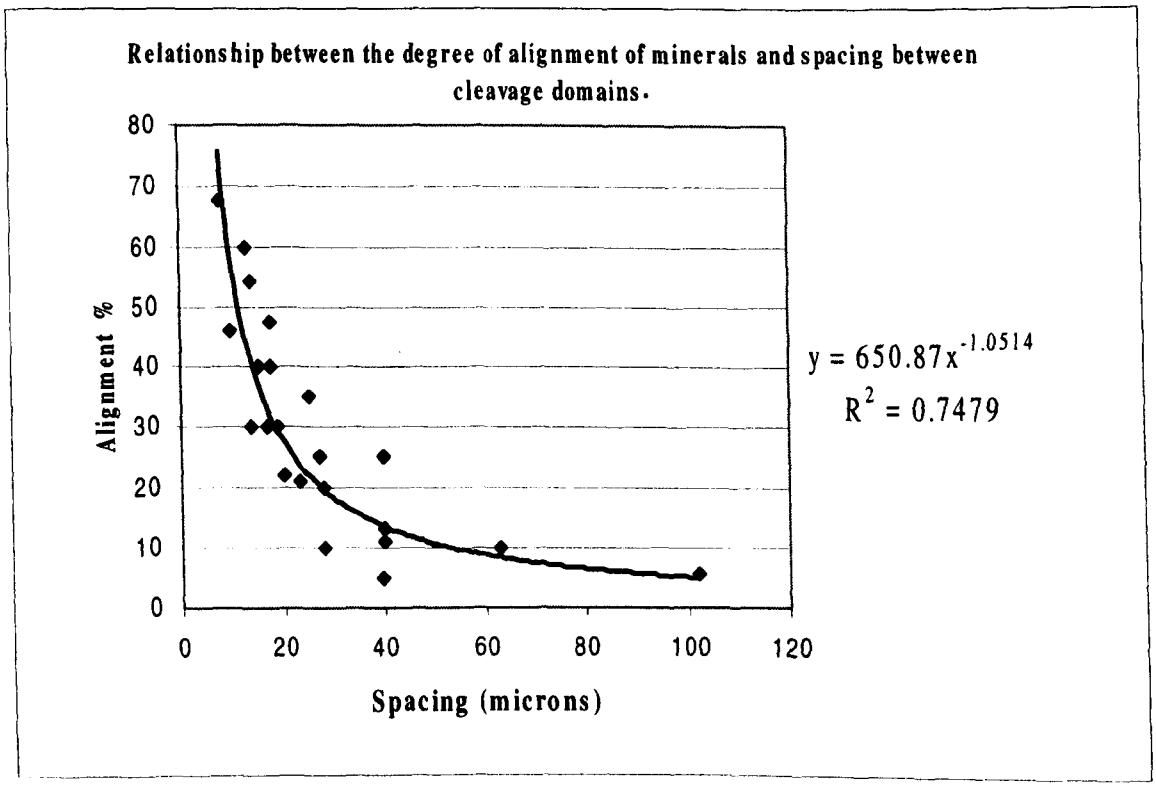

Fig. 4.13 Relationship between spacing of cleavage domains and the % area of aligned minerals in Welsh and Cumbrian slates.

4.3.2.3 Evaluation Procedure

In order to interpret the above measurements, a considered judgement was made regarding the relative importance of the different parameters to the splitting property of the slate. This ***relative importance*** is termed the ***weighting.*** A range of values was assigned to each parameter and then each parameter was varied systematically to get the optimum correlation between the points system and the minimum commercial thickness. As an illustration, the variation of the different weightings relative to a value of 5 at 15 μm for spacing is shown to get the final optimum conditions. The different measurements were assigned an initial weighting (Table 4.2) for each cleavage property as described in Section 4.3.2.1 and evaluated as follows:

- ***Spacing - Weighting 7.5***

It is assumed that the closer the spacing the thinner the slate can be split. Initially, the spacing of 15 μm observed in the sample from the *old vein* Ffestiniog W/F-1 was assigned a value of 5, and other samples were given values inversely proportional to their spacing, relative to this sample. Therefore the value of 7.5 is given to the minimum observed spacing of 10μm.

$$Value = \frac{15}{spacing} \times 5$$

- ***%Alignment - Initial Weighting 10***

The greater the degree of alignment the better the splitting potential of the slate. Initially the maximum value for this parameter was 10 but it was subsequently re-evaluated (Section 4.3.2.4) and a weighting value of 2 was assigned to this parameter (Table 4.2).

$$Value = \frac{\%alignment}{100} \times weighting$$

- ***Shape - Weighting 4 (Straightness 2 Continuity 2)***

The ideal shape of the CDs is deemed to be straight and continuous. Straight CDs are given a value of 2, anastomosing CDs a value of 1 and irregular CDs a value of

0, while interim values were allocated to slates which do not fall easily into the different categories. Continuity of the CDs was also considered important. A fabric where the CDs are predominantly continuous are given a value of 2 and those with less persistent CDs are given points *pro rata*.

- ***Microlithon Fabric - Weighting 3***

Where possible a figure was assigned to this parameter based on $\log_{10}$(length/width) of individual microlithons, but often a value in the range 1-3 was assigned subjectively.

- ***Homogeneity - Weighting 3***

This parameter was assigned a value between 0 and 3 in a semi-quantitative way, as discussed in Section 4.3.2.1 (Table 4.2).

The value given to the fabric is the sum of the values given to the different parameters above.

4.3.2.4 Verification of the Fabric Points Scheme (FPS)

A selection of the photographs used in the evaluation of slate is shown in Fig. 4.15 but these do not correspond directly to the results given in Appendices 4.1 and 4.2 which are the average values obtained for measurements taken at many locations. The validity of the proposed points scheme was tested by determining the degree of correlation between values found for different slates and the thickness of the finished product (Fig. 4.14). The correlation coefficients depend on the type of regression analysis used and the weightings given to the different parameters. For the regression analysis it was found that the best fit was given by an exponential relationship and this is used throughout the following evaluation. The weighting given to each parameter was assessed **independently** by determining the value which gave the highest correlation. Because of the interdependence of the weightings, the procedure was repeated until an optimum set of values was found for all the parameters (Table 4.2).

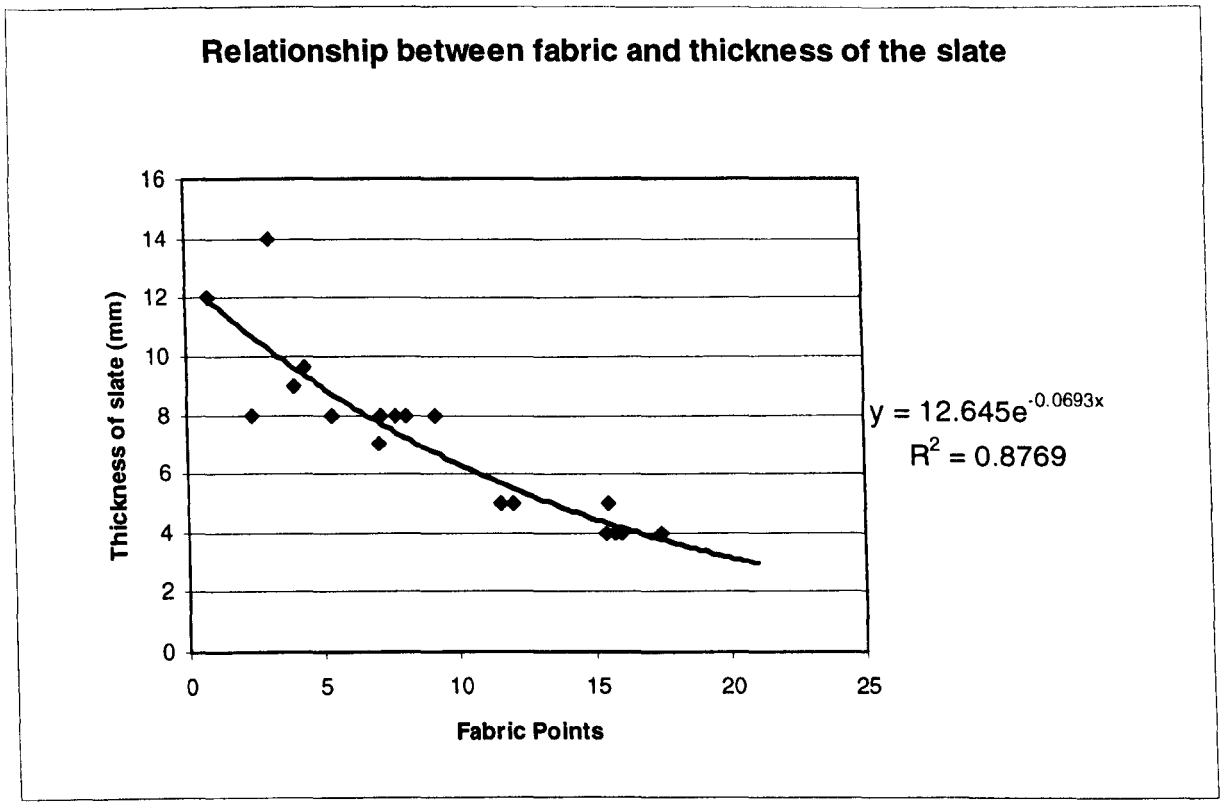

Fig. 4.14 Relationship between fabric and the thickness of the slate produced.

Parameter/weighting	Initial	Optimum	Final
Spacing w.r.t. 15μm	5	4.9	5
% alignment	10	2	2
Shape	2	3	2
Continuity	2	1.6	2
Microlithon	3	3.3	3
Homogeneity	3	6	3
R^2	0.8618	0.8820	0.8769

Table 4.2 Multivariant analysis of fabric, the effect of the final adjustments to the different weightings of the different parameters on the optimum correlation coefficient.

In this case study the initial weightings gave a correlation coefficient of $R^2 = 0.8618$. This figure was improved by reducing the contribution made by the degree of alignment, increasing that made by the homogeneity and making minor adjustments to the other parameters until an optimum correlation coefficient of $R^2 = 0.8820$ was obtained. The relationship between the minimum thickness of the slate produced and the number of points assigned to the fabric at optimum conditions is:

$$t = 12.371\, e^{-0.0503x}$$ **t** = thickness (mm) **x** = number of fabric points

This relationship was then used to assign a potential minimum thickness to Scottish slate The data set used for this work was limited to Welsh and Cumbrian slates because only working quarries were able to provide an assessment of splitting ability. This data set should be broadened before a more thorough discriminant analysis is carried out.

The optimum conditions were obtained by assigning a weighting of 6 to the parameter of homogeneity which is on a par with that assigned to spacing (Table 4.2). It is unfortunate that the parameter with the greatest control was least amenable to quantification. It could be that with a larger data set, which includes slates from other working quarries world-wide, this parameter would lose some of its relative weighting. However, homogeneity may well be a significant parameter and further work should be done to define this term more rigorously. At the present stage of this research, the degree of variance of other measurements, such as CD spacing, was used to assign a value to homogeneity. But this does not address the greater problem of determining homogeneity of a slate seam based on a few small samples. Because the principal aim of the procedure was to produce a rigorous and objective method of analysing the fabric of slate, it was decided to revert to a value of 3 for the parameter of homogeneity:

$$t = 12.645\, e^{-0693x}$$

t = thickness mm

x = number of fabric points

This was then applied to samples of Scottish slate and a second set of values for theoretical minimum thickness were obtained (Appendix 4.1) and used in the following discussion of Scottish slate.

(The equivalent values, calculated with a homogeneity weighting of 6 i.e. approximately the optimum weightings above, are given in parenthesis Appendix 4.2)

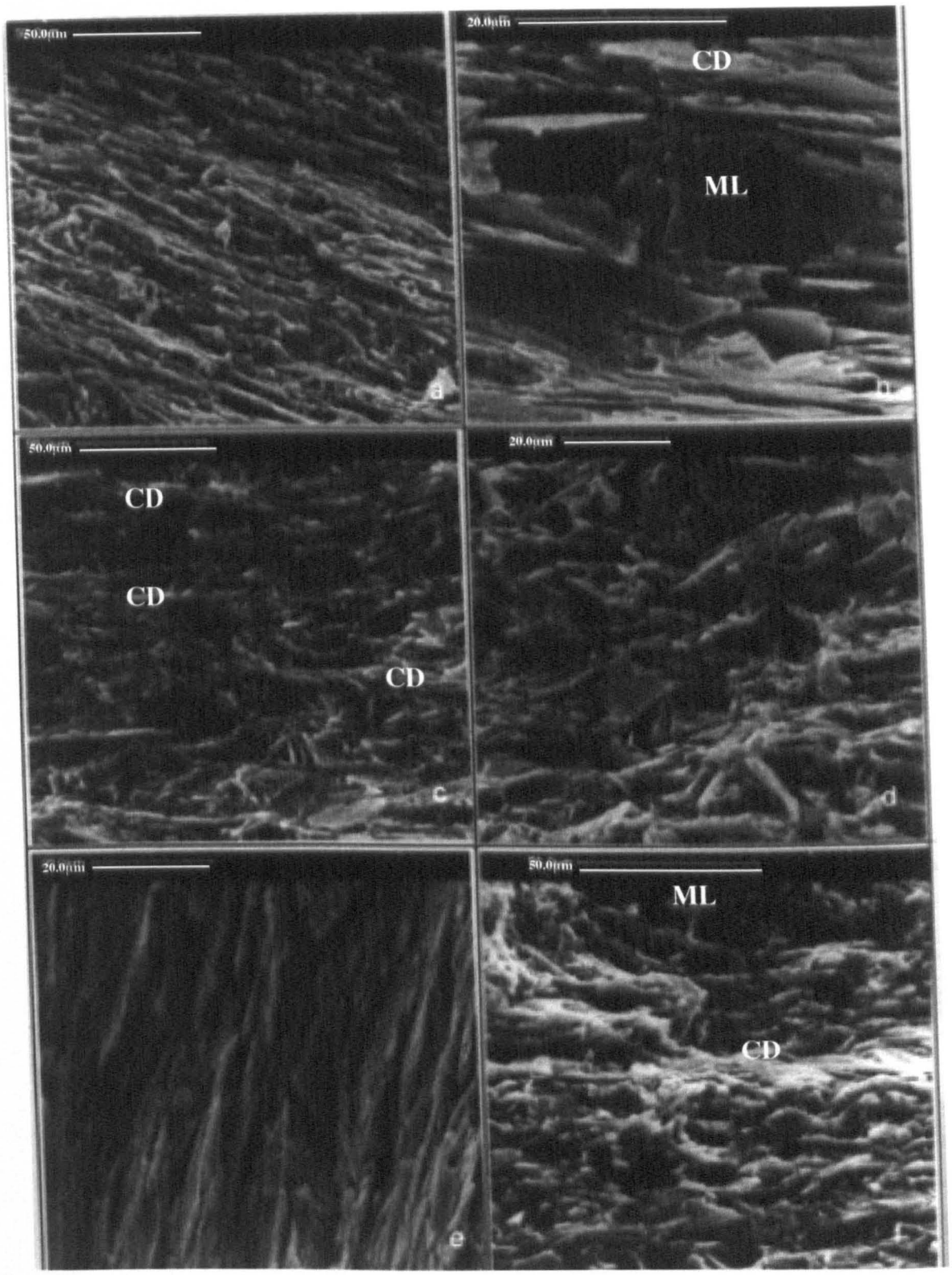

Fig. 4.15 Fabric of Welsh slate; a) Ffestiniog *old vein* W/F-1 *best* slate has straight closely-spaced cleavage domains. Slates 4mm thick are produced from this *vein*. b) Sample W/F-5 is also from the *old vein*. This figure is at a larger scale which highlights the domainal nature of the cleavage i.e. quartz-rich zones in the microlithons (ML) are separated by zones rich in platy minerals in the cleavage domains (CD). c) Ffestiniog *pigs vein* W/F-12 has straight but more widely-spaced cleavage domains than that found in samples from the *old vein*. Slates 8mm thick are produced from this *vein*. d)Ffestiniog sampleW/F-9 from between the producing *veins* has a poorly developed fabric. e) Cwt y Bugail sample W/CB-1 from the *best vein* has straight closely spaced cleavage domains and strongly aligned fabric in the microlithons. Slates 5mmthick are produced from this *vein*. Note the larger scale f) Cwt y Bugail sample W/CB-4 from the *new vein* from which slates 8mm thick are produced. The cleavage domains are more widely spaced than in slate from the *best vein*.

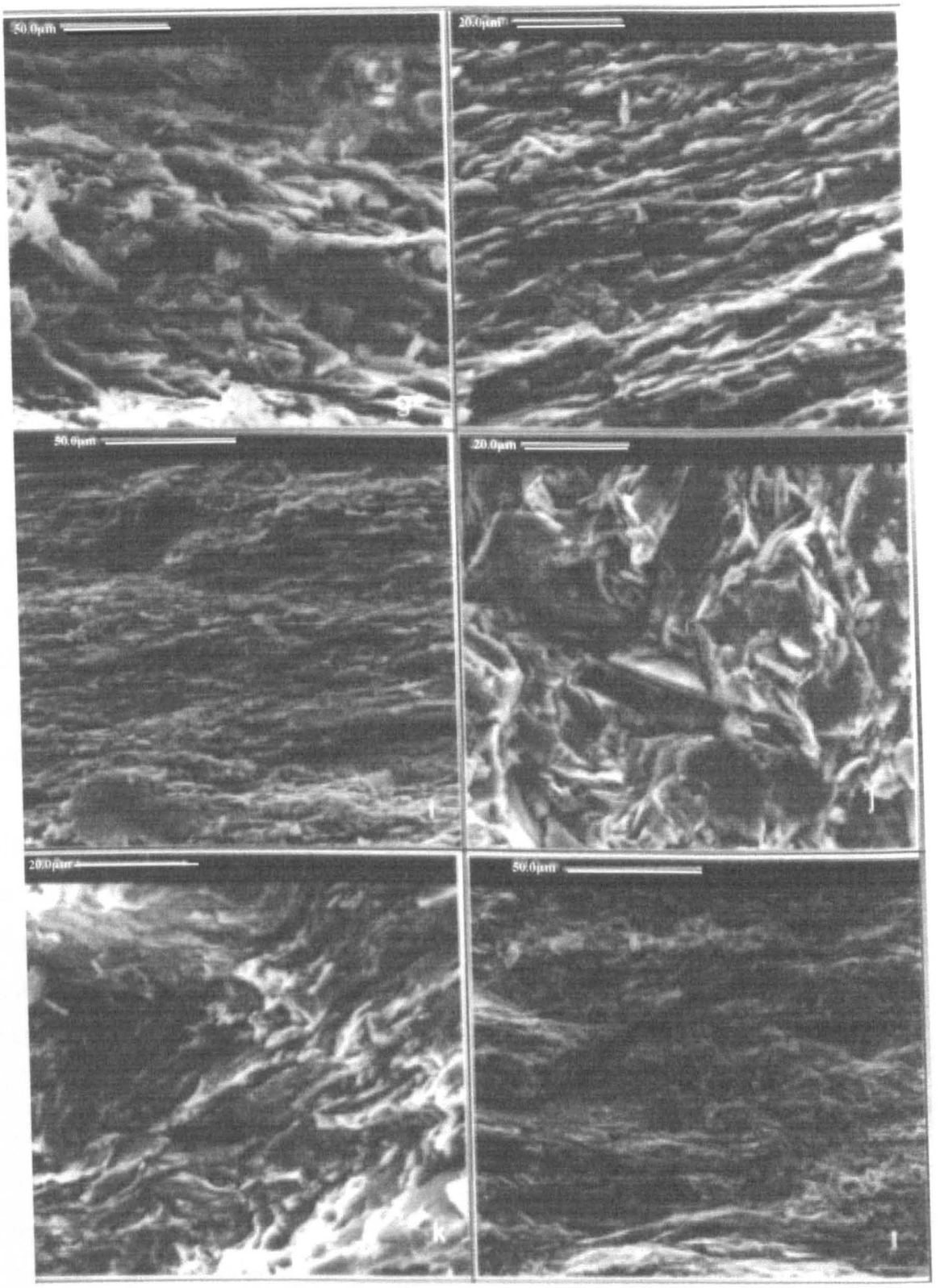

Fig. 4.15 continued g)Ffestiniog W/F-12 *new vein* has irregularly spaced cleavage domains. Slates 8mm thick are produced from this vein. h) Pen yr Orsedd W/PO-3 *best heather blue* has closely-spaced cleavage domains and strongly aligned fabric in the microlithons. Slates 5mm thick are produced from this *vein*. Note the larger scale i) Tyn y Weingladd W/PO-11 has closely spaced cleavage domains and well developed fabric in the microlithons. Slates 5mm thick are produced from this quarry.

Fabric of Cumbrian slate j) Kirby E/K-3 The fabric has anastomosing discontinious cleavage domains and minerals in the microlithons are non-aligned. Slates 9mm thick are produced from this quarry. k) Broughton Moor E/BM-1 The fabric has anastomosing discontinious cleavage domains and no alignment of minerals in the microlithons. Slates 12mm thick are produced from this quarry l) Brossan Stone E/BS -3 the fabric has anastomosing discontinious cleavage domains and non-aligned minerals in the microlithons. Slabs for cladding 14mm thick are produced from this quarry.

4.3.2.5 Discussion

The minimum thickness of a commercial slate is determined by the ability to be split, therefore if the fabric scheme has validity in predicting the commercial potential of a slate deposit, there should be good correlation between the points scheme values and the thickness of the produced slate.

As suggested, the database for the evaluation of the slaty fabric should be extended to include slate world-wide. However in general it was found that there is a high degree of interdependence between the different cleavage properties, similar to that between spacing and the degree of alignment of minerals (Fig. 4.13). For example fine-grained slates have finely spaced cleavage domains which are also straight and continuous. In addition these slates also show the greatest degree of homogeneity. For this reason the correlation coefficients are not sensitive to changes in the relative weightings of the different parameters.

However there are other factors besides the statistical approach above which need to be considered. While it is simple to measure the thickness of a finished slate, in the case of samples taken from the quarry face, the minimum commercial thickness value assigned to the slate by the quarry manager were taken. The relationship between this potential thickness of the slates and FPS values has correlation value $R^2 = 0.88$ (Fig. 4.14), which suggests that 88% of the variation in thickness can be attributed to the properties of fabric as assessed in the proposed points scheme. In this regression analysis no account was taken of the bias in the data, e.g. the thickness of the slate from the *old vein* Oakley Quarry, Ffestiniog is not as thin as possible but limited to 4mm for commercial reasons. However slates from other seams were split to produce the thinnest roofing slates possible without tapering. (Per. com. Mr E Williams Ffestiniog Slate Quarries. In fact there are several situations where a slate is not split to its minimum thickness, hence this data set does not reflect the true splitting ability of the slate but rather an effective splitting as determined by the economics of production, requirements of the industry etc. ***In spite of this bias, the high correlation value recommends the fabric points scheme***

as a useful procedure in determining the potential splitting ability of a slate deposit.

The minimum thickness to which a slate can be split has a direct bearing on the economics of a quarry. For example, a quarry with the potential to split slate to 4mm has twice the potential yield as a vein with an "8mm" fabric. This is why the *best* slate from each quarry refers to the thinnest slate in production and not to other properties such as durability etc.

Correlation of the grain size and the cleavage surface:

The grain size affects the spacing of the cleavage domains as well as affecting the surface of the slate. Fine grain size has a silky texture while a coarse grained slate has a rough and gritty feel. The limited data available for Scottish slate suggest that a larger grain size increases the ability of a slate to absorb water. This has important consequences to the durability of a slate and is discussed further in Chapter 5.

4.4 The Fabric of Scottish Slate

The fabric of Scottish slate, collected from the various quarries or from second-hand slate dealers, has been assessed according to the procedure described above. Using the relationship derived from the multivariate statistical analysis described (Section 4.3.2.4), the minimum commercial thickness of Scottish slate was calculated and where possible compared with actual thicknesses (Appendix 4.2).

$$t = 12.645 e^{-0.06933x}$$

t = thickness mm

x = number of fabric points

The fabric points scheme (FPS) relates the microscopic properties of the slate fabric to its splitting ability and does not take into account factors which are localised or only seen on a macroscopic scale. Such factors, relevant to Scottish slate, are:

- The presence of pyrites locally distorts the cleavage fabric and increases the minimum thickness of thicker slate.
- Crenulation cleavage common in Easdale slate.

- Refraction of cleavage due to changes in grain size.
- Undulating cleavage.

The assessment of Scottish slate is described in the various quarry reports (Appendix A) and only a limited discussion is given here to show how the FPS has been used to evaluate the fabric and where possible to support the assessment with anecdotal evidence. A selection of photographs of various fabrics of Scottish slate is shown in Figs. 17- 20, but no direct comparison can be made with the results in Appendices 4.1 and 4.2. The latter are based on the average measurements made at many locations, and not on the single location shown in the photographs.

4.4.1 The Fabric of Ballachulish slate

A selection of fabrics of Ballachulish slates from different quarries is shown in Fig. 4.16. These fabric range in FPS values from 15 to 7 (17 to 7), which equates to thicknesses of 4.4mm to 7.6mm (4.5mm to 8.0mm). The spacings of CDs at East Laroch (Appendix A 2.5.1) are 20μm (Fig. 4.16a) indicating a fine-grained material giving a smooth surface, while that from Khartoum (Appendix A 2.5.3) is coarser grained with CD spacing of 40μm (Fig. 4.16c). In general, CDs are planar and continuous and the degree of mineral alignment is high ranging from 50 to 60%. The microlithons also have a high degree of alignment. All of these characteristics point to a slate with good splitting potential. The one-hundred-year-old slate has the best fabric, closely followed by a sample collected from the *best seam* as described in the Wartime Pamphlet No 40 (Richey & Anderson 1944). These two samples have the most closely spaced CDs and highest degree of homogeneity. The lowest values were obtained for Khartoum due to the widely spaced cleavage domains and lower homogeneity. Historical records suggest that the Ballachulish slate was split to a thickness of 6-9mm which is slightly thicker than the potential thickness as predicted by the fabric points scheme (Appendix A 2.4.4.4).

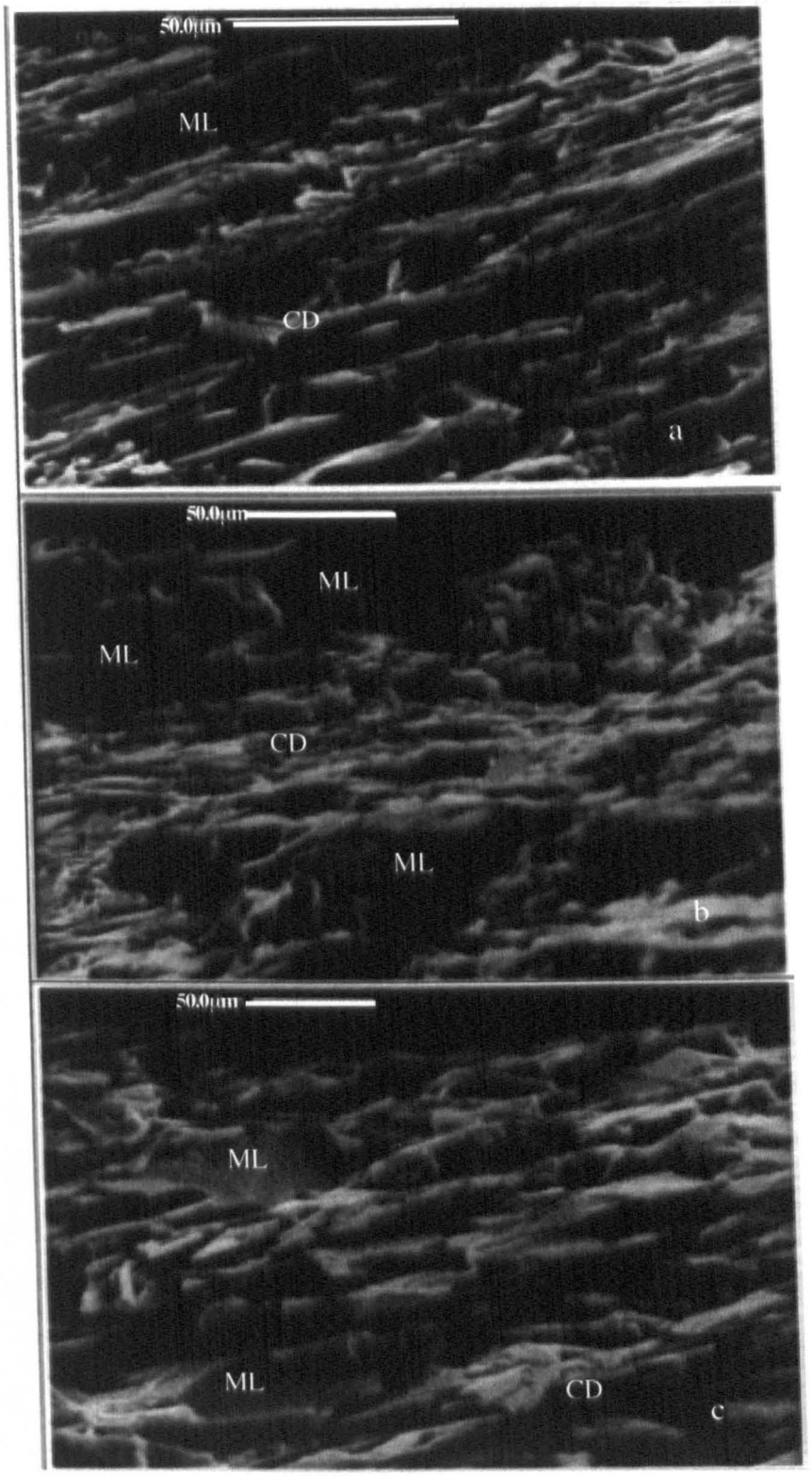

Fig. 4.16 Fabric of Ballachulish slate a) East Laroch EL-3 b) West Laroch WL-5 c) Khartoum K1 These slates have closely-spaced straight cleavage domains separated by zones of aligned minerals in the microlithons. Estimated commercial thickness of slates from these quarries is 6-7mm.

4.4.2 The Fabric of Easdale Slate

The fabric of the Easdale slate group varies considerably from quarry to quarry (Fig. 4.17). The FPS values vary from 14 to 5 (16 to 5), which equates to a potential minimum thickness of 4.9mm to 8.9mm (5.0mm to 9.2mm). Peach *et al.* (1909) report that the average thickness of Easdale slate is ¼ inch (6mm).

The finest grained material with the most closely spaced cleavage domains was found at Easdale Island (Fig. 4.17a, Appendix A 3.5.1), Toberonochy (Fig. 4.17e, Appendix A 3.5.5) and Port Mary (Fig. 4.17f, Appendix A 3.5.7), while the coarsest grained and hence most widely spaced CDs were found in a sample of Belnahua slate (Appendix A 3.5.11). CDs are generally straight and occasionally anastomosing.

Pyrite cubes are common at some locations in Easdale slate; in a sample of Balvicar slate it can be seen cutting across the cleavage fabric (Fig. 4.17b), while in a sample from Breine Phort it distorts the cleavage (Fig. 4.17c).

Judging from the few finished slates measured, the slates were not cut as thinly as that determined theoretically (Table 4.3). This may be due to a lack of accuracy of the fabric points scheme but is more likely due to the need for a thicker slate in Scotland's climatic conditions.

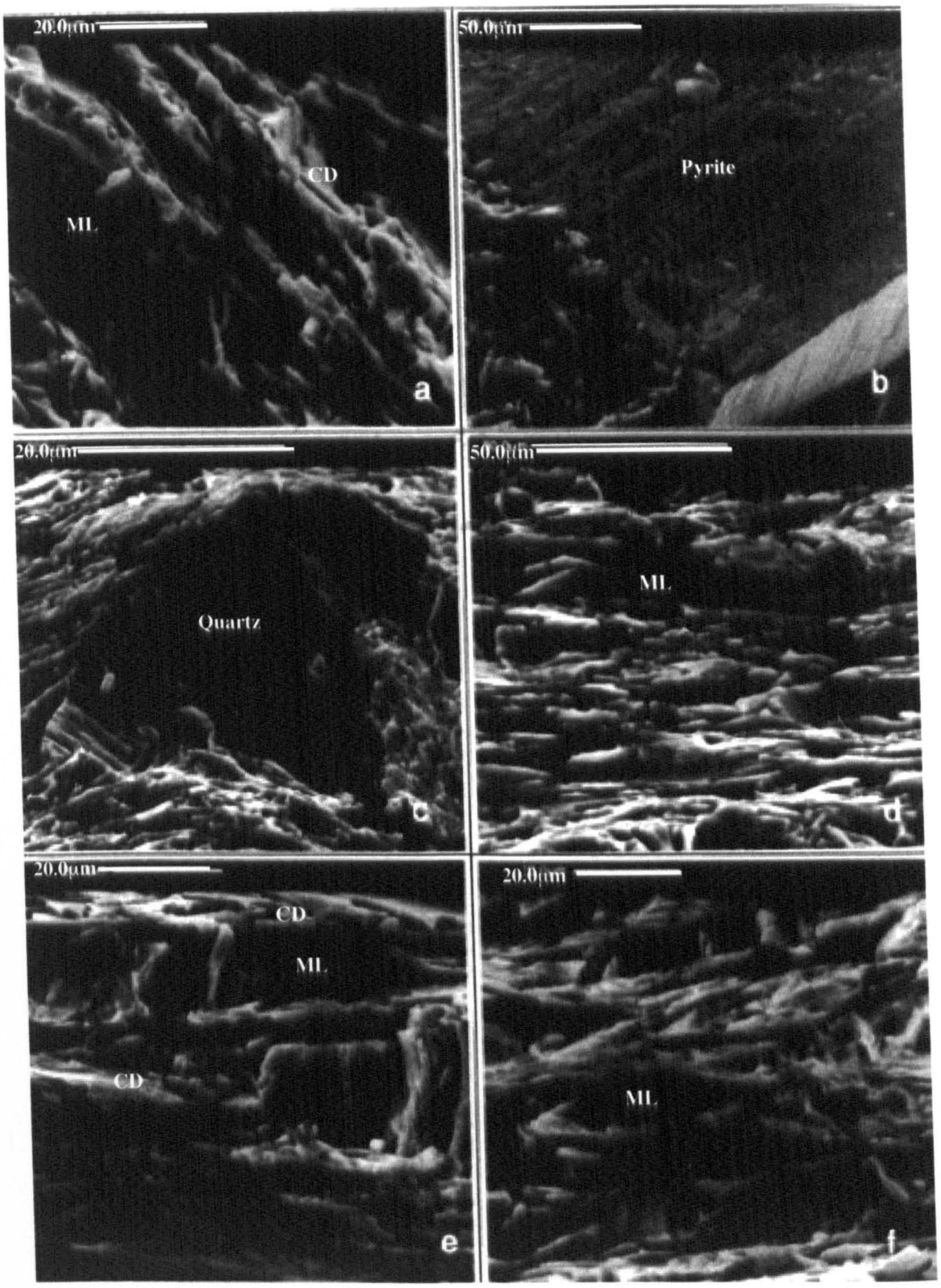

Fig. 4.17 Fabric of Easdale slate a) Easdale Island EE-3 used-slate. Although irregularly spaced, the cleavage domains are straight and continuous. This slate has an estimated commercial thickness of 6mm but is actually 9mm thick. b) Balvicar SB-2 This sample has an estimated commercial thickness of 8mm. This view shows an euhedral mineral of pyrite truncating the cleavage. c) Breine Phort SB-5 This view shows the cleavage domains wrapping around a grain of quartz. d) Breine Phort SB-5 In this view, the cleavage domains are straight and closely-spaced giving it an estimated commercial thickness of 5mm. e) Toberonochy LT-2 used-slate. Straight closely-spaced cleavage domains and microlithons with aligned minerals give this sample an estimated commercial thickness of 6mm. The actual thickness is 8mm. f) Port Mary LP-6 Straight and closely spaced at regular interval give this sample an estimated commercial thickness of 5mm.

4.4.3 The Fabric of Highland Border Slate

With only a few samples from individual quarries analysed it is not possible to know how representative the following comments are.

Arran (Fig.18a, Appendix A 4.5.1)
The samples collected were fine grained, cleavage domains closely spaced, straight and continuous and the degree of alignment of minerals low. The theoretical minimum thickness is 5.2mm (5.3mm)

Luss (Appendix A 4.5.3)
Fine grained, closely spaced cleavage domains were straight and continuous with 50% alignment of minerals suggesting good splitting. However on a larger scale the cleavage is undulating and this is indicated as low homogeneity slate. The theoretical minimum thickness is 5.8mm (6.1mm). A Luss slate, not assessed, had a thickness of 8mm.

Aberfoyle (Fig.18b & c, Appendix A 4.5.4)
Several samples of Aberfoyle slate were evaluated and showed a wide range of results, indicating the variation within one group of quarries. The slate is coarse grained, with spacing of cleavage domains of 30-40μm, anastomotic and fairly continuous. The degree of alignment varies from 40% in the *best seam* (as described by Mr Ferguson, a retired Aberfoyle quarrier) to 15% in AB-3. The microlithon has little fabric. The average theoretical minimum thickness is 7.4mm (7.2mm), which agrees with the actual thickness of a used slate (8mm) AB-6, estimated as over 100 years old by Mr. Cummings, second-hand slate dealer, Perth. The lowest values were obtained for AB-4 and AB-5 which substantiates the comments of the quarrymen e.g. AB-5 comes from the *best seam* as identified by Mr Ferguson and AB-4 was selected by Mr Williams as having the best potential from Lockout Quarry.

Aberuchill (Fig.18d, Appendix A 4.5.5)

The fabric in the Aberuchill quarries is poorly developed, CDs are spaced 25μm to 30μm and are discontinuous and irregular. There is a low degree of alignment of minerals and quartz grains in the microlithons are only slightly elongated. The FPS assigns a minimum theoretical thickness of 10.4mm (10.5mm) to the samples from this area. The sample of slate from a local Aberuchill farmhouse (not assessed) was 12 mm thick.

Craiglea (Fig. 18e, Appendix A 4.5.6)

The fabric of two samples of Craiglea slate was assessed, one collected from the quarry waste tips and the other from a local farmhouse. The latter had a considerably better fabric than that from the quarry. The CDs of the used slate sample have a spacing of 21μm and are straight and continuous, while those from the quarry are more widely spaced, anastomotic and discontinuous. The finished slate also had greater alignment of minerals both overall and within the microlithons and a higher degree of homogeneity. This variation highlights the problem of assessing the fabric of a quarry based on too small a data set. The FPS assigned a theoretical minimum thickness of 8.7mm (9.0mm) to the quarry sample and 6.1mm (6.9mm) to the finished slate which was actually 9-11mm thick.

Dunkeld (Fig. 18f, Appendix A 4.5.7)

The samples of Dunkeld slate collected in the quarries are fine grained with CD spacing of approximately 20μm and are straight and continuous with some alignment of minerals. The theoretical minimum thickness is 5.2 - 6.7mm (5.2 – 6.8mm). A used slate supposedly from a Dunkeld quarry (per. com. Mr. Cummings, second-hand slate dealer) had a poorer fabric, a theoretical minimum thickness of 8.9mm (9.2mm) and an actual thickness of 10mm.

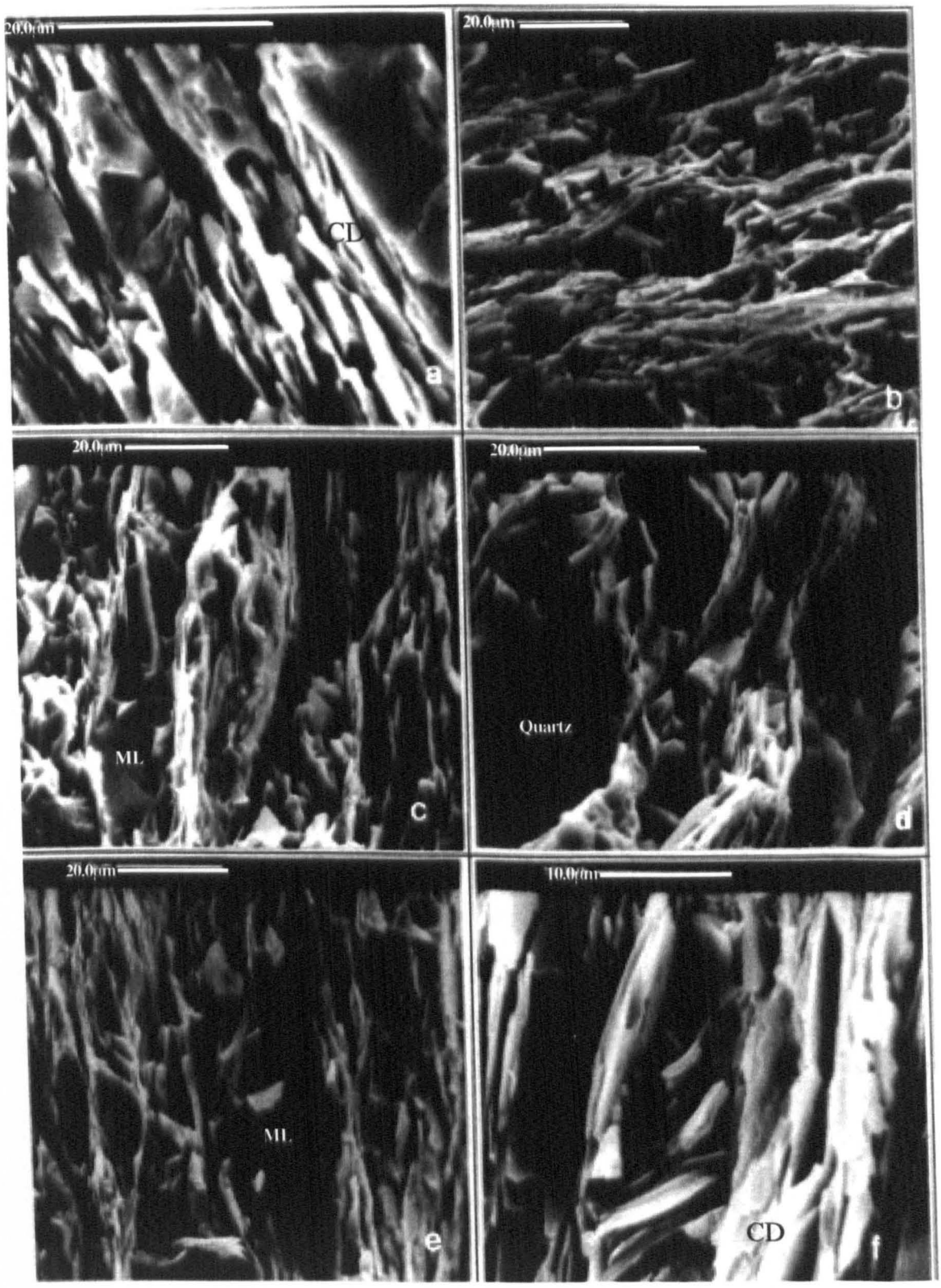

Fig. 4.18 Fabric of Highland Border Slate a) Arran A-1 The fabric has straight closely spaced cleavage donains. The estimated commercial thickness is 5mm b) Ab-5 Cleavage domains are anastomosing around the microlithons. The estimated commercial thickness is 7mm. c) Aberfoyle Ab-6 used-slate is 8mm thick. d) Aberuchill Au-1 Large quartz grains are separated by thin anastomosing cleavage domains. Estimated commercial thickness is 11mm. e) Craiglea Cr-3 used-slate. This slate has a relatively high proportion of aligned minerals giving it an estimated commercial thickness of 6mm although the actual thickness is 9mm. f) Newtyle DN-3 Straight closely-spaced cleavage domains give this an estimated commercial thickness of 5mm. Note the larger scale.

4.4.4 The Fabric of Macduff Slate

Macduff slate is relatively homogeneous over a large area including all the slate hills. The average CD spacing is 26 μm with a standard deviation of 6. The shape is anastomotic and about 50% continuous. The degree of alignment is fairly low in both the CDs and the microlithons. The overall homogeneity is medium. The FPS determined minimum thickness to be approximately 8mm.

Slates from Tillymorgan have minimum theoretical values of 8.5mm (7.9mm). A sample collected from a *bald patch,* which is assumed to be the location at which slates were dressed (see Appendix A), was examined to see if the quarrymen of old were able to select slate of above average fabric quality. However the sample had a minimum theoretical thickness of 8.6mm (8.1mm) which suggests no such selection. This was confirmed on examining MF-14, a slate from the barn at Greystone Farm on the Hill of Tillymorgan, which had a minimum theoretical thickness of 9.1mm (8.8mm). Again a finished slate did not have a better than average fabric. This slate sample was 14mm thick although it has a potential of being split to 9mm by modern production techniques as predicted by the FPS.

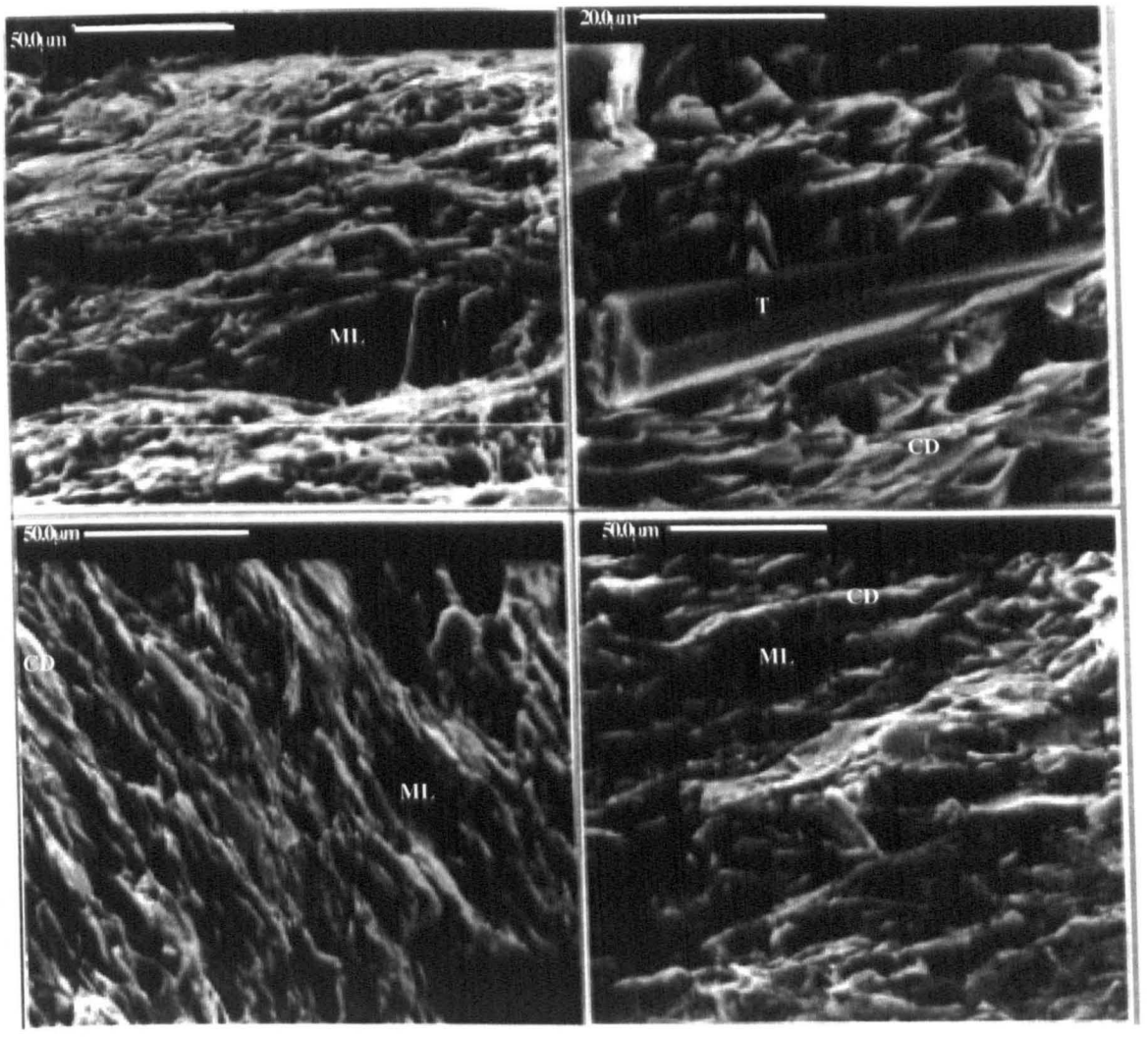

Fig. 4.19 Fabric of Macduff slate a) Corskie MC-2. Cleavage domains are anastomosing around the microlithons. The estimated commercial thickness is 10mm. b) Haining MH-2. The cleavage domains are straighter and more closely spaced than in the Corskie sample, giving it an estimated commercial thickness of 7mm. The euhedral mineral marked T is tourmaline. Note the larger scale. d) Foudland MF-2. This has straighter and more continuous cleavage domains than the average Macduff slate, giving it an estimated commercial thickness of 6mm. e) Foudland used-slate MF-14. Cleavage domains are widely spaced and anastomotic. This has an estimated commercial thickness of 8mm although the actual thickness is 14mm.

4.4.5 Discussion

The fabric points scheme was used to estimate the splitting ability of slate from Scottish quarries. In order to determine how well it achieved this objective, the thickness of finished slates was compared with the thickness as determined by the points scheme. The sources of slates used in this comparison were (i) from second hand sources where only the source area was known but not the actual quarry (ii) finished slates found in the quarry which were generally not split to their potential minimum thickness or (ii) finished slates found on local farm buildings where the source quarry was almost certainly known. The results of this comparison are shown in Table 4.3.

Slates which had reached the market are probably a truer guide to the average thickness of the finished slate produced from a particular quarry or group of quarries than rejects found in the quarry. In all cases the actually thicknesses were greater than that determined theoretically. This may suggest a faulty FPS but is more likely to suggest that slates were not split to their minimum thickness because of the need for thicker slate for Scottish climatic conditions.

Sample	Quarry or group of quarries	Source	Theoretical thickness mm	Actual thickness mm
BX-1	Ballachulish	2nd hand dealer	5	9
EE-3	Easdale Island	local building	6	9
EX-1	Easdale	2nd hand dealer	9	10
LC-3	Cullipool	quarry	8	9
BB-1	Belnahua	quarry	8	15
Ab-6	Aberfoyle	2nd hand dealer	8	8
Cr-3	Craiglea	local building	7	10
DX-1	Dunkeld	2nd hand dealer	10	10
MF-14	Macduff group	local building	9	14

Table 4.3 Comparison between the theoretical and actual thicknesses of Scottish slates.

Slate dimensions

The thickness is only one dimension of the slate, albeit a very important aspect. The other dimensions such as the length and breadth of a slate are controlled by geological factors in the quarry which govern the dimensions of the slate block which can be extracted. This is a function of spacing and orientation of discontinuities such as veins, joints etc. within the quarry. The effect of such discontinuities can only be investigated on a fresh quarry surface, and hence it is not possible in the weathered Scottish quarries. Instead, a theoretical approach is used in Section 6.5.4 to demonstrate the inter-relationship between size of slates produced and the spacing and orientation of discontinuities.

4.5 Conclusions

In this section the fabric of slates from producing quarries in North Wales and Cumbria was evaluated using a points scheme based on submicroscopic properties of the cleavage. The results were correlated with the actual thickness of the slate and the relationship between the potential minimum commercial thickness value assigned to the slate based in the points scheme and actual thickness was determined by regressional analysis.

This relationship was then used to predict the potential thickness of Scottish slate. The validity of the method was assessed by comparing the actual thicknesses of used Scottish slates with their theoretically determined potential thickness. It was found that there was a tendency for finished slates to be split thicker than a Welsh slate with a corresponding number of points but in several examples there was good agreement to within 1mm. However it is worth noting that the closest agreement between the potential commercial thickness and actual thickness was found in those slates which had been sold and used on a roof, rather than those found rejected within the environs of the quarry. No slate was split thinner than the theoretical limitation.

The relationship between fabric and thickness of finished slates was based on that observed for Welsh and Cumbrian slates. A wider range of samples from quarries world-wide should be studied to provide a broader data set to test this relationship more thoroughly.

The FPS was then applied to a few samples from all the slate quarries described in Appendix A and a potential splitting ability was determined. As in all aspects of this work, the data set was spread too thinly to allow a more rigorous statistical analysis to be made. This results in observations which may not be representative of the natural variation in the quarry. However it gives a preliminary estimate of the splitting quality of the slate from all of the Scottish slate quarries reviewed.

Chapter 5 Weathering Properties

5.1 Introduction

As slates are extensively used as a roofing material they are most exposed to severe weather conditions acting on the building. There is little or no protection from extremes of temperatures, rain, ice, snow and high winds. High winds can lift slates so that they rotate on their securing nails and can also deflect the rafters, straining the slates to breaking point if secured too tightly. Slates are also exposed to flue gases and leaching from deposits of soot as well as a polluted atmosphere in industrial areas.

In common with other exterior building materials slates are weathered by both chemical and physical methods:

Chemical weathering, where ionisation, hydrolysis and oxidation of minerals takes place as the system of slate, air and water approaches equilibrium. A major contributory factor to chemical weathering is acidic attack of susceptible minerals within the slate by polluted atmosphere.

Physical deterioration of slate is due principally to the mechanical action of wind. Although essentially a chemical agent, water also acts in a physical manner as it expands and contracts in cracks when subjected to freezing and thawing cycles.

The aim of this part of the research is to understand the changes which take place in a slate on a roof and then to devise a method which experimentally reproduces these change to enable prediction of the life-spans of new slates

5.2 Background - Weathering Reactions

There have been various studies of the chemical reactions that take place in the weathering of slate. Some have looked at the weathering reactions which take place *in situ* while other studies have examined those that have taken place in a finished

slate. An example of the former is that carried out by Bayliss and Loughman (1964) in slate in New South Wales. They examined the change in the mineral composition of the slate with depth i.e. a depth profile and found that of the three major minerals in slate quartz, crystallised illite and chlorite/montmorillonite, that chlorite is the least stable, being destroyed in the leached zone. In contrast quartz content is left unchanged while the degradation of illite is confine to the surface layer. Kaolinite is the end product of the breakdown of both chlorite/montmorillonite and illite. minerals.

Before looking at the weathering of Scottish slates it is necessary to discuss the processes involved. Chemical weathering of any building material is brought about by the actions of water, acid and oxygen.

5.2.1 Dissolution - Action of Water

The most important agent of weathering is water. In a dry atmosphere, the weathering of rocks proceeds extremely slowly as can be seen in the preservation of carved inscriptions dating from over three thousand years ago in the arid climate of Egypt, and by the slow decay of stone (including slate objects) in museums. Moisture performs a number of functions; it is the agent of transfer, bringing solutions into contact with solids and so allowing reactions to take place, it carries dissolved CO_2 and other atmospheric agents into the slate and is also a continuous supply of oxygen to facilitate reactions and biochemical activity.

Dissolution

Soluble minerals are dissolved by ionisation as in breakdown of feldspar to clay and quartz. In a strong leaching environment, clay minerals (Section 2.2.2.2, Fig. 2.3) such as kaolinite and halloysite are the common weathered products.

$$2NaAlSi_3O_8 + 9H_2O \rightarrow Al_2Si_2O_5(OH)_4.2H_2O + 4H_2SiO_3 + 2NaOH$$

Albite **Halloysite**

However in an environment that is only mildly leaching, illite (Table 2.1) or montmorillonite are produced.

$$3KAlSi_3O_8 + 8H_2O \rightarrow KAl_2(AlSi_3O_{10})(OH)_2 + 6H_2SiO_3 + 2KOH$$

Orthoclase **White mica**

(Montmorillonite has a dioctahedral structure similar the white micas but lacking potassium ions)

These reactions depend on the removal of the alkali cations to proceed which is not possible in slate having low porosity. Of the feldspars plagioclase is more vulnerable to weathering but this feldspar is not the generally found in slate. Hence the hydration of alkali silicates is not an important reaction in the weathering of slates.

The weathering of white micas depends on the ease at which potassium can be removed by dissolution. One approach is to compare the stability of white mica with another potassium bearing mineral such a biotite. It was found that there was considerable disparity in the rate of solution of potassium ions from dioctahedral muscovite and trioctahedral biotite, the former being much more stable (Loughnan 1969). This has been attributed to the differences in orientation of hydroxyl groups (Bassett 1960) to the presence of oxidisable iron in the latter (Walker 1949). Whatever the reason the conclusion is that potassium cations fixed in muscovite are not easily removed. This suggests that the closer the white mica (the dioctahedral phyllosillicate found in slate) approaches muscovite the less vulnerable to weathering. Therefore the white mica in Easdale slate, which has an alkali cation content of approximately 0.8 per formula unit, is more vulnerable to weathering than that found in the other Scottish slate areas, all of which have a alkali cation content greater than 0.9 per formula unit (Table 2.7).

Of greater significance is the weathering of carbonates

$$CaCO_3 + H_2CO_3 \rightarrow Ca^{2+} + 2HCO_3^-$$

and hydration of anhydrite to gypsum

$$Ca\,SO_4 + 2H_2O \rightarrow Ca\,SO_4.2H_2O$$

These are two important weathering reactions.

5.2.2 Weathering of Carbonates - Action of Acid

Pure water is neutral with a pH of 7 but natural water in equilibrium with the atmosphere contains dissolved carbon dioxide, resulting in a weak acid with a pH of 5.7, making it a much better dissolving agent. Other acids, such as nitric acid may also contribute to the acidity of natural water, but of greater importance are sulphur acids H_2SO_3 and H_2SO_4 which are strong acids and hence lower the pH considerably.

$$CO_2 + H_2O \leftrightarrow H_2CO_3$$

$$H_2CO_3 \leftrightarrow H^+ + HCO_3^-$$

5.2.2.1 Calcium carbonate

Calcium carbonate, found as two polymorphs, calcite and aragonite, is only slightly soluble in pure water but dissolves slowly in natural water due to the formation of calcium bicarbonate

$$CaCO_3 + CO_2 + H_2O \rightarrow Ca^{2+} + 2HCO_3^-$$

In the presence of a strong acid it reacts rapidly giving off carbon dioxide gas. Where that acid is sulphurous or sulphuric acid, hydrated calcium sulphate i.e. gypsum is produced.

$$CaCO_3 + H_2SO_4 \rightarrow CaSO_4 + H_2O + CO_2\uparrow$$

In a study of slate weathering, Roekens *et al.* (1991) took slates from St Rombout's Cathedral in Mechelen, Belgium constructed from the 13th to the 15th century. Mechelen is located in the polluted industrialised area between Antwerp and Brussels. They found that the un-weathered part of the slate contained micas, quartz and minor amounts of aragonite but no pyrite. In contrast the weathered portion of the slate showed fan-shaped splitting which on AAS (Atomic Absorption Spectroscopy) and EDXRF (Energy Dispersive X-ray Fluorescence) analysis revealed increased Ca^{2+} and SO_4^{2-} i.e. gypsum concentrations. The aragonite in the slate had reacted with atmospheric sulphur (in the form of sulphurous acid) to form gypsum which causes expansion and splitting due to its larger molar volume. In

their study Roekens *et al.* concluded that other acids found in the atmosphere such as NO_2 and HCl were of minor importance.

5.2.2.2 Other carbonates

Other carbonates such as magnesite, siderite and dolomite are also susceptible to weathering.

Siderite $FeCO_3$ is only deposited when a source of Fe^{2+} is available i.e. in reducing conditions (Section 5.2.3). It is less common in slate than calcite and its solubility constant is 1/100 of that of calcite, making it more resistant to weathering (Table 5.1). There is continuous solid solution between siderite and magnesite.

Magnesite $MgCO_3$ The magnesium carbonate has a greater solubility constant than calcite and is only precipitated in evaporites (Table 5.1). It can also form at high temperature or as a product of weathering of magnesium rich rocks. An epidiorite sill on the east coast of Luing and Seil close to Balvicar and Toberonochy slate quarries (Appendix A 3.5.) may well be the source of the magnesite found in the samples analysed from these quarries.

Dolomite $CaMg(CO_3)_2$ Dolomite is a very common rock yet it is not produced in the laboratory without extremes of pH or high concentrations of anions. The answer to this conundrum may lie in its organised crystalline structure of alternating Ca^{2+} and Mg^{2+} cations, which can only be produced slowly or at high temperature experimentally. It is often found in Scottish slate where its low solubility constant is very unreactive (Table 5.1).

Apatite $Ca_5(PO_4)_3(F,OH)$ Although not a carbonate, apatite is included here for completeness. It is a hydrated calcium phosphate salt, traces of which are found in most slates, but as can be seen from its solubility coefficient (Table 5.1), it is extremely insoluble and hence unreactive.

Solubility products of carbonates and apatite		
Magnesite	2.0×10^{-5}	
Calcite	4.5×10^{-9}	
Siderite	3.0×10^{-11}	
Dolomite	10^{-17} - 10^{-19}	No precise figure available.
Apatite	10^{-58}	fluoroapatite
	10^{-60}	hydroxyapatite

Table 5.1 Solubility products of the most common carbonates and apatite (Krauskopf 1967)

Ease of weathering is roughly in line with the solubility constants i.e.

magnesite >calcite >siderite >>dolomite >> apatite

When considering the effect the presence of carbonates has on the durability of a slate, the type of carbonate present should also be taken into account.

5.2.3 Oxidation - Action of Oxygen

Second only to water is the role oxygen plays in weathering reactions. Metals such as iron combine with oxygen to form soluble products.

5.2.3.1 Definition of Oxidation

When an element is oxidised, it losses one or more electrons, represented by the half equation,

$$M \rightarrow M^n + ne^-$$

Oxidation does not occur in isolation, but is always accompanied by reduction, where some compound or element accepts the released electrons. These two complementary processes are called a redox reaction. However it is oxidation and more specifically that of iron and sulphur compounds, that is relevant to the weathering of slate.

5.2.3.2 Oxidation of Iron Compounds

Iron can exist in one of three oxidation states, the metal, Fe^{2+} ferrous compounds and Fe^{3+}, ferric compounds. In slate, ferrous iron is found in chlorite, to a lesser extent in phengite and in iron sulphides, all of which are susceptible to oxidation, producing bright, usually rusty-coloured staining.

Any ferrous compound on prolonged exposure to air is oxidised e.g. the reaction for the weathering of a chlorite containing ferrous iron, such as ***brunsvigite*** (Table 2.6), shows the overall conversion of ferrous to ferric iron, the releasing of silica and ionisation of non-oxidisable metals like magnesium.

$$Mg_3Fe_2Al\,(AlSi_3O_{10})(OH)_8 + 1/2O_2 + H_2O \rightarrow 3Mg(OH)_2 + Fe_2O_3 + Al_2Si_2O_5(OH)_4 + SiO_2$$

This overall reaction takes part in stages, probably initiated by oxidation of the Fe^{2+} to Fe^{3+} thus upsetting the balance of the charges between the tetrahedral and the octahedral layers.

The oxidation state of iron in the iron sulphide minerals is also important in considering the vulnerability of slates to weathering i.e. the relatively reduced form pyrrhotite FeS is much more easily weathered than the more oxidised form pyrite FeS_2. This is discussed in greater detail in Section 5.2.3.5.

Ferric iron can be present in many forms such as oxides and hydrated oxides.

Anhydrous oxides	Fe_2O_3 haematite and its less common polymorph maghemite.
Hydrates	FeO.OH. nH_2O goethite and lepidocrocite.

Haematite is an iron ore mineral common in slate due to its great stability and insolubility. Field evidence (Appendix A) suggests that haematite-rich layers follow bedding and hence it is a diagenetic mineral and not always a product of weathering. Other ferric compounds such as goethite, or its fine-grained equivalent limonite, exist, although the precise conditions under which they form are largely unknown.

Although not susceptible to oxidation these minerals can be weathered by dissolution. Limonite is the field term used for hydrated iron minerals which cause the rusty-brown staining observed in the many Scottish slate quarries.

5.2.3.3 Oxidation of Manganese

Manganese (Mn) is also oxidisable, but in a more complicated manner than iron because of its numerous oxidation states. The reaction products are less conspicuous being black and less abundant because of the relative scarcity of the element.

5.2.3.4 Oxidation of Sulphur

The oxidation of sulphur is very relevant to the weathering of slate. Sulphur has a range of oxidation states from $^{-}2$ when bonded to a metal to $^{+}6$ when present as sulphuric acid.

$$FeS + 2H_2CO_3 \rightarrow Fe^{2+} + H_2S + 2HCO^{-}_3$$

$$H_2S + 2O_2 + Fe^{2+} + 2HCO^{-}_3 \rightarrow FeSO_4 + 2H_2CO_3$$

5.2.3.5 Oxidation of Iron and Sulphur

Iron and sulphur are found together in slate as pyrite FeS_2 and pyrrhotite $Fe_{1-x}S$ Pyrite is found as an euhedral mineral or disseminated throughout the rock. When present as crystalline cubes, pyrite is resistant to weathering, which accounts for slate with *diamonds* (term used by quarriers for cubes of pyrite) having a good reputation. When pyrite is present as small rounded grains disseminated throughout the rock it is less crystalline and hence readily altered to limonite. Pyrrhotite does not form euhedral crystals and alters readily to a mixture of iron minerals.

The type of sulphide found in a particular slate is controlled by its metamorphic history, the oxidation state of metamorphic fluids and the extent to which the following redox reaction has gone to completion.

$$2FeS \leftrightarrow FeS_2 + Fe^{2+} + 2e^-$$

Both pyrrhotite and pyrite are found in Ballachulish and Easdale slates. The former is often found as lenses within crystalline minerals such as quartz and pyrite. Pyrites are found as large porphyroblasts which post-date the growth of the matrix minerals and the development of cleavage. The source of the pyrrhotite is problematic. Pyrite is the iron sulphide which forms during the diagenesis of anoxic organic rich sediments (Section 5.3.1), therefore pyrrhotite must form at a later stage. One suggestion is that it formed during metamorphism due to the reduction of disseminated pyrite. One of many possible reactions suggested by Thompson (1972) is

$$2\ FeS_2 + C + (2FeO)_{silicates} \rightarrow 4FeS + CO_{2\ fluid}$$

which according to Hall (1982) is a low grade metamorphic reaction taking place at the achizone/ greenschist boundary.

At a later stage in its metamorphic history, possible during post-metamorphic uplift (Hall *et al.* 1988), microfractures formed allowing relatively oxidising fluids to penetrate the rock. This reversed the process causing pyrrhotite to dissolve, be oxidised and re-precipitate as large pyrite porphyroblasts.

Under different metamorphic conditions pyrites in the North Ballachulish slate quarries, have been converted to pyrrhotites during contact metamorphism (Section 5.3.1).

These few examples demonstrate the complexity of the history of pyrite/pyrrhotites The extent that this process has gone to completion controls the weathering properties of the slate. Pyrites are stable, as are pyrrhotites founds as lenses within pyrites but pyrrhotite, found as disseminated amorphous material, is easily weathered.

Slate No 1		
Fresh	Quartz chlorite muscovite pyrite paragonite feldspar	
Surface stain	Hydronium jarosite	$Fe_3(SO_4)_2(OH)_5.2H_2O$
Salt crust	Halotrichite	$FeAl_2(SO_4)_4.22H_2O$
Loose flakes	Melanterite	$FeSO_4.7H_2O$
Slate No 2		
Fresh	Quartz muscovite chlorite haematite goethite feldspar paragonite and kaolinite	
Upper layer	Gypsum	
Reddish stains	Increase in the amount of goethite and haematite at the loss of chlorite	
Lower layer	Gypsum, hydronium jarosite with a translucent crust of gypsum	

Table 5.2 Weathering products of slate after Shayan and Lancuck (1987)

The profiles of weathered slates studied by Shayan and Lancuck (1987) showed considerable disintegration on the upper surface and a globular salt on the under surface. The decrease in the amount of chlorite on the weathered portion relative to the fresh part of the slate showed that chlorite had weathered, producing hydrated sulphates of iron and aluminium (Table 5.2).

Both slates, one containing pyrite and one containing haematite, have very similar weathering products but in addition gypsum was formed in slate no 2, although the source of calcium needed to produce gypsum was not identified.

5.3 Weathering in the Scottish Slate Quarries

Alteration of slate *in situ* takes place as the rock is subjected to changing conditions during its metamorphism and subsequent uplift. Weathering takes place in the late stages of uplift as it nears the earth's surface until eventually it is exposed at the surface. Slate reactions, which occur on exposure to oxidising atmospheric conditions, are the subject of this Section. Scottish quarries have not been used for 50 to >200 years and the effect of superficial weathering can be seen in both the

remaining outcrops and in the reject tips. These observations have been described in the individual quarry reports (Appendix A).

5.3.1 Environment of Deposition

The conditions under which the original deposits were deposited and underwent diagenesis have a lasting effect on the properties of the slate. If it is assumed that the slate did not change its oxidation state during subsequent metamorphism, then the aspects of slate discussed here can be directly related to its earlier history.

The low energy environment necessary for the deposition of mudstone (the precursor of slate) is often associated with stagnant, reducing. One example of such conditions is the stagnant basin in which the Ballachulish deposits were laid down conditions (Hickman 1975). In such an environment, sulphates were reduced to sulphides and pyrite formed. Organic matter was not completely recycled and the residue became graphite when the rock was metamorphosed. When such deposits are exposed to the atmosphere millions of years later they are vulnerable to oxidation. At ordinary temperatures, oxidation is extremely slow, but the rate of the reaction is increased in the presence of water which dissolves minute amounts of the reactants.

The environment of deposition which produces the thinnest slate is also associated with the relatively un-oxidised minerals, pyrite and carbon, which lead to its deterioration. This is particularly true when the pyrite is disseminated throughout the rock and causes intensive brown staining e.g. in Balvicar Quarry (Appendix A 3.5.4). In the Ballachulish group of quarries the pyrites were converted to pyrrhotite during contact metamorphism associated with the intrusion of the Ballachulish granite (Hall 1982). These pyrrhotites have weathered out leaving large holes in the lower level quarries at North Ballachulish (Neumann 1950).

5.3.2 Effect of Environment of Deposition on Slate Properties

Scottish slate has characteristics which reflect the environment of deposition e.g. the reducing conditions under which Ballachulish (Appendix A 2.2.1.3) and Easdale (Appendix A 3.2.1.2) protoliths were formed produced a dark blue to black slate due to the presence of graphite. Some of the Easdale slate is less graphitic and consequently more blue slate was produced.

In contrast the slates of the Macduff area are derived from a sequence which included turbidites, which were laid down in relatively oxidising conditions and as a result the iron ore mineral found in such quarries is haematite (Sutton & Watson 1955). The colour of Macduff slate is typically grey due to a high white mica/chlorite ratio. Weathering in these quarries is due to the deterioration of chlorite. Light brown staining due to the weathering of chlorite is often noted along joint. Weathered chlorite is also associated with quartz veins in some quarries.

The situation is more variable in the Highland Border slate and in a few quarries, e.g. Aberfoyle (Appendix A 4.5.4) and Dunkeld (Appendix A 4.5.7), the colour of the slate can change abruptly from purple to green. This may reflect a sharp boundary between the oxidising and reducing conditions at the time of diagenesis. The best quality slate in several Highland Border quarries, such as Craiglea (Appendix A 4.5.6) and Dunkeld, is from fine-grained red deposits which are associated with deep water. In reducing conditions the ferrous iron combined to form chlorite while in the oxidising conditions the ferric iron was taken into haematite.

5.4 Experimental Weathering of Slate

It is difficult to assess how well a test or group of tests can predict the durability of a slate, and diverse methods have been used over the years to evaluate the quality of the material. One approach, and the one followed in this Report, ***is to determine***

how a slate deteriorates with time and then to devise tests which produce a similar deterioration experimentally. However, this should ideally be carried out using data from a range of slates with known history, which is not often available. In the absence of such a comprehensive data set, the results of the experiments can be verified to some extent by reference to the reputation of the slate in the trade.

5.4.1 Weathered Slate

While some work has been done on the chemical reactions which have taken place in weathered slate (Section 5.2) it is necessary to relate this to changes in properties of the roofing material.

Kessler & Sligh (1932) examined the effect of weathering on 61 samples of old slates exposed from 12 to 131 years and found that there was a loss of strength and an increase in water absorption with time (Fig.5.1). Comparing the data with those for fresh samples, it was possible to determine the average annual increase in water absorption and the average yearly decrease in strength. Some correlation was found between the two parameters ($R^2 = 0.69$) showing that both water absorption and loss of strength are a feature of weathering. This is substantiated by examination of data gathered by the Building Research Establishment BRE on weathered slate, where there is an increase in water absorption with the age of the slate (Fig.5.2), but there is no equivalent data for loss of strength with age. ***Therefore the test which simulates the weathering of slate experimentally should also produce an increase in water absorption and loss of strength as well as exhibiting chemical weathering as discussed in Section 5.2.1.***

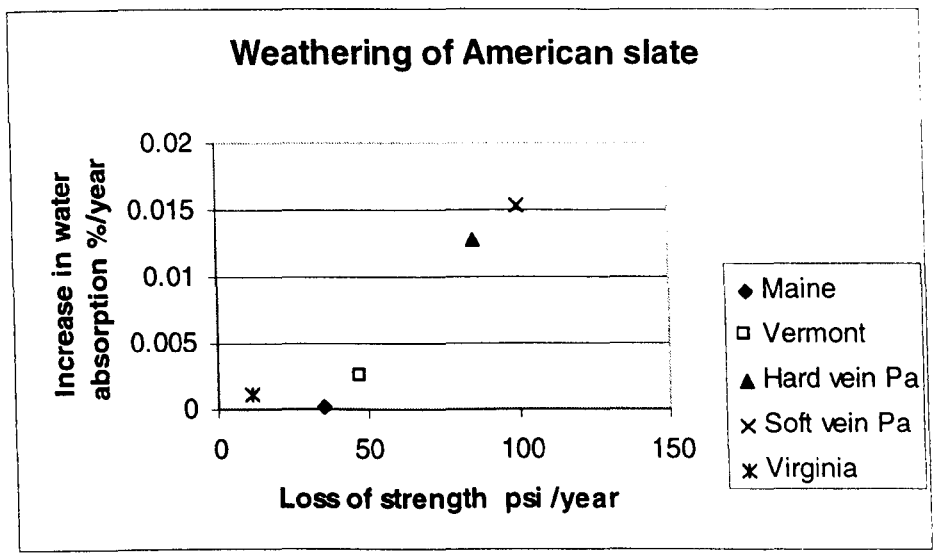

Fig. 5.1 Loss of strength and increase in water absorption observed with ageing after Kessler & Sligh (1932)

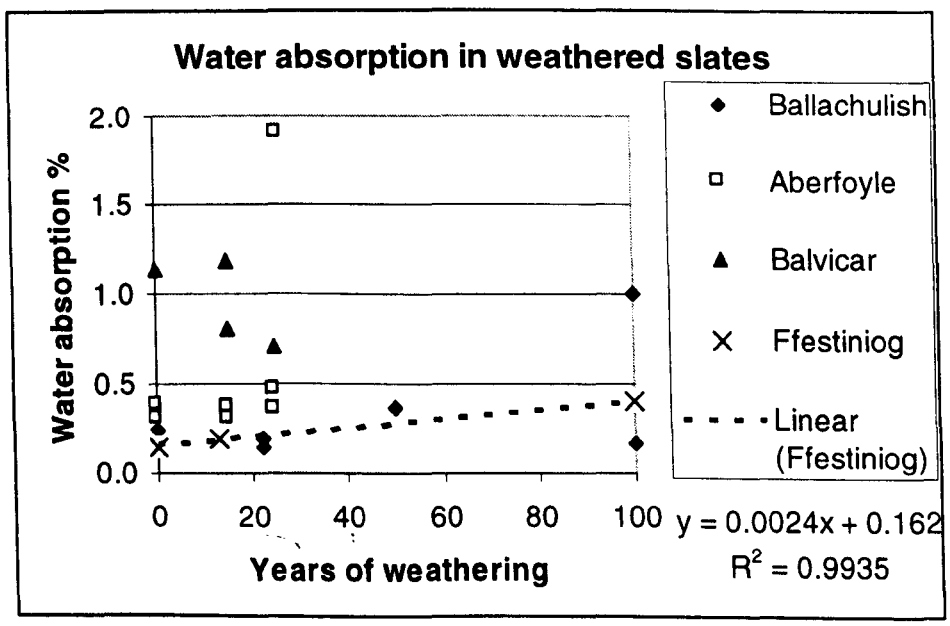

Fig.5.2 Increase in water absorption with years of natural weathering. Source of data BRE archives.

5.4.2 Unweathered Slate

Two studies of the best methods of evaluating the durability of roofing slates have been carried out. The first comprehensive study was carried out on American slates by Kessler and Sligh (1932) and the second was carried out in the preparation of the

British Standard for slate BS 680 (Watkins 1934, BRE archives). The first study, based on a data set of 343 samples, has provided a wealth of data against which it has been possible to compare the performance of Scottish slate.

Data collected from the BRE archives has been invaluable in providing a few results for fresh samples of Scottish slates as well as the source of the following opinions on the relative merits of slate from different Scottish quarries.

> *"In my opinion Ballachulish, Toberonochy and Easdale are best. At the same time the Ballachulish slate of today is not of the same quality as 20 years ago. Aberfoyle and Luss are next in quality and Balvicar in the third category. Aberfoyle is liable to be slightly soft after say 15 years under cover."* Mr Sommerville, Superintendent of Maintenance, Corporation of Glasgow 1947.

5/2/47

> *"Ballachulish is the best, Balvicar is very poor, Cullipool is good, Aberfoyle blue is soft, lasting for example 20 years on a Grangemouth roof, but the green is good. Luss is soft and of short life"*, (Mr Robertson, a slater with 50 years experience from a family of slaters).

30/1/47

> *Ballachulish has the best reputation, followed by Aberfoyle. The remainder, including Cullipool and Balvicar, are about the same quality. Aberfoyle and Cullipool have water absorption greater than .30 and fail BS 680 contrary to their good reputation.* (Mr McNecol, Director of Aberfoyle slate quarries)

In addition information from Mr Elfed Williams of Ffestiniog slates quarries on the quality of slates from different sources was found to be very reliable. Other sources of information were used when corroborating information was obtained.

5.4.3 National Standards for Slate

National standards for slate, designed to assess its durability, have been set by some countries. However, the considerable differences in approach adopted by the different countries gives some idea of the complexity of the problem, and limits set often reflect the type of slate produced in the particular country.

Synopses of the several different national standards for countries within the European Union are given in Appendix B, although these are soon to be replaced by a new European Standard prEN12326. Because this Report continually refers to the data published on American slate (Kessler & Sligh 1932) a précis of the American standard has also been included.

It is not possible to look at all the methods proposed to test slate and the following discussion has been limited to those tests which appear to fulfil the criteria in Section 5.4.1:

1. Flexural strength
2. Water absorption
3. Wetting and drying

5.4.3.1 Flexural Strength of a Slate. Modulus of Rupture Rα

Failure of a slate is often caused by tensional stresses due to gravity, or bending stresses resulting from the uplifting effect of the wind. Flexural strength is the usual criterion for the strength of a slate, as it is considered a more appropriate measure than the more standard compression test used in the evaluation of other building materials. Results are reported as the modulus of rupture, a measure of the intrinsic strength of a material (Appendix B 3.6 for details).

$$R\alpha = \frac{3Pl}{2be^2}$$

Rα = Modulus of rupture in newton/mm^2

P = Failure load in newtons

l = Distance between support bars of the three point bending machine

b = Width of test piece in mm

e = Thickness of slate in mm

As slate is an anisotropic material, the strength of a slate depends on the direction of applied stress, i.e. the strength of a slate along the grain is less than that across the grain (See Fig. 5.3). Kessler & Sligh (1932) found that the strength of a slate broken along the grain is on average 0.65 times that across the grain but the ratio was not characteristic of a slate producing region (Fig.5.4).

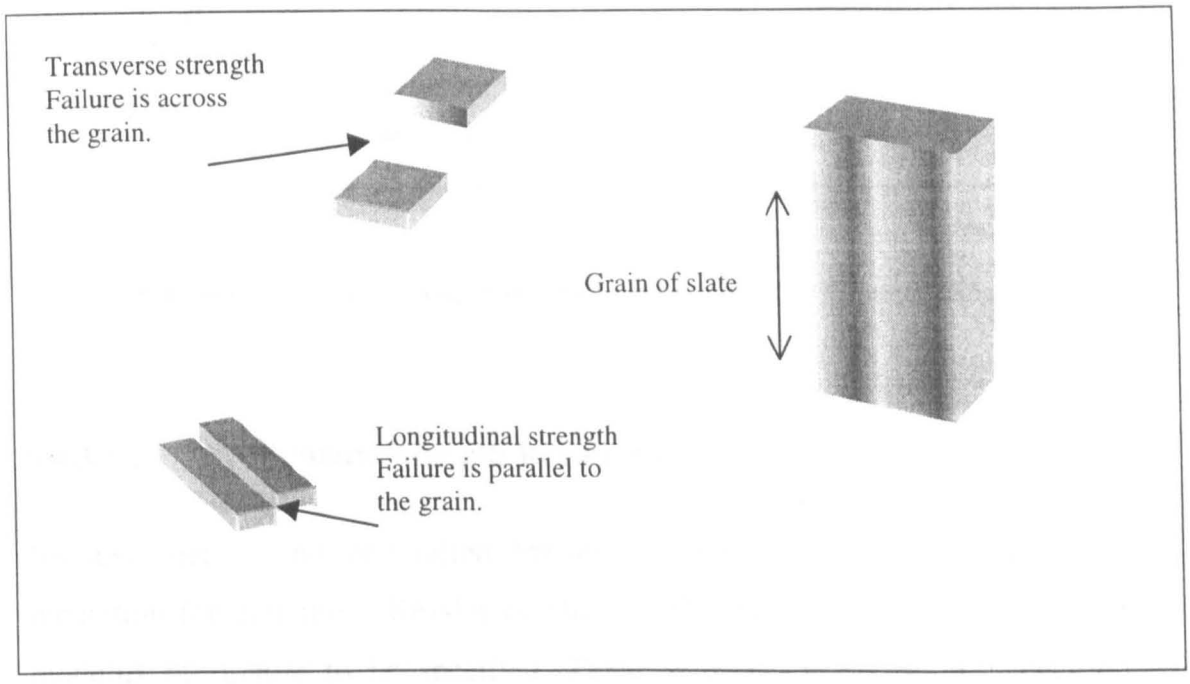

Fig. 5.3 Transverse strength; the slate fails across the grain, longitudinal strength failure is along the grain.

	Rα across grain	Rα along grain	Ratio
Mean Rα (MPa)	76	55	1.48
Standard Dev	14	12	0.45
Values range	52-97	20-87	1.1-2.6

Table 5.3 Variation in the Modulus of Rupture; data extracted from Kessler and Sligh (1932)

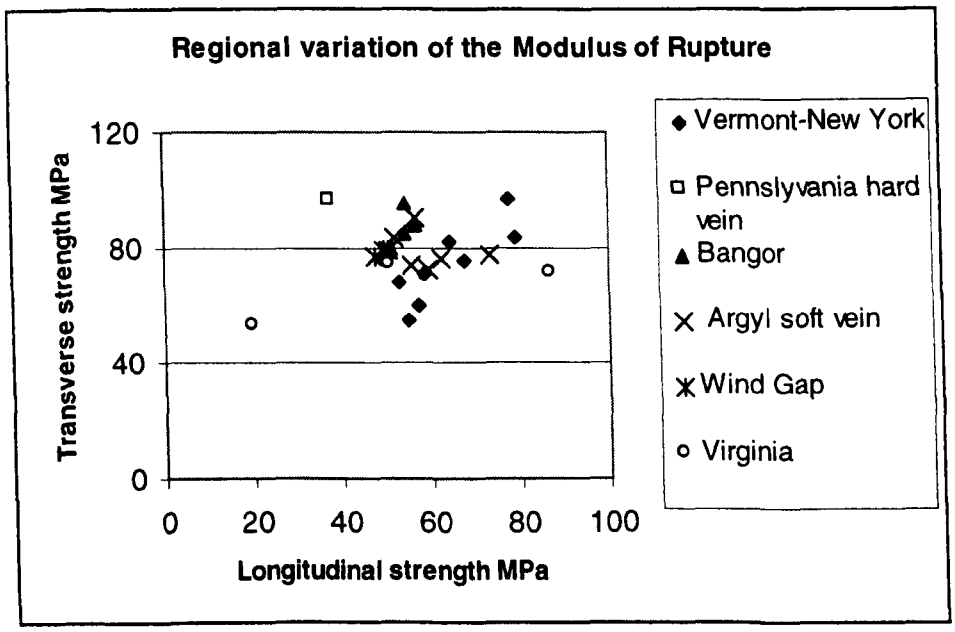

Fig.5.4 Variation in the strength of a slate with ageing after Kessler & Sligh (1932).

5.4.3.1.1 Minimum Strength Requirement

Because there is no correlation between intrinsic strength of a slate and its reputation for durability (Kessler & Sligh 1932), there is no case for a minimum modulus of rupture to be specified. There is however a case for specifying a minimum bending strength of the slate as produced. For example Spanish slate is reported (trade literature and press) to have a low intrinsic strength and when split too thinly for the British climate often fails. This has been rectified to some extent by producing a thicker slate for the British market.

As the strength of Welsh and English slate is greater than that specified for other roofing materials, the British Standard has no minimum requirement, and as a result it was possible to import weaker slates into Britain.

Several countries do have minimum requirement in their standards, but limits set vary considerably, e.g. that set by the Spanish is conspicuously lower than that set by the French and the American standards (Table 5.4).

To determine an appropriate minimum strength, that set for man-made tiles and slates was considered, but because of different testing conditions no direct comparison was possible.

Limits MPa		Grade 1	Grade2	Grade3
PrEN12326	E.U.	A function of the thickness		
BS 680	British	No requirement		
NF P32	French	70 dry 40 wet	50 dry 33wet	33 dry 24 wet
DIN 52 201	German			
UNI 8626 & 8635	Italian	A function of the thickness		
UNE 220 201 85	Spanish	28.4 dry 22.7 wet		
C119 -74	American	62	62	62

Table 5.4 Variation in the minimum requirement for the strength of a slate as specified by different national standards. To enable comparison all units were converted to MPa.

The European Commission for Standardisation CEN has effectively set a minimum apparent strength requirement by setting the minimum thickness as a function of the modulus of rupture (Appendix B 3.12). However, as the function also incorporates a factor taking into account the climate and construction techniques, no comparison with other national limits was possible.

5.4.3.1.2 Effect of Water Absorption on Strength

Modulus of rupture when wet

Both the British and American studies investigated the loss of strength due to absorbed water as a means of assessing the quality of slate. In each case the modulus of rupture was determined after prolonged immersion, the percentage loss of strength plotted against water absorbed, measured as a percentage of the dry weight, and correlation coefficients determined (Fig. 5.5). The American study showed a loss of strength of approximately 30% regardless of the source of slate, and no relationship with water absorption. The British study did however suggest some correlation with water absorption. The significance of this will be discussed in Section 5.4.3.2.1.

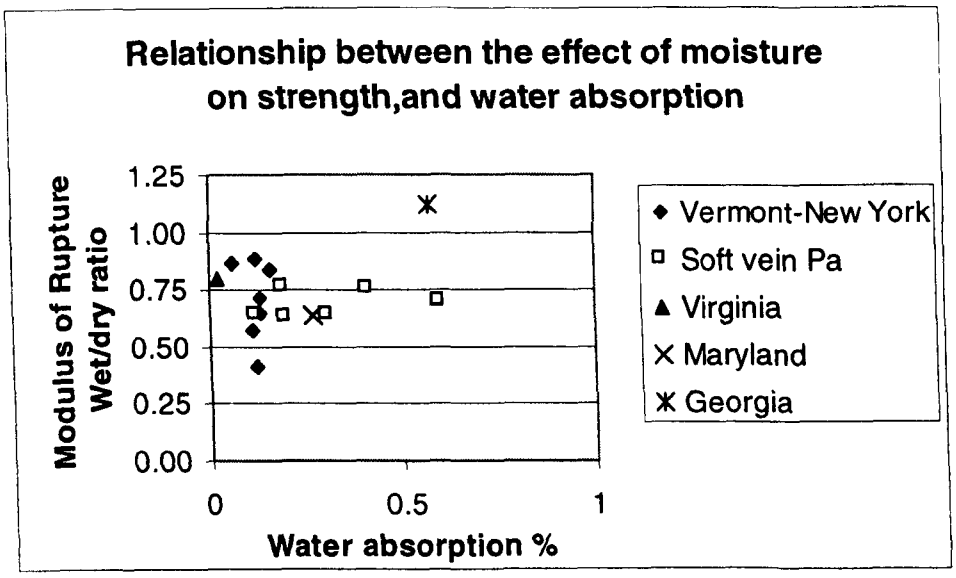

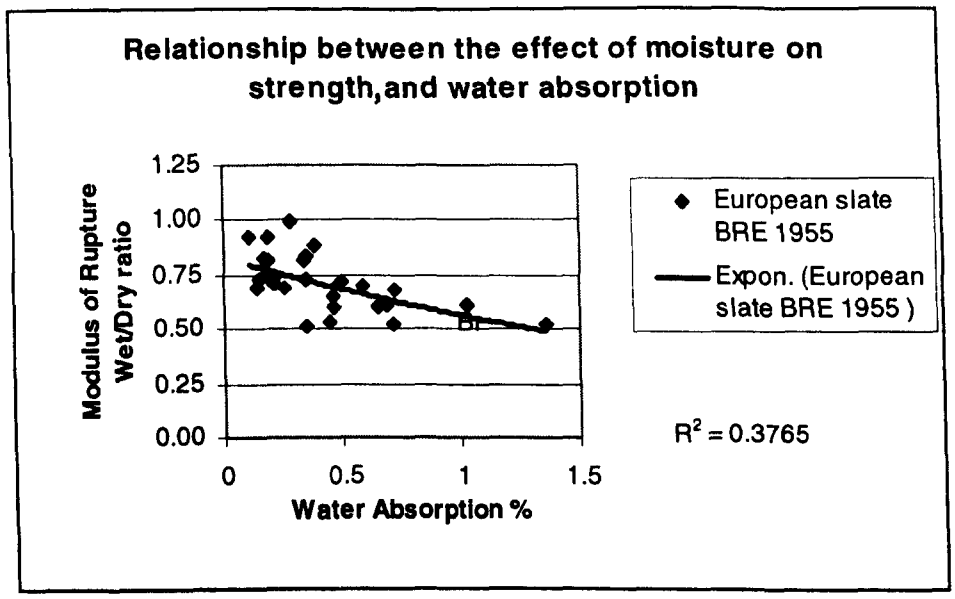

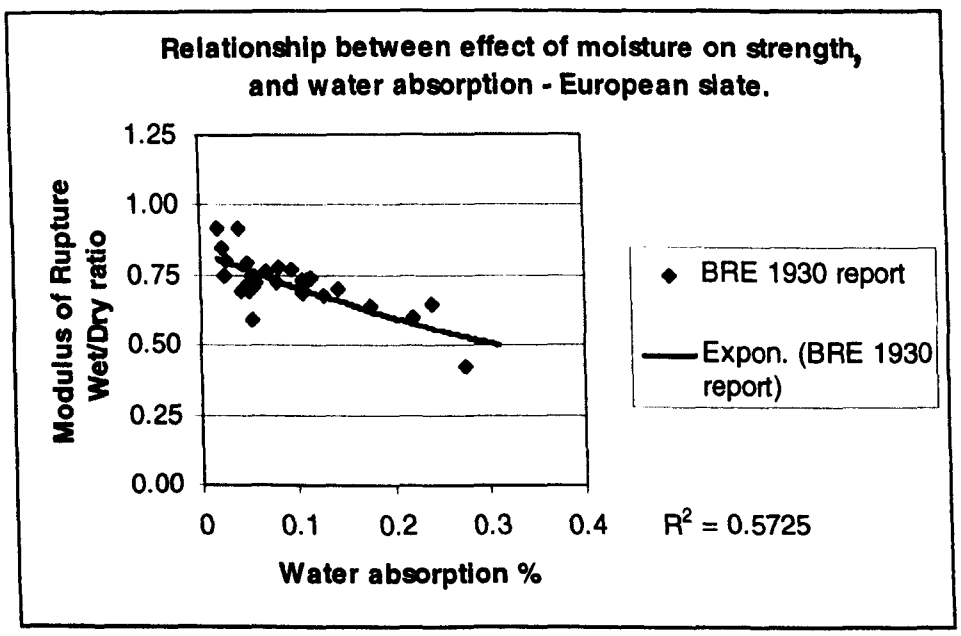

Fig. 5.5 Relationship between water absorption and loss of strength a) American slates after Kessler and Sligh (1932) b) European slates tested by BRE 1955 (BRE archives) c) European slates tested by BRE 1930 (BRE archives).

Rate of decrease in strength

It is not the initial strength of the material that is important but the rate of decrease of strength. Some standards test the strength of a slate before and after an experimental weathering procedure e.g. the Italian standard requires less than 20% reduction in strength for a slate subjected to a thermal cycle test (Appendix B 7.2). In theory this is valid, given that loss of strength is one of the characteristics of a weathered slate, but in practice it has its limitations. The test is destructive and hence the same slate cannot be tested before and after experimental weathering. As there is considerable natural variation in strength, even within one quarry, this is a serious problem.

5.4.3.2 Water Absorption

Water is present in slate in the pores and is also an essential constituent of some minerals such as clays. Because of the importance of water in all weathering reactions, the determination of porosity was considered important. Kessler & Sligh (1932) found an average porosity of 0.88% for all the slates in the American study. But of far greater importance is the amount of water absorption, which although related to porosity, is also controlled by permeability, pore size and other properties of the slate. Kessler & Sligh (1932) found a correlation figure $R^2 = 0.5$ between porosity and water absorption.

5.4.3.2.1 Limits of Water Absorption

One of the characteristics of weathered slate is an increase in the ability to absorb more water during a set period of time (Section 5.4.1). All national standards reviewed include a test of water absorption although there is considerable variation in the testing procedures as well as in the limits of absorption allowed (Table 5.5).

Values for absorption vary considerably depending on the testing procedure e.g. the BS 680 method of boiling increases the water absorption by 30 to 50% relative to simple immersion as carried out according to prEN12326 (Appendix 5.)

Report	Test conditions	Range of values found %	National Standard Limit %
American (Kessler and Sligh, 1932)	48 hours immersion at room temp	0-0.8	0.25
BRE 1930	24 hours at room temp	0-0.3	
BRE 1955	48 hours boiling	0-1.5	0.3
EU standard	48 hours immersion	no data	0.6

Table 5.5 Variation in water absorption test procedures

It is known from a memo in the BRE archives that the BS 680 limit was set at 0.3% to exclude foreign slate with a poor reputation. This resulted in excluding Scottish slate of good reputation (Table 5.5). Slates such as those from Aberfoyle which failed the test by a small margin (Appendix A 4.4.3) would pass the proposed European Standard test as the conditions are less stringent and the limit is set at 0.6%.

5.4.3.2.2 Rate of increase of water absorption

All national standards agree that the amount of water absorption is an important criterion in evaluating the quality of a slate. ***It is proposed here that of greater significance is the rate of increase in water absorption*** due to a period of weathering, either naturally on a roof or simulated experimentally.

From a limited number of points taken from the BRE study of naturally weathered slates (supplemented by some in-house work) it is possible to see that there is an increase in water absorption with time (Fig. 5.2).

- The Ffestiniog slate from the *old vein* in both the Greaves quarry and the Oakley quarry shows a very slow rate of increase, which is in keeping with its excellent reputation for durability.
- The Ballachulish slate shows a similar profile (in spite of the large discrepancy in the values for the 100-year-old slates).
- The Aberfoyle results shows an increase in absorption after a shorter time than the previous two types of slate which agrees with anecdotal evidence for softening after twenty years.
- The Balvicar slate has a poor reputation and the scatter of points reflects this.

This data set is too limited for any definite conclusions to be made but it is supplemented by experimental work as discussed in Section 5.5.

5.4.3.3 Experimental Weathering of Slate

There are many different procedures which aim to reproduce experimentally the deterioration observed in a slate on a roof. Some tests, such as the acid test, assess the effect of chemical weathering, while others, such as the freeze-thaw test, concentrate on the physical aspects. The wetting and drying test replicates an aspect of the environment on a roof and the results of experimental weathering mirror those seen in natural weathering.

5.4.3.3.1 Acid Testing Procedures

Many national standards try to reproduce the conditions experienced by a slate in a polluted atmosphere by incorporating an ***acid test*** either by immersion in acid as in BS 680 or exposure to acid vapour as in the proposed EU standard (Table 5.6). Although slates which fail the test exhibit softening and exfoliation as observed in natural weathering, there is much dissatisfaction with the inability of this test to discriminate between different qualities of slate.

The British Standard addresses this problem by making the test applicable only for slate destined for use in polluted areas. Even then exception is made for Westmorland slates which, although failing the acid test, are still found to perform well in industrial areas! The proposed European standard has two forms of the test depending on the amount of calcite present.

The alternative method of exposure to sulphurous acid is a closer representation of the conditions experienced by a slate in a polluted atmosphere and is the form of the test to be adopted by the prEN 12326.

Standard		Conditions	Grading	Time (days)	Method of inspection	Appendix B Reference
PrEN12326	E.U	Exposure to SO_2 at 2 different strengths	3 grades	21	Visual Abrasion for slates with >20% carbonate	3.10
BS 680	British	Immersion in 20% H_2SO_4		10	Visual inspection	
NF	French	No acid test				
DN 52 206	German	Exposure to SO_2		14 28	Visual and change of weight	6.8
UNI 8626	Italian	No acid test				
	Spanish	No acid test				
C119-74	U.S.	1% H_2SO_4		7	Depth of softening	

Table 5.6 Variation in acid test procedures for a selection of national standards

	No of slates	No of runs	Acid test BS 680	Exposure to SO_2	No of runs
Ballachulish	5	30	Most pass	All passed	3
Balvicar	2	6	All failed	All failed	6
Cullipool	1	6	All failed	All passed	3
Toberonochy	1	6	Failed		
Aberfoyle	2	12	All passed	All passed	9

Table 5.7 Effect of acid on a selection of Scottish slates (Source: BRE archives)

5.4.3.3.2 Wetting and Drying Test

The wetting/drying (W/D) test subjects a slate to repeated cycles of immersion in water and drying in an oven, which closely reflects the conditions experienced by a slate on a roof. In the American study the oven temperature was initially at 50°C which approximated to the maximum temperatures experienced by an in-service slate. However, because of the need to accelerate the experimental weathering procedure this was subsequently increased to 105°C, which has the problem of exposing the slate to conditions not normally experienced on a roof. All chemical

reactions are accelerated by an increase in temperature, but a minimum temperature is necessary for a reaction to get started. This minimum energy requirement may well be satisfied by the high temperature of the experimental conditions, and some chemical changes may proceed which would not take place naturally e.g. the increase in crystallinity observed experimentally (Section 5.5.2.4) is not seen in naturally weathered slates.

The changes of properties of a slate experimentally weathered by the wetting and drying procedure are:

- Increase in water absorption
- Loss of strength
- Formation of gypsum

These changes mirror those observed in naturally weathered slates. Especially important is the fact that gypsum, the principal mineral found in the weathered portions of slates, can be produced in the laboratory, suggesting that the test is useful in evaluating the quality of a slate.

Supporting evidence comes from the study by Kessler & Sligh (1932) who, on recognising the importance of the formation of gypsum, studied the reaction between iron sulphide and calcite in isolation. Again gypsum formed when a mixture of iron sulphide and calcite was subjected to 100 cycles of wetting/drying. Carbon was found to accelerate the reaction, showing the role that graphite plays in the chemical weathering of slates (Table 5.8).

Sample	$CaSO_4$ wt.%	$CaSO_4$ wt. %
		Little carbon added
Calcite and pyrite	7.0	14.9
Calcite and marcasite	2.3	6.0

Table 5.8 Formation of gypsum after 100 wetting/drying cycles after Kessler & Sligh (1932)

Their work also included the wetting and drying of many slates and found that those slates containing considerable amounts of both pyrite and calcite disintegrated almost completely. Slates also showed loss of strength and increased water

absorption similar to that observed in natural weathering. In spite of this, the test was not included in the American standard due to the time needed to carry out the procedure, and instead the effect of immersion in acid was tested by abrasion. (Appendix B 9.3).

Apart from the German procedure, there is a general consensus in the test conditions from one national standard to another. The BRE report (Watkins 1934) states that 10 cycles are sufficient to produce decay in slates with appreciable amounts of pyrite.

		Wetting cycle		Drying cycle			
National Standard		Temp °C	Time hrs	Temp °C	Time hrs	No of Cycles	Inspection
PrEN12362	E.U	23	6	110	17	20	Visual
BS 680	British	20	6	105	17	15	Visual
NF P32-302	French	18	8	105	15.5	25	Visual
Din 52204	German	20	0.25	Heated to 105		25	Change in strength
UN 22-197	Spanish	20	4	105	20	25	Change in weight

Table 5.9 Variation in conditions for the wetting/drying test

5.4.3.3.3 Other tests

The freeze-thaw

Frost action is considered to be one of the common causes of stone weathering, but given the low porosity and water absorption of slate, frost is not a serious problem in its weathering. In the American study only one sample failed after 1374 cycles and that sample had shown signs of weathering before the test commenced.

The thermal cycle test

A test involving cycles of heating and cooling is proposed by the European standard, to determine the effect the expansion and contraction of the component minerals. Kessler & Sligh (1932) found that the two samples that failed a similar test in their experiments contained calcite and sulphide and would have failed the wetting and drying test anyway.

5.4.3.4 Evaluation of Tests

Experimental weathering

The most reliable experimental test of weathering of slate is the wetting and drying test, as the slate shows the same signs of deterioration as naturally weathered material. Experimental exposure of slates to acid vapour also shows a similar effect to naturally weathered slate but special allowances have to be made for slate with considerable amounts of calcite. The American Standard assesses the degree of deterioration due to acid exposure by abrasion (Appendix B 9.3), which determines the depth of softening on the surface. Kessler & Sligh (1932) state that the acid test would give erroneous results for slates with considerable amounts of calcite but because American slates in production at the time had very little calcite the abrasion test was adopted. Yet the new EU Standard proposes to test slates with high calcite using an abrasion technique. It would be interesting to reconcile these two conflicting views by experimental work in the future.

Water absorption

The amount of water absorption varies considerably according the methods of testing. Watkin (1934) states that it takes a month for water absorption to stabilise at room temperature, a process which can be speeded up by boiling. This is the method used in BS 680 although most other national standards preferred a simple immersion technique, which is a better representation of natural conditions.

As discussed in Section 5.4.3.2.1, the limits set by different national standards vary considerably. Historically, limits of water absorption have been set pragmatically in an attempt to exclude slate of perceived poor quality. However it was recognised that this also excluded slates with a proven record, as can be seen in an extract from a memo in the BRE archives.

> *Some French and some Scottish slates of good reputation and Prescelly slates fail to meet the requirements of the Standard for no other reason than that their water absorption exceed by a small margin the present limiting value (0.3 per.cent). A simple*

> *relaxation of the water absorption requirement would have the effect of admitting for rural use slate of poor quality...*(Note C 330 BRE archives)

A more scientific approach to setting a water absorption limit will be discussed in Section 5.5.

Relationship between loss of strength and increase in water absorption

Given that an increase in the capacity of slate to absorb water and loss of strength are characteristics of natural weathering, it was expected that the reduction in strength due to soaking in water would correlate with the volume of water absorbed. Analysis of the data for American slates in Kessler & Sligh's study showed no such correlation (see Fig.5.5a). This may have been due to the time of immersion (48 hours at room temperature) being insufficient for equilibrium absorption. This idea is supported by data from the BRE 1955 Report where there is some correlation (R^2 = 0.39) between water absorption carried out by boiling and loss of strength (Fig. 5.5b). However the 1930 Report also showed some correlation too ($R^2 = 0.55$) when immersion lasted only 24 hours (Fig.5.5c). There are several reasons for inconsistency in these results such as (i) insufficient data or (ii) variation in the conditions under which the modulus of rupture tests were performed. It is clear that loss of strength due to immersion in water is not a useful method of assessing the quality of a slate.

The conclusion from the foregoing is that ***the best procedure for evaluating the durability of slate is to subject it to experimental weathering by repeated cycles of wetting and drying and to measure its deterioration by the increased ability to absorb water. This will be discussed further in Section 5.5.2.***

5.5 Experimental Weathering of Scottish Slate

5.5.1 Stability of Chlorite - Glycolation of Samples

From observations in the quarries, it was recognised that of the three major minerals (quartz, white mica and chlorite) found in slate, chlorite is the most vulnerable to weathering. This can be seen clearly in three samples of slate from Hilton Quarry, Bute (Appendix A 4.5.2).

Samples	XRD results	Quartz	White mica		Chlorite	
		24.26° 2θ	K	Na	14° 2θ	7° 2θ
Quarry sample B2	Area	2258	6708		4668	
	FWHM	0.136	0.184		0.162	
	Intensity	263	397	151	138	451
Slate from roof B3	Area	1980	7030		6412	
	FWHM	0.130	0.135		0.127	
	Intensity	238	631	133	235	784
Weathered sample B4	Area	2208	7672		2094	
	FWHM	0.170	0.181		0.133	
	Intensity	220	407	109	111	266

Table 5.10 X-ray analysis of Bute slate showing preferential weathering of chlorite

Two samples were collected from the Hilton Quarry: the first sample B2 showed the normal degree of weathering and the second B4 was from a band of badly weathered slate. The XRD analyses of the samples showed little difference in the intensities and areas of the quartz and white mica peaks, but significant decrease in area and intensity of the chlorite peaks in the weathered sample (Table 5.10, Fig. 5.6). Another sample B3 collected from a derelict farm shed nearby was analysed and identified as originating from the local quarry due to the distinctive paragonite (a sodium-rich white mica) peak. This sample showed approximately the same quartz content, slightly higher white mica peaks and substantially higher intensities and areas for chlorite than the typically weathered slate from the quarry. This suggests that the producing seam was more crystalline than the samples from the quarry or that the dressed slate weathers less than slate which is exposed in the quarry face. Broadening of peaks was also observed in the more weathered slates, so that the two white mica peaks became less distinct.

Chlorite is the least stable of the three major minerals found in slates This is substantiated by the depth profile made by Bayliss and Loughman (1964, Section 5.2), field observations made in the various quarries (Appendix A) and the mineral composition of Scottish slates determined from XRF analyses (Section 2.5). These XRF analyses show that there is an inverse relationship between amount of clay and chlorite found in Ballachulish slate (Fig. 2.7) R^2 = 0.5091 while the white mica

content appears to rise and quartz content is unchanged. This suggests that chlorite is being converted to clay as described in Section 5.2.3.2. There is a similar reciprocal relationship found in Easdale slate from the Seil quarries although the correlation is very poor.

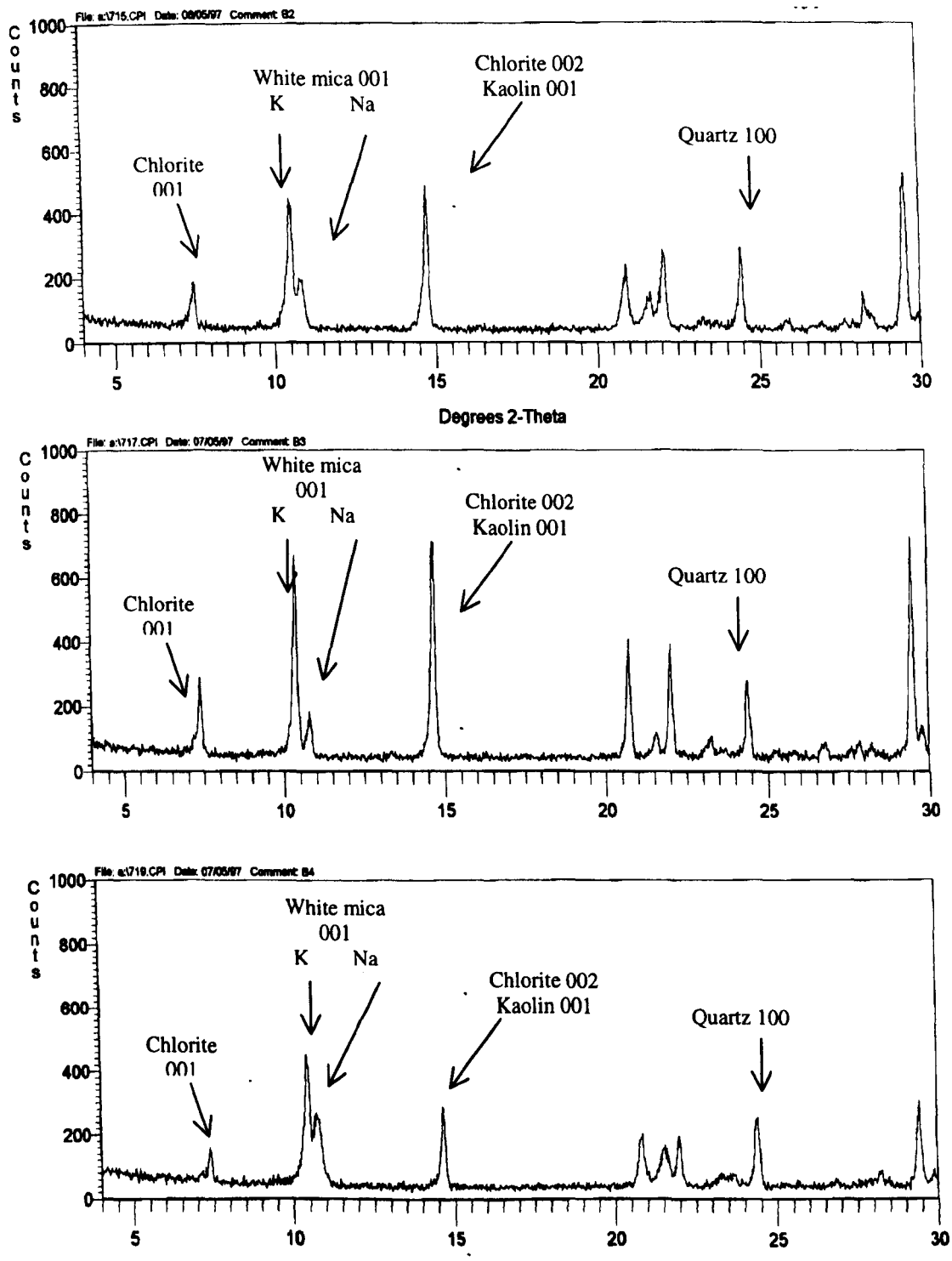

Fig. 5.6 Preferential weathering of chlorite observed in slate from Hilton Farm quarry Bute a) quarry sample b) sample from farm shed c) sample from a badly weathered band in the quarry.

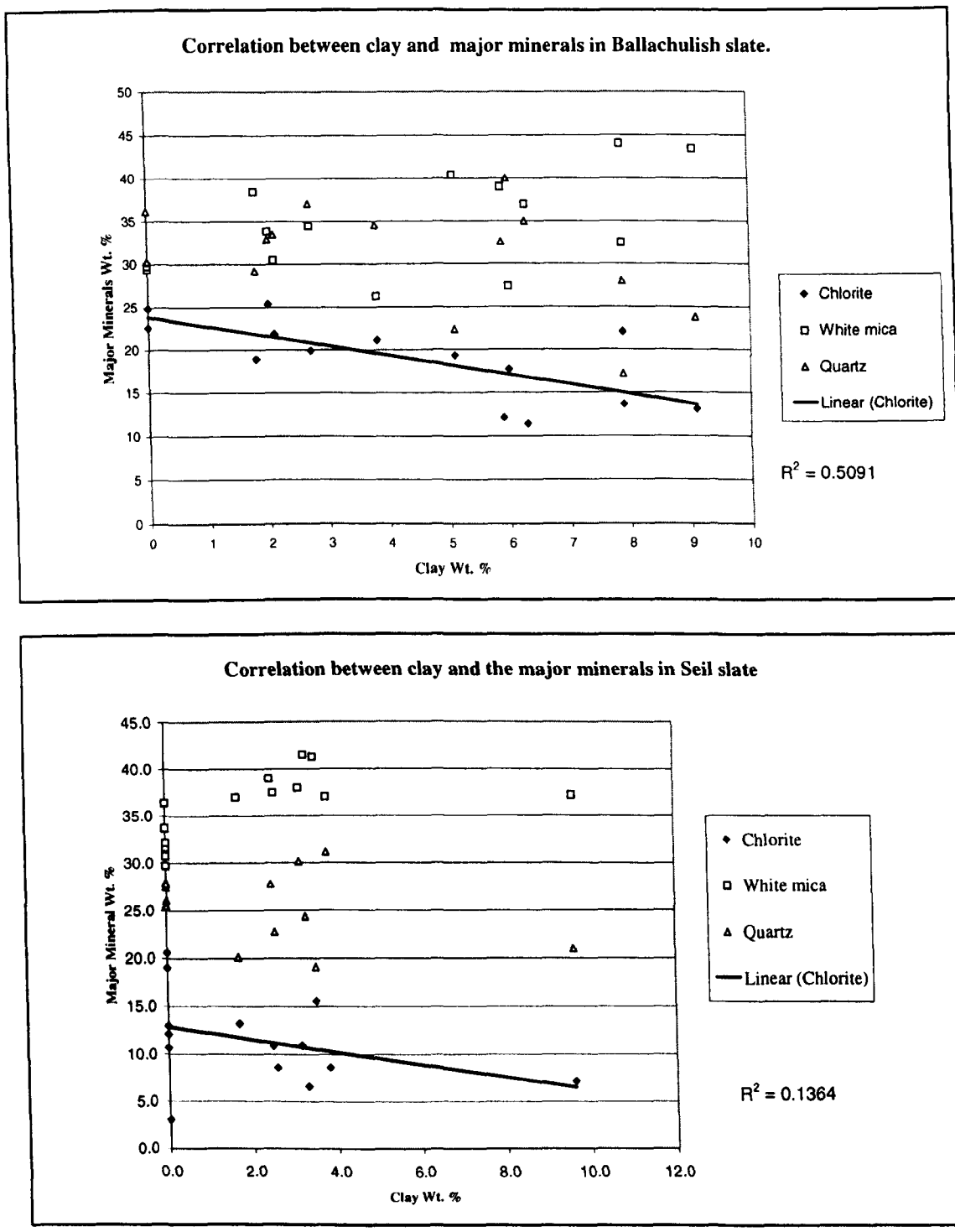

Fig. 5.7 Relationship between the weight of major minerals found in slate and clay.

Because of this tendency for chlorite to weather more readily than quartz and white mica, several samples of Scottish slate were tested for swelling by exposure to glycol for a period of 24 hours at 60°C. The effect of temperature was also determined by heating samples for one hour at 300°C. XRD scans were run on the untreated, the heated and glycolated samples and any changes in the properties of the chlorite [001] and [002] peaks and the [001] white mica peak were noted.

The following properties were checked:

- change in position of peaks due to loss/gain of water
- increase in intensity due to increase in crystallinity on heating
- decrease in intensity of the 14° 2θ peak due to kaolin becoming amorphous
- broadening of the peaks due to swelling.

Results

No general trend was observed and the variation in intensities was within the natural variation due to the imprecision of the XRD scans (Fig.5.8).

- no change in position of peaks i.e. no increase in the spacing between layers of the mineral due to glycolation (Section 2.4.1.3.1).
- variation in intensities was observed but no trend in change of crystallinity (Section 2.4.1.3.2 & 2.5.5).
- loss in intensity in the 14° 2θ for one Aberfoyle (AB-5) sample suggests that some clay became amorphous on heating (Section 2.4.1.3.2 & Section 2.5.5).
- FWHM values for Macduff slate increased by an average of 0.01 each (Section 2.4.1.3. & Section 3.4).

Discussion

Although some tentative observations have been made above, initial work suggests that none of the slates chosen were strongly affected either by heating or by exposure to glycol. Therefore considerably more work would need to be carried out to determine the statistical variation in this technique before deciding what trends are significant. The fact that the Scottish slates showed little change on glycolation does not rule out the technique as a method of assessing the stability of phyllosilicates.

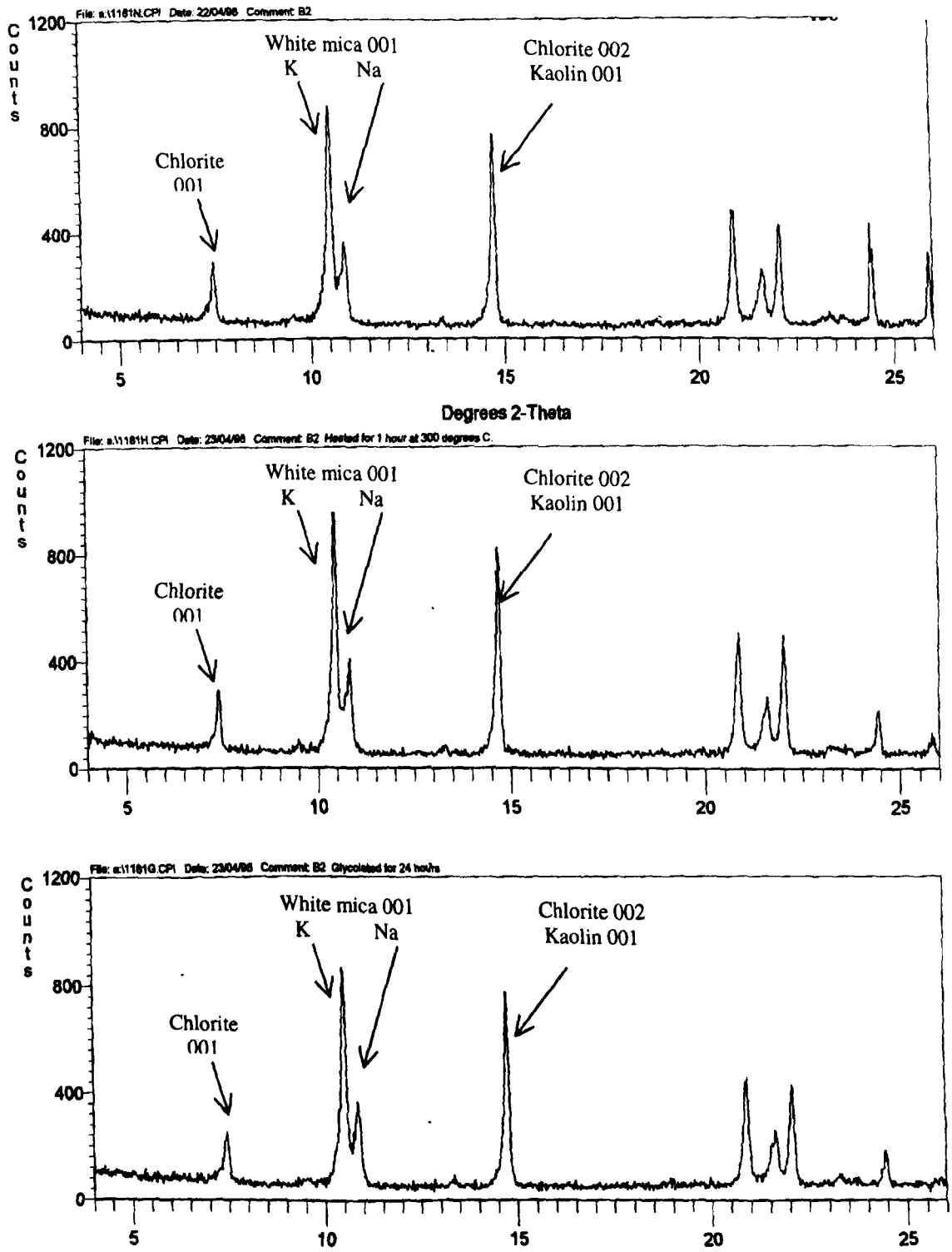

Fig. 5.8 XRD scans of a Bute slate B2 a) normal, b) effect of heating and c) effect of glycolation

5.5.2 Climatic Response

As already stated (Section 5.4.3.3.2), slates undergoing the wetting/drying test show increase in water absorption, loss of strength and formation of gypsum, i.e. the same deterioration as found in slates exposed to the elements. Therefore determining the percentage water absorption at intervals during the repeated cycles of wetting and drying would give a measure of the rate of increase in water absorption. The ***limit of water absorption*** could be set as that determined when the slate shows signs of failure. Ideally the increase in water absorption due to experimental weathering could provide a characteristic profile, which could then be compared with that observed in similar slates that have been naturally weathered and the experiment thereby calibrated. Then, given a suitable limit of water absorption, the life expectancy of the slate could be determined.

5.5.2.1 Method

The wetting-and-drying procedure followed that set out in BS 680. The periodic water absorption tests were carried out according to the procedure laid down by BS 680 and, with slight modification, that proposed in prEN 12326 (Appendix B).

- Four test pieces 5cm square were cut from each slate sample
- The cut edges of the test pieces were polished using 400 grit carborundum paste, followed by 600 grit until a smooth silky texture was obtained.
- Samples were then washed with water and scrubbed to remove any traces of carborundum paste and put in the oven for two days to dry.
- Samples were allowed to cool in a desiccator for an hour.
- Samples were then weighed to 0.0001gm. The thickness of the slate was measured to 0.1mm, at four locations using callipers.
- Two of the test pieces from each slate samples were immersed in water for 48 hours as prescribed by the prEN12326 test. The remaining two samples were placed in a flask of distilled water and refluxed for 48 hours as prescribed by the BS 680 method.

- Samples were dried with a cloth to remove surface water and weighed to 0.0001 gm (the refluxed samples having been allowed to cool for 30 minutes in a desiccator before weighing).
- The increase in weight was calculated and reported as a percentage of the dried sample weight.

When water absorption test was carried out on weathered slates with a flaky surface, loss of material during the test would give erroneous results, so the samples were dried for two days in the oven at 105°C after refluxing or immersion and re-weighed. The increase in water absorption was then calculated relative to this new weight.

Slate samples were then experimentally weathered using the wet/dry test procedure set out in BS 680, one cycle consisting of the following:

- Samples were placed in an oven at 105°C for 17 hours
- Samples were removed from the oven and allowed to stand for 1 hour before being placed in a beaker of distilled water at ambient temperature for 6 hours.

The percentage water absorption of the samples was tested four times at increasing intervals, using the prEN12326 or BS 680 method as appropriate, until approximately 100 - 150 cycles had been carried out. The thickness was measured at varying intervals throughout the test.

The test pieces were then assessed as follows:

- Visual check for signs of weathering.
- Thickness and weight changes.
- XRD analysis for change in position and intensity of peaks.

The BS 680 water absorption test, in which the samples are refluxed (boiled) for 48 hours, was thought to contribute to the deterioration of the slate. This effect was checked by performing additional water absorption tests as follows (Table 5.11):

1. According to BS 680 on those which had previously been tested only according to prEN12326.
2. According to prEN12326 on those which had previously been tested only according to BS 680.

No of previous BS 680 tests	IK3		W/F8	
	142 W/D cycles		140 W/D cycles	
	BS 680	prEN12326	BS 680	prEN12326
4	0.1293% wt.	0.1123% wt.	0.12173% wt.	0.13207% wt.
0	0.1290% wt.	0.0931% wt.	0.0977% wt.	0.0640% wt.

Table 5.11 Effect of previous BS 680 water absorption tests on the test itself

In the case of IK/3 the effect of previous water absorption test on the BS 680 result was negligible, but previous refluxing had a significant effect on the prEN12326 result. In the case of WF/8 the test was carried out at a stage when the sample was beginning to show increased variation in results and the effect of the extra refluxing was significant in both cases. Therefore the refluxing method of assessing the increase in water absorption also contributes to the deterioration of the slate. The prEN12326 method of assessing increase in water absorption does not have this problem. However, because of the need to differentiate between different quality slates in a reasonable length of time, the refluxing method is more suitable. Comparison between slates is therefore possible, providing the technique is standardised so that all slates undergo the same regime.

5.5.2.2 Results

Results are given in Appendix 5.1 and summarised in Fig. 5.9

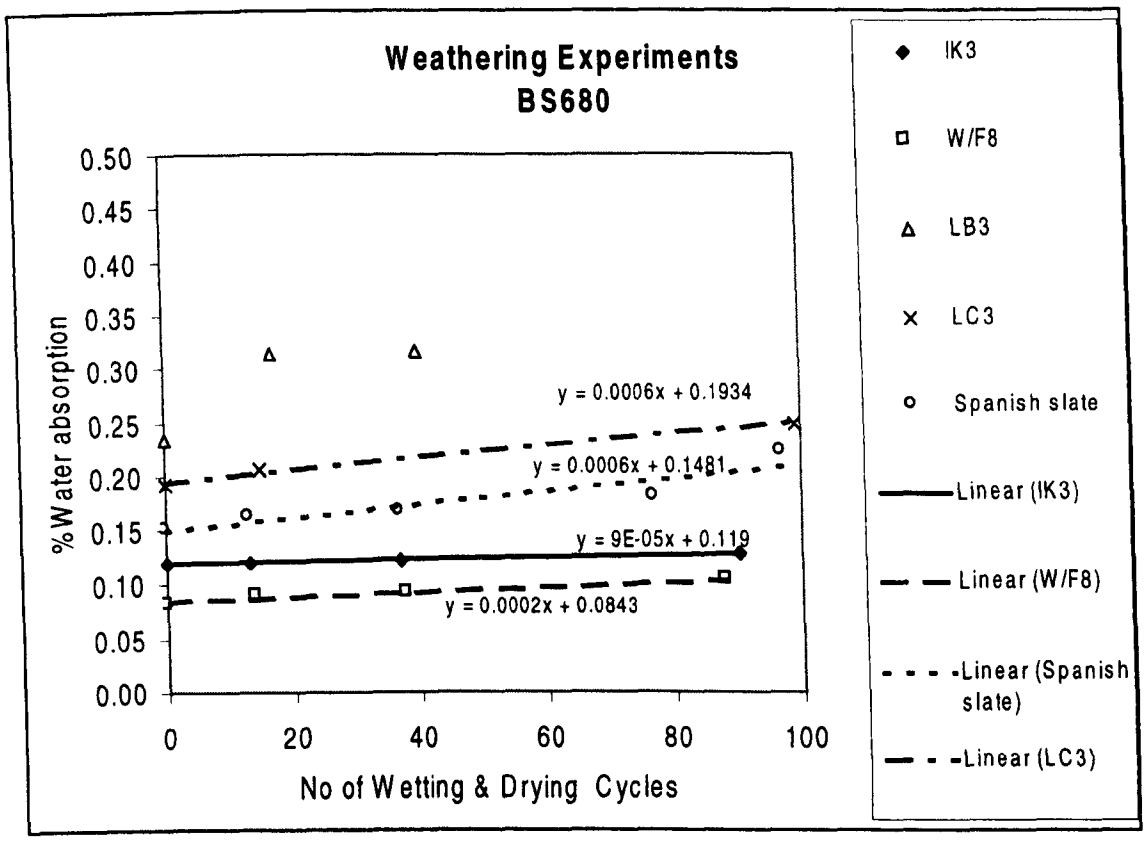

Fig. 5.9 Climatic response profile of a selection of old and new slates

1. **W/F-8 Welsh sample from the old vein Oakley Quarry, Ffestiniog. Data for slate from this vein, albeit from different quarries, had been gathered by BRE in 1944 when re-assessing the BS 680 standard for slate.**

2. **I/K-3 Killaloe slate from Killoran Quarry, Portroe near Nenagh in Ireland (Map: Tipperary, Sheet 19). This quarry was worked until the mid 19th century and then at intervals during this century, the most recent being in 1990 in a joint venture (by McAlpine, Capco Slate Co. and an Irish roofing company) making it possible to get fresh samples (per. com. M. Joy, local historian). Killaloe slate has been used as a roofing material in the surrounding area and is known for its durability.**

3. **LB-3 Slate from roof of Garsten Cottage, Blackmill Bay (Quarry Reports 3.5.10). Although the age of the slate is assumed to be that of the house, which was built in 1911, the source is not known. The quarries at Blackmill Bay were not being worked at this time so the slate may be from Tir na Oig 1 km to the north.**

4. **LC-3 Blue grey slate from Cullipool which looked new, and was definitely never on a roof as there was no nail hole. It is known that a local quarrier Mr D McKay continued to split slates in the area after the quarries were officially closed. This is the least weathered Scottish slate used in this Report.**

5. **Spanish slate, Glasgow roofing merchant. Little information about its source is available.**

5.5.2.3 Calibration of Results

An attempt was made to relate the increase in water absorption in the experiment which subjected the slates to repeated cycles of wetting and drying (Fig. 5.9), to that observed in slates which have experienced natural weathering on roofs.

A tentative calibration has been achieved based on data collected for the BRE study of weathered samples in 1948/49 (Fig. 5.2). A linear regression of the few data points for naturally weathered slate samples from the *old vein* in the Ffestiniog area gave the following relationship between water absorption y and years of natural weathering **x**

$$\mathbf{y = 0.0024x + 0.162}$$

This implies an initial water absorption figure of 0.162% and an annual increase of 0.0024% per year over a hundred year period. (Although the rate of increase in water absorption of 0.0024/year was comparable with the better types of American slate (Fig. 5.1), no conclusion can be drawn from this comparison due to different testing procedures).

The linear regression for the experimental weathering of a new slate from the *old vein,* gave the following relationship for the first 88 cycles (Fig. 5.9)

$$\mathbf{y = 0.0002x + 0.0843}$$

This gives a rate of increase in water absorption per W/D cycle of 0.0002%
By comparing this relationship with that found for the naturally weathered slates based on the BRE data, it is possible to get a rough equivalence between natural and experimental weathering as **12 W/D cycles per year.** However the rate of increase in water absorption is not linear but increases with time so that exponential or polynomial regressional lines give a better fit (Fig. 5.10). Therefore using a linear

relationship is an over simplification, as can be seen when the experimental weathering of the W/F-8 sample was continued to 181 W/D cycles and the best fit line was as follows:

$$y = 0.0003x + 0.0843$$

which equates to **8 W/D cycles per year.**

The more the climatic response profiles deviate from a straight line the greater the approximation, as can be seen for the experimental weathering of the Spanish slate Fig.5.9b. However, with limited data it was necessary to use the initial part of the curve, which approximates to a straight line, to compare the climatic response profiles of different slates.

An independent calibration was attempted by comparing the water absorption of a Killaloe slate supposedly 200 years old (per. com. Mr Tom O'Brien, used slate dealer, Killaloe) with a new Killaloe slate.

200 year old slate % water absorption		0.181
New Killaloe slate IK3	0.12	
Trade Literature (Hart 1991)	0.09	
Average value for new slate	0.10	0.10
Increase in % water absorption over 200 years		0.081
Annual increase in % water absorption		**0.00041**

Comparing this figure with that obtained for an experimentally weathered slate

$$y = 0.00009x + 0.119$$

this equates to **4.5 W/D cycles per year.**

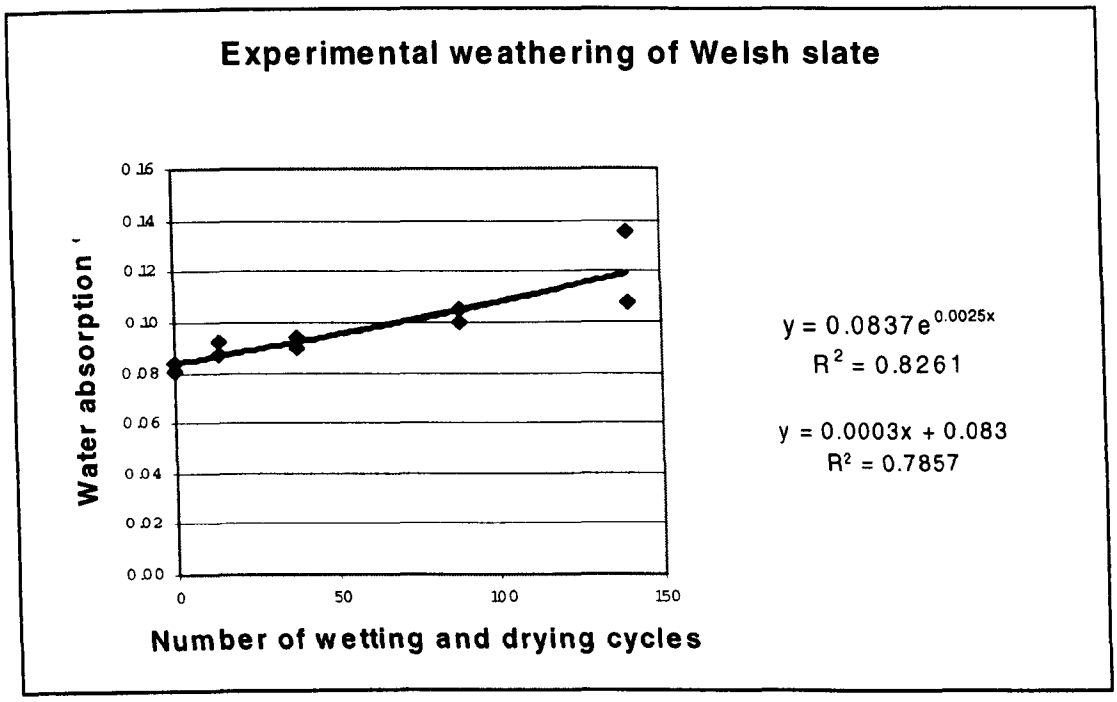

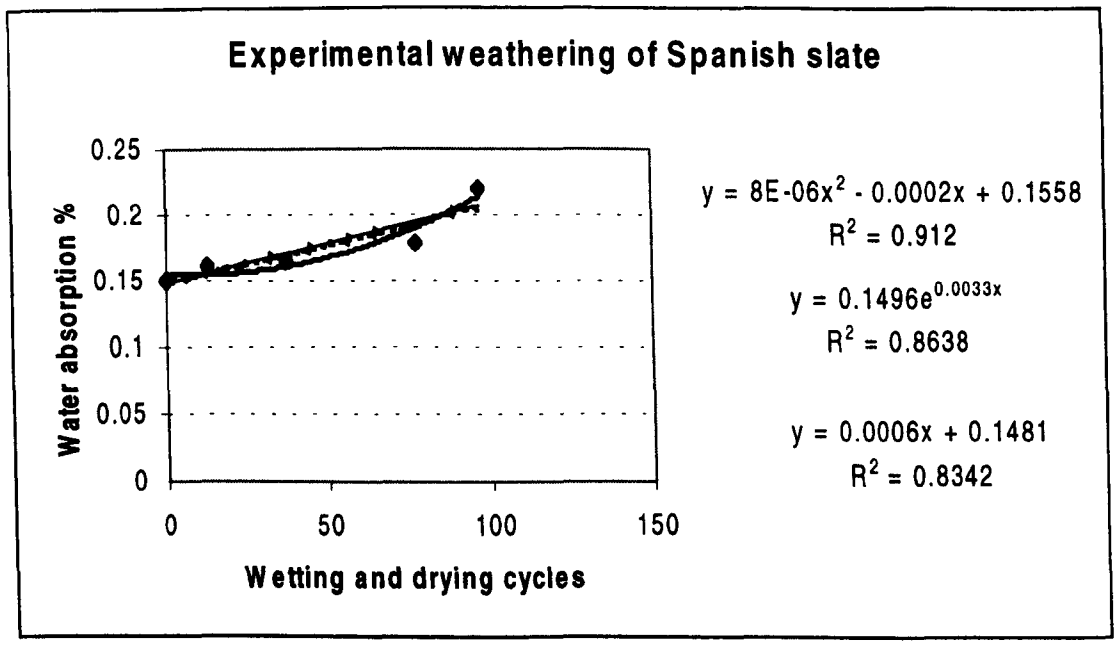

Fig. 5.10 Climatic response profiles of a) a Welsh slate b) a Spanish slate.

A different approach was taken with LB-3, a slate from Garsten Cottage, Blackmill Bay, Luing (Appendix A 3.5.10). The slate was assumed to have the same age as the house, which was built in 1911. The graph in Fig.5.8 was extrapolated backwards at the rate of 6W/D cycles per year to the origin and the following relationship was obtained. (A higher rate of 10 W/D cycles per year gave a negative result for the original water absorption figure and was discounted.)

$$y = 0.0004x + 0.10$$

Given all the variations possible in the history of the different slates, let alone their imprecise ages (based on information from second-hand slate dealers), it is only possible to say that ***5-12 experimental W/D cycles are equivalent to one year of natural weathering.***

5.5.2.4 Interpretation of Results

The limit of water absorption

There was insufficient time to test any of the slates to the point of observed failure, therefore it was not possible to define a level of water absorption indicative of failure and hence a value for a useful working life. W/F-8 showed measurable deterioration after 100 W/D cycles, i.e. there was an increase in the rate of water absorption with time, an increase in variance of the results, as well as a visual change in that brown staining developed. However, there was nothing to suggest that failure was imminent. Although the procedure was run for nearly a year, this was still insufficient time to bring it to a satisfactory conclusion.

Without a scientifically determined limit for water absorption, that set by BS 680 of 0.3% was used in the following determination of the longevity of a slate.

The climatic response profiles (Fig.5.8) were extrapolated to give the number of cycles necessary until a value of 0.3% water absorption was reached (Table 5.11). Then the life expectancy was calculated using a rate of 10 W/D cycles per year. There are several assumptions made in the above extrapolation which cannot be tested scientifically. However there is anecdotal evidence e.g. the Killaloe slate has a reputation of lasting over 200 years and one example of such longevity was seen on the roof of a row of terraced houses in Clonmel built in the late 18th century. Because the houses were in such a bad state of repair, it was assumed that the slates were original, and because distinctive banding similar to that found in Killaloe slate was visible, the slates were assumed to be from Killaloe. The usual figure used in the trade for Welsh slate is 100 years and Spanish slate has a life expectancy of 30 years (Table 1.1).

Climatic response profiles

As discussed in Section 5.5.2.3, the relationship between the increase in water absorption and experimental weathering time is non-linear, but to enable comparison between different slates the initial part of the graph was treated as linear (Table 5.12). The Killaloe slate has the lowest rate of increase in water absorption, while the highest rate of increase was found in the Spanish and unused Cullipool slate.

New slates	No of test cycles	Equation	Increase in thickness/ cycle ‰	Visual change	No. of cycles to 0.3%	Life expectancy at 10 cycles/yr
IK-3	127	y = 0.00009x+0.1195	0.167	No change	2005	200
WF-8	123	y = 0.0002x+0.0805	0.152	Brown stains	1095	109
	181	y = 0.0003x+0.0805	0.271			
LC-3*	99	y= 0.0006x +0.1938	0.455	Leaching of iron	177	18
Spanish	97	y = 0.0006x+0.1484	0.310	Brown stains	253	25
		$y = 0.1496e^{0.003x}$			231	23

Table 5.12 Experimental weathering of new slate. (*LC-3 may not be new Fig. 5.9).

While this Report has not succeeded in determining experimentally a suitable limit for water absorption it has pointed the way to setting a limit scientifically given sufficient length of time for the experiment. It has shown that a suitable method of assessing the durability and life expectancy of a slate is to measure the rate of increase in water absorption due to repeated cycles of wetting and drying.

The above discussion highlights the problems of determining the weathering properties of Scottish slate without access to fresh samples.

5.5.2.4 Understanding the Weathering of Slate

Most of the above discussion is based on water absorption figures obtained using the BS 680 method. A parallel set of results was obtained according to prEN12326 by water immersion. If, as reported by Watkins (1934), it takes a month of immersion in water at room temperature for the weight to stabilise, the prEN12326 test is

measuring only the *rate* at which the slate absorbs water. If, again according to Watkins, weight stability is achieved by the boiling method in 48 hours, the BS 680 test measures the *total* capacity of the slate to absorb water. Both methods are valid measures of deterioration in a slate, but the BS 680 method, if accepted as a proxy for natural weathering, gives larger values and earlier signs of significant change and therefore shortens the length of time needed to evaluate a new slate.

To understand the changes which take place in an experimentally weathered slate, and to see how they correspond with those observed in naturally weathered slate, XRD scans were run on the weathered and non-weathered samples.

The increase in thickness and loss of weight in the experimentally weathered Killaloe slate imply an increase in porosity and concomitant increase in water absorption, but the absence of changes in the position and intensity of peaks, including that of calcite, suggests that any changes are undetectable by XRD scans. The Welsh sample also showed no shift in the position of peaks and the intensity of the mica and chlorite peaks increased (no carbonate was detected in this slate). Therefore the mineralogical changes observed in these experimentally weathered slates do not reflect the changes observed in naturally weathered slate. Instead of loss of crystallinity, as observed in old slates, there was actually an increase in crystallinity and a concomitant decrease in FWHM. This was due to the samples being kept at >100°C for long periods, which does not mirror the natural weathering conditions.

However the Spanish slate, which showed the greatest increase in water absorption, also showed significant differences between its XRD scans of un-weathered and experimentally weathered samples (Table 5.13). There was a 26% -30% decrease in area and 20% -24% decrease in intensity of the chlorite [001] peak. Similar but smaller changes were found in the white mica [001] peak but no changes were observed in the quartz peak. This loss in area and intensity of the phyllosilicates cannot be accounted for by loss of weight, which was negligible (0.02%) but must be due to other changes in their crystalline nature. One suggestion is that chlorite is being converted to clay. This is supported by the fact that the chlorite [002] peak, which is also the principal clay peak, showed a smaller decrease in area than the

[001] peak i.e. 14%-20% and no decrease in intensity between the un-weathered and experimentally weathered samples. The FWHM of the chlorite [001] peak increased with weathering due to loss of crystallinity but that of the [002] peak decreased. This is interpreted an increase in the crystallinity of clay due to prolonged heating. More research is needed to establish the effect of experimental weathering on the phyllosilicates. No calcite was detected in this slate, therefore the changes observed can not be accounted for by the weathering reactions discussed in Section 5.2.2.1.

The overall crystallinity of the experimentally weathered Spanish samples decreased, which corresponds to what is observed in naturally weathered slates.

Chlorite [001] peak	**Intensity counts**	**Area counts**	**FWHM 2θ**	**Position 2θ**
S1-0	405	4958	0.156	7.26
un-weathered	373	4067	0.156	7.26
S1-19	305	3103	0.158	7.26
weathered	282	3029	0.166	7.26
S1-21	308	3346	0.178	7.25
weathered	308	3320	0.196	7.25

Chlorite [002] peak	**Intensity counts**	**Area counts**	**FWHM 2θ**	**Position 2θ**
S1-0	1482	16400	0.194	14.54
un-weathered	1428	16700	0.204	14.54
S1-19	1405	12801	0.140	14.56
weathered	1486	13024	0.130	14.57
S1-21	1395	14380	0.160	14.55
weathered	1416	13796	0.158	14.55

Table 5. 13 The effect of experimental weathering on the a) chlorite [001] and b) [002] XRD peaks: S1-0 is unweathered; S1-19 and S1-21 were weathered for 97 W/D cycles: S1-19 was tested according to BS 680, S1-21 was tested according to prEN12326

Recommendations:

1. Carry our experimental weathering of a wider range of new slate.
2. Refine the thickness measurements, which were only carried out using callipers to an accuracy of 0.1mm. If done more accurately, these could be used to predict the climatic response profiles.

3. Determine the changes in fabric of weathered slates using the SEM (Section 4).
4. Carry out chemical analysis to account for the loss of weight.

5.6 Conclusions

The aim of this Section was to identify a key method of testing a new slate with a view to predicting its performance on a roof. Other test procedures are supplementary but not redundant e.g. there is a need for a minimum strength requirement for different climatic environments and for an acid test to assess the effect of polluted atmosphere on a slate containing significant amounts of carbonate. Slates, experimentally weathered using wetting and drying cycles, show some of the characteristics of deterioration seen in naturally weathered slates. The increase in water absorption is one of the quantifiable effects which, when compared with that observed in a naturally weathered slate, gives an estimate of the number of cycles of wetting and drying equivalent to one year of natural weathering.

This Section has shown that experimentally weathered slates show an increase in volume and loss in weight, indicating an increase in porosity. Although the deterioration is exponential, it would be impractical to weather a good slate for a sufficiently long time until the climatic response profile is determined. However, it is possible to use the **initial rate** at which deterioration takes place as a relative measure of the vulnerability of the slate to weathering.

The proposed testing procedure is as follows:

- Determination of the percentage water absorption by refluxing the sample for 48 hours according to BS 680.
- Subjecting the slate to 20 repeated cycles of wetting and drying. The number of cycles needed to produce sufficient change is only approximate.
- Repeating the water absorption test and determining the average increase in water absorption per W/D cycle.

- The longevity of a slate can be assessed relative to a Welsh slate based on the increase in water absorption. A figure of 100 years is the usual figure used for the life span of a Welsh slate.

Chapter 6 Possible Revival of the Scottish Slate Industry

6.1 Introduction

The Scottish slate industry was centred in four areas:

1. *Ballachulish* on the shores of Loch Leven close to the Great Glen Fault.
2. The islands of *Easdale*, Seil, Luing and Belnahua in a belt stretching from Oban to Jura.
3. In the Southern Highlands close to the *Highland Boundary* Fault in a series of quarries from Arran to Dunkeld.
4. The *Macduff* quarries in Buchan and the *Keith* Quarries near Banff in the north east of Scotland.

Scottish slate has a distinctive appearance making an important contribution to the character of many Scottish houses. This partly arises from the slates being on the whole smaller, thicker and less regular than their Welsh counterparts as well as having a slight sheen due to the higher metamorphic grade. There is also greater variation in colour than more homogeneous imports. The smaller size has had an impact on the vernacular style of architecture whereby slates are fixed to sarking, instead of spanning from batten to batten as found in England and Wales. Similarly the practice of *graduated coursing,* so that the largest slates are used at the eaves and each subsequent course uses smaller sizes until the smallest *(peggies)* are used at the ridge, exaggerates the perspective of the roof and makes efficient use of irregular sizes. The practice of using even the smallest of slates is also significant from an environmental point of view, as a higher proportion of the quarry product is used. The irregular shape of the slates gave rise to the practice of shouldering, whereby the upper corners are mitred to enable them to lie flat. In addition the thicker Scottish slate is stronger and hence more suitable for the Scottish climate. (Most of the west coast of Scotland is in the highest zone for annual driving rain index (Harrison 1996), which was identified as the most significant climatic condition in the deterioration of buildings in general.)

Scottish slate is remarkably durable, often out-lasting the life of the building. This can be seen in the older parts of the towns and cities which are still substantially roofed with Scottish slate 50 years after the demise of the Scottish slate industry. But this townscape will not last without a new source of Scottish slate. Since the closure of the last of the producing quarries at Ballachulish in 1955, all maintenance has had to rely on salvaged second-hand slates, leading to diminishing stocks. Unless quarrying is revived soon, there will be an important change in the character of Scottish townscapes. Alternative materials, such as concrete tiles and resin-based and fibre cement replica slates, will have to be introduced and the special slating skills will be lost.

This Research Report is concerned with characterising and explaining the roofing properties of slate with particular reference to Scottish slate. One of the aims of this Research is to select a Scottish quarry with sufficient reserves, capable of supplying marketable roofing slates, which will help maintain the characteristics of Scottish buildings for future generations to appreciate.

In order to achieve this aim it is necessary to assess those properties which make a good slate and to determine whether there are adequate resources of good quality slate in Scotland.

6.2 Review of different Roofing Materials

The traditional roofing material in many parts of Scotland was slate, in particular in those areas with local availability and low transport costs. But there have been considerable inroads made by other roofing materials as can be seen in a recent survey of Scotland's housing (Scottish Homes 1991). The proportion of houses whose principal roofing material is slate now stands at approximately 35% or 657,000. By far the most common roofing materials are concrete and clay tiles which comprise over 60% of the total dwellings.

All roofing materials are subject to the same local climatic conditions and experience the same problems in their supporting structures and fixing methods e.g. clay tile roofs

may fail due to nail sickness in the same way as slate. Replacing slate with concrete tiles on a roof originally designed to support slate may lead to additional problems of sagging of the supporting timbers.

There is considerable difficulty in comparing the durability of different roofing materials, and estimates of service life vary considerably, especially as the more durable the material the longer the time-span and the less reliable the data. In the case of natural materials, such as slate and clay tiles, there is also considerable natural variation and one of the reasons for failure may be due to a disreputable source. In the case of manufactured materials, some, such as asbestos tiles, are being phased out and other newer materials have no proven record of durability.

Harrison (1996), in a recent survey of domestic housing in Scotland and England, presented data on the state of repair of roofs in general, but little information specific to slate (Table 6.1). He does however mention that slate roofs of houses built between 1900 and 1918 are in the greatest need of repair. Assuming that pre-1900 roofs have been repaired, this gives some idea that the life span of a slate roof is approximately 100 years.

The following discussion looks at the principal roofing materials used on short pitched domestic housing, which are:

1. Concrete tiles
2. Clay tiles
3. Slates
4. Manufactured slates

	Roofing Material	Number of Houses	%	Condition
Scotland	Concrete and clay tiles (not differentiated)	1.2 million	64	1 in 5 need repair
	Natural slate and stone	657,000	35	1 in 2 need repair*
	Manufactured slates	17,000	1	1 in 2 need repair
England	Clay tiles	4.2 million	26	1 in 3 need repair
	Concrete tiles	8.1 million	51	1 in 12 need repair
	Natural slate and stone	3 million	19	1 in 2 need repair
	Manufactured slates	689,000	4	1 in 2 need repair

Table 6.1 Classification of roofs of domestic housing in the U.K. Extracts from a survey of the roofs of domestic housing in Scotland and England as summarised by Harrison (1996)

6.2.1 Concrete Tiles

Concrete consists of cement mixed with water which react to produce hydrated silicates. This results in a hard matrix which binds together an aggregate.

Compliance with British Standards

Concrete tiles must comply with BS 473 550: 1990 *Specifications for concrete roofing tiles and fittings.*

This will be superseded by the new CEN BS EN 490 and BS EN 491.

Durability

Surveys of the durability of used concrete tiles suggest 30 to 50 years life (Table 6.2), although according to a BRE report (Harrison 1996) new concrete tiles are expected to last 100 years if all building regulations are satisfied.

6.2.2 Clay Tiles

Clay, shaped and burnt into tiles, has a long history. Fragments of burnt brick have been found in Egypt dating from 1200 BC (Prentice 1990), but it is the Romans who brought the process to a fine art. Clay tiles are similar to slates in that the raw material is derived from sedimentary deposits and the variation in the composition can affect the final product. The most important ingredient is quartz, which can make up to 90% of the total and which imparts its hardness and durability to the finished product. The other minerals present are phyllosilicates such as illite and chlorite as found in slate as well as smectite and kaolin (Section 2.2.2). The plastic nature of the phyllosilicates enables the tile to be moulded and then to form a glass during the firing part of the process. Iron minerals present are oxidised to haematite and impart the colour to the brick. Reducing conditions must be avoided by controlling the furnace temperature, as reduced iron minerals would have a similar detrimental effect as discussed for slate (Section 5.2.3.5).

Compliance with British Standards

Clay tiles must comply with BS402 Part I: 1990 *Clay roofing tiles and fittings.*

Durability

As with concrete tiles, the BRE survey states that clay tiles are expected to last 100 years if all building regulations are satisfied. Davis Langdon Consultancy estimate a life of 60 years based on commonly reported published figures. The Maol figure reported in Builder Feb 1995 is 40 years.

6.2.3 Slate

The name *slate* has been applied to all naturally occurring rocks which can be cut into slabs and used as a roofing material. Historical records do not distinguish between flagstones and true slate and many of the early records of roofing slate probably refer to flagstone. In Britain *true slates* in the geological sense are found in the mountainous

regions of North Wales, Cumbria and the Highlands of Scotland, remote from areas of habitation. In an age of poor roads, slates were only used in the most prestigious buildings close to sources of supply. One of the oldest examples of the use of slate in Britain is of slate-slabs used as flooring in the 3rd century Roman remains at Segontium (Caernarfon). There is only scant evidence of slate roofing until the 15th century. In the 14th century, slates were shipped to repair Chester Castle from near Bangor (Richards 1995) at about the same time as putative Easdale slates were used in the 14th century wall at Finlaggan, Islay (Section 1.4). It is only since the 15th century that the use of slate as a roofing material quickly developed. The history of the Scottish slate industry is discussed in Section 1.4.

6.2.3.1 Natural Slate

Natural slate is one of the most durable roofing materials available. Problems arise when impurities are present. Natural slates chosen and fixed in accordance with BS 5534 will withstand most wind loads and provide a watertight roof. Failure, when it occurs, is often due to nail sickness and a large proportion of the slates can be reused .

Compliance with British Standards

Natural slate must comply with BS 680 Part 2: 1971 *Specifications for roofing slates Metric Units.*

Durability

Natural slate of UK origin should last more than 100 years but inferior slate can fail within months. The Maol figure for the durability of imported slate is 30 years.

Building Regulation of Slate

This is covered by the following BS Codes of Practice

BS5534: Part 1: 1990 *Code of practice for slating and tiling*

BS8000: Part 6: 1990 *Workmanship on building sites. Code of practice for slating and tiling of roofs and claddings*

6.2.3.2 Man-made Slate

These are synthetic slates from a wide range of materials. Most of those found on roofs today are likely to be of obsolescent asbestos cement and at the end of their lifespan. Other materials are of relatively recent introduction.

Materials of manufacture include:

- Portland Cement and a variety of aggregates
- Portland Cement reinforced with man-made fibres
- Portland Cement reinforced with asbestos fibres (obsolete)
- Resins (thermosetting, polyester or acrylic) with crushed slate or other inert filler. The slate is ground to a fine powder, incorporated into a resin base and moulded against a natural slate to produce a realistic simulation of the natural product (Harrison 1996).

Compliance with British Standards

The following specifications are not strictly applicable to the slate but have been used in the BSE report

Concrete slate:	BS473 550 See concrete tiles above
Fibre reinforced slate	BS 690 Part 4: 1974 *Asbestos-cement slates and sheets.*
	BS 4624:1981 *Methods of test for asbestos-cement building products*
Glass-fibre reinforced slate	BS6432:1984 *Methods for determining properties of glass fibre reinforced cement material.*

Durability

The Maol figure reported in Builder Feb 1995 is 30 years for fibre cement slate and synthetic slates, comparable to the figure for concrete tiles. Asbestos tiles were introduced at the end of the 19th century but few roofs more than 50 years old still exist.

Man-made fibre reinforced slates often discolour, become distorted and crack.

6.2.4 Conclusions

Figures of comparative costs for plain areas of roofing, including battens and standard underfelt, were supplied by Everest.

Roofing Tiles and Slates		**£ (m^2)**	**Typical life span (years)***	
Clay Tiles	Machine made plain	30.00	60	40
	Handmade	45.00		
	Interlocking Pantiles	19.00		
Concrete Tiles	Plain	26.00	50	30
	Slate look-alike	17.00		
Natural Slates	Spanish	31.00	N/A	30
	Welsh Blue	45.00 - 50.00	100	100
Reconstituted slate				
Crushed slate with resin and glass fibre reinforcement,	Preweathered slate grey	35.00	N/A	
Ground slate and resin	Welsh grey colour	31.00		
Fibre Cement Slate	Blue/black	23.50	N/A	30
	Matt coated	27.50		

Table 6.2 Costs and estimated lifespans of different roofing materials from *Focus 1997 Products in Practice: Theme Roofing.*

*Estimates of life span vary considerably. The first set of figures is from "The current cost of roofing" compiled by Davis Langdon Consultancy and the second set is by Maol as published in Builder 1995.

When the cost of maintenance and the durability of the material are taken into account over a 100 year cycle, roofing with British slate is one of the cheapest methods available. Although the figures are based on Welsh slates, Scottish slates also have a proven durability record with slates lasting over 100 years. By increasing our understanding of the material this research project aims to give scientific backing to this reputation.

6.3 Assessment of Quality

Assessment of the quality of a slate is difficult due to the inherent variation of any natural material. Historically slate has been assessed qualitatively at source by relying on the experience of quarry managers. Yet often the criteria for selecting a particular source of slate were economic factors such as transport costs, accessibility to markets and availability of manpower. During World Wars I and II, the production of slate came to a standstill because of lack of manpower. One of the reason given for the closure of the Aberfoyle Quarry (Appendix A 4.5.4) was the higher wages paid locally by the Forestry Commission (Per. com. Mr Ferguson, retired quarrier).

The quality of the slate from a particular quarry was dependent on the expertise and knowledge of the quality controller. At a time of more stable population and local use of the material, it was possible to link the performance of a particular slate to its origin and pass this information from generation to generation. However this system did not prevent poor quality slates reaching the markets, and at various times different slate-producing countries addressed the problem by introducing national standards for slate which set out the minimum requirements on the basis of a set of tests. But the approach adopted by each of the different countries reflected the type of slate produced in that country and did not result in an independent standard capable of predicting performance. Even within one country such as Britain, different climatic conditions in different parts of the country require different types of slate. The *best* grade of Welsh slate is split too thinly for the Scottish weather.

With increasing international trade in slate, there is growing dissatisfaction with the ability of different standards to select satisfactory slates and exclude unsatisfactory ones. The lack of a minimum strength requirement in the British Standard, as British slates are stronger than most other roofing materials, leads to the importation of weaker slates. The lack of uniformity in standards is being addressed by the proposed introduction of a new European standard. However, without information on what scientific research is behind this standard, it was necessary to take an independent look at the different methods of assessing the quality of slates.

This Report places great emphasis on relating the physical properties of slate to its geological make up. Having addressed the problem of evaluating the mineral composition (Section 2), metamorphic grade (Section 3) and the fabric of slate (Section 4), it is now necessary to relate these parameters to the properties of Scottish slate and select the most suitable Scottish quarries for further investigation.

1. The first criterion in selecting a quarry is the ability of the slate rock to produce flat slabs

   Fabric (Chapter 4)

2. The second criterion is the quality of the rock in terms of its durability

   Crystallinity (Chapter 3)

   Mineral composition (Chapter 2)

6.3.1 Fabric of Slate

The economics of any particular quarry is controlled by the fabric of the slate and hence the ability to split the slate into thin slabs. Ease of splitting was evaluated in Chapter 4 and compared with the known splitting ability of slate from producing quarries. Scottish slate was assessed with reference to the splitting ability of Cumbrian and Welsh slates and its potential minimum commercial thickness is shown in Fig. 4.15. The size of the slate is controlled by the spacing and orientation of discontinuities such as joints and veins (Section 6.5.4).

6.3.2 Durability of Slate

By comparing the experimentally assessed properties of various slates with their reputation the following conclusions were reached in this Study,

The durability of slate is dependent on

1. Metamorphic grade
2. Mineral composition
3 Grain Size /Fabric

Slates with the highest metamorphic grades (as measured by the crystallinity of the material) have an excellent reputation for longevity (Section 3.4.2.2). This is because with increasing metamorphic grade there is an increased ordering of the minerals and an increase in grain size with regular grain to grain boundaries. Unlike sedimentary rocks, where an increase in grain size is associated with higher permeability, the regularity of grain boundaries is associated with a decrease in porosity and inability to absorb water. However, the increase in grain size due to increasing metamorphic grade is associated with a decrease in the splitting properties of the slate.

The greatest control on the durability of slate is low water absorption. As well as being found in slates with higher metamorphic grade as described above, this property is also associated with a fabric with closely spaced cleavage domains. These develop in slate from a fine grained protolith e.g. fresh Toberonochy slate has a low water absorption figure of 0.10% (BRE archives). In spite of the presence of the deleterious mineral magnesite, very little weathering was observed in the Toberonochy reject tips. In contrast at Balvicar, which also has magnesite present but with a water absorption value of 0.94-1.34%, weathering is extremely severe. This shows the important role of water absorption in weathering. However, in the absence of deleterious minerals a high degree of water absorption is less crucial. Although there are no water absorption values for fresh Macduff slate, it is assumed to have high water absorption due to the presence of algae etc on the roofs in the area. Yet the slate is very durable because of the absence of deleterious minerals.

Some slates have a reputation of softening when on a roof for 20 to 50 years. It was found that these slates have a low quartz content and a high chlorite content. Quartz has a hardness of 7 on the Mohs' scale while that of the phyllosilicates is 2 -3, giving some idea of the contribution quartz makes to the durability of slate. Chlorite is the most susceptible of the major minerals in slate to chemical weathering, followed by white mica. Quartz is the most durable.

6.3.2.1 Evaluation of the Durability of Slate

An attempt is made in this Section to reconcile all these observations and relate them to the durability of slate. In Chapter 3, the relationship between crystallinity and the quality of a slate was discussed, and Appendix 3.1 gives the XRD analysis results on which crystallinity measurements were based. These were then modified as follows to incorporate an empirical assessment of the relative contributions to durability made by the different minerals to arrive at a durability index..

1. The contribution made by quartz was increased threefold to take into account its hardness relative to the other major minerals. In addition, for a given mineral concentration, the intensity count of the XRD peak for quartz [100] is lower than those of the white mica and chlorite [001] peaks. This is due to non-random orientation of the minerals in the powder sample (Fig. 6.1).

2. The contribution made by chlorite was halved to take into account its greater vulnerability to weathering reactions.

3. The contribution made by calcite was removed but that of dolomite was retained due to its extremely low solubility product.

The results of this extension of the crystallinity measurements are also given in Appendix 3.1 and are summarised in Table 6.3 below.

It should be noted that this method cannot take any account of the effect of non-crystalline minerals such as graphite to the durability of slate. This is a serious omission as graphite acts as a catalyst and hence facilitates weathering reactions (Section 5.4.3.3.2).

Welsh Slate	Durability Index	Reputation	Source
Cwt y Bugail	543	Good	This Report and BRE archive
Pen yr Orsedd	731	Very good	
Ffestiniog	593	Good	
Twll Coed	462	Poor	
Cumbrian Slate			
Kirkby	788	Good	BRE archives
Elterwater	585		
Brossan Stone	691		
Broughton	637		
Brandy Crag	790		
Irish Slate			
Killaloe	582	Very good	This Report
Spanish slate	660	Poor	This Report
Scottish Slate			
Ballachulish	1354	Very good	This Report and BRE archives
Easdale Island	1152	Very good	
Balvicar	1134	Poor	

Table 6.3 Relationship between the reputation of a slate and its durability index

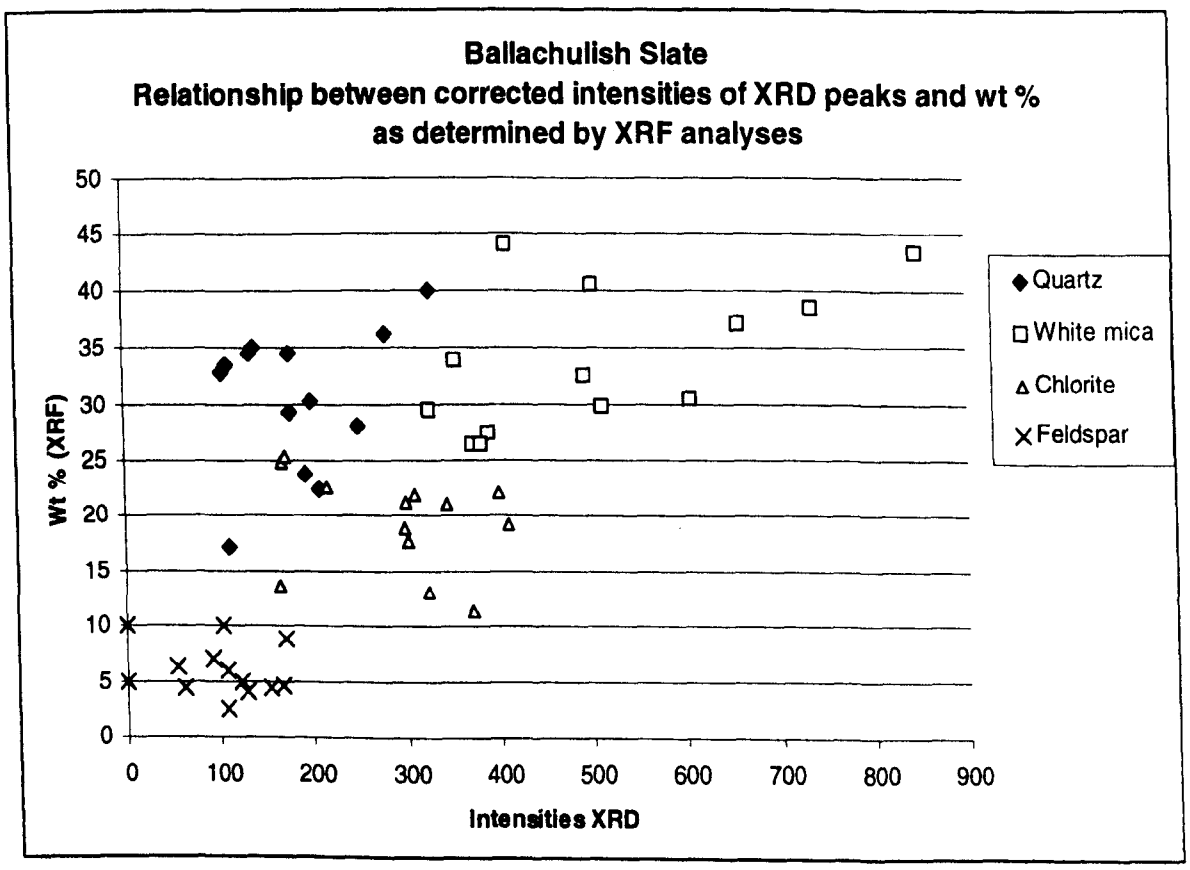

Fig. 6.1 Relationship between intensities of XRD peaks of the major minerals and their concentration.

Comment There appears to be some correlation **within an area** between the reputation of a slate and the durability index. However, the low value for Killaloe slate with an excellent reputation, and the high value for Spanish slate with a poor reputation, show the weakness of this method. Clearly other weightings might have been chosen to provide a better correlation between the index and reputed durability, but more research is needed to establish whether there is in fact a quantifiable link between the chemical and physical properties of a slate and its durability. This would need also to take account of the non-crystalline mineral content such as graphite. Until this is done, it must be concluded that the method described above is unsatisfactory for assessing slate durability.

6.4 Resources and Reserves

The ***resource*** is the overall volume of the slate deposit and ***reserves*** is the amount of slate which can be exploited and hence is dependent on many factors: geological, economic and environmental etc. However since not all of these factors have been explored in this Study no figure can be put to the reserves. In this Report therefore, any estimates, based solely on geological factors, of the proportion of useable rock are referred to as ***usable slate***.

In giving quantitative estimates of ***usable slate*** the following points have to be evaluated:

- Resource i.e. the volume of the available outcrop.
- Depth of workable slate.
- Proportion of rock suitable as slate.

6.4.1 Resources

The *Resource* is the area of the outcrop times the depth.

Area of the outcrop

The area of the outcrop can refer to the area in the immediate confines of the quarry or the limit of the slate outcrop in the surrounding areas. In some cases the limits of the

quarry are clearly defined such as on Easdale Island or Belnahua, but more often this is not the case. Except in one or two cases (which are clearly mentioned in individual quarry reports) the total area of outcrop is usually on so large a scale that it is not seen as a limiting factor.

No allowance is made in this Report for the availability of land for slate quarrying.

Depth of Outcrop

Without borehole information the depth of outcrop can only be inferred from geological maps. In general the depth of outcrop is not seen as a limiting factor.

6.4.2 Depth of Workable Slate

The depth to which a quarry can be economically worked is variable. It is generally noted that the quality of a slate improves with depth but the deeper the quarry the higher the cost of extraction. The limit of the *usable slate* is dictated by the engineering factors such as the need to pump out groundwater etc. For a quarry situated on high ground, the depth to which it can be worked is considerably more than for a quarry on low ground, especially if close to the sea. Yet several Easdale quarries were worked to a depth of greater than 50m, as the quality of the slate was good, but with dire consequences (see Ellenabeich Appendix A 3.5.2). For historical reasons none of the Macduff quarries was worked to much more than 10m depth, making their further exploitation feasible.

6.4.3 Exploitable Proportion of Slate Rock

Within a quarry the slate is often found interspersed with quartz veins, igneous bodies and other types of rock. Where there is a high concentration of such irregularities the amount of *useable slate* is low.

Slate quarries are generally worked along strike, following the line of a productive unit or *seam*. For this reason the possibility of extending the *seam* is given in individual quarry reports. For example at Toberonochy (Appendix A 3.5.5), the *seam* in the

quarry is of good quality but the resources within the confines of the quarry are limited, so the possibility of looking for an extension of the *useable slate* along strike is suggested.

Exploitation of *useable slate* in the surrounding area but outwith the immediate confines of the quarry would need much exploratory work such as boreholes etc. to determine the quality and extent of the slate.

In this preliminary study of all the Scottish slate quarries, it is possible in some cases to estimate the resource. Based on these estimates, quarries are described in this Report in the following terms: (These are the terms used in Appendix A and Section 6.5)

Resource (x100,000m^3)	
<10	Exhausted
10 – 100	Limited
100-1000	Medium
1000-10,000	Large
>10,000	Very large

For those quarries which appear to have substantial resources, the *usable slate* can then be estimated based on the size of the *seam* and other observations in the quarry. To make a more accurate assessment of the *useable slate* of a selected quarry would involve firstly surveying the area surrounding it to determine the extent of the available resources, and then a more detailed mapping inside the quarry to determine the ratio of *useable slate* to the total rock. This is beyond the scope of this Thesis.

6.4.4 Joints and Recovery

Having located a good *seam* of slate, the size of the blocks extracted is strongly influenced by the pattern of joints in the rock.

Joints are classified as systematic and irregular:

Systematic jointing consists of planar fractures, whose form and orientation are related to the deformation history of the rock and subsequent de-stressing associated with erosion. Superimposed on Scottish slate is ***irregular jointing*** associated with over 50 years of weathering, so that it is not often possible to determine the original systematic fractures. The type of joints most often identified are parallel to the cleavage surface J_0 and normal to the cleavage surface J_1. Occasionally other fractures, such as diagonal joints, form a pattern which is considered as characteristic of the original rock J_2 (The terms J_0, J_1 etc. are those used in the Appendix A).

Size of Slates

The spacing of joints and the angle (pitch) at which they cut the cleavage surface controls the dimensions of a slab produced in the quarry (Fig. 6.2). This in turn affects the size of slate produced (see Appendix A 2.3.4 for sizes of Ballachulish slates). Welsh quarries generally report around 5-10% recovery, yet Bailey *et al.*(1916) when describing the Ballachulish quarries reports *"6000 tons annually of finished material representing 30,000 to 35,000 tons of quarried rock"*, which equates to 15% recovery. Blaikie (1834) mentions 20% recovery when discussing Macduff slate. These figures reflect the difference in roofing practice between Scotland and the rest of the U.K. whereby the former makes use of different sizes of slate and is prepared to use even the smallest Peggies (228 x 150mm).

The relationship between size of slate and percentage recovery was calculated (Table 6.4) for different pitches of joints and for varying perpendicular spacing between them (Fig. 6.3). This shows how the use of smaller sizes increases the rate of recovery where jointing is fairly closely spaced (Fig. 6.3a), especially at higher angles of pitch (Fig. 6.3b).

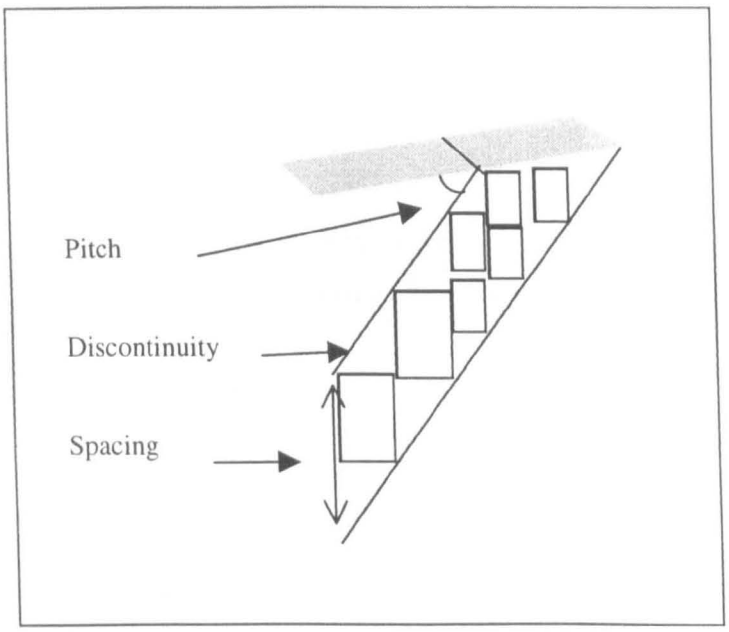

Fig. 6.2 Orientation of joints relative to the cleavage surface. Slates are cut along the pillaring line, which is the perpendicular line shown. The recovery is affected by the distance between joints and the angle or pitch of the joints.

6.4.5 Weathering of Quarry Faces

It should be borne in mind in considering the individual quarry reports which follow that all the faces of present day Scottish quarries have been exposed for at least 30 and in some cases more than 100 years. The effect of this exposure in terms of weathering is to some extent indicative of the likely durability of the slate. Weathering of the slate at the quarry faces has been assessed subjectively by reference to the extent of rusty staining, the softness of the surface rock etc.

Theoretical estimate of the rates of recovery of slate as a function of the following

1 Size of slate

2 Spacing of discontinuities such as joints

3 Angle at which the discontinuities cut the cleavage surface

Definition of terms

Spacing	S	Distance along the grain of the slate. The long edge of the slate is cut along this line, assumed to be vertical.
Width	W	Width of block, a constant
Length	L	Longer dimension of the slate
Breadth	B	Shorter dimension of the slate
Pitch α		Angle between the horizontal and the discontinuity measured on the cleavage surface.

Method

Effective spacing	E.S. = S - B x tan α
Effective width	E.W.= S/tan α
Minimum width	M.W. = B+L/tan α
	If E.W. > M.W. then W = W otherwise W = 0
Total area	T.A. = S x W
Number of slates =	Integer (E.S./L) x W/B
Recovery R =	N x L x B
% Recovery =	R/T.A. x 100

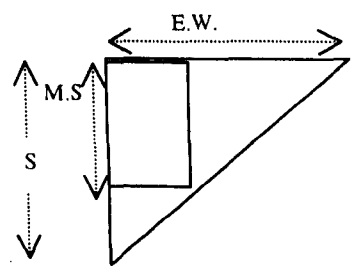

Note: Once there is sufficient width for one slate, there is no other width limitation

Table 6.4 Method of assessing the effect of size of slate on theoretical recovery rates.

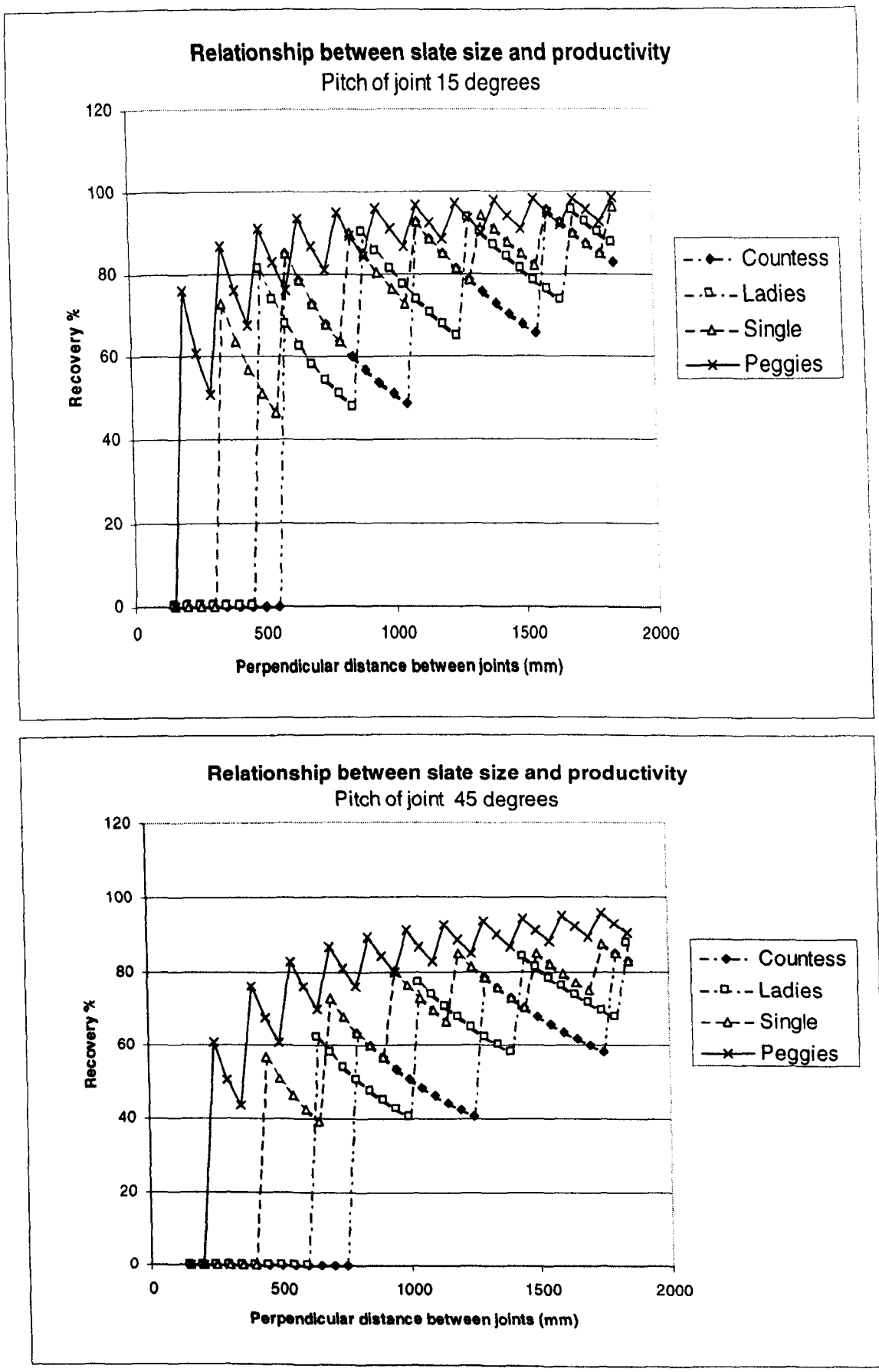

Fig. 6. 3 Relationship between the rate of recovery and the size of slate in mm a) Pitch of joint on the cleavage surface is 15 degrees b) Pitch of joint on the cleavage surface is 45 degrees

Countess	**510 x 260 mm**	**Ladies**	**405 x 200 mm**
Single	**255 x 180 mm**	**Peggies**	**228 x 150 mm**

6.5 Resources of Scottish Slate

An important aspect of this research Project was to update the last report on the Scottish slate quarries, which was carried out in 1944 (Wartime Pamphlet No 40). There have been many changes in the subsequent 55 years. Some quarries were substantially altered after that date due to continuing production for a further ten to twenty years, others no longer exist due to road building and landscaping. All quarries were considerably overgrown with gorse and heather making it impossible in many cases to assess them properly.

The approach taken in this work was to reassess all the quarries described in the Wartime Pamphlet and to update it in the light of subsequent developments in the understanding of the geology of the region. The following aspects of each quarry are described fully in Appendix A, with a summary in this Section:

- Site details
- Topography
- Geology
- History
- Mineralogy and crystallinity
- Slate description
- Cleavage and splitting properties
- Joints
- Imperfections
- Description of workings
- Usable slate

The quarries were grouped according to their geological location as follows:

1. Ballachulish
2. Easdale
3. Highland Border
4. Macduff

These are also the generic terms used and applied to all the quarries in the relevant group.

6.5.1 Ballachulish Slate Quarries

Quarry	**East Laroch**
Resources	***Medium.*** For small scale development, there are limited resources within the present confines of the quarry. For large scale development the problem of the large rockfall in the SE, which has limited exploitation in the past, would have to be addressed.
Weathering	Good
Access	Excellent
Environmental Sensitivity	This quarry has been landscaped and is now in the centre of a tourist area used for leisure activities.

Quarry	**Khartoum**
Resources	***Medium*** resources within the confines of the quarry.
Weathering	Good.
Access	Reasonable road and track for small scale development.
Environmental Sensitivity	The site is on Forestry Commission land and away from the main tourist attractions. However, large scale development would be conspicuous in an area much used for hill walking. The access road is narrow and passes through the village of East Laroch.
Comment	This is the quarry best suited for further investigation.

Quarry	**West Laroch Quarries**
Resources	***Large*** slate deposit continues south up the steep hill behind the two quarries, but the steepness of the slope and the

increasingly heavy overburden to the south make exploitation difficult.

Weathering Poor – medium.

Access Good.

Environmental Sensitivity

Close to the village and now being used as an industrial site (a roads depot, bus depot and other businesses).

Quarry **North Ballachulish**

Resources ***Very large.*** resources stretch many kilometres to the north of the quarries.

Weathering In the low-level quarries pyrites have been altered to pyrrhotite and have weathered badly, staining the rock in the process. Where the pyrrhotite has fallen out, large holes have been left. The high-level quarries are outside the range of this alteration (Neumann 1950) and have a less serious weathering problem.

Access Access to the low-level quarries is good; that to the high level is by a steep, poorly defined path.

Environmental sensitivity

The low level quarries are close to hotels in an area of outstanding natural beauty. The high level quarry is less conspicuous, while the resources to the north are remote from all habitation.

6.5.2 Easdale Slate Quarries

The slate from Easdale Island itself was once said to roof the world but resources on this small island are now ***exhausted.*** Resources of slate are available elsewhere in the area but considerable work would need to be done to select a quarry suitable for further exploitation. Only limited information from fresh samples is available and assessment of the weathering properties of the slate from different quarries is based on the appearance of the slate in the quarries after 50-100 years.

Location	**Easdale Island**
Quarries	**Easdale Island**
Resources	***Exhausted***

Location	**Seil Island**
Quarries	**Ellenabeich**
Resources	***Limited***
Weathering	Good
Access	Poor
Environmental Sensitivity	
	Ellenabeich is a conservation village with narrow streets.
Comment	No action due to its location.

Location	**Seil Island**
Quarry	**Breine Phort**
Resources	***Medium*** resources are available along the cliff face and below the level of the present workings, with possible extension to the east
Weathering	Slate in the tips and quarry faces shows extensive rusty weathering.
Access	Reasonably good.
Environmental Sensitivity	
	Low: apart from a few houses near the entrance this slate quarry is remote from the villages in the area and hidden from view behind the cliffs.
Comment	Re-opening this quarry is a possibility due to its location but further work would need to be done to determine the quality of the slate.

Location	**Seil Island**
Quarries	**Balvicar**
Resources	***Medium*** resources due to an epidiorite sill to the east and alluvium to the west.
Weathering	Poor to bad

Access	Good
Environmental Sensitivity	
	High, this area has been landscaped as a golf course.
Comment	Re-opening not recommended in view of the poor quality slate and high environmental sensitivity.

Location	**Luing Island**
Quarry	**Toberonochy**
Resources	Resources are ***limited*** in the immediate vicinity of the quarry as it has been worked to >60m and is now flooded.
Weathering	Excellent.
Access	Good; close to the road and the sea.
Environmental Sensitivity	
	The quarry is located in a village with narrow roads and surrounded by attractive former quarriers' cottages.
Comment	There is good quality slate in this area and it is worth exploiting if sufficient reserves can be found and the environmental problems overcome.

Location	**Luing Island**
Quarries	**Rubha na hEasgainne**
Resources	***Medium*** resources but the proportion of usable slate is expected to be low due to geological factors such as folding.
Weathering	Poor to medium.
Access	There is no road leading to these quarries.
Environmental Sensitivity	
	Low; this quarry is remote from all habitation.
Comment	Not recommended due to the inaccessibility of the quarries.

Location	**Luing Island**
Quarries	**Port Mary**
Resources	***Medium*** resources but reserves would be poor due to folding.
Weathering	Poor to medium.
Access	Good farm track to the north quarry.

Environmental Sensitivity

Low, this quarry is hidden from view in a remote area.

Comment It may be worth looking at this quarry in more detail given the good location.

Location **Luing Island**

Quarries **Cullipool**

Resources ***Medium*** resources within the confines of Quarry No 3

Weathering Medium - good

Access Poor, through the narrow street of the village.

Environmental Sensitivity

High, this quarry is close to the village.

Comment Possibility for small-scale development within the confines of the Quarry No 3.

Location **Luing Island**

Quarries **Tir na Oig**

Resources Although the slate resources are ***large*** in this area, the proportion of *usable slate* is low due to geological factors such as folding.

Weathering Medium.

Access Very inaccessible.

Environmental Sensitivity

Low, these quarries are in a very remote area.

Comment Not recommended due to the inaccessibility of the quarries.

Location **Luing Island**

Quarry **Black Mill Bay**

Resources ***Large*** resources of slate but proportion of *usable slate* is low.

Weathering Poor.

Access Good.

Environmental Sensitivity

Apart from one or two houses this quarry is in a remote area.

Comment Not recommended due to the poor quality of the slate

Location	**Belnahua Island**
Quarries	**Belnahua**
Resources	***Exhausted.***

6.5.3 Highland Border Slate Quarries

Giving a general summary for a slate area as diverse as that of the Highland Border has severe limitations, and the following should be read in conjunction with individual quarry reports.

Resources

As the slate belt stretches from Arran to Dunkeld, the total resource is obviously large. However it is not possible to estimate reserves of roofing slate. As a rough guide it is generally assumed that the resources continue along strike and that the size of the present workings is a guide to potential reserves. More accurate assessment would require more thorough mapping of individual quarries and their surrounding areas, which is outside the scope of this Report.

With these points in mind the following tentative summary is given:

Location	**Arran Island**
Quarries	**Arran**
Resources	***Limited***
Weathering	Good
Access	Very inaccessible
Environmental sensitivity	Low; these quarries are in a remote area.

Location	**Island of Bute**
Quarries	**Edinmore, Hilton and Ardmaleish**
Resources	***Medium.***
Weathering	The quality of this slate is very variable.

Access Edinmore and Ardmaleish are accessible but Hilton is not accessible.

Environmental sensitivity

Low, these quarries are in a remote area.

Location **Luss**

Quarry **Auchengavin**

Resources ***Limited to medium.***

Weathering Medium.

Access Reasonably accessible.

Environmental sensitivity

Medium. Although these quarries are hidden, the area around Loch Lomond is one of outstanding natural beauty and a tourist area.

Location **Aberfoyle**

Quarries **Aberfoyle**

Resources ***Medium.***

Weathering Medium - good.

Access Accessible.

Environmental sensitivity

Low.There are already extensive workings in this area and a relatively recent history of quarrying.

Location **Comrie**

Quarries **Aberuchill and Drummond**

Resources ***Medium.***

Weathering Good.

Access Very inaccessible.

Environmental sensitivity

Low, these quarries are in a remote area.

Location **Logiealmond**

Quarry **Craiglea**

Resources ***Medium.***

Weathering Good.

Access A good track leads to the quarries.

Environmental sensitivity

Low, these quarries are in a remote area.

Location **Dunkeld**

Quarries **Birnam and Newtyle**

Resources ***Variable***, see quarry reports.

Weathering Medium - good.

Access A good road leads to the lower level quarries at Birnam but the upper level quarries at Birnam are inaccessible. The Newtyle quarries are close to the public road.

Environmental sensitivity

Birnam low

Newtyle medium; these quarries are close to several houses.

6.5.4 Macduff Slate Quarries

Location **Kirkney Hill**

Quarries **Kirkney**

Resources ***Large*** resources are available for further exploitation. The present workings could be increased to a greater depth as well as extending along strike.

Weathering Good quality slate.

Access Poor, no roads lead to these quarries.

Environmental Sensitivity

Low, these quarries are fairly remote from all habitation.

Location **Corskie Hill**

Quarries **Corskie, Haining and Roughouster**

Resources	***Large*** resources are available for further exploitation. Present workings could be increased to a greater depth as well as extended along strike.
Weathering	Good quality slate with only slight weathering of chlorites observed.
Access	Medium. The forestry road leads to the lower level quarries (Corskie) and another track leads to the top of the hill which is fairly close to the higher level quarries (Haining).

Environmental Sensitivity

Low, these quarries are remote from all habitation.

Location	**Wishach Hill**
Quarries	**Wishach**
Resources	***Large*** resources are available for further exploitation. Present workings could be increased to a greater depth as well as extended along strike.
Weathering	Good quality slate.
Access	Poor. No road leads to this quarry although a forestry road is fairly close. At the time of writing, the vegetation was very dense making this quarry inaccessible.

Environmental Sensitivity

Low, these quarries are very remote.

Location	**Hill of Foudland**
Quarries	**Foudland**
Resources	***Large*** resources are available for further exploitation. Many of the quarries in this area are covered with large tips. The depth of workings is greater than observed elsewhere in the Slate Hills.
Weathering	Good quality slate.
Access	Medium; there is a good track to the top of the hill close to the high level quarries, but many of the other workings are quite some distance from any vehicular access.

Environmental Sensitivity

Low, these quarries are fairly remote from all habitation.

Location	**Tillymorgan Hill**
Quarries	**Tillymorgan**
Resources	Many of the quarries in this area are covered with large tips, but ***large*** resources are available for further exploitation.
Weathering	Good quality slate.
Access	Poor. No roads lead directly to the quarries.

Environmental Sensitivity

Low, these quarries are fairly remote from all habitation.

6.6 Conclusions and Recommendations for Further Investigation

The Terms of Reference for this research Project call for a recommendation for further investigation to be made for at least one quarry in each of the four main slate areas. The remainder of this Section goes on to fulfil this requirement. Selection of a quarry is assumed to depend primarily on the likely quantity and quality of slate which may be extracted. However, other factors such as accessibility and environmental sensitivity have also been taken into account. These are summarised for each site in the foregoing Section 6.5, and are given in greater detail in Appendix A.

The important criteria in assessing quantity and quality are:

1. Potential minimum commercial thickness of slate which is controlled by its fabric (Section 4.4)

2. Size of slate as determined by spacing and orientation of discontinuities such a joints within the quarry (Section 6.4.4).

3. Durability as influenced by crystallinity and mineralogy (Section 6.3.2 and Chapter 3).

Although at least one recommendation is made for each main slate area, for reasons which are given in each case, some areas offer much better prospects than others. Accordingly, the recommendations are set out below in order of their perceived potential for renewed exploitation.

6.6.1 Ballachulish

The best Scottish slate is found at Ballachulish, and there are sufficient resources to merit further investigation. However, some individual quarries have severe limitations in terms of access, proximity to centres of population, environmental sensitivity etc. Taking all the factors into account, the Ballachulish quarry proposed for further investigation is Khartoum for the following reasons:

Mineralogy: The mineralogy of the slate is good. There is a high quartz content and the ratio of white mica to chlorite is high. The iron ore mineral is pyrite but it is present as recrystallised cubes which show only superficial rusting. There is however some clay present in those samples analysed.

Crystallinity: The crystallinity of the slate is very high as measured by the intensity of XRD peaks and FWHM of between 0.12 and 0.14 2θ.

Size of slates: The cleavage is smooth and regular and would produce flat slates. However the slate is coarser grained than at other Ballachulish quarries and the potential commercial thickness, estimated at 7mm, is greater than the average for the area. Jointing is widely spaced; one set of organised joints spaced at 2m intervals, which pitch at a low angle relative to cleavage surface would place little constraint on the size on the slates.

Recovery: The proportion of the reserves that is ***usable slate*** is estimated as high. Wastage due to the presence of quartz veins would be localised while the slate in the accessible part of the quarry face is fairly homogeneous.

6.6.2 Macduff

There are large resources of slate on the north slopes of the Slate Hills. Apart from the intensity of spotting, which depends on the proximity to the Insch Intrusion, the quality of the slate was found to be remarkably homogeneous from one hill to the next. Selecting a quarry for further exploitation has depended largely on other factors such as access etc. In general, quarries that have at least rudimentary vehicular access are those worked extensively in the past and hence those which have the problem of large tips covering the working area. Hence the decision on further investigation has had to balance the advantage of easier access against the need to clear larger volumes of waste material.

With this in mind, of the several quarries in the area suitable for further investigation the group chosen in this Report is Kirkney Hill.

Mineralogy: The mineralogy is ideally suited to producing a durable slate, in that the quartz content is moderately high and there is a high white mica to chlorite ratio. More significantly there are no deleterious minerals, the iron ore mineral present is in the oxidised form of haematite, and no carbonate and graphite were detected in those samples analysed. Spotting was infrequent as compared to that observed in the slate hills to the east.

Crystallinity: The crystallinity is medium as measured by the intensity of XRD peaks and the FWHM is 0.17- 0.23 2θ.

Size of slates: Samples are fairly coarse grained and would produce a thick slate of approximately 7 to 10mm. In general the overhanging face has collapsed along the pillaring line and the inclined faces are obscured with debris. It was therefore not possible to assess the effect of density and orientation of jointing on the size of the slates.

Recovery: The proportion of slate that is usable is probably high, as quartz veins and igneous intrusions are infrequent. However density and orientation of jointing may also have a significant effect on recovery.

6.6.3 Highland Border

The mineralogy of Highland Border slate, in particular the lack of pyrites, suggests that it would have good potential as a roofing material. Other properties however, such as the degree of crystallinity, also control the durability of the slate and these vary considerably from quarry to quarry and for producing units within a quarry. Zones with poor crystallinity and low quartz content should be avoided.

The Highland Border quarries proposed for further investigation are Craiglea and Aberfoyle for the following reasons:

Other uses: The green slate of Craiglea and some of the Aberfoyle have attractive bedding features which suggest that the slate could be used for architectural purposes other than roofing, such as flooring and cladding.

Mineralogy: The mineralogy of Highland Border slate indicates lower durability than other Scottish slate in that there is a higher proportion of chlorite. In addition Aberfoyle has lower than average quartz content. However the iron ore mineral present is in the oxidised form of haematite and there is no graphite. The presence of small amounts of calcite in the absence of pyrite/pyrrhotite is not considered deleterious.

Crystallinity: The crystallinity of the Craiglea slate is high as measured by the intensity of XRD peaks and FWHM of between 0.12 and 0.14 2θ. The crystallinity of Aberfoyle is low to medium and FWHM is 0.16 2θ.

Size of slates: The Craiglea slate is fine to medium grained and would produce a slate 9-10mm thick. Because the waste tips have been left in a very unstable condition, it was not possible to assess the effect of density and orientation of jointing on the size of the slates. The Aberfoyle slate is finer grained and the commercial thickness is

estimated as 8mm. Joints are widely spaced and would not limit the size of slates.

Recovery: Grit bands delimit the Craiglea quarry, but it should be possible to extend the quarry into the high ground to the SW. Waste material has been dumped indiscriminately and would have to be cleared. Several seams were worked in the Aberfoyle quarries some of which could be extended along strike. These seams are separated by zones densely permeated by veins of quartz and calcite. There has also been indiscriminate dumping of waste in the Aberfoyle and reopening would involve major clearing of the area.

6.6.4 Easdale

There is no question that very durable slate has been produced from the Easdale area in the past, and those quarries which were worked extensively e.g. Easdale Island, show little superficial weathering. The quality of the slate in different quarries was assessed by looking at the effect of weathering on the quarry faces. Many quarries which were suitable in terms of their resources, location and access had badly weathered surfaces or complex geological features. Toberonochy slate appeared little weathered, but the confines of the present quarry are extensively worked. It may be worth investigating if the producing seam extends along strike.

No quarry is ideal for further investigation as a possible source of Easdale slate. Resources in quarries with the best quality slate are exhausted and Breine Phort is proposed as a compromise between quality and resource.

Mineralogy: Although the mineralogy of the slate is good in that there is a high quartz content and the ratio of white mica to chlorite is high, the white mica has low potassium plus sodium content making it more prone to weathering. The iron ore mineral is pyrite/pyrrhotite which is present as small crystals or is disseminated throughout the rock and is extensively weathered.

Crystallinity: The crystallinity of the slate is very high as measured by the intensity of XRD peaks and FWHM of 0.11 to 0.12 2θ.

Size of slates: Where the cleavage is smooth and regular it would be possible to produce thin flat slates. The fabric of the few samples analysed suggests potential commercial thickness at 5-6mm. However minor folding of the cleavage would increase the thickness and reduce the size of the slates. Jointing is closely spaced which would also limit the size on the slates produced. However the joints are generally orientated parallel to the cleavage and pillaring surfaces which would minimise this constraint.

Recovery: The proportion of the reserves in the present quarry that is *usable slate* is estimated as low due to the presence of igneous intrusions and quartz veins. However the large resources in the area outside the confines of the quarry may be worth investigating.

6.6.5 Summary

The brief for this Study calls for at least one quarry from each of the major areas to be recommended for further investigation. This is difficult in the case of Easdale, since all of the quarries have severe drawbacks. It is also difficult for Macduff for the opposite reason, that several quarries show good possibilities. Nevertheless, taking all the above factors into account, the following quarries are recommended for further investigation:

1	**Ballachulish**	**Khartoum**
2	**Macduff**	**Kirkney**
3	**Highland Border**	**Craiglea**
4	**"** **"**	**Aberfoyle**
5	**Easdale**	**Breine Phort**

Chapter 7 Conclusions and Recommendations

7.1 Introduction

In order to achieve the principal objective of this research Project, the identification of those Scottish slate quarries with potential for further exploitation, it has been necessary to determine ways of evaluating the quality of slate. The general approach has been to analyse slates from producing quarries in Wales and Cumbria and identify those parameters with the greatest effect on the performance of slate as a roofing material. The analytical methods developed were then applied to samples of slate from all the quarries reviewed in the Wartime Pamphlet No 40 to identify the most likely resources of good quality Scottish slate. Ideally, comparisons should have been made between fresh production-run slates, but without access to fresh Scottish samples this was not possible.

Because of the large number of quarries that needed to be included in this Report, the data sets for individual quarries for all aspects of this research are smaller than desirable.

Slate is a fine-grained material, which has only been metamorphosed to a very low level and falls into a grey area between sedimentary and metamorphic rocks. The techniques used to assess the properties of materials in both these areas were found to be unsatisfactory.

Evaluation of slate was based on the following properties:

1. Mineral composition
2. Metamorphic grade
3. Fabric
4. Weathering properties

The methods developed were then applied to the Scottish slate quarries with a view to selecting those suitable for further investigation.

7.2 Mineral Composition

In the past the composition of slate was described either in terms of major and minor minerals or as total oxides, without any information on their proportions. Recent progress has been made in the analysis of phyllosilicates in fine-grained material. This has enabled the mineral content of slate to be calculated from its total oxide composition. A representative sample from each group of quarries was analysed, the formulae of the component minerals established and hence the mineral composition. The mineral composition of other samples was then calculated from their total oxide content, using the formulae of the phyllosilicates from the standard. This technique appeared to give good results for samples taken in the immediate vicinity of the standard but when applied to samples from more remote sites in the area, unallocated oxides suggested that the formulae were no longer applicable. Thus the techniques developed would be better suited if the use of a single standard were limited to one quarry or group of closely spaced quarries.

Results were verified by comparison with those from other analytical techniques where possible.

It was found to be possible to relate the mineral composition of the slate loosely to the durability e.g. high quartz content and high white mica/chlorite ratio correlate with long service life. Ballachulish slate has a higher than average quartz content which may account for its longevity while some Aberfoyle slate has a reputation of softening after 20-30 years which may be due to some seams having lower than average quartz content. However, it may also be due to the presence of calcite but this was not assessed.

Minor minerals play a disproportionate role in the durability of slate. In general carbonates have a detrimental effect on durability but a distinction should be made between the different types of carbonate, e.g. dolomite is considerably more stable than

calcite. Similarly the type of iron ore mineral is also important. When present as an oxide (haematite) it is considerably more stable than as a sulphide (pyrite or pyrrhotite).

7.3 Metamorphic Grade

The second most important parameter in determining the properties of slate is the metamorphic grade, which controls the crystallinity and affects the grain size of the material. Traditionally for sedimentary rocks and soils both properties of crystallinity and grain size are evaluated by the sharpness of peaks in XRD analysis, using Full Width at Half Magnitude (FWHM) as the criterion. This work is usually carried out on a particular grain size fraction, which is an extremely time consuming procedure. However when applied to slate, the range of results is so small, with such high scatter, that the method is not effective for determining crystallinity. For these reasons an alternative method of determining the crystallinity of slate was developed, based on the intensities of peaks of the main minerals. Crystallinity values determined by this method vary from 200 to 1100, whereas the values given by FWHM range only from 0.25 to 0.1. Thus while both methods measure crystallinity, the greater sensitivity of the intensity of peaks method makes it of more practical use in discriminating between different quality slates.

The usefulness of the method was assessed by evaluating the results for a group of slates from working quarries. It was found that a given crystallinity value is characteristic of an area with coefficient of variation of approximately 10%. The technique was then applied to Scottish slate and the results were found to correlate with the reputation of the slate e.g. the crystallinity of weathered Ballachulish and Easdale samples was high to very high and these slates are known for their durability.

As with the FWHM method of assessing crystallinity, the results of this technique are dependent on the experimental methods and equipment used. Therefore results must be compared with values from samples with known properties.

7.4 Fabric

Much research has been carried out on the cleavage of slate and other low-grade metamorphic material with a view to understanding the tectonic regime under which the fabric developed. But little previous research has been done to relate the submicroscopic properties of the fabric to the ability to split it into thin sheets for use as a roofing material.

Building on the characteristics of slaty cleavage defined by Powell (1979) it was possible to develop a relationship between these and the thickness of the finished roofing slate. The fabrics of a selection of slates from producing quarries in North Wales and Cumbria were examined and the submicroscopic properties quantified wherever possible and assigned a value called the Fabric Point Scheme (FPS) value. The results were correlated with the actual thickness of the finished slates and a relationship established. This relationship was optimised by regressional analysis using multivariate statistics. It was then used to predict the potential minimum thickness of Scottish slate. The validity of the method was verified by comparing the actual thicknesses of used Scottish slates with their theoretical minimum thicknesses. It was found that there was a tendency for finished slates to be split thicker than Welsh slates with a corresponding number of points but in several examples there was good agreement to within 1mm. No slate was split thinner than the theoretical limit.

The relationship between FPS and thickness of the slate was then applied to a few samples from all the slate quarries described in Appendix A and a theoretical minimum thickness for each sample was determined. As in all aspects of this work, the data set was too small, so that observations may not be representative due to the natural variation in the quarry. However it gives a indication of the splitting quality of the slate from all the Scottish slate quarries reviewed.

7.5 Weathering Properties

Estimates of the durability of a slate were made by experimentally weathering new slates. The method which best mirrors the effect of natural weathering of slate on a roof is the wetting and drying test. The effect of weathering was assessed by measuring the increase in ability of the slate to absorb water with length of experimental weathering. This effect is also observed in slates which have been naturally weathered. The relationship between length of experimental weathering and water absorption (weathering profile) was determined for a few fresh slate samples and a few weathered Scottish samples. When the effect of natural weathering was compared to that of experimental weathering in terms of the rate of increase in water absorption with time it was found that 5 to 12 wetting and drying cycles were equivalent to one year of natural weathering. Applying this relationship to the weathering profiles, it was then possible to estimate the life of a slate to the point at which water absorption reached a value of 0.3% which is the limit specified by the British Standard for slate, BS 680.

It is proposed that routine testing of new slate should include the following:

- Determining the initial water absorption
- 25 cycles of wetting and drying to test for oxidisable compounds, such as pyrite (especially in the presence of carbonate)
- Determining the final water absorption after a set number of wetting and drying cycles.

Rate of increase in water absorption relative to a slate of known performance, such as from the old vein at Ffestiniog as used in this work, can be used to estimate the service life.

7.6 Conclusions

The geological parameters which affect the performance of slate have been used to select potentially viable quarries, as discussed at length in Appendix A. In evaluating the potential of a quarry to produce roofing slate the significant attributes are:

- Dimensional Considerations
- Durability

Dimensional Considerations

An important consideration in assessing the viability of a quarry is the potential minimum thickness and size of the finished slates. The Fabric Point Scheme (FPS) method has been used to assess the minimum potential thickness of slate from Scottish quarries.

The effect of spacing and orientation within the quarry of discontinuities such as joints on its ability to produce slates of usable size can be assessed theoretically. However it has only been possible to apply this approach to a limited number of Scottish slate quarries. In most cases, the quarries are overgrown, faces are obscured with waste tips or were left in an unstable condition and have collapsed in the intervening years..

Durability

The important determinants of the durability of slate are

- Crystallinity
- Mineralogy

In general low water absorption indicates high durability and the more crystalline the slate the less it absorbs water. In addition, any deleterious minerals present are in a crystalline form and hence are stable. However, in some cases fine-grained slates with low crystallinity have low water absorption due to their grain size and are also durable. When mineralogy is good i.e. minerals are present in their oxidised form, the effect of

high water absorption is substantially reduced and minerals are stable even if water can penetrate the slate. This is the case for Macduff slate.

Other, non geological, factors affecting the viability of a quarry are touched on briefly in the Quarry Reports Appendix A.

Ballachulish Slate

The best Scottish slate is found at Ballachulish, and there are sufficient resources to merit further investigation. However there are many other factors to consider. Individual quarries have their limitations in terms of access, proximity to centres of population, environmental sensitivity etc.

Macduff

There are large resources of slate on the north slopes of the Slate Hills. The quality of the slate was found to be remarkably uniform from one hill to the next. Areas between worked veins were not investigated. Selecting a quarry for further exploitation will depend on other factors such as access etc. In general, quarries that have at least rudimentary vehicular access are those worked extensively in the past and hence they have the problem of large tips covering the working area. The splitting properties of the slate rock deteriorate to the south due to increasing proximity to the Insch igneous intrusion.

Highland Border

The mineralogy of Highland Border slate, in particular the lack of pyrites, suggests that it would have good potential as a roofing material. Other properties however, such as the degree of crystallinity, also affect the durability of the slate and these vary considerably from quarry to quarry and for producing units within a quarry. Zones with poor crystallinity and low quartz content which are present in some quarries should be avoided.

Easdale

There is no question that very durable slate has been produced from the Easdale area in the past, and those quarries which were worked extensively e.g. Easdale Island, show little superficial weathering.

Many quarries which were suitable in terms of their resources, location and access had badly weathered surfaces or complex geological features. No quarry in this area was particularly suitable for further investigation. Toberonochy slate appeared little weathered, but the confines of the present quarry are extensively worked. It may be worth investigating if the producing seam extends along strike. A more practical alternative for further investigation is Breine Phort, even though the slate is badly weathered on the surface.

Taking all these factors into account, the following quarries merit further investigation:

1.	Ballachulish	Khartoum
2.	Macduff	Kirkney
3.	Highland Border	Craiglea
4.	" "	Aberfoyle
5.	Easdale	Breine Phort

Bibliography

Ager D V. 1980. *The Geology of Europe* McGraw-Hill London 275-282.

Aller J, Bastida F, Brime C & Perez-Estaun A. 1987 Cleavage and its relation with metamorphic grade in the Cantabrian zone (Hercynian of north-west Spain). *Sciences de Geologie Bulletin (Strasbourg)* **40** 255-272.

Anderton R. 1985 Sedimentation and tectonics in the Scottish Dalradian. *Scottish Journal of Geology* **21** 407-436.

Anderton R. 1976. Tidal-shelf sedimentation: an example from the Scottish Dalradian. *Sedimentology.* **23** 429-458.

Avery B W & Bullock P 1977 Mineralogy of clayey soils in relation to soil classification *Soil Survey Techniques. Monograph* **10** 1-64.

Bailey S W & Brown B E. 1962 Chlorite Polytypism: 1 Regular and semi-regular one-layer structures. *American Mineralogy* **47** 819-850.

Bailey S W. 1984 Classification and Structures of the Micas; Reviews in Mineralogy **13** *Editor* S. W. Bailey; *Mineralogical Society of America.*

Barrow G. 1893 On an intrusion of muscovite biotite gneiss in the S. E. Highlands of Scotland and its accompanying metamorphism. *Quarterly Journal of the Geological Society, London.* **49** 350-358.

Barrow G. 1912 On the geology of lower Deeside and southern highland border. *Proceedings of the Geologists' Association* **23** 268-284.

Bayliss P & Loughnan F C. 1964 Mineralogical transformation accompanying the chemical weathering of clay slate from New South Wales. *Clay Mineral Bulletin* **5** 353-362.

Bell T H, Rubenach M J & Flemming P D. 1986. Porphyroblast nucleation, growth and dissolution in regional metamorphic rocks as a function of deformation partitioning during foliation development. *Journal of Metamorphic Geology.* **4** 37-67.

Blaikie J. 1834 Essay III on the slate quarries of Aberdeenshire. *Prize Essays and Transactions of the Highland and Agriculture Society* **10** 98-106.

Borradaile G J, Bayly M B & Powell C McA. 1982 Atlas of deformational and Metamorphic Rock Fabrics. *Publishers* Springer-Verlag.

Bremmer D. 1869 *Industries of Scotland Publishers* Black, Edinburgh.

Brindley G W. 1980 Quantitative mineral analysis of clays in crystal structures of clay minerals and their X-ray identification *Editors* Brindley G W & Brown G *Mineralogical Society*, London 2nd edition.

Carroll D. 1974 Clay Minerals: a guide to their X-ray identification *Publishers The Geological Society of America Special Paper 126.*

Cathelineau M & Nieva D. 1985 A chlorite solid solution geothermometer; the Los Azufres (Mexico) geothermal system. *Contribution to Mineralogy and Petrology* **91** 235-244.

Cloos E 1947. Oolite deformation in South Mountain fold, Maryland. *Geological Society of America Bulletin.* **58** 843-918.

Crockett R N 1975 Slate – Mineral Dossier 12 *Publishers* Mineral Resources Consulting Committee, London.

Deer W A, Howie R.A & Zussman J. 1992 *An introduction to the rock-forming minerals. Publishers;* Longman Group UK.

Dempster T J & Tanner P W G. 1997 The biotite isograd, Central Pyrenees: a deformation-controlled reaction. *Journal of Metamorphic Geology* **15** 531-548.

Department of the Environment. 1993 *English House Condition Survey 1991. Publishers* HMSO London.

Dunoyer de Segonzac G. 1969. Les mineraux argileux dans la diagenese. Passage au metamorphisme *Thesis, University of Strasbourg.*

Dunoyer de Segonzac G. 1970 The transformation of clay minerals during diagenesis: A Review. *Sedimentology* **15** 281-346.

Erslev E A. 1998 Limited localized nonvolatile element flux and volume change in Appalachian slates. *Geological Society of America Bulletin* **100** 900-915.

Eslinger E V & Savin S M. 1971 Mineralogy and oxygen isotope ratios of hydrothermal and low-grade metamorphic argillaceous rocks *PhD thesis, Case Western Reserve University Clevland Ohio.*

Esquevin J. 1969 Influence de la composition chimique des illites sur leur cristallinite. *Bulletin du Centre de Recherches de Pau, Societe Nationale des Petroles d'Aquitaine* **3** 147-154.

European Standard 1996 prEN12407 Draft Test on natural stone-Petrographic description of natural stone.

Fairweather B 1994 The 300-year story of Ballachulish slate *Publishers* Glencoe and North Lorn Folk Museum Glencoe Fort William.

Fitton F 1997 X-ray fluorescence spectrometry. In *Modern analytical geochemistry Editor* Gill R. *Publishers* Longman

Flinn D 1962 On folding during three dimensional progressive deformation. *Quarterly Journal of the Geological Society, London* **118** 385-433.

Flinn D 1962. On the symmetry principle and the deformation ellipsoid. *Geological Magazine* **102** 36-45.

Foster M D. 1962 Interpretation of the composition and a classification of the chlorites. *U.S. Geol Survey Prof Paper* **414-A** 33.

Frey M. 1970 The step from diagenesis to metamorphism in pelitic rocks during Alpine Orogenesis. *Sedimentology* **15** 261-279.

Gibbons W & Harris A L. 1994 *A revised correlation of Precambrian rocks in the British Isles* Special Report No 22. *Publishers* Geological Society London

Hall A J. 1982 Gypsum as a Precursor to Pyrrhotite in Metamorphic Rocks. Evidence from the Ballachulish Slate in Scotland. *Mineralium Deposita* 17 401-409.

Hall A J. 1986 Pyrite-pyrrhotine redox reaction in nature. *Mineralogical Magazine* **50** 223-229.

Hall A J, Boyce A J & Fallick A E. 1988 A sulphur isotope study of iron sulphides in the Late Precambrian Dalradian Easdale Slate Formation Argyll Scotland. *Mineralogical Magazine* **52** 483-490.

Harries-Rees 1991 Slate Market Split - Niche develops for prestige products. *Industrial Minerals.* **284** 44-55.

Harrison H W 1996 *Roofs and Roofing Publishers* Building Research Establishment.

Hart D 1991 *The building slate of the British Isles. Publishers* Building Research Establishment.

Hewison J K. 1845 *The Isle of Bute in the olden Times Vol II, Publishers* William Blackwood Edinburgh.

Hickman A H. 1975 The stratigraphy of late Precambrian metasediments between Glen Roy and Lismore. *Scottish Journal of Geology* **11** 117-142.

Kemp A E S, Oliver G H J & Baldwin J R. 1985 Low grade metamorphism and accretion tectonics: Southern Upland Terrane, Scotland. *Mineralogical Magazine* **49** 335-344.

Kessler D W & Sligh W H. 1932 Physical properties and weathering characteristics of slate *Bureau of Standards Journal of Research* **9** 377-411.

Kisch H J. 1983 Mineralogy and petrology of burial diagenesis (burial metamorphism) and incipient metamorphism in clastic rocks *Diagenesis in sediments and sedimentary rocks 2 Editors* Larsen and Chilingar *Publishers* Elsevier - New York.

Kisch H J. 1990. Calibration of the anchizone: a critical comparison of illite 'crystallinity' scales used for definition. *Journal of Metamorphic Geology* **8** 31-46.

Kisch H.J. 1991 Development of slaty cleavage and degree of very low-grade metamorphism: a review *Journal of Metamorphic Geology* **9** 735-750.

Klingebiel A & Latouche C. 1962 Etude cristallographique des illites dans les series Eocenes du Bordelais *C R Acad Sce Ser D 255* 142-144.

Klug H P & Alexander L E 1974 X-ray Diffraction Procedures for Polycrystalline and Amorphous Materials *Publishers* John Wiley and Sons, 2nd edition, New York

Krauskopf K 1953 *Fundamentals of Physical Science* 3rd Edition *Publishers* McGraw-Hill Co. New York.

Krauskopf K B 1967 Introduction to geochemistry, International series in earth and planetary sciences *Publishers* McGraw-Hill U.S.A.

Kubler B 1967 La cristallinite de l'illite et les zones tout a fait superieures du metamorphisme *Etages Tectoniques* **105-121** A la Baconniere, Neuchatel Suisse.

Le Corre C. 1970 Bases methodologiques pour la recherche ardoisiere dans le massif Armoricain. *Bulletin, Societe Geologique et Mineral. Bretagne* **2** 73-87.

Marty J 1980 Géologie de l'ardoise. *Industrie Minérale* 552-558.

Maxwell D & Hower J. 1967 High grade diagenesis and low grade metamorphism of illite in the Precambrian belt series. *American Mineralogist* **52** 843-857.

Maxwell J C 1962 Origin of slaty cleavage in the Delaware Water Gap area, New Jersey and Pennsylvania . *Geological Society of America Memoirs* Buddington Volume 281-311.

McEwan D M C, Ruiz Amil A & Brown G. 1961 Interstratified clay minerals. *The X-ray Identification and Crystal Structures of Clay Minerals. Editor* Brown G. *Publishers* Mineralogical Society London 393-445.

Merriman R J & Roberts B. 1985 A survey of white mica crystallinity and polytypes in pelitic rocks of Snowdonia and Llyn, North Wales. *Mineralogical Magazine* **49** 305-319.

Moore M M & Reynolds R C. 1989 & 1997 (First and second editions) *X-ray diffraction and the identification and analysis of clay minerals Publishers* Oxford University Press, Oxford.

Naismith R J. 1985 Buildings of the Scottish Countryside. *Publishers* Gollancz, London.

Norris R J & Rupke N A. 1986 Development of slaty cleavage in a mudstone unit from the Cantabrian Mountains, northern Spain. *Journal of Structural Geology* **8** 871-878.

Neumann H. 1950 Pseudomorphs after Pyrite in the Ballachulish Slates. *Mineralogy Magazine* **29** 234-238.

Nuffield E W 1966 *X-Ray Diffraction Methods. Publishers* John Wiley and Sons New York.

Oertel G. 1970. Deformation of a slaty, lapillar tuff in the Lake District, England. *Geological Society of America Bulletin.* **81** 1173-1178.

Peach B N., Kynaston H. & Muff H B. 1909 *The Geology of the seaboard of Mid Argyll. Memoirs of the Geological Survey of Scotland. Publishers* HMSO Glasgow U.K.

Powell C McA. 1979 A morphological classification of rock cleavage *Tectonophysics* **58** 21-34.

Prentice J E. 1990 *Geology of Construction Materials Publishers* Chapman and Hall, London.

Ramsay J G 1976 Displacement and strain. *Phil Transactions Royal Society London* **A283**: 3-25.

Richards A J. 1995 *Slate quarrying in Wales Publishers* Gwasg Carreg Gwalch, Wales.

Reed S J B 1996 *Electron microprobe analysis and scanning electron microscopy in geology Publishers* Cambridge University Press

Richey J E & Anderson J G. 1944 *Scottish Slate Wartime Pamphlet No 40. Publishers* Geological Survey of Great Britain.

Riley J P 1958 The rapid analysis of silicate rocks and minerals *Analytica Chemica Acta* **19** 413-428.

Riley J P. 1958 Simultaneous determination of water and carbon dioxide in rocks and minerals *The Analyst* **83** 42-46.

Roberts B & Merriman R J. 1985. Caledonian metamorphism in North Wales. *Journal of the Geological Society, London* **142** 615-624.

Robinson D & Bevins R. 1986 Incipient metamorphism in the lower Palaeozoic marginal basin of Wales. *Journal of Metamorphic Geology* **1986** 101-113.

Robinson D, Warr L N & Bevins R E. 1990 The illite 'crystallinity' technique: a critical appraisal of its precision. *Journal of Metamorphic Geology* **8** 333-344.

Roekens E J,Keppens E C & Van Grieken R E. 1991 Air pollution-induced weathering of slates The Science of the Total Environment 121-126 *Publishers* Elsevier Science B.V Amsterdam.

Roy R.B. 1978. Evolution of slaty cleavage in relation to diagenesis and metamorphism: A study from the Hunsruckschiefer. *Geological Society of America Bulletin.* **89** 1775-1785.

Schultz L G 1964 Quantitative interpretation of mineralogical composition from X-ray and chemical data from the Pierre Shale *U.S Geological Survey Prof. Paper* **391-C** 1-31.

Scottish Homes 1993 Scottish House condition survey 1991. Survey Report. Publishers Scottish Homes Edinburgh.

Shayan A. Lancuck C J 1987 Deterioration of slate tiles containing iron sulphides. *Fourth international conference on durability of building materials and components,* Singapore.

Smith G (c1835) Accounts of the Principal Slate Quarries in Scotland *Prize Essays and Transactions of the Highland and Agriculture Society* **10** 98-106.

Sorby H C. 1908. On the application of quantitive methods to the study of the structure and history of rocks. *Quarterly Journal of the Geological Society, London.* 64 171-232.

Srodon J. & Eberl D.D 1984 *Illite: Reviews in Mineralogy 13 Editor.* Bailey S.W Mineralogical Society of America.

Stephen I & MacEwan D M C. 1950 Swelling chlorites. *Geotechnique* **2** 82-83.

Stephen I & MacEwan D M C. 1951 Some chloritic clay minerals of unusual type. *Clay Mineral Bulletin* **1** 157-163

Sutton S J. 1989 Orientation dependent metamorphic grade in phyllosilicates belonging to a slaty cleavage fabric. *Journal of Geology* **97** 197-208.

Sutton J & Watson J V. 1955 The deposition of the Upper Dalradian rocks of the Banffshire coast. *Proceedings of the Geologists' Association.* **66** 101-133.

Taboada J, Vaamonde A, Saavedra A & Alejano L. 1997 Application of geostatistical techniques to exploitation planning in slate quarries. *Engineering Geology* **47** 269 –278.

Tilley C E. 1925 Metamorphic zones in the southern Highlands of Scotland. *Quarterly Journal of Mineralogy* **81** 100-112.

Tucker D G. 1977 The slate islands of Scotland: The History of the Scottish Slate Industry *Business History* **19** 18-36.

Twiss R J & Moores E M. 1992 *Structural Geology Publishers* Freeman and Co., New York.

Wagner W, Le Bail R, Hagar- Rodriguez M. P. & Stanek S. 1994 European Roofing Slates Part 1: Remarks to the Geology of Mineral Deposits *Zeitschrift fur Angewordte Geologie* **40** 68-74.

Wagner W, Le Bail R, Hagar-Rodriquez & Stanek S. 1995 European Roofing Slates Part 2 Geology of Selected Examples of Slate Deposits *Zeitscrift fur Angewordte Geologie* **41** 21 - 25.

Watkins C M. 1934 The Durability of Slates for Roofing *Building Research Bulletin No 12 Publishers* HMSO for Department of Scientific and Industrial Research.

Weaver C E & Associates 1984 *Shale Slate Metamorphism in Southern Appalachians. Publishers* Elsevier Science Amsterdam.

Weaver C E. 1960. Possible uses of clay minerals in search for oil. *Bulletin of American Association of Petroleum Geology* **44** 1505-1518.

Weaver C E. 1965 Potassium content of illite. *Science* **147** 603-605.

Weber K. 1981. Kinematic and metamorphic aspects of cleavage formation in very low-grade Metamorphic slates. *Tectonophysics* **78** 291-306.

Weber K. 1972 Notes on determination of illite crystallinity. *Neues Jahrbuch for Mineralogie Monatshasste* **6** 267-278.

West A R. 1984 *Solid State Chemistry and its Application Publishers* John Wiley & sons 115-186.

Wood D. 1971 Studies of strain and slaty cleavage in the Caledonides of northwest Europe and the eastern United States. *PhD thesis, University of Leeds, England.*

Wood D S. 1974 Current views of the development of slaty cleavage. *Annual Review of Earth and Planetary Sciences* **2** 369-401.

Yoder H S & Eugster H P. 1955 Synthetic and natural muscovites. *Geochemica et Cosmochimica Acta* **8** 225-280.

Appendix 1.1a	Sample Set of non-Scottish slates and the procedures for which they were used.								
Quarry	**Source**	**Sample Code**	**Grid Reference**	**Colour**	**WR**	**Total Oxides**	**Fabric**	**FWHM Crystal-linity**	**Misc**
Cwt y Bugail			**SH732 456**	Dark-grey,					
	Fine-grained slates produced in thicknesses of 5mm to 8mm								
	"Medium strong" from quarry face	WCB-1			Yes	Yes	Yes	Yes	
	"Medium strong" from quarry face	W/CB-2			Yes			Yes	
	Weathered sample from waste tips	W/CB-3			Yes			Yes	
	"Extra heavy" finished slate	W/CB-4			Yes		Yes	Yes	
	"Medium strong" finished slate	W/CB-5			Yes		Yes	Yes	
Pen yr Orsedd			**SH510 538**						
	Fine-grained in a variety of colours, thicknesses of 4mm to 8mm								
	Tips	W/PO-1		Green/purple	Yes			Yes	
	Reject from dressing shed	W/PO-3		Purple	Yes	Yes			
	Slate from quarry face	W/PO-5		Purple	Yes			Yes	
	"Best" heather blue finished slate	W/PO-6		Purple	Yes			Yes	
	"Best" heather blue finished slate	W/PO-7		Red	Yes			Yes	
	"Best" Bangor blue finished slate	W/PO-8		Red	Yes			Yes	
	"Best" red finished slate	W/PO-9		Red	Yes			Yes	
	"Best" finished slate	W/PO-10		Red	Yes			Yes	
Tyn y Weirglodd			**SH494 523**						
	Sample from quarry face	W/PO-11		Plum -red	Yes	Yes	Yes	Yes	

Quarry	Source	Sample Code	Grid Reference	Colour	WR	Total Oxides	Fabric	FWHM Crystal-linity	Misc
Ffestiniog and Gloddfa Ganol Quarries			**SH 694 473**						
	Fine grained slates produced in thicknesses from 4mm to 8mm								
	Old *vein* finished slate	W/F-1		Blue-grey	Yes	Yes	Yes	Yes	Thin sections H&L, FeO
	Old *vein* finished slate	W/F-4		Blue-grey	Yes			Yes	Thin sections H&L
	Old *vein* finished slate	W/F-5		Blue-grey	Yes		Yes	Yes	
	Old *vein* finished slate	W/F-8		Blue-grey	Yes		.	Yes	Weathering
	Between old and new *vein*	W/F-9		Blue-grey	Yes	Yes	Yes	Yes	Thin sections H&L
	Old *vein* outcrop	W/F-10		Blue-grey	Yes			Yes	
	Old *vein* frost damaged sample	W/F-11		Blue-grey	Yes			Yes	Thin sections H&L
	North or pigs *vein* sample	W/F-12		Blue-grey	Yes		Yes	Yes	
	North or pigs *vein*	W/F-13		Blue-grey	Yes		Yes	Yes	
	Between old and north (pigs) *vein*	W/F-15		Blue-grey	Yes			Yes	
	New *vein* finished slate	W/F-16		Blue-grey	Yes		Yes	Yes	
Twill Coed			**SH 494 524**						
	Sample from quarry	W/TC-1		Red	Yes			Yes	
Penrhyn			**SH623 650**						
	Fine grained slates in a variety of colours range of thicknesses from 5mm to 8mm								
	Sample from quarry	W/P-1		Purple	Yes		Yes		Thin sections H&L
	Reject from quarry	W/P-2		Purple	Yes				Thin sections H&L

Quarry	Source	Sample Code	Grid Reference	Colour	WR	Total Oxides	Fabric	FWHM Crystal-linity	Misc
Spanish slate supplied by Mr Elfed Williams of Ffestiniog Quarries									
W/X-1	Quarry unknown			Blue-grey	Yes			Yes	
W/X-2				Blue-grey	Yes			Yes	
W/X-3				Blue-grey	Yes			Yes	

Burlington Slate Company produces "Burlington Blue" and Burlington Green Slates
The Burlington quarries produce three grades of slates

1) "Best" 7-9mm
2) "Strong" 9-12mm
3) "Extra strong" > 12mm and imperfects of any thickness

Burlington Quarry Kirkby-in-Furness			**SD 250 837**						
Trade Name	**Burlington Blue**								
	"Best" roofing slate from quarry face	E/K-1		Blue-grey	Yes		Yes	Yes	CO_2 & H_2O
	poor potential from quarry face	E/K-2		Blue-grey	Yes			Yes	CO_2 & H_2O
	Finished "strong"	E/K-3		Blue-grey	Yes		Yes	Yes	
	"strong" slate from dressing shed	E/K-4		Blue-grey	Yes			Yes	
Broughton Moor			**SD 254 646**						
Trade Name	**Burlington Green or Westmorland**								
	"Extra strong" coarse grain 12mm	E/BM-1		Olive green	Yes		Yes	Yes	
	"Best" 9mm thick	E/BM-2		Olive green	Yes			Yes	

Quarry	Source	Sample Code	Grid Reference	Colour	WR	Total Oxides	Fabric	FWHM Crystal-linity	Misc
Elterwater			**NY 324 048**						
Trade Name	Burlington Green or Westmorland								
	Finished "strong" slate	E/EW-1		Dark green	Yes			Yes	CO_2 & H_2O
	Finished "strong" slate	E/EW-2		Dark green	Yes			Yes	CO_2 & H_2O
	Finished " extra strong" slate	E/EW-3		Dark green	Yes			Yes	Thin section L
	Finished "best" slate	E/EW-4		Dark green	Yes		Yes	Yes	
	Finished slate from slate merchant	E/W-1			Yes				Thin sections H&L
Brossan Stone			**SD278 974**						
Trade Name	"Silver grey" coarse grained slate used for cladding								
	Weathered sample	E/BS-1		Grey green	Yes			Yes	
	Dark Brossan Stone	E/BS-2		Grey green	Yes			Yes	
	Light Brossan Stone	E/BS-3		Grey green	Yes			Yes	
	Dark Brossan Stone	E/BS-4		Grey green	Yes			Yes	
Brandy Crag			**SD284 984**						
Trade Name	"Silver grey" coarse grained slate 9-10mm thick used for floors and roofs								
		E/BC-1		Grey green	Yes			Yes	

Quarry	Source	Sample Code	Grid Reference	Colour	WR	Total Oxides	Fabric	FWHM Crystal-linity	Misc
Irish Slate									
Killaloe Slate from Killoran Quarry, Portroe Nr Nenagh Co. Tipperary Ireland.									
The following samples were collected from a slate dealer									
	Slate > 200 yrs old	I/K-1	Tipperary Sheet 19 R770 785	Blue grey occasionally with distinctive banding	Yes			Yes	
	New slate from Killoran quarry	I/K-3			Yes			Yes	Weathering
	Killaloe old slate	I/K-4			Yes			Yes	
French Slate									
The following Ardoisieres d'Angers were collected by Mr Robin Kent of Historic Scotland. The Noyant Slate Mine is 60km NW Angers, Maine et Loire, The Grand Carreau and the Fresnal slate mines are 20 Km SE of Angers									
	Noyant Grade A	F/N-1		Blue-grey	Yes			Yes	
	Noyant Grade B	F/N-2		Blue-grey	Yes			Yes	
	Grand Carreau Grade A	F/G-1		Blue-grey	Yes			Yes	
	Grand Carreau Grade B	F/G-2		Blue-grey	Yes			Yes	
	Fresnal Grade B	F/F-1		Blue-grey	Yes			Yes	
	Fresnal Grade A	F/F-2		Blue-grey	Yes			Yes	

Quarry		Sample Code	Grid Reference	Colour	WR	Total Oxides	Fabric	FWHM Crystal-linity	Misc
Miscellaneous samples from different importers of roofing slates									
	Spanish Cupa sample fine grained with pyrite cubes	S/C-1		Dark-grey	Yes			Yes	
		S/C-2		Dark-grey	Yes			Yes	
	Unweathered spanish	S1-0		Dark-grey	Yes			Yes	Weathering
	Chinese slate	C/C-1		Dark grey	Yes				
Trade Name	Vermont slate cut 7mm thick. "Heather Purple"	U/V-1		Purple	Yes			Yes	Thin sections H&L
	Garnet Mica schist	S/A-1		Dark grey	Yes			Yes	
Non-slate from Grampian Highlands of Scotland									
	Garnet mica hornfels	CS 7			Yes			Yes	
	Garnet mica hornfels	CC34			Yes			Yes	

Appendix 1.1b	Sample Set of Scottish slates and procedures carried out								
				Miscellaneous					
				Thin section	WR	Fabric	Total	FWHM	FeO
				H horizontal			Oxides		
				L perpendicular					
Ballachulish Slate									
East Laroch Quarry			**NN085 582**						
North face	Dark grey fine to medium grained from kink in cleavage	EL-2	NN0849 5836	L	yes				
	Dark grey fine-grained slate with pyrites from face	EL-3	NN0862 5828	L	yes	yes	yes	yes	
	Dark grey fine-grained slate with pyrites from seam	EL-4	NN0862 5828	L	yes		yes	yes	
	Dark grey fine-grained slate from face	EL-5	NN0844 5844		yes	yes			
Upper galleries	Dark grey fine-grained slate with large pyrites clusters	EL-6	NN0853 5805		yes		yes	yes	
	Dark grey fine-grained with some rusty weathering from tips	EL-7	NN0845 5843		yes	yes	yes	yes	
	Dark grey fine-grained with some rusty weathering from face	EL-8	NN0848 5810		yes		yes	yes	
	Dark grey fine-grained with some silty bands from face	EL-9	NN0858 5811		yes		yes	yes	
Best vein	Medium grey fine-grained from working face	EL-10	NN0863 5813	CO2 & H2O	yes	yes	yes	yes	yes
West Laroch			**NN075 582**						
Middle Quarry	Dark grey fine to medium grained from face	WL-1	NN0750 5820	L	yes	yes	yes	yes	
	Dark grey fine to medium grained from face	WL-3	NN0744 5819	L	yes		yes	yes	
	Dark grey fine to medium grained from tips	WL-5	NN0743 5822		yes	yes	yes	yes	
Khartoum			**NN084 572**						
	Dark grey medium-grained with rusty weathered bands	K-1	NN0838 5720		yes	yes	yes	yes	
	Dark grey medium-grained with rusty spots from tips	K-2	NN0828 5722		yes		yes	yes	
	Dark grey medium-grained with rusty spots from tips	K-3	NN0828 5722		yes	yes	yes	yes	
2nd-hand-slate dealer	Dark grey medium grained roofing slate	BX-1	unknown		yes	yes	yes		
Easdale Slate									
Easdale Island			**NM735 169 to NM740 174**						
Craig na h-uamha Q.	Dark grey fine-medium grained with pyrites cubes from seam	EE-1	NM7631 1732	H & L	yes		yes		
	A similar slate from the tips	EE-2	NM7659 1709		yes	yes	yes		
	Used slate from the island with 5mm pyrites rusty but no leaching	EE-3	unknown		yes	yes	yes		
Seil Island									
Breine Phort			**NM754 166**						
	Dark grey medium grained slate form face, crenulated cleavage	SB-5	NM7538 1662	CO2 & H2O	yes	yes	yes	yes	
	pyrites bimodal some superficial weathering from face	SB-6	NM7542 1659		yes		yes	yes	yes
	Similar slates from the tips	SB-7	NM7534 1660		yes		yes	yes	yes
	Similar slates from the tips	SB-8	NM7534 1660		yes		yes	yes	

				Miscellaneous					
				Thin section	WR	Fabric	Total	FWHM	FeO
				H horizontal			Oxides		
				L perpendicular					
Balvicar			**NM766 164 to NM769 168**						
Quarry No 1	SB1-3 are dark grey slates medium grained slates from the	SB-1	NM7685 1662		yes	yes	yes		
	working face. Pyrites are small (<1mm) rusty but no leaching	SB-2	NM8684 1662	CO2 & H2O	yes	yes	yes	yes	
		SB-3	NM7679 1659	CO2 & H2O	yes		yes	yes	
	Graphitic dark grey slate from face	SB-4	NM7678 1656		yes		yes	yes	
2nd-hand-slate dealer		EX-1	unknown		yes		yes		
Island of Luing									
Toberonochy	These slates are dark grey fine-grained with small sparsely		**NM747085**						
	spaced pyrites from the working face	LT-1	NM7488 0854	L	yes		yes	yes	
	a used slate from village hall	LT-2	unknown	L	yes	yes	yes	yes	
	from the tips	LT-3	NM7499 0866	CO2 & H2O	yes	yes	yes	yes	
Rubha na hEasgainne	These are dark grey fine to medium grained slates graphitic in places		*NM748145*						
	with ubiquitous pyrites, badly weathered from the tips.	LP-1	NM7483 1452		yes		yes		
	Tips	LP-2	NM7481 1441		yes				
	Tips	LP-3	NM7476 1439	L	yes		yes	yes	
Port Mary	These are blue-grey, fine to medium-grained slates with crenulated	LP-5	NM7451 1402		yes	yes	yes	yes	yes
	cleavages, pyrites are 4mm in size, fresh in LP-5 but rusty in LP-6	LP-6	NM7411 1332	CO2 & H2O	yes	yes	yes	yes	
	Both samples from working faces								
Cullipool			**NM739129 to NM742138**						
Quarry No 3	These are blue-grey, fine to medium-grained slates with crenulated	LC-1	NM7397 1345	L	yes		yes	yes	
Quarry No 2	cleavages, pyrites are 5mm in size, with superficial weathering	LC-2	NM7400 1352		yes	yes	yes	yes	
	An almost new slate similar to the LC-1 and 2	LC-3	unknown	Weathering	yes	yes	yes		
Tir na Oig	North quarry tips	LT-5	**NM733 103**	CO2 & H2O		yes	yes	yes	
Blackmill Bay			**NM732082**						
	These slates are dark grey medium-grained, crenulated surface, the	LB-1	NM73250832		yes	yes	yes	yes	
	pyrites are 5mm in size are rusty, leached and or have fallen out	LB-2	NM73290832		yes		yes		
	LB-1 and 2 are from the tips while LB-3 is a used slate from local house	LB-3	unknown	Weathering	yes		yes	yes	
Bellnahua	Medium grey medium grained slate with crenulated surface		NM714 128						
	A used slate, pyrites a 1-2mm in size and rusty but no leaching	BB-1	unknown		yes	yes	yes	yes	
	a similar slate from the tips	BB-2	NM7148 1268	CO2 & H2O	yes	yes	yes	yes	

				Miscellaneous					
				Thin section	WR	Fabric	Total	FWHM	FeO
				H horizontal			Oxides		
				L perpendicular					
Highland Border Slate									
Arran			**NR963 504 & NR961 503**						
Main Quarry	Blue-grey fine grained from tips	A-1	NR963 504		yes				
	Green medium grained slate from tips	A-3	NR96 3504		yes	yes	yes	yes	
	Light grey medium grained slate from tips	A-5	NR963 504		yes	yes	yes		
	Dark grey medium grained slate	A-6	NT963 504		yes		yes	yes	
Bute									
Ardmaleish Quarry	Grey-blue fine -medium grained crenulated surface	B-1a	NS0749 6967		yes		yes	yes	
	Green medium grained slate from seam	B-1b	NS0749 6967		yes		yes	yes	
Hilton Quarry	Grey blue fine grained from face	B-2	NS0582 6842		yes		yes	yes	yes
	Blue-grey slate from collapsed roof - Hilton farm	B-3	NS0622 6844		yes		yes	yes	
	Weathered band in quarry face	B-4	NS0583 6842		yes			yes	
Edinmore Quarry	Blue grey fine-medium grained from tips	B-5	NS052 681		yes		yes	yes	
Luss	These slates show little superficial weathering								
Auchengavin Quarry	Grey-blue fine -medium grained crenulated cleavage surface	LS-1	NS349 09273		yes	yes	yes		
	Blue-grey fine grained from seam	LS-2	NS349 09273		yes		yes		
Aberfoyle	These slates show little superficial weathering								
West Quarry	Green medium grained slate from seam	AB-1	NN5030 0289		yes	yes	yes	yes	
	Green/Purple slate separated by quartz vein from seam	AB-2	NN5031 0289						
Lochout Quarry	Grey medium grained slate from face	AB-3	NN5041 0304		yes	yes	yes	yes	
	Grey medium grained slate from lower level tips	AB-4	NN50 6032		yes	yes	yes	yes	
No 1 vein	Blue-grey medium grey slate from seam	AB-5	NN5054 0302		yes	yes	yes	yes	yes
2nd hand slate dealer	Dark green fine-medium grained slate flaking on the under surface.	AB-6	unknown		yes	yes	yes	yes	
Comrie	These slates show little superficial weathering								
Aberuchill Quarry	Green coarse grained slate from face, ripple marks visible	Au-1	NN7160 1970		yes		yes		
	Blue grey medium grained slate from seam	Au-2	NN7163 1971		yes		yes		
	A similar slate from a local roof	Au-3	unknown		yes	yes	yes		
Drummond Quarry	Green coarse grained slate from seam	Dr-1	NN7081 1873		yes	yes	yes		
Logiealmond									
Craiglea Quarry	These slates show little superficial weathering								
	Green coarse grained slate from seam	Cr-1	NN9492 3219		yes	yes	yes		
	Blue medium grained from worked seam	Cr-2	NN9492 3219		yes		yes		

				Miscellaneous					
				Thin section	WR	Fabric	Total	FWHM	FeO
				H horizontal			Oxides		
				L perpendicular					
	Slate from local roof	Cr-3	unknown		yes	yes	yes		
Dunkeld	These slates show little superficial weathering								
Birnam	Green medium-grained slate from the tips	DB-1	NO037 94049		yes	yes	yes	yes	
Birnam	Blue fine-medium grained slate	DB-2	NO0383 4043		yes		yes	yes	
Birnam	Blue fine-medium grained slate	DB-3	NO0374 4029		yes		yes	yes	
Newtyle South	Green medium grained from worked seam	DN-1	NO0470 4110		yes	yes	yes	yes	yes
Newtyle South	Blue fine-medium grained slate	DN-2	NO0470 4110		yes		yes	yes	
Newtyle North	Green medium grained from seam	DN-3	NO0452 4124		yes		yes	yes	
Newtyle North	Blue fine-medium grained from seam	DN-4	NOO454 4126		yes	yes	yes	yes	yes
Second-hand slate dealer		DX-1	unknown		yes	yes	yes		
Macduff Slate									
Kirkney Hill	These slates show little superficial weathering		**NJ503 317 to NJ510 320**						
Kirkney Quarry	Grey fine-medium grained slate from face	MK-2	NJ5105 3198	CO2 & H2O	yes	yes	yes	yes	
Kirkney Quarry	Grey medium grained slate from face	MK-4	NJ5094 3197		yes	yes	yes	yes	yes
Hill of Corskie			**NJ533 328 & NJ544 328 to NJ549 329**						
Haining Quarry	Grey fine to medium grained slate from face	MH-1	NJ547 13283		yes		yes	yes	
Haining Quarry	Grey medium grained slate from tips	MH-2	NJ545 43285	CO2 & H2O	yes	yes	yes	yes	
Haining Quarry	Sample from a yellow weathered seam	MH-3	NJ545 43284		yes			yes	
Corskie Quarry	These are grey fine to medium grained slate from the tips	MC-1	NJ529 13268		yes	yes	yes	yes	
	Silty bands are frequent,	MC-2	NJ529 13268		yes	yes		yes	
		MC-3	NJ529 13268		yes	yes		yes	
Wishach Hill			**NJ577 331 to NJ579 334**						
Wishach Quarry	Tips	MW-1	NJ5775 3330		yes		yes		
Hill of Foudland	These are grey fine to medium grained slates with occasional spotting		**NJ590 327 to NJ620 340**						
South Quarries	Sample from face	MF-1	NJ6181 3358		yes		yes	yes	
	Spotted sample from tips	MF-2	NJ6178 3357		yes	yes		yes	
	Spotted sample not *in situ*	MF-3	unknown		yes			yes	
Upper Quarries	Spotted sample from tips	MF-5	NJ6130 3372		yes	yes		yes	
	Green-grey medium grained slate from face	MF-6	NJ6117 3368		yes			yes	
	Tips	MF-7	NJ6117 3368		yes			yes	
Western Quarries	From a pinnacle of intact rock	MF-9	NJ6009 3322		yes			yes	
	From a pinnacle of intact rock	MF-10	NJ6010 3322		yes			yes	

				Miscellaneous					
				Thin section	WR	Fabric	Total	FWHM	FeO
				H horizontal			Oxides		
				L perpendicular					
	From seam	MF-11	NJ6018 3325		yes		yes		yes
	Weathered sample	MF-12	NJ6021 3353		yes				
	Wall of intact rock	MF-13	NJ60663 372		yes			yes	
	Slate from local roof	MF-14	unknown		yes	yes		yes	
Skirts of Foudland	These are grey medium-grained slates with frequent silty bands and								
	occasional spotting	MX-1	NJ5907 3319			yes			
	MX-1 from seam and 2 - 3 from tips.	MX-2	NJ5907 3319				yes	yes	
		MX-3	NJ5907 3319				yes	yes	
Hill of Tillymorgan	These are grey medium-grained slates with frequent silty bands and								
	occasional spotting		NJ646 345 to NJ659 351						
Willamston Quarry	From working face	MT-1	NJ6523 3469		412			yes	
	Working face	MT-2b	NJ6524 3471		401		yes	yes	
Watery Quarry	Tips	MT-4	NJ6522 3484			yes			
	Working face	MT-5	NJ6521 3482					yes	
	Seam	MT-6	NJ6516 3483	Weathering			yes		
	Area used for dressing slates	MT-BALD	NJ6478 3453			yes			

Appendix 2.1 XRD Analyses -Identification of minerals present in slate

Mineral	XRD Peaks	White mica			Chlorite		Quartz		Feldspar		Haematite		Carbonate	
	Intensity	K rich		Na rich					K feld	Plag	/Pyrite	Calcite		34.31
Angle	2 theta	10.4		10.9	7.3	14.8	24.44		32.2	32.6-32.8	38.8	Dolomite		36.1
											41.5/43.6°	Magnesite		38.07
												Siderite		37.55
Ballachulish Slate														
East Laroch														
EL-2	North face	230	trace		187	635	136				65			
EL-3		253			103	327	111				90			
EL-4		468		54	201	733	194				104	Siderite		57
EL-6		241	trace		188	567	330				69	Siderite		
EL-7	Upper galleries	304			249	761	250				87	Siderite		
EL-8		202			135	339	281				110	Siderite		
EL-9		316			105	312	201				63	Siderite		
EL-10	*Best vein*	236			215	510	179				137	Dolomite		75
West Laroch														
WL-1	Middle quarry	374			193	531	111				65	Siderite		39
WL-3		219			108	366	106				93	Siderite		25
WL-5		310			255	671	208				32			
Khartoum														
K-1	Khartoum	406			231	782	139				70	Siderite		47
K-2		454			186	553	178				73	Siderite		50
K-3		457			165	474	232				65	Siderite		46
BX-1	2nd hand slate	252			106	383	116				100	Siderite		46
Easdale Slate														
EE-1	Easdale Q	212		36	80	194	77				74			
EE-2	tips	346		36	96	317	154				129			
EE-3	2nd hand slate	313		39		223	151				144	Dolomite		146
Luing														
LP-1	Port Mary HS	270			114	287	84				98			
		325			102	250	128				67			
		197			77	181	123				86			
LP-2		123			24	63	97				68	Dolomite		340
LP-3	North of island	298				321	295				102	55	Pyrite	
LP-5	Port Mary North	449			133	399	132				123			
LP-6	Porth Mary South	393			88	268	222				130			93
	Cullipool													
LC-1	Quarry 1	304			55	119	101				118	Dolomite		71
LC-2		313			56	177	89				72			
LC-2	Quarry 2	324			71	244	182				97			
LC-3	Nearly new slate	262			50	197	101				111			
	Toberonochy													
LT-1	slate from quarry	353			0		123				87	Magnesite		220
LT-2	slate from village hall	331		41	105	293	157				133	144	Dolomite	100
LT-3	tips	455			0		130				80	Magnesite		190
Luing														
LT-5	quarry face	476			72	168	90		129		107	Dolomite		115
Luing														
LB-1		383			127	285	189				135	Dolomite		168
LB-2		360			37	100	137				122	Dolomite		461
LB-3		413			94	255	195				155			0
Belnahua														
BB-1	quarry face	217			145	451	270				85	Dolomite		93
BB-2	tips	283		61	120	307	183				148	Dolomite		98
Seil	**Balvicar Q1**													
SB-1	face	256			120	280	188				72	Dolomite		60
SB-2	recent landslide	234			143	365	258				125			
SB-3	cliff face	222			53	144	148				94	Dolomite		282
SB-4	carbonaceous layer	250			83	209	104				89	Dolomite		160
	Breine Phort													
SB-5	North side of Q	478			125	400	114				166	Dolomite		98
SB-6	south	477			88	252	188				189			
SB-7	tips	325			91	250	253				149	Dolomite		
SB-8	tips	398			109	351	196				197			
EX-1	2nd hand slate	104			39	102	176				115	67	Siderite	25
Arran														
Sample														
A1	Main Quarry	287			66	193	133				125	48	Haematite	
A3		55			38	143	126				99			
A6	Minor Quarry	180			66	166	139				112	64	Haematite	
Bute														
B1a	Ardmaleish Point	194		67	44	180	81				185	71	Haematite	
B1b		120			80	328					161			
B2	Hilton Farm Q.	182		87	75	208	138				203	71	Haematite	
B3	Shed Hilton Farm	328		73	128	382	130				164			
B4	Hilton Farm Q.	207		122	51	113	122				238	72	Haematite	
B4-w	Hilton Farm Q.	143		70	50	147	88				147	31	Haematite	
B5	Edinmore Q.	257		48	135	578	118				109			
											64			
Luss														
Ls-1	AuchingavinQ.	310		42	98	415	94				237	66	Haematite	
Ls-2	AuchingavinQ.	354		18	112	453	213				106			

Mineral	XRD Peaks	White mica		Chlorite	Quartz	Feldspar		Haematite	Carbonate	
	Intensity	K rich	Na rich			K feld	Plag	/Pyrite	Calcite	34.31
Angle	2 theta	10.4	10.9	7.3	14.8	24.44	32.2	32.6-32.8	38.8 Dolomite	36.1
									41.5/43.6* Magnesite	38.07
									Siderite	37.55
Aberfoyle										
AB-1	Green slate	62	33	71	234	87		67		
		71	44	68	306	55		146		
AB-3	Purple	169		50	197	64		136	7	
AB-4	slate with a good ring	121		61	203	80		127	99	
AB-5	standard from "best vein"	100	46	82	331	193		136		
AB-6	2nd hand slate Cummings	98		65	209	122		186		
Craigiea										
Cr-1	Green slate	168		163	575	165		155	120	
Cr-2	Blue slate	232		100	324	134		165	60	
Cr-3	Slate from local roof	251		129	36	129		173	57	
Comrie										
Au-1	Aberuchill Q	106		118	404	96		189		
Au-2	Aberuchill Q	182		81	286	110		182	44	
Au-3	slate	188		126	461	170		228		
Dr-1	Drummond Q.	186			449	151		145		
Dunkeld										
DB-1	Birnam	256		95	403	158		87		
DB-2	Birnam	178		40	113	130		122	117	
DB-3	Birnam	191		0	87	99		106	95	
DN-1	Newtyle South	93		66	230	81		139		
DN-2	Newtyle South	120		38	125	118		123	64	
DN-3	Newtyle North	240		86	381	89		115		
DN-4	Newtyle North	79		28	80	112		137	32	
DX-1	Cummings	123		91	282	124		202	30	
MK-2	Kirkney	230		75	152	161		71	112	Haematite
MK-4	Kirkney	142	31	92	182	123		64	96	Haematite
MF-1	Foudland Q no 1	250	54	50	111	123		89	84	Haematite
MF-1	Lower quarries	212	45	40	92	114		87	127	Haematite
MF-1'		191	48	24	79	109		88	403	Haematite
MF-2	Foudland	130			140	82		33	87	Haematite
MF-3	Foudland	125	trace	56	210	86		58	74	Haematite
MF-5	Foudland upper quarries	146	trace	64	131	131		54	82	Haematite
MF-9	Foudland western quarries	143	trace	58	192	144		49	70	Haematite
MF-10	Foudland weathered seam	138	trace	59	213	115		67	64	Haematite
MF-6	Foudland green/grey band	136		64	206	167				
MF-7	Foudland	142	29	73	254	155		48	70	Haematite
MF-13	Foudland	100		44	134	138		56	43	Haematite
MF-11	West quarry	133	42	66	154	99		51	76	Haematite
		217	trace	104	344	171			96	Haematite
MF-12	Weahtered seam	132		0	54	123		71		
MF-14	Slate from local roof	217		38	115	155		92	127	Haematite
MH-1	Haining Quarry	141		0	34	77		70	82	Haematite
MH-1		262		0	71	111		86	101	Haematite
MH-2	Haining Quarry	219		0	44	88		73	81	Haematite
MH-2		191		0	30	69		72	91	Haematite
MH-3	Haining Q weathered seam	153		91	314	107		70		
MH-3w	Weathered surface	50		44	176	67		36		
MC-1	Corskie Quarry	112	29	38	158	129		72	95	Haematite
MC-2		128	trace	82	267	94				
MC-3		157	trace	45	103	100		64	137	Haematite
MW-1	Wishach Quarry	291	47	79	159	150		91	169	Haematite
MT-1	Tillymorgan Williamston Q	177	trace	66	206	109		68	56	Haematite
MT-2b	"	216	trace	41	111	109		61	101	Haematite
Mean (excluding the weathered samples)										
STDEV (excluding the weathered samples)										
A5w		212	23	93	311	105		109		
Cwt y Bugail										
WCB-1	*Medium strong* from face	82		30	135	94	21	30		
W/CB-2	*Medium strong* from face	113		59	245	91	23	37		
W/CB-3	Weathered from tips	97		45	233	115		42		
W/CB-4	*Extra heavy*	102		57	228	99		31		
W/CB-5	*Medium strong*	119		71	269	83	23	31		
Pen yr Orsedd										
		The following all have haematite at 38.86-38.88 very clean runs								
W/PO-1	tips	179			88	162		77	55	Haematite
W/PO-5	purple slate	142			56	175		40	106	Haematite
W/PO-6	*Best heather blue*	120			45	131		51	80	Haematite
W/PO-7	*Best heather blue*	72				132		56	56	Haematite
W/PO-8	*Best Bangor blue*	84		38	93	110		103	59	Haematite
W/PO-9	Best red	91			50	137		67	121	Haematite
W/PO-10	*Best*	67				131		44	77	Haematite
W/PO-11	Tyn y Weingladd	147		21	77	135		82	84	Haematite

Mineral	XRD Peaks	White mica		Chlorite	Quartz	Feldspar		Haematite	Carbonate	
	Intensity	K rich	Na rich			K feld	Plag	/Pyrite	Calcite	34.31
Angle	2 theta	10.4	10.9	7.3	14.8	24.44	32.2	32.6-32.8	38.8 Dolomite	36.1
									41.5/43.6° Magnesite	38.07
									Siderite	37.55
Oakley Quarry Ffestiniog		Traces of K feldspar d		Most of the following have a trace of anatase at 29.84-29.91						
W/F-1	old vein standard	155		73	312	103		42		
		170		65	280	69		41		
		164		72	293	88		46		
		140		50	272	82		35		
W/F-1	old vein standard	157		65	289	86		41		
W/F-4	Old vein poor splitting	96		54	251	100		40		
W/F-9	Between old and new	123		53	248	102		56		
W/F-10	old vein outcrop	147		57	284	83		51		
W/F-11	old vein frost damaged	196		63	330	121	trace			
W/F-12	pigs vein	130		69	281	104		36		
W/F-15	between old and north pigs ve	148		63	357	111		62		
W/F-16	new vien	91		59	241	91		51		
W/F-2	old vein	158		59	232	89		45		
W/F-5	old vein	93		20	158	81		42		
W/TC-1	Twill Coed	83			33	76		46	70 Haematite	
W/X-1	unknowns from Wales	173		80	303	91		72		
W/X-2		154		41	170	106		96		
W/X-3		169		72	363	46	33	56		
	Kirby Burlington blue									
E/K-1	good potential	121		34	101	167		113	Calcite	134
E/K-2	poor potential	99		39	103	193		125	Calcite	117
E/K-3	9mm slate	85		36	112	163		113	Calcite	115
E/K-4		61		28	70	150		105	Calcite	111
	Elterwater									
E/EW-1	Coarse grained	57		55	180	111		102	Calcite	165
E/EW-2	Strong coarse grained	green		52	203	197		69	Calcite	170
E/EW-3	Extra strong coarse grain	46		75	231	117		84	Calcite	232
E/EW-4	"best"	39		56	164	104		99	Calcite	209
	Brossan Stone used for cladding									
E/BS-1		68		68	221	223		88	Calcite	106
E/BS-2		0		107	240	94		73	Calcite	83
E/BS-3				119	314	137		98	Calcite	231
E/BS-4		67		59	160	187		102	Calcite	210
	Broughton Moor									
E/BM-1	Extra strong coarse grain	24		104	314	129		119	Calcite	110
E/BM-2	"best"	61		85	261	109		158	Calcite	102
	Brandy Crag									
E/BC-1		63		53	171	189		83		
E/W-1	UNKNOWN	35		54	146	94		45	Calcite	86
	Irish Slate									
I/K-1	Killaloe >100yrs old	58		26	152	123		111	Calcite	151
I/K-3	Killaloe New slate	68		41	152	114		78	Calcite	135
I/K-4	Killaloe old	66		45	180	126		85	Calcite	101
	French Slate									
F/N-1	Noyant Grade A	148		85	329	133	47	41		
F/N-2	Noyant grade B	61		43	183	93	52	47		
F/G-1	Grand Carreau grade A	150		112	514	139	46	60		
F/G-2	Grand Carreau grade B	117		72	360	95	trace	67		
F/F-1	Fresnal grade B	151		82	352	77	49	49		
F/F-2	Fresnal grade A	246		128	570	115	trace	51		
	Misc slate									
S/C-1	Cupa sample	163		99	425	50	30	85		
S/C-2	Glades ?	185		71	288	116		57		
C/C-1	Chinese slate	91		32	98	63		62	Calcite	223
U/V-1	Vermont slate	93		0	48	81		51		51
S/A-1	Garnet Mica schist	443		37	104	108		60		60

Appendix 2.2 Determination of Mineral Composition of a Ballachulish Slate (EL-10)

DATA BASE	Total	Si	Ti	Al	Mg	Ca	Mn	Fe	Na	K	O	H
Chlorite												
EL10+	15.599	4.160	0.006	4.586	3.886	0.007	0.012	2.826	0.002	0.114		
EL10+	15.672	4.084	0.000	4.518	4.172	0.006	0.021	2.838	0.009	0.024		
EL10+	15.605	4.133	0.007	4.526	4.122	0.004	0.031	2.768	0.000	0.014		
EL10+	15.373	4.572	0.006	4.115	3.717	0.003	0.011	2.932	0.002	0.015		
EL-10	15.840	4.022	0.007	4.398	4.196	0.018	0.047	3.016	0.089	0.047		
EL-10	15.639	4.169	0.008	4.465	4.015	0.013	0.036	2.838	0.033	0.062		
EL-10	15.564	4.235	0.000	4.524	3.856	0.001	0.000	2.828	0.045	0.076		
EL-10	15.684	4.117	0.006	4.502	3.928	0.000	0.016	3.002	0.038	0.076		
EL-10	15.620	4.167	0.007	4.471	4.061	0.000	0.027	2.830	0.020	0.037		
EL-10	15.737	4.220	0.011	4.146	4.212	0.008	0.020	3.037	0.073	0.009		
EL-10	15.706	4.121	0.016	4.374	4.223	0.003	0.022	2.887	0.029	0.031		
EL-10	15.759	4.140	0.009	4.281	4.191	0.002	0.031	3.007	0.057	0.040		
Mean	**15.650**	**4.178**	**0.007**	**4.409**	**4.048**	**0.005**	**0.023**	**2.901**	**0.033**	**0.045**		
St Dev	**0.117**	**0.136**	**0.004**	**0.153**	**0.168**	**0.005**	**0.013**	**0.093**	**0.029**	**0.031**		
C of V		**0.033**		**0.035**	**0.041**			**0.032**				
Charge	44.000	16.713	0.028	13.226	8.096	0.011	0.046	5.802	0.033	0.045		
Formula based on O10 (OH)8	28.000	2.659	0.004	2.806	2.576	0.003	0.015	1.846	0.021	0.029	18.000	8.000
Molecular Weight	614.459	74.714	0.211	75.751	62.136	0.136	0.800	103.098	0.485	1.127	288.000	8.000
μiWi	28459.30	7501.33	63.33	5870.71	3945.62	0.00	0.00	5794.12	22.86	250.13	5011.20	0.00
μ	46.316											
Oxide	614.459	159.798	0.352	143.085	103.354	0.191	1.034	132.634	0.654	1.357		72.000
%Oxide	100.000	26.006	0.057	23.286	16.820	0.031	0.168	21.585	0.106	0.221	0.000	11.718
White Mica											Na+K	
EL-10+	13.857	6.544	0.028	5.061	0.195	0.000	0.000	0.113	0.216	1.700	1.916	
EL-10+	14.016	6.319	0.038	5.215	0.314	0.000	0.000	0.171	0.191	1.768	1.959	
EL-10+	13.976	6.222	0.032	5.433	0.256	0.002	0.003	0.138	0.233	1.657	1.890	
EL-10+	14.026	6.155	0.034	5.531	0.216	0.000	0.000	0.129	0.289	1.672	1.961	
EL-10+	14.007	6.153	0.026	5.560	0.224	0.013	0.001	0.098	0.411	1.521	1.932	
EL-10	14.055	6.104	0.020	5.519	0.331	0.001	0.005	0.200	0.275	1.601	1.876	
EL-10	13.945	6.210	0.042	5.504	0.192	0.001	0.000	0.097	0.292	1.605	1.897	
EL-10	13.919	6.371	0.028	5.186	0.338	0.000	0.015	0.159	0.225	1.596	1.821	
EL-10	13.919	6.371	0.028	5.186	0.338	0.000	0.015	0.159	0.225	1.596	1.821	
Mean	13.969	6.272	0.031	5.355	0.267	0.002	0.004	0.140	0.262	1.635	1.635	
St Dev	0.064	0.141	0.007	0.191	0.063	0.004	0.006	0.035	0.066	0.072	0.072	
C of V	**0.005**	**0.022**		**0.036**					**0.252**	**0.044**	**0.044**	
Total Charge	**44.00**	**25.09**	**0.12**	**16.07**	**0.53**	**0.00**	**0.01**	**0.28**	**0.26**	**1.64**		
Formula based on O10 (OH)2	**22**	**3.136**	**0.015**	**2.677**	**0.134**	**0.001**	**0.002**	**0.070**	**0.131**	**0.818**	**12**	**2**
Molecular Weight	397.428	88.120	0.736	72.292	3.222	0.040	0.120	3.920	3.012	31.967	192	2
μiWi	25674.868	8847.201	220.735	5602.638	204.595	0.000	0.000	220.302	141.855	7096.742	3340.800	0.000
μ	**64.603**											
Wt of Oxide/mole	397.428	188.469	1.227	136.552	5.359	0.055	0.154	5.043	4.059	38.508		18.000
%Oxide	100	47.422	0.309	34.359	1.348	0.014	0.039	1.269	1.021	9.689	0.000	4.529

	Total	Si	Ti	Al	Mg	Ca	Mn	Fe	Na	K	O	H
Chlorite EL-10	614.459	2.659	0.004	2.806	2.576	0.003	0.015	1.846	0.000	0.000	18	8
Phengite EL-10	397.428	3.136	0.015	2.677	0.134	0.001	0.002	0.070	0.131	0.818	12	2
Reduced Iron/Total Iron (Wt)	0.89											Volatiles
EL-10	91.731	57.600	0.578	16.280	5.260	2.080	0.094	6.410	0.800	2.560		8.897
Normalized XRF	100	57.241	0.574	16.178	5.227	2.067	0.093	6.370	0.795	2.544	0	8.841
No. of moles of cation		0.952	0.007	0.317	0.130	0.037	0.001	0.089	0.026	0.054		0.982
Moles of Apatite	0.00032					0.002						
Residue		0.952	0.007	0.317	0.130	0.035	0.001	0.089	0.026	0.054		0.982
Moles of dolomite	0.03530				0.035	0.035						0.345
Residue		0.952	0.007	0.317	0.095	0.000	0.001	0.089	0.026	0.054		0.637
Moles of Phengite	0.06607	0.207	0.001	0.177	0.009		0.000	0.005	0.009	0.054		0.132
Residue		0.745	0.006	0.140	0.086	0.000	0.001	0.084	0.017	0.000		0.505
Moles of Albite	0.01699	0.051		0.017					0.017			
Residue		0.694	0.006	0.123	0.086	0.000	0.001	0.084	0.000	0.000		0.505
Moles of Chlorite	0.03345	0.089	0.000	0.094	0.086	0.000	0.000	0.062	0.000	0.000		0.268
Residue		0.605	0.006	0.030	0.000	0.000	0.001	0.022	0.000	0.000		0.237
Halloysite	0.02950	0.030		0.030								0.059
Quartz	0.57583	0.576										
Pyrite	0.02228							0.022				0.156
Residue	.	0.000	0.006	0.000	0.000	0.000	0.001	0.000	0.000	0.000		0.023
Residue in wt	0.726	0.000	0.482	0.000	0.000	-0.006	0.049	0.000	0.000	0.000		0.203
EL-10	Total	Quartz	Phengite	Chlorite	Pyrite	Albite	Apatite	Dolomite	Halloysite	Unallocated		
%Oxide	**99.61**	**34.61**	**26.26**	**21.15**	**2.67**	**4.46**	**0.16**	**6.50**	**3.81**	**0.73**	**100.34**	

Appendix 2.3 XRF Major element analyses

Sample Numbers as in Appendix 2.1unless otherwise stated

Sample	SiO2	Al2O3	Fe2O3	MgO	CaO	Na2O	K2O	TiO2	MnO	P2O5	Total	LOI
Ballachulish Slate												
EL3	52.56	23.46	7.18	2.85	0.07	1.66	4.295	0.9	0.063	0.046	93.08	6.92
EL4	55.44	22.48	6.35	2.74	0.08	0.99	4.229	0.894	0.073	0.063	93.33	6.67
EL6	63.58	16.71	7.16	3.29	0.07	0.77	2.678	0.688	0.067	0.046	95.06	4.94
EL7	57.2	20.61	8.38	4.09	0.09	1.05	3.172	0.833	0.077	0.068	95.57	4.43
EL8	62.29	16.71	6.19	4.14	0.14	1.35	2.868	0.728	0.062	0.084	94.55	5.45
EL9	54.63	14.41	11.46	4.55	0.11	0.89	2.917	0.686	0.29	0.049	89.99	10.01
EL10	57.6	16.28	6.41	5.26	2.09	0.8	2.56	0.578	0.094	0.069	91.73	8.27
WL1	62.75	18.26	5.56	3.74	0.07	0.81	3.358	0.756	0.041	0.045	95.39	4.61
WL3	61.77	18.31	5.69	4.01	0.13	1.51	2.967	0.768	0.03	0.1	95.29	4.71
WL5	58.51	18.83	7.29	4.67	0.1	0.65	3.312	0.763	0.06	0.053	94.24	5.76
K1	53.5	21.66	6.75	3.73	0.07	1.17	3.939	0.906	0.028	0.054	91.8	8.2
K2	61.11	19.67	5.53	2.51	0.08	1.07	3.797	0.806	0.031	0.065	94.67	5.33
K3	62.2	18.87	6.06	2.37	0.07	0.97	3.61	0.82	0.027	0.055	95.05	4.95
BX-1	58.33	19.72	6.53	3.67	0.12	1.23	3.754	0.842	0.072	0.057	94.32	5.68
Easdale Slate												
EE1	56.37	18.93	10	2.68	0.5	1.7	3.64	0.979	0.132	0.221	95.15	4.85
EE2	51.95	19.14	7.15	3.67	2.49	1.65	2.678	0.688	0.096	0.123	89.63	10.37
EE3	52.03	20.07	7.31	3.2	2.71	1.49	3.043	0.7	0.094	0.136	90.78	9.22
SB1	60.54	17.26	6.72	7.1	0.66	1.33	2.462	0.668	0.05	0.156	96.95	3.05
SB2	59.27	15.8	5.72	6.81	0.56	1.34	2.103	0.7	0.046	0.144	92.5	7.5
SB3	50.37	12.34	4.81	6.88	6.25	1.64	2.062	0.51	0.13	0.536	85.52	14.48
SB4	48.52	15.08	5.42	7.39	4.36	2.24	2.174	0.629	0.099	0.219	86.13	13.87
SB5	53.64	21.45	7.34	3.01	0.78	2.1	3.416	0.776	0.059	0.169	92.76	7.24
SB-6	59.56	20.15	4.88	2.24	0.22	2.33	3.308	0.759	0.03	0.107	93.58	6.42
SB7	66.17	16.42	5.3	2.04	0.16	1.78	2.492	0.69	0.047	0.158	95.26	4.74
SB8	56.75	19.71	6.28	2.9	1.19	2.08	3.107	0.688	0.068	0.179	92.96	7.04
LC1	56.89	19.59	5.61	2.72	1.62	1.94	3.397	0.763	0.091	0.173	92.8	7.2

Sample	SiO2	Al2O3	Fe2O3	MgO	CaO	Na2O	K2O	TiO2	MnO	P2O5	Total	LOI
LC2	59.86	18.72	6.28	2.55	0.41	1.53	3.11	0.921	0.087	0.19	93.66	6.34
LC-3	58.86	19.13	6.4	2.63	0.51	1.75	3.193	0.906	0.099	0.184	93.66	6.34
LP1	55.6	18.46	6.59	5.3	0.62	1.64	2.763	0.769	0.121	0.15	92.01	7.99
LP3	54.29	17.57	8.96	4.71	0.59	1.71	2.597	0.664	0.092	0.139	91.31	8.69
LP5	54.51	21.83	7.32	3.41	0.37	2.03	3.383	0.835	0.067	0.143	93.9	6.1
LP6	61.75	18.58	5.95	2.01	0.17	1.81	3.031	1.06	0.029	0.17	94.57	5.43
LB1	55.53	16.45	4.81	5.74	2.48	1.8	2.631	0.637	0.05	0.244	90.38	9.62
LB2	44.04	11.8	4.55	7.39	9.07	0.85	2.429	0.465	0.093	0.223	80.9	19.1
LB3	53.2	19.44	7.77	3.43	1.07	2.2	3.033	0.759	0.086	0.155	91.14	8.86
LT1	54.12	15.59	5.4	6.44	0.61	1.67	2.518	0.638	0.103	0.095	87.18	12.82
LT2	52.46	20.17	6.82	3.3	2.38	1.54	3.047	0.709	0.101	0.172	90.7	9.3
LT3	53.07	16.36	6.02	6.49	0.66	1.21	2.981	0.633	0.089	0.1	87.62	12.38
LT5	56.43	19.21	6.34	3.16	1.79	2.4	3.07	0.81	0.081	0.146	93.43	6.57
BB1	61.62	14.33	7.16	4.08	1.42	1.49	1.776	0.651	0.128	0.121	92.79	7.21
BB2	54.73	18.1	7.54	3.75	1.66	1.61	2.486	0.648	0.186	0.167	90.87	9.13
EX-1	61.47	17.99	7.07	2.19	1.06	1.9	2.95	0.869	0.133	0.079	95.71	4.29
Highland Border Slate												
A3	61.58	17.33	7.99	2.6	0.1	2.25	2.973	0.828	0.155	0.073	95.88	4.12
A5	61.05	18.42	6.75	2.33	0.2	1.56	4.611	0.861	0.078	0.089	95.96	4.04
A6	61.08	17.67	8.24	2.18	0.14	1.98	4.119	0.851	0.069	0.1	96.41	3.59
B1	53.31	23.2	9.58	2.02	0.52	2.11	3.358	1.245	0.094	0.177	95.6	4.40
B2	48.1	25.78	9.43	2.72	0.75	2.63	4.07	1.679	0.107	0.243	95.52	4.48
B2-	63.84	18.31	5.03	2.51	0.73	1.82	2.777	1.061	0.11	0.137	96.32	3.68
B3	48.28	23.34	9.34	4.3	0.29	1.49	3.311	0.738	0.195	0.164	91.44	8.56
B5	52.58	26.52	9.94	2.31	0.2	1.37	3.973	1.221	0.114	0.144	98.36	1.64
LS1	55.57	22.08	9.42	1.8	0.15	2.06	4.096	1.37	0.125	0.101	96.77	3.23
LS2	58.76	19.98	7.49	1.95	0.15	1.5	3.832	1.192	0.175	0.11	95.15	4.85
AB1	54.08	18.81	10.27	2.47	1.01	2.83	2.913	1.215	0.128	0.672	94.4	5.6
AB3	54.48	21.36	9.44	2.71	0.31	2.72	2.311	1.409	0.15	0.182	95.08	4.92
AB4	51.45	21.24	11.29	2.27	0.62	3.04	3.512	1.57	0.103	0.249	95.35	4.65
AB5	55.14	19.65	9.78	2.46	0.66	2.51	3.043	1.346	0.128	0.2	94.91	5.09

Sample	SiO2	Al2O3	Fe2O3	MgO	CaO	Na2O	K2O	TiO2	MnO	P2O5	Total	LOI
AB-6	58.44	20.11	7.12	2.39	0.61	2.67	2.588	1.308	0.162	0.128	95.54	4.46
AU1	56.57	18.78	9.62	2.56	0.66	2.99	2.745	1.229	0.148	0.248	95.56	4.44
AU2	55.63	19.14	10.76	2.34	0.33	2.19	3.769	1.108	0.105	0.24	95.62	4.38
AU-3	58.22	19.35	8.03	2.29	0.76	2.84	3.258	1.304	0.107	0.207	96.36	3.64
DR1	55.25	20.75	6.82	2.34	0.36	1.65	3.145	0.696	0.073	0.124	91.21	8.79
CR1	54.75	20.34	10.4	2.87	0.58	2.14	2.697	1.262	0.143	0.276	95.46	4.54
CR2	57.1	18.98	10.24	2.26	0.52	2.14	3.368	1.355	0.094	0.174	96.21	3.79
CR-3	53.1	21.13	10.25	2.74	0.69	2.24	3.422	1.281	0.127	0.229	95.21	4.79
DB1	57.49	19.25	9.28	2.26	0.38	1.25	4.144	1.169	0.085	0.158	95.46	4.54
DB2	59.11	17.88	9.43	2.04	0.28	1.99	3.97	1.132	0.163	0.175	96.18	3.82
DB3	55.11	20.66	10.72	1.64	0.24	1.68	4.719	1.135	0.064	0.174	96.14	3.86
DN1	58	19.09	8.08	2.95	0.25	2.28	3.465	1.195	0.098	0.138	95.54	4.46
DN2	56.61	19.29	9.51	2.38	0.48	2.06	3.749	1.385	0.08	0.237	95.77	4.23
DN3	53.9	21.3	8.79	2.62	0.37	1.64	5.061	1.463	0.092	0.243	95.48	4.52
DN4	56.11	20.27	8.14	2.45	0.87	2.19	3.821	1.281	0.072	0.229	95.43	4.57
DX-1	56.06	19.24	7.16	2.31	1.6	2.36	3.218	1.234	0.119	0.151	93.95	6.05
Macduff Slate												
MK2	53.64	21.83	10.27	1.93	0.19	1.1	4.449	1.048	0.041	0.143	94.64	5.36
MK4	52.1	22.61	11.88	1.6	0.18	1.63	3.287	0.916	0.047	0.109	94.36	5.64
MH1	52.95	24.71	9.2	1.1	0.14	1.12	5.5	0.808	0.019	0.116	95.67	4.33
MH2	52.84	24.99	9.63	0.92	0.16	1.18	5.558	0.781	0.021	0.139	96.22	3.78
MC1	49.64	23.79	10.8	1.82	0.28	1.12	4.503	0.975	0.102	0.212	93.24	6.76
MW1	55.12	22.98	10.18	1.7	0.25	1.51	4.028	0.931	0.053	0.118	96.87	3.13
MX2	55.31	22.52	9.78	1.94	0.33	1.39	3.237	0.894	0.136	0.121	95.66	4.34
MX3	56.32	22.6	8.74	1.8	0.39	1.21	3.219	0.9	0.16	0.099	95.44	4.56
MF1	53.17	24.57	9.2	1.44	0.62	1.75	3.674	0.98	0.084	0.144	95.63	4.37
MF11	54.51	22.84	9.74	1.65	0.2	1.53	3.236	0.908	0.071	0.12	94.8	5.20
MT2	53.2	26.33	9.48	1.46	0.65	1.74	3.217	0.931	0.068	0.157	97.24	2.76
MT6	55.77	23.04	9.95	1.48	0.23	1.77	3.289	0.93	0.05	0.123	96.65	3.35
MF-14	52.82	23.70	9.08	1.47	0.59	1.6	3.612	1.011	0.074	0.147	94.11	5.89

Sample	SiO2	Al2O3	Fe2O3	MgO	CaO	Na2O	K2O	TiO2	MnO	P2O5	Total	LOI
Cumbrian Slate												
E/K-1	58.5	13.69	5.56	3.5	4.77	1.58	3.326	0.692	0.068	0.127	91.81	8.19
E/BS-3	51.98	14.62	9.11	6.63	4.95	1.45	1.603	0.966	0.239	0.212	91.75	8.25
Welsh Slate												
W/PO-3	58.81	18.97	8.08	2.15	0.47	1.58	3.063	0.882	0.106	0.127	94.24	5.76
W/PO-11	58.67	19.88	8.45	2.45	0.19	1.56	3.586	0.762	0.121	0.071	95.74	4.26
W/F-1	54.5	22.91	8.75	1.93	0.32	0.69	4.3	0.998	0.335	0.212	94.94	5.06
W/F-9	55.68	22.24	8.39	1.84	0.35	0.96	4.115	0.994	0.287	0.229	95.07	4.93
W/P-1	60.89	18.56	6.98	2.31	0.81	2.11	2.991	0.783	0.179	0.103	95.72	4.28
W/CB-1	54.71	22.73	8.91	1.81	0.33	0.86	3.923	1.028	0.334	0.213	94.83	5.17
Precision of XRF measurements												
AB-5A	51.42	21.28	11.3	2.23	0.61	3.06	3.509	1.58	0.104	0.248	95.34	4.660
AB-5B	51.33	21.34	11.26	2.27	0.62	3.14	3.512	1.575	0.104	0.245	95.4	4.600
AB-5C	51.57	21.32	11.22	2.26	0.62	3.13	3.507	1.57	0.103	0.248	95.55	4.450
AB-5D	51.68	21.41	11.19	2.27	0.62	3.05	3.493	1.569	0.099	0.247	95.64	4.360
AB-5E	51.55	21.29	11.15	2.26	0.61	3.07	3.459	1.557	0.103	0.248	95.3	4.700
AB-5E	51.59	21.25	11.14	2.26	0.62	3.07	3.471	1.568	0.105	0.247	95.32	4.680
AB-5E	51.53	21.27	11.15	2.24	0.62	3	3.46	1.562	0.101	0.244	95.17	4.830
AB-5E	51.55	21.23	11.18	2.24	0.61	3.05	3.465	1.556	0.103	0.245	95.24	4.760
AB-5E	51.62	21.28	11.16	2.25	0.61	3.04	3.461	1.551	0.103	0.247	95.33	4.670

Appendix 2.4 Precision of XRD and XRF Analyses

Table 1 Precision of XRD results based on the spiking of MK-4 with quartz

Proportion	% wt	Area of peaks Chlorite	White Mica		
by weight	50	1535	1730	3070	3460
of sample	50	2358	1631	4716	3262
	50	1973	1641	3946	3282
	60	2208	2293	3680	3822
	60	2432	2070	4053	3450
	60	2429	2310	4048	3850
	70	2023	2359	2890	3370
	70	2786	3299	3980	4713
	70	2268	2494	3240	3563
	80	2858	4217	3573	5271
	80	2838	3986	3548	4983
	80	2827	2829	3534	3536
	90	3750	3277	4167	3641
	90	3899	3361	4332	3734
	90	4128	3820	4587	4244
	100	5213	4128	5213	4128
	100	5243	3848	5243	3848
	100	4527	3501	4527	3501
Mean				4019	3870
St Dev				672	586
C of V				0.2	0.2

Table 2 Precision of XRD results based on three different sample preparations from one standard and several scans at intervals over two years

	Quartz	White mica	Chlorite
	2426	4107	4017
	2593	4068	3840
	2605	4139	3683
	2636	4486	3898
	2711	3918	4082
	2581	4428	4078
Mean	2592	4191	3933
St Dev	94	220	157
C of V	0.04	0.05	0.04

Table 3 Precision of traces software in determining the area of peak

	Quartz	White mica	Chlorite
	2933	3959	4335
	2848	4094	4132
	2970	4130	3995
	2932	4047	3980
	2996	4086	4273
	2986	3997	4215
	2967	3930	4234
	2878	4024	4111
	2848	4024	4142
	2882	4137	4179
Mean	2924	4042.8	4159.6
St Dev	56	70	113.2
C of V	0.02	0.02	0.03

Table 4 Precision of XRF measurements

AB-5A	51.42	21.28	11.3	2.23	0.61	3.06	3.509	1.58	0.104	0.248	95.34	4.660
AB-5B	51.33	21.34	11.26	2.27	0.62	3.14	3.512	1.575	0.104	0.245	95.4	4.600
AB-5C	51.57	21.32	11.22	2.26	0.62	3.13	3.507	1.57	0.103	0.248	95.55	4.450
AB-5D	51.68	21.41	11.19	2.27	0.62	3.05	3.493	1.569	0.099	0.247	95.64	4.360
AB-5E	51.55	21.29	11.15	2.26	0.61	3.07	3.459	1.557	0.103	0.248	95.3	4.700
Mean	51.51	21.328	11.224	2.258	0.616	3.09	3.496	1.5702	0.1026	0.2472	95.446	4.554
St Dev	0.14	0.05	0.06	0.02	0.01	0.04	0.02	0.01	0.00	0.00	0.14	0.14
C of V	0.003	0.002	0.005	0.007	0.009	0.014	0.006	0.005	0.020	0.005	0.002	0.032
AB-5E	51.55	21.29	11.15	2.26	0.61	3.07	3.459	1.557	0.103	0.248	95.3	4.700
AB-5E	51.59	21.25	11.14	2.26	0.62	3.07	3.471	1.568	0.105	0.247	95.32	4.680
AB-5E	51.53	21.27	11.15	2.24	0.62	3	3.46	1.562	0.101	0.244	95.17	4.830
AB-5E	51.55	21.23	11.18	2.24	0.61	3.05	3.465	1.556	0.103	0.245	95.24	4.760
AB-5E	51.62	21.28	11.16	2.25	0.61	3.04	3.461	1.551	0.103	0.247	95.33	4.670
Mean	51.568	21.264	11.156	2.25	0.614	3.046	3.4632	1.5588	0.103	0.2462	95.272	4.728
StDev	0.04	0.02	0.02	0.01	0.01	0.03	0.00	0.01	0.00	0.00	0.07	0.07

Appendix 2.5 Mineral Composition of Scottish slate samples as calculated from XRF data

Ballachulish Slate

		Total	Quartz	White mica	Chlorite	Pyrite	Albite	Apatite	Dolomite	Clay	Unallocated		Ilmenite	Volatiles
East Laroch	Standard	99.6	34.6	26.3	21.2	2.7	4.5	0.2	6.5	3.8	0.7	100.3	0.5	0.2
	EL3	99.2	17.2	44	13.6	6.2	10.1	0.1	0	7.9	0.4	99.6	0.8	-0.3
	EL4	99.1	23.8	43.4	13.1	5	4.6	0.1	0	9.1	0.6	99.7	0.7	-0.1
	EL6	100.5	40	27.4	17.7	5.1	4.1	0.1	0	6	-0.6	99.9	0.6	-1.2
	EL7	102	28	32.5	22.1	5.4	6	0.2	0	7.9	-2	100	0.7	-2.7
	EL8	99.1	36.2	29.4	22.6	1.7	8.8	0.2	0.1	0	1.4	100.4	0.6	1.1
	EL9	99.6	30.3	29.8	24.9	9.6	4.9	0.1	0.1	0	-0.1	99.5	0.6	1.7
	EL10	99.6	34.6	26.3	21.1	2.7	4.5	0.2	6.5	3.8	0.6	100.3	0.5	0.2
West Laroch	WL1	99.7	37.1	34.5	19.9	1.5	3.8	0.1	0	2.7	0.7	100.4	0.6	0.1
	WL3	99.4	33.5	30.5	21.9	1.1	10.1	0.2	0	2.1	1	100.5	0.7	0.5
	WL5	99.5	32.9	33.9	25.4	2.5	2.5	0.1	0.1	2	0.9	100.4	0.6	0.4
Khartoum	K1	97.3	22.4	40.4	19.3	3.6	6.3	0.1	0	5.1	2.9	100.1	0.8	2.2
	K2	99.5	32.6	39	12.1	4.1	5.6	0.2	0	5.9	0.3	99.8	0.7	-0.3
	K3	100.1	35	37	11.4	5.3	5	0.1	0	6.3	-0.5	99.7	0.7	-1.1
Used slate	BX-1	99.2	29.2	38.5	18.9	3.4	7	0.1	0.1	1.8	0.9	100.1	0.7	0.3
	Mean	**99.6**	**31**	**33.6**	**19.6**	**3.9**	**5.8**	**0.1**	**1**	**4.3**	**0.5**	**100.1**	**0.6**	**0.1**
	St. Dev.	**1.0**	**6.5**	**6.3**	**4.3**	**2.3**	**2.4**	**0**	**2.4**	**3**	**1.1**	**0.3**	**0.7**	**0.0**

Easdale Slate

Seil		Total	Quartz	White mica	Chlorite	Pyrite	Albite	Apatite	Dolomite	Clay	Unallocated		Ilmenite	Volatiles
Balvicar	*SB1*	*99.1*	*32.7*	*32.7*	*21.8*	*1.6*	*8.4*	*0.4*	*1.5*	*0.0*	*0.7*	*99.8*	*0.5*	*-2.2*
	SB2	*93.1*	*33.9*	*28.0*	*20.0*	*0.8*	*8.9*	*0.3*	*1.2*	*0.0*	*6.8*	*99.9*	*0.6*	*3.1*
	SB3	*100.2*	*24.3*	*27.4*	*17.1*	*0.5*	*11.4*	*1.3*	*18.2*	*0.0*	*-0.3*	*100.0*	*0.4*	*2.5*
	SB4	*96.7*	*17.8*	*28.9*	*18.9*	*0.7*	*16.4*	*0.5*	*13.3*	*0.0*	*3.2*	*99.9*	*0.5*	*3.8*
Breine Phort	SB5	98.7	17.9	45.4	12.7	5.7	13.7	0.4	1.8	1.1	-0.1	98.6	0.6	-0.7
	SB7	98.9	38.2	33.2	10.2	3.7	12.1	0.4	0.0	1.1	0.6	99.5	0.5	0.1
	SB-6	97.3	24.3	44.0	9.9	2.8	15.8	0.3	0.3	0.0	2.1	99.5	0.6	1.7
	SB8	98.9	23.3	41.3	10.4	5.0	13.9	0.4	3.1	1.4	0.1	99.0	0.5	-0.4
Easdale Island	EE2	98.8	21.1	35.6	9.6	6.9	10.8	0.3	7.6	6.9	0.0	98.8	0.5	-0.6
	EE3	101.0	20.5	40.4	4.7	8.9	9.0	0.3	8.3	8.9	-2.6	98.4	0.5	-3.2
Used Slate	EX-1	102.1	30.8	39.2	5.7	8.2	12.6	0.2	3.1	2.3	-3.2	98.9	0.7	-4.0
	EE1	104.0	22.3	48.3	11.7	10.4	10.1	0.5	0.7	0.0	-5.8	98.3	0.8	-4.5
	Mean	**100.0**	**24.8**	**40.9**	**9.3**	**6.5**	**12.3**	**0.3**	**3.1**	**2.7**	**-1.1**	**98.9**	**0.6**	**-1.4**
	ST Dev	**2.2**	**6.6**	**5.0**	**2.8**	**2.6**	**2.2**	**0.1**	**3.2**	**3.3**	**2.6**	**0.4**	**0.1**	**2.2**

SB-1-SB-4, Pyrite based on sulphur XRF, chlorite based on residual Fe.

Seil		Total	Quartz	White mica	Chlorite	Pyrite	Albite	Apatite	Dolomite	Clay	Unallocated		Ilmenite	Volatiles
Balvicar	*SB1*	*98.2*	*33.3*	*32.7*	*19.3*	*2.6*	*8.4*	*0.4*	*1.5*	*0.0*	*0.6*	*98.8*	*0.5*	*-3.3*
	SB2	*92.8*	*34.0*	*28.0*	*19.5*	*0.8*	*8.9*	*0.3*	*1.2*	*0.0*	*7.1*	*99.9*	*0.6*	*3.2*
	SB3	*90.4*	*28.0*	*27.4*	*3.6*	*0.5*	*11.4*	*1.3*	*18.2*	*0.0*	*9.6*	*100.0*	*0.4*	*4.1*
	SB4	*89.4*	*20.6*	*28.9*	*9.0*	*0.7*	*16.4*	*0.5*	*13.3*	*0.0*	*10.5*	*99.9*	*0.5*	*5.0*
	Value of chlorite based on the amount of residue Al													
Luing		**Total**	**Quartz**	**White mica**	**Chlorite**	**Pyrite**	**Albite**	**Apatite**	**Dolomite**	**Clay**	**Unallocated**		**Ilmenite**	**Volatiles**
Toberonochy	LT1	87.8	27.9	30.7	12.1	3.8	11.4	0.2	1.6	0.0	11.8	99.5	0.6	7.6
	LT2	99.9	21.0	37.2	7.1	7.8	9.7	0.4	7.0	9.6	-0.9	99.0	0.6	-1.6
	LT3	88.7	27.4	36.4	10.7	5.2	7.0	0.2	1.7	0.0	10.6	99.4	0.6	6.3
Port Mary	LP1	95.5	26.1	33.7	20.6	2.5	10.9	0.4	1.4	0.0	4.2	99.7	0.7	2.5
& Rubha na	LP3	96.6	25.6	31.6	19.0	7.1	11.6	0.3	1.3	0.0	2.5	99.1	0.6	1.3
hEasgainne	LP5	99.3	19.1	41.3	15.6	5.4	13.5	0.3	0.6	3.5	0.0	99.3	0.7	-0.7
	LP6	98.8	31.1	37.0	8.6	5.8	12.0	0.4	0.0	3.8	0.5	99.3	1.0	-0.5
Cullipool	LC1	99.4	24.4	41.5	6.6	5.9	12.7	0.4	4.6	3.3	-0.1	99.3	0.7	-0.8
	LC2	98.3	30.1	38.0	11.0	5.5	9.6	0.4	0.5	3.2	1.1	99.3	0.8	0.2
	LC-3	98.5	27.7	39.0	10.9	5.7	11.4	0.4	0.9	2.5	0.8	99.3	0.8	0.0
Tir na Oig	LT5	100.4	22.8	37.5	8.6	6.5	17.0	0.3	5.2	2.6	-1.2	99.2	0.7	-2.0
Black Mill Bay	LB1	95.4	27.8	32.1	13.0	2.4	12.4	0.6	7.1	0.0	4.3	99.7	0.6	2.3
	LB2	97.8	25.4	29.7	3.0	5.8	4.6	0.5	28.8	0.0	1.5	99.3	0.4	0.9
	LB3	97.6	20.1	37.0	13.2	7.1	15.3	0.4	2.8	1.7	1.5	99.1	0.7	0.8
	Mean	**96.7**	**25.5**	**35.9**	**11.4**	**5.5**	**11.4**	**0.4**	**4.5**	**2.1**	**2.6**	**99.3**	**0.7**	**1.1**
	St Dev	**3.9**	**3.6**	**3.7**	**4.8**	**1.6**	**3.1**	**0.1**	**7.4**	**2.6**	**4.0**	**0.2**	**0.1**	**2.8**
Belmahua														
	BB1	99.0	38.0	21.7	16.5	5.2	10.7	0.3	4.1	2.5	0.4	99.4	0.6	-0.3
	BB2	98.5	25.8	30.3	13.2	6.9	10.9	0.4	4.7	6.2	0.7	99.1	0.6	-0.1

Highland Border Slate		Total	Quartz	White mica	Chlorite	Haematite	Albite	Apatite	Calcite	Clay	Unallocated		Ilmenite	Volatiles
Arran	A3	98.5	30.8	34.5	8.5	5.4	14.3	0.2	4.9	2.1	1.5	100.5	0.7	1.3
	A5	98.0	30.9	53.6	4.6	3.8	5.8	0.2	-0.9	2.4	2.0	100.4	0.7	1.5
	A6	98.7	30.2	47.8	4.6	5.8	10.2	0.2	0.0	1.8	1.3	100.6	0.7	1.3
Bute	B1b	99.1	5.4	47.3	7.4	6.5	15.7	0.6	16.1	1.6	100.7	1.6	-0.5	
	B1	99.6	16.0	39.0	5.0	7.6	12.5	0.4	19.1	1.2	100.8	1.2	-0.3	
	B3	96.8	13.3	38.5	16.5	5.0	7.3	0.4	15.8	3.7	100.5	0.6	3.0	
	B5	90.5	25.7	46.2	5.5	7.6	5.3	0.3	0.0	10.3	100.8	1.1	-0.8	
	B2-	98.6	33.7	32.3	8.3	2.2	10.9	0.3	10.8	1.6	100.2	1.0	0.0	
Luss														
Auchengavin	LS1	99.3	22.7	51.1	8.5	5.8	6.7	0.2	0.0	4.3	1.0	100.3	1.3	-0.3
	LS2	102.7	32.1	50.4	10.3	3.6	2.8	0.3	0.0	3.1	-2.7	100.0	1.2	-3.9
Aberfoyle														
	AB-5	97.9	15.4	43.6	12.3	7.0	16.9	0.6	0.5	1.5	2.6	100.4	1.5	1.1
	AB3	98.6	19.5	28.8	16.8	4.5	16.9	0.4	0.1	11.6	1.7	100.3	1.3	0.3
	AB4	97.8	15.7	43.8	12.4	7.1	16.4	0.6	0.5	1.3	2.7	100.4	1.5	1.2
	AB-6	98.6	25.2	32.3	14.2	2.5	15.8	0.3	0.8	7.5	1.5	100.1	1.2	0.2
	Mean	**98.2**	**19.0**	**37.1**	**13.9**	**5.3**	**16.5**	**0.5**	**0.5**	**5.5**	**2.1**	**100.3**	**1.4**	**0.7**
	Std Dev	**0.4**	**4.6**	**7.7**	**2.1**	**2.2**	**0.5**	**0.1**	**0.3**	**5.0**	**0.6**	**0.2**	**0.1**	**0.5**
Comrie														
Aberuchil	AU1	98.2	22.4	31.8	15.3	5.3	21.0	0.6	0.6	1.2	2.4	100.6	1.2	1.2
	AU2	99.2	22.8	43.7	12.7	6.8	12.6	0.6	0.0	0.0	1.6	100.7	1.1	1.4
	AU-3	98.8	23.8	37.8	12.9	4.0	18.9	0.5	0.9	0.1	1.7	100.5	1.3	0.4
Drummond	DR1	95.3	23.8	36.5	13.4	2.6	9.1	0.3	0.4	9.3	5.1	100.3	0.7	4.4
Logiealmond														
Craiglea	CR1	99.1	22.0	31.3	17.6	5.6	13.9	0.6	0.4	7.8	1.5	100.6	1.2	0.3
	CR2	98.8	25.7	39.0	12.6	6.4	12.8	0.4	0.5	1.3	1.9	100.7	1.3	0.6
	Cr3	98.6	18.9	39.7	15.9	5.5	13.6	0.5	0.7	3.8	2.0	100.6	1.2	0.7

Dunkeld		Total	Quartz	White mica	Chlorite	Haematite	Albite	Apatite	Calcite	Clay	Unallocated		Ilmenite	Volatiles
Birnam	DB1	98.6	28.6	48.0	11.8	5.3	4.1	0.4	0.3	0.0	2.0	100.6	1.1	1.3
	DB2	100.6	27.1	46.0	10.4	5.9	10.6	0.4	0.1	0.0	0.1	100.6	1.1	0.9
	DB3	99.3	22.5	54.7	6.8	7.9	6.9	0.4	0.0	0.0	1.6	100.8	1.1	1.0
Newtyle	DN1	99.4	24.8	40.2	17.4	2.7	13.9	0.3	0.1	0.0	1.0	100.4	1.1	0.9
	DN2	98.8	24.5	43.5	13.1	5.3	11.6	0.6	0.3	0.0	1.8	100.6	1.3	1.0
	DN3	101.0	18.3	58.7	13.4	3.9	6.0	0.6	0.1	0.0	-0.5	100.5	1.4	0.6
	DN4	98.4	22.8	44.3	13.5	3.7	12.6	0.5	1.0	0.0	2.0	100.4	1.2	0.9
Used slate	DX-1	97.6	23.0	37.3	13.1	3.0	14.9	0.4	2.5	3.3	2.8	100.4	1.2	1.6
	Mean	**99.2**	**24.0**	**46.6**	**12.4**	**4.7**	**10.1**	**0.4**	**0.6**	**0.4**	**1.3**			
	ST Dev	**1.1**	**3.1**	**7.1**	**3.0**	**1.7**	**3.9**	**0.1**	**0.8**	**1.2**	**1.1**			

Macduff Slate		Total	Quartz	White mica	Chlorite	Haematite	Albite	Apatite	Calcite	Clay	Unallocated		Ilmenite	Volatiles
Kirkney Hill	MK2	98.6	24.9	46.4	17.6	4.8	4.6	0.3		0.0	1.9	100.5	1.0	1.5
	MK4	98.4	22.5	41.5	14.6	7.6	5.4	0.3		6.5	2.4	100.8	0.8	1.5
Corksie Hill	MH1	99.6	18.6	47.3	9.7	6.1	10.4	0.3		7.3	1.0	100.6	0.7	0.3
	MH-2	100.2	18.4	49.8	7.9	7.0	9.5	0.3		7.1	0.6	100.7	0.7	-0.1
	MC-1	97.2	19.2	47.2	16.6	5.7	4.5	0.5		3.5	3.4	100.6	0.9	2.6
Wishach Hill	MW-1	100.2	26.3	50.9	15.4	5.3	2.6	0.3		-0.4	0.3	100.5	0.8	-0.6
	MX-2	99.5	26.8	40.9	17.8	4.3	3.5	0.3		5.8	1.0	100.4	0.8	0.0
	MX-3	99.2	28.4	40.7	16.5	3.6	2.1	0.2		7.8	1.2	100.4	0.8	0.1
Hill of Foudland	MF-1	99.2	21.1	46.4	12.9	5.1	5.5	0.3		7.8	1.3	100.5	0.9	0.0
	MF-11	98.8	25.0	40.9	15.0	5.1	4.7	0.3		7.7	1.7	100.5	0.8	0.9
Tillymorgan Hill	MT-2	101.9	18.7	40.6	13.2	5.4	6.6	0.4		17.0	-1.4	100.5	0.9	-2.6
	MT-6	100.5	25.1	41.5	13.4	5.9	6.6	0.3		7.7	0.1	100.6	0.8	-0.8
	Mean		**22.9**	**44.5**	**14.2**	**5.5**	**5.5**	**0.3**		**6.5**				
	Std Dev		**3.6**	**3.9**	**3.0**	**1.1**	**2.5**	**0.1**		**4.4**				
	Min		**18.4**	**40.6**	**7.9**	**3.6**	**2.1**	**0.2**		**-0.4**				
	Max		**28.4**	**50.9**	**17.8**	**7.6**	**10.4**	**0.5**		**17.0**				

Appendix 2.6 Attenuation Coefficients of minerals commonly found in slate

Haematite	**Fe**	**O**	**Total**
Formula	2.00	3.00	
Atomic wt	55.85	16.0	
Molecular Wt	111.70	48.00	159.70
μ	56.2	17.4	
$\mu_i w_i$	6277.54	835.20	7112.74
μ			**44.54**

Quartz	**Si**	**O**	**Total**
Formula	1.00	2.00	
Atomic wt	28.1	16.0	
Molecular Wt	28.10	32.00	60.10
μ	100.4	17.4	
$\mu_i w_i$	2821.24	556.80	3378.04
μ			**56.21**

Albite	**Na**	**Al**	**Si**	**O**	**Total**
Formula	1.00	1.00	3.00	8.00	
Atomic wt	23.0	27.0	28.1	16.0	
Molecular Wt	23.00	27.00	84.30	128.00	262.30
μ	47.1	77.5	100.4	17.4	
$\mu_i w_i$	1083.30	2092.50	8463.72	2227.20	13866.72
μ					**52.87**

Orthoclase	**K**	**Al**	**Si**	**O**	**Total**
Formula	1.00	1.00	3.00	8.00	
Atomic wt	39.1	27.0	28.1	16.0	
Molecular Wt	39.10	27.00	84.30	128.00	278.40
μ	222	77.5	100.4	17.4	
$\mu_i w_i$	8680.20	2092.50	8463.72	2227.20	21463.62
μ					**77.10**

Calcite	**Ca**	**C**	**O**	**Total**
Formula	1	1	3	
Atomic Wt	40	12	16	
Molecular wt	40	12	48	100
μ	257	6.68	17.4	
$\mu_i w_i$	10280	80.16	835.2	11195
μ				**112**

Dolomite	**Ca**	**Mg**	**C**	**O**	**Total**
Formula	1	1	2	6	
Atomic Wt	40	24	12	16	
Molecular wt	40	24	24	96	184
μ	257	63.5	6.68	17.4	
$\mu_i w_i$	10280	1524	160.32	1670.4	13635
μ					**74.1**

Magnesite	**Ca**	**Mg**	**C**	**O**	**Total**
Formula		1	1	3	
Atomic Wt	40	24	12	16	
Molecular wt	0	24	12	48	84
μ	257	63.5	6.68	17.4	
$\mu_i w_i$	0	1524	80.16	835.2	2439
μ					**29.0**

Siderite	**Fe**	**Mg**	**C**	**O**	**Total**
Formula	1	0	1	3	
Atomic Wt	55.8	24	12	16	
Molecular wt	55.8	0	12	48	115.8
m	56.2	63.5	6.68	17.4	
$\mu_i w_i$	3135.96	0	80.16	835.2	4051
μ					**35.0**

Pyrite	**Fe**	**S**	**Total**
Formula	1	2	
Atomic Wt	55.8	32	
Molecular wt	55.8	64	119.8
μ	56.2	141	
$\mu_i w_i$	3135.96	9024	12160
μ			**101.5**

Appendix 3.1a Determination of the relative crystallinity based on XRD intensitites

Mineral	White Mica K rich	White Mica Na rich	Chlorite	Quartz	Feldspar	Haematite /Pyrite	Carbonate Calcite	2θ 34.31
						38.8	Dolomite	36.10
Angle 2θ	10.4	10.9	7	24.44	32.6-32.8	41.5/43.6*	Magnesite	38.07
Correction factors								
Low diffraction angle	0.71		0.5	1				
Attenuation coefficient	64.81		45.14	56.21				
Correction factor	91.28		90.28	56.21	52.9	44.54	Calcite	112
Cwt y Bugail								
WCB-1	82		30	94	21	30		
WCB-2	113		59	91	23	37		
WCB-3	97		45	115		42		
WCB-4	102		57	99		31		
WCB-5	119		71	83	23	31		
Mean								
St Dev								
Pen yr Orsedd								
W/PO-1	179			162		77	55 Haematite	
W/PO-5	142			175		40	106 Haematite	
W/PO-6	120			131		51	80 Haematite	
W/PO-7	72			132		56	56	
W/PO-8	84		38	110		103	59	
W/PO-9	91			137		67	121	
W/PO-10	67			131		44	77 Haematite	
W/PO-11	147		21	135		82	84	
Mean								
St Dev								
			Most of the following have a trace of anatase at 29.84-29.91					
W/F-1	155		73	103		42		
	170		65	69		41		
	164		72	88		46		
	140		50	82		35		
	157		65	86		41		
W/F-1 average values	96		54	100		40		
W/F-4	123		53	102		56		
W/F-9	147		57	83		51		
W/F-10	196		63	121				
W/F-11	130		69	104		36		
W/F-12	148		63	111		62		
W/F-15	91		59	91		51		
W/F-16	158		59	89		45		
W/F-2	93		20	81		42		
W/F-5								
Mean								

Corrected Intensities White Mica	Chlorite	Quartz	Feldspar	Haematite	Carbonate	Crystallinity	Durability
Weighting given to the different minerals in determining the durability							
1	0.5	3	1	1	0		
						323	487
133	48	94	48	0	0	426	560
184	95	91	56	0	0	384	578
158	72	115	40	0	0	385	538
166	92	99	29	0	0	441	550
193	114	83	51	0	0	**392**	**543**
						46	**34**
						569	893
291	0	162	72	44	0	527	877
231	0	175	38	84	0	437	699
195	0	131	48	63	0	346	610
117	0	132	53	44	0	451	641
136	61	110	97	47	0	444	718
148	0	137	63	96	0	342	604
109	0	131	41	61	0	551	804
239	34	135	77	67	0	**458**	**731**
						86	**115**
						484	603
255	104	86	39	0	0	380	537
156	87	100	38	0	0	440	601
200	85	102	53	0	0	461	581
239	92	83	48	0	0	540	732
318	101	121	0	0	0	460	612
211	111	104	34	0	0	511	682
240	101	111	58	0	0	382	516
148	95	91	48	0	0	483	613
257	95	89	42	0	0	304	450
151	32	81	40	0	0	**444**	**593**

Mineral	White Mica		Chlorite	Quartz	Feldspar		Haematite	Carbonate	2θ	Corrected Intensities							
	K rich	Na rich					/Pyrite	Calcite	34.31	White Mica	Chlorite	Quartz	Feldspar	Haematite	Carbon-ate	Crystal-inity	Durability
Angle 2θ	10.4	10.9	7	24.44	32.6-32.8		38.8	Dolomite	36.10								
							41.5/43.6°	Magnesite	38.07								
Correction factors																	
Low diffraction angle	0.71		0.5	1													
Attenuation coefficient	64.81		45.14	56.21						Weighting given to the different minerals in determining the durability							
Correction factor	91.28		90.28	56.21	52.9		44.54	Calcite	112	1	0.5	3	1	1	0		
St Dev																71	80
W/TC-1	83		76		46	70				135	0	76	43	55	0	310	462
W/X-1	173		80	91		72				281	128	91	68	0	0	568	686
W/X-2	154		41	106		96				250	66	106	90	0	0	512	691
W/X-3	169		72	46	33	56				274	116	46	84	0	0	520	554
																533	644
E/K-1	121		34	167		113		Calcite	134	196	55	167	106	0	267	791	831
E/K-2	99		39	193		125		Calcite	117	161	63	193	118	0	233	767	889
E/K-3	85		36	163		113		Calcite	115	138	58	163	106	0	229	694	762
E/K-4	61		28	150		105		Calcite	111	99	45	150	99	0	221	614	670
																717	788
E/EW-1	57		55	111		102		Calcite	165	93	88	111	96	0	329	717	566
E/EW-2			52	197		69		Calcite	170	0	84	197	65	0	339	684	698
E/EW-3	46		75	117		84		Calcite	232	75	120	117	79	0	462	853	565
E/EW-4	39		56	104		99		Calcite	209	63	90	104	93	0	416	767	513
																755	585
E/BS-1	68		68	223		88		Calcite	106	110	109	223	83	0	211	737	917
E/BS-2	0		107	94		73		Calcite	83	0	172	94	69	0	165	500	437
E/BS-3			119	137		98		Calcite	231	0	191	137	92	0	460	881	599
E/BS-4	67		59	187		102		Calcite	210	109	95	187	96	0	418	905	813
																756	691
E/BM-1	24		104	129		119		Calcite	110	39	167	129	112	0	219	666	621
E/BM-2	61		85	109		158		Calcite	102	99	137	109	149	0	203	696	643
																743	637
E/BC-1	63		53	189		83				102	85	189	78	0	0	455	790
E/W-1	35		54	94		45		Calcite	86	57	87	94	42	0	171	451	425
I/B-1	187		123	122		63		Calcite	151	304	198	122	59	0	301	983	828
I/B-2	215		135	142		80		Calcite	135	349	217	142	75	0	269	1052	959
I/K-1	58		26	123		111		Calcite	151	94	42	123	104	0	301	664	588
I/K-3	68		41	114		78		Calcite	135	110	66	114	73	0	269	633	559
I/K-4	66		45	126		85		Calcite	101	107	72	126	80	0	201	587	601

Mineral	White Mica K rich	White Mica Na rich	Chlorite	Quartz	Feldspar		Haematite /Pyrite	Carbonate Calcite	2θ 34.31	Corrected Intensities White Mica	Chlorite	Quartz	Feldspar	Haematite	Carbon-ate	Crystal-inity	Durability
Angle 2θ	10.4	10.9	7	24.44	32.6-32.8		38.8	Dolomite	36.10								
							41.5/43.6°	Magnesite	38.07								
Correction factors																	
Low diffraction angle	0.71		0.5	1													
Attenuation coefficient	64.81		45.14	56.21						Weighting given to the different minerals in determining the durability							
Correction factor	91.28		90.28	56.21	52.9		44.54	Calcite	112	1	0.5	3	1	1	0		
F/N-1	148		85	133	47	41				240	137	133	83	0	0	593	790
F/N-2	61		43	93	52	47				99	69	93	93	0	0	354	506
F/G-1	150		112	139	46	60				244	180	139	100	0	0	662	850
F/G-2	117		72	95		67				190	116	95	63	0	0	464	596
F/F-1	151		82	77	49	49				245	132	77	92	0	0	546	634
F/F-2	246		128	115		51				399	206	115	48	0	0	763	895
S/C-1	163		99	50	30	85				265	159	50	108	0	0	582	602
S/C-2	185		71	116		57				300	114	116	54	0	0	584	759
																583	681
C/C-1	91		32	63		62		Calcite	223	148	51	63	58	0	444	765	421
U/V-1	93		0	81		51				151	0	81	48	0	0	280	442
S/A-1	443		37	108		60				719	59	108	56	0	0	943	1130
CS 7 bulk	197			250	96					320	0	250	90	0	0	660	1160
	31.4	12.8 bio		22.4	7	12											
CC34 bulk	141			163	134					229	0	163	126	0	0	518	844
S1	285		204	158						463	328	158	0	0	0	948	1101

Appendix 3.1b Intensities of XRD peaks and crystallinity measurements

Mineral	White mica K rich	White mica Na rich	Chlorite	Quartz	Feldspar Plag	Haematite /Pyrite	Carbonate Calcite	2θ	μ	White Mica	Chlorite	Quartz	Feldspar	Haematite	Carbonate	Crystallinity	Durability
										Corrected Intensities							
Angle	10	10.9	7	24.26	32.6-32.8	38.8	Dolomite	36.1	74								
						41.5/43.6°	Magnesite	38.1	29	Weighting for durability assessment				Calcite	0		
							Siderite	37.6	35	1	0.5	3	1	Dolomite	1		
Correction due to low angle	0.71	0.71	0.5														
Attenuation Coefficient μ	64.81		45.1	56.2	52.9	44.5											
Correction factor	**91.28**		**90.20**	**56.2**	**52.9**	**44.5**	**35**	**74**									
EL-2	230	trace	187	136	65					374	300	136	61	0	0	871	993
EL-3	253		103	111	90					411	165	111	104	0	0	791	931
EL-4	468	54	201	194	104		Siderite	57		848	323	194	167	0	35	1566	1793
EL-6	241	trace	188	330	69		Siderite			391	302	330	128	0	0	1151	1660
EL-7	304		249	250	87		Siderite			494	400	250	107	0	0	1250	1550
EL-8	202		135	281	110		Siderite			328	217	281	170	0	0	996	1450
EL-9	316		105	201	63		Siderite			513	168	201	123	0	0	1006	1324
EL-10	236		215	179	137		Dolomite	75		383	345	179	154	0	99	1160	1345
WL-1	374		193	111	65		Siderite	39		607	310	111	0	0	24	1052	1119
WL-3	219		108	106	93		Siderite	25		356	173	106	108	0	16	758	883
WL-5	310		255	208	32					503	409	208	53	0	0	1174	1385
K-1	406		231	139	70		Siderite	47		659	371	139	0	0	29	1198	1291
K-2	454		186	178	73		Siderite	50		737	298	178	91	0	31	1336	1543
K-3	457		165	232	65		Siderite	46		742	265	232	84	0	29	1352	1684
Mean										**525**	**289**	**190**	**96**	**0**	0	**1119**	**1354**
St Dev										**167**	**82**	**67**	**54**	**0**	0	**226**	**287**
BX-1	252		106	116	100		Siderite	46		409	170	116	0	0	29	724	871
EE-1	212	36	80	77	74					403	128	77	77	0	0	685	775
EE-2	346	36	96	154	129					620	154	154	154	0	0	1082	1313
EE-3	313	39		151	144		Dolomite	146		572	0	151	151	0	192	1066	1368
Mean																**944**	**1152**
Luing																	
LP-1	270		114	84	98					438	183	84	84	0	0	789	866
	325		102	128	67					528	164	128	128	0	0	947	1122
	197		77	123	86					320	124	123	123	0	0	689	874
LP-2	123		24	97	68		Dolomite	340		200	39	97	97	0	448	880	1055
LP-3	298			295	102	55	Pyrite			484	0	295	295	44	0	1118	1664
LP-5	449		133	132	123					729	213	132	132	0	0	1207	1364
LP-6	393		88	222	130			93		638	141	222	222	0	0	1223	1597
Mean																**979**	**1220**

Mineral	White mica K rich	White mica Na rich	Chlorite	Quartz	Feldspar Plag	Haematite /Pyrite	Carbonate	2θ	μ	Corrected Intensities White Mica	Chlorite	Quartz	Feldspar	Haematite	Carbonate	Crystallinity	Durability
Angle	**10**	**10.9**	**7**	**24.26**	**32.6-32.8**	**38.8**	**Calcite**	34.3	112								
						41.5/43.6°	**Dolomite**	36.1	74								
							Magnesite	38.1	29	**Weighting for durability assessment**				**Calcite**	0		
							Siderite	37.6	35	1	0.5	3	1	**Dolomite**	1		
LC-1	304		55	101	118		Dolomite	71		494	88	101	101	0	93	877	1035
LC-2	313		56	89	72					508	90	89	89	0	0	776	909
LC-2	324		71	182	97					526	114	182	182	0	0	1004	1311
LC-3	262		50	101	111					425	80	101	101	0	0	708	870
Mean																**841**	**1031**
LT-1	353		0	123	87		Magnesite	220		573	0	123	123	0	114	933	1179
LT-2	331	41	105	157	133	144	Dolomite	100		604	168	157	157	114	132	1332	1448
LT-3	455		0	130	80		Magnesite	190		739	0	130	130	0	98	1097	1357
Mean																**1121**	**1328**
LT-5	476		72	90	129/107°		Dolomite	115		773	116	90	90	0	151	1220	1342
										0							
LB-1	383		127	189	135		Dolomite	168		622	204	189	189	0	221	1425	1701
LB-2	360		37	137	122		Dolomite	461		585	59	137	137	0	607	1525	1769
LB-3	413		94	195	155			0		671	151	195	195	0	0	1212	1526
Mean										0						**1387**	**1665**
BB-1	217		145	270	85		Dolomite	93		352	233	270	270	0	122	1248	1671
BB-2	283	61	120	183	148		Dolomite	98		559	193	183	183	0	129	1246	1516
Mean										0						**1247**	**1594**
Sell										0							
SB-1	256		120	188	72		Dolomite	60		416	193	188	188	0	79	1063	1343
SB-2	234		143	258	125					380	229	258	258	0	0	1125	1527
SB-3	222		53	148	94		Dolomite	282		361	85	148	148	0	371	1113	1366
SB-4	250		83	104	89		Dolomite	160		406	133	104	104	0	211	958	1099
Mean										0						**1065**	**1334**
SB-5	478		125	114	166		Dolomite	98		776	201	114	114	0	129	1334	1462
SB-6	477		88	188	189					775	141	188	188	0	0	1292	1597
SB-7	325		91	253	149		Dolomite			528	146	253	253	0	0	1180	1613
SB-8	398		109	196	197					646	175	196	196	0	0	1213	1518
Mean										0						**1255**	**1547**
EX-1	104		39	176	115	67	Siderite	25		169	63	176	176	53	16	652	920
										0							
Arran			**45.14**														
Sample																	
A1	267		66	133	125	48	Haematite			434	106	133	133	38	0	844	1095
A3	55		38	126	99					89	61	126	126	0	0	402	624
A6	180		66	139	112	64	Haematite			292	106	139	139	51	0	727	1003
Mean																**658**	**907**
Bute																	

Mineral	White mica		Chlorite	Quartz	Feldspar	Haematite	Carbonate	2θ	μ	Corrected Intensities							
	K rich	Na rich			Plag	/Pyrite	Calcite	34.3	112	White Mica	Chlorite	Quartz	Feldspar	Haematite	Carbon-ate	Crystal-inity	Durability
Angle	10	10.9	7	24.26	32.6-32.8	38.8	Dolomite	36.1	74								
						41.5/43.6°	Magnesite	38.1	29	Weighting for durability assessment				Calcite	0		
							Siderite	37.6	35	1	0.5	3	1	Dolomite	1		
B1a	194	67	44	81	185	71	Haematite			424	71	81	81	56	0	713	896
B1b	120		80		161					195	128	0	0	0	0	323	259
B2	182	87	75	138	203	71	Haematite			437	120	138	138	56	0	889	1162
B3	328	73	128	130	164					651	205	130	130	0	0	1117	1274
B4	207	122	51	122	238	72	Haematite			534	82	122	122	57	0	917	1177
B4-w	143	70	50	88	147	31				346	80	88	88	25	0	627	787
B5	257	48	135	118	109					495	217	118	118	0	0	948	1076
					64											**791**	**947**
Luss																	
Ls-1	310	42	98	94	237	66	Calcite	54		572	157	94	94	52	108	1077	1238
Ls-2	354	18	112	213	106		Calcite	47		604	180	213	213	0	94	1303	1640
Mean																**1190**	**1439**
Aberfoyle																	
AB-1	62	33	71	87	67					154	114	87	87	0	0	442	559
	71	44	68	55	146					187	109	55	55	0	0	406	461
AB-3	169		50	64	136	7				274	80	64	64	6	0	488	582
AB-4	121		61	80	127	99				196	98	80	80	78	0	533	722
AB-5	100	46	82	193	136					237	132	193	193	0	0	755	1075
AB-6	98		65	122	186					159	104	122	122	0	0	507	699
Mean															0	**522**	**683**
Craiglea															0		
Cr-1	168		163	165	155	120	Siderite	47		273	262	165	165	95	29	989	1283
Cr-2	232		100	134	165	60				377	160	134	134	48	0	853	1088
Cr-3	251		129	129	173	57	Siderite	37		408	207	129	129	45	23	941	1140
Mean															0	**927**	**1171**
Comrie															0		
Au-1	106		118	96	189					172	189	96	96	0	0	553	651
Au-2	182		81	110	182	44				296	130	110	110	35	0	680	870
Au-3	188		126	170	228		Siderite	31		305	202	170	170	0	19	867	1106
Dr-1	186			151	145					302	0	151	151	0	0	604	906
Mean																**676**	**883**
Dunkeld																	
DB-1	256		95	158	87					416	152	158	158	0	0	884	1124
DB-2	178		40	130	122	117				289	64	130	130	93	0	706	1027
DB-3	191		0	99	106	95				310	0	99	99	75	0	583	857
DN-1	93		66	81	139					151	106	81	81	0	0	419	528
DN-2	120		38	118	123	64				195	61	118	118	51	0	543	799
DN-3	240		86	89	115		Siderite	45		390	138	89	89	0	28	734	843
DN-4	79		28	112	137	32				128	45	112	112	25	0	423	649
DX-1	123		91	124	202	30				200	146	124	124	24	0	618	816
Mean																**614**	**830**

Mineral	White mica		Chlorite	Quartz	Feldspar	Haematite	Carbonate	2θ	μ	Corrected Intensities							
	K rich	Na rich			Plag	/Pyrite	Calcite	34.3	112	White Mica	Chlorite	Quartz	Feldspar	Haematite	Carbon-ate	Crystal-inity	Durability
Angle	10	10.9	7	24.26	32.6-32.8	38.8	Dolomite	36.1	74								
						41.5/43.6°	Magnesite	38.1	29	Weighting for durability assessment				Calcite	0		
							Siderite	37.6	35	1	0.5	3	1	Dolomite	1		
Macduff																	
MK-2	230		75	161	71	112				374	120	161	161	89	0	905	1255
MK-4	142	31	92	123	64	96				281	148	123	123	76	0	751	999
MF-1	250	54	50	123	89	84				494	80	123	123	67	0	886	1159
MF-1	212	45	40	114	87	127				417	64	114	114	101	0	810	1107
MF-1'	191	48	24	109	88	403				388	39	109	109	319	0	964	1482
MF-2	130			82	33	87				211	0	82	82	69	0	444	677
MF-3	125	trace	56	86	58	74				203	90	86	86	59	0	523	709
MF-5	146	trace	64	131	54	82				237	103	131	131	65	0	667	942
MF-9	143	trace	58	144	49	70				232	93	144	144	55	0	669	966
MF-10	138	trace	59	115	67	64				224	95	115	115	51	0	599	833
MF-6	136		64	167						221	103	167	167	0	0	658	940
MF-7	142	29	73	155	48	70				278	117	155	155	55	0	760	1067
MF-13	100		44	138	56	43				162	71	138	138	34	0	543	818
MF-11	133	42	66	99	51	76				284	106	99	99	60	0	648	854
	217	trace	104	171		96				352	167	171	171	76	0	937	1272
MF-12	132		0	123	71					214	0	123	123	0	0	460	706
MF-14	217		38	155	92	127				352	61	155	155	101	0	824	1204
MH-1	141		0	77	70	82				229	0	77	77	65	0	448	667
MH-1	262		0	111	86	101				425	0	111	111	80	0	728	1030
MH-2	219		0	88	73	81				356	0	88	88	64	0	596	836
MH-2	191		0	69	72	91				310	0	69	69	72	0	520	730
MH-3	153		91	107	70					248	146	107	107	0	0	608	749
MH-3w	50		44	67	36					81	71	67	67	0	0	286	385
MC-1	112	29	38	129	72	95				229	61	129	129	75	0	623	926
MC-2	128	trace	82	94						208	132	94	94	0	0	527	650
MC-3	157	trace	45	100	64	137				255	72	100	100	109	0	636	908
MW-1	291	47	79	150	91	169				549	127	150	150	134	0	1110	1480
MT-1	177	trace	66	109	68	56				287	106	109	109	44	0	656	865
MT-2b	216	trace	41	109	61	101				351	66	109	109	80	0	715	980
Mean (excluding the weathered samples)																685	957
STDEV (excluding the weathered samples)																170	234

Appendix 3.2 Full Width at Half Magnitude measurements				
FWHM	**Chlorite**		**White mica**	**Quartz**
Peak 2θ	**~7**	**~14**	**~10**	**24.26**
Ballachulish				
EL-3	0.088	0.122	0.119	0.122
EL-4	0.097	0.118	0.120	0.143
EL-6	0.142	0.165	0.159	0.180
EL-7	0.177	0.194	0.189	0.182
EL-8	0.097	0.096	0.101	0.112
EL-9	0.112	0.136	0.143	0.115
EL-10	0.112	0.140	0.132	0.136
K-1	0.125	0.140	0.127	0.152
K-2	0.098	0.116	0.122	0.134
K-3	0.131	0.142	0.140	0.150
WL-1	0.164	0.122	0.151	0.110
WL-3	0.147	0.147	0.140	0.158
WL-5	0.145	0.115	0.137	0.127
Mean	**0.126**	**0.135**	**0.137**	**0.140**
St Dev	**0.028**	**0.025**	**0.022**	**0.024**
C of V	**0.22**	**0.19**	**0.16**	**0.17**
Luing				
LT-1			0.15	0.16
LT-2		0.14	0.14	0.17
LT-3			0.12	0.14
LT-5	0.11	0.11	0.1	0.12
LB-1	0.12	0.14	0.14	0.14
LB-3	0.11	0.12	0.12	0.1
LP-3	0.15	0.18	0.16	0.2
LP-5	0.13	0.14	0.14	0.17
LP-6	0.12	0.15	0.13	0.15
LC-1	0.14	0.18	0.17	0.18
LC-2	0.18	0.2	0.2	0.17
Mean	**0.13**	**0.15**	**0.143**	**0.15**
St Dev	**0.02**	**0.03**	**0.027**	**0.03**
C of V	**0.18**	**0.20**	**0.19**	**0.18**
Seil				
SB-2	0.11	0.14	0.12	0.11
SB-3	0.11	0.16	0.13	0.18
SB-4	0.12	0.12	0.1	0.14
SB-5	0.1	0.14	0.12	0.12
SB-6	0.1	0.12	0.12	0.13
SB-7	0.11	0.1	0.1	0.1
SB-8	0.1	0.12	0.11	0.13
Beinahua				
BB-1	0.12	0.15	0.14	0.13
BB-2	0.11	0.11	0.11	0.14
Mean	**0.11**	**0.13**	**0.117**	**0.13**
St Dev	**0.01**	**0.020**	**0.013**	**0.02**
C of V	**0.07**	**0.15**	**0.11**	**0.17**

FWHM	Chlorite		White mica	Quartz
Peak 2θ	**~7**	**~14**	**~10**	**24.26**
Arran				
A3		0.145	0.184	0.136
A6		0.162	0.183	0.174
Bute				
B1a		0.111	0.122	0.127
B1-b		0.317	0.329	
B2		0.167	0.172	0.133
B3		0.127	0.136	0.13
B4		0.133	0.181	0.17
B5		0.166	0.172	0.146
B4-w		0.141	0.161	0.17
Mean		**0.166**	**0.182**	**0.146**
St Dev		**0.070**	**0.068**	**0.020**
C of V		**0.42**	**0.38**	**0.13**
Aberfoyle				
AB-1	0.127	0.109	0.19	0.121
AB-3	0.12	0.139	0.159	0.131
AB-4	0.101	0.12	0.15	0.099
AB-5	0.129	0.138	0.159	0.136
AB-6	0.136	0.14	0.16	0.157
Mean	**0.123**	**0.129**	**0.164**	**0.129**
St Dev	**0.013**	**0.014**	**0.015**	**0.021**
C of V	**0.11**	**0.11**	**0.09**	**0.16**
Dunkeld				
DB-1	0.215	0.192	0.184	0.175
DB-2	0.152	0.164	0.166	0.185
DB-3	0.206	0.168	0.164	0.167
DN-1	0.15	0.173	0.17	0.174
DN-2	0.136	0.132	0.162	0.163
DN-3	0.128	0.141	0.14	0.161
DN-4	0.154	0.132	0.15	0.123
Mean	**0.163**	**0.157**	**0.162**	**0.164**
St dev	**0.034**	**0.023**	**0.014**	**0.020**
C of V	**0.21**	**0.15**	**0.09**	**0.12**

FWHM	Chlorite		White mica	Quartz
Peak 2θ	~7	~14	~10	24.26
Macduff				
MF-1	0.201	0.149	0.182	0.204
MF-2	0.085	0.15	0.182	0.177
MF-3	0.155	0.212	0.215	0.225
MF-5	0.178	0.194	0.216	0.162
MF-9	0.187	0.155	0.168	0.143
MF-10	0.175	0.197	0.227	0.168
MF-6	0.134	0.176	0.213	0.191
MF-7	0.138	0.155	0.169	0.158
MF-13	0.174	0.155	0.184	0.153
MF-12		0.141	0.189	0.153
MH-1		0.216	0.236	0.211
MH-2		0.149	0.182	0.155
MC-1	0.176	0.129	0.176	0.119
MC-2	0.129	0.143	0.167	0.163
MC-3	0.231	0.163	0.216	0.18
MH-3	0.157	0.182	0.185	0.2
MK-2	0.122	0.132	0.131	0.14
MX-2	0.146	0.148	0.197	0.145
MX-3	0.146	0.16	0.182	0.158
MT-1	0.169	0.158	0.166	0.153
MT-2	0.152	0.16	0.196	0.172
MT-5	0.185	0.166	0.229	0.193
Mean	**0.160**	**0.163**	**0.191**	**0.169**
ST DEV	**0.031**	**0.016**	**0.028**	**0.025**
C of V	**0.20**	**0.10**	**0.14**	**0.15**

Appendix 4.1 Fabric and minimum commercial thickness at non-optimum conditions

Sample	Space	Alignment	Shape		Microlithon	Homogeneity	Fabric	Eqtn	Thickness
	15	%	Straight/2	Continuity/2	Fabric /3	/3	Points	12.645	(mm)
	5	50	1	1	1	1		-0.0693	
								Theoretical	Actual
Cumbrian									
E/K-1	62.8	9.8	1	0	0	0	2	10.7	8
E/K-3	39.7	5	1	0	0	1	4	9.6	9
E/BS-3	40	13	1	0	0	0	3	10.2	14
E/EW-4	28	10	1	0.5	0	0	4	9.3	9.6
E/BM-1	102	5.8	0	0	0	0	1	11.9	12
Welsh									
W/CB-1	13	60	1.5	2	2	3	15	4.3	5
W\CB-4	20	22	1	0	1	1	7	7.7	8
W\CB-5	17	30	2	1	1.5	2	12	5.7	5
W/P-1	18	48	1	0	0	1	7	7.7	7
W/F-1	10	46	2	2	2.5	2.5	17	3.8	4
	14	54	2	2	2.5	2.5	15	4.3	4
W/F-9	19	30	1	0	0	1	7	8.0	
W/F-16	40	25	1	0	1	1	5	8.7	8
W/PO-3	23.3	21	1.5	1.5	1.3	1	9	6.8	
W/PO6	18	40	2	2	2	1	12	5.5	5
W/PO-11	8	68	2	2	3	3	21	2.9	
W/TC-1	40	11	0.5	0	0	0	3	10.6	
Sample									
W/F-5	15.3	40	2	2	3	3	16	4.3	4
	14	30	2	2	3	3	16	4.2	4
W /F-12	28	20	1	1	2	1	8	7.2	8
	27.5	25	2	1	0.5	1	8	7.4	8
W/F-13	25.4	35	2	1	1.5	1	9	6.7	8

Sample	Space	Alignment	Shape		Microlithon	Homogeneity	Fabric	Eqtn	Thickness
	15	%	Straight/2	Continuity/2	Fabric /3	/3	Points	12.645	(mm)
	5	50	1	1	1	1		-0.0693	
								Theoretical	Actual
Ballachulish									
EL-3	30	31	2	2	2	2	11	5.9	
EL-4									
EL-5	21	60	2	1.5	2.5	1	12	5.6	
EL-6									
EL-7	20	53	2	2	2	1	12	5.6	
EL-10	21	60	2	2	2.5	2.5	14	4.9	
WL-1	20.4	55	2	2	1	1.5	11	5.8	
WL-3									
WL-5	30	60	2	2	2.5	2	12	5.4	
K-1	40	50	2	2	1	2	10	6.4	
K-3	40	50	2	1.5	1	0	7	7.6	
BX-1	13.3	60	2	2	2.5	2	15	4.4	9
Easdale									
EE-3	20.6	32	2	2	1	2	11	5.8	9
EX-1	21	26	0	0	0	1.5	6	8.6	10
LC-1									
LC-2	26	40	2	2	1	1	10	6.5	
LC-3	25.9	30	1.5	1	0.5	1	7	7.5	9
LT-1									
LT-2	16	40	1.5	1.5	0	2	10	6.1	8
LT-3	16	64	1.5	2	2.5	2	14	4.8	
LT-5	22	32.5	0	0	1	0	5	8.9	
LB-1	15.5	41	2	2	2	2	14	4.9	
BB-1	66	31	1	1.5	2	1.5	8	7.4	15
SB-1	30.2	25	1	1.5	0.5	0	6	8.4	
SB-2	27	35	1	1	0	1.5	7	7.8	
SB-3									
SB-5	25	56	2	2	2	2	12	5.5	

Sample	Space	Alignment	Shape		Microlithon	Homogeneity	Fabric	Eqtn	Thickness
	15	%	Straight/2	Continuity/2	Fabric /3	/3	Points	12.645	(mm)
	5	50	1	1	1	1		-0.0693	
								Theoretical	Actual
Highland Border									
A3 x	13	30	2	2	1	2	13	5.0	
A5 y	9	20	1	1	0	1.5	12	5.4	
A-6									
B-1									
B-2	0	26	0	0	0	0			
B-3	0	0	No measurements possible						
AB-1	29	20	1	2	1	1.5	8	7.0	
AB-4	28	41	1.5	1.5	1	1	8	7.0	
AB-5	28.8	40	1	2	0	2	8	7.1	
"	35	33	1.5	2	1	2	9	6.6	
AB-6	31.2	40	1	1	1	1	7	7.7	8
AU-1	35	15	0	0	0	0	2	10.7	
AU-2									
AU-3	28	10	0	0	0	0	3	10.4	
DR-1	24.4	13	0	0	0	0	3	10.0	
CR-1	28	11	1	0.5	0	1	5	8.7	
Cr-3	21	25	2	1.5	2	1	11	6.1	9
LS-1*	20	50	1	2	2.5	1	11	5.8	
LS-2									
DB-1	21	25	1.5	1	2	1	10	6.5	
DB-2									
DB-3									
DN-3	21	62	2	2	2	2	13	5.2	
DN-4									
DX-1	35.5	20	1	1.5	0	0	5	8.9	10

Sample	Space	Alignment	Shape		Microlithon	Homogeneity	Fabric	Eqtn	Thickness
	15	%	Straight/2	Continuity/2	Fabric /3	/3	Points	12.645	(mm)
	5	50	1	1	1	1		-0.0693	
								Theoretical	Actual
Macduff Slate									
MK-2	16	20	1	1.5	0.5	1.5	10	6.5	
MK-4	35	15	1	1	1	1	6	8.1	
MC-1+1	30	15	1	1	0.5	1.5	7	7.9	
MC-2	30	30					3	10.2	
MC-3	18	25	1.5	1	1	2	10	6.3	
MH-1									
MH-2	20	25	1	1	1	1.5	9	6.9	
MX-1	30	30	1.5	1	1	1	8	7.5	
MF-2'	28	30	2	1.5	1.5	2	10	6.2	
MF-5	20	20	1	1	1.5	1	9	6.9	
MF-14	30	13	0	0	1	1	5	9.1	14
MT-4	30	15	1.5	0.5	1	1	7	7.9	
MT-BALD	30	13	1	0.5	0	1.5	6	8.5	

Appendix 4.2 Fabric and minimum commercial thickness at optimum conditions

Sample	Space	Alignment	Shape		Microlithon	Homogeneity	Fabric	Eqtn	Thickness
	15	%	Straight/2	Continuity/2	Fabric /3	/3	Points	12.36	(mm)
	4.9	50	1	1	1	2		-0.059	
								Theoretical	Actual
Cumbrian									
E/K-1	62.8	9.8	1	0	0	0	2	10.7	8
E/K-3	39.7	5	1	0	0	1	5	9.2	9
E/BS-3	40	13	1	0	0	0	3	10.3	14
E/EW-4	28	10	1	0.5	0	0	4	9.6	9.6
E/BM-1	102	5.8	0	0	0	0	1	11.8	12
Welsh									
W/CB-1	13	60	1.5	2	2	3	18	4.2	5
W\CB-4	20	22	1	0	1	1	8	7.7	8
W\CB-5	17	30	2	1	1.5	2	13	5.6	5
W/P-1	18	48	1	0	0	1	8	7.7	7
W/F-1	10	46	2	2	2.5	2.5	20	3.8	4
	14	54	2	2	2.5	2.5	18	4.3	4
W/F-9	19	30	1	0	0	1	7	8.0	
W/F-16	40	25	1	0	1	1	6	8.5	8
W/PO-3	23.3	21	1.5	1.5	1.3	1	10	6.9	
W/PO6	18	40	2	2	2	1	13	5.8	5
W/PO-11	8	68	2	2	3	3	24	3.0	
W/TC-1	40	11	0.5	0	0	0	3	10.6	
Sample									
W/F-5	15.3	40	2	2	3	3	19	4.1	4
	14	30	2	2	3	3	19	4.1	4
W /F-12	28	20	1	1	2	1	9	7.3	8
	27.5	25	2	1	0.5	1	9	7.4	8
W/F-13	25.4	35	2	1	1.5	1	10	6.8	8

Sample	Space	Alignment	Shape		Microlithon	Homogeneity	Fabric	Eqtn	Thickness
	15	%	Straight/2	Continuity/2	Fabric /3	/3	Points	12.36	(mm)
	4.9	50	1	1	1	2		-0.059	
								Theoretical	Actual
Ballachulish									
EL-3	30	31	2	2	2	2	13	5.7	
EL-4									
EL-5	21	60	2	1.5	2.5	1	13	5.8	
EL-6									
EL-7	20	53	2	2	2	1	13	5.8	
EL-10	21	60	2	2	2.5	2.5	16	4.8	
WL-1	20.4	55	2	2	1	1.5	13	5.8	
WL-3									
WL-5	30	60	2	2	2.5	2	14	5.4	
K-1	40	50	2	2	1	2	12	6.1	
K-3	40	50	2	1.5	1	0	7	8.0	
BX-1	13.3	60	2	2	2.5	2	17	4.5	9
Easdale									
EE-3	20.6	32	2	2	1	2	13	5.7	9
EX-1	21	26	0	0	0	1.5	7	8.2	10
LC-1									
LC-2	26	40	2	2	1	1	11	6.6	
LC-3	25.9	30	1.5	1	0.5	1	8	7.5	9
LT-1									
LT-2	16	40	1.5	1.5	0	2	12	5.9	8
LT-3	16	64	1.5	2	2.5	2	16	4.8	
LT-5	22	32.5	0	0	1	0	5	9.2	
LB-1	15.5	41	2	2	2	2	16	4.9	
BB-1	66	31	1	1.5	2	1.5	9	7.2	15
SB-1	30.2	25	1	1.5	0.5	0	6	8.7	
SB-2	27	35	1	1	0	1.5	8	7.5	
SB-3									
SB-5	25	56	2	2	2	2	14	5.4	

Sample	Space	Alignment	Shape		Microlithon	Homogeneity	Fabric	Eqtn	Thickness
	15	%	Straight/2	Continuity/2	Fabric /3	/3	Points	12.36	(mm)
	4.9	50	1	1	1	2		-0.059	
								Theoretical	Actual
Highland Border									
A3 x	13	30	2	2	1	2	15	5.0	
A5 y	9	20	1	1	0	1.5	14	5.6	
A-6									
B-1									
B-2	0	26	0	0	0	0			
B-3	0	0	No measurements possible						
AB-1	29	20	1	2	1	1.5	10	6.9	
AB-4	28	41	1.5	1.5	1	1	9	7.1	
AB-5	28.8	40	1	2	0	2	10	6.7	
"	35	33	1.5	2	1	2	11	6.4	
AB-6	31.2	40	1	1	1	1	8	7.6	8
AU-1	35	15	0	0	0	0	2	10.7	
AU-2									
AU-3	28	10	0	0	0	0	3	10.5	
DR-1	24.4	13	0	0	0	0	3	10.2	
CR-1	28	11	1	0.5	0	1	6	8.5	
CR-2									
Cr-3	21	25	2	1.5	2	1	12	6.3	9
LS-1*	20	50	1	2	2.5	1	12	6.0	
LS-2									
DB-1	21	25	1.5	1	2	1	11	6.7	
DB-2									
DB-3									
DN-3	21	62	2	2	2	2	15	5.2	
DN-4									
DX-1	35.5	20	1	1.5	0	0	5	9.2	10

Sample	Space	Alignment	Shape		Microlithon	Homogeneity	Fabric	Eqtn	Thickness
	15	%	Straight/2	Continuity/2	Fabric /3	/3	Points	12.36	(mm)
	4.9	50	1	1	1	2		-0.059	
								Theoretical	Actual
Macduff Slate									
MK-2	16	20	1	1.5	0.5	1.5	11	6.5	
MK-4	35	15	1	1	1	1	7	8.0	
MC-1+1	30	15	1	1	0.5	1.5	8	7.6	
MC-2	30	30					3	10.3	
MC-3	18	25	1.5	1	1	2	12	6.1	
MH-1									
MH-2	20	25	1	1	1	1.5	10	6.8	
MX-1	30	30	1.5	1	1	1	9	7.5	
MF-2'	28	30	2	1.5	1.5	2	12	6.0	
MF-5	20	20	1	1	1.5	1	10	7.0	
MF-14	30	13	0	0	1	1	6	8.8	14
MT-4	30	15	1.5	0.5	1	1	8	7.8	
MT-BALD	30	13	1	0.5	0	1.5	7	8.1	

Appendix 5.1 Weathering Experiments

Slates tested according to BS680 and prEN12326

							BS680	prEN12326	BS680	Increase in water absorption/cycle
IK3										
No of cycles		0	13	24	53	52				
Cumulative Total		0	13	37	90	142				
%water absorption	1	0.1174	0.1177	0.1204	0.1236	0.1255		0.1083		
	2	0.1212	0.1224	0.1242	0.1314	0.1331		0.1164		
Mean BS680		**0.1193**	**0.1200**	**0.1223**	**0.1275**	**0.1293**		**0.1123**		**0.070**
	3	0.0929	0.0959	0.0951	0.0959	0.0962	0.1303			
	4	0.0889	0.0938	0.0928	0.0917	0.0901	0.1278			
Mean prEN12326		**0.0909**	**0.0948**	**0.0939**	**0.0938**	**0.0931**	**0.1290**			**0.015**
W/F8										
No of cycles		0	14	24	50	52			5	
Cumulative Total		0	14	38	88	140			145	145
%water absorption	5	0.0804	0.0875	0.0897	0.0997	0.1077		0.1124	0.1263	0.16516
	6	0.0839	0.0921	0.0943	0.1046	0.1357		0.1512	0.1652	
Mean BS680		**0.0821**	**0.0898**	**0.0920**	**0.1022**	**0.1217**		**0.1318**		**0.283**
	7	0.0583	0.0628	0.0628	0.0692	0.0665	0.0997			
	8	0.0541	0.0595	0.0608	0.0653	0.0616	0.0957			
Mean prEN12326		**0.0562**	**0.0612**	**0.0618**	**0.0673**	**0.0640**	**0.0977**			
LB3										
No of cycles		0	17	23	47	46				
Cumulative Total		0	17	40	87	133				
% water absorption	9	0.2410	0.3453	0.3571	0.3830	0.3933				
	10	0.2253	0.2830	0.2759	0.2956	0.3342				
Mean BS680		**0.2331**	**0.3142**	**0.3165**	**0.3393**	**0.3637**				**0.982**

							BS680	prEN12326	BS680	Increase in water absorption/cycle
LC3										
No of cycles		0	15	31	53					
Cumulative Total		0	15	46	99					
% water absorption	11	0.1837	0.1948	0.2233	0.2408					
	12	0.1985	0.2141		0.2551					
Mean BS680		**0.1911**	**0.2045**		**0.2480**					0.5741
	13	0.1757	0.1677		0.1802					
	14	0.1928	0.2017		0.2437					
Mean prEN12326		**0.1842**	**0.1847**		**0.2120**					0.2799
MT6										
Cumulative Total		0	9	26	95					
% water absorption	15	0.2748	0.2909		0.3049					0.3171
	16	0.0821		0.0961	0.0929					0.1134
Mean BS680										
	17	0.1773	0.1882		0.1956					
	18	0.0538	0.0556		0.0521					
Mean prEN12326										
Spanish slate										
No of cycles		0	13	24	40	20				
Cumulative Total		0	13	37	77	97				
% water absorption	19	0.148	0.160	0.164	0.180	0.221				
	20	0.152	0.162	0.166	0.178	0.219				
Mean BS680		**0.1500**	**0.1611**	**0.1654**	**0.1788**	**0.2201**				0.3747
	21	0.1013	0.1084	0.1035	0.1033	0.1128				
	22	0.1098	0.1143	0.1084	0.1250	0.1537				
Mean prEN12326		**0.1056**	**0.1113**	**0.1060**	**0.1141**	**0.1332**				

Appendix B

Précis of National Standards for Slate

Appendix B: Précis of National Standards for Slate

1. Introduction

In the past, the selection of good roofing slate relied on the expertise of the quarryman at the quarry face. Different quarries relied on their local reputation which could rise and fall depending on their own quality control. As markets expanded each country built up its own set of standards, which to some extent were dependent on the type of slate produced in that country. With the onset of international markets, there is a greater need to find a standard that is applicable to all, and independent of national traits. To this end a new European Standard is being devised for use in the countries of the E.U. and is planned to supersede the national standards of member states. This has not been without teething problems, as the present draft requires a series of most complex tests, lacking the simplicity of the national standards and making the testing of slates an expensive and time consuming procedure.

This review of national standards covers the following

European Standard	prEN 12326-1 & prEN 12326-2
Britain	BS 680 Part 2 1971
France	NF P32 301 & NF P32-302
Germany	DIN 52 201
Italy	UNI 8626 & UNI 8635
Spain	UNE 220 201 85
U. S. A.	C119-74

2. Testing of slate as a roofing material

In an attempt to replicate the conditions experienced by a slate on a roof and to anticipate its life span, various tests have been devised. These tests can be grouped under three headings:

1. *Mechanical tests,* such as the freeze thaw, water absorption, hardness and strength tests.
2. *Chemical tests,* including determination of the concentration of carbonates,

presence of iron ores and graphite.

3. *Dimensional tests,* which limit the degree of irregularity allowed in the slates for use as roofing material.

3. European Standard prEN 12326-2 Draft Feb 1997 (Slate and stone products for discontinuous roofing and cladding)

Part 2 Methods of test

This draft European Standard for slate was prepared by the European Committee for Standardisation (CEN).

Sampling Clause No 4 of prEN 1236-2

Slates are selected randomly from each lot, preferably by the recipient or in the presence of his representative. In the case of dispute, samples are taken from each lot of 50,000 slates.

The following tests are proposed for the new Standard:

i Dimensional Tests Nos 5- 9

ii Mechanical Tests Nos 10-12 &16

iii Chemical Tests Nos 13-15

iv Petrographic examination and interpretation are covered in Annexes A & B.

3.1 Determination of length and width and deviation from specified length and width; Clause No 5 of prEN 1236-2

Samples required: 1 whole slate.

Deviation of the measurements from that specified is calculated as a percentage.

3.2 Determination of straightness of edges; Clause No 6 of prEN 1236-2

Samples required: 1 whole slate.

The deviation from straightness is measured and calculated as a percentage of the length of the edge.

3.3 Determination of rectangularity; Clause No 7 of prEN 1236-2

Samples required: 1 whole slate.

The deviation from squareness is measured and calculated as a percentage of the length.

3.4 Determination of thickness; Clause No 8 of prEN 1236-2

Samples required: 100 whole slates.

The average thickness of a 100 closely packed slates is determined. This figure is then adjusted according to the texture of the surface, e.g. the thickness of a smooth 2-4mm slate is reduced by 10% as compared to a textured slate which is reduced by 20%

3.5 Determination of deviation from flatness; Clause No 9 of prEN 1236-2

Samples required : 1 whole slate.

The curvature of a slate is defined as the height of the highest point of the slate when measured convex side uppermost less the height of the same point when concave side up.

$$\%Curvature = \frac{Curvature}{Length} X100$$

3.6 Determination of bending strength and modulus of rupture; Clause No 10 of prEN 1236-2

Samples required: 30 large or 60 small slates.

The modulus of rupture is a measure of the bending moment needed to rupture a slate and is in effect a measure of the tensile strength of the slate. Because of its anisotropic nature, the strength of a slate depends on the direction of the grain in relation to the direction of testing. Therefore the test is carried out in the cleavage plane both with and across grain. The elasticity of the slate can be measured at the same time, i.e. the amount of flexure as the slate is progressively loaded. Flexure testing is considered a more appropriate measure of the strength of a slate than the more normal compression tests used in the evaluation of other building materials.

The modulus of flexure is calculated as follows:

$$R = \frac{3Pl}{2be^2}$$

where R = modulus of rupture in newtons/mm^2

P = failure load in newtons

l = distance between the support bars of the three point bending test machine

b = width of the test piece in mm

e = mean thickness of the slate in mm

This test is carried out on test pieces 125mm long both parallel and perpendicular to the edge of the slate. The load required to break the slate is determined and the modulus of rupture R is calculated as described above.

The **mean modulus of rupture R_m** is determined for 30 tests in both directions.

The **characteristic modulus of rupture** is defined as

$R_c = R_m - 1.7\,R_{SD}$ where SD = standard deviation

$$R_{SD} = \frac{\sqrt{\Sigma(R_i - R_m)^2}}{(n-1)}$$

3.7 Determination of water absorption; Clause No 11 of prEN 1236-2

Samples required: 5 test pieces dried to a constant weight.

The amount of water absorbed by a slate is a measure of its porosity and would be expected to indicate its vulnerability to chemical attack.

Dried test pieces 100mm x 100mm with smooth edges are immersed in water for 48 hours and the increase in weight is determined.

$$\%Waterabsorption = \frac{m_s - m_0}{m_0} x100$$

3.8 Freeze - thaw test; Clause No 12 of prEN 1236-2

Samples required: 30 large or 60 small slates pre-soaked for 48 hours.

The difference in bending strength is determined between untreated samples and those subjected to 100 cycles of freezing at -20°C and thawing at +23°C. The mean value and the standard deviation of the modulus of rupture of the treated samples is compared to that of the untreated batch using a two-sided Student t-Test at the 95% confidence level. The difference between the two is reported.

3.9 Carbon Content

Carbon may be present in two forms; either as carbonate, assumed to be calcium carbonate, or as non-carbonate carbon assumed to be graphite. Carbon dioxide gas is given off on the addition of acid to a carbonate, while graphite is unaffected. This fact is used to distinguish between the two forms of carbon by carrying out the same tests on two samples, one pre-treated with acid and one untreated. The result for the former gives the graphitic carbon alone while the result from the latter gives the total carbon. The amount of gas is determined by one of several methods.

Determination of non-carbonate carbon content; Clause No 13 of prEN 1236-2

Samples required: 3 slate samples ground to a specified sieve size.

Having removed all the carbonate with HCl, graphitic carbon content may be determined by one of two methods:

i Graphite is converted to CO_2 by catalytic thermal conversion and the amount of gas given off is detected by infra-red detector.

ii Graphite is again converted to CO_2, this time in a stream of oxygen, and the amount of gas is determined coulometrically and compared with a standard.

Determination of carbonate content; Clause No 14 of prEN 1236-2

i The total amount of carbon is determined using the first method above without the pre-treatment with acid and the difference gives the carbonate content

ii The amount of carbonate present may be determined directly by comparing the amount of gas given off on the addition of HCl acid with that from standards such as calcium carbonate and silica.

iii A similar test using phosphoric acid as specified in EN 196-21 is also proposed.

iv CO_2 gas may also be detected by absorption in a solution of NaOH and comparing the conductivity of the resultant solution with standards of known concentration.

Results

The results are reported as percentage weight of carbon or calcium carbonate by the appropriate formula:

$$\%C = \frac{CO_2 x12}{44}$$

$$\%\,CaCO_3 = \frac{\%Cx100.1}{12}$$

3.10 Sulphur Dioxide exposure tests; Clause No 16 of prEN 1236-2

Samples required: 12 test pieces, 6 dry and 6 soaked in distilled water.

3 wet and 3 dry test pieces are placed above the sulphurous acid solution at two different strengths for 21 days. They are then dried and inspected for flaking, colour change, swelling and softening. Slates which have a carbonate content of >20% are tested using an abrasion method.

3.11 Thermal Cycle test; Clause No 16 of prEN 1236-2

Samples required: 6 test pieces.

Test pieces are subjected to 20 cycles of immersion in water at 23°C for 6 hours followed by drying for 17 hours at 110°C. They are then inspected for physical changes indicative of the presence of harmful mineral inclusions.

3.12 European Standard prEN 12326-1 Slate and stone products for discontinuous roofing and cladding: Part 1 Product Specifications Aug 1995

Requirements

Minimum thickness

The absolute minimum thickness of a slate must be 2.0mm.

The minimum acceptable thickness of a slate is a function of its inherent strength and dimensions as well as of climate. The basic nominal thickness is given by the greater of e_L or e_T, where:-

$$e_L = X\sqrt{\frac{L}{R_L}}$$

$$e_T = X\sqrt{\frac{L}{R_T}}$$

e_L, e_T = thickness mm

L = length mm

b = width mm

R_L, R_T = modulus of rupture, either longitudinal or traverse value, newtons/mm^2

X = constant determined as a function of the climate and construction techniques.

This value is adjusted to take into account the carbonate content and the classification of the slate in the $S0_2$ exposure test.

$$e_{CaC03\ >20\%} = e + 0.5mm + 7S^2$$

e = minimum nominal thickness mm

S = thickness of the softened layer mm

Variation of thickness from the nominal must be less than ± 35%.

Traditional building techniques may be specified.

Strength

The minimum breaking load and the characteristic modulus of rupture as specified by the manufacturer.

Water absorption

A1	≤	0.6 %
A2	>	0.6 %

Freeze thaw resistance

No reduction in strength

Thermal Cycle Test

T1	No change in appearance	Acceptable
T2	Oxidation but no structural change	Acceptable
T3	Oxidation of metallic minerals which penetrate the slate	Conditional
T4	Exfoliation, splitting and structural changes	Not acceptable

Carbonate Content

No higher than specified by the manufacturer.

Sulphur Dioxide test

Three grades:

S1 The best, unaffected by the concentrated acid	Acceptable
S2 Unaffected by the weaker acid	Conditional
S3 Affected by the weaker acid	Undecided

Carbon Content

Carbon content < 2.00%

Dimensions

Length and Width	± 5 mm of specification
Squareness	± 1% of length
Curvature	Smooth slates <1.0%
	Normal slates <1.5%
	Textured slates<2.0%

3.13 Conclusions

In the European Standard for slate:

Tests of **mechanical properties**, e.g. water absorption, freeze-thaw and the thermal cycle test, attempt to reproduce the temperature changes and humidity conditions suffered by a roofing slate. No information is given on how results correlate with known life expectancies of slates.

Chemical tests for deleterious minerals are the carbonate test, and exposure to sulphur dioxide to detect the presence of iron ore minerals. While the presence of carbonates and iron ore minerals certainly contributes to the weathering of slate, more information is needed on how the limits set in the draft Standard are derived.

The **dimensional requirements** are dictated by roofing regulations and practice in different countries. The assessment of how the compliance requirements affect Scottish slate is best done by the Dundee Town Planning Group and is outside the scope of this brief.

4. British Standard BS 680 Part 2 1971 Specification for Roofing Slates Part 2 Metric units

4.1 Thickness

Measured as the average thickness of 100 slates closely packed.

One slate should not deviate by >25%.

Slates that do not conform are deemed ungraded.

4.2 Marketing Description

A full description of the slate, including the source vein, quarry, thickness and whether graded or ungraded, should be given.

Test Samples required: 3 per test, 50mm x 50mm with edges ground to a smooth finish.

4.3 Water Absorption Test

Dried to a constant weight before being refluxed in boiling water for 48hrs and weighed. Results reported as a percentage increase in weight.

4.4 Wetting and Drying Test

Samples required: 3 prepared as described.

Immersed in distilled water at room temperature for 6 hours and dried for 17 hours at 105°C. Cycle repeated 15 times or until signs of splitting, flaking or delamination appear.

4.5 Sulphuric acid immersion test

Samples are soaked at room temperature in sulphuric acid diluted at 1: 7.

4.6 Compliance

Water Absorption Test	≤ 0.3%
Wetting and Drying Test	No visual signs of deterioration
Sulphuric Acid Immersion Test	No signs of delamination, swelling, softening or flaking and no gaseous evolution.

4.7 Comment

The principle advantage of the British Standard is its simplicity, in sharp contrast to the proposed European Standard. The British Standard is based on the research done by BRE in 1934 at the time of the first edition of the Standard. **For an unbiased view it would be necessary to see the background research done in the preparation of the other national standards.**

Strength

The British Standard has no compliance requirement as it was decided that there is no correlation between durability and strength. According to trade literature the slate produced in Britain would actually comply with other countries' requirements. However the lack of this requirement may well be one of the reasons that imported slate liable to fail has entered the British Market.

The roofing practice in Britain of nailing slates as opposed to fixing with hooks which is more common in other European countries makes the slate more likely to fail either by tension of uplift.

5. French Standard
Norme française NF P 32-301 Avril 1988
Norme française NF P 32-302 Avril 1989

A selection of slates chosen at random from each batch of 50,000 is subjected to various tests for their appearance and physical and chemical characteristics. Tests are carried out on whole slate specimens. The slates are classified into three categories A, B and C depending on how the average value obtained in the test results corresponds to the a minimum value as prescribed in NF P 32-301 **and** NF P 32-302. See Table 1.

5.1 Sampling and Testing

Sampling: 50 slates are selected from each batch of 50,000, i.e. 0.1%.

Appearance: The 50 hand specimens are examined for imperfections
Few irregularities are allowed in class A, however there is increasing tolerance of their presence in classes B and C.

Physical Characteristics: 14 specimens are examined for

i Density

ii Water Absorption

iii Effect of Freezing, measured as weight loss after 25 cycles of freezing at -25°C for 1 hour followed by thawing.

iv Strength of the slate or Modulus of flexure
7 wet and 7 dry slate tested according to NF P 18-411

Chemical Characteristics: 7 samples are tested for:

Oxidisable pyrites

Calcium carbonate

5.2 Compliance Requirements

Test	units	Class A	Class B	Class C
Density	gm/cm^3	≥ 2.75	≥ 2.70	≥ 2.65
Water Absorption	%	≤ 0.4	≤ 0.7	≤ 0.9
Loss of mass after freezing	%	≤ 0.3	≤ 0.6	≤ 1.0
Modulus of Flexure dry	MPa	≥ 70	≥ 50	≥ 33
wet		≥ 40	≥ 33	≥ 24
Minimum reference thickness	mm	2.6	3	4
Oxidisable Pyrites				
Non-penetrating and no leaching		yes	yes	yes
Non-penetrating with leaching		no	yes	yes
Penetrating pyrites		no	partial exclusion	
Micropyrites with leaching		no	no	yes
Calcium Carbonate with oxidisable pyrites	%	≤ 1.5	≤ 5.0*	≤ 10.0*
Calcium Carbonate with no oxidisable pyrites	%	≤ 3	≤ 5*	≤10*

Table B.1 NF P 32 301 Compliance Requirements for the different categories of slate

*Higher concentrations of calcium carbonate are allowed when the reference thickness is increased.

6. Germany DIN 52 201: Test methods

This is the general test standard for slate in which all relevant standards for roof slates are mentioned when not covered by the standard itself.

6.1 DIN 52 101 Testing of natural stone and mineral aggregates: Sampling 1988

Procedures to carry out sampling so that the resultant population is representative and adequate to characterise the rock and its variance.

6.2 Petrographical examinations

a Hand specimen

The samples are examined for structures such as fissures, stratification, cleavage and accessory minerals such as pyrites and marcasite.

b Microscopic

Thin sections are prepared and examined for mineral content, grain size and shape, and approximate composition as well as their relationship to the overall fabric of the rock.

Micaceous Minerals	The dispersal and how they are they linked
Chlorites	Clastic or porphyroblastic
Carbonates	Dispersed or concentrated in veins
Pyrites	Difficult to distinguish from other opaque minerals of carboniferous material

6.3. Chemical Investigation

Quantitative determination of:

i Loss on glow (equivalent to loss on ignition)

ii Carbon dioxide

iii Sulphur in the form of sulphides and sulphates

6.4 Determination of the Specific Gravity DIN 52 102 1988

Procedure for determining density, gross density, net density, degree of density, and porosity of the rock

6.5 Determination of Water Absorption DIN 52 103 1972

Procedure to determine the percentage increase in weight on absorption of water.

6.6 Frost Thaw Alternation Test DIN 52 104 Part 1, 1982

Samples which have been soaked in water are cooled to -20°C for 4 hours and then stored in a water bath at 20°C.

After the required number of cycles the specimen is dried and weighed.

The specimens are examined visually.

6.7 Flexural strength test DIN 52 112

Samples: 200mm X 100mm with span of 180mm

Load is increased at $0.2N/mm^2/s$

Calculation of results in the usual manner

6.8 Temperature Alternating Test DIN 52 204 1982

25 cycles of the sample being heated to 105°C followed by quenching in a water bath at 20°C for 15 min.

The samples are examined visually and determination of the change in flexure strength is optional.

6.9 Acid Test DIN 52 206 1975

Samples consisting of 5 air dried and 5 water saturated specimens are stored for 28 days in sulphurous acid vapour. After 14 and then 28 days the relative change in weight and condition is noted (weight is usually increased).

6.10 Compliance

Not available

7. Italy UNI 8626 1984

Pardotti per coperture discontinue; Charatteristiche, piani di campionamento e limiti do accettazione

(Products for discontinuous roofing - Characteristics, sampling plans and acceptance limits)

7.1 Sampling

5 per lot of 1200 randomly chosen

7.2 Method of testing UNI 8635

Impermeability Test

Slate sample forms the bottom of a watertight box containing water to a depth of 5mm. No drops of water should appear on the underside after 24 hrs.

Thermal cycle

The sample is subjected to 25 cycles of the following:

48 hrs at 15°C in a water bath, after which the sample is left for 2 hours to reach room temperature. It is then subjected to -15°C for 1 hour. On completion of the 25 cycles the sample is tested for appearance, impermeability and resistance to flexure.

Modulus of Rupture

A sample on supports 200mm apart is subjected to a load at the mid point increasing at 10 ± 2N/s. The force required to break the slate is noted and the modulus of flexure is calculated in the usual way:

$$R_f = \frac{3Pl}{2bs^2}$$

7.3 Compliance

The following tests, with corresponding limits of acceptability, are applicable to slate:

Appearance and geometry	Method of testing	Limit of acceptability
Appearance	UNI 8635.1	nodules <2mm
Length	UNI 8635. 2	as agreed
Width	UNI 8635.3	"
Thickness	UNI 8635.4	"
Planarity	UNI 8635.5	±1.5% of length
Density	UNI 8635.8	± 10% specifications

7.4 Characteristics in response to atmospheric and mechanical action

Impermeability	UNI 8635.10	No drops of water after 24hrs
Thermal cycle	UNI 8635.11	Strength reduced <20%
Modulus of flexure	UNI 8635.13	See Table 7.2

Nominal Thickness mm	Minimum pressure N/cm^2
2.7	8
3.0	10
3.3	12
3.6	14
4.0	16
4.4	19
4.8	22

Table B.2 Limits of acceptance of resistance to flexure for slate

8. Spain UNE 220201-85

Norma Española Pizarra ornamentales; Pizarras para cubiertal

The following requirements must be met:

8.1 Origin and Composition

Source: The quarry and vein from which the slate originated must be specified.

Composition: Carbon or clay <1%, carbonate <10%.

8.2 Dimensions and Curvature

Dimensions: No slate must vary by >50% of the nominal thickness.

Curvature: <1.5%

8.3 Colour and surface features

1. The colour should be uniform with only natural changes in tone.
2. Knots should not protrude greater than half the thickness of the slate.
3. No joint or line should penetrate more than half the thickness of the slate.
4 No imperfection which would damage the solidity of the slate.
5 No broken corners or flaking defects.

8.4 Inclusions

1. Metallic minerals, whether aggregates or bands, should not penetrate the slate.
2. The composition of the mineral inclusion should be determined.

8.5 Physical characteristics and alterations

1. Weight should not vary by >10% from the nominal weight.
2. Specific gravity >2.6 gm/cm^3. Method of test specified in UNE 22-191.
3. Water absorption <3%. Method of test specified in UNE 22-191.
4. The dry slate without alteration must have a modulus of flexure >290Kg/cm^2. Method of test specified in UNE 22-195.

5. The wet slate must show no visible signs of alteration and the modulus of flexure must not be less than 80% of that determined in 4.
6. After the freezing test as specified in UNE 22-193 there should be no visible signs of alteration and the loss of weight must not be >3%.
7. The reduction of the modulus of flexure after the freeze test must not be greater than 20% of that determined in 4.
8. Slates with > 5% carbonate must be thicker that 5mm.

8.6 Classification of slates

Quarries are classified. Samples are taken from intact rock; a minimum of 5 samples per stratum but depending on the complexity.

Characteristics and properties of the slate are determined based on a sample of 100 slates from each batch of 10,000.

Colour is specified e.g. black, grey and special colour.

Texture is described as smooth, undulating or rough.

Vulnerability to alteration is qualified as follows:

PAC Pizarras poco alterables No mineral inclusion such as pyrite, pyrrhotite or marcasite, and carbonates <1%. No appreciable alteration after the heat and acid test.

PAI Pizarras de mediana alterabilidad Must not contain excessive inclusions vulnerable to polluted atmosphere. Little alteration after the heating (UNE 22-197) and acid (UNE 22-198) tests, but some discoloration and spotting is allowed. Carbonates <5%.

PAS Pizarras muy atlerables Samples which contain many minerals unstable in polluted atmosphere or carbonate >5%.

8.7 Methods of testing

These are specified in the following standards:

UNE22-190	Ornamental Slates, Plaques and Slabs	General
UNE 22-191	"	Absorption and Specific gravity
UNE 22-193	"	Resistance to freezing
UNE 22-195	"	Resistance to flexure
UNE 22-197	"	Resistance to temperature change
UNE 22-198	"	Resistance to oxidation
UNE 22-199	"	Carbonate content
UNE 22-200	"	Curvature of the surface

9 United States of America Standards

C406 - 58 (re-approved 1970) Standard Specification for Roofing Slate
C119-74 Standard Definitions of Terms Relating to Natural Stones

The following standards relating to slate are under the jurisdiction of American Society for Testing and Materials (ASTM) Committee C-18 on Natural Building Stones

9.1 Classification of slates

Slates are classified into three grades with the following life expectancy

S_1	75-100 years
S_2	40- 75
S_3	20- 40

9.2 Compliance

Slate should conform to the following physical requirements:-

	Modulus of Rupture across the grain psi (MPa)	**Absorption of Water %**	**Depth of Softening (mm)**
Grade S_1	>9000 (62)	<0.25	<0.002 (0.05)
Grade S_2	>9000 (62)	<0.36	<0.008 (0.20)
Grade S_3	>9000 (62)	<0.45	<0.014 (0.36)

9.3 Methods of testing of mechanical properties

Modulus of Rupture: Testing methods are specified in **C120-52** (re-approved 1970) Standard Methods of Flexure Testing of Slate (Modulus of Rupture, Modulus of Elasticity)

Water Absorption of Slate: Testing methods are laid out in **C121 -48** (re-approved 1970) Standard Test Method for Water Absorption of Slate.

Depth of Softening This is a measure of the durability of a slate. Slate which contains pyrites, calcite and carbon can undergo chemical weathering e.g.

pyrite + calcite ------> gypsum

This reaction can cause swelling and lead to disintegration of the slate. The susceptibility of slate to weathering is estimated by standard abrasive techniques as described in **C217-58** (re-approved 1970) Standard Test Method for Weather Resistance of Natural Slate.

9.4 Specifications of appearance and dimensions

Sizes and Thicknesses

Sizes and allowable deviation from the oblong are laid out.

Thickness of 3/16 in (4.8mm) is treated as standard.

Texture: Smooth and rough are described.

Colour: Nine colours are specified.

Nail Holes: Method and position are specified

Imperfections

Curvature: <1/8" in 12" (0.1 mm in 10mm)

Knots and Knurls: Protuberances on the lower surface must not project more than 1/16" (1.5mm)

Ribbons: Grades S_1 and S_2 should be free from ribbons of carbonaceous material while S_3 should be free from ribbons near the nail holes.

Bibliography

Watkins C M 1934 The Durability of Slates for Roofing, Building Research Bulletin No 12 *Publishers* HMSO for Department of Scientific and Industrial Research

Appendix C

Selection of XRD Scans

Sample numbers are shown on the top left corner of each scan. For further information on sources etc. see Appendix 1.1.

Whole Rock Analyses
(Machine conditions: from 4° to 60° at 2° 2θ/min)

Slate Area	Quarry	Sample Ref.	Page
Ballachulish	East Laroch	EL-6	309
	"	EL-10	"
	West Laroch	WL-5	"
	Khartoum	K-1	310
	"	K-2	"
	"	K-3	"
Easdale	Easdale Island	EE-2	311
	Balvicar	SB-1	"
	Breine Phort	SB-5	"
	Toberonochy	LT-1	312
	Rubha na hEasgainnne	LP-3	"
	Port Mary	LP-5	"
	"	LP-6	313
	Cullipool	LC-1	"
	Tir na Oig	LT-5	"
	Black Mill Bay	LB-1	314
	Belnahua	BB-1	"
	"	BB-2	"
Highland Border	Arran	A1	315
	Bute	B-3	"
	"	B-5	"
	Luss	Ls-1	316
	Aberfoyle	Ab-6	"
	Comrie	Au-1	"
	"	Dr-1	317
	Craiglea	Cr-1	"
	"	Cr-2	"
	Dunkeld	DB-1	318
	"	DN-1	"
	"	DN-3	"
Macduff	Kirkney	MK-4	319
	Corskie	MH-2	"
	"	MH-1	"
	"	MC-1	320
	Foudland	MF-1	"
	"	MF-11	"
	Wishach	MW-1	321
	Tillymorgan	MT-1	"
	Skirts of Foudland	MX-2	"

Quantification (Machine Conditions from 4° to 30° at 2° 2θ/min)			
Slate Area	**Quarry**	**Sample Ref.**	**Page**
Ballachulish	East Laroch	EL-6	322
	"	EL-10	"
	West Laroch	WL-5	"
	Khartoum	K-1	323
	"	K-2	"
	"	K-3	"
Easdale	Toberonochy	LT-1	324
	Rubha na hEasgainnne	LP-3	"
	Port Mary	LP-5	"
	"	LP-6	325
	Cullipool	LC-1	"
	Tir na Oig	LT-5	"
	Black Mill Bay	LB-1	326
	Belnahua	BB-1	"
	"	BB-2	"
Highland Border	Arran	A1	327
	Bute	B-3	"
	"	B-5	"
	Dunkeld	DB-1	328
	"	DN-1	"
	"	DN-2	"
Macduff	Kirkney	MK-4	329
	Corskie	MH-2	"
	"	MH-1	"
	"	MC-1	330
	Foudland	MF-1	"
	"	MF-5	"
	Wishach	MW-1	331
	Tillymorgan	MT-1	"
	Skirts of Foudland	MX-2	"

Glycolation and Heating
(Machine Conditions from 4° to 25° at 1° 2θ/min)

Quarry	Sample Ref.	Treatment	Page
Aberfoyle	Ab-5	Normal	332
		Heated for 1 hour at 300° C	"
		Exposed to glycol for 24 hours	"
Bute	B2	Normal	333
		Heated for 1 hour at 300° C	"
		Exposed to glycol for 24 hours	"
Twill Coed	TC-1	Normal	334
		Heated for 1 hour at 300° C	"
		Exposed to glycol for 24 hours	"

Weathering Experiments
(Machine Conditions from 4° to 25° at 1° 2θ/min)

Source	Sample Ref.		Page
Spanish	S1	Unweathered	335
		Weathered artificially	"
		Weathered artificially	"
Welsh	W/F-8	Unweathered	336
		Weathered artificially	"

Full Width at Half Magnitude
(Machine Conditions from 9.5° to 11.5° at 1° 2θ/min)

Quarry	Sample Ref.	Grain Size	Page
East Laroch	EL-4	<2 micron	337
		<6 micron	"
		<10 micron	"
Cullipool	LC-2	<2 micron	338
		<6 micron	"
		<10 micron	"
Ffestiniog	W/F-1	<2 micron	339
		<6 micron	"
		<10 micron	"

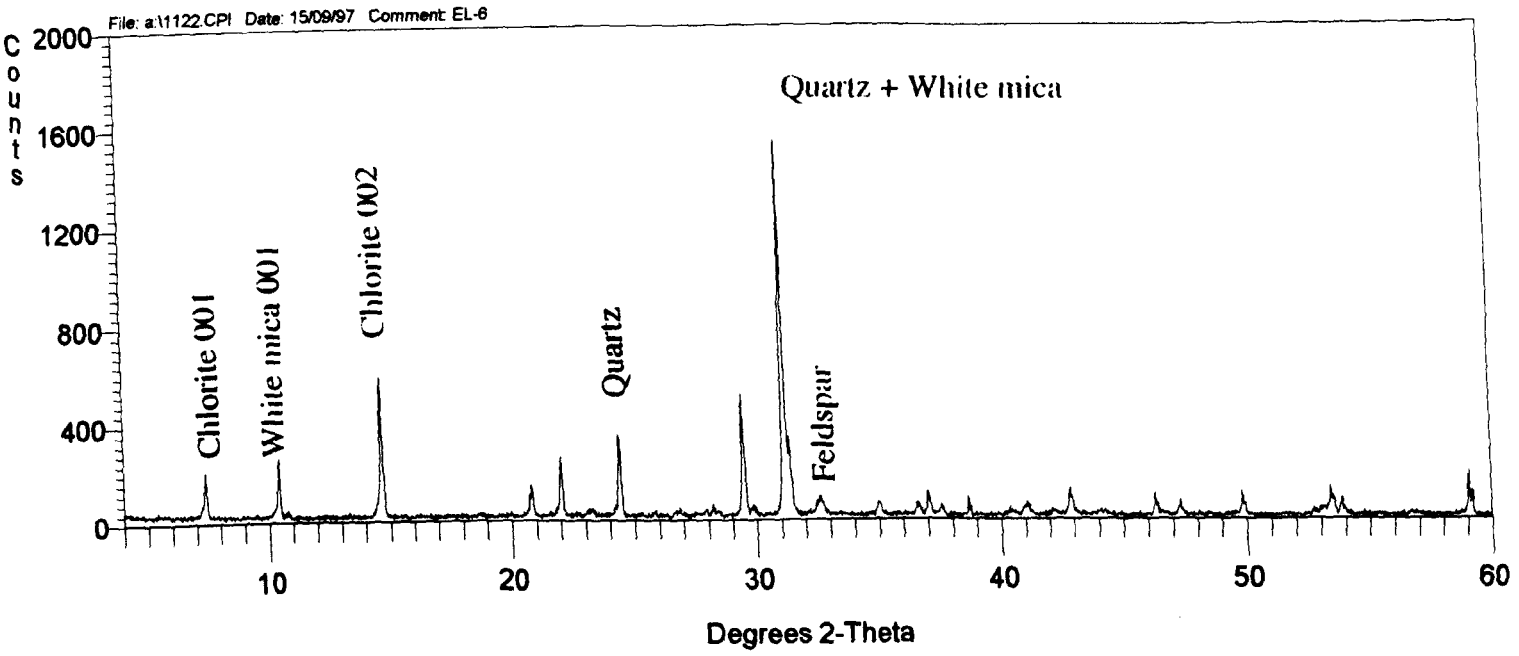
File: a:\1122.CPI Date: 15/09/97 Comment: EL-6
Counts
2000
1600
1200
800
400
0
Quartz + White mica
Chlorite (0 0 1)
White mica (0 0 1)
Chlorite (0 0 2)
Quartz
Feldspar
10
20
30
40
50
60
Degrees 2-Theta

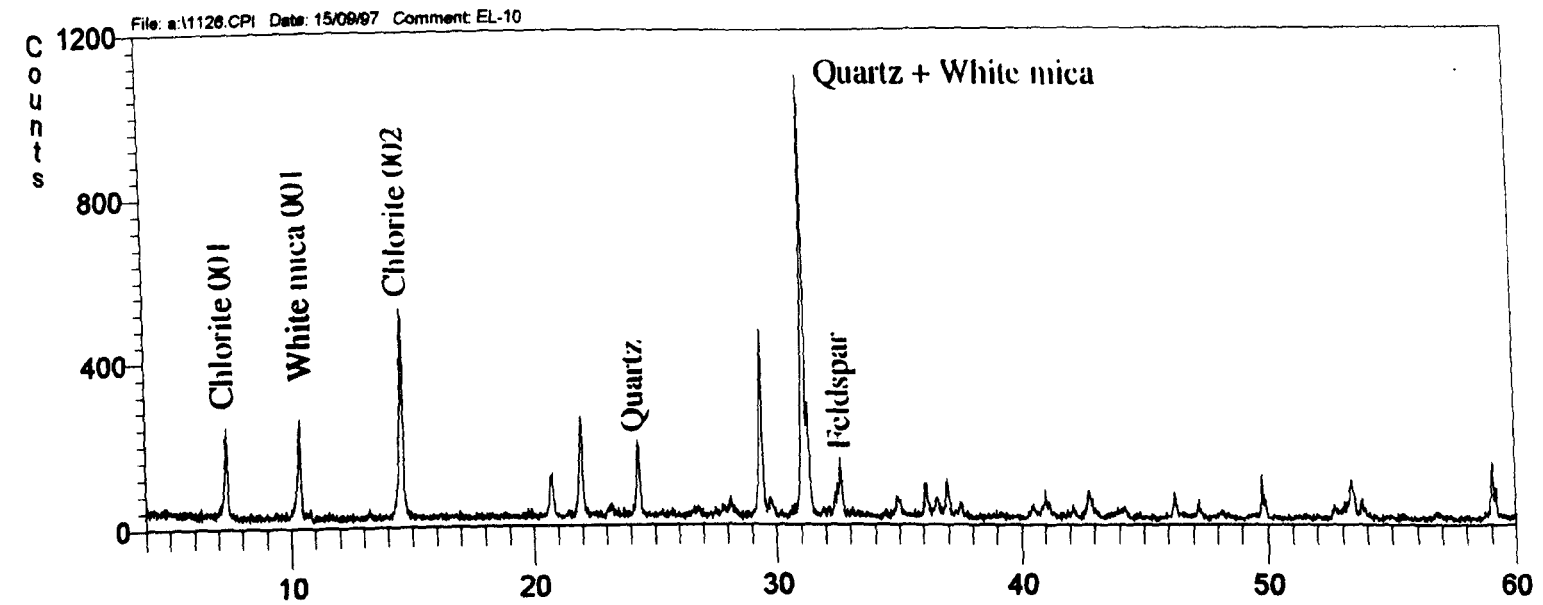
File: a:\1126.CPI Date: 15/09/97 Comment: EL-10
Counts
1200
800
400
0
Quartz + White mica
Chlorite (0 0 1)
White mica (0 0 1)
Chlorite (0 0 2)
Quartz
Feldspar
10
20
30
40
50
60

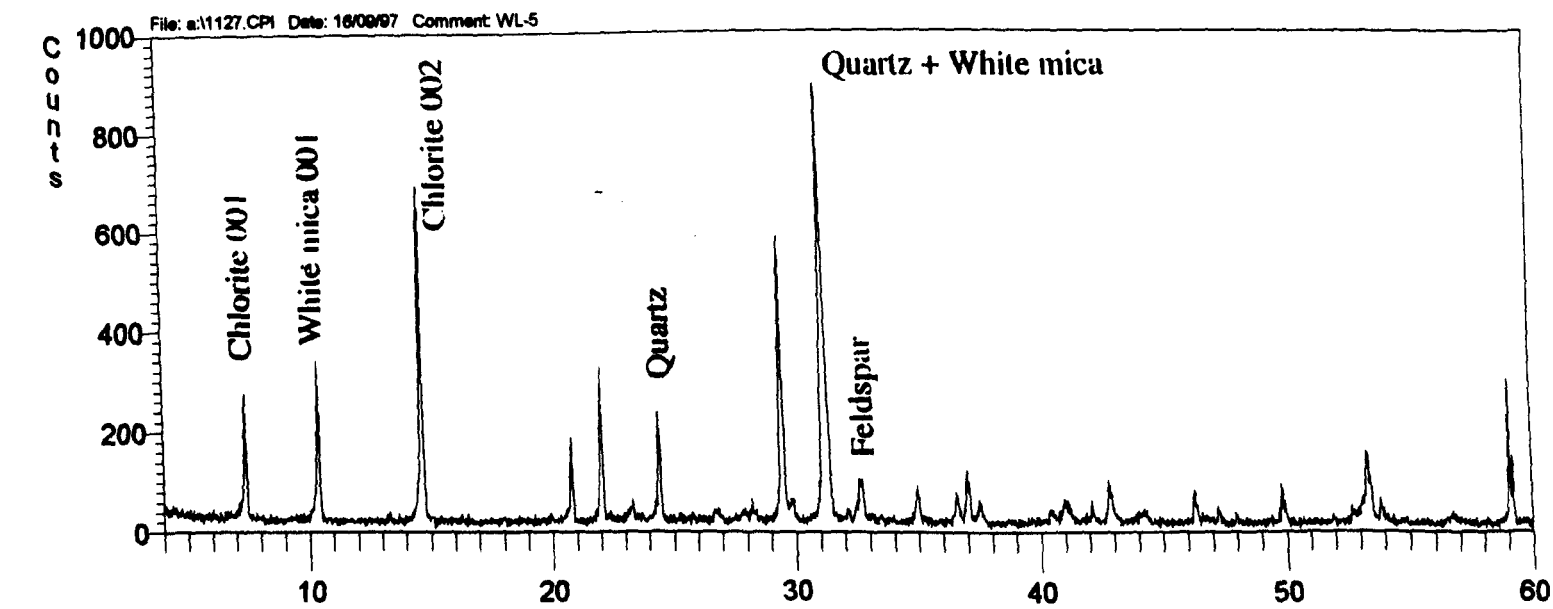
File: a:\1127.CPI Date: 16/09/97 Comment: WL-5
Counts
1000
800
600
400
200
0
Quartz + White mica
Chlorite (0 0 1)
White mica (0 0 1)
Chlorite (0 0 2)
Quartz
Feldspar
10
20
30
40
50
60

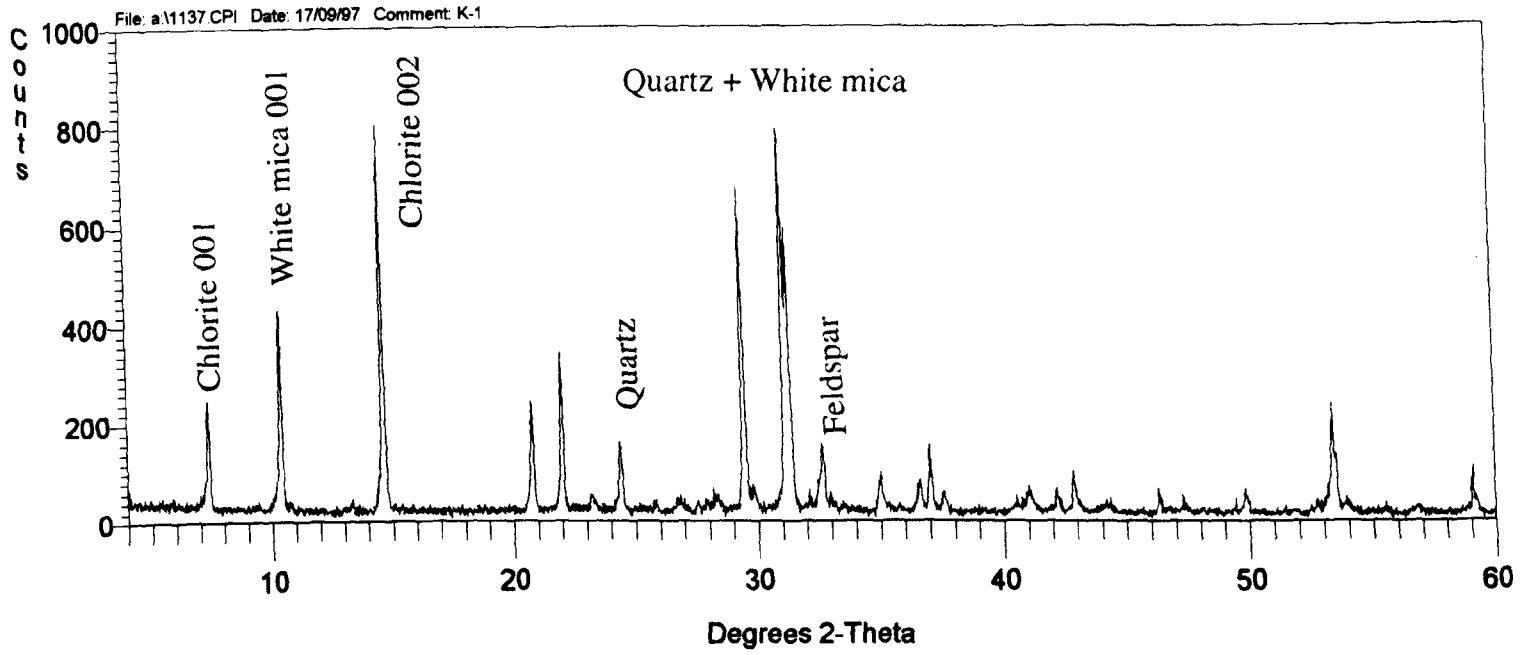
File: a:\1137.CPI Date: 17/09/97 Comment: K-1
Counts
1000
800
600
400
200
0
Quartz + White mica
Chlorite 001
White mica 001
Chlorite 002
Quartz
Feldspar
10
20
30
40
50
60
Degrees 2-Theta

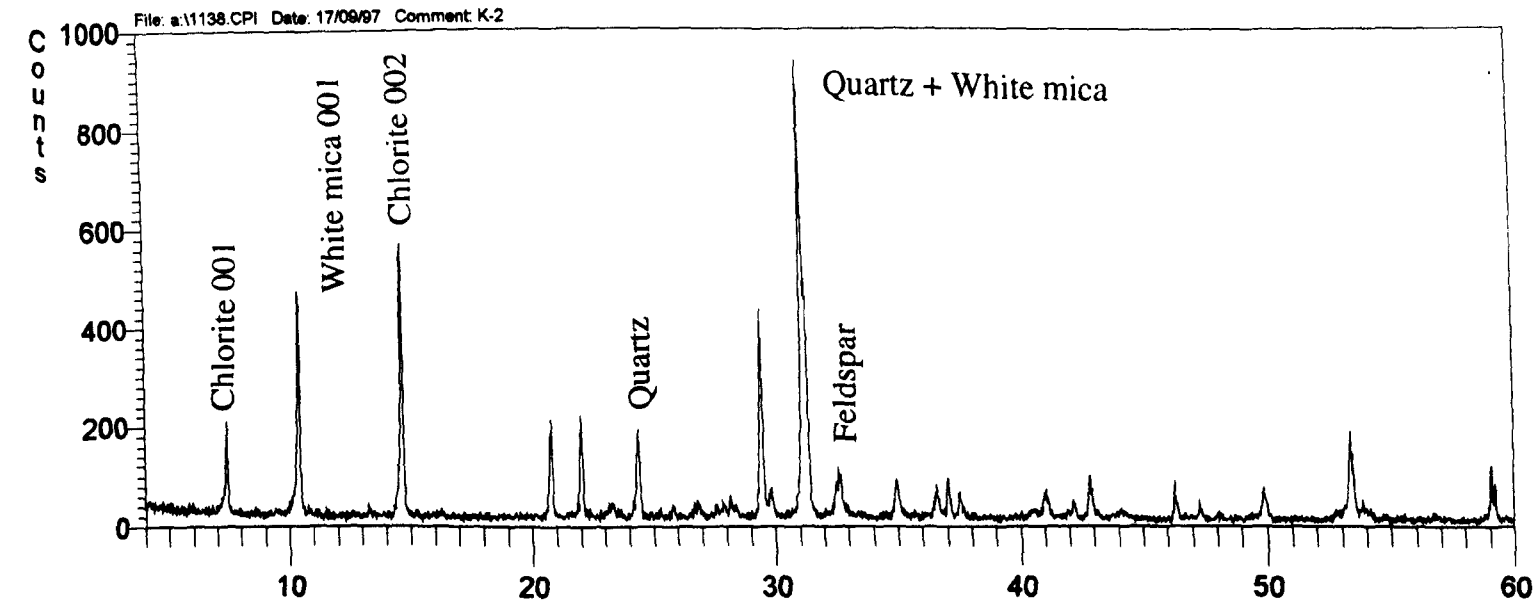
File: a:\1138.CPI Date: 17/09/97 Comment: K-2
Counts
1000
800
600
400
200
0
Quartz + White mica
Chlorite 001
White mica 001
Chlorite 002
Quartz
Feldspar
10
20
30
40
50
60

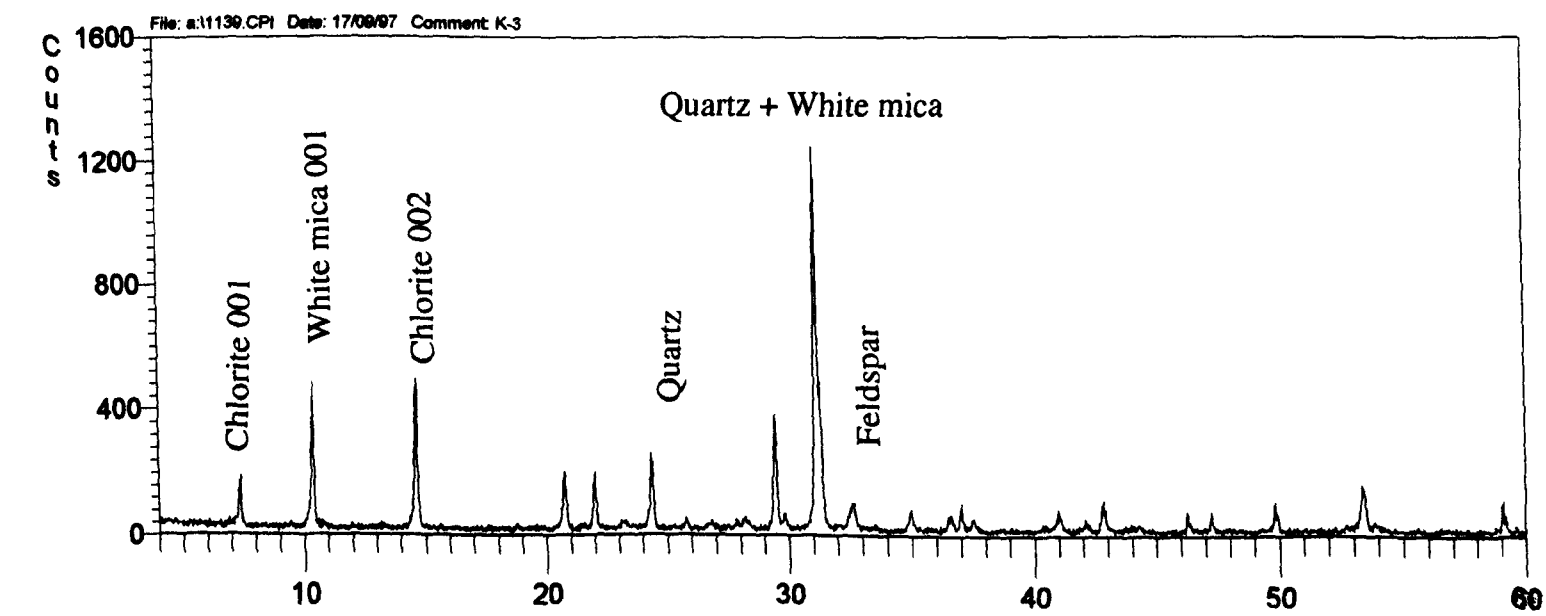
File: a:\1139.CPI Date: 17/09/97 Comment: K-3
Counts
1600
1200
800
400
0
Quartz + White mica
Chlorite 001
White mica 001
Chlorite 002
Quartz
Feldspar
10
20
30
40
50
60

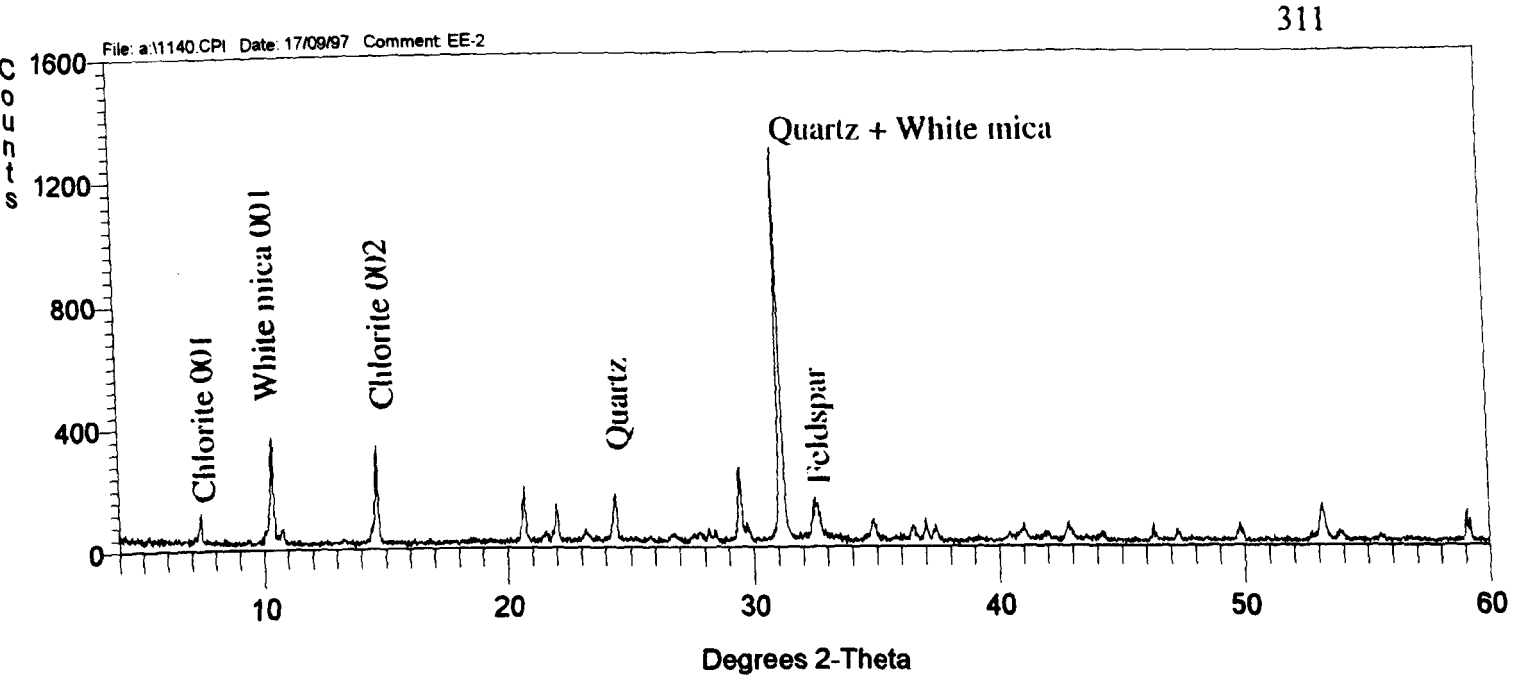
File: a:\1140.CPI Date: 17/09/97 Comment: EE-2
Counts
1600
1200
800
400
0
Chlorite 001
White mica 001
Chlorite 002
Quartz
Quartz + White mica
Feldspar
10
20
30
40
50
60
Degrees 2-Theta

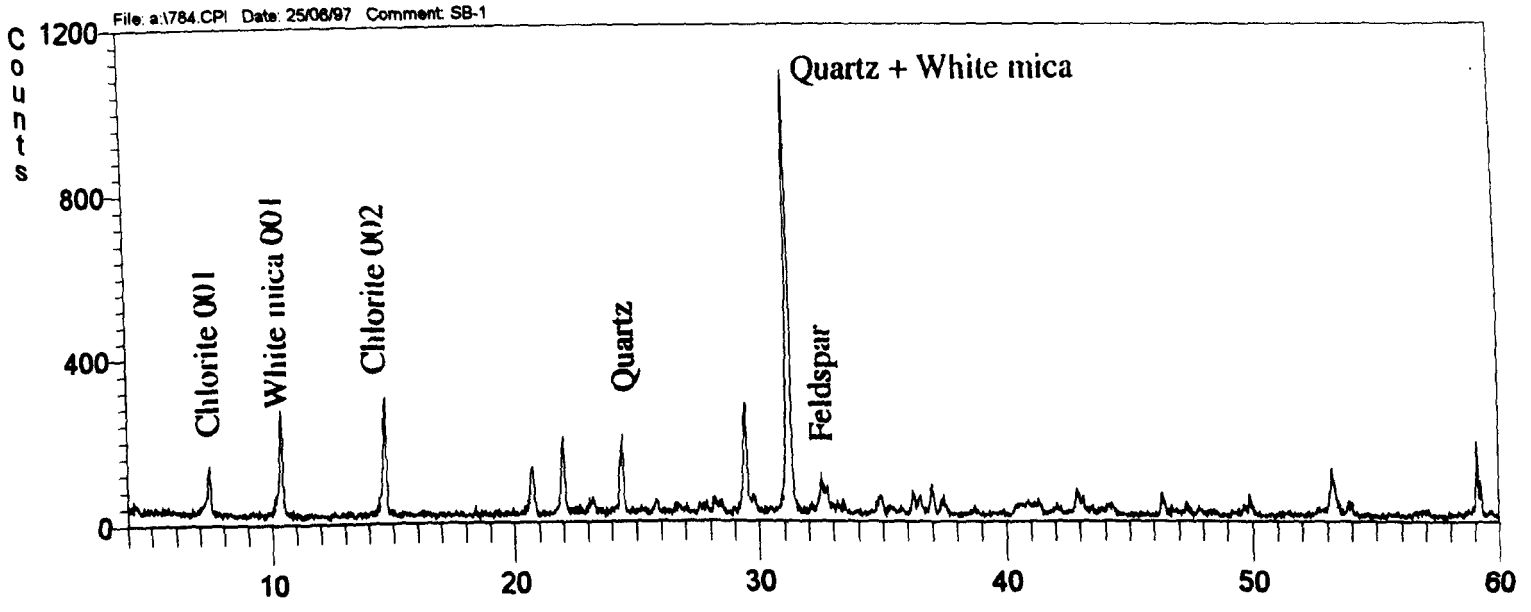
File: a:\784.CPI Date: 25/06/97 Comment: SB-1
Counts
1200
800
400
0
Chlorite 001
White mica 001
Chlorite 002
Quartz
Quartz + White mica
Feldspar
10
20
30
40
50
60

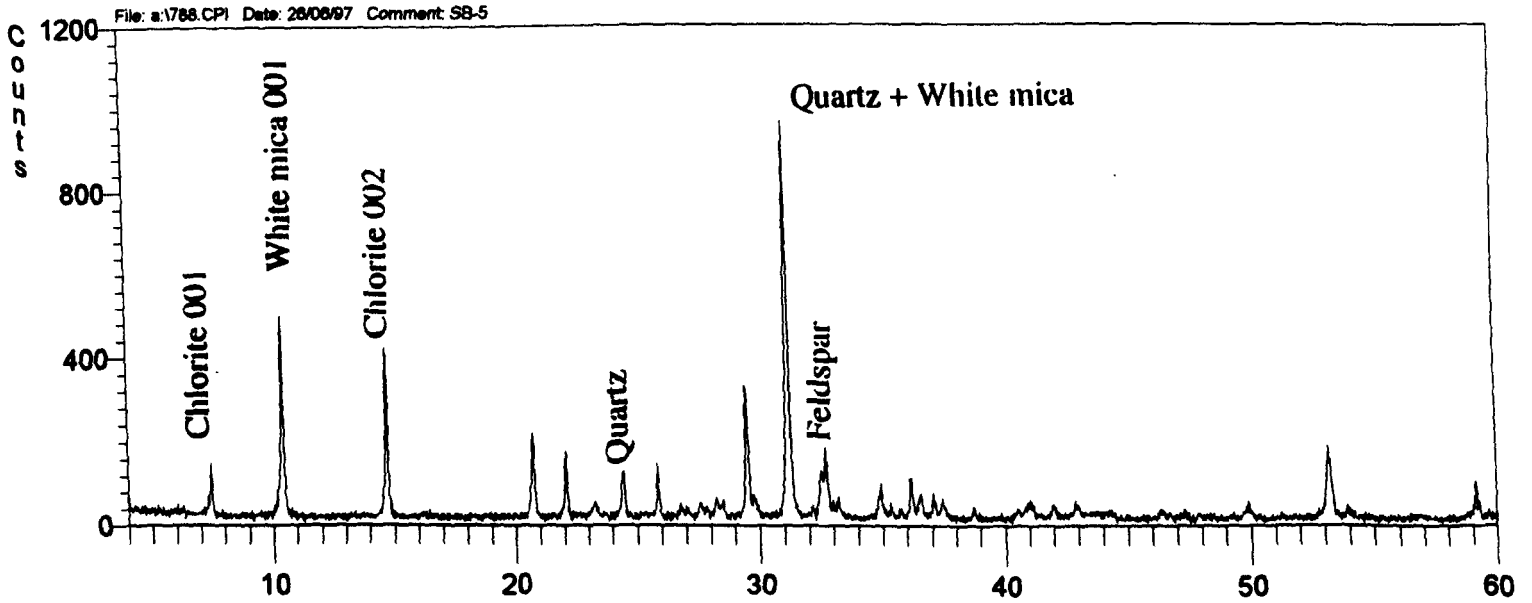
File: a:\788.CPI Date: 26/06/97 Comment: SB-5
Counts
1200
800
400
0
Chlorite 001
White mica 001
Chlorite 002
Quartz
Quartz + White mica
Feldspar
10
20
30
40
50
60

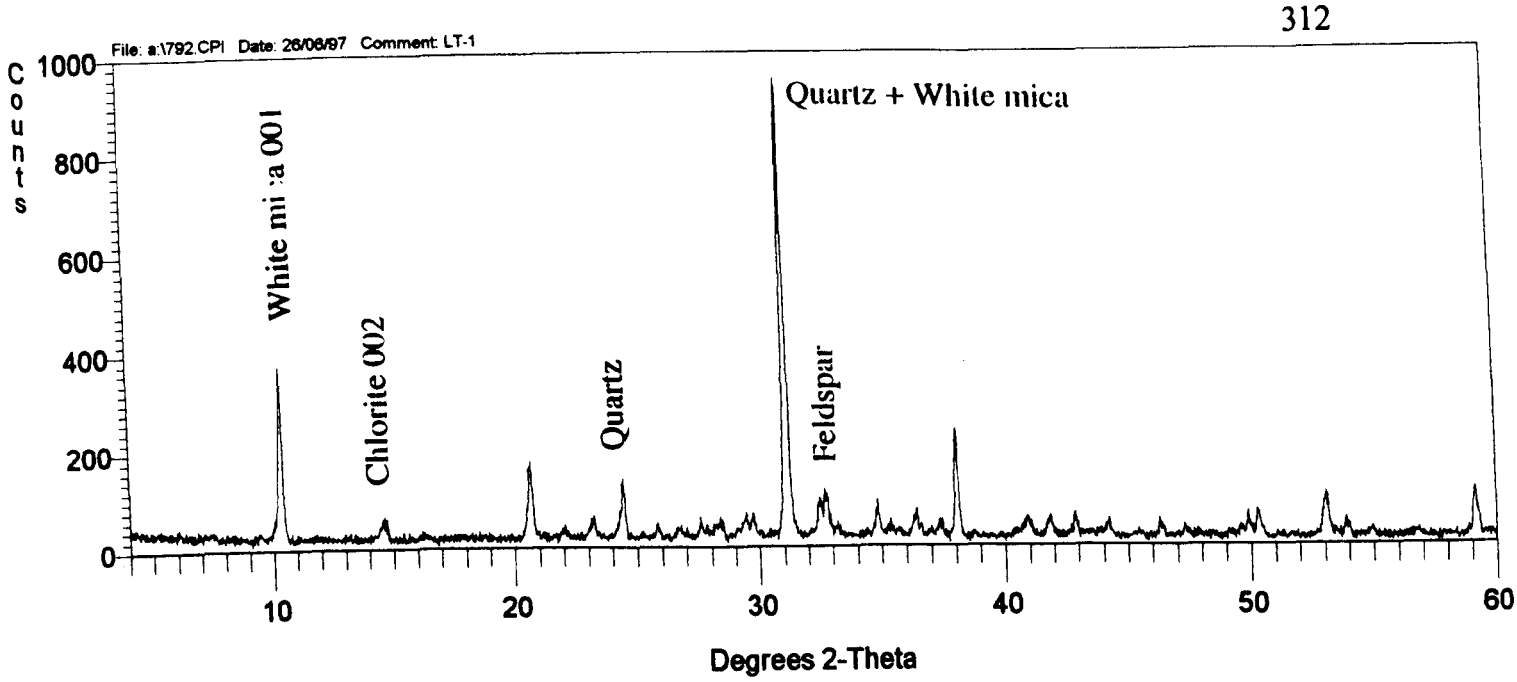
File: a:\792.CPI Date: 26/06/97 Comment: LT-1
Counts
1000
800
600
400
200
0
White mi :a 001
Chlorite 002
Quartz
Quartz + White mica
Feldspar
10
20
30
40
50
60
Degrees 2-Theta

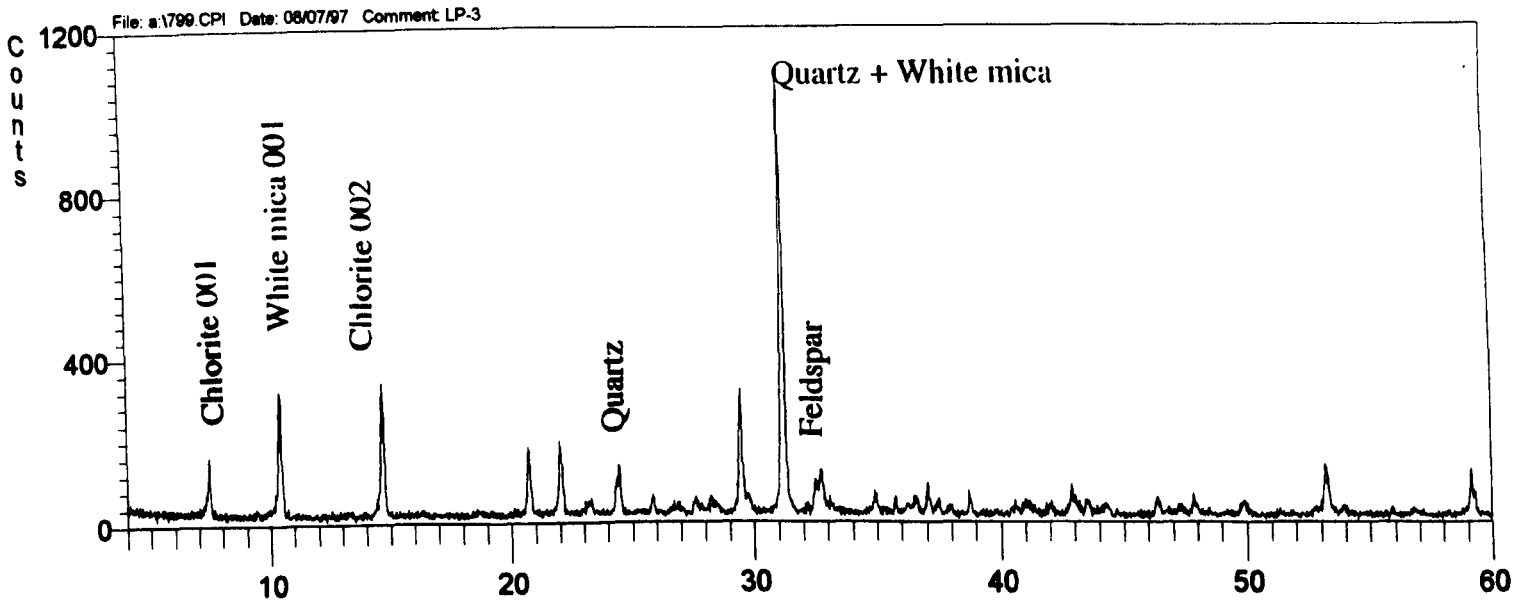
File: a:\799.CPI Date: 08/07/97 Comment: LP-3
Counts
1200
800
400
0
Chlorite 001
White mica 001
Chlorite 002
Quartz
Quartz + White mica
Feldspar
10
20
30
40
50
60

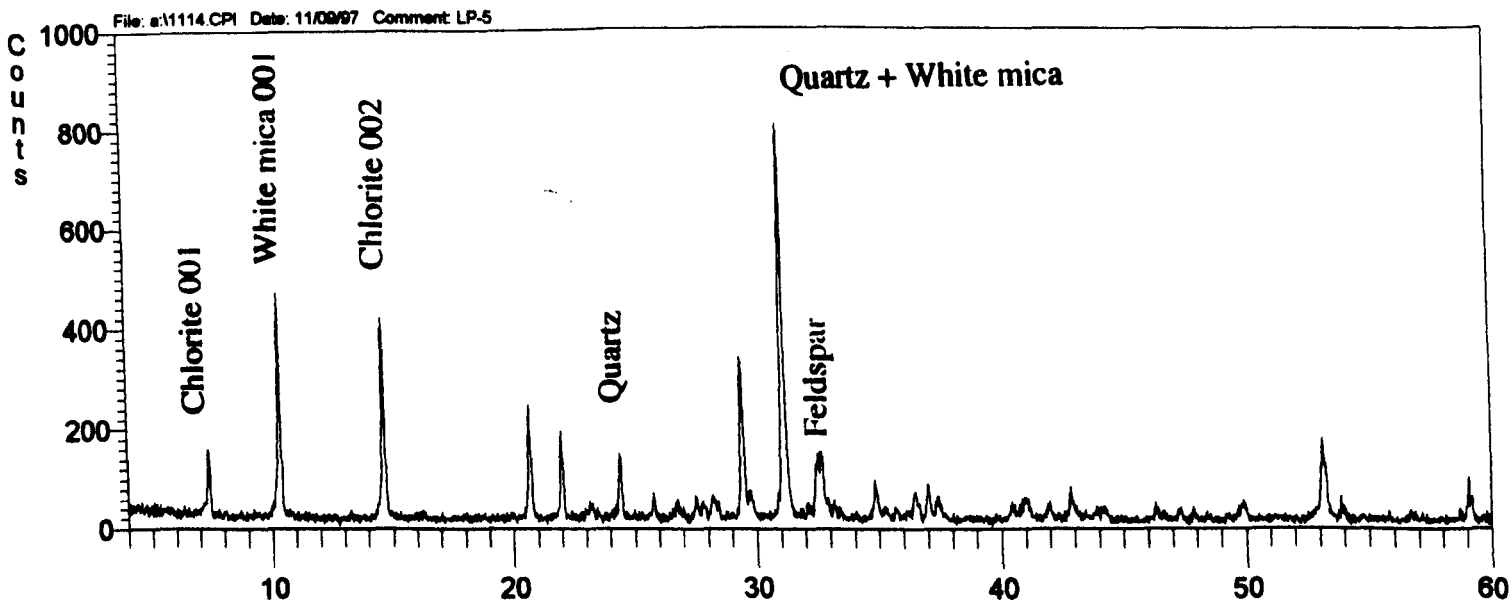
File: a:\1114.CPI Date: 11/09/97 Comment: LP-5
Counts
1000
800
600
400
200
0
Chlorite 001
White mica 001
Chlorite 002
Quartz
Quartz + White mica
Feldspar
10
20
30
40
50
60

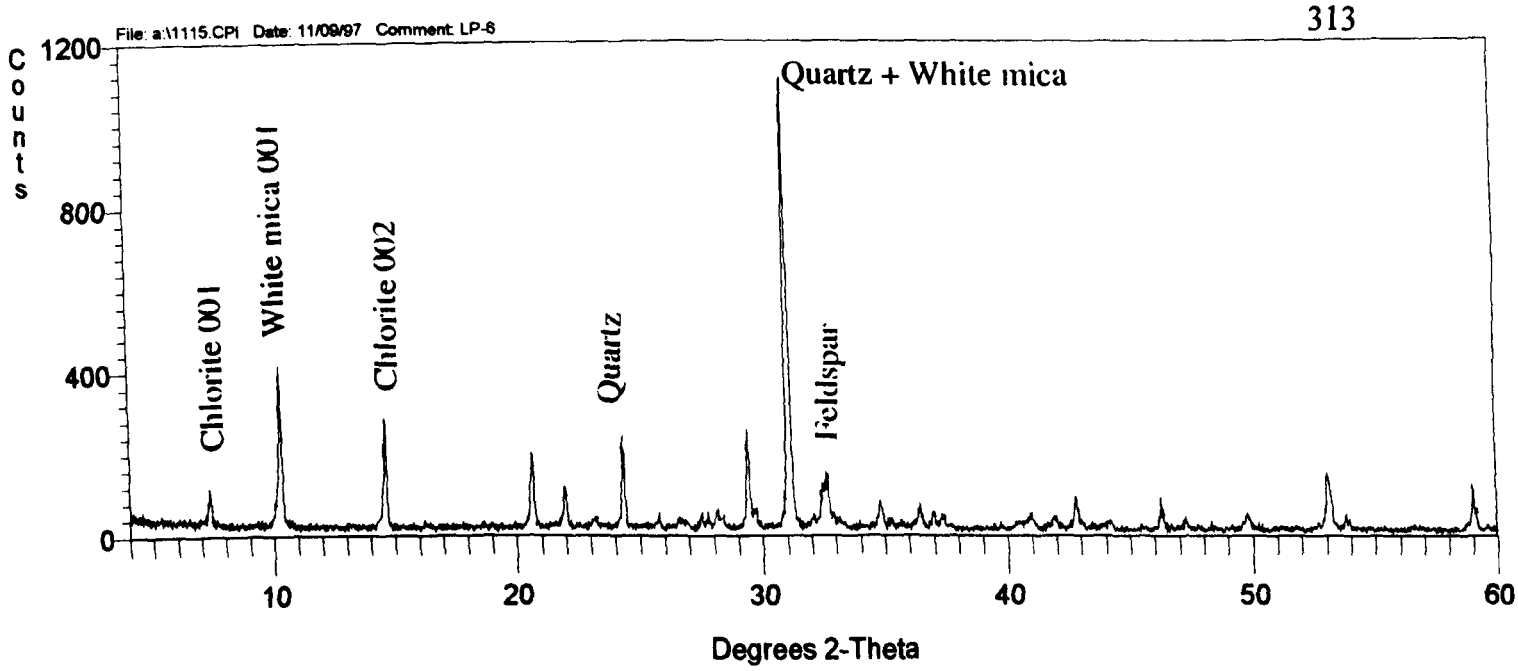
File: a:\1115.CPI Date: 11/09/97 Comment: LP-6
Counts
1200
800
400
0
Chlorite 001
White mica 001
Chlorite 002
Quartz
Quartz + White mica
Feldspar
10
20
30
40
50
60
Degrees 2-Theta

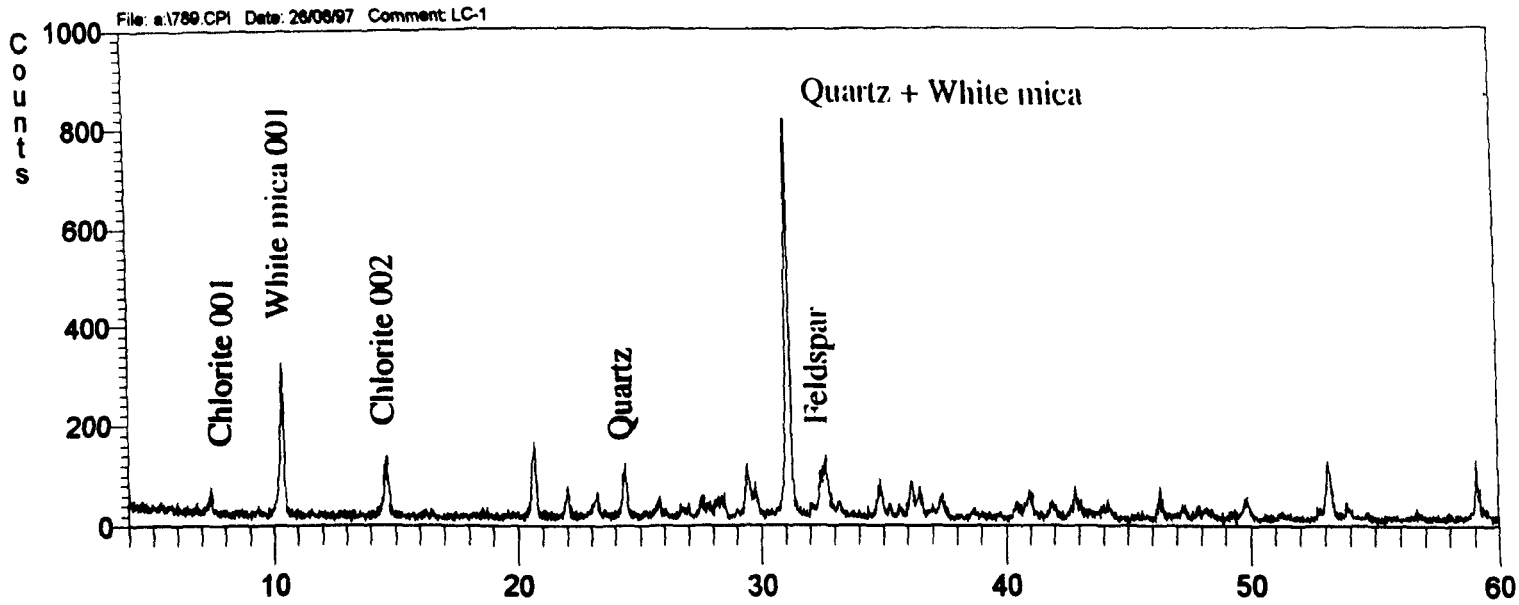
File: a:\789.CPI Date: 26/08/97 Comment: LC-1
Counts
1000
800
600
400
200
0
Chlorite 001
White mica 001
Chlorite 002
Quartz
Quartz + White mica
Feldspar
10
20
30
40
50
60

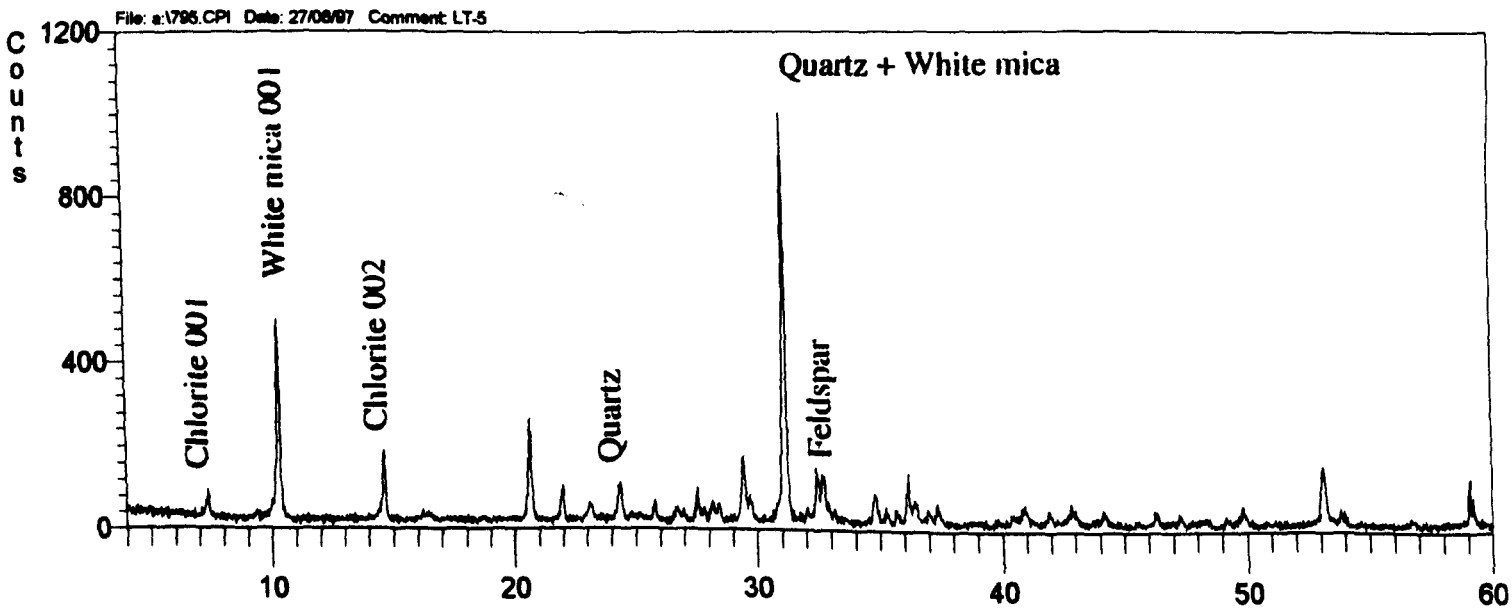
File: a:\795.CPI Date: 27/08/97 Comment: LT-5
Counts
1200
800
400
0
Chlorite 001
White mica 001
Chlorite 002
Quartz
Quartz + White mica
Feldspar
10
20
30
40
50
60

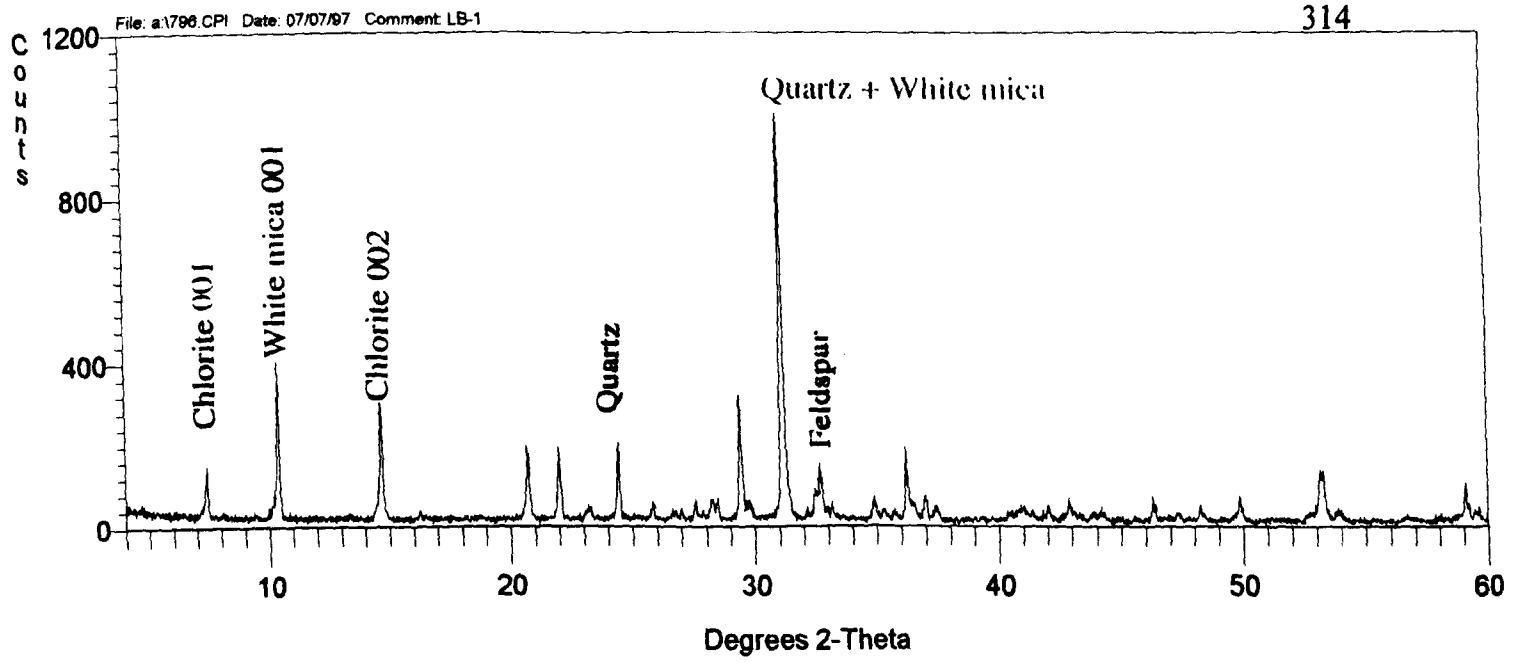
File: a:\796.CPI Date: 07/07/97 Comment: LB-1
Counts
1200
800
400
0
Chlorite (0)1
White mica 001
Chlorite 002
Quartz
Quartz + White mica
Feldspar
10
20
30
40
50
60
Degrees 2-Theta

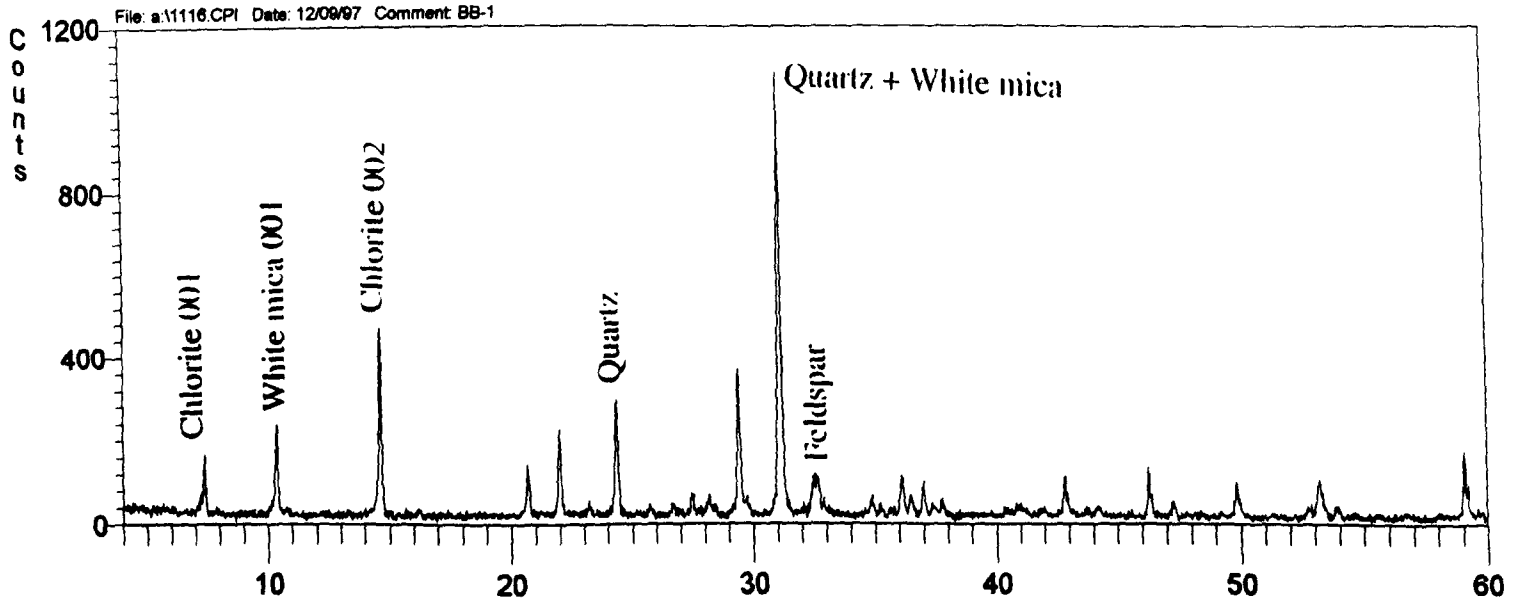
File: a:\1116.CPI Date: 12/09/97 Comment: BB-1
Counts
1200
800
400
0
Chlorite (0)1
White mica (0)1
Chlorite (0)2
Quartz
Quartz + White mica
Feldspar
10
20
30
40
50
60

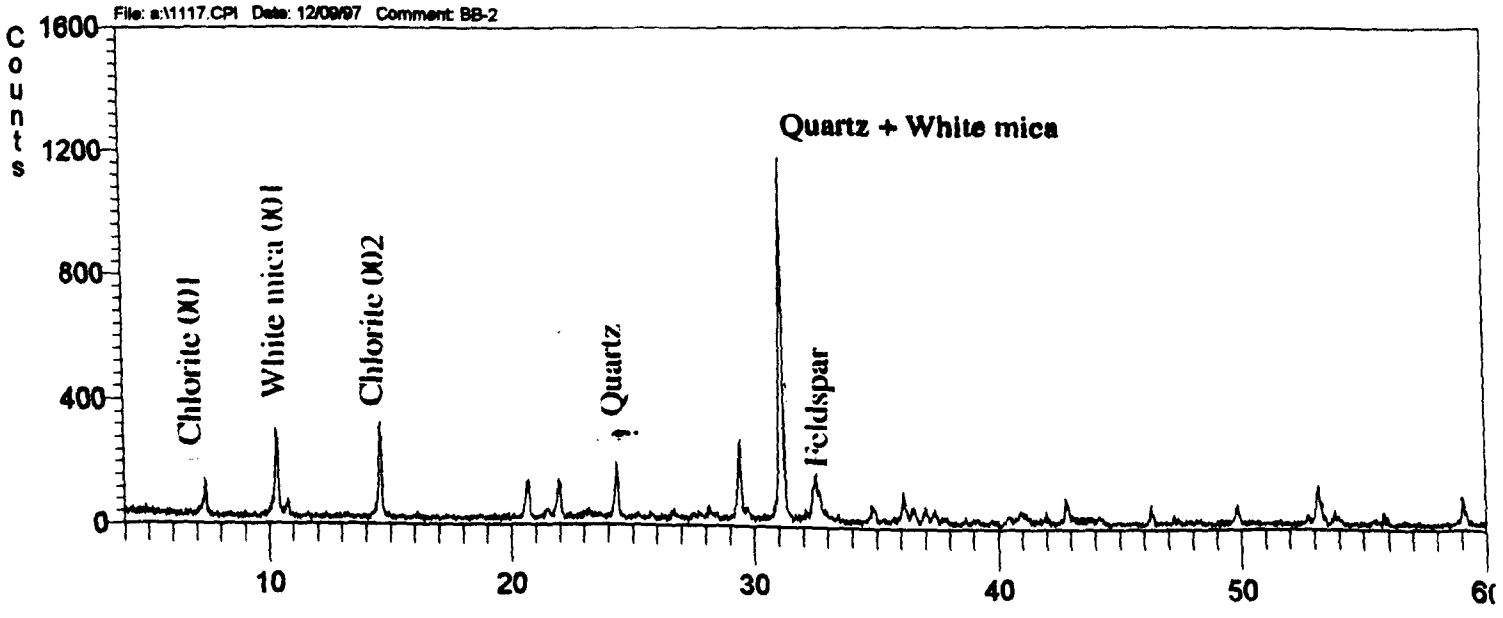
File: a:\1117.CPI Date: 12/09/97 Comment: BB-2
Counts
1600
1200
800
400
0
Chlorite (0)1
White mica (0)1
Chlorite (0)2
Quartz
Quartz + White mica
Feldspar
10
20
30
40
50

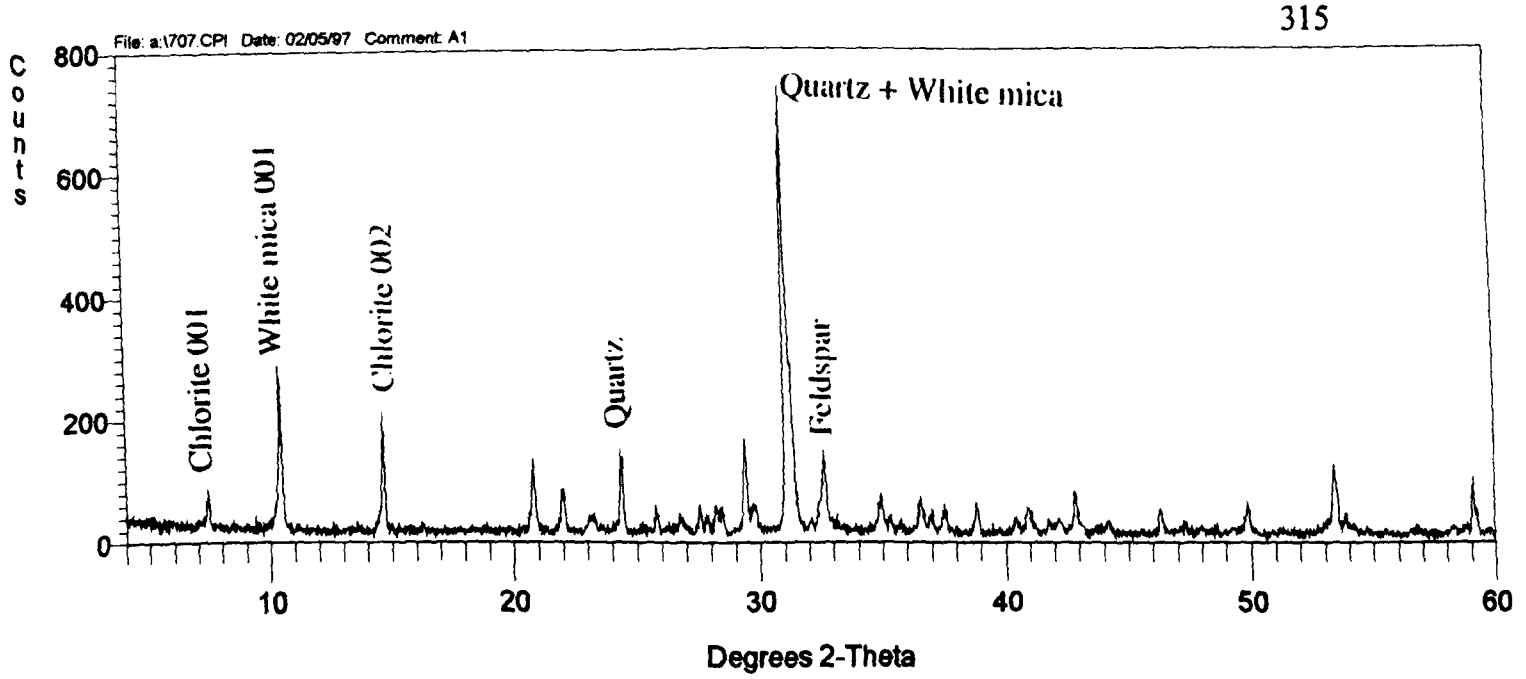
File: a:\707.CPI Date: 02/05/97 Comment: A1
Counts
800
600
400
200
0
Chlorite (001)
White mica (001)
Chlorite (002)
Quartz
Quartz + White mica
Feldspar
10
20
30
40
50
60
Degrees 2-Theta

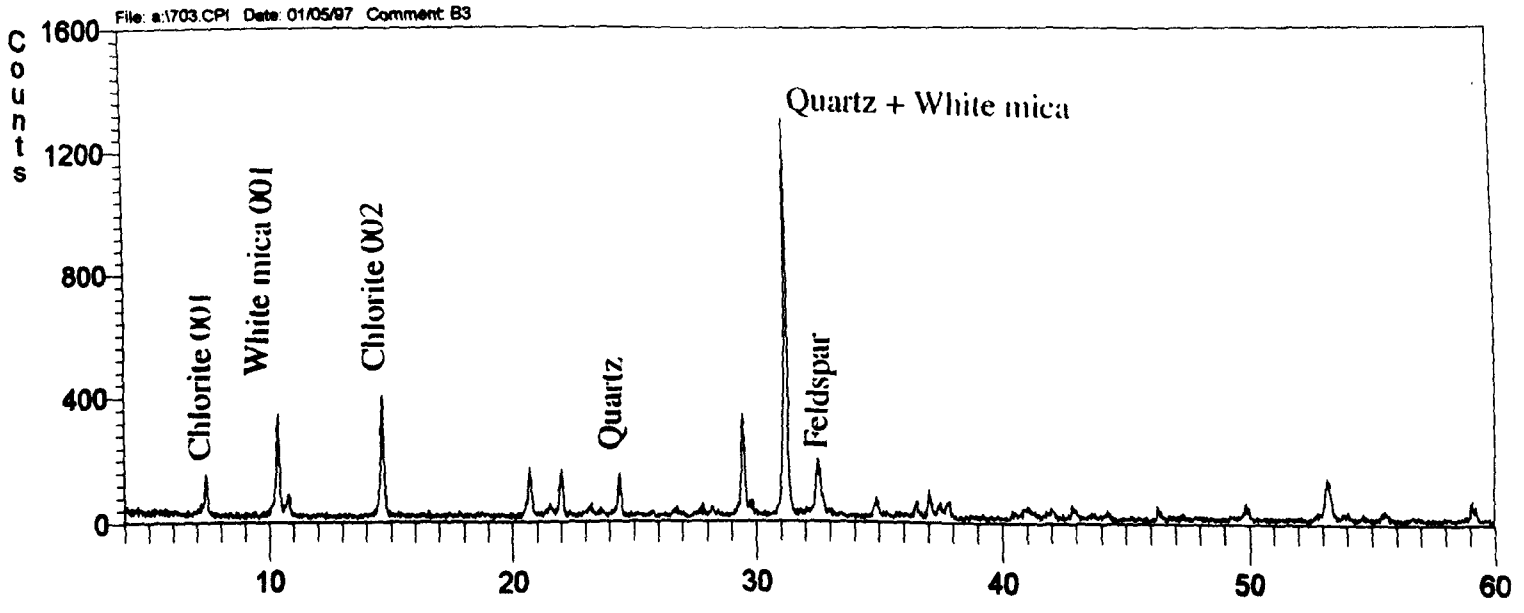
File: a:\703.CPI Date: 01/05/97 Comment: B3
Counts
1600
1200
800
400
0
Chlorite (001)
White mica (001)
Chlorite (002)
Quartz
Quartz + White mica
Feldspar
10
20
30
40
50
60

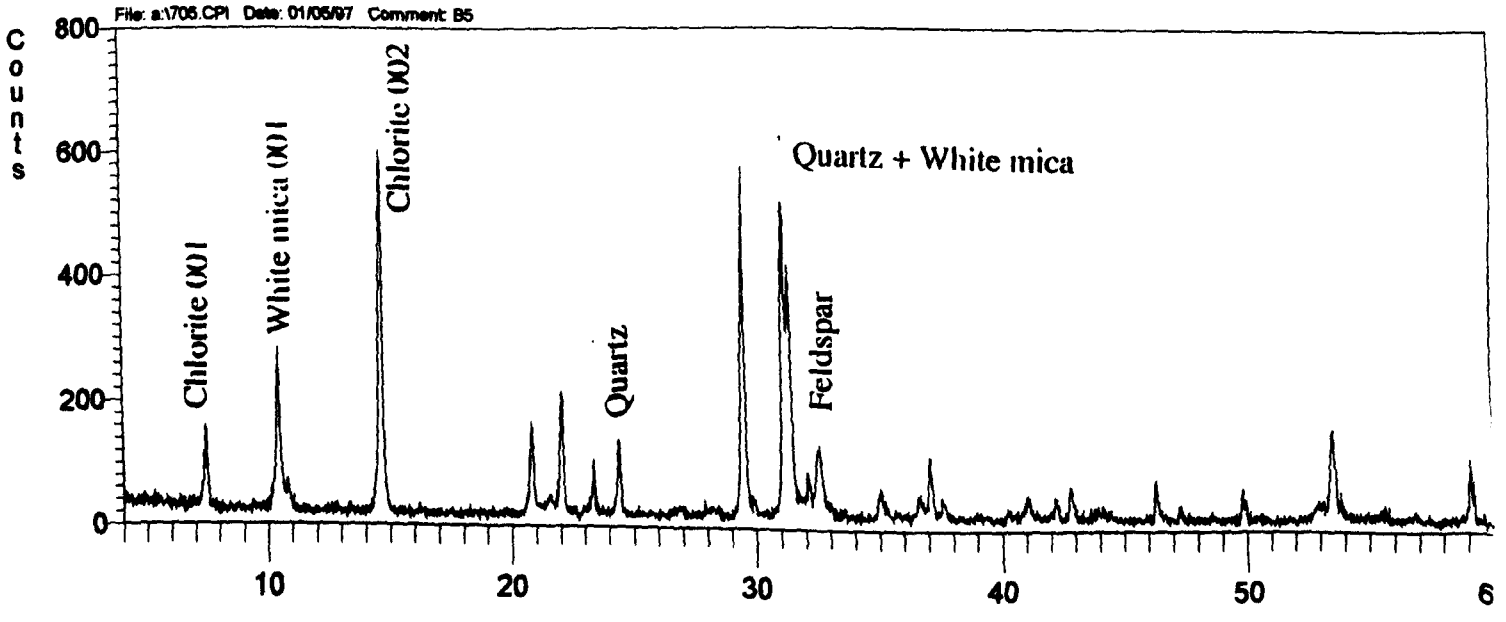
File: a:\706.CPI Date: 01/05/97 Comment: B5
Counts
800
600
400
200
0
Chlorite (001)
White mica (001)
Chlorite (002)
Quartz
Quartz + White mica
Feldspar
10
20
30
40
50
6

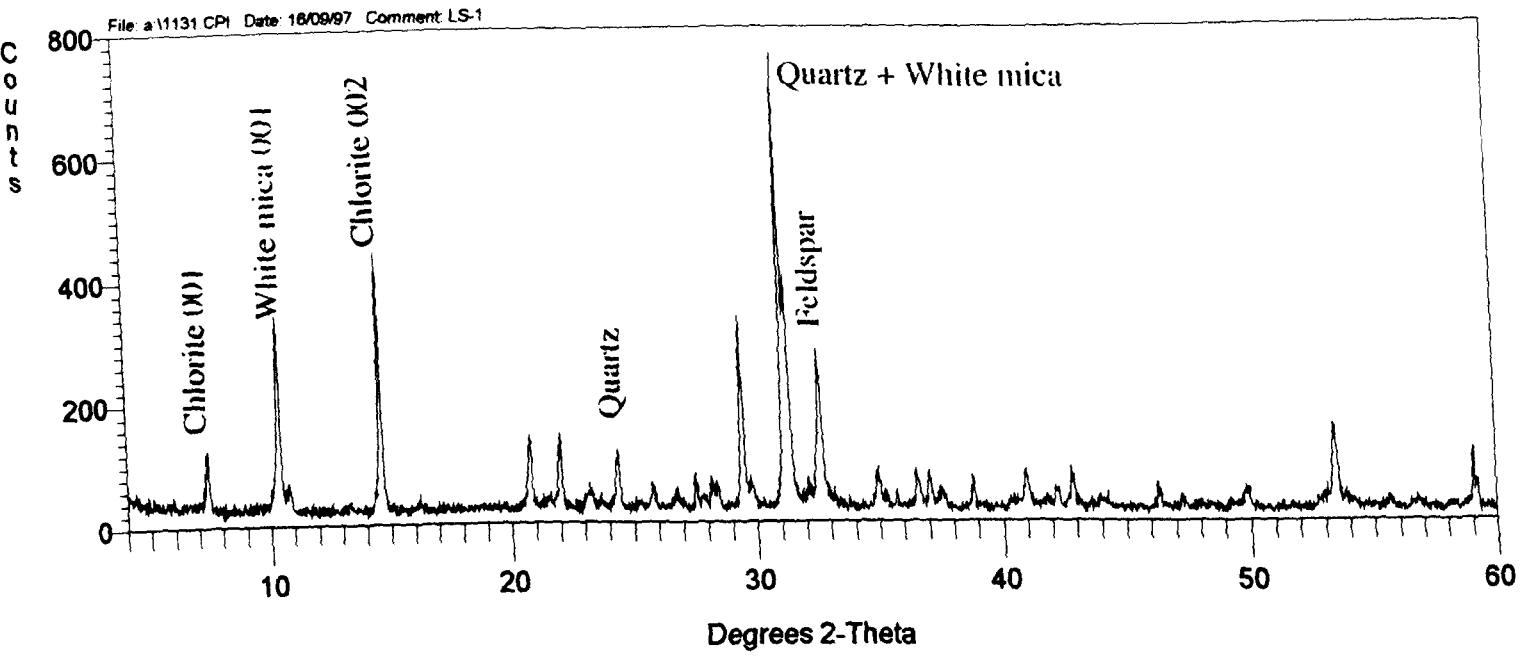
File: a:\1131.CPI Date: 16/09/97 Comment: LS-1
Counts
800
600
400
200
0
Chlorite (001)
White mica (001)
Chlorite (002)
Quartz
Quartz + White mica
Feldspar
10
20
30
40
50
60
Degrees 2-Theta

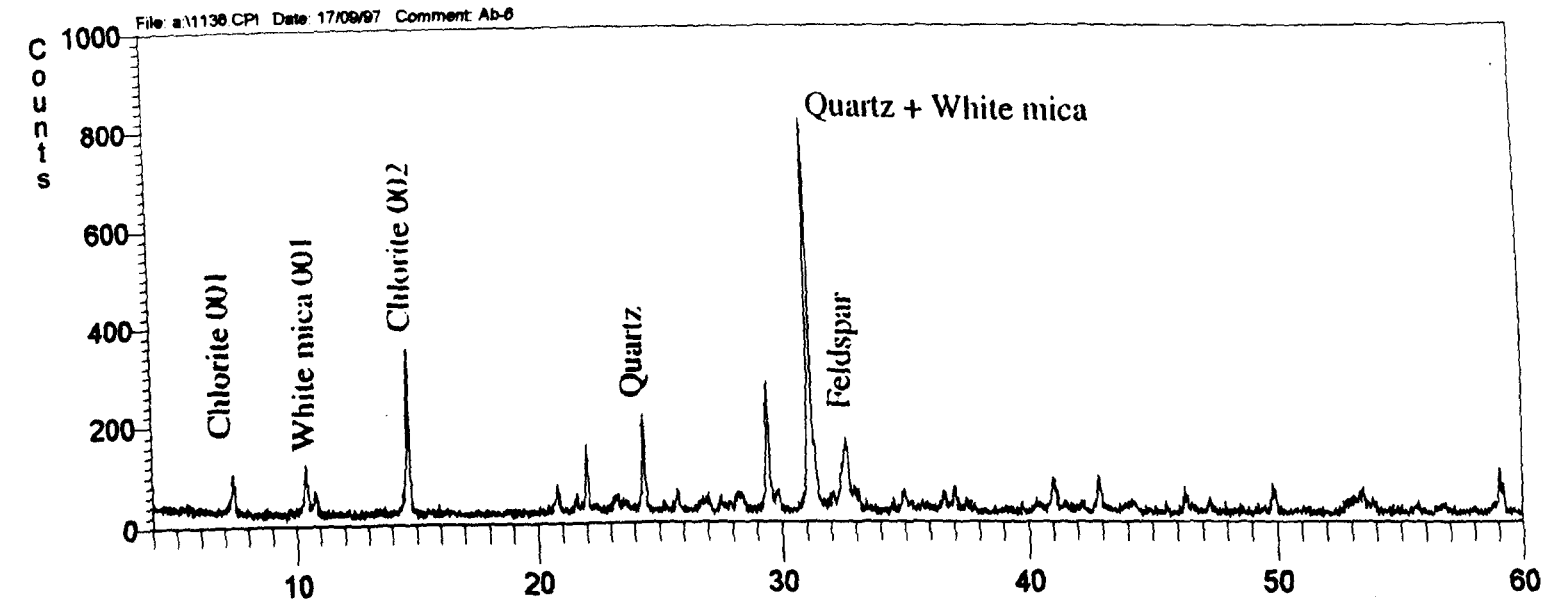
File: a:\1136.CPI Date: 17/09/97 Comment: Ab-6
Counts
1000
800
600
400
200
0
Chlorite (001)
White mica (001)
Chlorite (002)
Quartz
Quartz + White mica
Feldspar
10
20
30
40
50
60

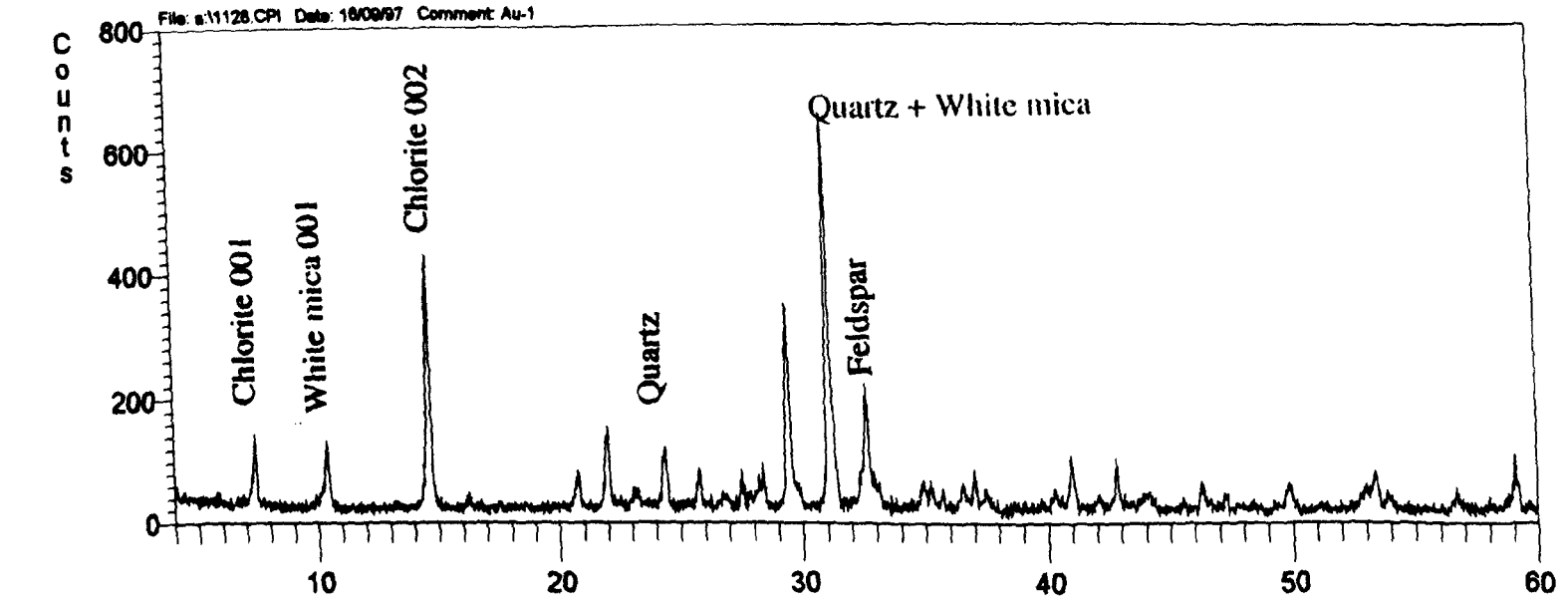
File: a:\1128.CPI Date: 16/09/97 Comment: Au-1
Counts
800
600
400
200
0
Chlorite (001)
White mica (001)
Chlorite (002)
Quartz
Quartz + White mica
Feldspar
10
20
30
40
50
60

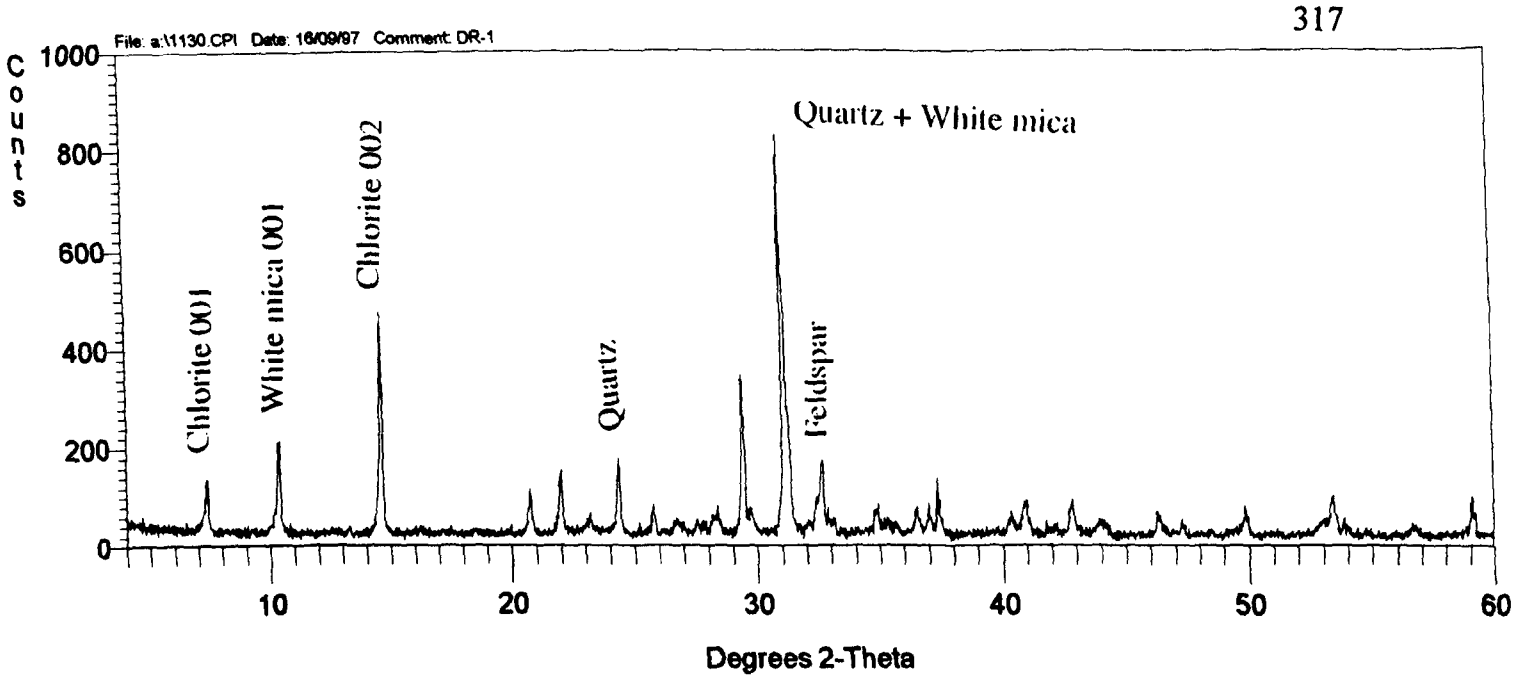
File: a:\1130.CPI Date: 16/09/97 Comment: DR-1
Counts
1000
800
600
400
200
0
Chlorite 001
White mica 001
Chlorite 002
Quartz
Quartz + White mica
Feldspar
10
20
30
40
50
60
Degrees 2-Theta

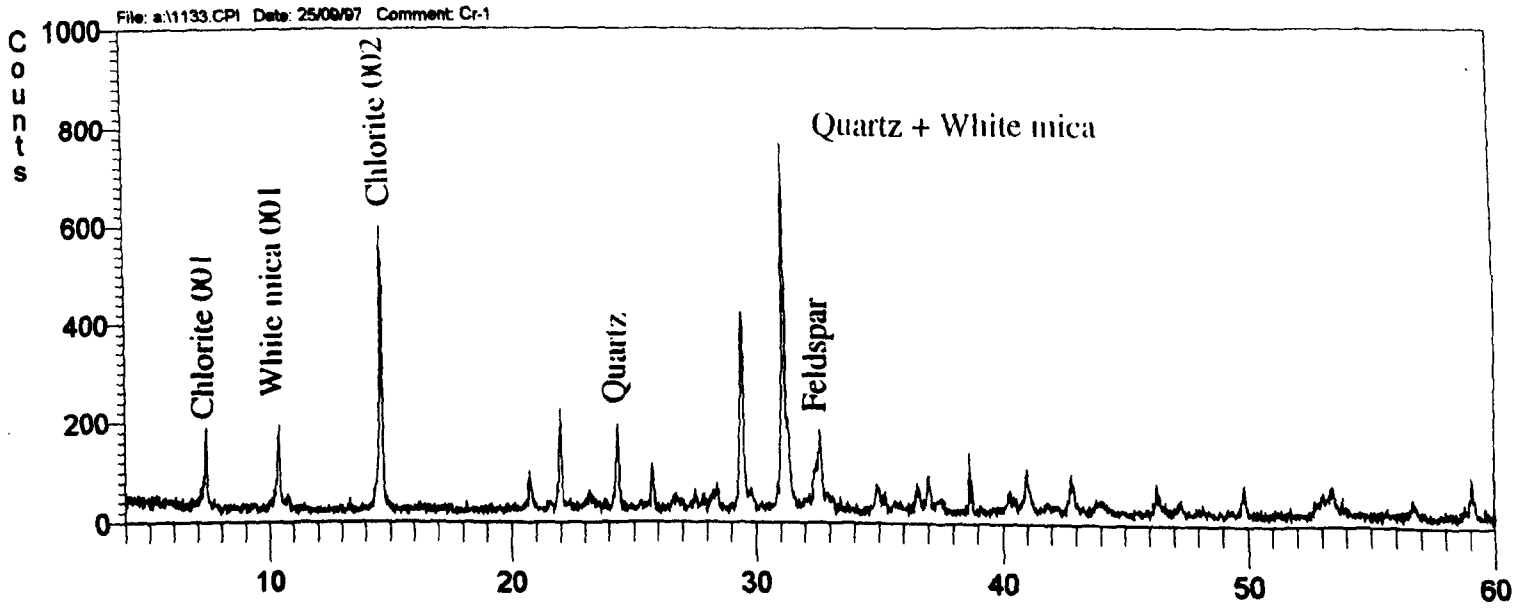
File: a:\1133.CPI Date: 25/09/97 Comment: Cr-1
Counts
1000
800
600
400
200
0
Chlorite 001
White mica 001
Chlorite 002
Quartz
Quartz + White mica
Feldspar
10
20
30
40
50
60

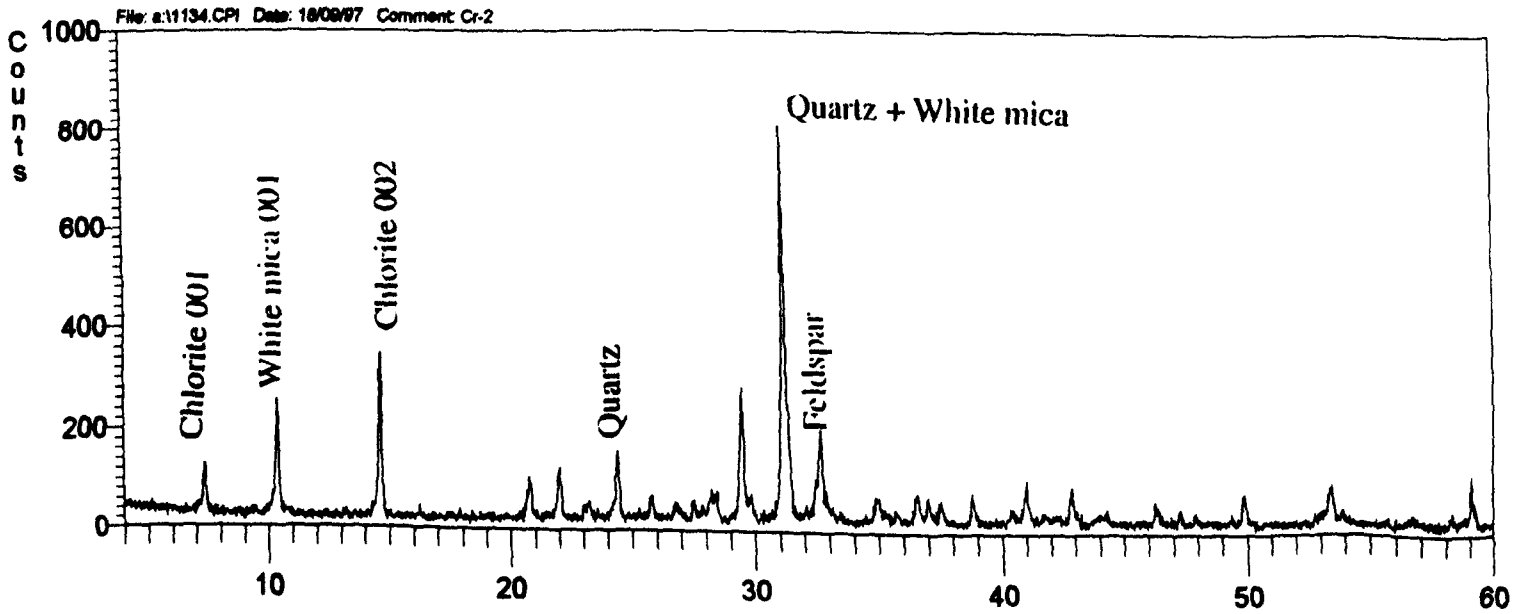
File: a:\1134.CPI Date: 18/09/97 Comment: Cr-2
Counts
1000
800
600
400
200
0
Chlorite 001
White mica 001
Chlorite 002
Quartz
Quartz + White mica
Feldspar
10
20
30
40
50
60

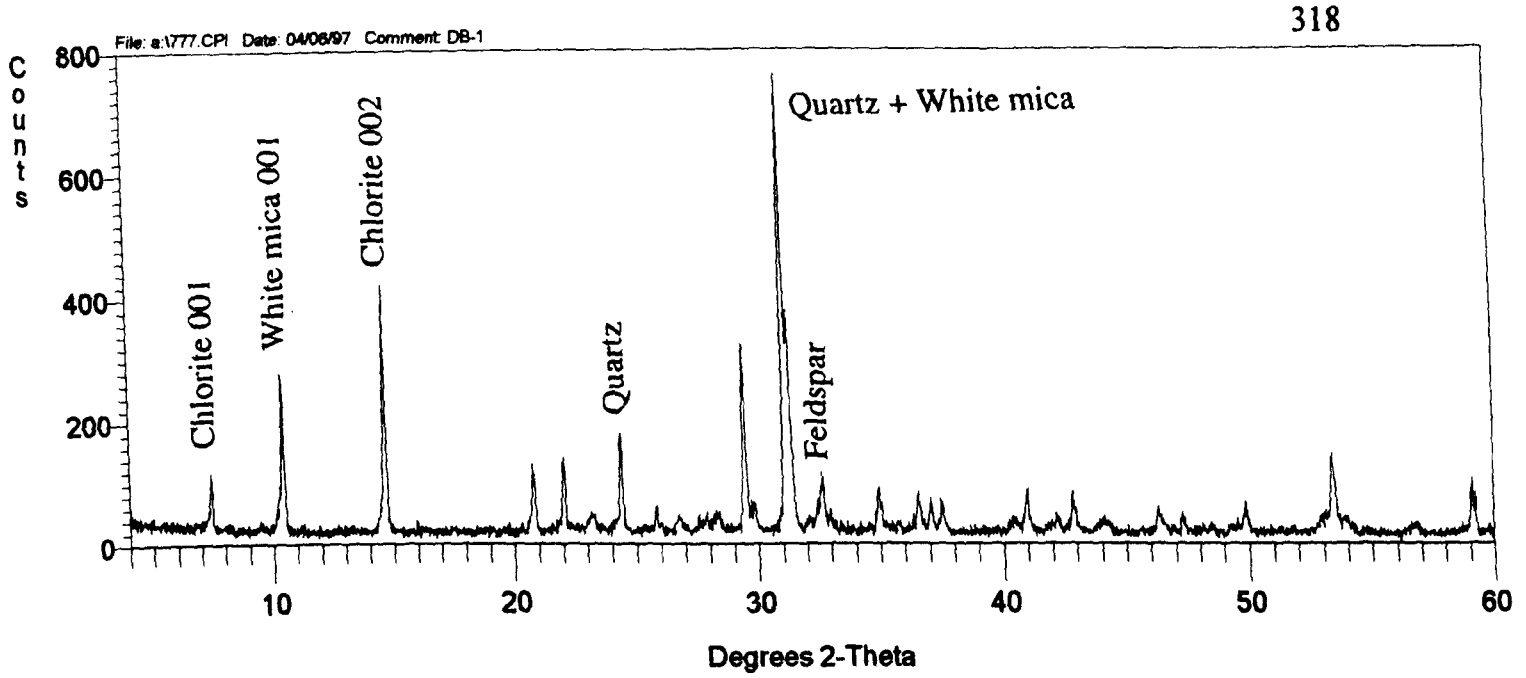
File: a:\777.CPI Date: 04/08/97 Comment: DB-1
Counts
800
600
400
200
0
Chlorite 001
White mica 001
Chlorite 002
Quartz
Quartz + White mica
Feldspar
10
20
30
40
50
60
Degrees 2-Theta

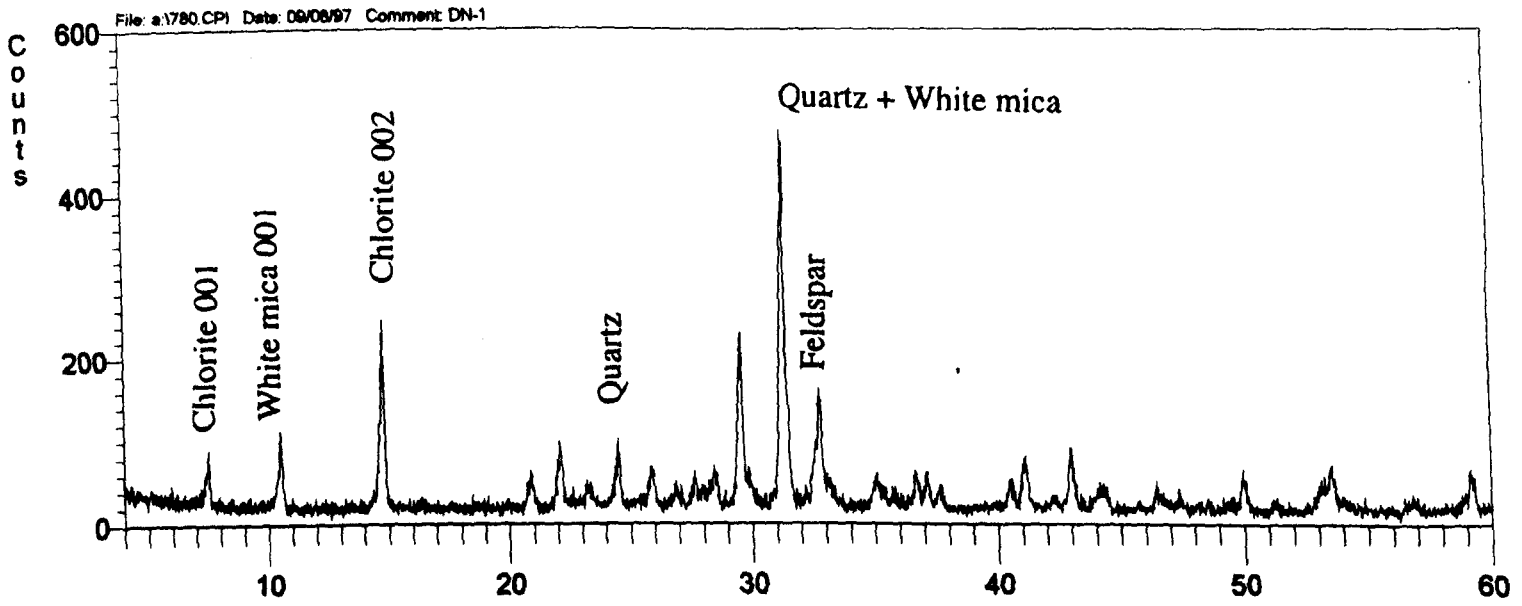
File: a:\780.CPI Date: 09/08/97 Comment: DN-1
Counts
600
400
200
0
Chlorite 001
White mica 001
Chlorite 002
Quartz
Quartz + White mica
Feldspar
10
20
30
40
50
60

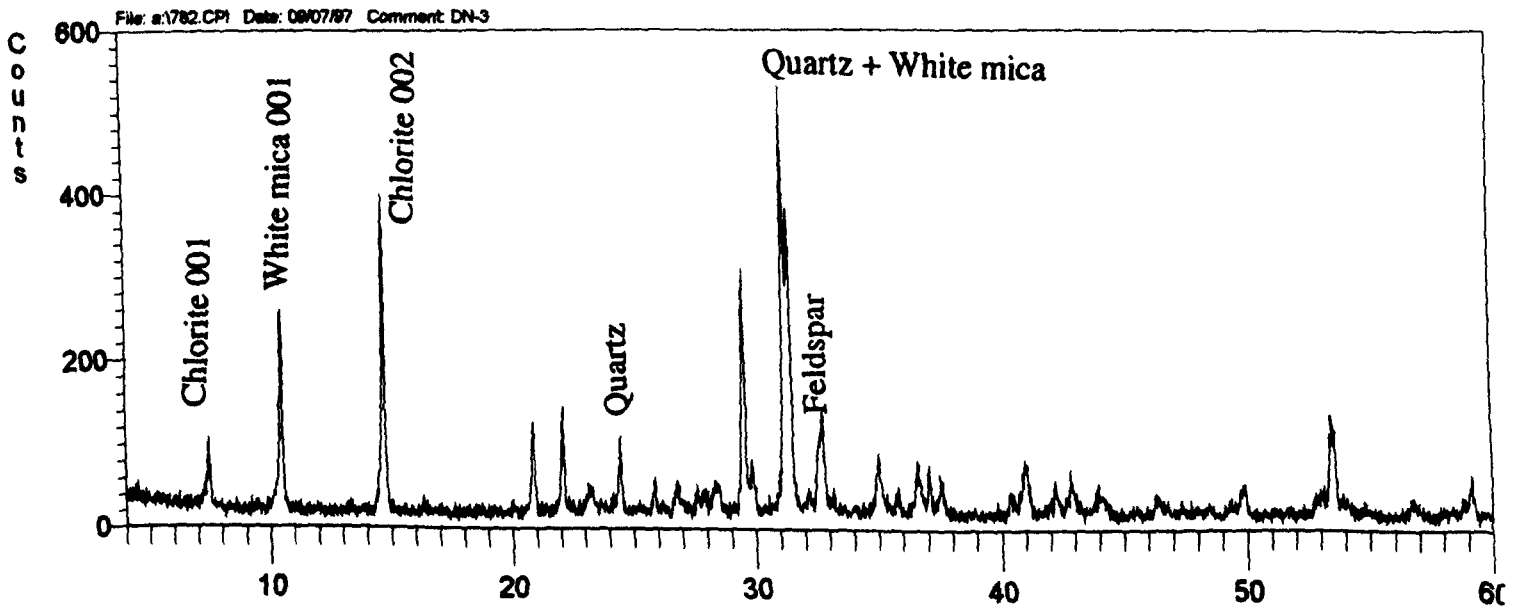
File: a:\782.CPI Date: 09/07/97 Comment: DN-3
Counts
600
400
200
0
Chlorite 001
White mica 001
Chlorite 002
Quartz
Quartz + White mica
Feldspar
10
20
30
40
50

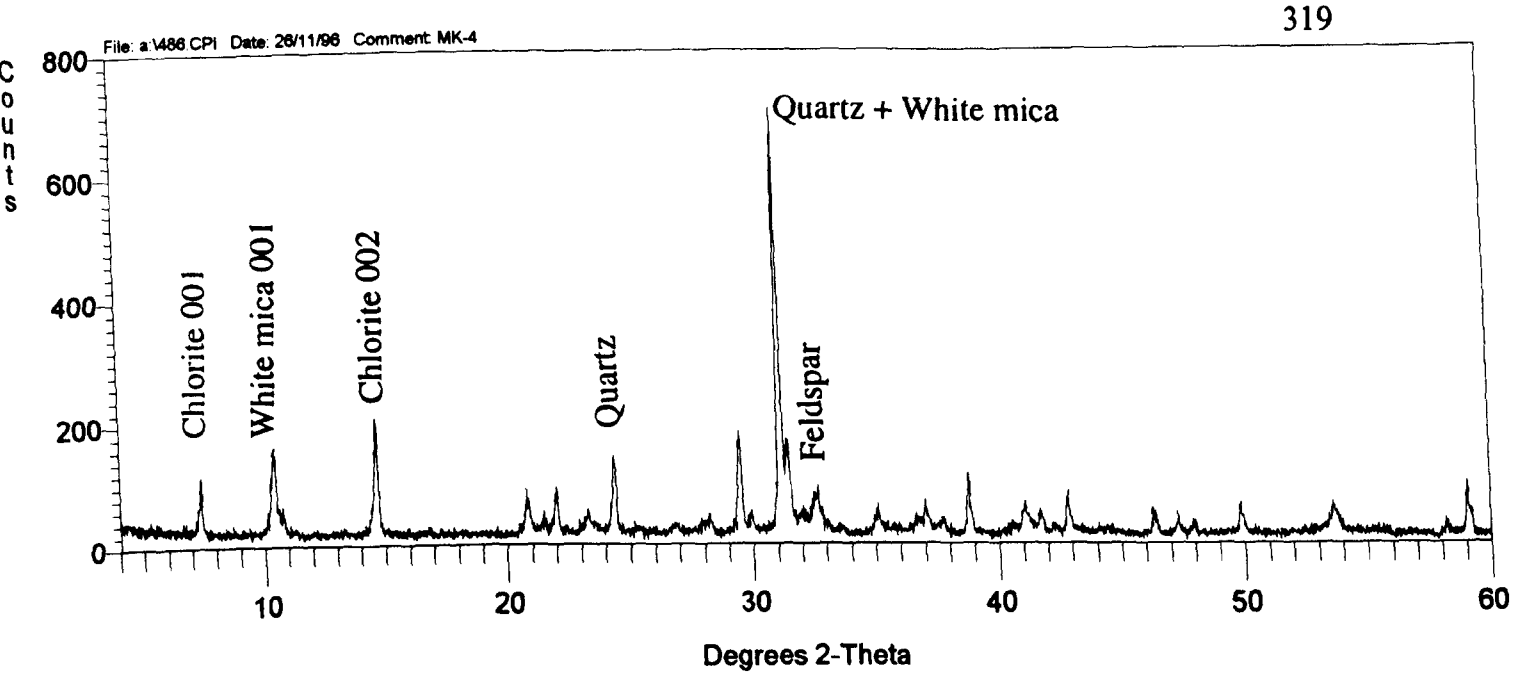
File: a:\486.CPI Date: 26/11/96 Comment: MK-4
Counts
800
600
400
200
0
Chlorite 001
White mica 001
Chlorite 002
Quartz
Quartz + White mica
Feldspar
10
20
30
40
50
60
Degrees 2-Theta

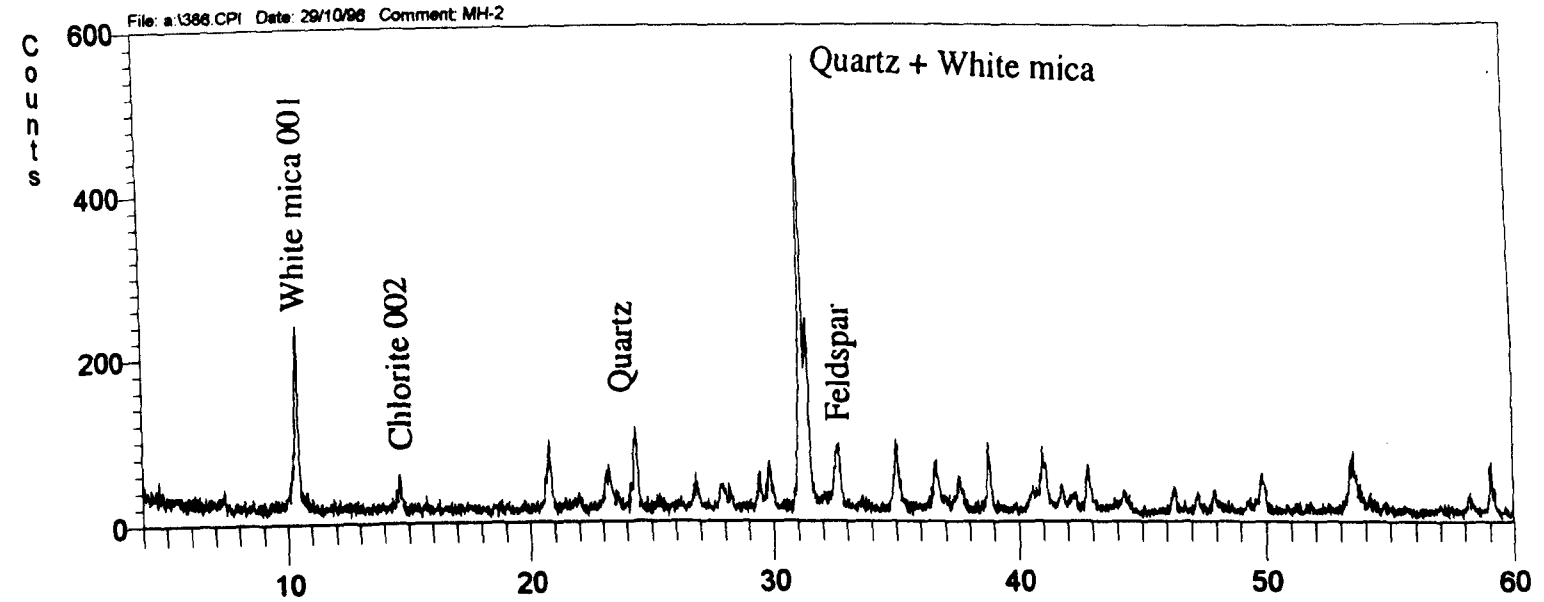
File: a:\386.CPI Date: 29/10/96 Comment: MH-2
Counts
600
400
200
0
White mica 001
Chlorite 002
Quartz
Quartz + White mica
Feldspar
10
20
30
40
50
60

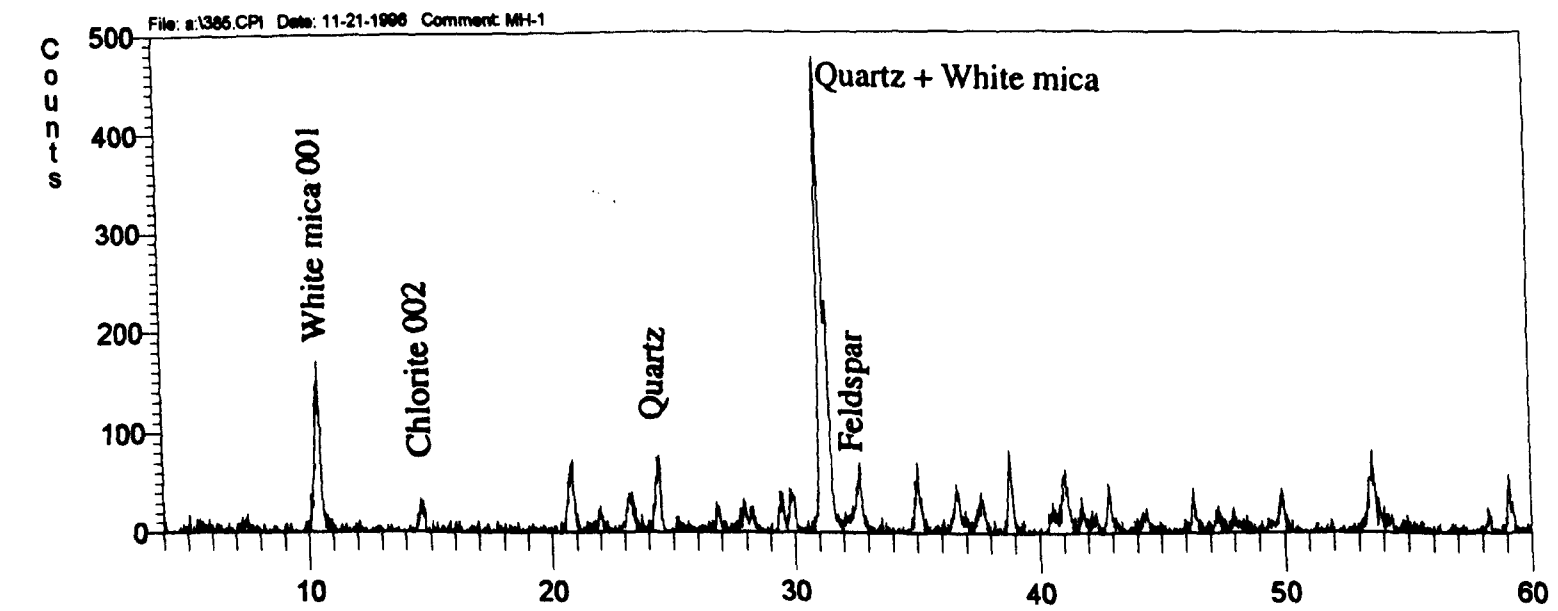
File: a:\386.CPI Date: 11-21-1996 Comment: MH-1
Counts
500
400
300
200
100
0
White mica 001
Chlorite 002
Quartz
Quartz + White mica
Feldspar
10
20
30
40
50
60

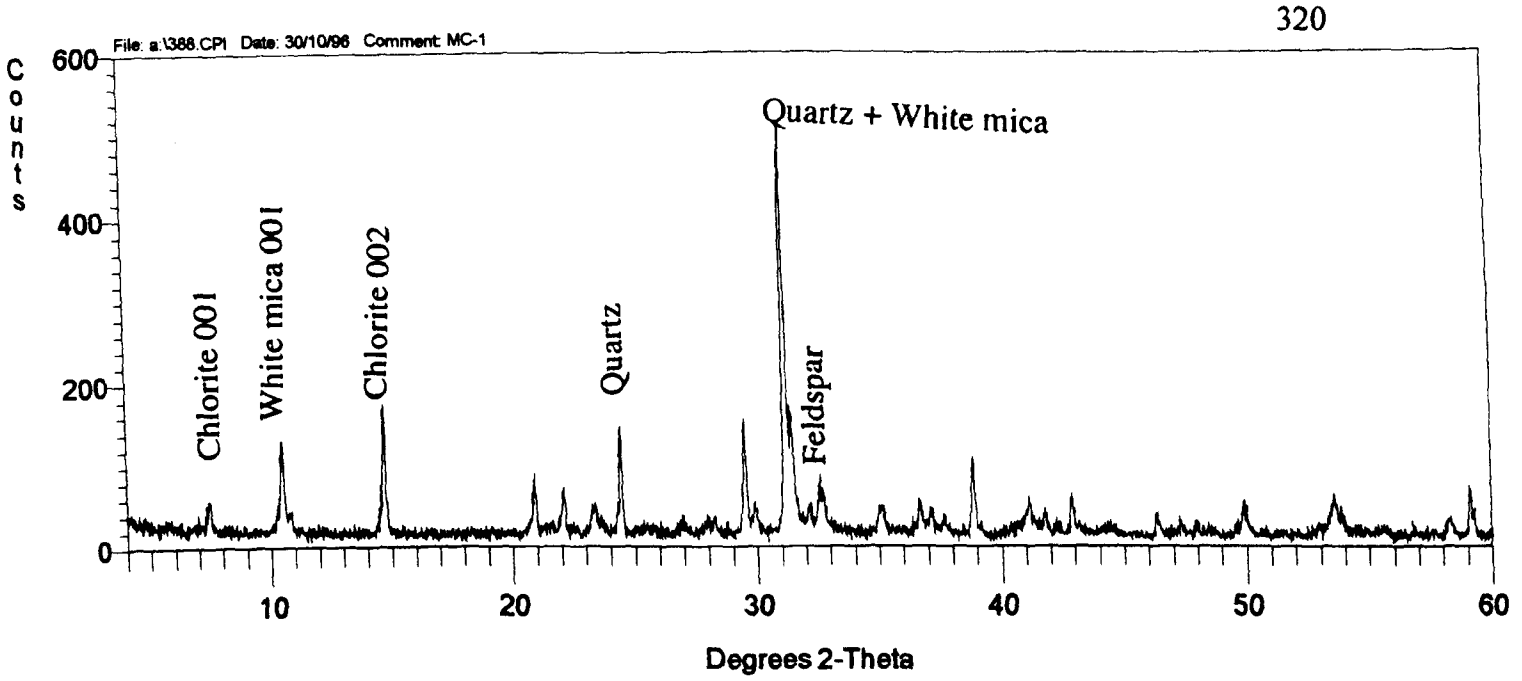
File: a:\388.CPI Date: 30/10/96 Comment: MC-1
Counts
600
400
200
0
Chlorite 001
White mica 001
Chlorite 002
Quartz
Quartz + White mica
Feldspar
10
20
30
40
50
60
Degrees 2-Theta

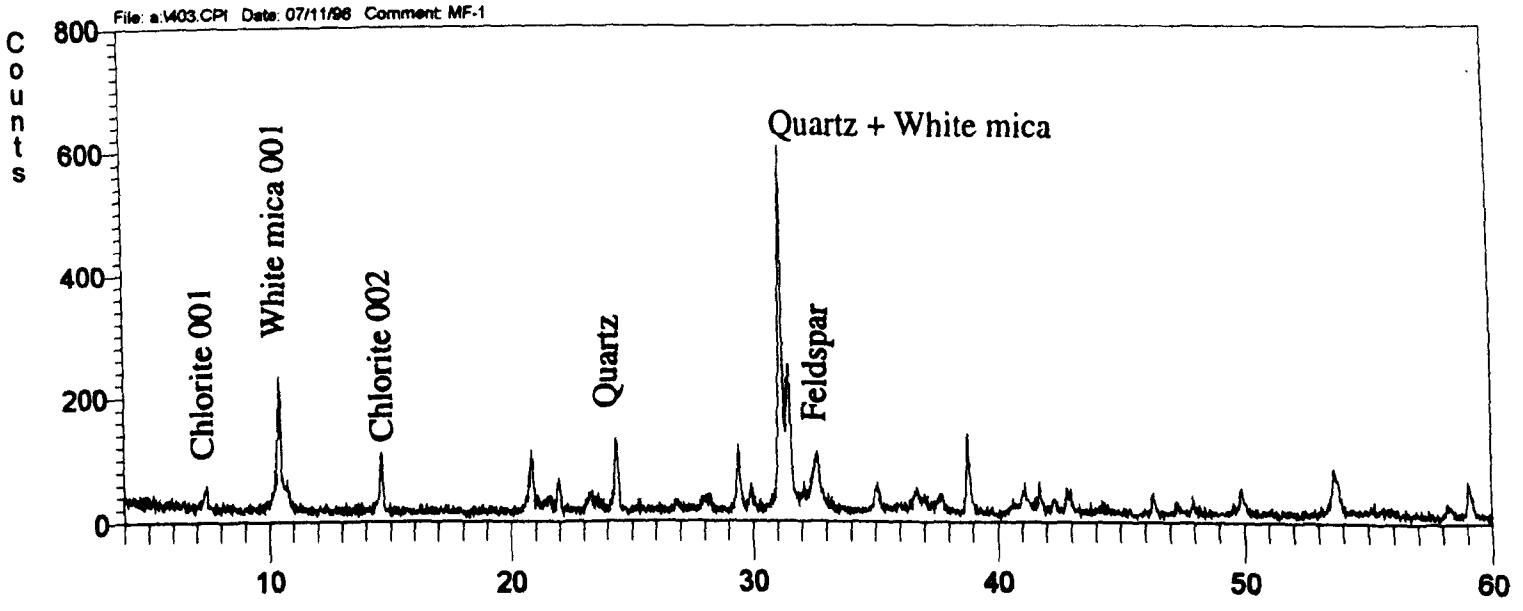
File: a:\403.CPI Date: 07/11/96 Comment: MF-1
Counts
800
600
400
200
0
Chlorite 001
White mica 001
Chlorite 002
Quartz
Quartz + White mica
Feldspar
10
20
30
40
50
60

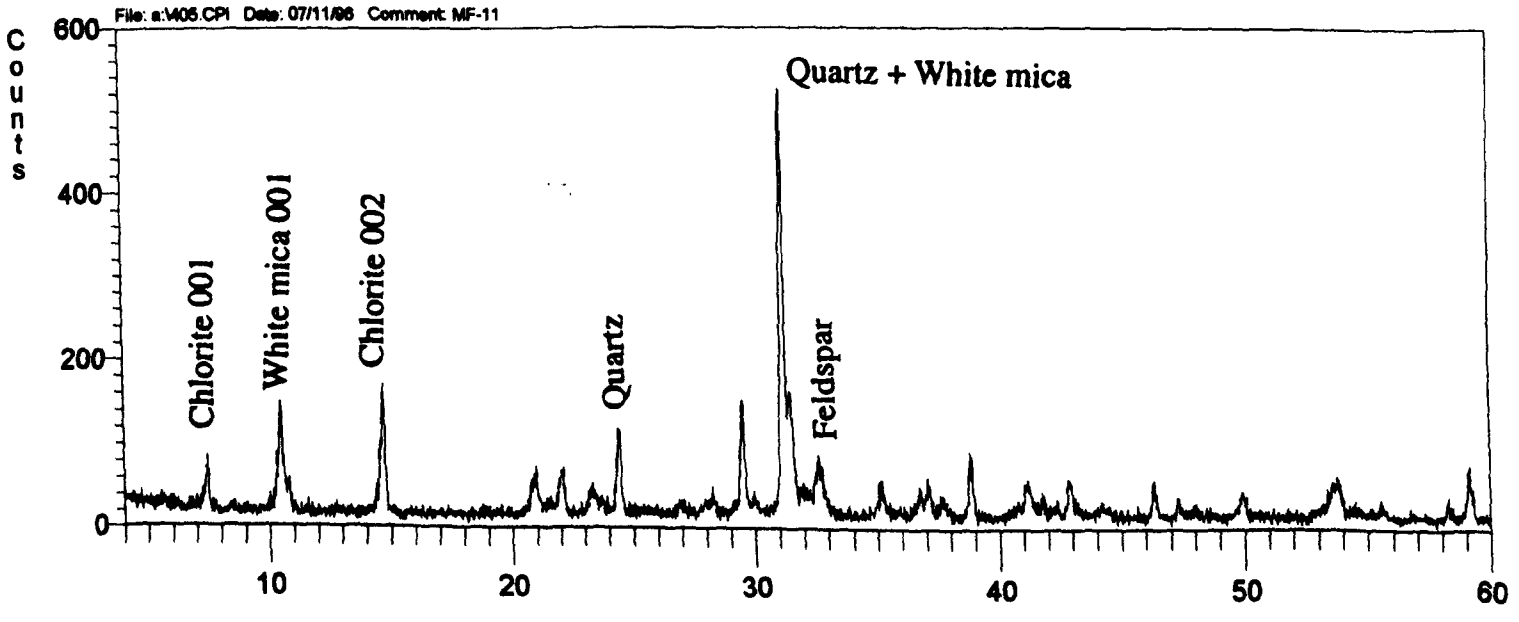
File: a:\405.CPI Date: 07/11/96 Comment: MF-11
Counts
600
400
200
0
Chlorite 001
White mica 001
Chlorite 002
Quartz
Quartz + White mica
Feldspar
10
20
30
40
50
60

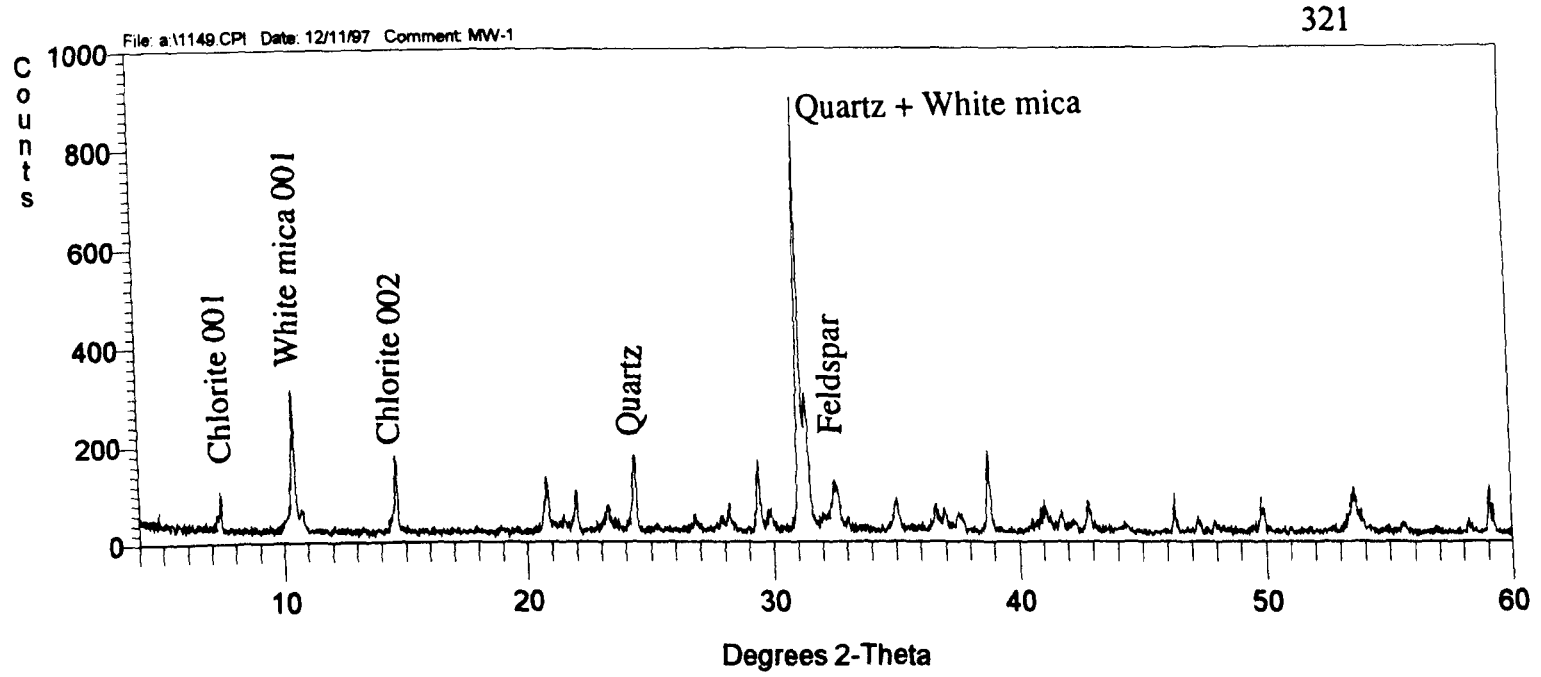
File: a:\1149.CPI Date: 12/11/97 Comment: MW-1
Counts
1000
800
600
400
200
0
Chlorite 001
White mica 001
Chlorite 002
Quartz
Quartz + White mica
Feldspar
10
20
30
40
50
60
Degrees 2-Theta

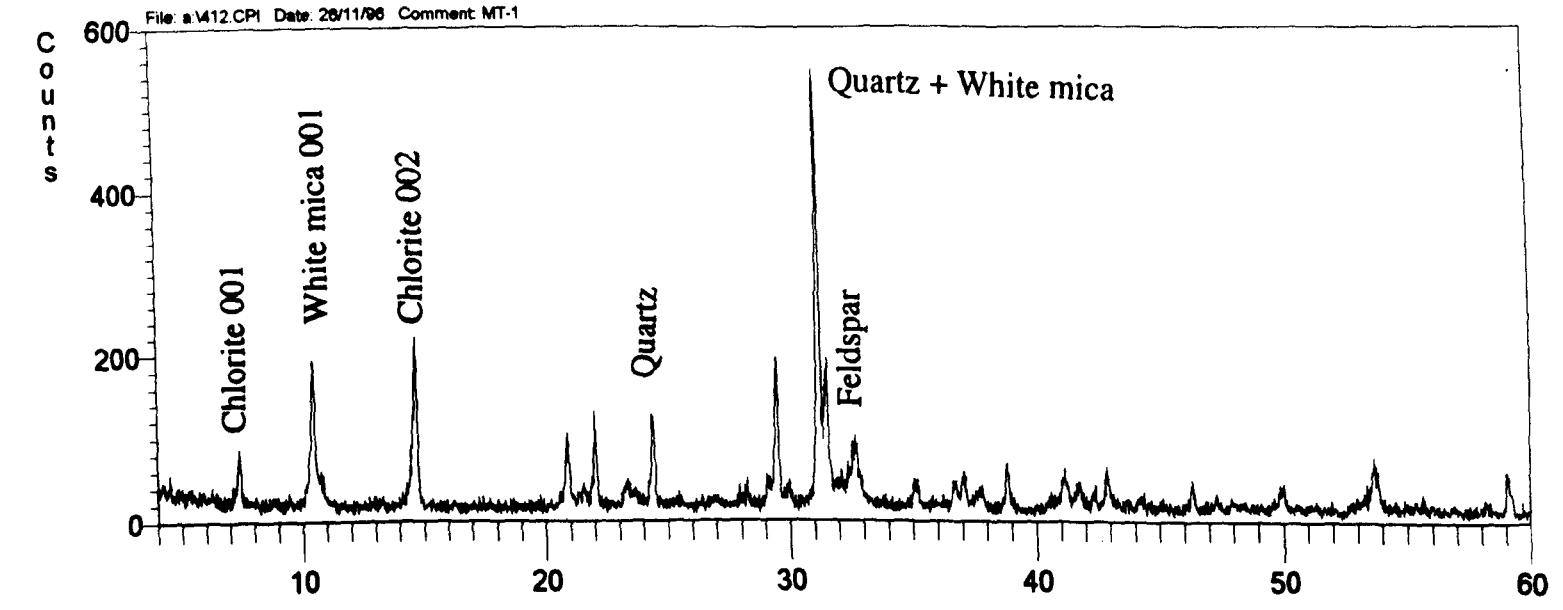
File: a:\412.CPI Date: 26/11/96 Comment: MT-1
Counts
600
400
200
0
Chlorite 001
White mica 001
Chlorite 002
Quartz
Quartz + White mica
Feldspar
10
20
30
40
50
60

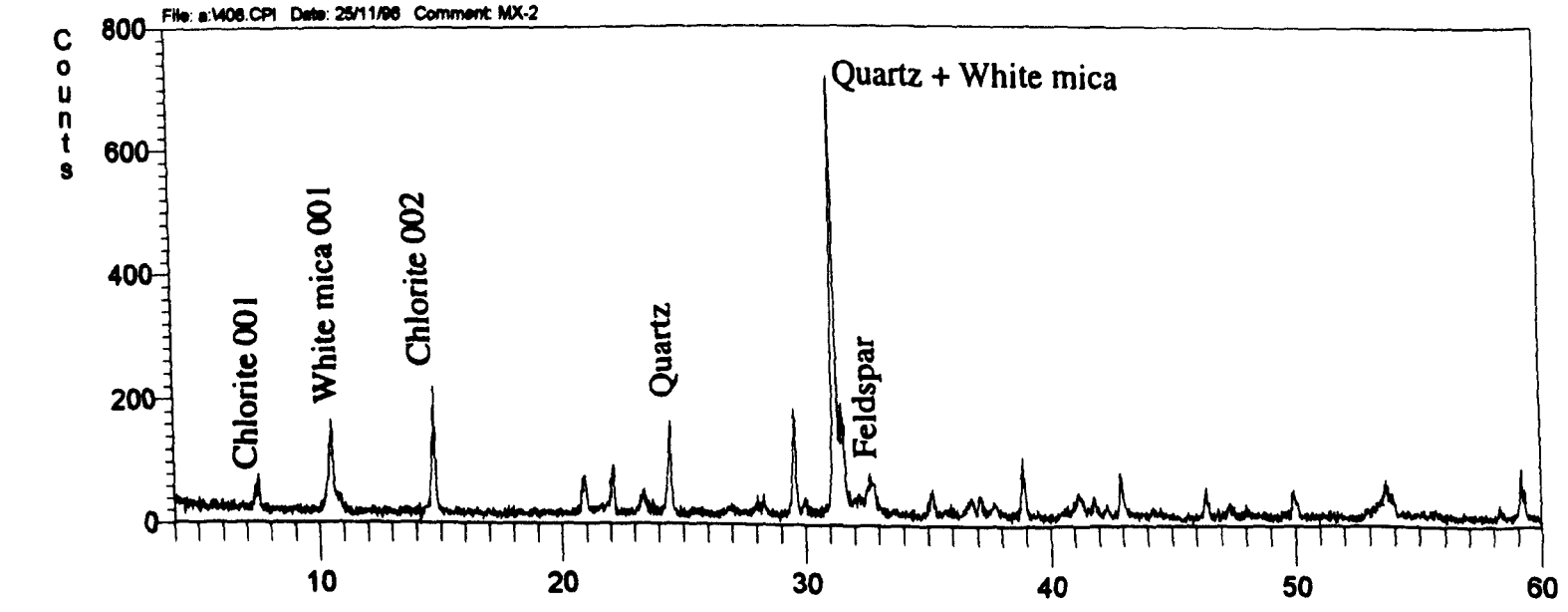
File: a:\406.CPI Date: 25/11/96 Comment: MX-2
Counts
800
600
400
200
0
Chlorite 001
White mica 001
Chlorite 002
Quartz
Quartz + White mica
Feldspar
10
20
30
40
50
60

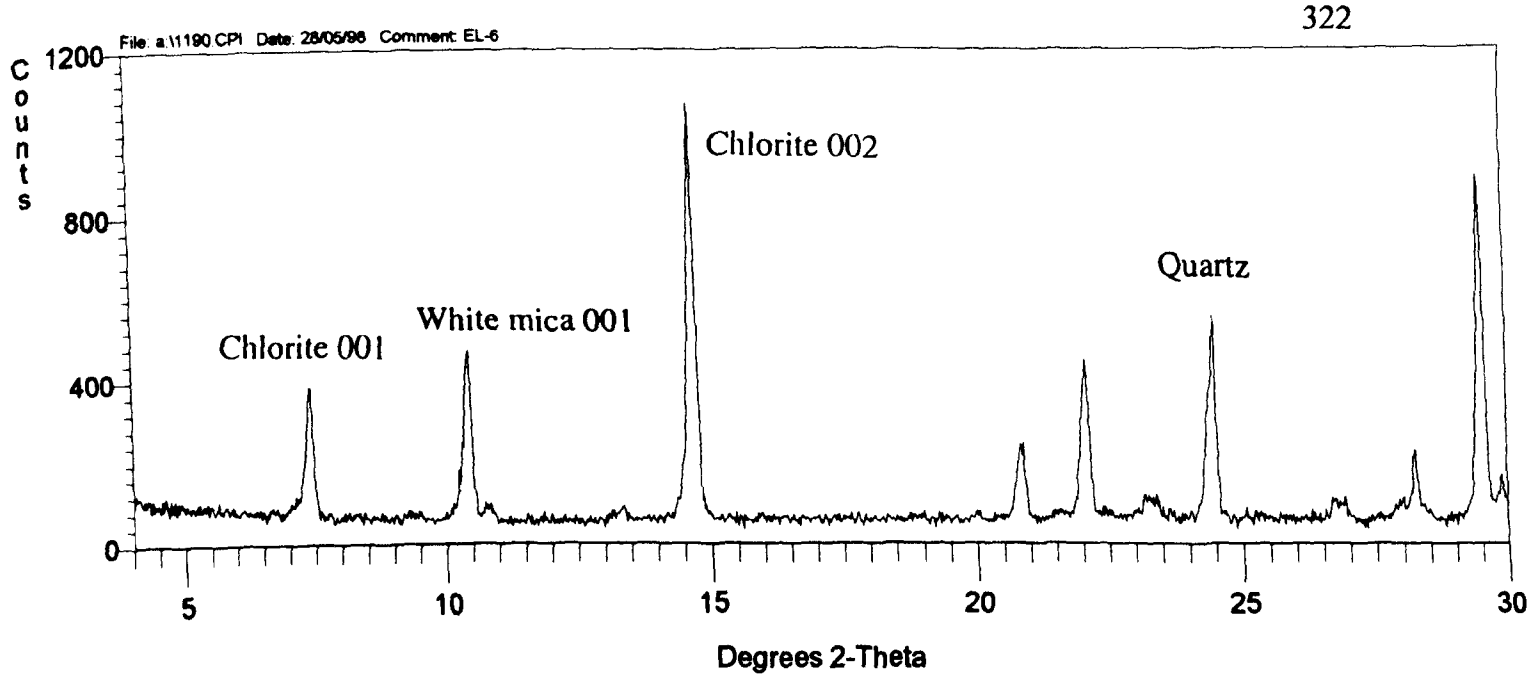
File: a:\1190.CPI Date: 28/05/96 Comment: EL-6
Counts
1200
800
400
0
Chlorite 001
White mica 001
Chlorite 002
Quartz
5
10
15
20
25
30
Degrees 2-Theta

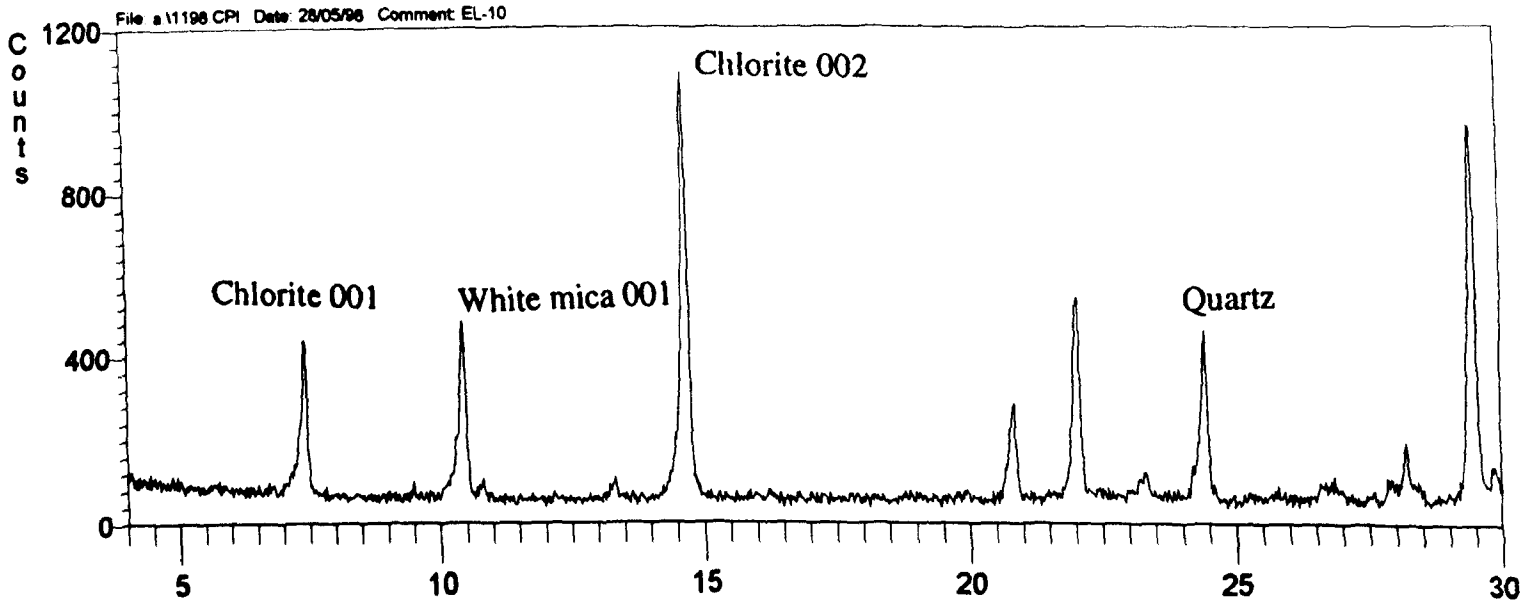
File: a:\1198.CPI Date: 28/05/96 Comment: EL-10
Counts
1200
800
400
0
Chlorite 001
White mica 001
Chlorite 002
Quartz
5
10
15
20
25
30

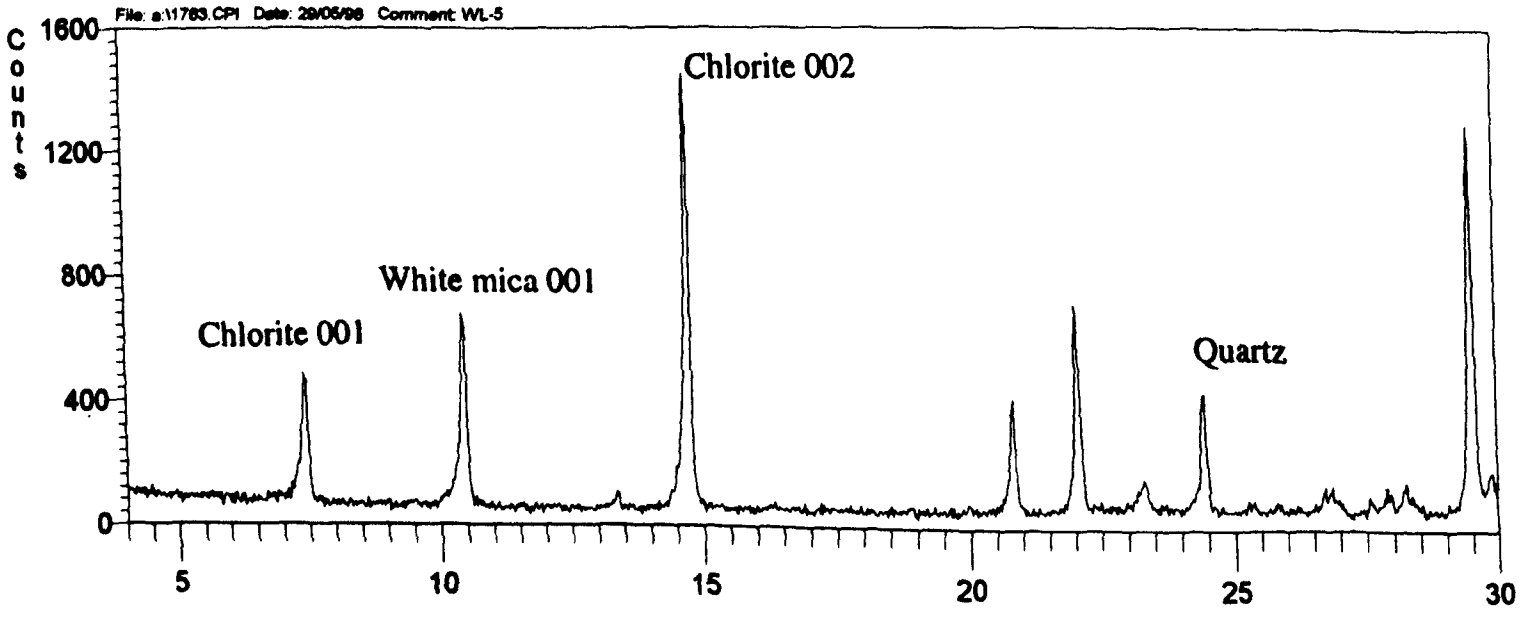
File: a:\1763.CPI Date: 29/05/96 Comment: WL-5
Counts
1600
1200
800
400
0
Chlorite 001
White mica 001
Chlorite 002
Quartz
5
10
15
20
25
30

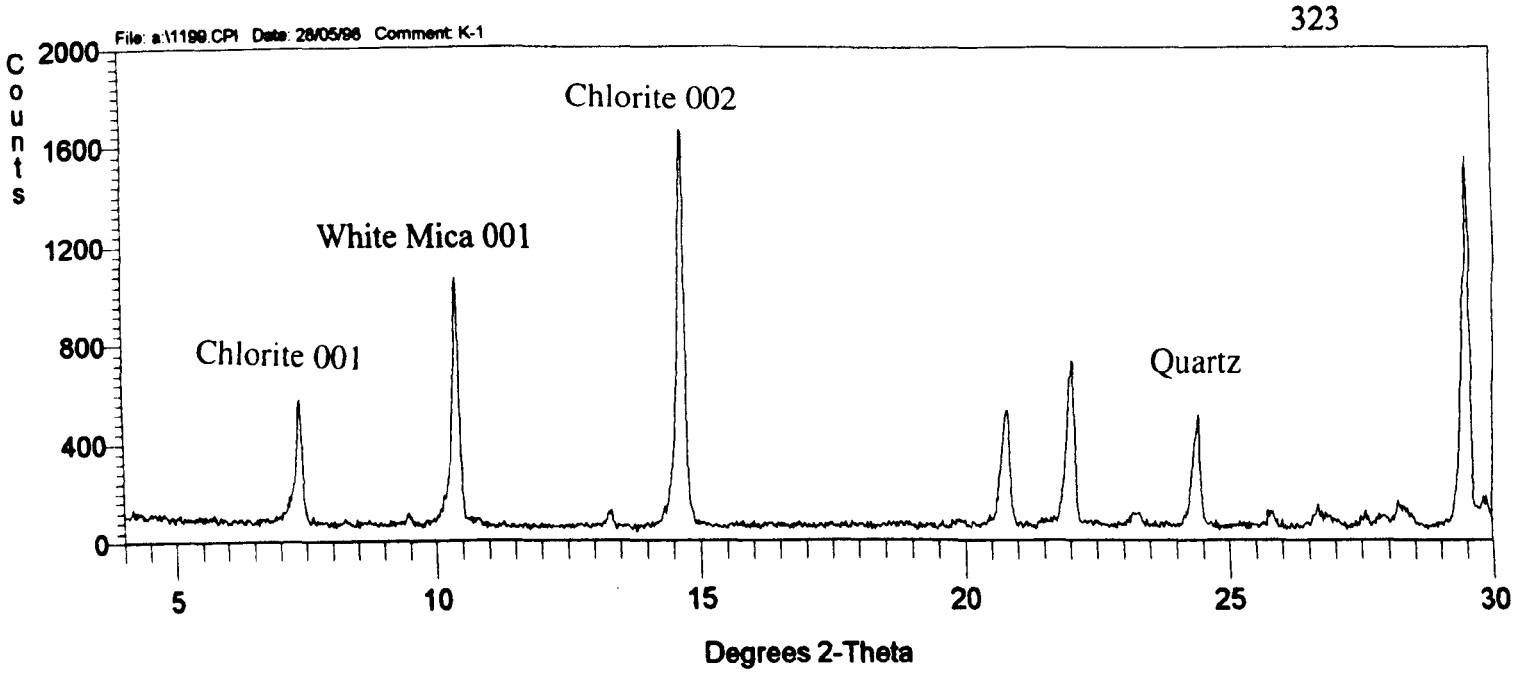
File: a:\1199.CPI Date: 28/05/96 Comment: K-1
Counts
2000
1600
1200
800
400
0
Chlorite 002
White Mica 001
Chlorite 001
Quartz
5
10
15
20
25
30
Degrees 2-Theta

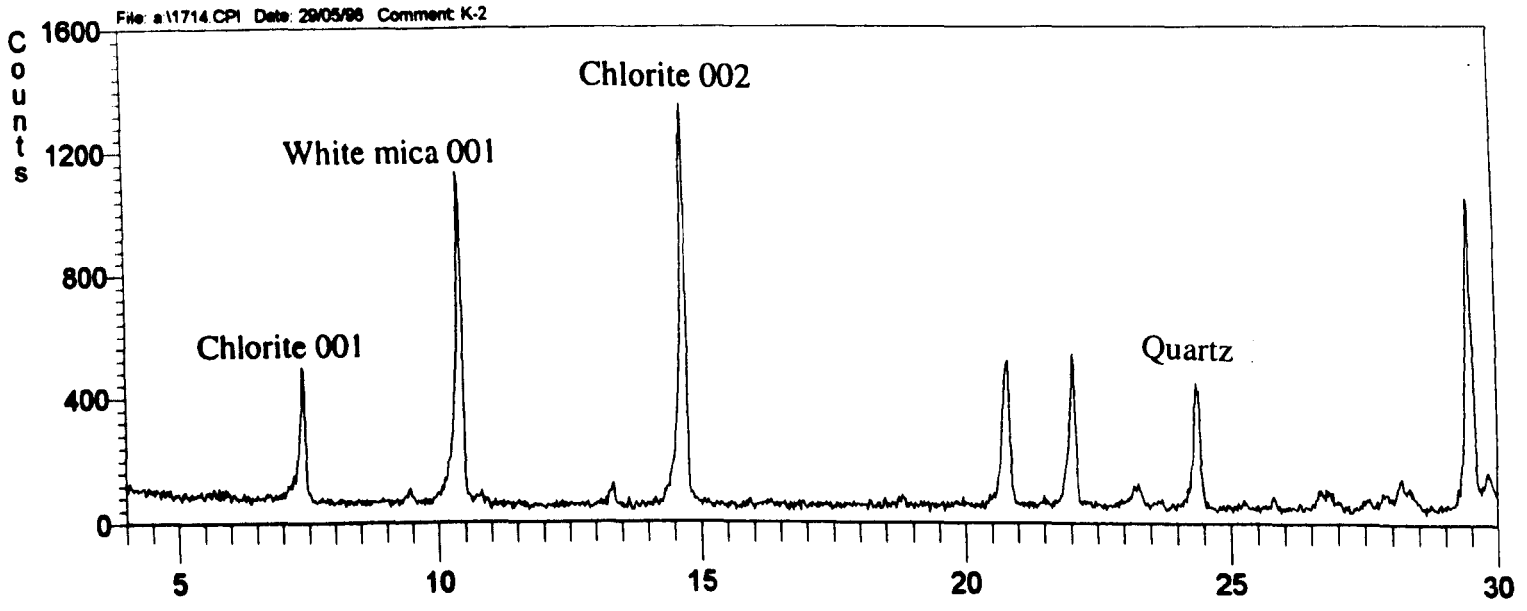
File: a:\1714.CPI Date: 29/05/96 Comment: K-2
Counts
1600
1200
800
400
0
Chlorite 002
White mica 001
Chlorite 001
Quartz
5
10
15
20
25
30

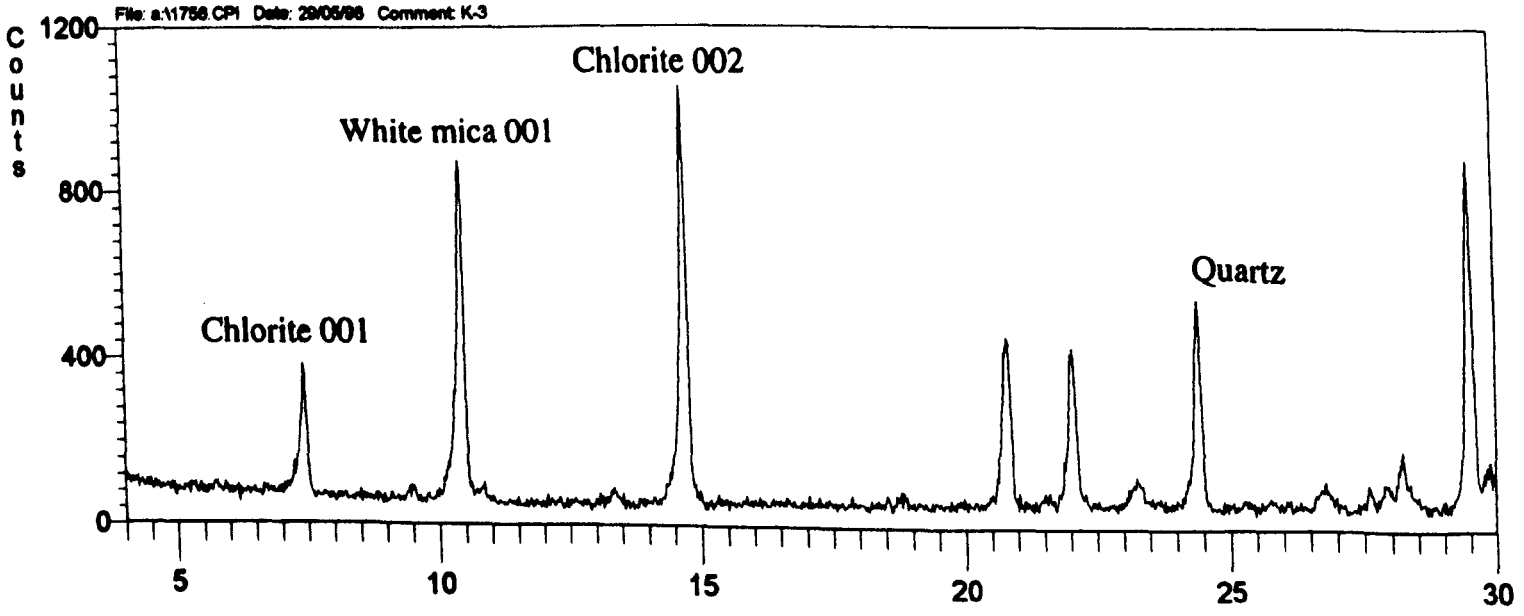
File: a:\1756.CPI Date: 29/05/96 Comment: K-3
Counts
1200
800
400
0
Chlorite 002
White mica 001
Chlorite 001
Quartz
5
10
15
20
25
30

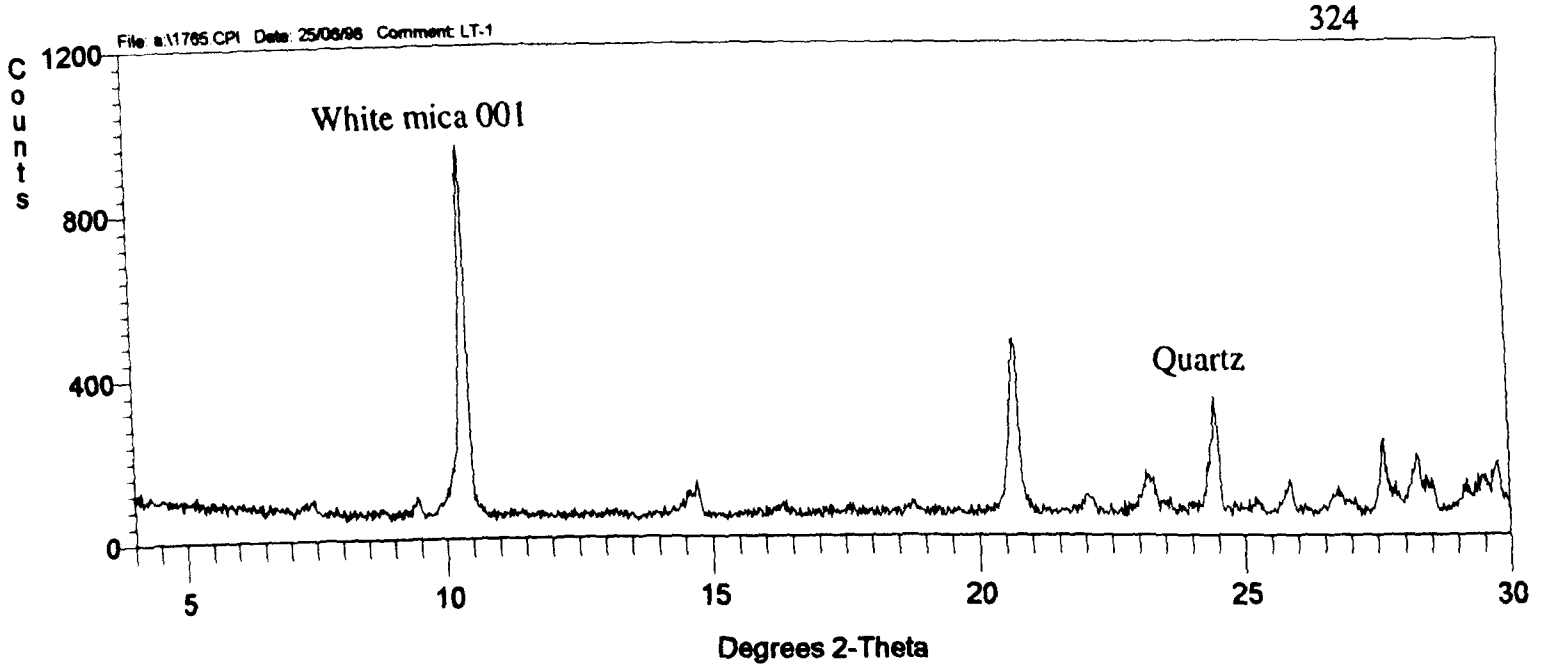
File: a:\1765.CPI Date: 25/06/96 Comment: LT-1
Counts
1200
800
400
0
White mica 001
Quartz
5
10
15
20
25
30
Degrees 2-Theta

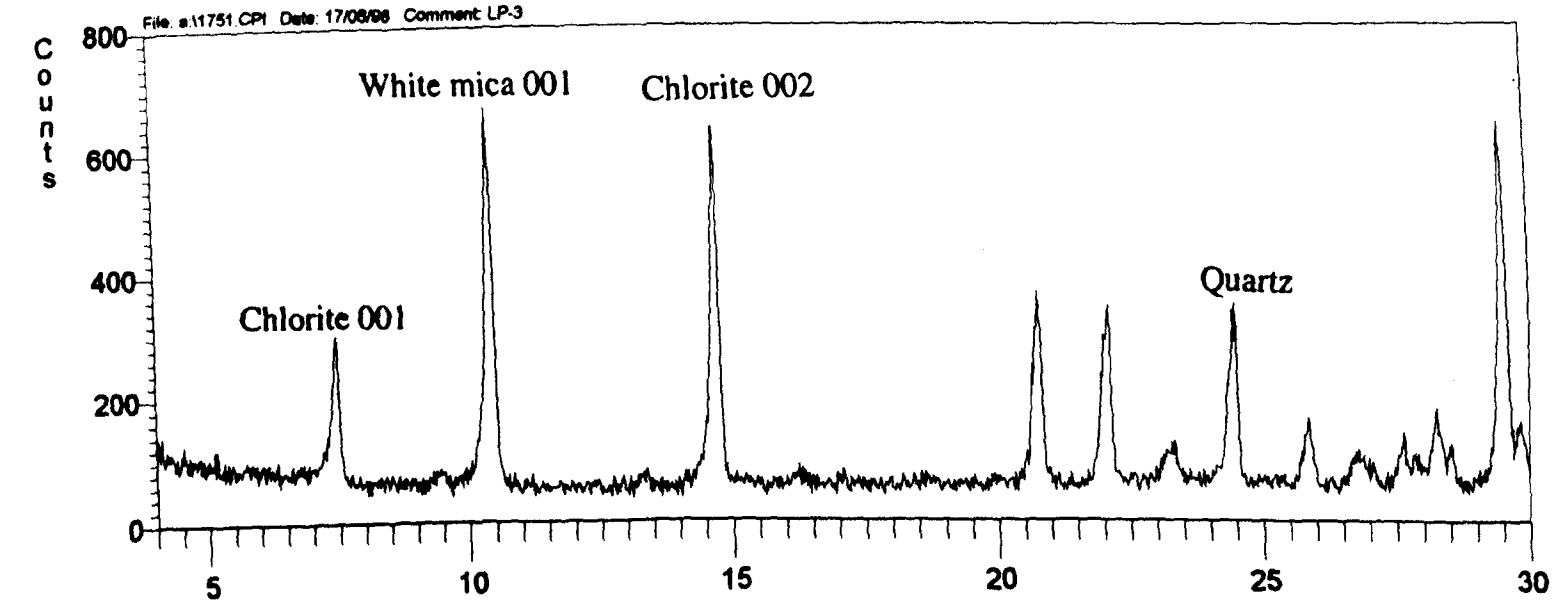
File: a:\1751.CPI Date: 17/06/96 Comment: LP-3
Counts
800
600
400
200
0
White mica 001
Chlorite 002
Chlorite 001
Quartz
5
10
15
20
25
30

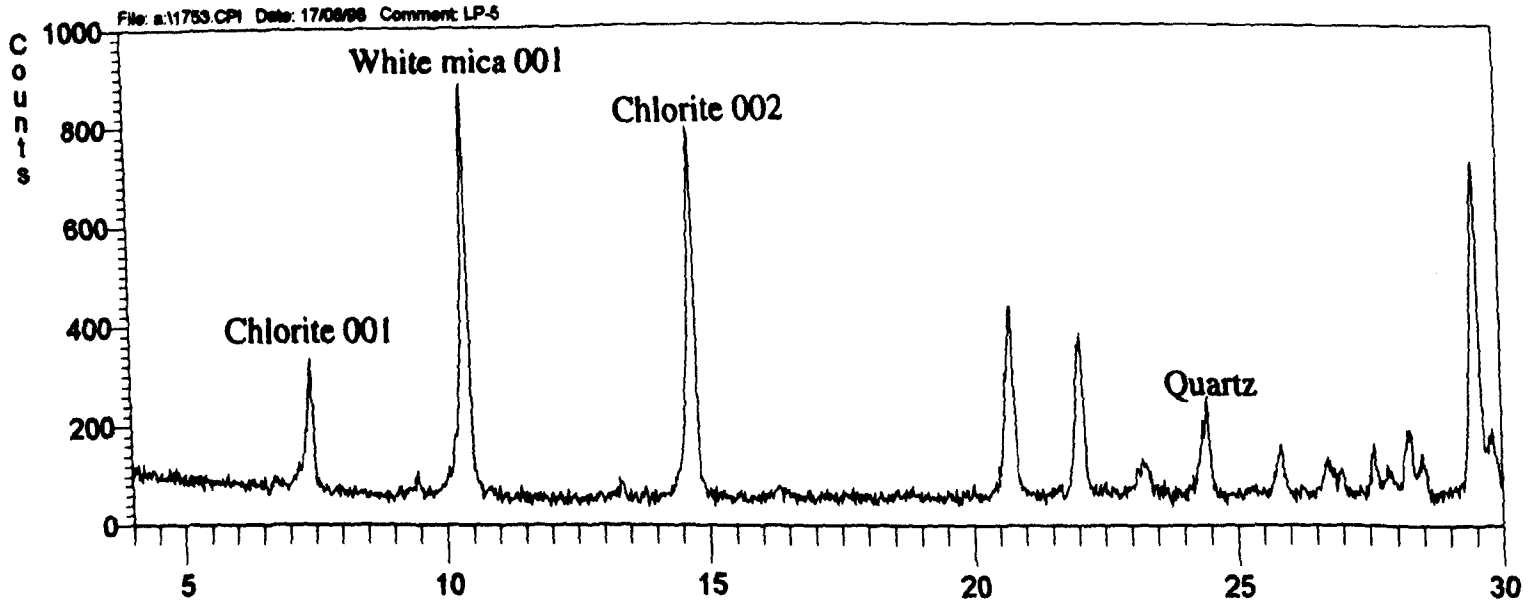
File: a:\1753.CPI Date: 17/06/96 Comment: LP-5
Counts
1000
800
600
400
200
0
White mica 001
Chlorite 002
Chlorite 001
Quartz
5
10
15
20
25
30

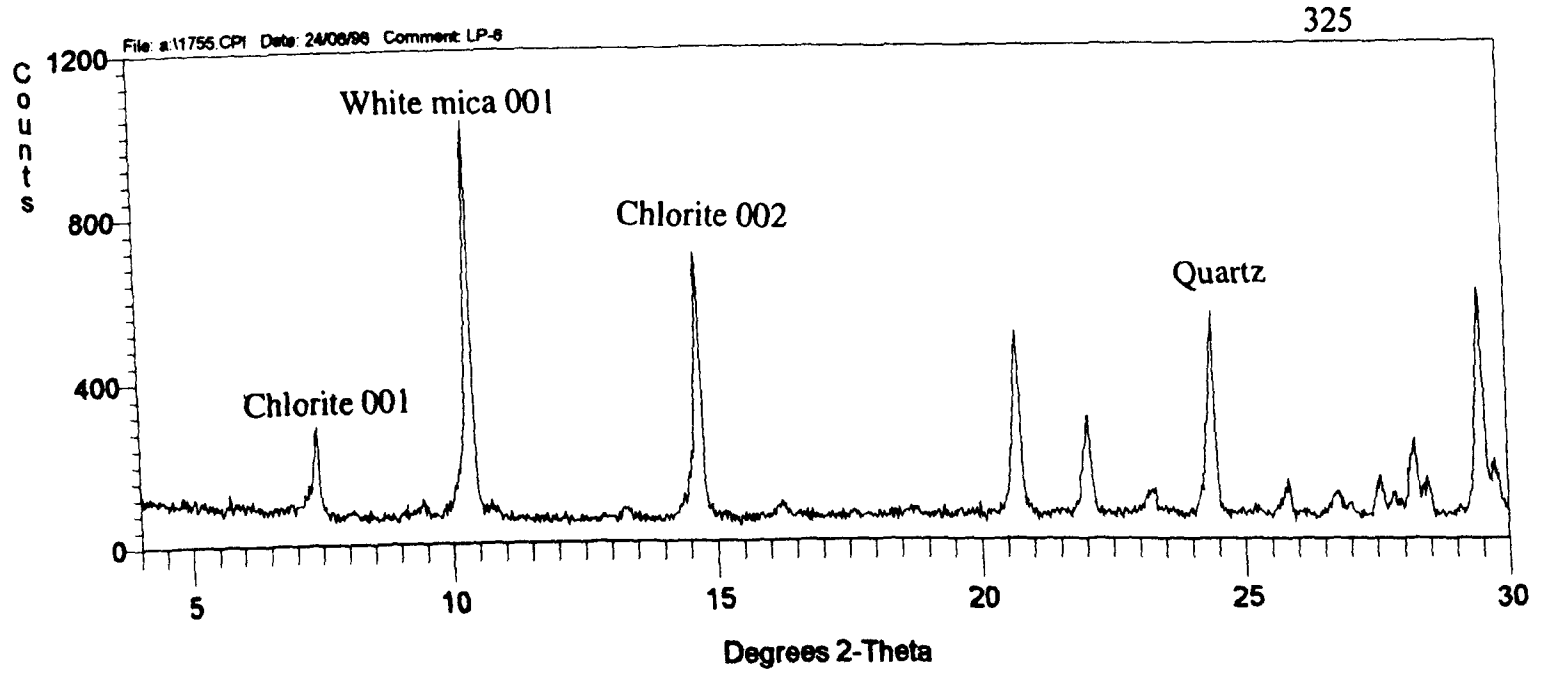
File: a:\11755.CPI Date: 24/06/96 Comment: LP-6
Counts
1200
800
400
0
White mica 001
Chlorite 002
Quartz
Chlorite 001
5
10
15
20
25
30
Degrees 2-Theta

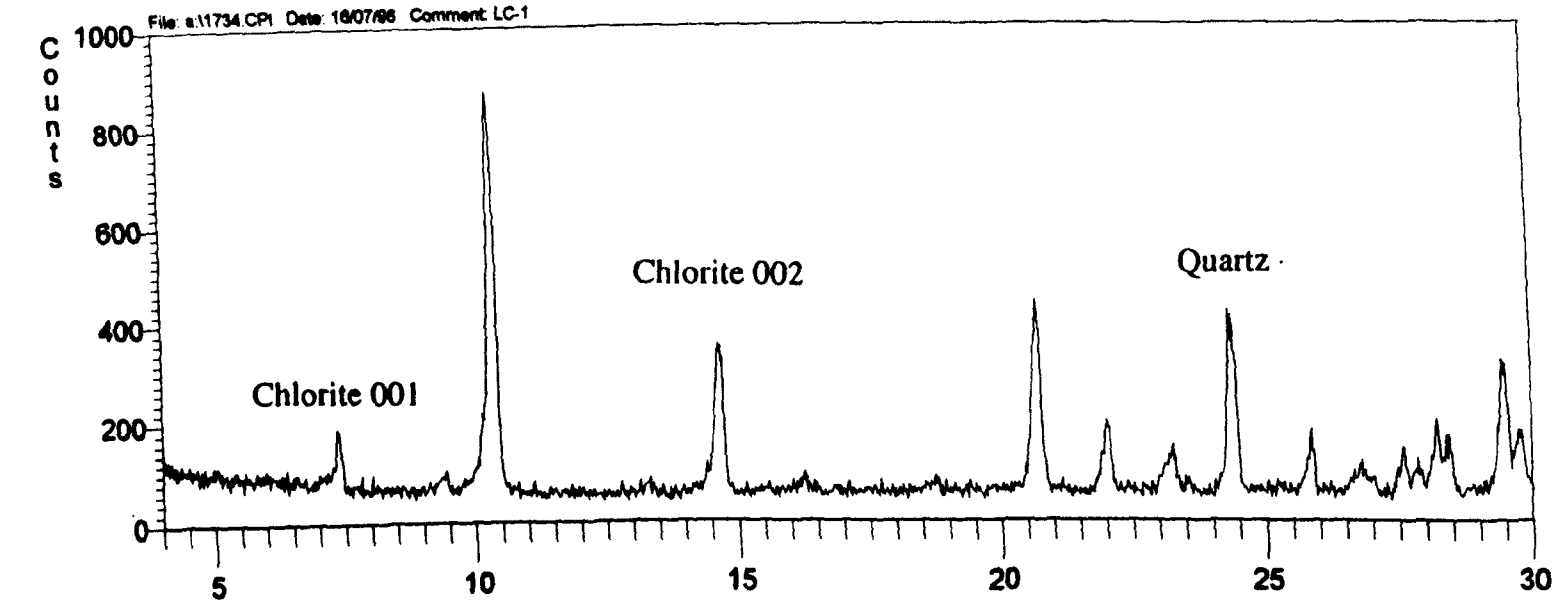
File: a:\11734.CPI Date: 16/07/96 Comment: LC-1
Counts
1000
800
600
400
200
0
Chlorite 002
Quartz
Chlorite 001
5
10
15
20
25
30

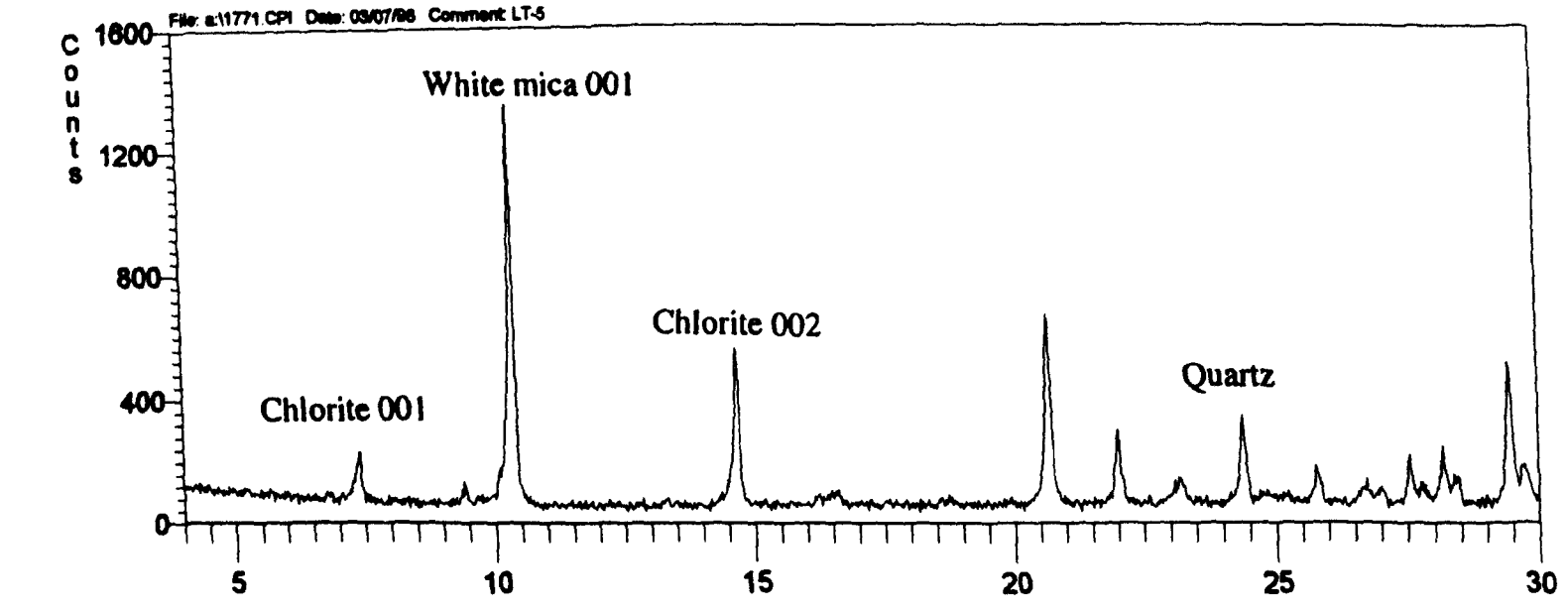
File: a:\11771.CPI Date: 03/07/96 Comment: LT-5
Counts
1600
1200
800
400
0
White mica 001
Chlorite 002
Quartz
Chlorite 001
5
10
15
20
25
30

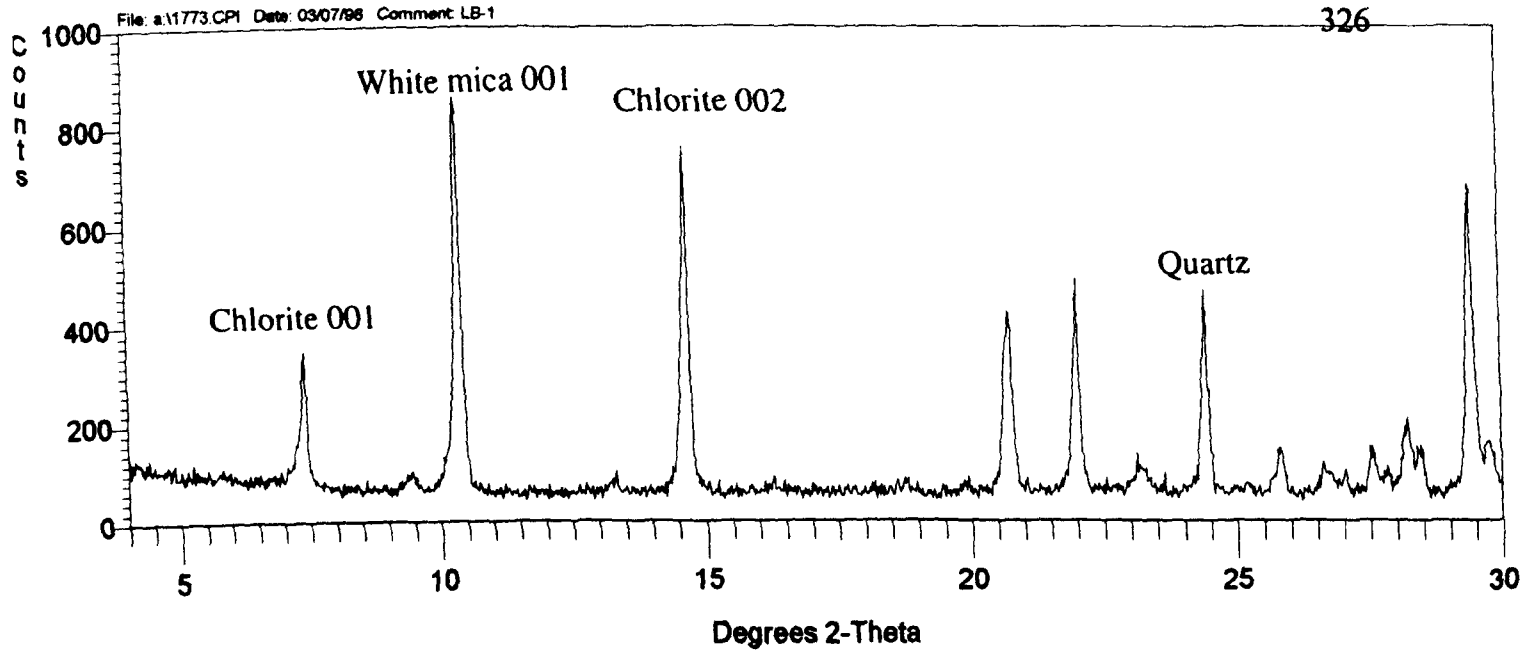
File: a:\1773.CPI Date: 03/07/96 Comment: LB-1
Counts
1000
800
600
400
200
0
White mica 001
Chlorite 002
Chlorite 001
Quartz
5
10
15
20
25
30
Degrees 2-Theta

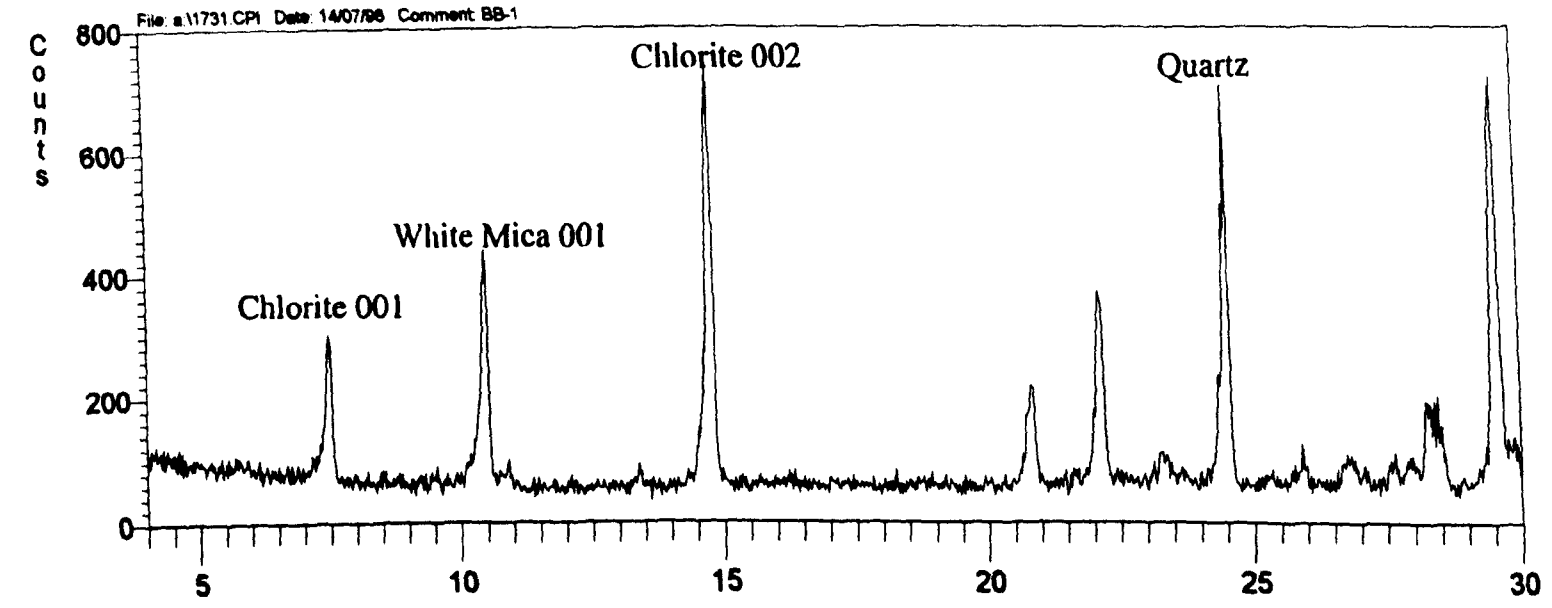
File: a:\1731.CPI Date: 14/07/96 Comment: BB-1
Counts
800
600
400
200
0
Chlorite 002
Quartz
White Mica 001
Chlorite 001
5
10
15
20
25
30

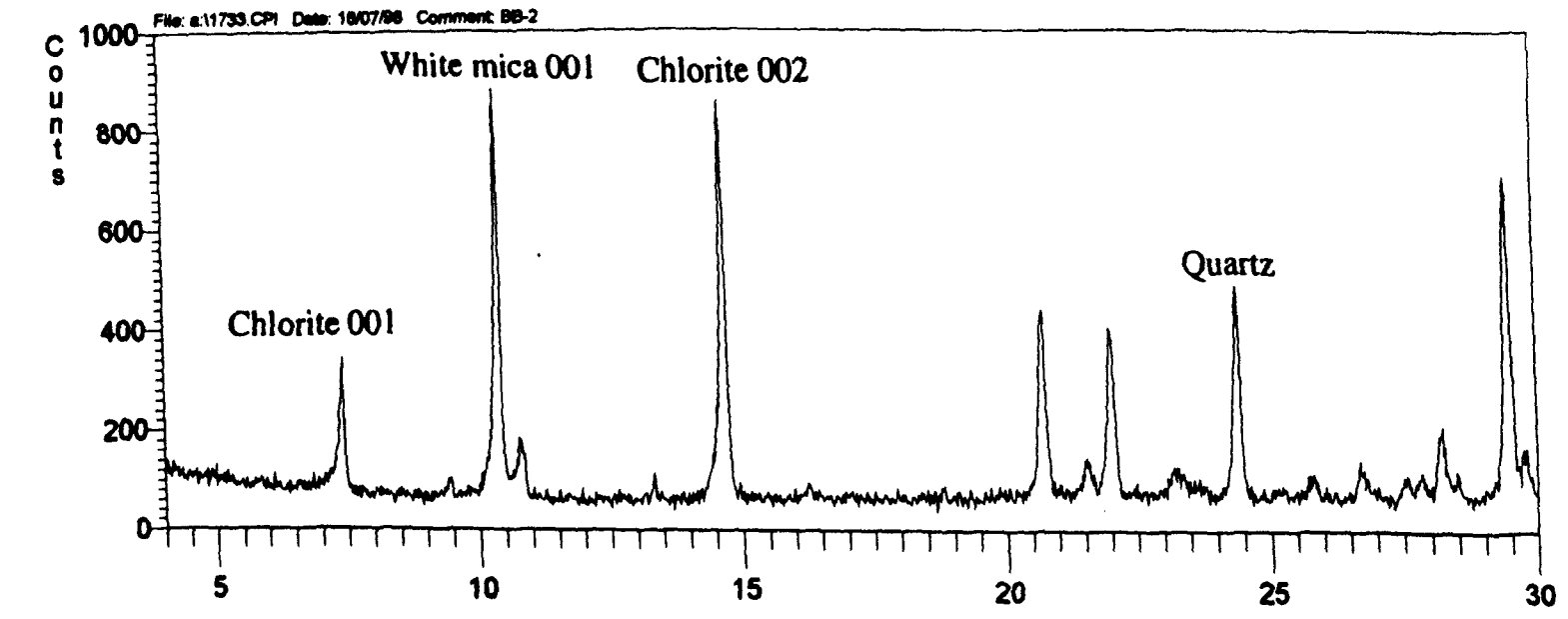
File: a:\1733.CPI Date: 16/07/96 Comment: BB-2
Counts
1000
800
600
400
200
0
White mica 001
Chlorite 002
Quartz
Chlorite 001
5
10
15
20
25
30

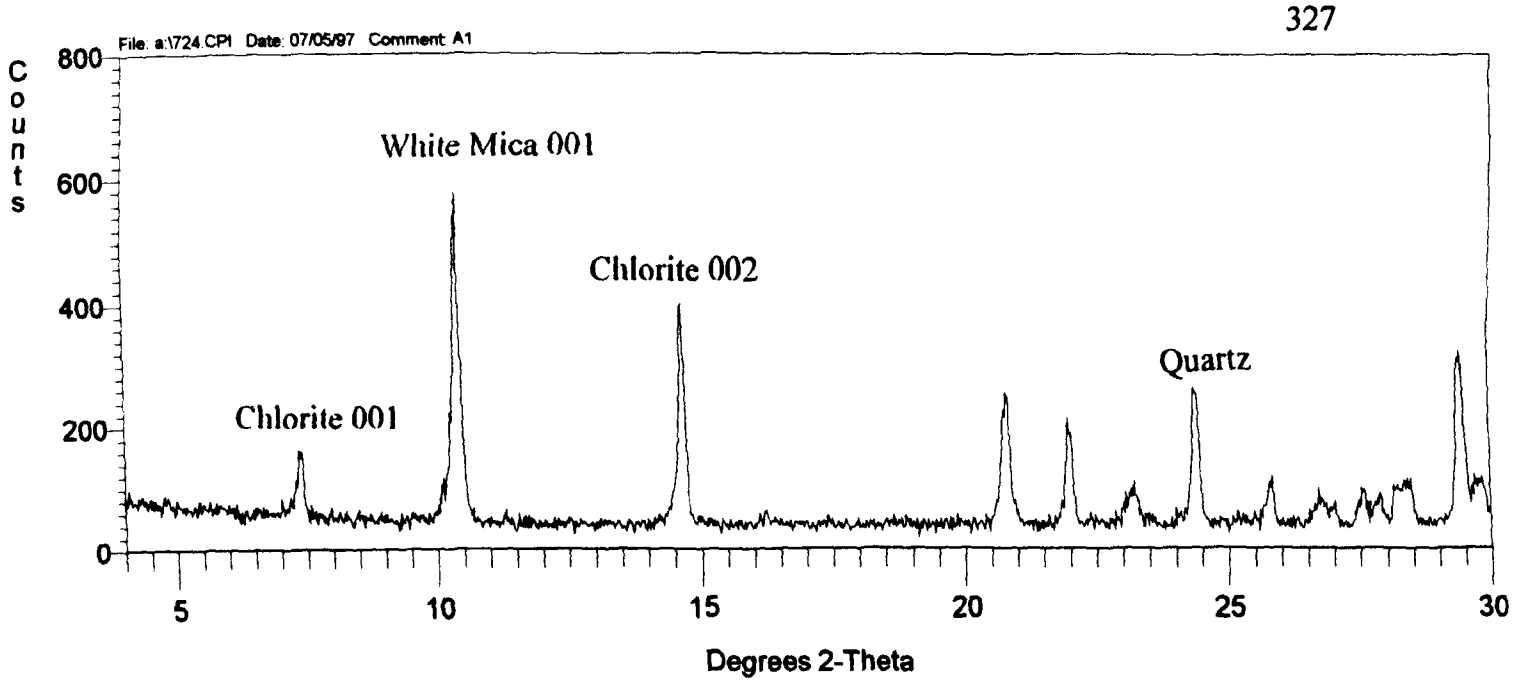
File: a:\724.CPI Date: 07/05/97 Comment: A1
Counts
800
600
400
200
0
White Mica 001
Chlorite 002
Quartz
Chlorite 001
5
10
15
20
25
30
Degrees 2-Theta

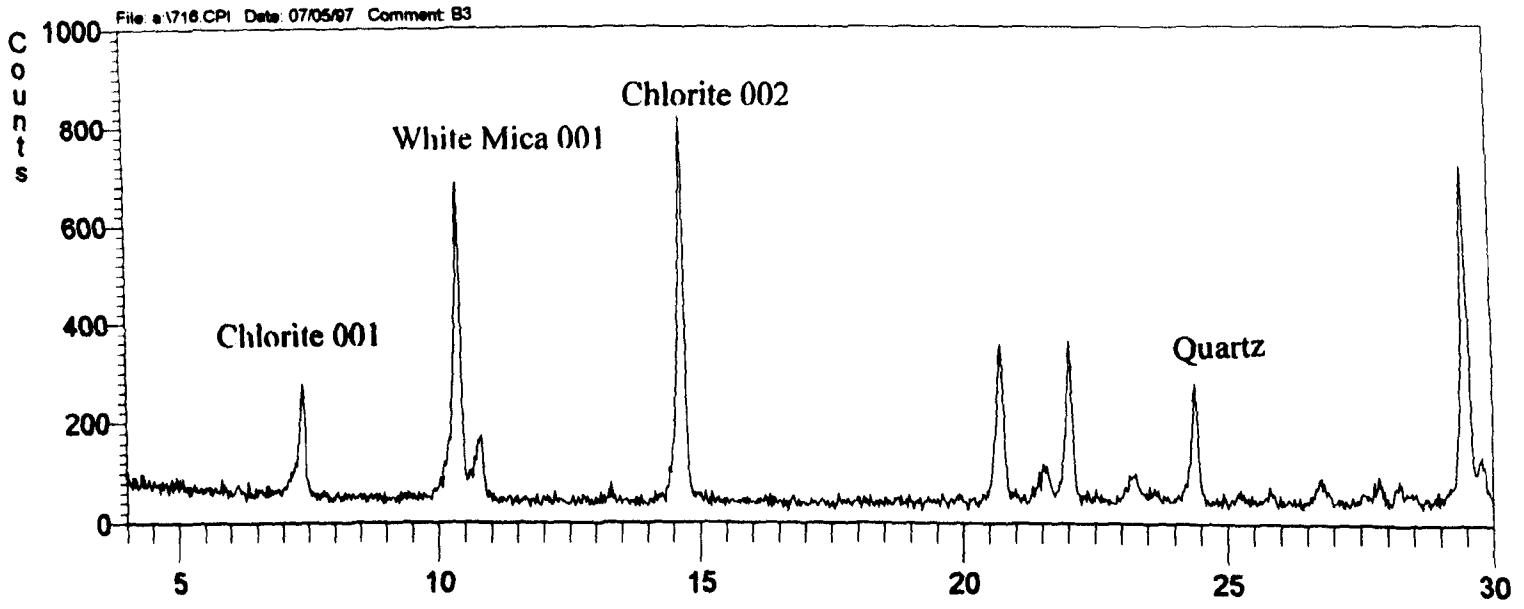
File: a:\716.CPI Date: 07/05/97 Comment: B3
Counts
1000
800
600
400
200
0
Chlorite 002
White Mica 001
Chlorite 001
Quartz
5
10
15
20
25
30

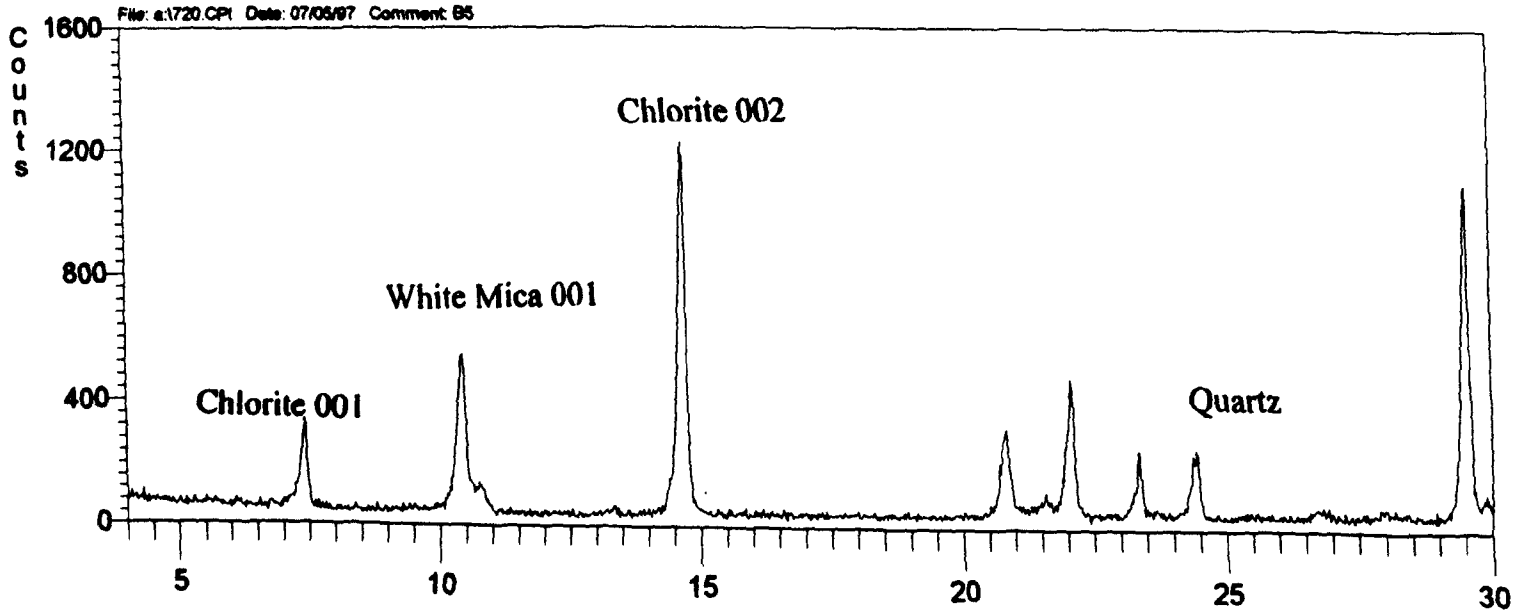
File: a:\720.CPI Date: 07/05/97 Comment: B5
Counts
1600
1200
800
400
0
Chlorite 002
White Mica 001
Chlorite 001
Quartz
5
10
15
20
25
30

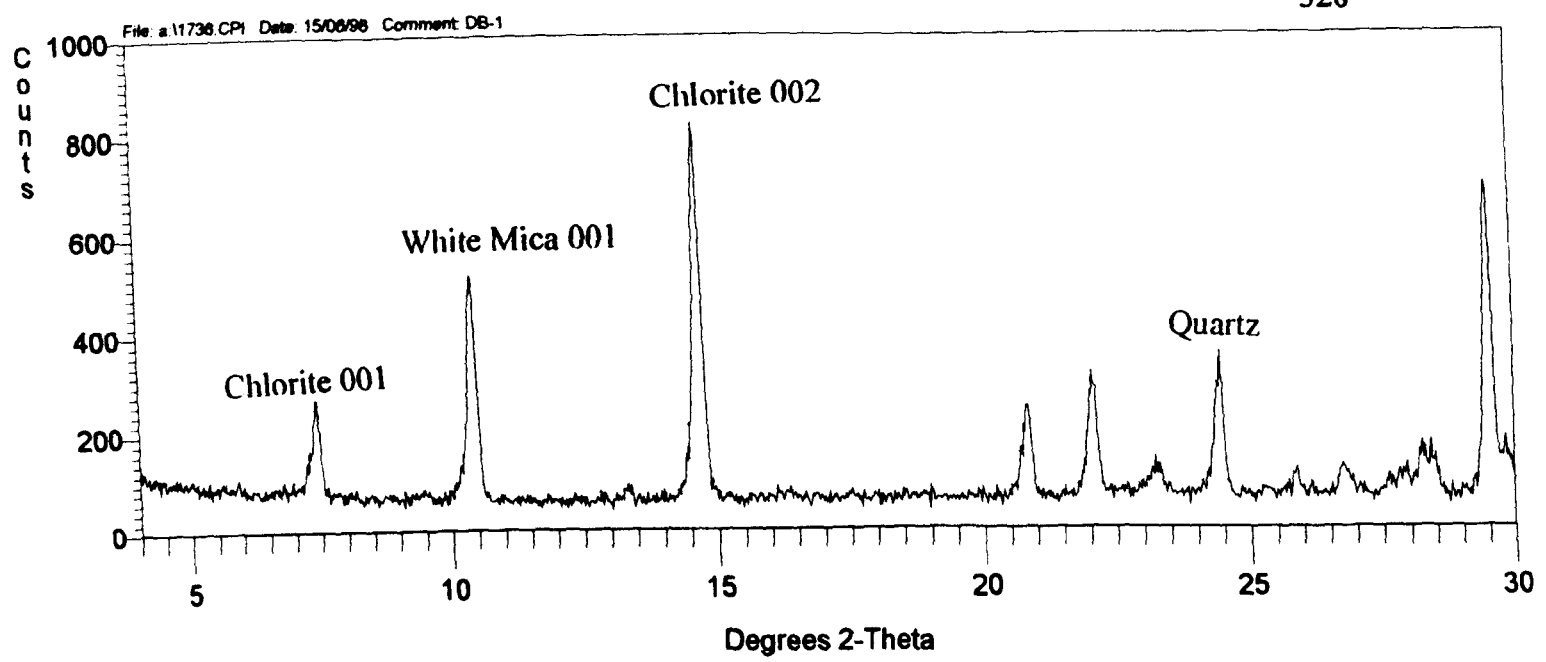
File: a:\1736.CPI Date: 15/06/96 Comment: DB-1
Counts
1000
800
600
400
200
0
Chlorite 002
White Mica 001
Chlorite 001
Quartz
5
10
15
20
25
30
Degrees 2-Theta

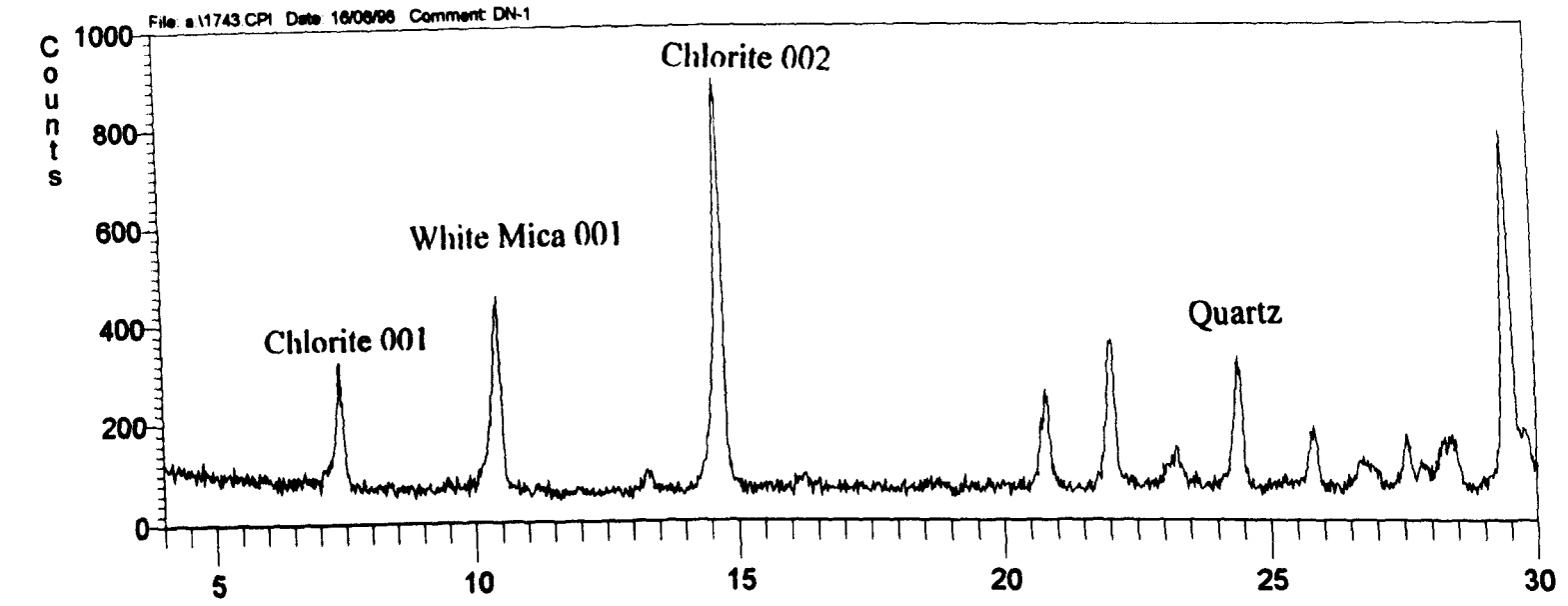
File: a:\1743.CPI Date: 16/06/96 Comment: DN-1
Counts
1000
800
600
400
200
0
Chlorite 002
White Mica 001
Chlorite 001
Quartz
5
10
15
20
25
30

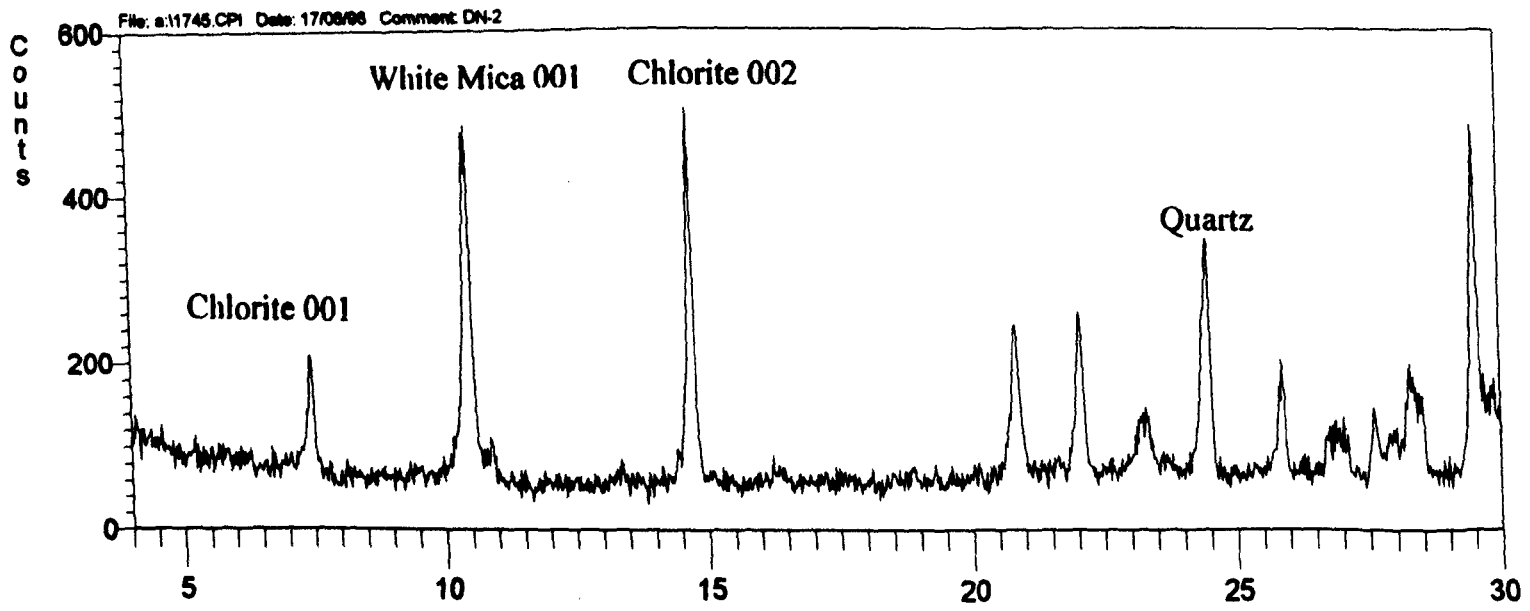
File: a:\1745.CPI Date: 17/06/96 Comment: DN-2
Counts
600
400
200
0
White Mica 001
Chlorite 002
Quartz
Chlorite 001
5
10
15
20
25
30

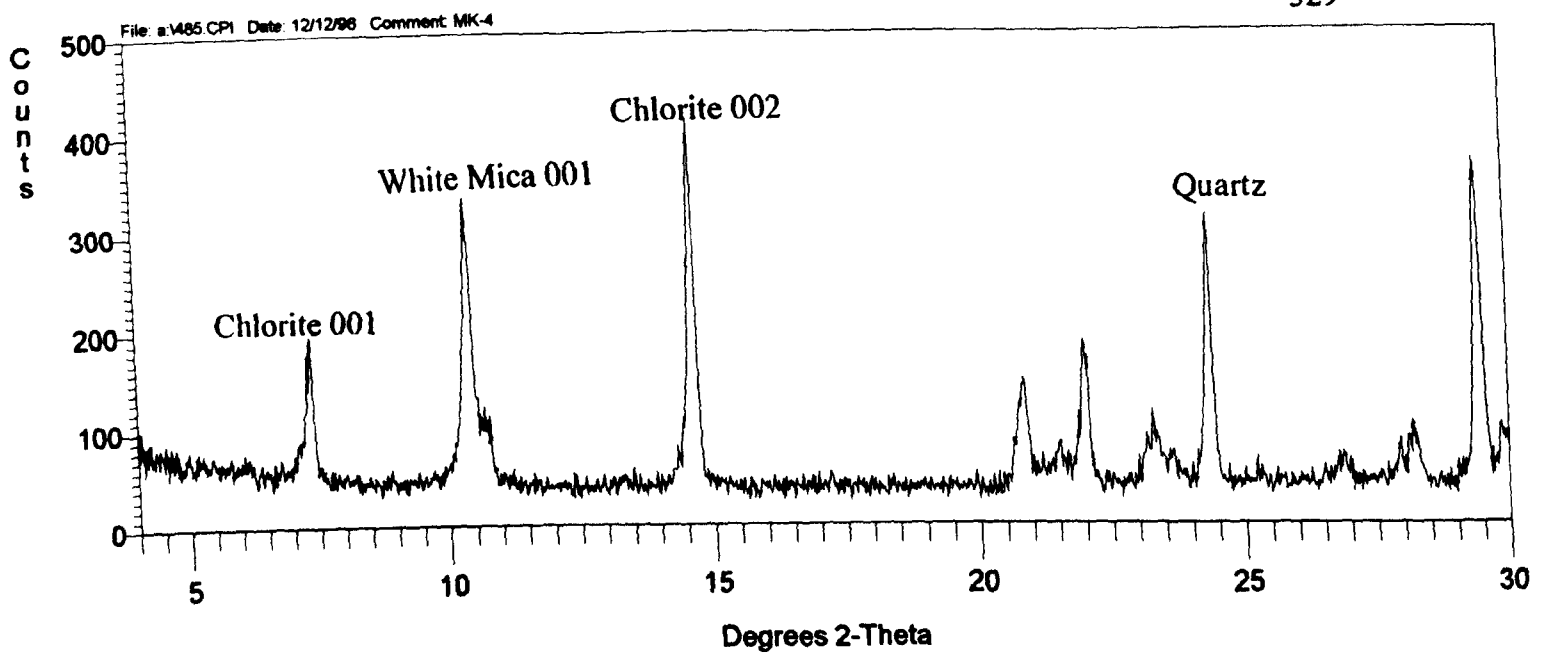
File: a:\485.CPI Date: 12/12/96 Comment: MK-4
Counts
500
400
300
200
100
0
Chlorite 001
White Mica 001
Chlorite 002
Quartz
5
10
15
20
25
30
Degrees 2-Theta

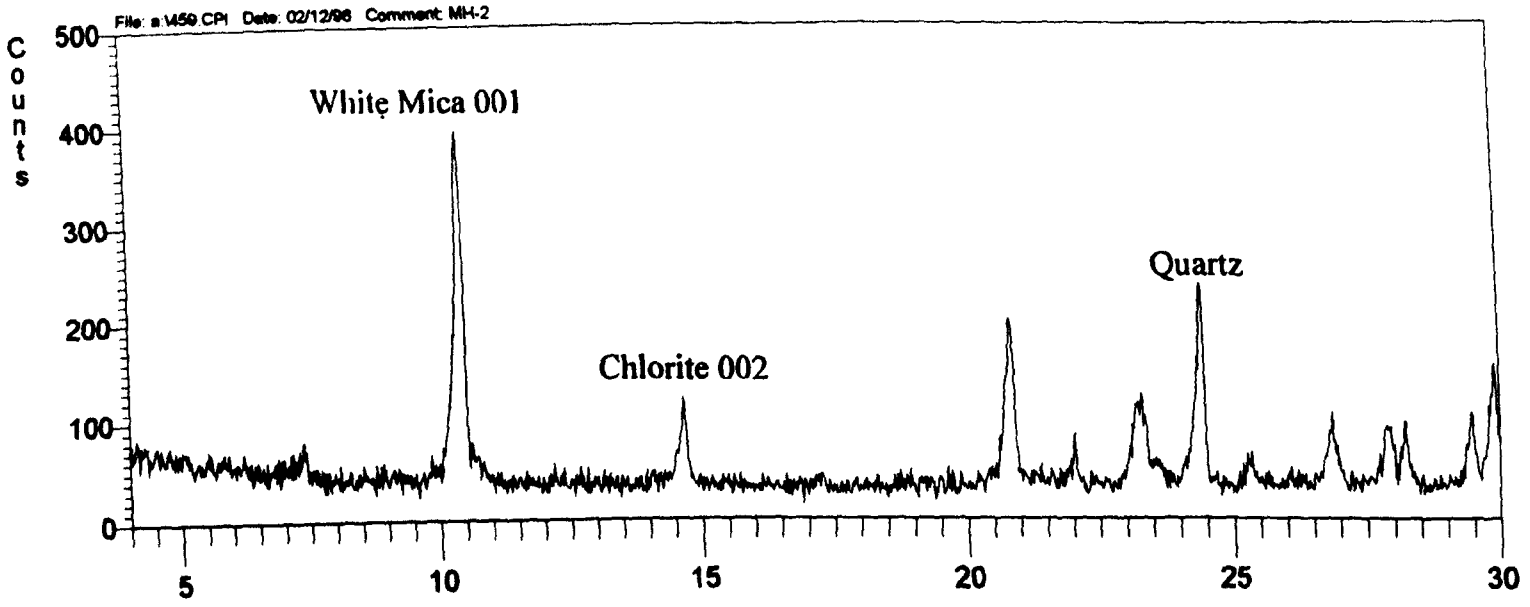
File: a:\459.CPI Date: 02/12/96 Comment: MH-2
Counts
500
400
300
200
100
0
White Mica 001
Chlorite 002
Quartz
5
10
15
20
25
30

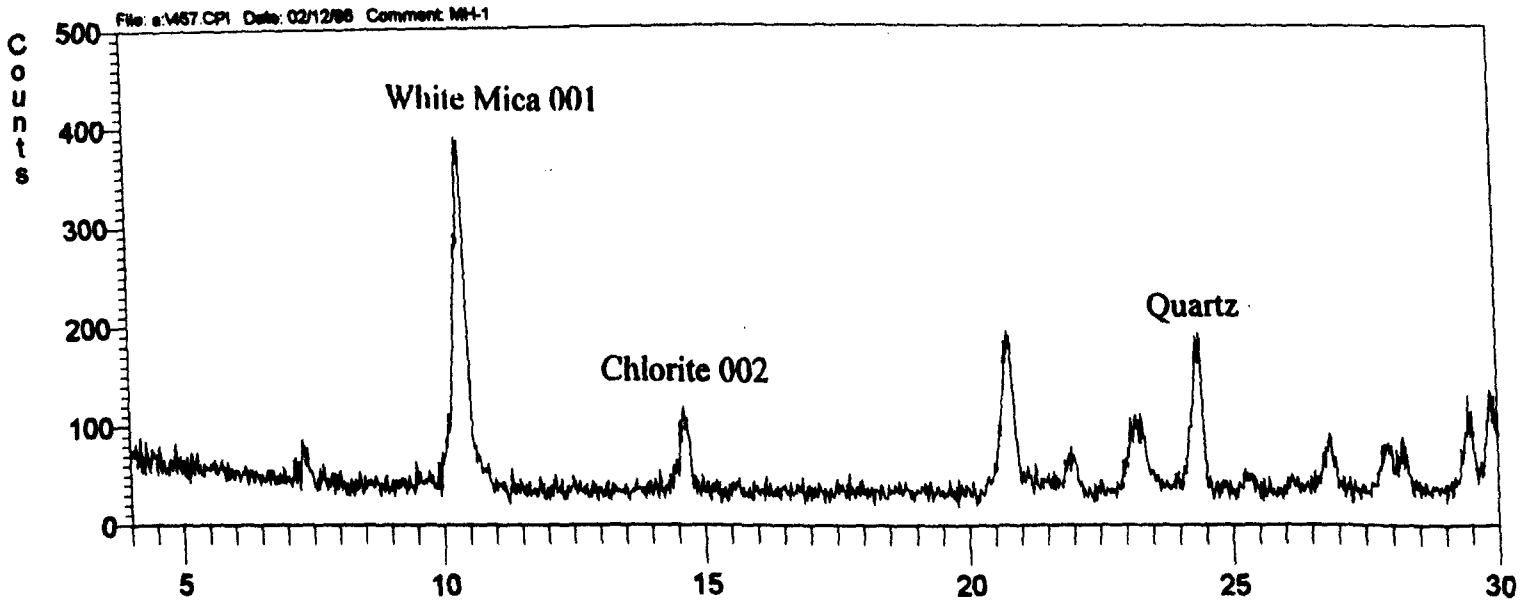
File: a:\457.CPI Date: 02/12/96 Comment: MH-1
Counts
500
400
300
200
100
0
White Mica 001
Chlorite 002
Quartz
5
10
15
20
25
30

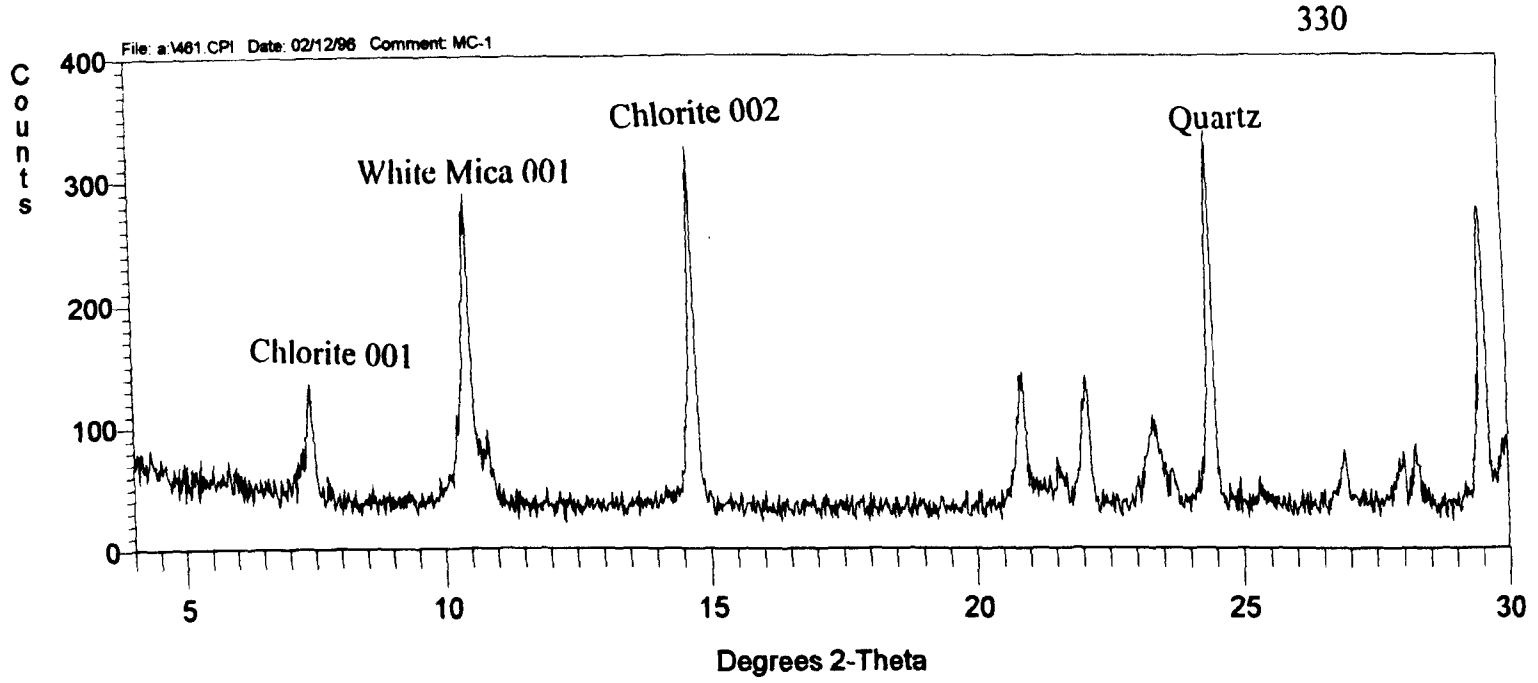
File: a:\461.CPI Date: 02/12/96 Comment: MC-1
Counts
Chlorite 002
Quartz
White Mica 001
Chlorite 001
Degrees 2-Theta

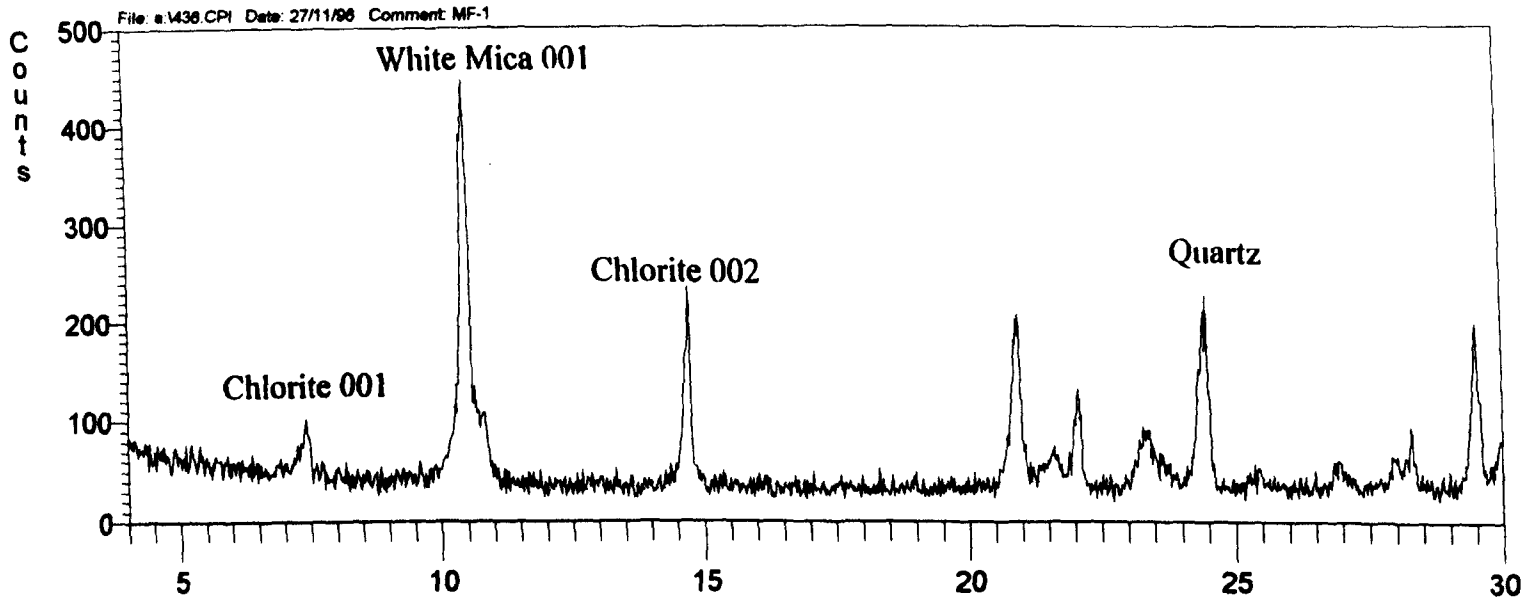
File: a:\436.CPI Date: 27/11/96 Comment: MF-1
Counts
White Mica 001
Chlorite 002
Quartz
Chlorite 001

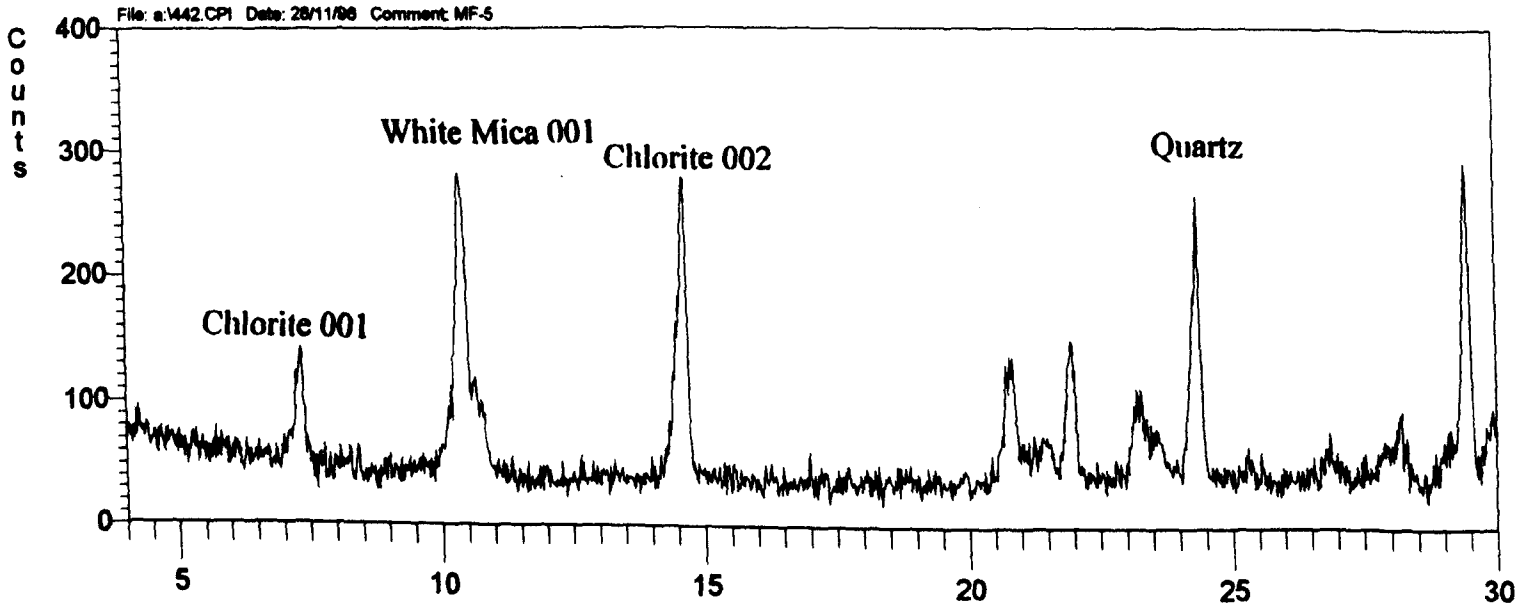
File: a:\442.CPI Date: 28/11/96 Comment: MF-5
Counts
White Mica 001
Chlorite 002
Quartz
Chlorite 001

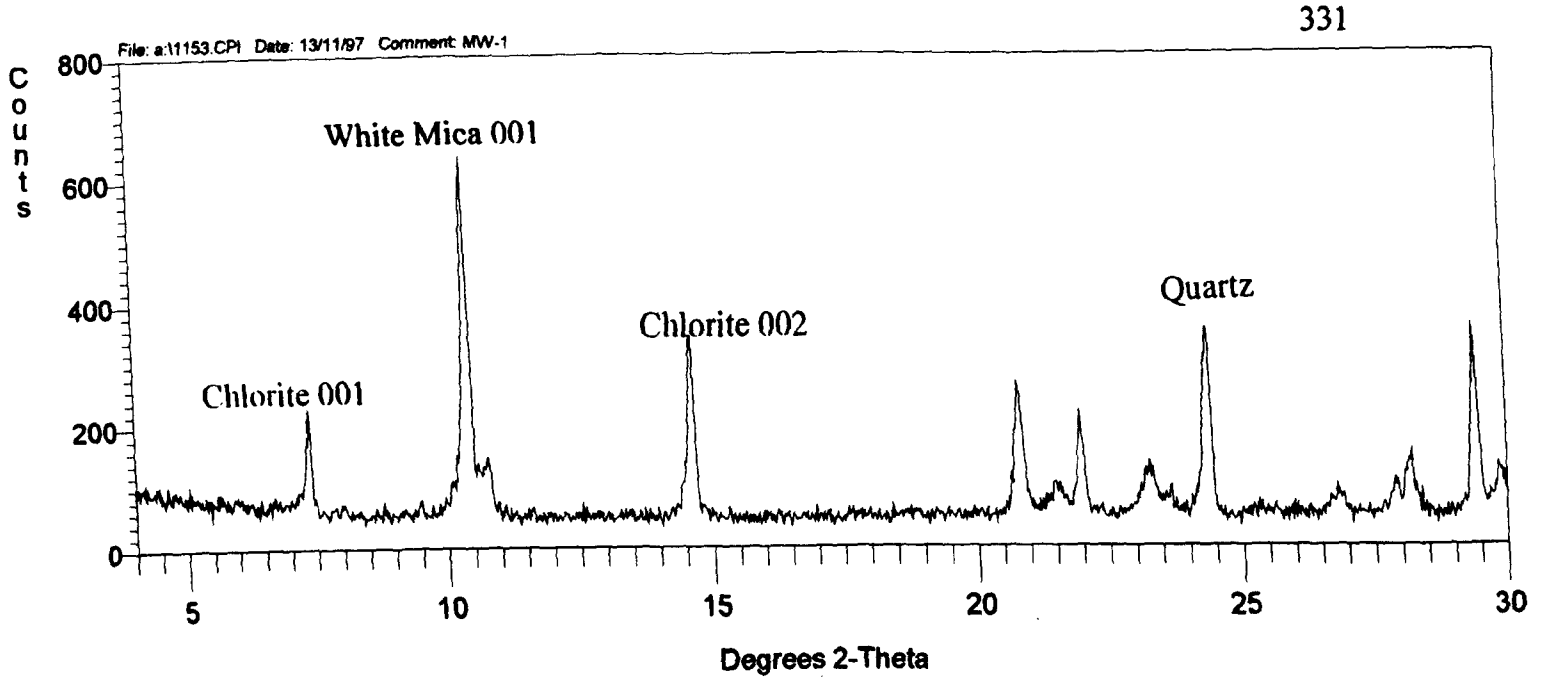
File: a:\1153.CPI Date: 13/11/97 Comment: MW-1
Counts
800
600
400
200
0
White Mica 001
Chlorite 002
Quartz
Chlorite 001
5
10
15
20
25
30
Degrees 2-Theta

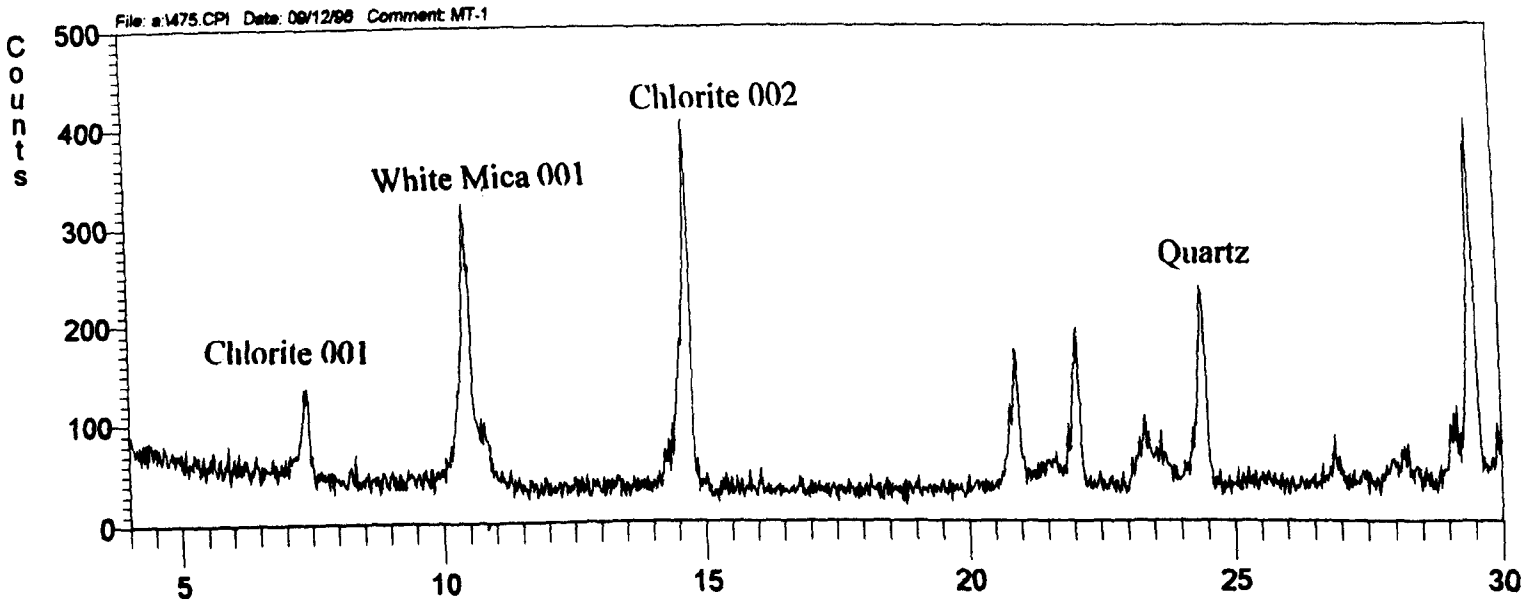
File: a:\475.CPI Date: 09/12/98 Comment: MT-1
Counts
500
400
300
200
100
0
Chlorite 002
White Mica 001
Quartz
Chlorite 001
5
10
15
20
25
30

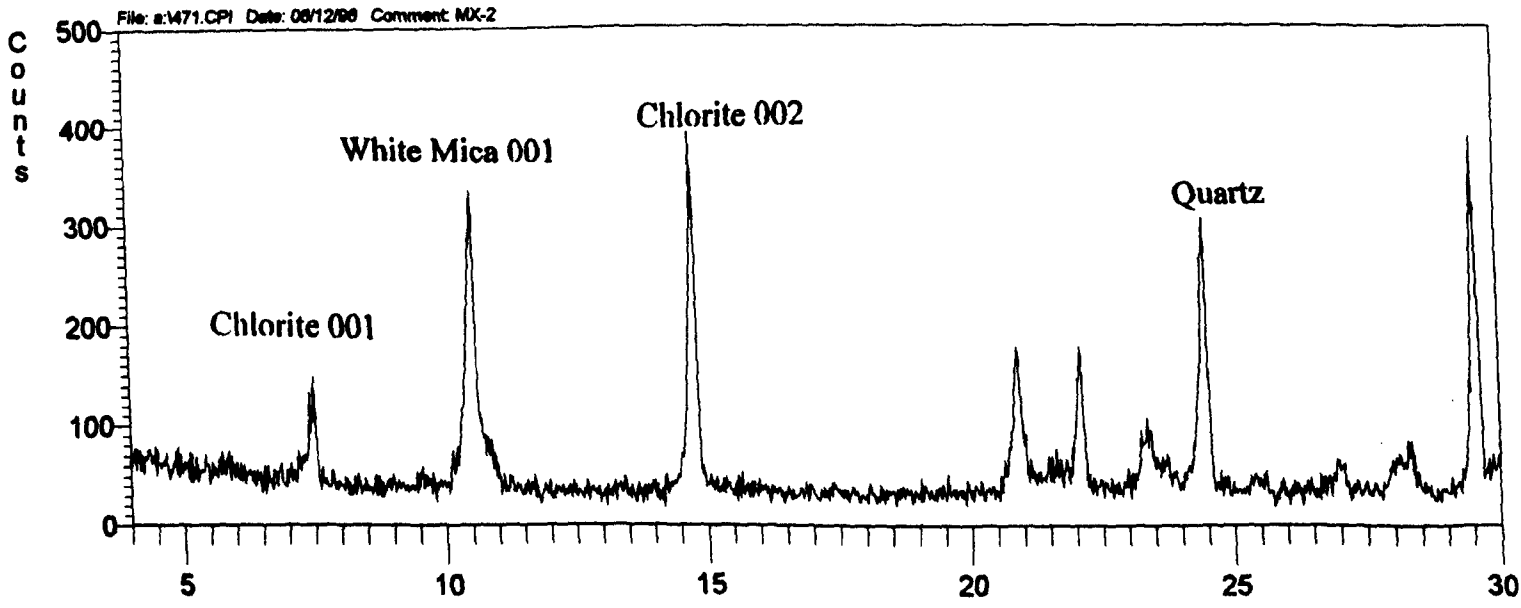
File: a:\471.CPI Date: 09/12/98 Comment: MX-2
Counts
500
400
300
200
100
0
Chlorite 002
White Mica 001
Quartz
Chlorite 001
5
10
15
20
25
30

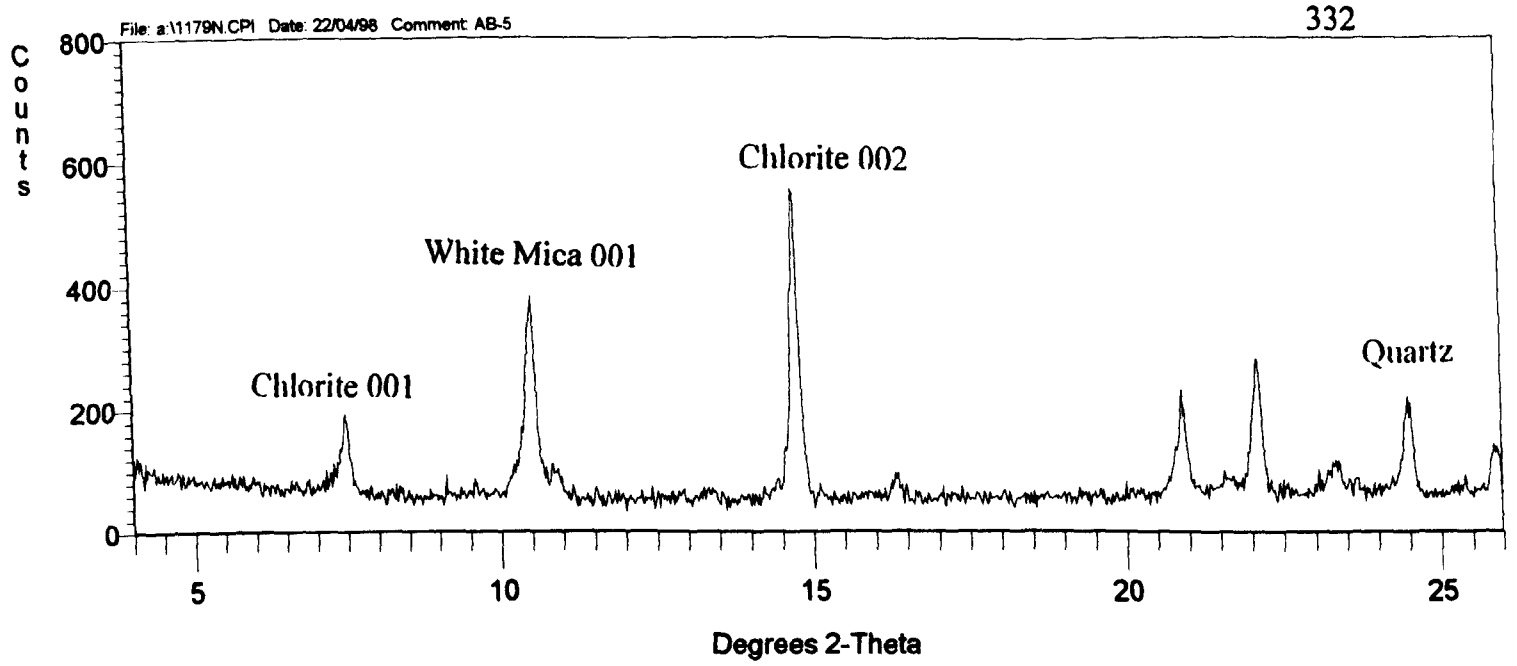
File: a:\1179N.CPI Date: 22/04/98 Comment: AB-5
Counts
800
600
400
200
0
Chlorite 002
White Mica 001
Chlorite 001
Quartz
5
10
15
20
25
Degrees 2-Theta

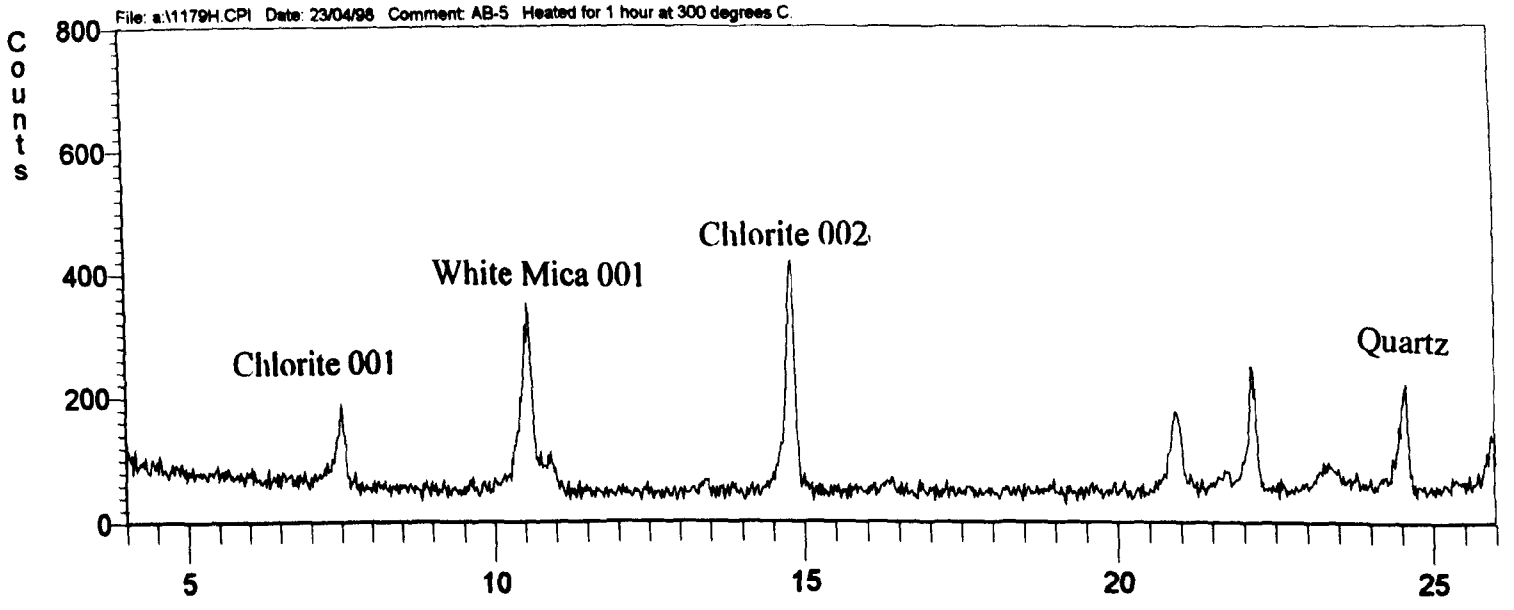
File: a:\1179H.CPI Date: 23/04/98 Comment: AB-5 Heated for 1 hour at 300 degrees C.
Counts
800
600
400
200
0
Chlorite 002
White Mica 001
Chlorite 001
Quartz
5
10
15
20
25

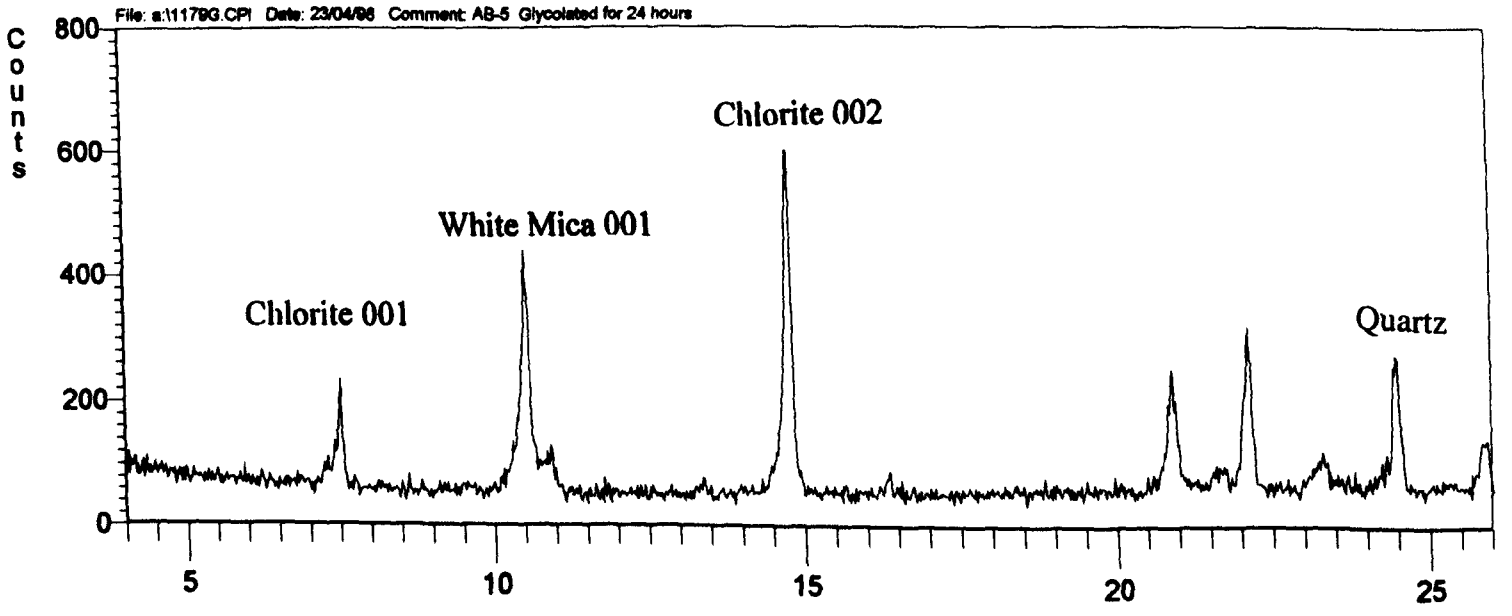
File: a:\1179G.CPI Date: 23/04/98 Comment: AB-5 Glycolated for 24 hours
Counts
800
600
400
200
0
Chlorite 002
White Mica 001
Chlorite 001
Quartz
5
10
15
20
25

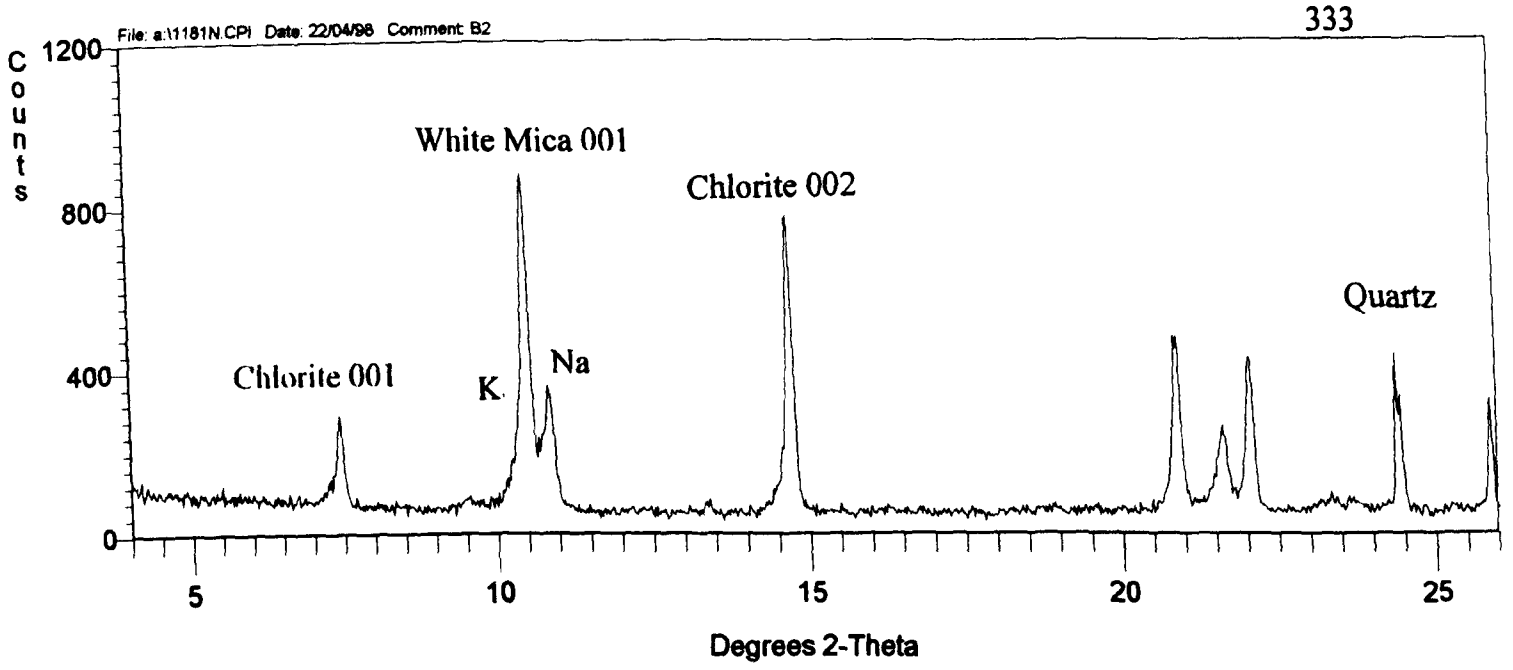
File: a:\1181N.CPI Date: 22/04/98 Comment: B2
Counts
1200
800
400
0
White Mica 001
Chlorite 002
Quartz
Chlorite 001
K
Na
5
10
15
20
25
Degrees 2-Theta

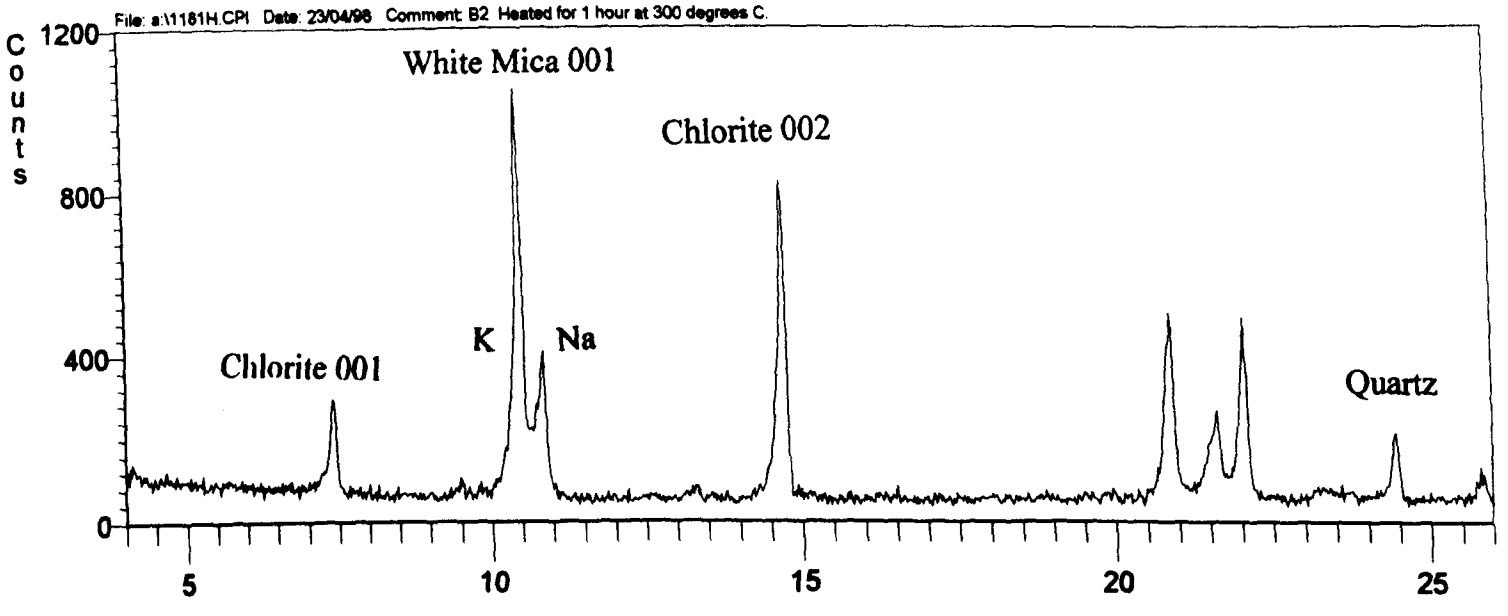
File: a:\1181H.CPI Date: 23/04/98 Comment: B2 Heated for 1 hour at 300 degrees C.
Counts
1200
800
400
0
White Mica 001
Chlorite 002
K
Na
Chlorite 001
Quartz
5
10
15
20
25

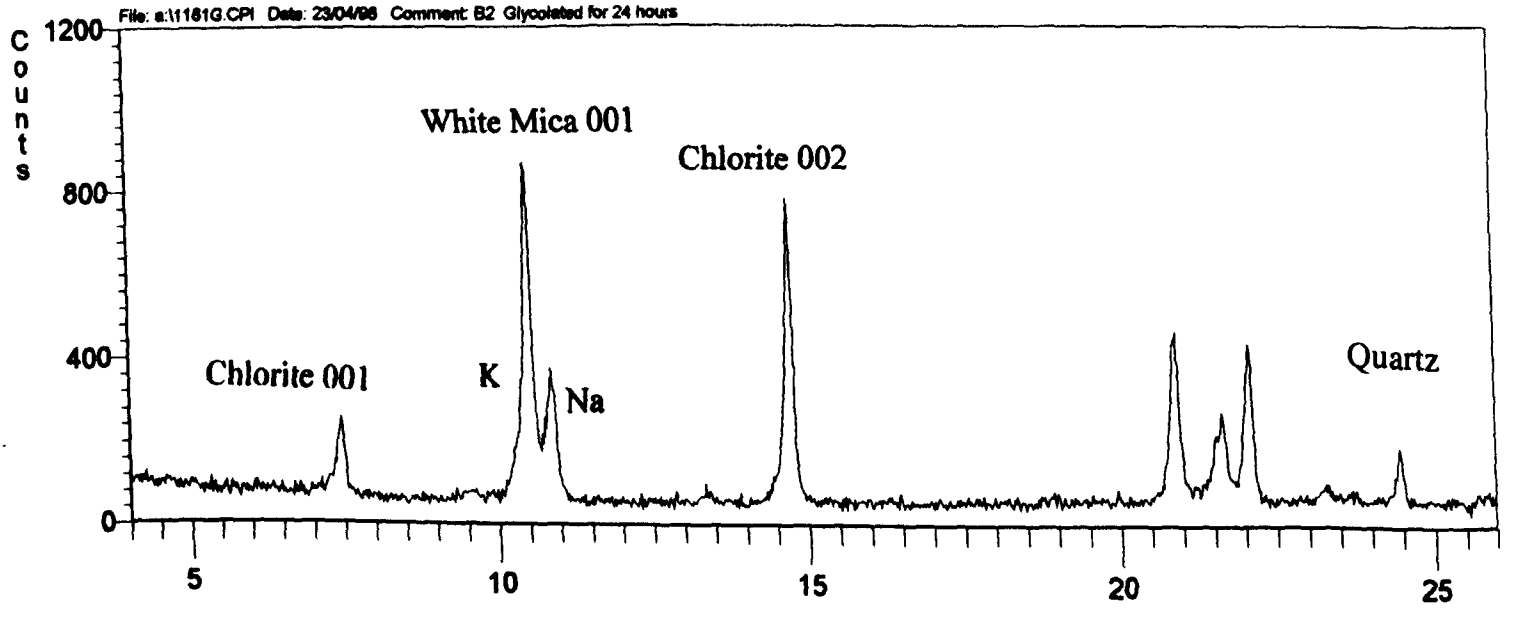
File: a:\1181G.CPI Date: 23/04/98 Comment: B2 Glycolated for 24 hours
Counts
1200
800
400
0
White Mica 001
Chlorite 002
Chlorite 001
K
Na
Quartz
5
10
15
20
25

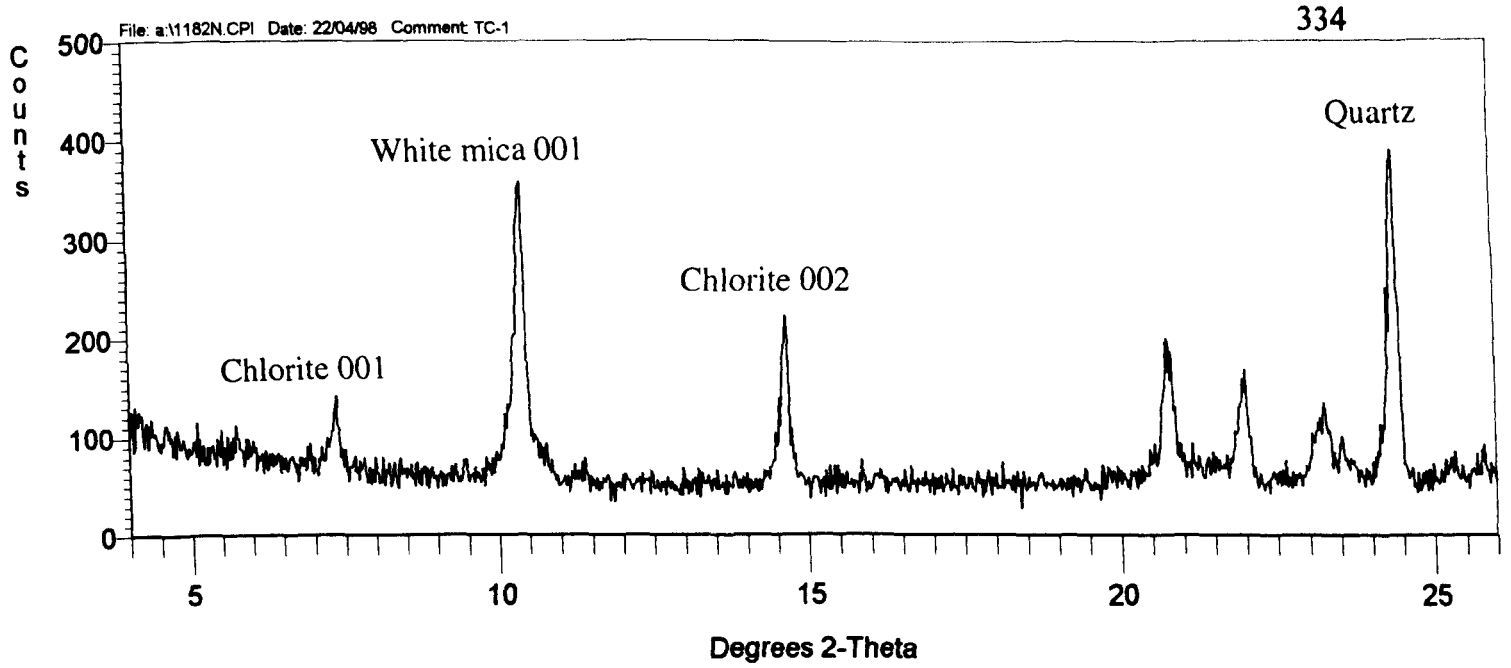
File: a:\1182N.CPI Date: 22/04/98 Comment: TC-1
Counts
500
400
300
200
100
0
White mica 001
Chlorite 002
Chlorite 001
Quartz
5
10
15
20
25
Degrees 2-Theta

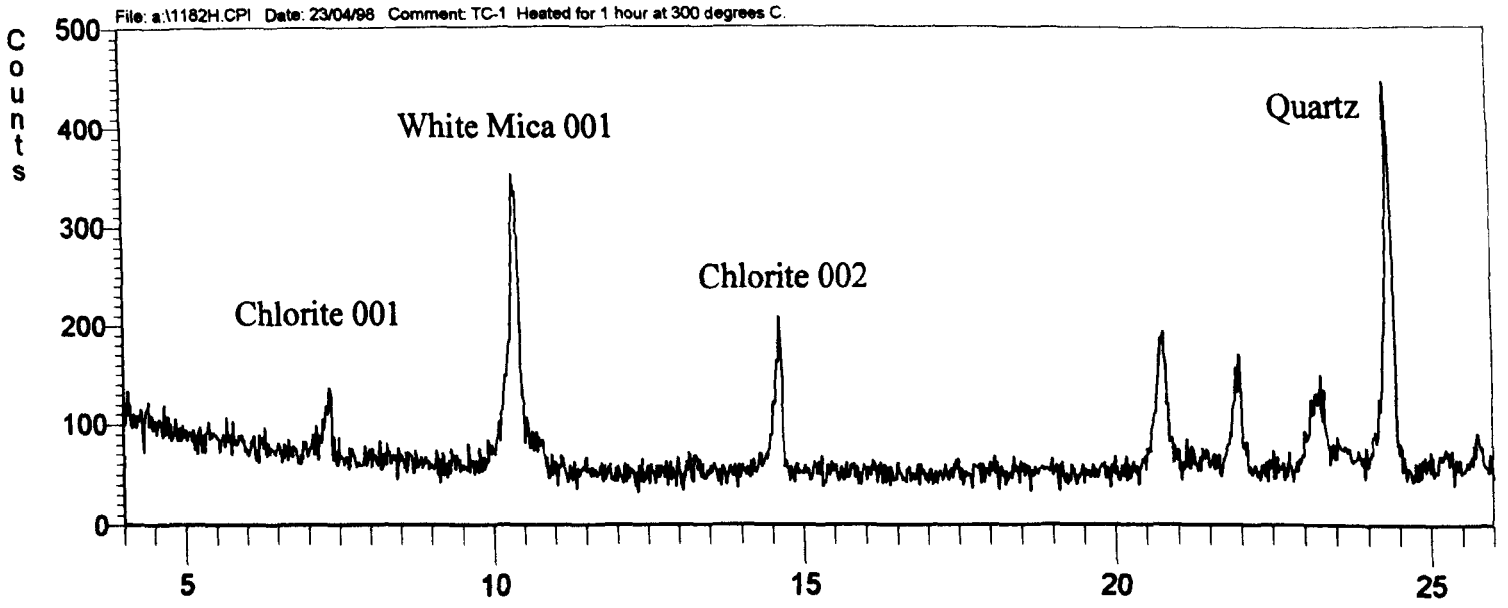
File: a:\1182H.CPI Date: 23/04/98 Comment: TC-1 Heated for 1 hour at 300 degrees C.
Counts
500
400
300
200
100
0
White Mica 001
Chlorite 002
Chlorite 001
Quartz
5
10
15
20
25

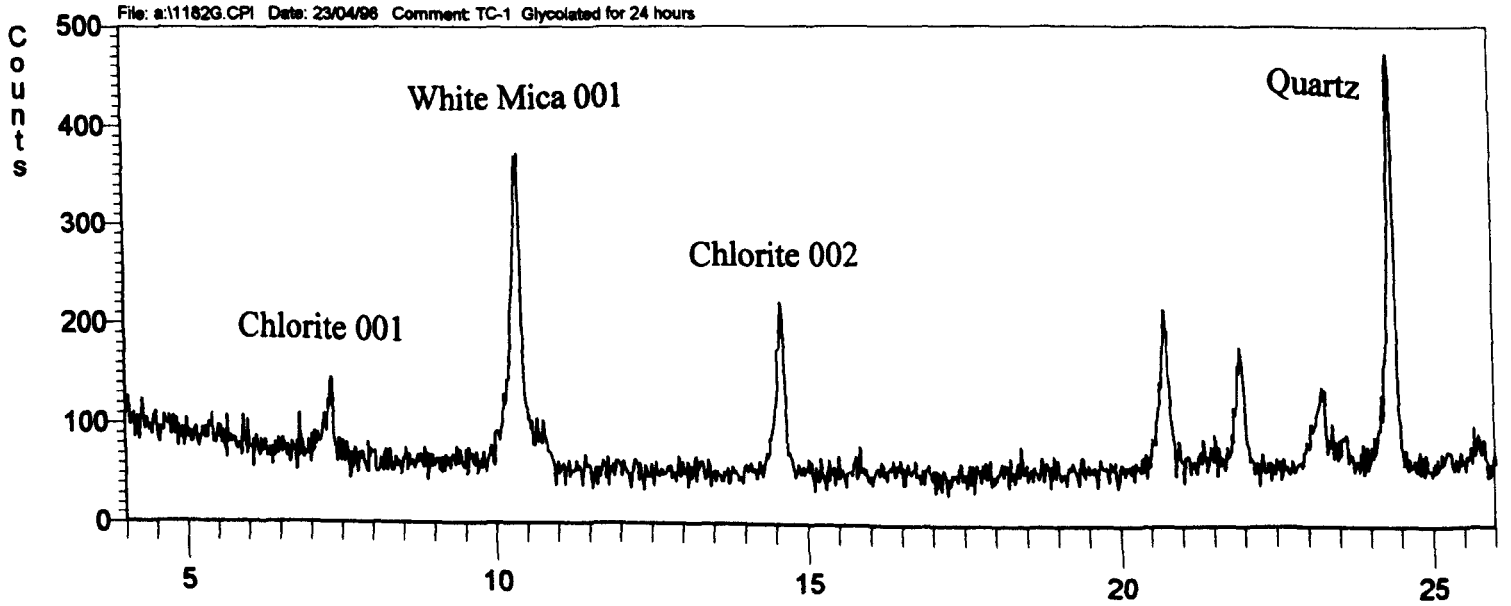
File: a:\1182G.CPI Date: 23/04/98 Comment: TC-1 Glycolated for 24 hours
Counts
500
400
300
200
100
0
White Mica 001
Chlorite 002
Chlorite 001
Quartz
5
10
15
20
25

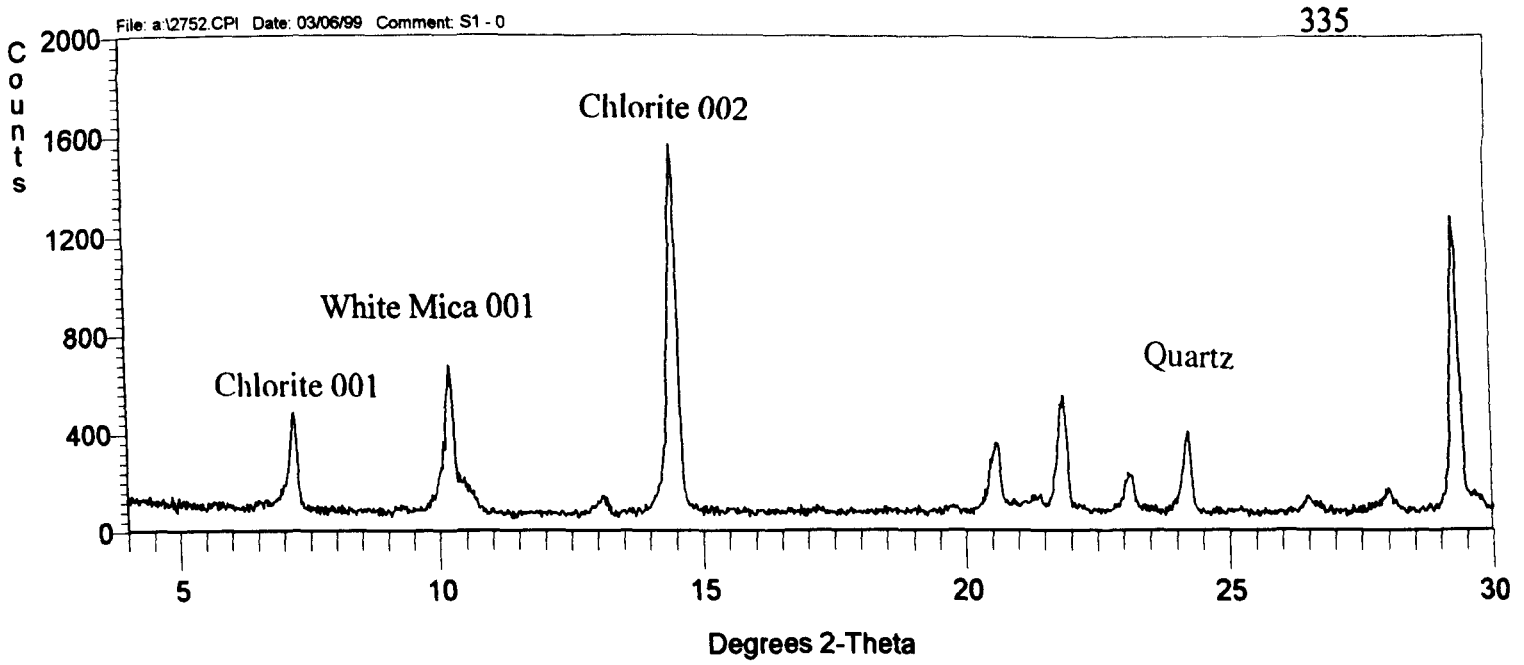
File: a:\2752.CPI Date: 03/06/99 Comment: S1 - 0
Counts
2000
1600
1200
800
400
0
Chlorite 002
White Mica 001
Chlorite 001
Quartz
5
10
15
20
25
30
Degrees 2-Theta

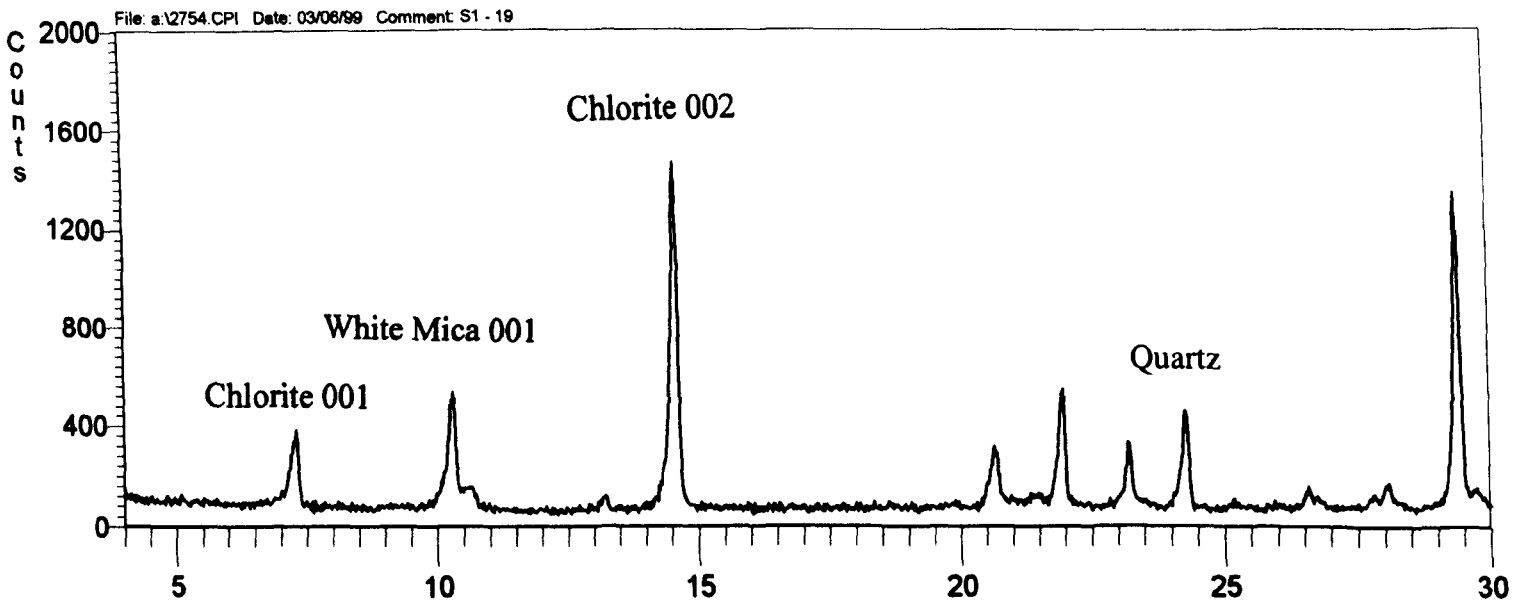
File: a:\2754.CPI Date: 03/06/99 Comment: S1 - 19
Counts
2000
1600
1200
800
400
0
Chlorite 002
White Mica 001
Chlorite 001
Quartz
5
10
15
20
25
30

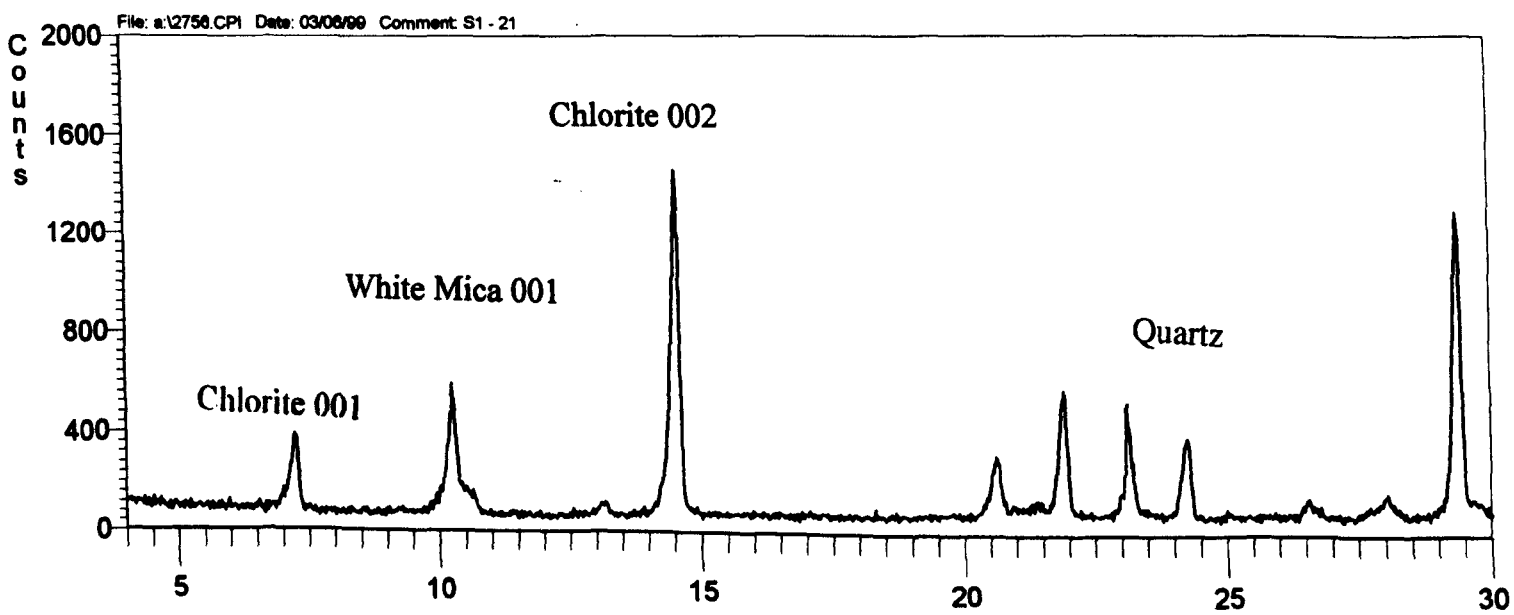
File: a:\2756.CPI Date: 03/06/99 Comment: S1 - 21
Counts
2000
1600
1200
800
400
0
Chlorite 002
White Mica 001
Chlorite 001
Quartz
5
10
15
20
25
30

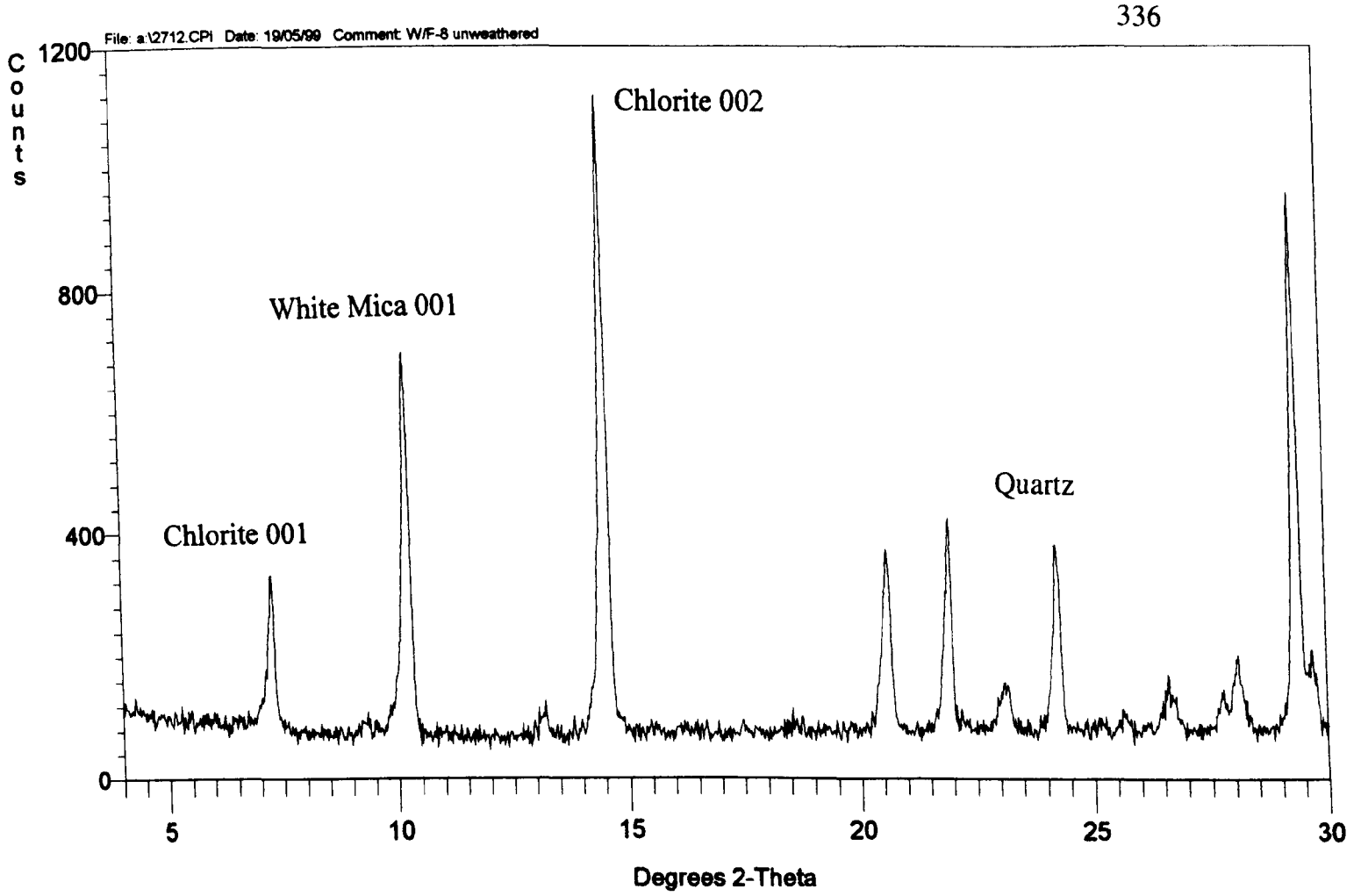
File: a:\2712.CPI Date: 19/05/99 Comment: W/F-8 unweathered
Counts
1200
800
400
0
Chlorite 002
White Mica 001
Chlorite 001
Quartz
5
10
15
20
25
30
Degrees 2-Theta

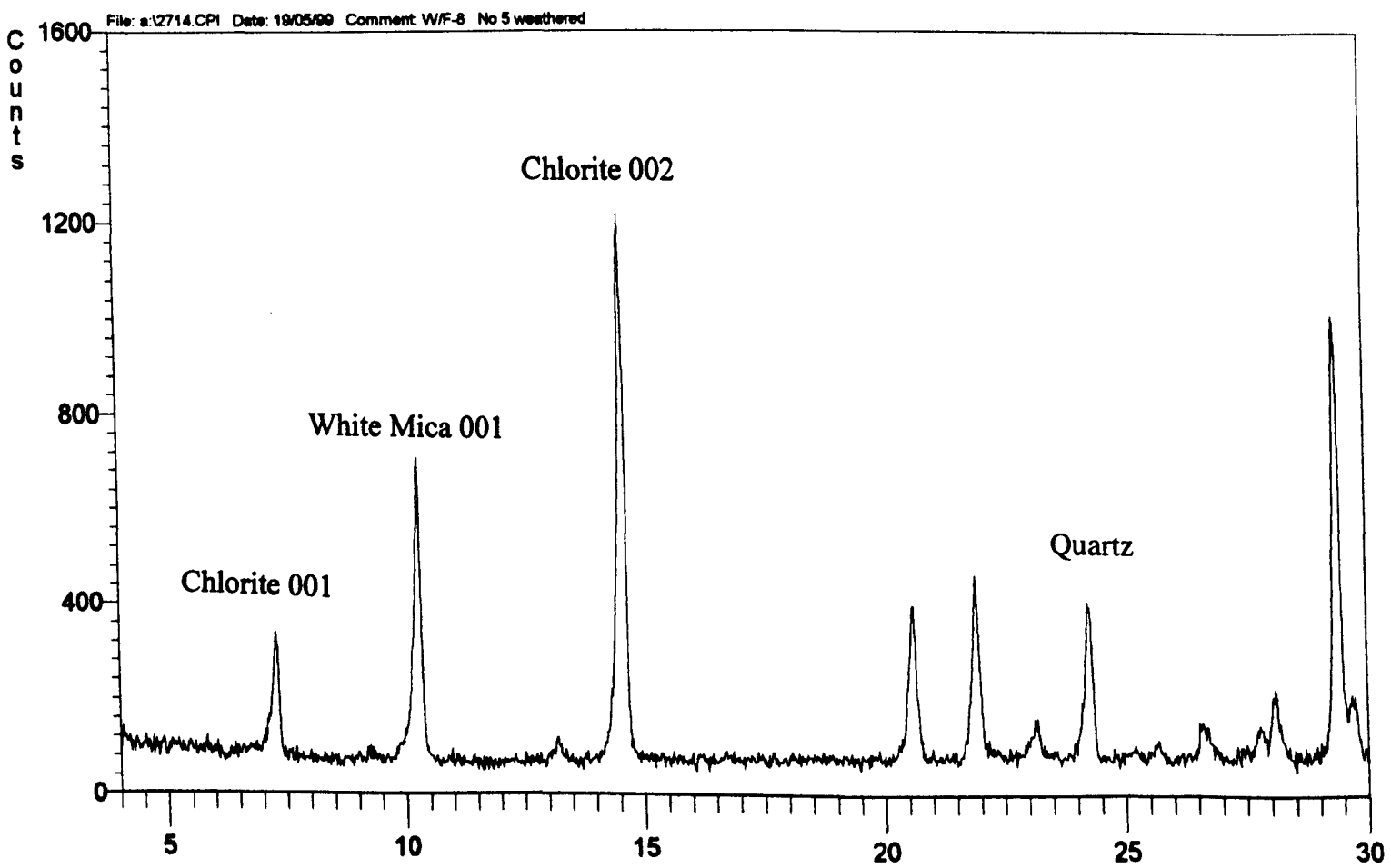
File: a:\2714.CPI Date: 19/05/99 Comment: W/F-8 No 5 weathered
Counts
1600
1200
800
400
0
Chlorite 002
White Mica 001
Chlorite 001
Quartz
5
10
15
20
25
30

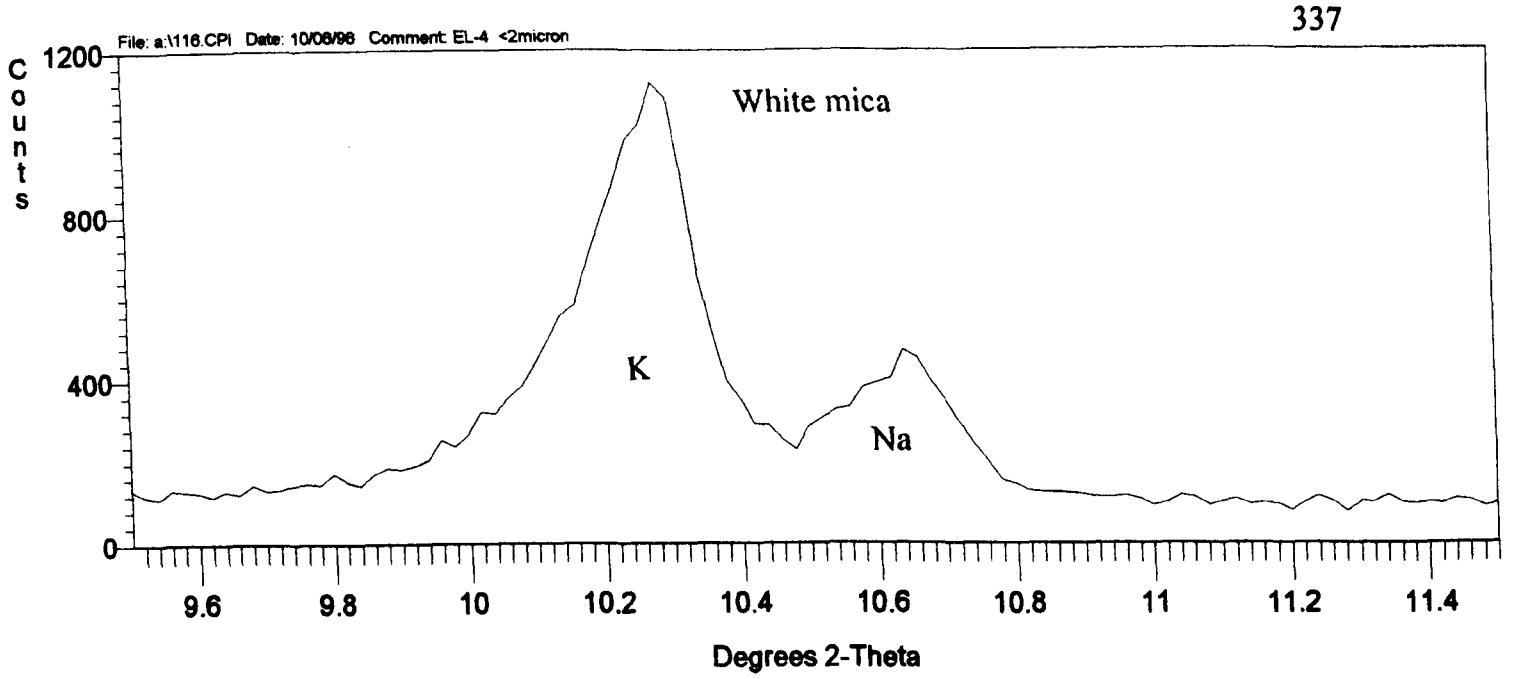
File: a:\116.CPI Date: 10/08/96 Comment: EL-4 <2micron
Counts
1200
800
400
0
White mica
K
Na
9.6
9.8
10
10.2
10.4
10.6
10.8
11
11.2
11.4
Degrees 2-Theta

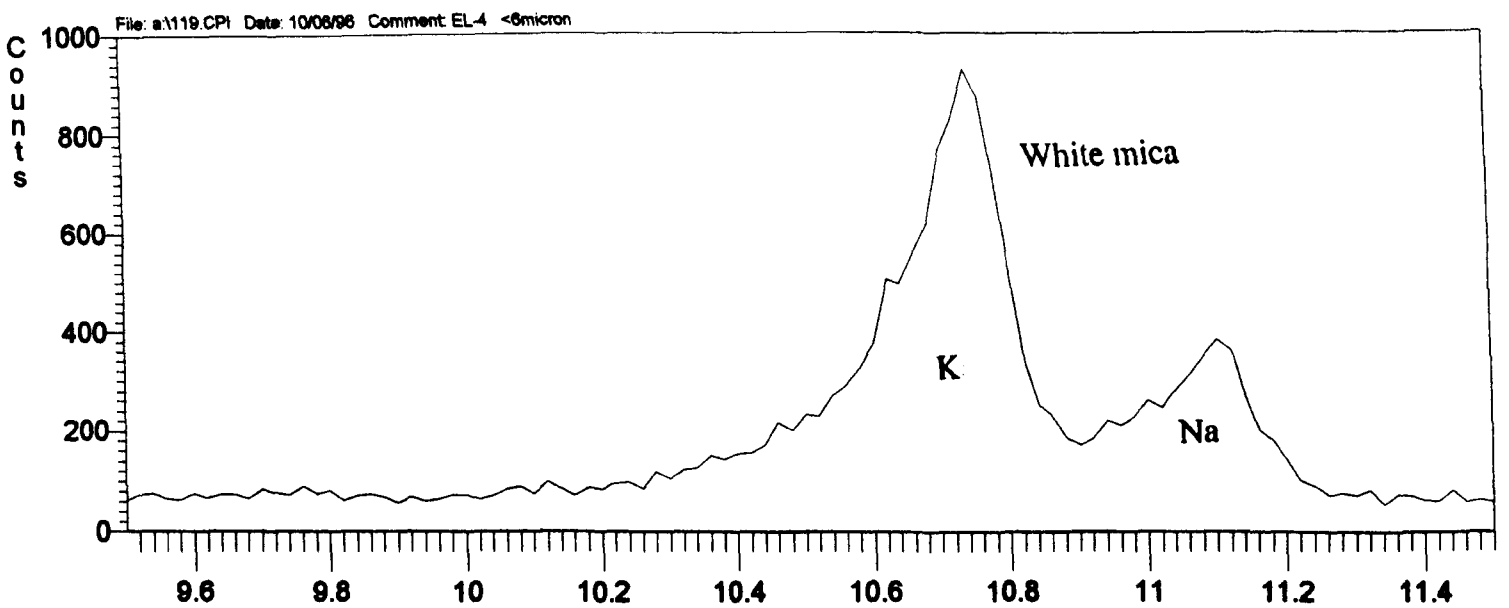
File: a:\119.CPI Date: 10/08/96 Comment: EL-4 <6micron
Counts
1000
800
600
400
200
0
White mica
K
Na
9.6
9.8
10
10.2
10.4
10.6
10.8
11
11.2
11.4

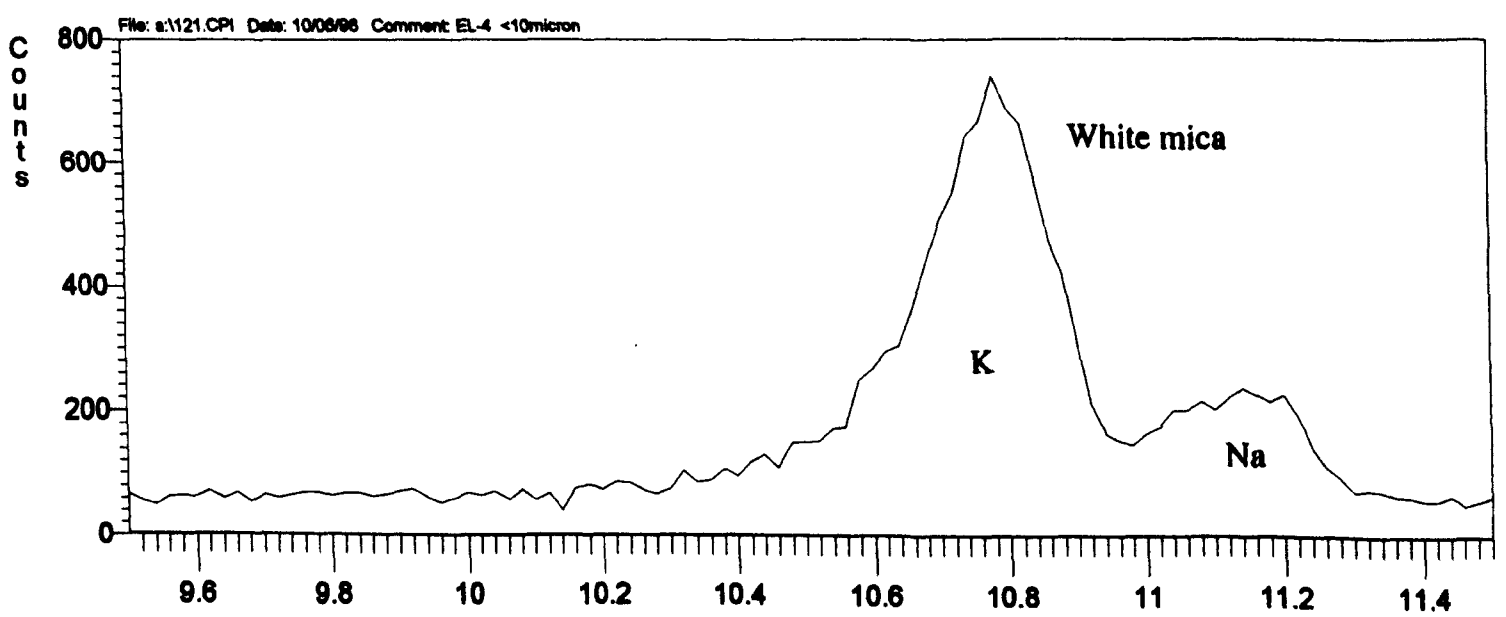
File: a:\121.CPI Date: 10/08/96 Comment: EL-4 <10micron
Counts
800
600
400
200
0
White mica
K
Na
9.6
9.8
10
10.2
10.4
10.6
10.8
11
11.2
11.4

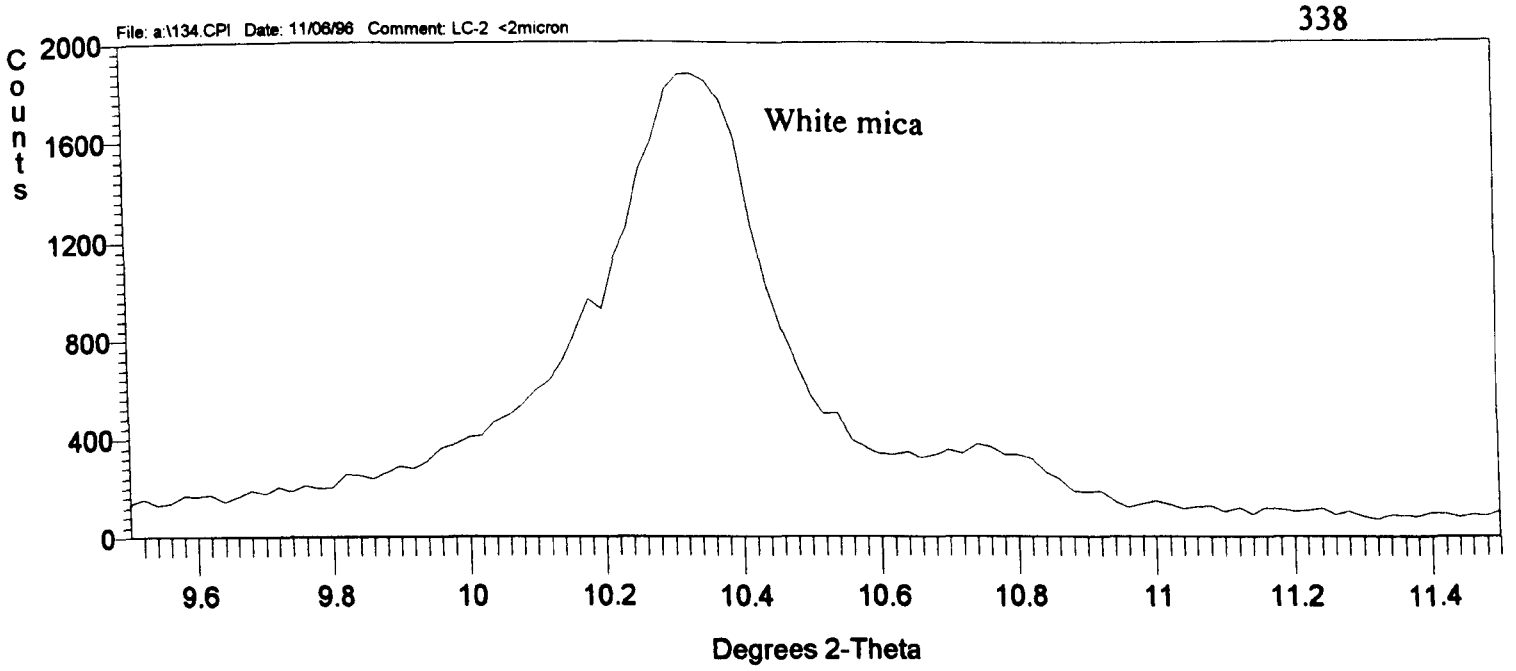
File: a:\134.CPI Date: 11/06/96 Comment: LC-2 <2micron
Counts
2000
1600
1200
800
400
0
White mica
9.6
9.8
10
10.2
10.4
10.6
10.8
11
11.2
11.4
Degrees 2-Theta

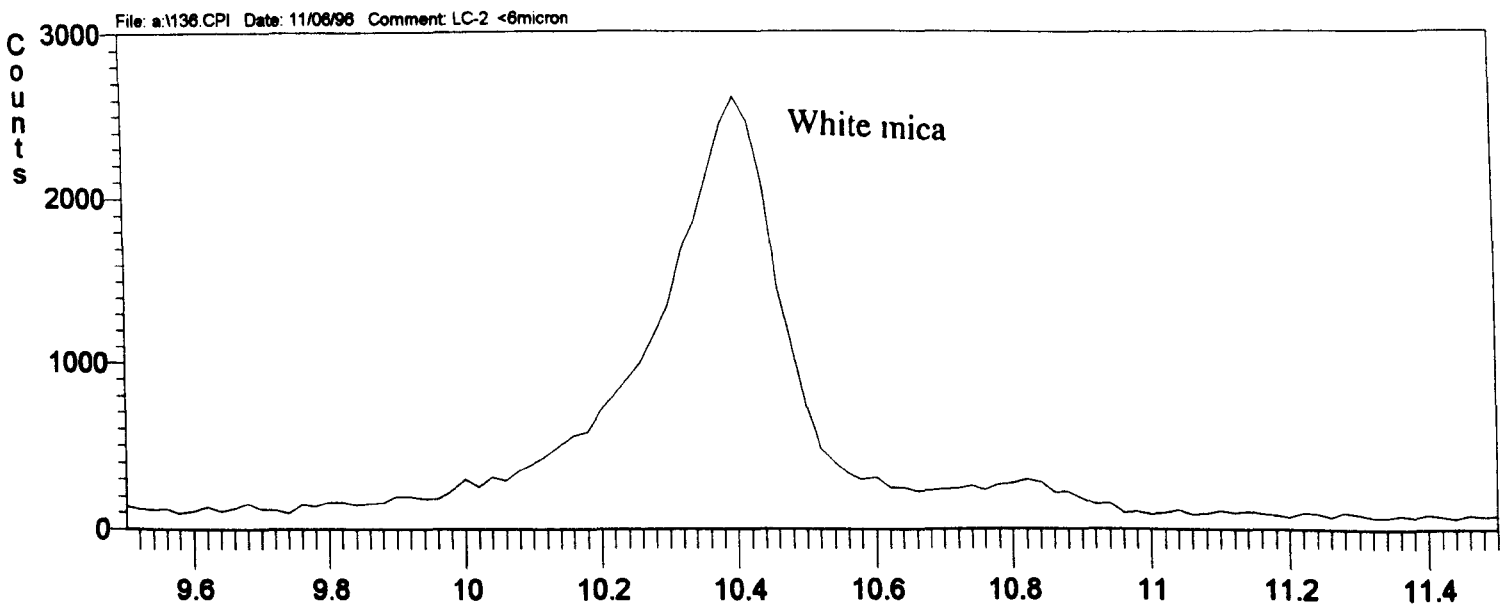
File: a:\136.CPI Date: 11/06/96 Comment: LC-2 <6micron
Counts
3000
2000
1000
0
White mica
9.6
9.8
10
10.2
10.4
10.6
10.8
11
11.2
11.4

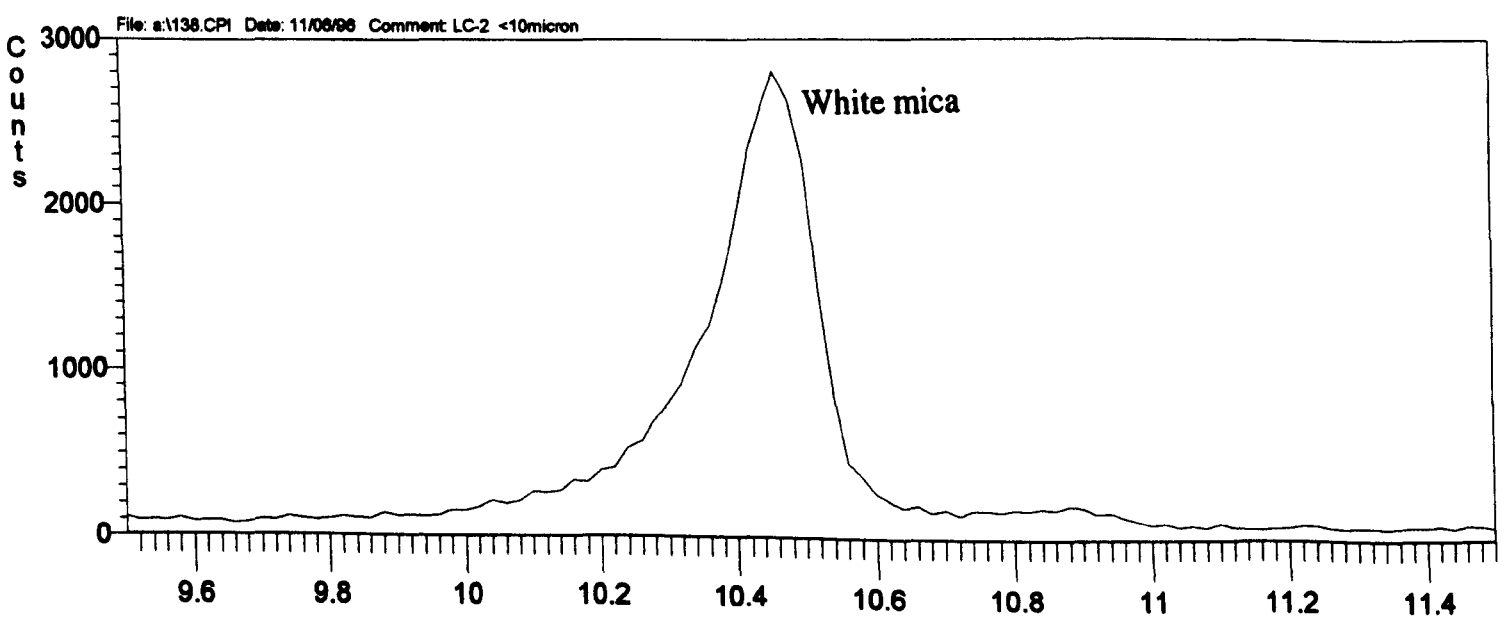
File: a:\138.CPI Date: 11/06/96 Comment: LC-2 <10micron
Counts
3000
2000
1000
0
White mica
9.6
9.8
10
10.2
10.4
10.6
10.8
11
11.2
11.4